BIOSEPARATIONS SCIENCE AND ENGINEERING

Second Edition

ROGER G. HARRISON
PAUL W. TODD
SCOTT R. RUDGE
DEMETRI P. PETRIDES

BIOSEPARATIONS SCIENCE AND ENGINEERING

TOPICS IN CHEMICAL ENGINEERING: A SERIES OF TEXTBOOKS AND MONOGRAPHS

SERIES EDITOR
Keith E. Gubbins, North Carolina State University

ASSOCIATE EDITORS
Mark A. Barteau, University of Delaware
Douglas A. Lauffenburger, MIT
Manfred Morari, ETH
W. Harmon Ray, University of Wisconsin
William B. Russel, Princeton University

Deen, *Analysis of Transport Phenomena*
Doraiswamy, *Organic Synthesis Engineering*
Floudas, *Nonlinear and Mixed Integer Optimization: Fundamentals and Applications*
Friedlander, *Smoke, Dust, and Haze, Second Edition*
Fuller, *Optical Rheometry of Complex Fluids*
Harrison, *Todd, Rudge, and Petrides, Bioseparations Science and Engineering*
Larson, *The Structure and Rheology of Complex Fluids*
Lauffenburger and Linderman, *Receptors: Models for Binding, Trafficking, and Signalling*
Morrison, *Understanding Rheology*
Ogunnaike and Ray, *Process Dynamics, Modeling, and Control*
Pearson, *Discrete-Time Dynamic Models*
Phan-Thien and Kim, *Microstructures in Elastic Media*
Pozrikidis, *An Introduction to Theoretical and Computational Fluid Dynamics*
Pozrikidis, *Numerical Computation in Science and Engineering*
Schmidt, *The Engineering of Chemical Reactions*
Varma and Morbidelli, *Mathematical Methods in Chemical Engineering*

BIOSEPARATIONS SCIENCE AND ENGINEERING

SECOND EDITION

Roger G. Harrison, Paul W. Todd, Scott R. Rudge,
and
Demetri P. Petrides

OXFORD
UNIVERSITY PRESS

OXFORD
UNIVERSITY PRESS

Oxford University Press is a department of the University of
Oxford. It furthers the University's objective of excellence in research,
scholarship, and education by publishing worldwide.

Oxford New York
Auckland Cape Town Dar es Salaam Hong Kong Karachi
Kuala Lumpur Madrid Melbourne Mexico City Nairobi
New Delhi Shanghai Taipei Toronto

With offices in
Argentina Austria Brazil Chile Czech Republic France Greece
Guatemala Hungary Italy Japan Poland Portugal Singapore
South Korea Switzerland Thailand Turkey Ukraine Vietnam

Oxford is a registered trademark of Oxford University Press
in the UK and certain other countries.

Published in the United States of America by
Oxford University Press
198 Madison Avenue, New York, NY 10016

© Oxford University Press 2015

All rights reserved. No part of this publication may be reproduced, stored in
a retrieval system, or transmitted, in any form or by any means, without the prior
permission in writing of Oxford University Press, or as expressly permitted by law,
by license, or under terms agreed with the appropriate reproduction rights organization.
Inquiries concerning reproduction outside the scope of the above should be sent to the
Rights Department, Oxford University Press, at the address above.

You must not circulate this work in any other form
and you must impose this same condition on any acquirer.

Library of Congress Cataloging-in-Publication Data
Harrison, Roger G., 1944— author.
Bioseparations science and engineering / Roger G. Harrison, Paul W. Todd, Scott R. Rudge, and Demetri P. Petrides. — 2nd edition.
p. ; cm.
Preceded by: Bioseparations science and engineering / Roger G. Harrison ... [et al.]. c2003.
Includes bibliographical references and index.
ISBN 978–0–19–539181–7 (alk. paper)
1. Biomolecules—Separation. 2. Biochemical engineering. 3. Separation (Technology) 4. Extraction (Chemistry) I. Todd, Paul, 1936– author. II. Rudge, Scott R., author. III. Petrides, Demetri P., author. IV. Title.
[DNLM: 1. Biotechnology—methods. 2. Biochemical Processes. 3. Bioengineering—methods. 4. Chemistry Techniques, Analytical. TP 248.25.S47]
TP248.25.S47B55 2015
660′.2842—dc23
2014014226

9 8 7 6 5 4 3 2 1
Printed in the United States of America
on acid-free paper

To Kathy, Mike, and Zack
RGH

To Judy
PT

To Kathy, Cutter, and Davis
SRR

To Elpida, Petros, and Savvas
DPP

CONTENTS

Preface *xix*

1. Introduction to Bioproducts and Bioseparations **1**

1.1 Instructional Objectives 3

1.2 Broad Classification of Bioproducts 3

1.3 Small Biomolecules 4
1.3.1 Primary Metabolites 4
1.3.2 Secondary Metabolites 9
1.3.3 Summary of Small Biomolecules 12

1.4 Macromolecules: Proteins 13
1.4.1 Primary Structure 13
1.4.2 Secondary Structure 14
1.4.3 Tertiary Structure 14
Example 1.1. Effect of a Reducing Agent on Protein Structure and Mobility 17
1.4.4 Quaternary Structure 17
1.4.5 Prosthetic Groups and Hybrid Molecules 17
1.4.6 Functions and Commercial Uses of Proteins 19
1.4.7 Stability of Proteins 21
1.4.8 Recombinant Protein Expression 25

1.5 Macromolecules: Nucleic Acids and Oligonucleotides 31

1.6 Macromolecules: Polysaccharides 33

1.7 Particulate Products 34

1.8 Introduction to Bioseparations: Engineering Analysis 35
1.8.1 Stages of Downstream Processing 35
Example 1.2. Initial Selection of Purification Steps 36
1.8.2 Basic Principles of Engineering Analysis 37

1.8.3 Process and Product Quality 39
1.8.4 Criteria for Process Development 39

1.9 The Route to Market 40
1.9.1 The Chemical and Applications Range of the Bioproduct 40
1.9.2 Documentation of Pharmaceutical Bioproducts 41
1.9.3 GLP and cGMP 42
1.9.4 Formulation 42

1.10 Summary 42
Nomenclature 43
Problems 44
References 46

2. Analytical Methods and Bench Scale Preparative Bioseparations 48

2.1 Instructional Objectives 49

2.2 Specifications 49

2.3 Assay Attributes 51
2.3.1 Precision 51
2.3.2 Accuracy 52
2.3.3 Specificity 52
2.3.4 Linearity, Limit of Detection, and Limit of Quantitation 53
2.3.5 Range 54
2.3.6 Robustness 55

2.4 Analysis of Biological Activity 55
2.4.1 Animal Model Assays 55
2.4.2 Cell-Line-Derived Bioassays 56
2.4.3 *In vitro* Biochemical Assays 57
Example 2.1. Coupled Enzyme Assay for Alcohol Oxidase 58

2.5 Analysis of Purity 59
2.5.1 Electrophoretic Analysis 60
Example 2.2. Estimation of the Maximum Temperature in an Electrophoresis Gel 63
2.5.2 High-Performance Liquid Chromatography (HPLC) 76
2.5.3 Mass Spectrometry 79
2.5.4 Coupling of HPLC with Mass Spectrometry 80
2.5.5 Ultraviolet Absorbance 80
Example 2.3. Determination of Molar Absorptivity 81
2.5.6 CHNO/Amino Acid Analysis (AAA) 82
Example 2.4. Calculations Based on CHNO Analysis 82

2.5.7 Protein Assays 83
2.5.8 Enzyme-Linked Immunosorbent Assay 84
2.5.9 Gas Chromatography 86
2.5.10 DNA Hybridization 86
2.5.11 ICP/MS (AES) 87
2.5.12 Dry Weight 87

2.6 Microbiology Assays 88
2.6.1 Sterility 88
2.6.2 Bioburden 88
2.6.3 Endotoxin 89
2.6.4 Virus, Mycoplasma, and Phage 89

2.7 Bench Scale Preparative Separations 90
2.7.1 Preparative Electrophoresis 90
2.7.2 Magnetic Bioseparations 96

2.8 Summary 101
Nomenclature 103
Problems 104
References 108

3. Cell Lysis and Flocculation 111

3.1 Instructional Objectives 111

3.2 Some Elements of Cell Structure 112
3.2.1 Prokaryotic Cells 112
3.2.2 Eukaryotic Cells 113

3.3 Cell Lysis 114
3.3.1 Osmotic and Chemical Cell Lysis 116
3.3.2 Mechanical Methods of Lysis 117

3.4 Flocculation 120
3.4.1 The Electric Double Layer 121
Example 3.1. Dependence of the Debye Radius on the Type of Electrolyte 124
3.4.2 Forces Between Particles and Flocculation by Electrolytes 125
Example 3.2. Sensitivity of Critical Flocculation Concentration to Temperature and Counterion Charge Number 127
3.4.3 The Schulze-Hardy Rule 128
3.4.4 Flocculation Rate 129
3.4.5 Polymeric Flocculants 129

3.5 Summary 131
Nomenclature 131
Problems 133
References 133

4. Filtration 135

4.1 Instructional Objectives 136

4.2 Filtration Principles 137
4.2.1 Conventional Filtration 137
Example 4.1. Batch Filtration 138
4.2.2 Crossflow Filtration 143
Example 4.2. Concentration Polarization in Ultrafiltration 146
Example 4.3. Comparison of Mass Transfer Coefficient Calculated by Boundary Layer Theory Versus by Shear-Induced Diffusion Theory 150

4.3 Filter Media and Equipment 152
4.3.1 Conventional Filtration 152
4.3.2 Crossflow Filtration 156

4.4 Membrane Fouling 160

4.5 Scale-up and Design of Filtration Systems 162
4.5.1 Conventional Filtration 163
Example 4.4. Rotary Vacuum Filtration 164
Example 4.5. Washing of a Rotary Vacuum Filter Cake 166
4.5.2 Crossflow Filtration 171
Example 4.6. Diafiltration Mode in Crossflow Filtration 173

4.6 Summary 176
Nomenclature 178
Problems 179
References 184

5. Sedimentation 185

5.1 Instructional Objectives 185

5.2 Sedimentation Principles 186
5.2.1 Equation of Motion 186
5.2.2 Sensitivities 187

5.3 Methods for Analysis of Sedimentation 189
5.3.1 Equilibrium Sedimentation 190
5.3.2 Sedimentation Coefficient 191

Example 5.1. Application of the Sedimentation Coefficient 191
5.3.3 Equivalent Time 192
Example 5.2. Scale-up Based on Equivalent Time 193
5.3.4 Sigma Analysis 193

5.4 Production Centrifuges: Comparison and Engineering Analysis 194
5.4.1 Tubular Bowl Centrifuge 195
Example 5.3. Complete Recovery of Bacterial Cells in a Tubular Bowl Centrifuge 199
5.4.2 Disk Centrifuge 200

5.5 Ultracentrifugation 203
5.5.1 Determination of Molecular Weight 204

5.6 Flocculation and Sedimentation 205

5.7 Sedimentation at Low Accelerations 206
5.7.1 Diffusion, Brownian Motion 206
5.7.2 Isothermal Settling 207
5.7.3 Convective Motion and Péclet Analysis 207
5.7.4 Inclined Sedimentation 207
5.7.5 Field-Flow Fractionation 209

5.8 Centrifugal Elutriation 210

5.9 Summary 210
Nomenclature 212
Problems 214
References 217

6. Extraction 219

6.1 Instructional Objectives 219

6.2 Extraction Principles 220
6.2.1 Phase Separation and Partitioning Equilibria 220
6.2.2 Countercurrent Stage Calculations 226
Example 6.1. Separation of a Bioproduct and an Impurity by Countercurrent Extraction 230
Example 6.2. Effect of Solvent Rate in Countercurrent Staged Extraction of an Antibiotic 230

6.3 Scale-up and Design of Extractors 232
6.3.1 Reciprocating-Plate Extraction Columns 233
Example 6.3. Scale-up of a Reciprocating-Plate Extraction Column 235

6.3.2 Centrifugal Extractors 237
Example 6.4. Increase in Feed Rate to a Podbielniak Centrifugal Extractor 238

6.4 Summary 239
Nomenclature 240
Problems 241
References 243

7. Liquid Chromatography and Adsorption 245

7.1 Instructional Objectives 247

7.2 Adsorption Equilibrium 248

7.3 Adsorption Column Dynamics 251
7.3.1 Fixed-Bed Adsorption 251
Example 7.1. Determination of the Mass Transfer Coefficient from Adsorption Breakthrough Data 256
7.3.2 Agitated-Bed Adsorption 258

7.4 Chromatography Column Dynamics 259
7.4.1 Plate Models 260
7.4.2 Moment Analysis 262
7.4.3 Chromatography Column Mass Balance with Negligible Dispersion 264
Example 7.2. Chromatographic Separation of Two Solutes 264
Example 7.3. Calculation of the Shock Wave Velocity for a Nonlinear Isotherm 266
Example 7.4. Calculation of the Elution Profile 267
7.4.4 Dispersion Effects in Chromatography 269
7.4.5 Computer Simulation of Chromatography Considering Axial Dispersion, Fluid-Phase Mass Transfer, Intraparticle Diffusion, and Nonlinear Equilibrium 275
7.4.6 Gradients and Modifiers 277
Example 7.5. Equilibrium for a Protein Anion in the Presence of Chloride Ion 277

7.5 Membrane Chromatography 279
Example 7.6. Comparison of Time for Diffusion Mass Transfer in Conventional Chromatography and Membrane Chromatography 282

7.6 Simulated Moving Bed Chromatography 284

7.7 Adsorbent Types 288
7.7.1 Silica-Based Resins 288
7.7.2 Polymer-Based Resins 289
7.7.3 Ion Exchange Resins 290
7.7.4 Reversed-Phase Chromatography 291
7.7.5 Hydrophobic Interaction Chromatography 292
7.7.6 Affinity Chromatography 292
7.7.7 Immobilized Metal Affinity Chromatography (IMAC) 293
7.7.8 Size Exclusion Chromatography 293

7.8 Particle Size and Pressure Drop in Fixed Beds 294

7.9 Equipment 295
7.9.1 Columns 295
7.9.2 Chromatography Column Packing Procedures 296
7.9.3 Detectors 297
7.9.4 Chromatography System Fluidics 298

7.10 Scale-up 299
7.10.1 Adsorption 299
Example 7.7. Scale-up of the Fixed-Bed Adsorption of a Pharmaceutical Product 302
7.10.2 Chromatography 306
Example 7.8. Scale-up of a Protein Chromatography 308
Example 7.9. Scale-up of Protein Chromatography Using Standard Column Sizes 309
Example 7.10. Scale-up of Elution Buffer Volumes in Protein Chromatography 310
Example 7.11. Consideration of Pressure Drop in Column Scaling 311

7.11 Summary 311
Nomenclature 314
Problems 317
References 324

8. Precipitation 327

8.1 Instructional Objectives 327

8.2 Protein Solubility 328
8.2.1 Structure and Size 328
8.2.2 Charge 329

8.2.3 Solvent 331
Example 8.1. Salting Out of a Protein with Ammonium Sulfate 333

8.3 Precipitate Formation Phenomena 334
8.3.1 Initial Mixing 335
8.3.2 Nucleation 335
8.3.3 Growth Governed by Diffusion 336
Example 8.2. Calculation of Concentration of Nuclei in a Protein Precipitation 337
Example 8.3. Diffusion-Limited Growth of Particles 340
8.3.4 Growth Governed by Fluid Motion 341
Example 8.4. Growth of Particles Limited by Fluid Motion 342
8.3.5 Precipitate Breakage 343
8.3.6 Precipitate Aging 343

8.4 Particle Size Distribution in a Continuous-Flow Stirred Tank Reactor 344
Example 8.5. Dependence of Population Density on Particle Size and Residence Time in a CSTR 348

8.5 Methods of Precipitation 348

8.6 Design of Precipitation Systems 352

8.7 Summary 354
Nomenclature 356
Problems 358
References 360

9. Crystallization 362

9.1 Instructional Objectives 363

9.2 Crystallization Principles 363
9.2.1 Crystals 363
9.2.2 Nucleation 364
9.2.3 Crystal Growth 366
9.2.4 Crystallization Kinetics from Batch Experiments 367

9.3 Batch Crystallizers 368
9.3.1 Analysis of Dilution Batch Crystallization 369
Example 9.1. Batch Crystallization with Constant Rate of Change of Diluent Concentration 371

9.4 Process Crystallization of Proteins 373

9.5 Crystallizer Scale-up and Design 375
9.5.1 Experimental Crystallization Studies as a Basis for Scale-up 375
9.5.2 Scale-up and Design Calculations 377
Example 9.2. Scale-up of Crystallization Based on Constant Power per Volume 378

9.6 Summary 379
Nomenclature 379
Problems 381
References 383

10. Evaporation 384

10.1 Instructional Objectives 384

10.2 Evaporation Principles 385
10.2.1 Heat Transfer 385
Example 10.1. Evaporation of a Butyl Acetate Stream Containing a Heat-Sensitive Antibiotic in a Falling-Film Evaporator 388
10.2.2 Vapor-Liquid Separation 394

10.3 Evaporation Equipment 396
10.3.1 Climbing-Film Evaporators 397
10.3.2 Falling-Film Evaporators 398
10.3.3 Forced-Circulation Evaporators 398
10.3.4 Agitated-Film Evaporators 399

10.4 Scale-up and Design of Evaporators 399

10.5 Summary 402
Nomenclature 403
Problems 404
References 405

11. Drying 407

11.1 Instructional Objectives 407

11.2 Drying Principles 408
11.2.1 Water in Biological Solids and in Gases 408
Example 11.1. Drying of Antibiotic Crystals 411
11.2.2 Heat and Mass Transfer 412
Example 11.2. Conductive Drying of Wet Solids in a Tray 414
Example 11.3. Mass Flux During the Constant Rate Drying Period in Convective Drying 420

Example 11.4. Time to Dry Nonporous Biological Solids by Convective Drying 421

11.3 Dryer Description and Operation 422
11.3.1 Vacuum-Shelf Dryers 422
11.3.2 Batch Vacuum Rotary Dryers 423
11.3.3 Freeze Dryers 424
11.3.4 Spray Dryers 426

11.4 Scale-up and Design of Drying Systems 427
11.4.1 Vacuum-Shelf Dryers 427
11.4.2 Batch Vacuum Rotary Dryers 428
11.4.3 Freeze Dryers 428
11.4.4 Spray Dryers 431
Example 11.5. Sizing of a Spray Dryer 432

11.5 Summary 435
Nomenclature 436
Problems 437
References 440

12. Bioprocess Design and Economics 441

12.1 Instructional Objectives 441

12.2 Definitions and Background 442

12.3 Synthesis of Bioseparation Processes 445
12.3.1 Primary Recovery Stages 445
12.3.2 Intermediate Recovery Stages 450
12.3.3 Final Purification Stages 451
12.3.4 Pairing of Unit Operations in Process Synthesis 453

12.4 Process Analysis 454
12.4.1 Spreadsheets 454
12.4.2 Process Simulators and Their Benefits 454
12.4.3 Using a Biochemical Process Simulator 457

12.5 Process Economics 460
12.5.1 Capital Cost Estimation 461
12.5.2 Operating Cost Estimation 466
12.5.3 Profitability Analysis 471

12.6 Illustrative Examples 472
12.6.1 Citric Acid Production 472
12.6.2 Human Insulin Production 479
12.6.3 Therapeutic Monoclonal Antibody Production 495

12.7 Summary 502
Problems 503
References 507

13. Laboratory Exercises in Bioseparations 511

13.1 Flocculant Screening 511
13.1.1 Background 512
13.1.2 Objectives 512
13.1.3 Procedure 512
13.1.4 Report 513
13.1.5 Some Notes and Precautions 514

13.2 Crossflow Filtration 514
13.2.1 Background 514
13.2.2 Objectives 515
13.2.3 Procedure 515
13.2.4 Report 515

13.3 Centrifugation of Flocculated and Unflocculated Particulates 516
13.3.1 Background 516
13.3.2 Objectives 517
13.3.3 Procedure 517
13.3.4 Report 519

13.4 Aqueous Two-Phase Extraction 520
13.4.1 Physical Measurements 520
13.4.2 Procedure 521
13.4.3 Calculations and Report 522
13.4.4 Inverse Lever Rule 524

13.5 Chromatography Scale-up 525
13.5.1 Background 525
13.5.2 Objectives 525
13.5.3 Procedure 526
13.5.4 Report 528
References 530

APPENDIX: Table of Units and Constants 531

Index 535

PREFACE

The field of bioseparations has developed as a significant, separate discipline within the general field of biochemical engineering that involves the separation and purification of compounds of biological origin, which are derived from cells grown in bioreactors or from cells contained in animal or plant tissue. The biotechnology industry, which originated in the late 1970's, gave added importance to bioseparations, because many of the products of biotechnology are proteins that often are difficult to purify and frequently must be purified to homogeneity or near homogeneity, leading to high costs. The market for biotechnology products is now in the tens of billions of dollars per year and is forecast to more than triple in size over the next twenty-five years. By far the largest sector of biotechnology products is the one for human therapeutics. The increasing demand for human therapeutics has put even more emphasis on the bioseparation processes that lead to very high purity, such as chromatography.

Practitioners of bioseparations include biochemical engineers and biochemists in the pharmaceutical, biotechnology, food, and chemical industries. This text focuses on the science and engineering aspects of bioseparations and is designed for juniors, seniors, and graduate students. The book is also intended to be useful for practitioners in industry.

The first chapter contains introductory material in two parts, the first of which is basic information about biochemistry. Bioprocess engineers need to know about the physical properties of the materials they must purify, which include antibiotics, vitamins, and vaccines, and, in the field of biotechnology, proteins, nucleic acids, antibodies, subcellular particles, and whole cells. An understanding of cell structure and function is necessary for the intelligent choice of early post-fermentation processes. The second part of this chapter is a brief review of engineering analysis, which is used in various forms throughout the book.

Because we believe that good analytical methods are the foundation of any effort to develop, optimize, and then operate and troubleshoot any bioprocess, the introductory chapter is followed by a chapter on analytical methods. A good understanding of these analytical methods is important for anyone involved in bioseparations process development or production.

The important unit operations are thoroughly covered in separate chapters that follow (Chapters 3-12), with the order of the chapters being similar to the order in which the operations are used in a typical bioseparations process. The approach in each of the chapters on unit operations is to start with a qualitative description indicating the importance and general application of the unit operation, then to describe the scientific foundation of the operation, develop the necessary mathematical theory, and finally describe the applications of the theory in engineering practice with an emphasis on design and scale-up.

In deciding on the subject matter in each of the chapters on unit operations, we have been guided by a desire to emphasize those aspects of unit operations most important as applied to bioseparations at the commercial scale. For example, we have not discussed all methods of industrial drying, just those that are the most important in general for drying bioproducts.

A comprehensive treatment of bioseparations process design (Chapter 12) follows the unit operations chapters and focuses on how to integrate the individual unit operations in developing a process design that is the "best" among several plausible alternatives. The use of a process simulator (SuperPro Designer) is illustrated to analyze and evaluate the production of three biological products—citric acid, recombinant human insulin, and monoclonal antibodies. All the problems in this chapter are intended as open-ended assignments, which can be worked either with or without a biochemical process simulator. The use of a bioprocess simulator, however, will greatly facilitate the process analysis, including generating flowsheets, carrying out material balances, and analyzing costs. It is recommended that students have 6 to 8 weeks to complete their problems.

SuperPro Designer is our strong preference for a biochemical process simulator that can handle batch as well as continuous processes. A functional evaluation version of SuperPro Designer can be accessed at the website www.intelligen.com. A site license (one time fee) of SuperPro Designer can be obtained at a discount for courses at universities adopting *Bioseparations Science and Engineering* (Intelligen, Inc., Scotch Plains, New Jersey).

In the second edition of this text, several topics have received added emphasis. In keeping with the current increased importance of biotechnology products that are proteins, such as monoclonal antibodies, considerable new coverage of chromatography has been added. Compared to the first edition, the following topics were added or major changes were made:

- moment analysis in chromatography
- computer simulation of chromatography
- membrane chromatography
- simulated moving bed chromatography
- bench scale preparative separations using electrophoresis and magnetic separations

- evaporation, a process commonly used for bioproducts such as antibiotics, steroids, and peptides
- updating of the bioprocess design and economics for the production of a therapeutic monoclonal antibody
- updating of all of the costs in the chapter on bioprocess design and economics

Illustrative example problems are included within the text throughout Chapters 1 to 12. The purpose of these examples is often to show how to apply previously presented theory, or in some cases to extend the theory to other situations. One way that these examples can be effectively used in the classroom is as follows: The student reads through the solution of the problem and then (1) formulates a question that someone might have about the problem's solution and discusses this question and possible answers to the question with another student or students in the course, or (2) discusses a key point in the solution with another student or students in the course. Then, the instructor asks one or more students about the questions or key points that have been raised.

Problems developed for this book are given at the ends of Chapters 1 to 12, now totaling 130 for the second edition. These problems are intended to help the student both understand and be able to apply the material presented. Several of the problems are deliberately underspecified or of an open-ended nature. The problems can be assigned as out-of-class homework, or can be worked in class by students working in groups (of two, three, or four, depending on the complexity of the problem). Groups in class respond to the task in the following way: (1) each student formulates his or her answer, (2) students share their answer with their partner or partners, (3) students listen carefully to partner's or partners' answers, and (4) groups create a new answer that is superior to each member's initial formulation through the process of association, building on each other's thoughts, and synthesizing.

The practicum (Chapter 13) describes a set of bioseparations experiments that has been thoroughly tested by students (University of Colorado). A few selected experiments, or all of them, could be used in a course on bioseparations.

Additional information supporting this textbook and bioseparations in general can be found at the website http://www.biosep.ou.edu. Material at this website includes (1) a link to the bioprocess simulation software used in the bioprocess design and economics chapter; (2) new problems and examples, which are added periodically; (3) links to useful databases (such as for proteins); and (4) links to manufacturers of bioseparations equipment and supplies.

We are grateful for the contributions that many people made, either directly or indirectly, to this book. University of Oklahoma undergraduate students Emily Burdett and Kevin Dyer contributed new problems in the chapter on liquid chromatography and adsorption. Jean Hunter gave us encouragement and feedback in her review of the prospectus of the second edition. Jean-Bernard Gros read the final draft of the second edition and gave use valuable feedback. We again thank those who contributed in various ways to the first edition, including Ed Cussler, Robert Davis,

Eric Dunlop, Larry Erickson, Antonio Garcia, Jean-Bernard Gros, Dale Gyure, Juan Hong, Harold Monbouquette, Harold Null, Todd Przybycien, Subhas Sikdar, Geoffrey Slaff, and Richard Willson. We appreciate the feedback we have received over several years from students taking courses and the teaching assistants in these courses at the Universities of Colorado and Oklahoma where material on bioseparations was presented.

We are also grateful for being selected by the American Society for Engineering Education in 2006 to receive the Meriam/Wiley Distinguished Author Award for the first edition of *Bioseparations Science and Engineering*, an award given for writing the outstanding engineering textbook in the previous four years.

Finally, we are thankful for the patience and support from our families during the writing of this book.

Roger G. Harrison
Paul Todd
Scott R. Rudge
Demetri Petrides

BIOSEPARATIONS SCIENCE AND ENGINEERING

/// 1 /// INTRODUCTION TO BIOPRODUCTS AND BIOSEPARATIONS

Bioproducts—chemical substances or combinations of chemical substances that are made by living things—range from methanol to whole cells. They are derived by extraction from whole plants and animals or by synthesis in bioreactors containing cells or enzymes. Bioproducts are sold for their chemical *activity:* methanol for solvent activity, ethanol for its neurological activity or as a fuel, penicillin for its antibacterial activity, taxol for its anticancer activity, streptokinase (an enzyme) for its blood clot dissolving activity, hexose isomerase for its sugar-converting activity, and whole *Bacillus thuringiensis* cells for their insecticide activity, to name a few very different examples. The wide variety represented by this tiny list makes it clear that bioseparations must encompass a correspondingly wide variety of methods. The choice of separation method depends on the nature of the product, remembering that purity, yield, and activity are the goals, and the most important of these is activity.

This first chapter therefore reviews the chemical properties of bioproducts with themes and examples chosen to heighten awareness of those properties that must be recognized in the selection of downstream processes that result in acceptably high final purity while preserving activity. The final part of this chapter is an introduction to the field of bioseparations, which includes a discussion of the stages of downstream processing, the basic principles of engineering analysis as applied to bioseparations, and the various factors involved in developing a bioproduct for the marketplace.

The pharmaceutical, agrichemical, and biotechnology bioproduct industries account for many billion dollars in annual sales—neglecting, of course, commodity foods and beverages. By "bioproduct" we mean chemical substances that are produced in or by a biological process, either *in vivo* or *ex vivo* (inside or outside a living organism). Figure 1.1 indicates a clear inverse relationship between bioproduct market size and cost.

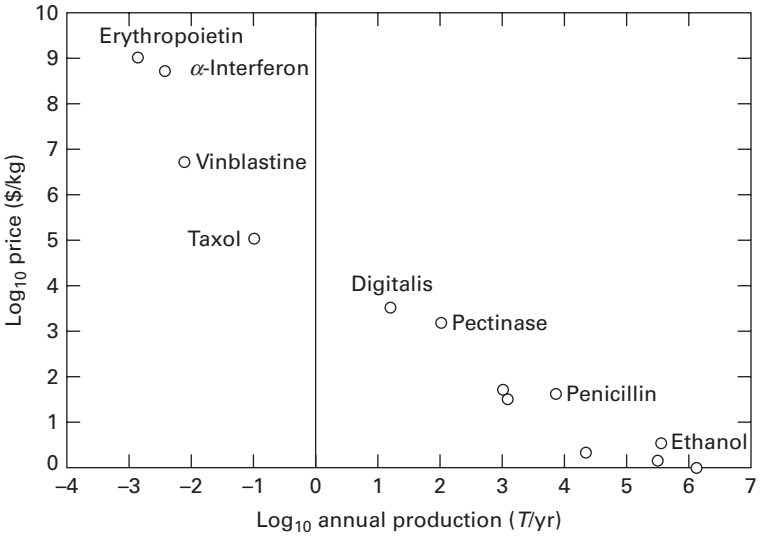

FIGURE 1.1 World production levels and prices of bioproducts, showing the inverse relationship between price and production. *(Data from sources in the early 1990s time frame.)*

TABLE 1.1 Summary of U.S. Biotechnology Product Sales Forecasts (Millions of 2000 Dollars) by Key Market Sectors: 2008–2050[a]

	Sales forecasts ($ million)			
Key sectors	**2008**	**2025**	**2050**	**Average annual growth, 2008–2050 (%)**
Human therapeutics	$27,000	63,500	215,000	5
Human diagnostics	4,300	8,400	18,000	3
Agriculture	2,300	8,600	58,000	8
Specialty chemicals	2,000	4,750	26,700	6
Nonmedical diagnostics	600	1,050	2,300	3
Totals	36,200	86,300	320,000	5

[a] Data from reference 2.

Owing to intense competition, cost, price, and value are very closely related, except in the case of completely new products that are thoroughly protected by patents, difficult to copy, and of added value to the end user. Products with these characteristics—"biotechnology products"—have typically been developed at considerable cost (over $800 million for R&D alone in the case of pharmaceutical products requiring clinical trials [1]) and marketed at prices that allow for the recovery of the development, production, and marketing costs. Their total contribution to the bioproduct market is also in the tens of billions of dollars annually (see Table 1.1) [2]. Such products must recover their development costs within a few years of initial sales, owing to potential competing products, expiration of patents, and economic pressures. Eventually such products move "down" the curve of Figure 1.1, but they

stay on the curve. In the future, movement down the curve will require increased scale and reduced cost of production. Therefore, while existing processes meet many of the requirements of the current market, innovation will eventually be required for the economic large-scale production of biotechnology products. Thus, the following chapters are a practical guide to biochemical separations as currently practiced and as might be practiced in the future.

1.1 INSTRUCTIONAL OBJECTIVES

After completing this chapter, the reader should be able to do the following:

- Broadly classify bioproducts as small molecules, macromolecules, and particulate products including cells.
- Explain the differences between the structures of the various bioproducts.
- Explain the difference between a primary metabolite and a secondary metabolite.
- Outline the structure of proteins at four levels and their stability and functions.
- Explain the structures of other macromolecular substances that are commercial bioproducts, such as nucleic acids and polysaccharides.
- Outline the four stages of downstream processing, the objectives of each stage, and typical unit operations for each stage.
- Explain the engineering analysis concepts of material balance, equilibria, and transport phenomena.
- Calculate purity, specific activity, and yield as quality indicators in purification.

1.2 BROAD CLASSIFICATION OF BIOPRODUCTS

Bioproducts can be broadly classified into the following categories: small molecules, consisting of fine chemicals, antibiotics, hormones, amino acids, and vitamins; large molecules, consisting of proteins, polysaccharides, and nucleic acids; and particulate products, consisting of cells, spores, liposomes, and subcellular particles or organelles. Table 1.2 indicates the sizes and masses of each category of product. These three broad categories correspond to three broad categories of separation procedures for purifying them. As we shall see in this book, small molecules cannot be sedimented, but they can be separated by extraction; many large molecules cannot withstand the conditions of solvent extraction, but they are highly adsorptive; and particulate products can be collected by sedimentation or filtration. In addition, separation processes depend on property differences. Therefore it is important to learn as much as we can about the physical properties and chemical characteristics of the categories of products for which we must design separation procedures. The following subsections summarize the bioproduct types in order of increasing molecular size and complexity, which is also in increasing order of complexity of processing.

TABLE 1.2 Broad Categories of Bioproducts and Their Sizes

Bioproduct	Examples	Molecular weight (Da)	Typical radius
Small molecules	Sugars	200–600	0.5 nm
	Amino acids	60–200	0.5 nm
	Vitamins	300–600	1–2 nm
	Organic acids	30–300	0.5 nm
Large molecules	Proteins	10^3–10^6	3–10 nm
	Polysaccharides	10^4–10^7	4–20 nm
	Nucleic acids	10^3–10^{10}	2–1,000 nm[a]
Particles	Ribosomes		25 nm
	Viruses		100 nm
	Bacteria		1 μm
	Organelles		1 μm
	Yeast cells		4 μm
	Animal cells		10 μm

[a]Single pieces of genetic DNA can have end-to-end lengths up to millimeters, depending on method of isolation; the diameter of the DNA double-stranded α helix is 2.5 nm.

1.3 SMALL BIOMOLECULES

Small biomolecules include naturally occurring compounds and metabolites such as citric acid, vitamins, amino acids, and antibiotics. Besides their importance in fermentation processes, many of these compounds are important commercial products, some of them at very large production rates. Small biomolecules can be divided into two categories—primary metabolites and secondary metabolites.

1.3.1 Primary Metabolites

A primary metabolite is one that is formed during the primary growth phase of the organism. Figure 1.2 shows the key central metabolic intermediates of biosynthetic pathways in heterotrophs, organisms that use organic compounds as carbon sources. The intermediates shown in this overview are used in catabolism, the processes by which microorganisms obtain energy from organic compounds, as well as in biosynthesis, also called anabolism.

Sugars

Naturally occurring sugars are found as monosaccharides, disaccharides, or polysaccharides. One of the world's highest tonnage bioproducts is one of these, sucrose, a disaccharide, whose structure is shown in Figure 1.3. In the food industry, sucrose has been refined from sugarcane for centuries by using an aqueous solution and crystallization process. Mono- and disaccharides are also used in the biochemical

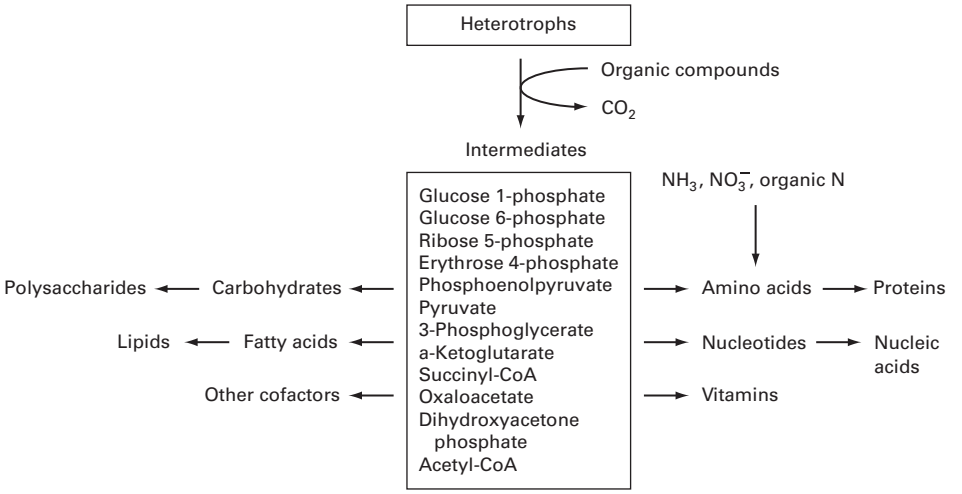

FIGURE 1.2 Overview of the biosynthetic pathways in heterotrophs, organisms that use organic compounds as carbon sources, showing the key central metabolic intermediates.

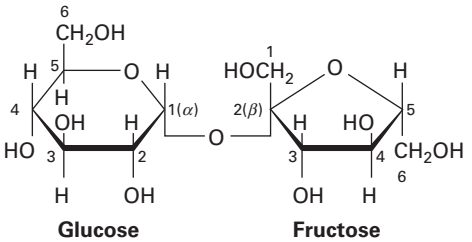

FIGURE 1.3 Sucrose, or table sugar, is a disaccharide composed of the monosaccharides glucose and fructose.

process industry as solutes for the control of osmotic pressure and, most importantly, as carbon sources for the growth of organisms in fermenters. Glucose, a monosaccharide (Figure 1.3), is the most common fermentation nutrient, and lactose (milk sugar) and maltose are popular commercial disaccharides.

Sugars can also be obtained as products in bioprocesses. For example, the enzyme glucose isomerase can convert glucose to fructose, which is much sweeter than glucose. This latter process is being used commercially to produce large amounts of high-fructose corn syrups, which are used as sweeteners in soft drinks.

Organic Alcohols, Acids, and Ketones

Organic alcohols, acids, and ketones can be produced by the anaerobic fermentation of microorganisms. Many of these organisms proceed from glucose to pyruvic acid and then on to the final bioproduct. Ethanol, isopropanol, acetone, acetic acid, lactic acid, and propionic acid are some of the organic alcohols, acids, and ketones that have been produced in anaerobic fermentations [3]. The most economically important of these processes is the production of ethanol. Another way of producing

organic alcohols, acids, and ketones is by using the acetic acid bacteria to perform partial oxidation. For example, the acetic acid product produced by *Acetobacter* bacteria with ethanol as a substrate is vinegar.

Vitamins

The name for vitamins was originally derived from "vital amines," but we have known for decades that not all vitamins are amines, and some are not even vital. Generally, animals do not synthesize vitamins, but generalizations have exceptions. For example, humans and guinea pigs do not synthesize vitamin C (ascorbic acid), while nearly all other mammals do. Vitamin C has many more functions than originally thought. While it is required as a catalyst to support the hydroxylation of proline in collagen, which gives collagen its strength and low solubility, its presence at high concentrations supports antioxidant functions and the sulfation of cholesterol. Biological antioxidants are thought to prolong life and promote health, so vitamin C and its fat-soluble counterparts, vitamins A and E, have become popular consumer products. Both natural and synthetic forms are produced and marketed.

The B vitamins are water soluble and are metabolic precursors of cofactors involved in enzymatically catalyzed reactions. For example, vitamin B_6, pyridoxine, becomes phosphorylated inside the cell and serves as a nitrogen atom shuttle in transamination reactions, which convert keto acids into amino acids and vice versa. Niacin becomes nicotinamide adenine dinucleotide (NAD), the cell's principal redox compound and carrier of hydrogen atoms. The water-soluble vitamins are not phosphorylated because cell membranes cannot transmit organic phosphates; instead, the cell phosphorylates them after they enter. After phosphorylation (and in some cases additional modifications) they become cofactors, or "coenzymes." Folic acid, also water soluble and named for its origin from leaves, is required in minute quantities for hydrogen atom transfer in very special chemical reactions, such as methyl group transfer in the synthesis of the important amino acid methionine and the important DNA base thymine. Folic acid is present in plant tissues in extremely low quantities and was among the earliest challenges in bioprocessing in terms of purifying usable amounts of a product initially present at minuscule concentrations. Folic acid is now synthesized in bacterial or fungal fermentations and is sold as a common ingredient in daily vitamin tablets.

Vitamin A, a carotenoid, becomes the energy transducer of the pigment proteins of the retina. Vitamin D, perhaps more appropriately called hormone D, is a steroid that regulates the passage of calcium ions in and out of cells. Vitamins A and D are derived from carrots and milk, respectively, and are sold after extraction and purification (or after laboratory synthesis) as over-the-counter consumer products.

Vitamins are an excellent example of a present-day market tension: natural versus synthetic. Most vitamins can be synthesized in organic chemical reactions, but some argue that unnatural solvents and reagents used in these syntheses could be present as impurities, possibly harming the consumer. Extraction from plants and fermentation produces vitamins naturally—at higher cost. This issue is important in

bioseparation technology, because the downstream processes are very different in the two approaches. In the latter case, hundreds of unknown contaminating solutes are present, and the product itself is at a low concentration. In the former case (synthesis), fewer impurities are present, but in some cases these may be more objectionable. The chapters that follow will give much more attention to natural products.

Amino Acids

Amino acids are the building blocks of proteins; understanding their chemistry is critical to an understanding of the stability of protein bioproducts. The general structure of an α-amino acid is given in Figure 1.4, where it is seen that every such amino acid has a side chain, or "R group," a negatively charged carboxyl group, and a protonated (positively charged) amino group bonded to a carbon atom, which is called the α carbon because it is adjacent to the carboxyl group. At neutral pH, all amino acids are zwitterionic; that is, they carry positive and negative charges simultaneously.

Table 1.3 lists the amino acids, the three-letter and one-letter abbreviations of each, and their respective side chain structures. This table is grouped according to side chain class. The single-letter code allows easy representation of the primary structure of proteins. It can be seen that all the α-amino acids except glycine contain asymmetric carbon atoms, indicating that amino acids, like sugars, should be optically active. With almost no exceptions, the amino acids synthesized by living things are levorotatory and not racemic, so proteins can be studied on the basis of optical rotary dispersion (ORD); each protein, made of a different combination of amino acids, will have a unique ORD spectrum.

When amino acids are polymerized to form proteins, their carboxyl carbons are linked to their neighbors' amino nitrogens in a classical amide linkage called the *peptide bond*. This occurs through a dehydration condensation, and equilibrium laws dictate that this reaction is highly unlikely in aqueous solutions. However, living cells solve this problem with a catalytic unit known as a *ribosome*. This reaction and a resulting peptide backbone are depicted in Figure 1.5.

Specific properties of amino acid side groups can be exploited in purification methods. A protein rich in acidic or basic amino acids on its surface can be adsorbed by ion exchange or separated by electrophoresis. Many aliphatic side chains can result in preferential adsorption onto or extraction into nonpolar separation media. The free–SH (sulfhydryl) group of cysteine can be used to bind proteins to immobilized mercury. Histidine forms coordination complexes with metals, a fact that is being heavily exploited in protein purification by adsorption methods, as we shall see in Chapter 7.

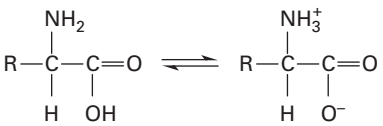

FIGURE 1.4 α-Amino acid structure showing zwitterionic equilibrium at neutral pH.

TABLE 1.3 List of α-Amino Acids Indicating R Group (Side Chain) Structure, Abbreviations, p*K* of R Group,[a] and Class: For General Structure, See Figure 1.4

R Group	Name	Abbreviations	p*K* of R group	Class
—H	Glycine	Gly, G		Aliphatic
—CH_3	Alanine	Ala, A		
—$CH(CH_3)_2$	Valine	Val, V		
—$CH_2CH(CH_3)_2$	Leucine	Leu, L		
—$CHCH_3CH_2CH_3$	Isoleucine	Ile, I		
—CH_2OH	Serine	Ser, S		Hydroxyl or sulfur containing
—$CHOHCH_3$	Threonine	Thr, T		
—CH_2SH	Cysteine	Cys, C	8.3	
—$(CH_2)_2SCH_3$	Methionine	Met, M		
—CH_2COOH	Aspartic acid	Asp, D	3.9	Acids and corresponding amides
—CH_2CONH_2	Asparagine	Asn, N		
—$(CH_2)_2COOH$	Glutamic acid	Glu, E	4.3	
—$(CH_2)_2CONH_2$	Glutamine	Gln, Q		
—$(CH_2)_3CH_2NH_2$	Lysine	Lys, K	10.5	Basic
—$(CH_2)_3NHCNHNH_2$	Arginine	Arg, R	12.5	
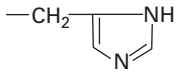	Histidine	His, H	6.0	
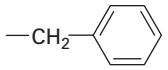	Phenylalanine	Phe, F		Aromatic
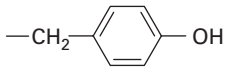	Tyrosine	Tyr, Y	10.1	
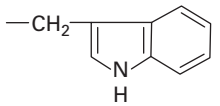	Tryptophan	Try, W		
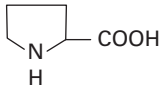	Proline	Pro, P		Imino acid
—CH_2—S—S—CH_2—	Cystine	—		Disulfide

[a] See reference 4. *pK* is the pH at which the R group is half dissociated.

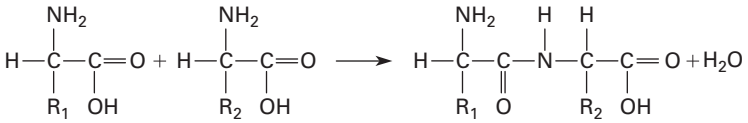

FIGURE 1.5 The formation of a peptide bond (amide linkage) between two amino acids and the resulting peptide backbone of proteins that results from polymerization.

Lipids

The natural fats consist of fatty acids, lipids, steroids, and steroid precursors. This family of bioproducts is highly extractable into nonpolar solvents. Fatty acids are synthesized by cells by building up two-carbon fragments contributed by a precursor compound known as acetyl-coenzyme A (acetyl-CoA), the cell's principal mechanism of acetyl group transfer. Fatty acids are usually esterified to glycerol to form di- and triglycerides, and diglycerides are usually esterified to a phosphate group (hence "phospholipids"), which may in turn be esterified to ethanolamine or choline, rendering the phosphate "head" zwitterionic or amphoteric (having both charges). Fatty acids and phospholipids are *amphiphilic,* having a strongly polar "head" and a strongly nonpolar tail. Such molecules form layers at liquid-liquid interfaces, and just such layers form the membranes that surround living cells and are also found inside eukaryotic cells (fungi, algae, protozoa, and animal and plant cells).

Steroids are heterocyclical compounds, and the most common is cholesterol. Many steroids have hormone activity, partly because they are able to penetrate the nonpolar cell membrane and get inside cells, where they bind and modify the activity of an intracellular protein. It is no surprise that steroids are important bioproducts. Similarly, a family of very potent lipids can profoundly affect the activities of animal cells, namely prostaglandins and leukotrienes; these are also significant commercial bioproducts. Figure 1.6 gives typical structures of four classes of compounds: fatty acid, phospholipid, steroid, and prostaglandin.

Commercial Uses

Many primary metabolites are important commercially; some important examples are given in Table 1.4. The products listed in Table 1.4 are sold in the fermentation, food, and biochemical research marketplaces, and several fine-chemical houses have adopted the sale of primary metabolites as a specialty or as a product line in a warehouse of general chemicals. The biochemical research market demands high variety and low volume. This market is served by a small number of large repackaging or distribution firms who purchase from specialty producers, some of whom also sell directly to customers.

Exemplified by ethanol at the bottom of Figure 1.1, these low molecular weight compounds are the easiest products to purify, mainly owing to their thermal stability. Not surprisingly, they are produced in highest quantity and are used in the beverage, food, feed, solvent, and specialty chemicals industries. Some of the alcohols are traditionally purified using distillation. This is true of none of the other substances discussed in the paragraphs that follow. The highest volume fermentation products in this category include ethanol, acetic acid, butyric acid, lactic acid, citric acid, glutamic acid, tryptophan, and glycine. Two examples are given in Figure 1.7.

1.3.2 Secondary Metabolites

Secondary metabolites are not produced during the primary growth phase of a microorganism, but at or near the beginning of the stationary phase. Antibiotics are the best

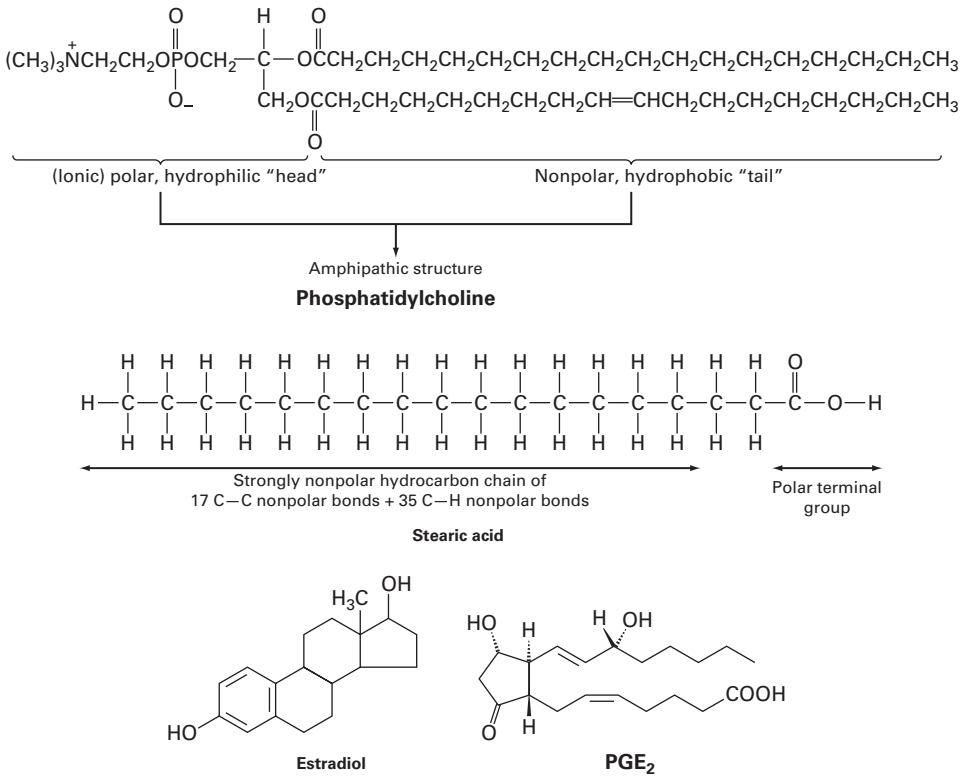

FIGURE 1.6 Structures of typical compounds: a phospholipid (phosphatidylcholine), a fatty acid (stearic acid), a steroid (estradiol), and a prostaglandin (PGE_2).

TABLE 1.4 Some Examples of Primary Metabolites That Are Marketed and Their Uses

Primary metabolite	Commercial uses
Citric acid	Beverages
Acetic acid	Food (vinegar) and fine chemicals
Glutamic acid	Food flavoring (as monosodium glutamate, or MSG)
Lactic acid and Glycolic acid	Reactants for production of biodegradable polymers
Glycerol	Solvent
Butanol	Solvent
Fructose	Food, fermentation
Formic acid	Fine chemicals

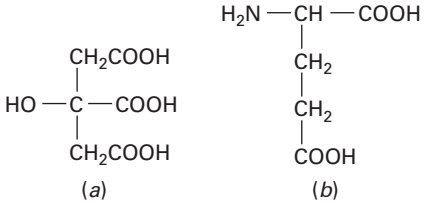

FIGURE 1.7 Structures of (*a*) citric acid and (*b*) glutamic acid (an amino acid).

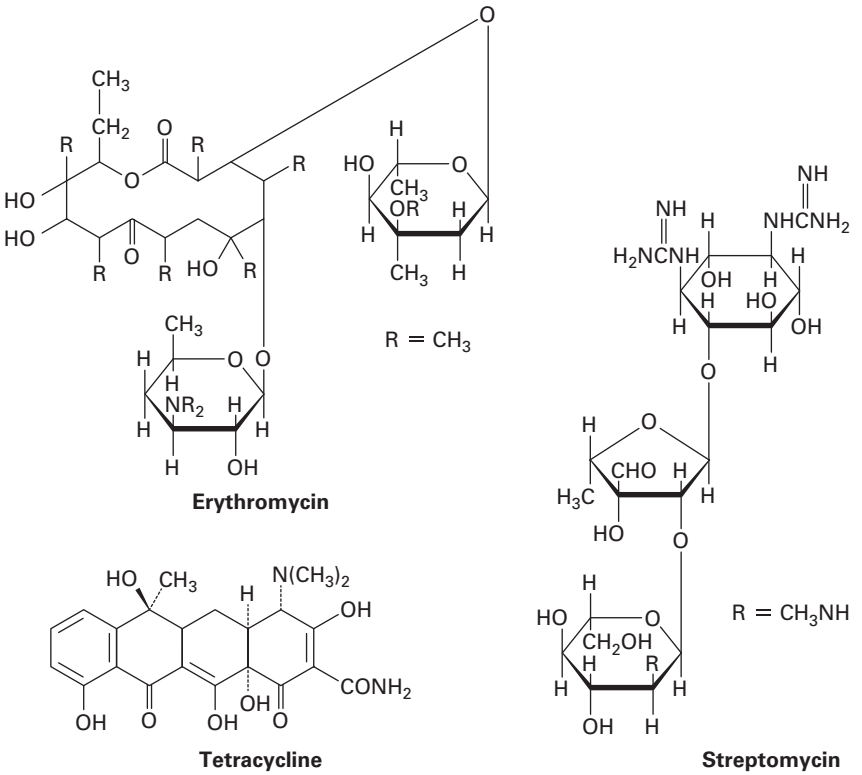

FIGURE 1.8 Structures of three well-known antibiotics: erythromycin, tetracycline, and streptomycin. The choice of purification method is influenced by the profound differences in the chemical structure of these compounds, which have, respectively, macrocycle, polycyclic aromatic, and oligosaccharide structures.

known and most extensively studied secondary metabolites. They are synthesized by fungi as a successful means of competing with bacteria (and sometimes other fungi) for unimpeded growth in natural (dirty) environments. Most primitive eukaryotes are heavily endowed with mechanisms of defense against prokaryotic intrusion, and humans have learned to discover and use these mechanisms. While some antibiotics can be prepared by chemical synthesis, Figure 1.8 illustrates, on the basis of molecular complexity, that their synthesis is more profitably performed by fungal cultures in fermentation vessels. Indeed, large-scale fermentation of any product other than ethanol began with the penicillin industry. Fungi are not the only sources of antibiotics, and bacteria, higher plants, and even animal tissues that produce them can be found.

A number of different secondary metabolites and their general routes of synthesis are shown in Figure 1.9. Clearly, primary metabolites are the raw material for the synthesis of secondary metabolites. The primary metabolites, the level of phosphate in the culture medium, and the cell's energy charge are important modulators of the pathways leading to secondary metabolites [3].

Secondary metabolites made by plants and fungi have found many roles in human culture. Apart from steroid hormones, hallucinogens, and other psychoactive drugs,

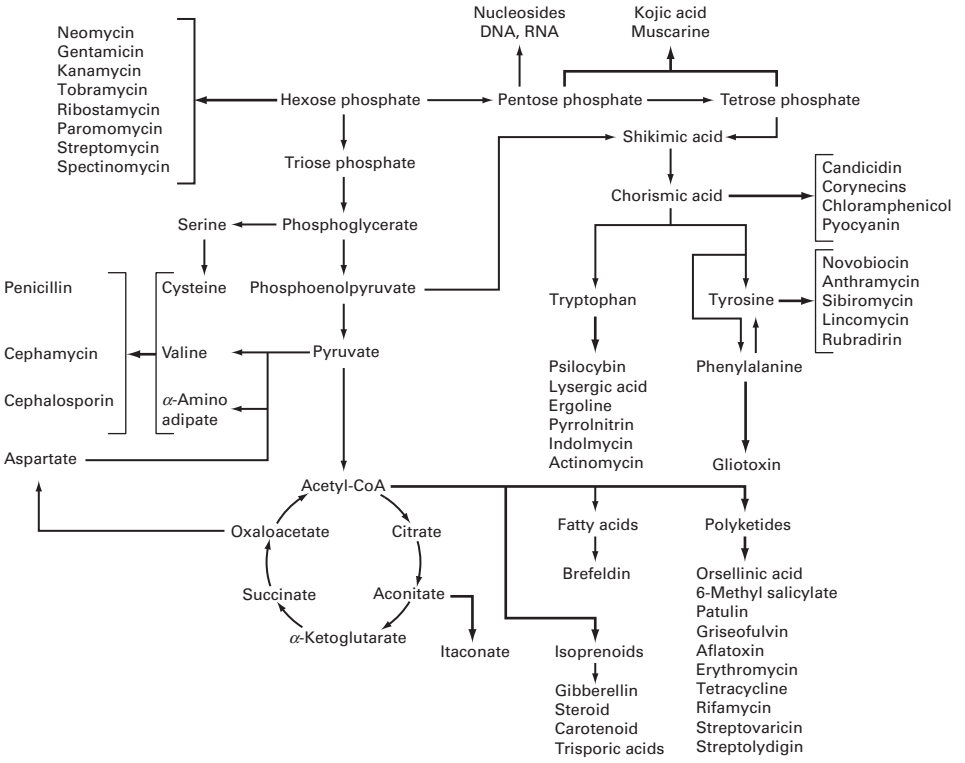

FIGURE 1.9 General routes of biosynthesis of secondary metabolites. The heavy arrows signify enzyme-catalyzed reaction sequences, and the products at the end of these arrows are secondary metabolites.

there are numerous cytotoxic secondary metabolites that have found their way into cancer therapy, cell and biochemical research, and physiological applications.

1.3.3 Summary of Small Biomolecules

Any small-molecule bioproduct could, given suitable conditions, be synthesized by a chemist from petroleum-derived shelf reagents. Where there is large bulk demand, as in the cases of methanol, acetone, and aspirin, chemical synthesis has displaced extraction of natural products as the primary source. Many steroids, especially those popular in preventive gynecology, are synthesized, whereas they were once extracted in large quantities from the tubers of a variety of beets.

In many cases, bioprocess technology is still economically superior. Examine, for example, the structure of taxol in Figure 1.10. Its complete synthesis is extremely difficult, and laboratories are actively pursuing an economical synthetic route owing to its potential importance in cancer therapy and its limited supply from trees. All three upstream methods are used to produce small-molecule bioproducts: extraction from plant and animal tissues, synthesis by fermentation, and conversion in

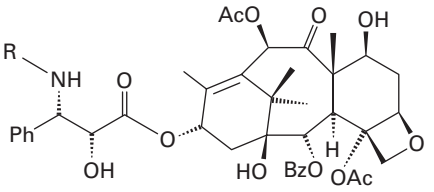

FIGURE 1.10 Structure of taxol, an anticancer compound extracted from the bark of *Taxus brevifolia,* the Pacific yew tree, and certain other natural sources. It functions by immobilizing microtubules in dividing cells and preventing the redissolution of the mitotic spindle.

enzyme-based catalytic reactors. Concerning the last, enantioselective synthetic methods are important, and enantioselective separation methods have been developed for bioproducts with a specific active enantiomer.

1.4 MACROMOLECULES: PROTEINS

The principal source of excitement in the biotechnology industry during the past decades has been the production of biological macromolecules. From presoak laundry enzymes to therapeutic peptides for the treatment of rare diseases, the world of protein chemistry has undergone remarkable metamorphosis. Protein purification is now approaching billion-dollar-industry status on its own. Vendors of adsorption equipment, ultrafiltration technology, and large-scale fermentors are moving rapidly to capture the "picks-and-shovels" market of biotechnology.

Nearly all biological macromolecules are characterized at four levels of structure: primary (the covalent amino acid sequence), secondary (the hydrogen-bonded structures), tertiary (the folding pattern of hydrogen-bonded and disulfide-bonded structures), and quaternary (the formation of multimeric complexes by individual protein molecules).

1.4.1 Primary Structure

Primary structure is the sequence of amino acids established by the sequence of nucleotide codons of the messenger RNA for that protein. The amino acids are held together in strictly linear sequence (just as mRNA is strictly linear), and all backbone bonds are covalent. The peptide bond is illustrated in Figure 1.5. Any polymer of α-amino acids is called a *polypeptide*. When peptides are synthesized by cells, using ribosomes and several enzymes as catalysts, all polymer chains are linear; there are no branched peptides, despite the existence of amino and carboxyl side chains capable of forming amide linkages. Even after translation, branching amide linkages are not formed. In nearly all protein molecules having more than about 70 amino acids, the –SH groups of cysteines *might* react with each other to form disulfide bonds and produce peptide rings; such rings can become branches if the cell deletes a portion of the peptide sequence, as in the case of insulin, shown in Figure 1.11.

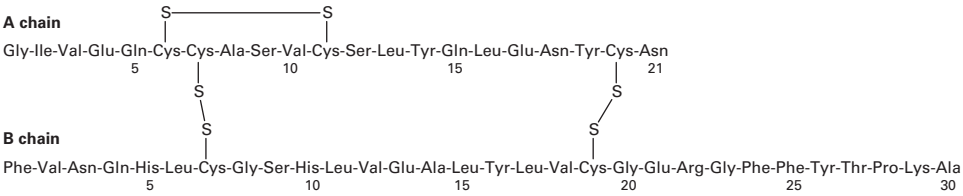

FIGURE 1.11 Amino acid sequence of bovine insulin. The two polypeptide chains are held together by disulfide bridges, but they originated from a single chain, a portion of which was excised by the cell. The A and B chains are connected by interchain disulfide bonds. The chains are numbered, by convention, from their N-terminal ends.

1.4.2 Secondary Structure

There are two main forms of secondary structure, both due to the formation of hydrogen bonds between oxygen and nitrogen atoms in the peptide backbone. Since these are regularly spaced, a repeating pattern of interaction is expected. Indeed, the two structures that form are the α helix and the β sheet (or "pleated sheet"), shown schematically in Figures 1.12 and 1.13, respectively. In the α helix, each peptide CO group is hydrogen-bonded to a peptide NH group four residues further up the chain, and there are 3.6 residues per turn [4]. For the β sheet, the side-by-side polypeptide chains are aligned by interchain hydrogen bonds; all the peptide linkages participate in this hydrogen bond alignment, thus giving the structure great stability [4]. Another secondary structural element that occurs in proteins is the β turn, which is a hairpin turn of the polypeptide chain. This turn is stabilized by the CO group of residue n of the polypeptide being hydrogen bonded to the NH group of residue $(n + 3)$ [4]. This kind of turn allows proteins to have compact three-dimensional structures. β turns often connect antiparallel strands in β-sheet structures.

A commonly used means of following changes in the secondary structure of a protein is the circular dichroism (CD) method, which measures the difference in the absorbances of left circularly polarized light and right circularly polarized light. This difference occurs because secondary structures, such as α helices, interact one way with a left circularly polarized beam and differently with a right circularly polarized beam. CD can be used to estimate the fraction of a protein in α-helix, β-sheet, and random coil configurations [5].

1.4.3 Tertiary Structure

A complete protein molecule will consist of various combinations of various secondary structures, with each helix or sheet called a *domain*. The three-dimensional folding of the coiled or pleated polypeptide chain establishes the following:

- Surface properties
- Catalytic activity
- Stability

- Mechanical strength
- Shape

In protein synthesis, once secondary structures have been established, in most cases the hydrophobic amino acids fold inward, owing to entropic organization of the surrounding polar water molecules. The outcome of the folding step may be constrained by the strong covalent disulfide bonds between cysteine amino acid residues; some proteins, like trypsin inhibitor, can still be hydrophobic on the outside, owing to a large number of covalent disulfide bonds per mole, which stabilize the molecule against folding according to polarity. Finally, the polar and charged amino acids fold toward the surface and confer a net charge on the protein molecular surface that depends on the numerical combination of Asp, Glu, Lys, and Arg on the surface, as well as on the pH. Depending on the pH, His is sometimes counted as a charged amino acid; it has a side chain pK of 6.0 and is only ~10% protonated at pH 7.0.

In globular proteins in aqueous solution, for example, many of the amino acids with non-polar side chains are forced to the inside of the ball-shaped molecule

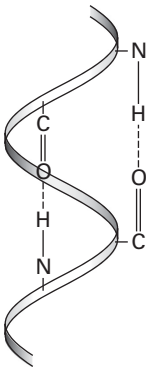

FIGURE 1.12 Schematic representation of a peptide chain in an α-helix configuration, showing hydrogen bonding (dashed lines) that stabilizes the structure.

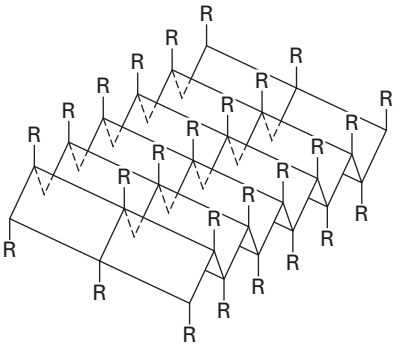

FIGURE 1.13 Representation of three parallel peptide chains in a β-sheet structure. All the R groups (side chains) project above or below the β-sheet structure.

owing to the affinity of the other, polar amino acids for the aqueous environment. Temperature, pH, surfactants, and organic solvents can reverse this picture, leading to *denaturation* of globular protein molecules, a subject discussed in greater detail in Section 1.4.7. Once formed, a tertiary structure is often stabilized by the formation of disulfide bridges between cysteine residues that have folded to positions near one another. A ribbon model of the three-dimensional structure of ribonuclease, determined by x-ray diffraction analysis, is shown in Figure 1.14.

Beyond these simple thermodynamic rules, the tertiary structure of a protein depends highly upon the way in which it is synthesized. For example, the eukaryotic cell takes great care to fold a protein properly during synthesis. In many cases, as the growing peptide chain rolls off the polyribosome translation assembly, an early synthesized part of the chain is extracted into the adjacent lipid-phase membrane. This "signal sequence" holds the N-terminus of the peptide in place while the rest of the molecule is synthesized, glycosylated, and folded. If the same gene is expressed in a prokaryotic cell, which has no internal lipid membranes, however, these things do not happen, and the growing peptide chain folds according to simpler, more "thermodynamic" rules that might apply in free solutions. Heterologous proteins expressed in prokaryotic cells often do not fold correctly, leading to a precipitate called an "inclusion body." Synthesis in other environments can lead to yet other results. The stability of the tertiary structure is discussed later, in Section 1.4.7.

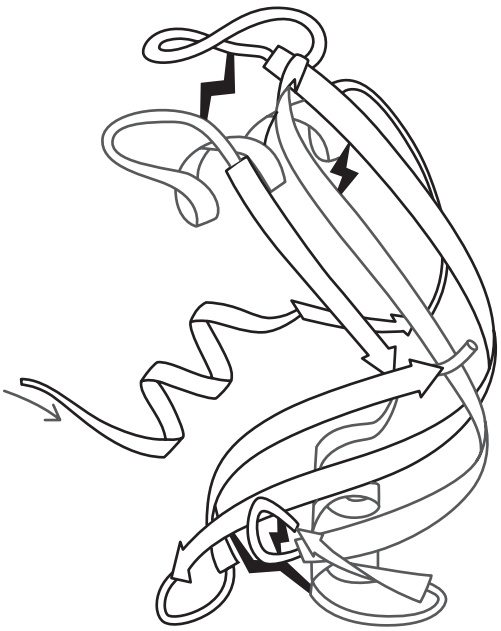

FIGURE 1.14 Ribbon model of ribonuclease. Sections of α helix are shown as helices, β sheets as parallel ribbons, and disulfide bridges in solid black. *(Reproduced by permission of Professor Jane Richardson.)*

EXAMPLE 1.1

Effect of a Reducing Agent on Protein Structure and Mobility Upon the addition of 1 mM dithiothreitol (a reducing agent), the relative mobility of a protein decreases by 10% during the migration of the protein through a polyacrylamide gel under the influence of an electric potential. What is the likely reason for this shift?

Solution

Dithiothreitol is a reducing agent that causes the disulfide bonds between cysteines in the protein to be broken. The breaking of the disulfide bonds causes the protein to unfold and the three-dimensional structure to become less compact, which causes the protein to move more slowly in the polyacrylamide gel. The analysis of proteins by electrophoresis is discussed further in Chapter 2 on analytical methods.

1.4.4 Quaternary Structure

Quaternary structure specifies the way in which the individual, folded peptide chains interact with one another in the native conformation of an oligomeric protein. Thus, a complete hemoglobin molecule contains two α-globin and two β-globin peptide chains (total of four), and bacterial RNA polymerases contain several subunits, one of which confers specificity based on the gene being transcribed. Cytochrome oxidase, located in mitochondria, can have up to 13 peptide chains. Quaternary structure is maintained by intermolecular bonds, including ionic and covalent linkages. In the latter case, cysteine residues form disulfide bridges; in the former case, opposite charges attract (e.g., Lys and Asp).

1.4.5 Prosthetic Groups and Hybrid Molecules

Not all proteins are pure peptides, and the majority of them are *conjugated proteins* that contain not only amino acids, but other organic and inorganic compounds. The non–amino acid portion of a conjugated protein is called its *prosthetic group*. Conjugated proteins are classified on the basis of the chemical nature of their prosthetic groups (Table 1.5). Proteins containing lipids or sugar moieties have also been called *hybrid* compounds.

As the cell synthesizes each new peptide chain by the process of translation, highly specific chemical steps occur that determine whether chemical derivatives of the peptide will be made. Any changes to protein molecules other than the addition of amino acids via peptide bond formation are called *posttranslational modifications*.

A great deal of attention has been given to glycosylation, in which oligosaccharides (usually branched) are added to active side chains of specific amino acids (serine, asparagine, or threonine) while the nascent peptide is in the Golgi apparatus and

TABLE 1.5 Classification of Proteins According to Prosthetic Group

Class	Prosthetic group	Example
Lipoprotein	Lipids such as triglycerides or cholesterol esters	β_1-lipoprotein of blood
Glycoproteins	Oligosaccharides, typically containing mannose, *N*-acetylglucosamine, and galactose, often with sialic acid as a capping residue	Gamma globulin
Phosphoproteins	Phosphate	Protein kinase C
Hemoproteins	Iron porphyrin	Hemoglobin
Flavoproteins	Flavin nucleotides	Succinate dehydrogenase
Metalloproteins	Iron, zinc	Ferritin, alcohol dehydrogenase

being prepared for secretion. The immunogenicity of certain peptides is established by their oligosaccharide content.

Side chain oligosaccharides added during glycosylation serve extremely important functions, such as stability, catalytic function, binding specificity, solubility, targeting, and transport. Glycosylation is extremely important in bioprocessing, since many commercial proteins must be properly glycosylated to function and be marketable. An excellent example is human erythropoietin, which is normally made in cells of the kidney and transported via the blood to the bone marrow, where the target cells reside. Since bacteria do not glycosylate peptides, this valuable product cannot be manufactured by recombinant bacteria; rather, it is made in large cultures of animal cells. Animal or yeast cells are chosen to perform syntheses when the product is a glycosylated protein.

Antibodies are hybrid molecules that have become a major product of biotechnology companies, and many start-up biotechnology companies have initiated their revenue streams by selling antibodies, mainly to be used in diagnostic kits. There is also hope that the "seek and destroy" function of antibodies can be exploited in therapeutic medicine, and clinical trials of antibodies that can carry poisonous or radioactive compounds to tumors, for example, have been under way for some years.

Antibodies are globular proteins synthesized by B lymphocytes in animals. All B lymphocytes that are members of a "clone" produce identical antibody molecules, but different clones produce different antibodies, with a combinatorial number of possibilities, perhaps more than 10^8 different possible peptide sequences. How do they do that? Genes that code for proteins are supposed to be constant and stable, but antibody genes are an exception; they are susceptible to internal rearrangements of DNA base sequences that encode the "hypervariable" region of antibodies, the part that binds antigens. Once the immune system has recognized a substance as "foreign," the B lymphocytes that make antibodies against it expand their clone at the request of specific T lymphocytes, and the blood is flooded with one kind of antibody.

Antibodies that bind to only one epitope (specific molecular region of an antigen) are called "monoclonal antibodies"; they were originally produced by a hybridoma cell that consists of one B lymphocyte cell hybridized with a lymphoma (blood tumor) cell. Monoclonal antibodies for commercial use and clinical studies are now produced by mammalian cell culture using genetically engineered cells. Chinese hamster ovary (CHO) cells are predominantly used now for the large-scale production of monoclonal antibodies [6]. Monoclonal antibodies can also be purified and sold as diagnostic reagents or as affinity reagents for downstream processing, about which we shall learn more later (Chapter 7).

A basic element of the structure of all antibodies, or immunoglobulins, consists of two identical heavy chains and two identical light chains, held together by disulfide bonds to form a Y-shaped structure. The structure of immunoglobulin G, or IgG, is shown in Figure 1.15. The stem of the Y does not vary and is part of the "constant region" of the antibody. The stems are not essential to antigen binding, so sometimes reagents are made without them.

1.4.6 Functions and Commercial Uses of Proteins

Proteins are of interest to biotechnology only on the basis of their function. Table 1.6 lists some functions of proteins, with examples. The ten proteins produced commercially by recombinant DNA technology that had the highest worldwide sales in 2011 are shown in Table 1.7, along with the activity or use of each protein.

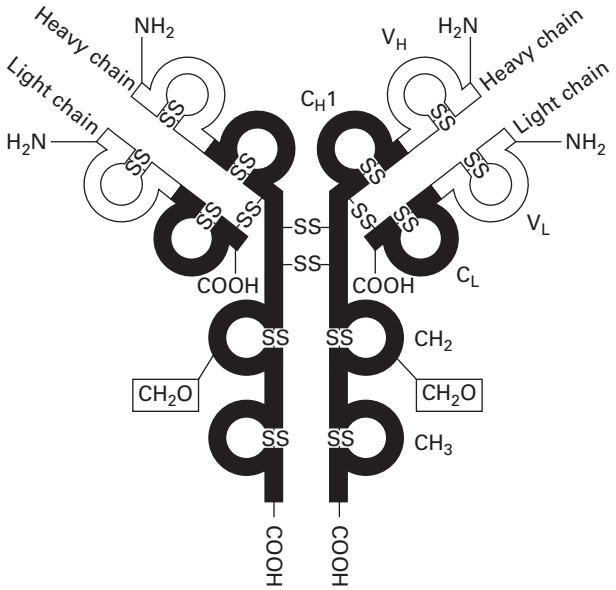

FIGURE 1.15 Structural features of an antibody (immunoglobulin G, or IgG). Each pair of N-terminal residues constitutes an antigen binding site. The variable and constant regions are shown in white and black, respectively. V_H, variable region of the heavy chain; V_L, variable region of the light chain; C_H1, C_H2, and C_H3, constant regions of the heavy chain; C_L, constant region of the light chain. CH_2O denotes carbohydrate, and SS denotes a disulfide bond.

TABLE 1.6 Classification of Proteins According to Function

Class	Examples
Enzymes	Ribonuclease
	Trypsin
	Urokinase
	DNA polymerase
	Cellulase
Transport proteins	Hemoglobin
	Serum albumin
	Myoglobin
	β_1-Lipoprotein
Nutrient, storage protein	Ovalbumin
	Casein
Contractile or motile	Actin
	Myosin
	Tubulin
Structural	Keratin (skin)
	Fibroin (silk)
	Collagen (tendons, ligaments)
	Elastin (joints)
	Proteoglycans (cell walls)
Defense	Immunoglobulin (antibodies)
	Venom proteins
	Ricin
	Interferon
Regulatory	Insulin
	Growth hormone
	Lymphokines/cytokines
	Protein kinases (signal transduction)
	DNA binding repressors and activators
Inhibitors	Soybean trypsin inhibitor
	Plasminogen activator inhibitor
	HIV protease inhibitor

Enzymes are catalysts of reactions, usually involving organic substrates. Enzymes are highly specific both in the reaction catalyzed by each and in the substrates utilized. The most important feature of every enzyme is an *active site* that binds substrates and contains the amino acid residues that are directly involved in the making and breaking of bonds. The active site of an enzyme is typically a cleft or crevice in its three-dimensional structure [5].

TABLE 1.7 The 10 Leading Biotechnology Proteins, in Order of Worldwide Sales in 2011[a]

Protein	Activity/use
Anti-TNF monoclonal antibody	Arthritis relief
Anti-TNF receptor monoclonal antibody	Arthritis relief
Anti-VEGF monoclonal antibody	Cancer
Anti-CD20 monoclonal antibody	Cancer
Anti-HER2 receptor monoclonal antibody	Cancer
Insulin	Diabetes
Colony stimulating factor, PEGylated	White blood cell stimulation
Erythropoietin	Red blood cell growth
Anti-VEGF monoclonal antibody fragment	Macular degeneration
Interferon β-1a	Multiple sclerosis

[a]See reference [7].

From the biotechnology point of view, it is crucial that a protein product be purified without destroying any of its functions. Therefore, tertiary and quaternary structures must be preserved. Recombinant proteins that are produced in bacteria are often in a nonnative state, and this problem is solved by "refolding." Refolding is a reversible denaturing-renaturing process, about which more is explained in Section 1.4.8.

Human growth hormone (hGH) is an excellent example of a commercial *polypeptide hormone*. For several decades it was prepared in the United States from hemipituitaries extracted from human cadavers (the other half of the anterior pituitary lobe was used for research) under auspices of the National Pituitary Agency. A few cases of fatal virus infection discouraged the medical profession from continuing to use this source, and recombinant sources were sought. As a nonglycosylated peptide, hGH is ideally suited for production by recombinant fermentation. It should be added that the first recombinant human peptide produced in bacteria was another peptide hormone, somatostatin, for which the gene was synthesized chemically and transfected into laboratory bacterial strains. In addition to endocrine peptide hormones and their releasing factors, and in addition to tissue-targeted monoclonal antibodies, there exists a broad category of "biological response modifiers" (BRMs), proteins that cause a biological response to a particular environmental insult, such as infection, wounding, clotting, or cancer.

1.4.7 Stability of Proteins

One important aspect of quality control in bioprocessing is the production and monitoring of active proteins. Since the active function of proteins is dependent on tertiary and quaternary structures (which in turn depend on primary and secondary structures), the three-dimensional configuration of each molecule must be maintained; denaturation

is to be prevented if possible, but if it occurs, it must be detected. Proteins degrade via several pathways: deamidation of asparagine and glutamine, oxidation of methionine, oligomerization, aggregation, fragmentation (depolymerization), cross-linking, inter- and intramolecular rearrangements involving cysteine disulfide exchanges, and denaturation (breakdown of hydrogen bonds and ionic bonds that determine tertiary structure). In the United States, the legal evaluation of recombinant and other protein products is the responsibility of subdivisions of the U.S. Food and Drug Administration (FDA), including the Center for Drug Evaluation and Research (CDER) and the Center for Biologics Evaluation and Research (CBER), located in Rockville, Maryland. This agency is responsible for, among other things, authorizing processes used for testing the stability of biopharmaceutical protein preparations.

It is possible to test samples for each of these chemical modifications by fairly routine methods of analytical biochemistry. For example, gel electrophoresis can detect changes in molecular weight and hence aggregation, oligomerization, or fragmentation; isoelectric focusing, which depends on charge, can detect deamidation on the basis of the appearance of dissociating carboxyl groups [8]. High-performance liquid chromatography (HPLC), using several adsorption chemistries, provides information on both purity and structure. Thus, methods used to purify proteins are also used as analytical methods for quality control and for off-line product analysis following purification steps. For this reason, some of our chapters include a discussion of the analytical applications of each separation method, and Chapter 2 emphasizes these applications.

It is important to be aware of the variables that have effects on the stability of proteins. Variables that most commonly affect protein stability are temperature, pH, mechanical shear, chemical agents, and irradiation.

Temperature

As temperature is increased, denaturation of a protein will start to occur at some point. Thermal denaturation for many proteins begins to occur at 45 to 50ºC [3]. An example of the thermal denaturation of the protein ribonuclease is shown in Figures 1.16 and 1.17. When the temperature is high enough, the hydrogen bonds (dotted lines in Figure 1.16) are broken, and the β-pleated sheet structure of the protein is disrupted. Heating, however, still leaves the disulfide bonds intact. As observed in Figure 1.17, the denaturation of ribonuclease (as monitored by the change in absorbance) is an S-shaped function of temperature and depends strongly on the solution pH. Chromophores buried deep in the interior of the protein become exposed to the solvent when the protein is denatured and cause the absorbance to change. Some enzymes are still active at temperatures much higher than 45 to 50ºC. For example, enzymes isolated from thermophilic bacteria inhabiting hot springs are active at temperatures above 85ºC.

pH

Solution pH is a parameter that is often varied during the downstream processing of proteins. The impact of pH on the protein ranges from mild denaturation that is

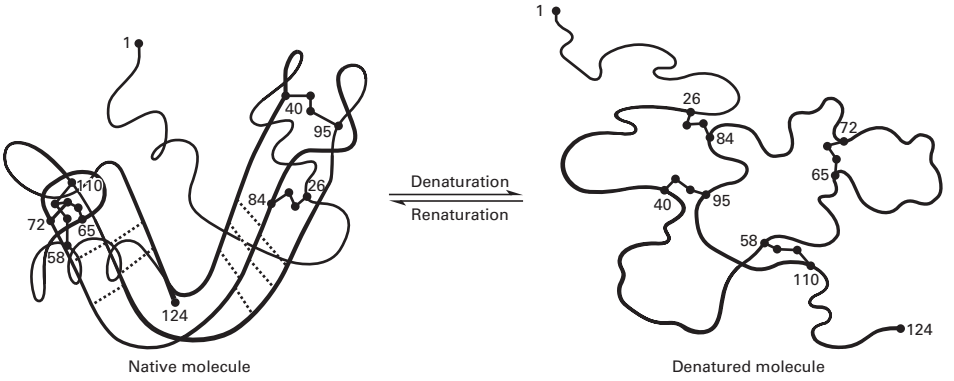

FIGURE 1.16 Schematic drawing showing the conformational change that occurs when ribonuclease is heated above its thermal denaturation temperature. Dotted lines indicate hydrogen bonds, and numbers indicate the positions of the amino acid cysteine, which forms disulfide bonds between chains. *(Copyright © 1996 by the Benjamin/Cummings Publishing Company, Inc. Reprinted by permission of Pearson Education, Inc.)*

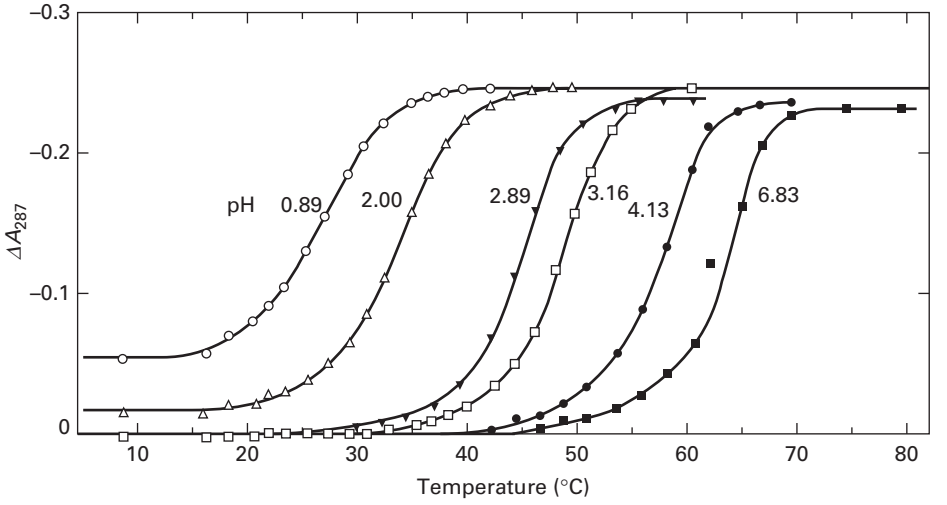

FIGURE 1.17 Thermal denaturation of ribonuclease as measured by ΔA_{287}, the change in absorbance at 287 nm, compared with a reference solution at zero absorbance. The pH values of the solutions (ribonuclease concentration 1.90 mg/ml, and ionic strength 0.16 M) are indicated. *(Data from J. Hermans and H. A. Scheraga, "Structural studies of ribonuclease. V. Reversible change of configuration,"* J. Am. Chem. Soc., *vol. 83, p. 3283, 1961.)*

reversible to complete hydrolysis of the protein. In mild denaturation, protonation or deprotonation of the protein leads to a change in the structure of the protein. Figure 1.18 illustrates the phenomenon for four enzymes for which the effect of pH on the relative activity of the enzymes has been determined. In these cases the pH changes are leading to a change in the ionization state and structure of the active site. Changing the pH, however, can lead to more than just a perturbation of the active site of an enzyme. Studies with serum albumin, for example, have shown that this

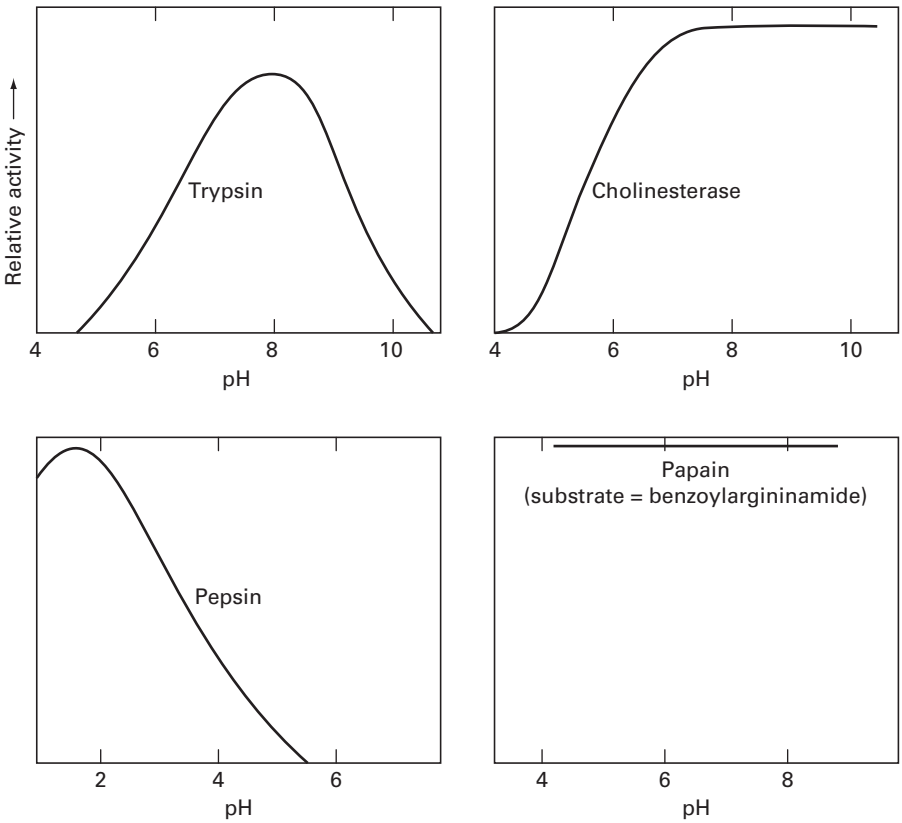

FIGURE 1.18 The effect of pH on the relative activity of the enzymes trypsin, cholinesterase, pepsin, and papain. *(Data from A. L. Lehninger,* Biochemistry, *2nd ed., p. 196, Worth, New York, 1975.)*

protein undergoes several major reversible conformational changes when the pH is varied [9]. Albumin, which usually exists in a compact globular form, undergoes an abrupt opening of the molecule at pH 4.0 that involves unfolding of one of the three molecular domains (domain III) from the rest of the molecule. Below pH 4.0, there is a significant expansion of the molecule to a form that resembles a series of balls and strings.

At extremes of pH, proteins are not only denatured but can be completely hydrolyzed to their constituent amino acids. Typically, 6 M hydrochloric acid, having a pH of −0.8, is used for acid hydrolysis, while 4 M sodium hydroxide, having pH of 14.6, is used for alkaline hydrolysis [10]. To obtain complete hydrolysis of proteins, the temperature is usually elevated to 110ºC. If strong acids or bases are used in adjusting the pH of protein solutions during a processing step, transient high concentrations of acid or base are present; and since some dipeptides are more readily hydrolyzed than others, the possibility of at least limited hydrolysis of protein exists. Thus, strong acids or bases should be avoided when even a slight amount of protein hydrolysis is undesirable. Strategies that have been developed to avoid extremes of pH during pH adjustment of protein solutions include the following: (1) using dilute

weak acids or bases (1 M acetic acid or Tris) in the pH range of 5 to 8; and (2) for pH values below 5 or above 8, using 5 M acetic acid at pH 4.0 (NaOH) to lower the pH, and 5 M ammonia at pH 9.5 (HCl) to raise the pH [11].

A final possible effect of pH is aggregation. At their isoelectric points, proteins have a net charge of zero, and therefore the electrostatic repulsion between protein molecules is gone (see Section 8.2, Protein Solubility). This may lead to formation of aggregates. Quite often, purification strategies involve the use of both anion exchange and cation exchange chromatography. If the target protein is to be bound to the resin in both cases, the pH will need to be adjusted from above the isoelectric point to below the isoelectric point. Since aggregate formation is typically a function of protein concentration and kinetics, adjusting pH quickly through the pI usually minimizes the aggregation. However, if weak or dilute acids or bases are used to minimize hydrolysis and denaturation, as discussed above, aggregation may become an issue.

Shear

The effect of mechanical shear on proteins has been extensively studied, and the general conclusion is that shear effects are not significant except when gas-liquid interfaces are present [12, 13]. In one study with alcohol dehydrogenase, no loss of enzyme activity was observed even at shear rates up to 26,000 s^{-1} using a completely filled concentric cylinder (Couette) shear device. Significant activity losses were, however, observed in a rotating disk reactor that had a gas phase caused by incomplete filling of the reactor [13]. This loss of activity was attributed to the proteins being adsorbed to the gas-liquid interfaces in an unfolded partially active or inactive state; if the turbulence in the solution is sufficiently high, the interface with protein adsorbed breaks, causing unfolded protein to be entrained in the bulk solution. As this process continues, more and more protein becomes inactivated. Therefore, it is important that gas-liquid interfaces be avoided or minimized in general, particularly when mechanical shear is present. Also, it should be recognized that shear rates experienced by proteins in process scale separation and purification processes are much less than in the alcohol dehydrogenase study, typically no more that 1000 s^{-1}.

1.4.8 Recombinant Protein Expression

Recombinant proteins can be synthesized in a variety of organisms, which can vary from bacteria to mammalian cells. For bacteria, typically the host organism is transfected with a plasmid (circular DNA) that contains an efficient promoter sequence for expression of the desired protein at high levels. There are many strategies for integrating genes into mammalian cells, including transfection with a plasmid, but also via transduction with a virus or translocation, by which one gene is targeted for replacement with another. Two issues that can be encountered early in the development of a purification process for a recombinant protein are whether the protein should be genetically engineered to aid in the purification and whether the protein

must be solubilized and refolded from "inclusion bodies," insoluble and inactive aggregates of protein. Inclusion bodies can sometimes be prevented, however, by the coexpression of folding modulators, or chaperones.

Genetic Engineering to Improve Protein Purification

Various approaches can be taken to genetically engineer proteins to aid the purification process. Affinity peptide or protein "tags" can be genetically attached to recombinant protein molecules by splicing a gene that creates a "fusion protein" consisting of the product and its tag. One attractive tag is a histidine oligomer, the most commonly used of which has six histidines. Histidine tags have been added to either terminus of the protein or in the linker region between two segments of a fusion protein. Histidine binds transition metals such as nickel, zinc, and copper. The histidine tag will therefore bind to metal ions immobilized in a purification medium such as a chromatography column, membrane, filter, precipitant, or extraction solvent [14].

Genetic engineering has been applied to avoid the expression of insoluble inclusion bodies through the expression of the target insoluble protein as part of a fusion protein. The target heterologous protein is expressed as a C-terminal fusion with another protein called a carrier protein, which has a higher solubility than the target protein. Carrier proteins that have been used to solubilize target heterologous proteins as part of fusion proteins include glutathione-*S*-transferase (GST) [15], maltose-binding protein (MBP) [16], NusA protein [17], and thioredoxin [18]. GST and MBP are themselves affinity tags that are also used to facilitate purification of fusion proteins containing GST and MBP. Histidine tails have been used to purify NusA and thioredoxin fusion proteins. The target protein can be removed from the fusion protein during purification either by proteases such as bovine enterokinase that specifically cleave a short peptide sequence inserted at the N-terminus of the target protein, or by self-cleaving proteins called inteins that are also inserted at the N-terminus of the target protein [19]. A number of fusion partners classified by affinity purification or solubility improvement are shown in Table 1.8.

Solubilization and Refolding of Proteins in Inclusion Bodies

Inclusion bodies have been commonly observed in the expression of heterologous proteins in bacteria and yeast cells. Inclusion bodies are recovered by lysing the cells and then washing the inclusion bodies by centrifugation. Inclusion bodies typically have a density higher than cell fragments. The larger the inclusion body, the more favorable the centrifugal properties (see Chapter 5), but there are no rules of thumb for increasing inclusion body size within the cell. After washing, inclusion bodies can be very enriched in the protein of interest, but they are by no means pure. An inclusion body is a heterogeneous mixture of precipitated proteins, and not solely the recombinant protein of interest. Although initial purification of inclusion body material by cell lysis and centrifugation is relatively simple, the

TABLE 1.8 Fusion Protein Partners for Improvement of Protein Purification

Purpose	Fusion partner	Number of amino acids	Affinity/capture method
Affinity	His	5–15	Immobilized metal ions
	FLAG	8	Immobilized anti-FLAG monoclonal antibody (mAb), Ca-dependent
	Strep-II	8	Immobilized Strep-Tactin protein, elution with biotin
	Hemagglutinin tag, Softag, c-myc, T7-tag	9–16	Immobilized mAb
	S-tag	15	Immobilized S-protein
	Elastin-like peptides (ELP)	18–320	Temperature shift, ELP is repeating pattern of VPGXG
	Calmodulin-binding peptide (CBP)	26	Immobilized calmodulin
	Chitin-binding domain (CBD)	51–52	Chitin beads
	Xylanase 10A	163	Cellulose, elution with glucose
	Glutathioine-*S*-transferase (GST)	211	Immobilized glutathione
	Protein A	280	Immobilized IgG
	Maltose-binding protein (MBP)	396	Cross-linked amylose
Solubility	Solubility-enhancing peptide (SEP), containing hydrophilic amino acids	5–20	Require additional tag for capture specificity
	IgG domain B1 of streptococcus Protein G (GB1)	56	
	Small ubiquitin modifier (SUMO)	~100	
	Thioredoxin (Trx)	109	
	NusA protein	495	

agglomerated protein must be resolubilized by strong denaturants; and the protein must be refolded to its correct three-dimensional conformation. The success in refolding is protein dependent, and for some proteins, relatively high refolding yields can be obtained.

Solubilization Inclusion bodies are found in the cell sediment after the cells have been lysed and centrifuged. The proteins in these inclusion bodies are usually solubilized by the addition of buffer containing a chaotropic agent such as

guanidinium chloride or urea or with a detergent like Sarkosyl. One protocol calls for incubating the inclusion bodies in 6 M guanidium chloride or 8 M urea with 0.1 M phosphate buffer at pH 7 for 0.1 to 1 h at 20ºC (1 ml of denaturing solution per 5 mg of protein) [20]. For proteins that contain cysteine, it is advisable to also add a reducing agent such as β-mercaptoethanol, dithiothreitol (DTT), dithioerythritol, or cysteine, to allow reduction of the interchain disulfide bonds by thiol-disulfide exchange. This is done to ensure that improper disulfide bonds that may have formed in the protein translation and intracellular precipitation processes are completely broken so that they can be reformed during the refolding process.

Refolding After having resolubilized an inclusion body, two conditions must be realized in order for the protein to spontaneously refold. The first is that the denaturant must be removed or reduced in concentration, and the second is that oxidizing conditions must exist to reform the correct disulfide bonds. The first objective is achieved by dilution or dialysis. Flash dilution is often the method of choice in industry because of its simplicity; in this method, the denatured protein is added quickly to the refolding buffer [21]. However, the optimal method of dilution is to add the denatured protein to the refolding buffer very slowly, which leads to the protein always refolding at minimal protein concentration [22]. Since the refolding half-life to the native state is small (1–3 min), the concentration of partially folded protein will be very low with this procedure, so that the tendency for protein aggregation will be low. Dialysis, which involves the use of ultrafiltration membranes to slowly change the composition of the solution containing the denatured protein to that of the refolding buffer (see Chapter 4, Filtration), is used instead of dilution when the protein concentration is too low for further dilution or when it is necessary to perform a complete buffer exchange [23].

The choice of the refolding buffer is the most essential part of the development of an efficient protein refolding process. Many proteins can be refolded only under very specific conditions; therefore, the approach to finding the optimal conditions for refolding is an empirical one. There are many variables to consider in designing a refolding process, including pH, temperature, salt concentration, redox environment, presence of divalent ions such as copper and manganese, and the use of additives such as arginine and other amino acids, glycerol and sugars, detergents, and chaotropic agents [22]. Commercial refolding screens are now available to aid researchers in finding optimal refolding conditions.

During refolding to the native state N, there is a kinetic competition of folding and aggregation of denatured state D according to the following sequence of reactions [20]:

$$N \rightleftharpoons D \longrightarrow \text{aggregates}$$

To minimize aggregation during the refolding process, the refolding usually must be performed at low protein concentrations (<100 mg/liter) [24]. An example

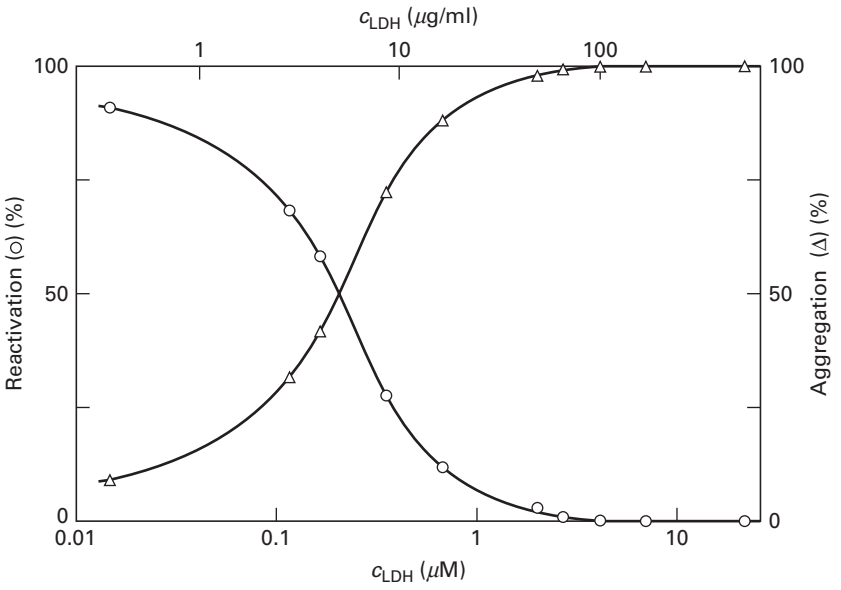

FIGURE 1.19 Effect of protein concentration *c* on the renaturation of lactate dehydrogenase (LDH) from pig muscle. Acid-denatured lactate dehydrogenase was renatured in 0.1 M phosphate buffer at pH 7 and 20°C with 1 mM EDTA and 1 mM dithioerythritol. After 192 h, reactivation (circles) and aggregation (triangles) were quantified. *(Data from A. Mukhopadhyay, "Inclusion bodies and purification of proteins in biologically active forms."* Adv. Biochem. Eng. Biotechnol.*, vol. 56, p. 61, 1997.)*

is shown for the refolding of lactate dehydrogenase in Figure 1.19. For this enzyme, it is seen that the enzyme concentration should be 1 to 3 mg/liter for reasonably good refolding yields. If it is desired to refold a large quantity of protein, it may not be reasonable to refold the entire batch at such a low concentration. Excessive volume for refolding can be avoided by doing successive additions of the denatured protein solution to the renaturation solution [20]. Using lactate dehydrogenase as an example, the protein concentration in the renaturation buffer should not increase by more than 1 to 3 mg/liter upon each addition to achieve good refolding yields. The time interval between successive additions should be the time required for renaturation of 90% of the final value.

While refolding to the final tertiary structure is the goal of refolding steps, the formation of disulfide bonds (oxidation) is typically the most critical and limiting aspect. Proteins without disulfide bonds will typically refold spontaneously and with limited aggregation under fairly standard conditions. Methods that are commonly used to achieve the correct folding of proteins with disulfide bonds are slow air oxidation and the use of buffer supplemented with a redox system. For proteins with disulfide bonds, the best strategy is to have a redox buffer present during protein refolding [22]. Adding a mixture of the reduced and oxidized forms of low molecular weight thiol reagents, such as glutathione, cysteine, or cysteamine, usually provides the appropriate redox potential to allow the formation and reshuffling of disulfides

[24]. The concentrations of reduced and oxidized reagents are commonly in the ranges of 1 to 5 mM and 0.01 to 0.5 mM, respectively, and optimal regeneration usually occurs with a tenfold molar excess of the reduced component [20].

Use of Folding Modulators for Expression of Functional Proteins

Another approach for achieving the expression of functional recombinant proteins is the concurrent expression of folding modulators, or chaperones. A number of these chaperones have been studied for expression in the bacterium *Escherichia coli*, which is commonly used for the expression of recombinant proteins. The use of a single modulator is usually not successful, so it is common to express a number of modulators simultaneously. Plasmid systems for *E. coli* are now available for the coproduction of as many as seven folding modulators with a heterologous protein (see the following section for a discussion of DNA plasmids). Some of the most important *E. coli* folding chaperones are the following [25]:

- DnaK, DnaJ, and GrpE—These proteins belong to the heat shock protein 70 family whose main feature is the ability to bind short, linear hydrophobic regions of polypeptides. These are cytoplasmic proteins that have improved the solubility of recombinant proteins expressed both in the cytoplasm and periplasm.
- GroEL and GroES-GroEL, a member of the heat shock protein 60 family, has a double-ring shaped structure made up of 14 subunits that form a hollow cylinder. An unfolded polypolypeptide binds at either of the outer ends of the inner cavity of GroEL through hydrophobic interactions. The cavity containing the polypeptide is capped by GroES, a heat shock 10 family protein composed of seven identical subunits to make up a single ring with a hollow dome-shaped structure for the creation of a closed environment in which protein folding is favored. Expression of recombinant proteins along with GroEL and GroES has led to correct folding in the cytoplasm but not in the periplasm.
- Peptidyl-prolyl *cis-trans* isomerase (PPIase)—This enzyme catalyzes the isomerization of peptidyl-prolyl bonds, which is required by some proteins for proper folding. Enzymes with this isomerization activity are found in both the cytoplasm and periplasm of *E. coli.* One of these is trigger factor, which is expressed in the cytoplasm and has been found to be synergistic with heat shock protein 70 family members DnaK, DnaJ, and GrpE.
- Skp—This is an *E. coli* periplasmic protein that has led to recombinant proteins being expressed in soluble form in the periplasm.
- DsbA, DsbB, DsbC—These are *E. coli* periplasmic proteins that assist with the formation of disulfide bonds. DsbC has been used without its leader sequence to assist in correctly folding proteins in the cytoplasm using *E. coli* cells that have been mutated to give an oxidative environment in the cytoplasm (*trx* or *gor* mutations).

The use of folding chaperones for large-scale protein refolding could be practical using immobilization methods. For example, GroEL, DsbA, and PPIase were

immobilized on a chromatography adsorbent, and a protein very recalcitrant to refolding, scorpion toxin Cn5, was refolded by passing it through a column of this adsorbent [26].

1.5 MACROMOLECULES: NUCLEIC ACIDS AND OLIGONUCLEOTIDES

Nucleic acids are polynucleotides whose primary structures consist of repeating units of nucleotides that are joined by a phosphodiester linkage between the 3′-hydroxyl group of one ribose (or deoxyribose) and the 5′-hydroxyl group of an adjacent ribose (or deoxyribose). A nucleotide consists of a nitrogenous base, a ribose or deoxyribose sugar, and one or more phosphate groups (Figure 1.20). Ribonucleic acid (RNA) is a polynucleotide containing only ribose sugar, while deoxyribonucleic acid (DNA) contains only deoxyriboses (where a hydroxyl group at the 2′ position is replaced by

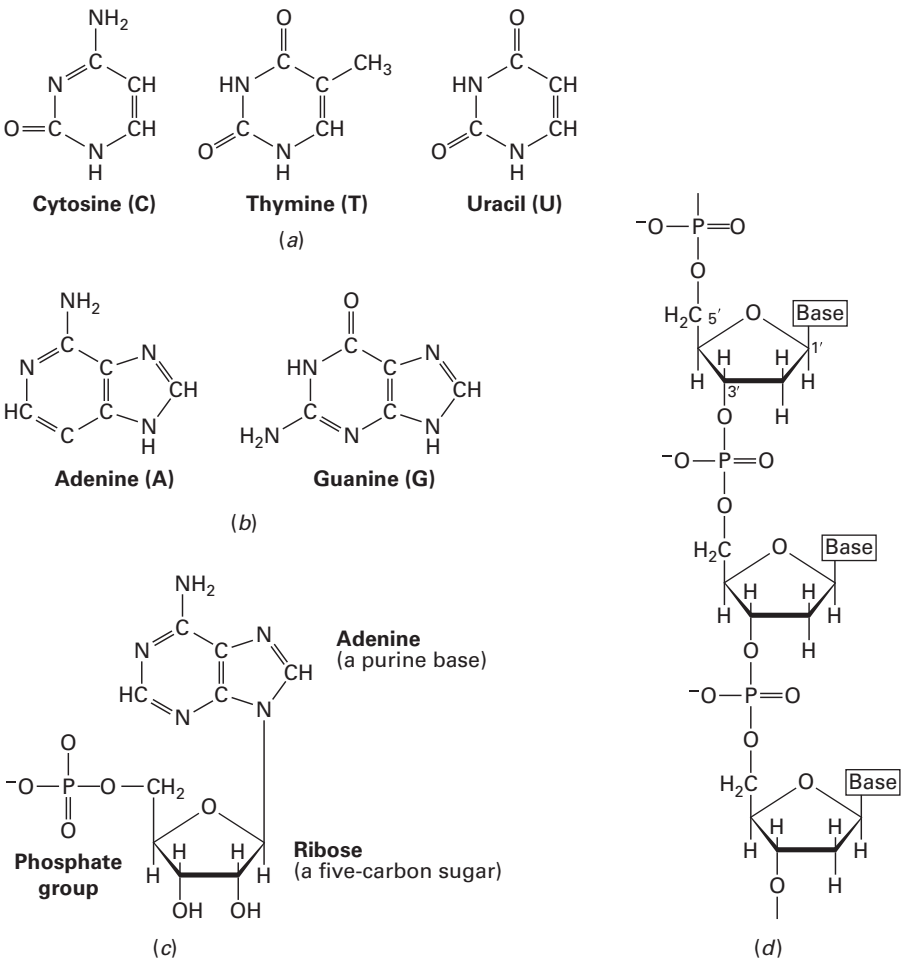

FIGURE 1.20 The basic structures present in nucleic acids: (*a*) pyrimidine bases, (*b*) purine bases, (*c*) the nucleotide adenosine monophospate (AMP), and (*d*) a section of a DNA chain.

hydrogen). The structure of a DNA chain is shown in Figure 1.20. The structure of a DNA molecule—two antiparallel polynucleotide chains coiled into a double helix—was deduced by James Watson and Francis Crick in 1953. The nitrogenous bases are on the interior of the helix, with one base on one strand being hydrogen-bonded to an adjacent base on the other strand. Adenine-thymine and guanine-cytosine are the possible base pairs in DNA, while in RNA, thymine is replaced by uracil. In shorthand notation, a DNA oligonucleotide can be written as follows:

5′ATCGGCATCGCCGAT3′
3′TAGCCGTAGCGGCTA5′

The use of DNA in tiny quantities is common in the genetic engineering industry and the gene therapy and DNA vaccines fields. Today, there are several products in development or marketed as therapies that require purification at reasonably large scale. Antisense sequences, ribozymes, and aptamers represent the three major categories of oligo- and polynucleotides that have commercial potential. Antisense molecules can bind to mRNA and inactivate it; ribozymes can react with RNA and catalyze its cleavage at sequence-specific sites, and aptamers are oligonucleotides that bind with high affinity to chosen ligands because they have undergone *in vitro* evolution under selective pressure during several rounds of enzymatic replication. Aptamers are thus considered combinatorial products. These three categories of nucleic acid products are targeted for the therapeutics and diagnostics fields. The synthesis of these products is not, in general, achieved by fermentation. Except for aptamers, the field is dominated by automated polynucleotide synthesizers. Pegaptanib, a 38 base aptamer that is "PEGylated" (has polyethylene glycol, or PEG, attached), is currently approved for treating macular degeneration. An important antisense product is small interfering RNA (siRNA). These 20 to 30 base-pair segments of double-stranded RNA contain sequences that are complementary to specific mRNAs and "knock down" expression of the corresponding gene by a pathway known as RNA inhibition (RNAi). These molecular products are purified for use in testing gene-targeting pharmaceuticals and other molecular biology applications. Some siRNAs have undergone preclinical testing in the treatment of macular degeneration and certain dangerous virus infections.

The genetic engineering industry, on the other hand, consists of patented DNA sequences that are sold to customers or used as vectors for recombinant genes in a company's own processes. Vectors (plasmids) containing genes for human insulin, human α-interferon, and human erythropoietin are well-known examples of the latter category. Some plasmids are extremely sophisticated and contain the structural gene for the protein product, one or more promoter sequences recognized by the transcription enzyme complex, enhancer elements, origins of replication for bacteria and animal cells, and operator sequences for switching on and off transcription of RNA for the protein product. All these products are generated in recombinant bacteria, characterized by gel electrophoresis (see Chapter 2), and partially purified

for transfection into bacterial, yeast, or animal cells that will generate the product. Products used for gene therapy are also produced in this fashion. The most popular means of purifying plasmid DNA and portions thereof is gel electrophoresis, a very low-capacity method that is useful in the gene industry because only very small amounts (nanograms) of material are needed to transform cells.

Nucleic acids are chemically more robust than proteins. Their secondary structures are highly stable, being based on base-pairing hydrogen bonds. A word of caution, however: nucleic acids are hydrolyzed by enzymes that are ubiquitous in nature, and RNA, in particular, is susceptible to ribonuclease molecules that seem to be everywhere.

1.6 MACROMOLECULES: POLYSACCHARIDES

Of all bioproducts in use, the polysaccharides have the highest molecular weight and the longest end-to-end polymer length. Most naturally derived polysaccharides are branched to various degrees—they are not necessarily linear like peptides and oligonucleotides.

The most familiar polysaccharides are starch, glycogen, and cellulose. These are very high molecular weight polymers of a small number of different sugars. Owing to the numerous hydroxyl groups attached to sugar carbons, some polysaccharides can be highly branched via typical glycosidic linkages. Polysaccharides find uses in industrial chemistry (e.g., agar) and foods (e.g., carrageenan). Figure 1.21 depicts two more polysaccharides, amylose (a linear form of corn starch) and chitin (a

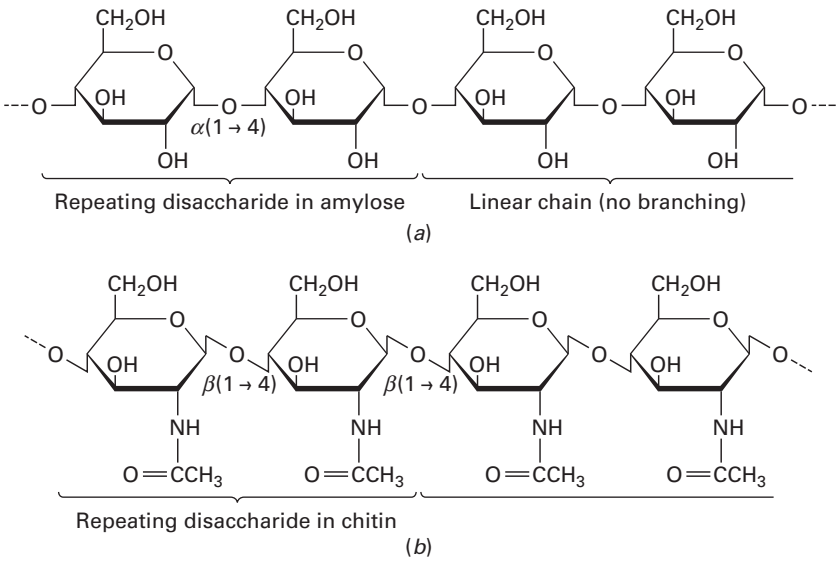

FIGURE 1.21 Two polysaccharides. (*a*) Amylose, which is poly[α(1 → 4) glucose] (straight chain); it has polarity, and the free C_1 end is the "reducing sugar." (*b*) Chitin, which is poly-*N*-acetylglucosamine, a mucopolysaccharide.

TABLE 1.9 Some Polysaccharides, Their Sources and Uses

Polysaccharide name	Polysaccharide source	Uses
Starch	Potatoes, corn	Food, clothing
Cellulose	Wood, cotton	Paper, clothing
Carrageenan	Mycophyta (algae)	Food
Agar	Mycophyta	Microbiology, food
Dextran	Corn	Food, medicine
Agarose	Mycophyta	Biochemistry
Xanthan gum	*X. campestris*	Food, industrial chemical, oil field drilling

mucopolysaccharide containing *N*-acetylamino sugars found in fungal cell walls and invertebrate exoskeletons). Bacterial polysaccharides are the active component of a number of vaccines.

Although most polysaccharides are extracted from plants, several are produced microbially, the most important of which is xanthan gum. Other important microbial polysaccharides include dextran, alginate, and pullulan [27]. Except for applications in biochemical research and in the bioprocessing industry itself, highly purified polysaccharides are seldom sold. Sources and uses of selected polysaccharides are listed in Table 1.9. It is of some interest to the field of this textbook that cellulose, agarose, and dextran are used in media for bioseparations, including electrophoresis, chromatography, and extraction (see Chapters 2, 6, and 7).

1.7 PARTICULATE PRODUCTS

Novel products of biotechnology include particulate materials. These take the form of subcellular particles, bacterial inclusion bodies, whole cells, and insoluble macromolecular aggregates. Theoretically, the logical way to purify these products is by centrifugation. In an increasing number of cases of subcellular particles, this approach fails. Some very small particles have very low sedimentation rates, and therefore require ultracentrifugation—a satisfactory method only at bench scale. Some particle suspensions are contaminated with unwanted particles having identical sedimentation velocities. The reasons for purifying suspended animal and plant cells are numerous, including obtaining pure populations for biochemical study and for food or feed applications, purified living material for transplantation, and starting material for pure bioproducts.

Numerous activities require or involve the separation or purification of cells: using purified cells for relating cell structure to cell function, obtaining rare plant and animal clonogenic cell subpopulations, isolating hybrid (fused) cells for genetic engineering, separating nonclonogenic cells, obtaining cell subsets for transplantation, separating productive from nonproductive bioreactor cells, and removing cells that produce unwanted products from fermentor harvests.

Microbial cells grown for food or feed applications are sources of “single-cell proteins” (SCP). Microorganisms that have been grown for SCP include algae,

bacteria, yeast, and filamentous fungi. Raw materials for the production of SCP by fermentation have varied from hydrocarbons, cellulosic materials, and saccharides to carbon-containing wastes [27].

Subcellular components that have been of recent interest include bacterial inclusion bodies (100–1000 nm), ribosomes (25 nm), liposomes or natural vesicles (100 nm), and natural hormone granules (200 nm). Sometimes these products differ in subtle ways from their contaminants, and a pure separation could be challenging. At some point in the life of a number of fermentation products, the product is a component of a particle, such as a cell or organelle. The cell or organelle may not itself be the product, but when it houses the product it must be successfully isolated from the impurity-laden fluid that surrounds it. As will be seen in Chapters 3 to 5, the early bioseparation steps can include flocculation, sedimentation, and filtration—methods designed to isolate particulate separands.

1.8 INTRODUCTION TO BIOSEPARATIONS: ENGINEERING ANALYSIS

Modern biotechnology is built on the genetic manipulation of organisms, *genetic engineering,* to produce commercial products or processes. The implementation of these products or processes is dependent upon *biochemical engineering,* which is in turn divided into two disciplines, upstream engineering (fermentation) and downstream engineering (purification, or bioseparations). Purification of bioproducts typically involves a long sequence of steps, and each step requires the use of one or more *unit operations,* such as sedimentation, adsorption, and drying.

Bioproducts have unique properties. The earlier part of this chapter listed several bioproducts and their properties. For bioseparation purposes, important properties data include thermal stability, solubilities, diffusivities, charge, isoelectric pH, reaction rate constants, and separation thermodynamics. A considerable amount of downstream process planning is based on the lability of most bioproducts. Temperature, pH, and concentration must be maintained within specific ranges to assure product bioactivity.

1.8.1 Stages of Downstream Processing

Removal of solids (or recovery), isolation of product, purification, and polishing constitute a sequence of events applied to nearly every product as it is prepared. These four stages make use of various unit operations. A “unit operation” is a single process and the equipment used therefor. These operations are applied in varying combinations to the four stages, approximately as indicated in Table 1.10.

In the unit operations approach used in this book, a separate chapter will be devoted to the analysis and applications of each unit operation. The unit operations can be divided by function into:

- Liquid–solids separations (dewatering, concentration, particle removal)
- Solute–solute separations (isolation, purification)
- Solute–liquid separations (polishing).

TABLE 1.10 Objectives and Typical Unit Operations of the Four Stages in Bioseparations

Stage	Objective(s)	Typical unit operations
Separation of insolubles	Remove or collect cells, cell debris, or other particulates Reduce volume (depends on unit operation)	Filtration, sedimentation, extraction, adsorption
Isolation of product	Remove materials having properties widely different from those desired in product Reduce volume (depends on unit operation)	Extraction, adsorption, ultrafiltration, precipitation
Purification	Remove remaining impurities, which typically are similar to the desired product in chemical functionality and physical properties	Chromatography, affinity methods, crystallization, fractional precipitation
Polishing	Remove liquids Convert the product to crystalline form (not always possible)	Drying, crystallization

EXAMPLE 1.2

Initial Selection of Purification Steps You have been given the assignment to purify the antibiotic erythromycin. You have at your disposal the *Merck Index*, which has the information on erythromycin shown in Figure E1.2. What do you think are the most likely unit operations that should be used for the isolation and purification of erythromycin?

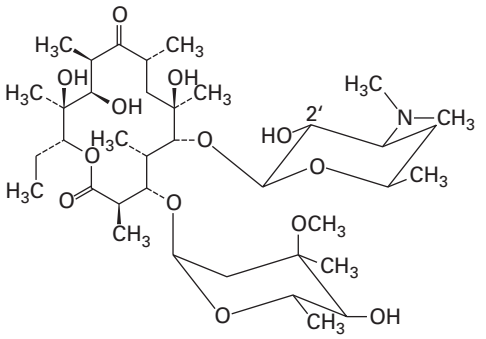

Erythromycin A

FIGURE E1.2 The *Merck Index* entry for a widely used antibiotic. *(Data from S. Budavari, M. J. O'Neill, A. Smith, P. E. Heckelman, and J. F. Kinneary, eds.,* The Merck Index, *12th ed., p. 625, Merck Research Laboratories, Whitehouse Station, NJ, 1996.)*

Solution

Erythromycin has limited solubility in water but is soluble in several solvents, including amyl acetate. Since the solubility of amyl acetate in water is low, isolation could be performed by a liquid-liquid extraction of erythromycin using a water–amyl

acetate system. For the extraction, it would be desirable to raise the pH of the aqueous phase above the pK_a of erythromycin of 8.8, so that the secondary amino group is converted from the positively charged form to the neutral free-base form. For the purification step, crystallization is a good choice, since hydrated crystals have been obtained from water.

This example illustrates how laboratory data can guide the formulation of a sequence of unit operations to purify a bioproduct. Chapter 12, Bioprocess Design and Economics, elaborates further on the selection of unit operations for a bioseparations process.

1.8.2 Basic Principles of Engineering Analysis

It is said that any good engineering calculation ends with a number bearing a dollar sign. The purpose of engineering analysis, therefore, is to determine "how much" and "how fast." These questions are answered in the form of equations that can be solved for product capacity, processing rate, and possibly product purity. To obtain values for such variables, a set of *governing equations* derived from the three principal ingredients of engineering analysis is required: *equilibria, material balance,* and *flux (or transport phenomena)*. The translation of processing rates into cost is detailed in Chapter 12.

Material balance

Operating curves (for each unit operation) are built on the basis of material balances and used in consort with equilibrium curves. The material balance equation states

$$\text{Accumulation} = \text{inflow} - \text{outflow} + \text{amount produced} - \text{amount consumed} \tag{1.8.1}$$

Examples of Equilibria

Traditionally, a chemical reaction that is at equilibrium,

$$A + B \rightleftharpoons C \tag{1.8.2}$$

can be characterized by an equilibrium constant

$$K_{eq} = \frac{[C]}{[A][B]} \tag{1.8.3}$$

where all concentrations are in mole fractions, molarity, or molality. Likewise, in an extraction process that has gone to equilibrium,

$$K = \frac{y}{x} \tag{1.8.4}$$

where y is the concentration of a separand in the extract phase, and x is the concentration of the same separand in the raffinate (usually heavy) phase, and K is called the partition coefficient or distribution coefficient. In the case of adsorption, the equilibrium constant relates the concentration in the adsorbent phase, $[CS]$, to the concentration in the liquid phase, $[C]$, at equilibrium, where C is a chemical species and S is an adsorption site. When the adsorption equilibrium is linear, for example, the following relation is valid at low concentrations:

$$[CS] = K_{\text{eq}}[C] \tag{1.8.5}$$

Examples of Flux Relationships (Transport Phenomena)

Flux relationships abound in chemistry and physics, and they all state that

$$\text{Flux} = \text{coefficient} \times \text{driving force} \tag{1.8.6}$$

where flux is in units flowing per unit area per unit time, driving force is a gradient down which units flow, and the "coefficient" is a permeability or the inverse of a resistance, derivable from properties of the medium. Thus, we have Ohm's law

$$J_e = CE \tag{1.8.7}$$

where J_e is current density, C is electrical conductivity (property of the medium), and E is electrical potential gradient. Fick's first law applies for diffusive flux due to a concentration gradient dc/dx in one dimension

$$J_D = -\mathscr{D}\frac{dc}{dx} \tag{1.8.8}$$

where $\mathscr{D}$, the diffusion coefficient, is also a property of the medium and in some cases calculable from the Stokes-Einstein equation for spheres

$$\mathscr{D} = \frac{kT}{6\pi\mu a} \tag{1.8.9}$$

where k is the Boltzmann constant, T is absolute temperature, μ is viscosity, and a is particle radius. Equation (1.8.9) is particularly useful when property data are not available.

Of great interest in downstream processing is the empirical law (Darcy's law) of flow through a porous medium

$$J_w = L_p \Delta p \tag{1.8.10}$$

where J_w is the fluid flux, L_p is Darcy's law permeability, and Δp is pressure drop across the porous medium, such as a filter or a column of adsorbent resin—systems very frequently used in bioprocessing.

1.8.3 Process and Product Quality

The measures of product quality due to processing are purity, fold purification, specific activity, and yield. Purity is defined as follows:

$$\text{Purity} = \frac{\text{amount of product}}{\text{amount of product} + \text{amount of total impurities}} \tag{1.8.11}$$

Fold purification is the ratio of the purity at any stage in the process to the purity at the start of the purification process. Another measure of purity is

$$\text{Specific activity} = \frac{\text{units of biological activity}}{\text{mass}} \tag{1.8.12}$$

where units of biological activity are assayed by means of a biological test, such as moles of substrate converted per second per liter or fraction of bacterial cells killed. Examples of analytical measurements are given in Chapter 2. For proteins, the mass in Equation (1.8.12) is usually total protein; on this basis, the specific activity reaches a constant value when the protein is pure.

Yield is given by

$$\text{Yield} = \frac{\text{amount of product produced}}{\text{amount of product in feed}} \tag{1.8.13}$$

Purity is a strictly quantitative measure and not always an expression of the quality of the product. A therapeutic protein can be 99.99% pure but still unacceptable if any pyrogen (a substance that produces a fever) is present. On the other hand, if the product is not a therapeutic protein but an industrial enzyme, then practically any impurities that do not inhibit the activity of the product or endanger the user are allowed. Figure 1.22 indicates this principle by comparing the level and range of purity acceptable for three different protein products. In short, two kinds of measurements of purity are required: activity, composition, and structure on the product itself; and host-cell materials, degraded product, and excipients (additives) on the impurities.

1.8.4 Criteria for Process Development

Approaches to process development (also known as process synthesis) must be made with future scale-up in mind. A biotechnology product production process is a set of connected unit operations that produces a final product able to meet defined levels of quality, yield, and cost. The following criteria should therefore be used in evaluating and developing a bioseparation process:

- Product purity
- Cost of production as related to yield

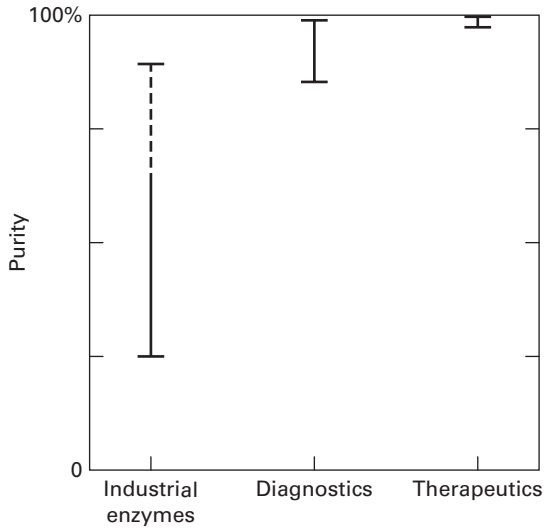

FIGURE 1.22 Different levels of purity are required for different products.

- Scalability
- Reproducibility and ease of implementation
- Robustness with respect to process stream variables

The integration of unit operations for the efficient synthesis of bioseparation processes is discussed fully in Chapter 12, Bioprocess Design and Economics.

1.9 THE ROUTE TO MARKET

The route for a biotechnology product being on the market is complex and can be lengthy. Figure 1.23 charts the pathway to market for a recombinant biotechnology product. Note that several years are required for the completion of the route from genetic discovery to marketing.

Besides identifying the market for the product and determining the optimal process for the expected production rate, the personnel involved in this effort must make sure that all the regulatory requirements are met. This is clearly an interdisciplinary task, involving not only engineers and bioscientists but also marketing and regulatory personnel. Often, applications personnel, such as medical doctors and veterinarians, must also be involved. Now we turn to some of the factors that are important to consider on the route to market.

1.9.1 The Chemical and Applications Range of the Bioproduct

As mentioned earlier, modern biotechnology produces the full range of substances for a wide range of applications; some well-known examples help emphasize this point:

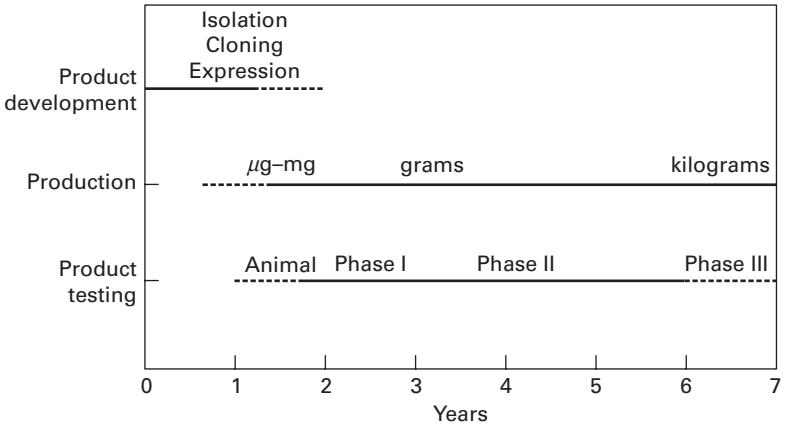

FIGURE 1.23 Pathway to market, beginning with the discovery of a recombinant biopharmaceutical product.

Aspartame, a dipeptide nonnutritive sweetener

Paclitaxel, a triterpene from plants used in cancer treatment

Erythropoietin, a peptide hormone that stimulates red cell production in the bone marrow

Oligonucleotides, which can be made to function according to shape and according to catalytic activity

Bacillus thuringiensis (Bt), whole bacterial cells that when dried can be sprayed on crops to prevent insect damage

Note the categories: food, medicine, and agriproducts. While most of the excitement in biotechnology and bioprocessing today is in the area of biopharmaceuticals produced by genetically engineered organisms, a much wider variety of products exists, usually with lower value per mass unit, including biopesticides, novel food products, polymer components, hydrogel polymers, industrial enzymes, commodity enzymes (laundry products), and fine chemicals. To know what product purity, cost, and FDA requirements must be met, the exact application of the proposed bioproduct must be identified early in process development, or even beforehand.

1.9.2 Documentation of Pharmaceutical Bioproducts

Medical products are catalogued in numerous commercial handbooks, including the *Merck Index* and *Physician's Desk Reference* (PDR). The official documentation of all compounds sold for medication must appear in the *U.S. Pharmacopeia*. For each substance, the following data are given: structural formula, empirical formula, Geneva name (to the extent possible), potency, packaging and storage, reference standards, labeling, chemical identification methods, and assays for identity and purity. Validations of these properties are the responsibility of the manufacturer; in

the United States, the FDA grants permits, first to manufacture for testing, then to test, and then to manufacture for sale and to sell.

1.9.3 GLP and cGMP

GLP refers to "good laboratory practice," and cGMP refers to "current good manufacturing practice." These are guidelines of procedure in research and manufacturing mandated by the Food and Drug Act of 1976, which states, in part (Paragraph 210.1): "This chapter contains the minimum current good manufacturing practice for methods to be used in, and the facilities or controls to be used for, the manufacture, processing, packing, or holding of a drug to assure that such drug meets the requirements of the act as to safety, and has the identity and strength and meets the quality and purity characteristics that it purports or is represented to possess."

Once a product has met the requirements of the act, it may be considered an "investigative new drug" (IND) for which a license is issued. The most important matter for the engineer is the fact that the process in part defines the product. Thus a published description of a pharmacological product in the *U.S. Pharmacopeia* (USP) includes a structural formula and Geneva name (if applicable), methods of analysis, and definitions of units of activity (if applicable).

1.9.4 Formulation

Formulation is that postpolishing process whereby a drug or other chemical is converted to a dosage form. It is combined with *excipients* that contribute to its stability under storage conditions, deliverability in medical applications, or final concentration. Thus excipients can be stabilizers (reducing compounds, polymers, etc.), tablet solids or parenteral diluents [a gum, water for injection, poly(ethylene glycol), penetrant oil, etc.], or a liquid diluent (water for injection). Formulation is also subject to cGMP and usually defines a commercial product.

1.10 SUMMARY

Bioseparations is an essential component of the production of bioproducts, the market for which is large and continuing to grow rapidly. Bioproducts encompass human therapeutics and diagnostics, agriculture specialty chemicals, and nonmedical diagnostics.

- The products in this market are identifiable as small biomolecules, macromolecules, and particulate products, including cells.
- Much of the recent effort in bioseparations has focused on proteins produced by recombinant DNA technology. Purification of recombinant proteins can be simplified by the addition through genetic engineering of a peptide "tag" that enables affinity purification, such as the addition of a histidine oligomer that

selectively binds to immobilized transition metals. Some recombinant proteins are expressed as insoluble inclusion bodies and must be resolubilized and then refolded. Refolding can sometimes be avoided by expressing the target protein as part of a fusion protein that includes a soluble carrier protein, or by the concurrent expression of folding modulators.

- The structure of proteins is established at up to four levels: primary (amino acid sequence), secondary (hydrogen-bonded structures), tertiary (the folding pattern of hydrogen-bonded and disulfide-bonded structures), and quaternary (the formation of multimeric complexes by individual protein molecules). The stability and functions of proteins are established on the basis of these structure determinants.
- Product stability is a criterion for selecting unit operations. Some processes, especially those involving excess heat, bubble formation, pH extremes, or untimely drying, can destroy the function of bioactive substances such as enzymes, hormones, antibiotics, and some vitamins.
- Once synthesized, nearly all bioproducts are separated using a sequence of processes usually consisting of separation of insolubles, product isolation, purification, and polishing.
- Material balance, equilibrium, and transport equations form the scientific foundation of engineering calculations in biochemical separations.
- Purity specified as [product]/([product] + [contaminants]), specific activity (biological activity/mass), and yield (mass after purification/initial mass) are calculated as quality indicators in purification.

NOMENCLATURE

a	particle radius (μm)
c	solute concentration (M, or g liter^{-1})
C	electrical conductivity (ohm^{-1} cm^{-1})
$\mathscr{D}$	diffusion coefficient (cm^2 s^{-1})
E	electrical potential gradient (V cm^{-1})
J_D	diffusive flux of a solute (mol cm^{-2} s^{-1}, or g cm^{-2} s^{-1})
J_e	electrical current density or flux (A cm^{-2})
J_w	fluid flux (liter cm^{-2} h^{-1})
k	Boltzmann constant (1.3807×10^{-23} J K^{-1})
K	partition or distribution coefficient (dimensionless)
K_{eq}	equilibrium constant (units vary)
L_p	permeability coefficient (liter cm^{-2} h^{-1} Pa^{-1})
p	pressure (Pa)
T	absolute temperature (K)
x	linear distance (cm)
x	raffinate phase concentration of a separand in extraction (M, or g liter^{-1})
y	extract phase concentration of a separand in extraction (M, or g liter^{-1})
μ	viscosity (g cm^{-1} s^{-1})

PROBLEMS

The solution to the following problems may require the use of information not in the textbook (which is part of the exercise).

1.1 Product Molecular Weight and Value Rearrange the following five bioproducts approximately according to molecular size (left column) and according to cost per kilogram in the right column: recombinant human growth hormone for injection (hGH), lactic acid (LA), riboflavin for animal feed (B_2), goat antibodies for AIDS testing kits (gAb), and yeast phospholipase C for laundry presoaks (yPLc).

MW	$/kg

1.2 Product Concentrations A 10^{-3} M solution of gamma globulin (antibodies) is called a "concentrated solution." Why is it called a concentrated solution? Support your answer with a calculation.

1.3 pH-Dependent Change of Conformation of Poly-L-glutamic Acid A synthetic polypeptide made up of L-glutamic acid residues is in a random coil configuration at pH 7.0 but changes to α helical when the pH is lowered to 2.0. Explain this pH-dependent conformational transition.

1.4 Properties for Processing Riboflavin (vitamin B_2) is isolated by filtration and polished by spray drying. The efficiency of both processes (higher yield per unit time) increases with increasing temperature. Find the necessary handbook data and determine the maximum temperature at which you could run these two unit operations.

1.5 Process Sequencing Arrange the following products in order of increasing molecular weight (i.e., smallest first), and write after each product the most likely separation process to be useful in its isolation, using the list of processes given in Table P1.5.

TABLE P1.5

Product	Process
Insulin	Distillation
Citric acid	Filtration
B lymphocytes	Adsorption
Vaccine virus	Extraction
Gamma globulin	Centrifugation

Product	Process
Bacitracin	Precipitation
Ethanol	Ultrafiltration
Ribozyme	
Hemoglobin	
Riboflavin	

1.6 Properties: Diffusivity Estimate the molecular diameter and diffusion coefficient for the proteins ribonuclease (MW 13,700 Da), hemoglobin (MW 68,000), and urease (MW 480,000), assuming the molecules are spherical and the density of each protein molecule is 1.3 g/cm^3.

1.7 Preliminary Selection of Purification Steps Based on information in the *Merck Index,* what do you think are the most likely unit operations that should be used for the isolation and purification of the following bioproducts?

(a) Lincomycin
(b) L-Lactic acid
(c) L-Asparaginase

1.8 Calculations for the Purification of a Recombinant Protein The purification of a recombinant protein is carried out starting with 100 liters of a clarified cell lysate (i.e., the cells have been lysed, and the cell debris has been removed to give a clarified solution), which has a total protein concentration of 0.36 mg/ml and a recombinant protein concentration of 2.2 U/ml, where U denotes units of biological activity of the recombinant protein. It is known that the completely pure recombinant protein has a specific activity of 40.0 U/mg. Purification is continued until a chromatography step that yields 2.0 liters of a fraction containing the protein, with a total protein concentration of 1.11 mg/ml and a recombinant protein concentration of 43.2 U/ml.For the recombinant protein, calculate the starting and ending purity, the starting and ending specific activity, and the percentage yield and fold purification through the chromatography step.

1.9 Process Synthesis A process for isolating an antibody against insulin has, as a unit operation, the reaction of the antibody with the antigen in a continuous-stirred tank reactor. The reaction product is a precipitate that is continuously removed from the reactor with 10% of the solution, which is mouse serum. Since insulin is an expensive reagent, only stoichiometric amounts can be added to the mouse serum, which contains 8 mg/liter of anti-insulin. If this particular monoclonal antibody precipitates with its antigen in a 1:1 ratio, how many milligrams of insulin must be added to the reactor per hour to process 100 ml of mouse serum per hour? (Assume that equilibrium is achieved in this reactor.) Sketch a flowchart of this process.

1.10 Product Concentrations Using the *Handbook of Biochemistry and Molecular Biology* (G. Fasman, ed., CRC Press, Cleveland, 1976) or a similar source or a suitable biochemistry textbook (in other words, looking up information), find the necessary information to determine the amount of material required to make 1 ml of each of the following aqueous solutions:

(a) 0.01 M cytochrome c
(b) 1×10^{-7} M β-galactosidase
(c) 0.01 M porcine insulin

(d) 0.01 M human hemoglobin
(e) 0.1 M streptomycin
(f) 1×10^{-6} M oligonucleotide with 10 nucleotides

Also calculate the concentrations in terms of the following additional standard means of expressing bioproduct concentrations: percent (weight per volume) and milligrams per milliliter. Assuming that the solutions are in pure water, also express the concentrations as mole fractions. Discuss the feasibility of making each one of these solutions.

REFERENCES

1. DiMasi, J. A., Hansen, R. W., and Grabowski, H. G. (2003). The price of innovation: new estimates of drug development costs. *J. Health Econ*., vol. 22, p. 151.
2. Palomares, L. A., Kuri-Brena, F., and Ramirez, O. T. (2002). Industrial recombinant protein production. In *Encyclopedia of Life Support Systems*, EOLSS Publishers, Oxford, p. 203.
3. Bailey, J. E., and Ollis, D. F. (1986). *Biochemical Engineering Fundamentals*, 2nd ed., McGraw-Hill, New York.
4. Garrett, R. H., and Grisham, C. M. (2013). *Biochemistry*, 5th ed., Brooks/Cole, Belmont, CA.
5. Mathews, C. K., Van Holde, K. E., Appling, D. R., and Anthony-Cahill, S. J. (2013). *Biochemistry*, 4th ed., Benjamin/Cummings, Menlo Park, CA.
6. Li, F., Vijayasankaran, N., Shen, A. Y., Kiss, R., and Amanullah, A. (2010). Cell culture processes for monoclonal antibody production, *mAbs*, vol. 2, p. 466.
7. Rader, R. A. (2012). Top 50 (or so) biopharma products, *Contract Pharma*, July/August.
8. Weiss, M. (1992). Stability data prove critical for assuring biopharmaceutical shelf life. *Gen. Eng. News*, vol. 14, no. 2, p. 10.
9. Carter, D. C., and Ho, J. X. (1994). Structure of serum albumin. In *Advances in Protein Chemistry*, vol. 45, V. N. Schumaker, ed., Academic Press, New York, p. 153.
10. Kellner, R., Meyer, H. E., and Lotspeich, F. (1994). Amino acid analysis. In *Microcharacterization of Proteins*, R. Kellner, F. Lotspeich, and H. E. Meyer, eds., VCH, Weinheim, p. 93.
11. Scopes, R. K. (1994). *Protein Purification*, 3rd ed., Springer-Verlag, New York.
12. Maa, Y. F., and Hsu, C. C. (1996). Effect of high shear on proteins. *Biotechnol. Bioeng*., vol. 51, p. 458.
13. Virkar, P. D., Narendranathan, T. J., Hoare, M., and Dunnill, P. (1981). Studies of the effects of shear on globular proteins: Extension to high shear fields and to pumps. *Biotechnol. Bioeng*., vol. 23, p. 425.
14. Arnold, F. H. (1991). Metal-affinity separations: A new dimension in protein processing. *Bio/Technology*, vol. 9, p. 152.
15. Smith, D. B., and Johnson, K. S. (1988). Single-step purification of polypeptides expressed in *Escherichia coli* as fusions with glutathione S-transferase. *Gene*, vol. 67, p. 31.
16. di Guan, C., Li, P., Riggs, P. D., and Inouye, H. (1981). Vectors that facilitate the expression and purification of foreign peptides in *Escherichia coli* by fusion to maltose-binding protein. *Gene*, vol. 67, p. 21.
17. Davis, G. D., and Harrison, R. G. (1999). New fusion protein systems designed to give soluble expression in *Escherichia coli*. *Biotechnol. Bioeng*., vol. 65, p. 382.
18. LaVallie, E. R., DiBlasio, E. A., Kovacic, S., Grant, K. L., Schendel, P. F., and McCoy, J. M. (1993). A thioredoxin gene fusion expression system that circumvents inclusion body formation in the *E. coli* cytoplasm. *Bio/Technology*, vol. 11, p. 187.
19. Southworth, M. W., Amaya, K., Evans, T. C., Xu, M.-Q., and Perler, F. B. (1999). Purification of proteins fused to either the amino or carboxy terminus of the *Mycobacterium xenopi* gyrase A intein. *BioTechniques*, vol. 27, p. 110.

20. Rudolph, R., Bohm, G., Lilie, H., and Jaenicke, R. (1997). Folding proteins. In *Protein Function. A Practical Approach*, T. E. Creighton, ed., IRL Press, Oxford, p. 57.
21. Jungbauer, A., and Kaar, W. (2007). Current status of technical protein refolding. *J. Biotechnol*., vol. 128, p. 587.
22. Burgess, R. R. (2009). Refolding solubilized inclusion body proteins, *Meth. Enzymol*., vol. 463, p. 259.
23. Basu, A., Li, X., and Leong, S. S. (2011). Refolding of proteins from inclusion bodies: rational design and recipes. *Appl. Microbiol. Biotechnol*., vol. 92, p. 241.
24. Lilie, H., Schwarz, E., and Rudolph, R. (1998). Advances in refolding of proteins produced in *E. coli*. *Curr. Opin. Biotechnol*., vol. 9, p. 497.
25. Kolaj, O., Spada, S., Robin, S., and Wall, G. (2009). Use of folding modulators to improve heterologous protein production in *Escherichia coli*. *Microb. Cell Fact*., vol. 8, p. 9.
26. Altamirano, M. M., Garcia, C., Possani, L. D., and Fersht, A. R. (1999). Oxidative refolding chromatography: folding of the scorpion toxin Cn5. *Nature Biotechnol*., vol. 17, p. 187.
27. Blanch, H. W., and Clark, D. S. (1996). *Biochemical Engineering*, Dekker, New York.

/// 2 /// ANALYTICAL METHODS AND BENCH SCALE PREPARATIVE BIOSEPARATIONS

The development of efficient and reliable processes for bioseparations is dependent on the availability of suitable analytical methods. This means it is important that work on analytical methodology for the bioproduct of interest starts at the very beginning of process development. Analytical studies are important throughout the development and scale up of the process, as changes can occur either to the product or to its associated impurities from what may be thought of as minor changes in the process.

This chapter gives access to the vocabulary and techniques used in quality control and analytical development activities, starting with a description of specifications typically set for a pharmaceutical and the rationale behind them. Then, before discussing the assays themselves, we describe assay attributes, which can be measured and used to help not only the assay developer but also the biochemist and engineer responsible for developing downstream processes determine the usefulness and meaning of the assay. Finally, we turn to assays that are commonly applied in biotechnology, as they apply to biological activity, identity, and purity.

These assays are the ultimate yardsticks by which the process is measured. Purification methods are developed for their ability to remove a contaminant from the product of interest, whether it is a related molecule, a contaminant related to a host organism, such as DNA or endotoxin, or a process contaminant, such as a residual solvent or water. Critical to understanding process performance is an understanding of how the assays that measure these contaminants have been developed, what the assay strengths and limitations are, and what they indicate and why.

Electrophoresis and magnetic separation are two methods that are now used for the bench scale preparative purification of bioproducts, including living cells. The electrophoresis systems with the highest capacity are free-flow electrophoresis, density gradient electrophoresis, recycling free-flow isoelectric focusing, and rotating isoelectric focusing, and the principles of operation of these are discussed.

The physical principles of magnetic separations are presented, as well as magnetic reagents and applications of magnetic separators.

2.1 INSTRUCTIONAL OBJECTIVES

After completing this chapter, the reader should be able to do the following:

- Identify "specifications" that are desired, especially by regulatory agencies, in the definition of a product.
- Define assay attributes in terms of precision, accuracy, specificity, linearity, limits of detection, range, and robustness.
- Identify and select laboratory methods for assaying biological activity.
- Determine enzyme activity from absorbance measurements.
- Identify and select laboratory methods for assaying purity.
- Predict the maximum temperature in electrophoresis gels.
- Define measurements made in microbiological assays.
- Explain the principles of separation for free-flow electrophoresis, density gradient electrophoresis, recycling free-flow isoelectric focusing, and rotating isoelectric focusing.
- Explain the physical principles of magnetic separations.

2.2 SPECIFICATIONS

The specifications that are set for any product that is expected to be sold are important for assuring the quality and consistency of the product. When the product is to be sold as a pharmaceutical, specifications (among other things) must be reviewed and approved by the U.S. Food and Drug Administration. The FDA is interested in a well-specified product, whose manufacturer assures through routine measurements such product attributes as biological activity, purity, identity, physical characteristics (including color and other appearance qualities), and product safety. The example specification for a therapeutic protein shown in Table 2.1 shows examples of the following:

- Identity determination (identity by HPLC, identity by peptide map, and identity by amino terminal sequencing)
- Biological activity (bioassay: specific activity)
- Purity [content by ultraviolet, purity by reversed-phase HPLC (RP-HPLC), total and individual related substances by RP-HPLC, multimeric forms by ion exchange HPLC, residual organic solvents by gas chromatography, trace metals, host-cell proteins, endotoxin, moisture, bioburden, particulates, and sterility]
- Physical/appearance qualities (general inspection, physical appearance, solubility, pH, and content uniformity)

TABLE 2.1 Example Specification for a Therapeutic Protein[a]

Specification type and method	Drug substance (frozen solution)	Drug product (10 mg vial, lyophilized)
Identity by HPLC	Coelutes with reference standard	Coelutes with reference standard
Identity by peptide map	Conforms to reference standard	
Identity by amino terminal sequencing	70–90% [1–55] form	
Content by ultraviolet	≥10.0 mg/ml	90–110% label claim
Bioassay: specific activity	≥1,000 IU/mg	≥9000 IU/vial
Purity by RP-HPLC	≥97.6%	
Total and individual related substances by RP-HPLC	Total RS ≤2.5% (relative to active) truncated [5–55] form ≤1.0%	Total RS ≤1250 μg/vial truncated [5–55] form ≤150 μg/vial
Multimeric forms by IE-HPLC	≤5.0% multimeric forms	
Residual organic solvents by gas chromatography	Isopropanol ≤150 ppm, acetonitrile ≤100 ppm	
Trace metals	Copper ≤15 ppm	
Host-cell proteins	≤200 ppm	
Endotoxin	≤2.5 EU/mg protein	≤200 EU/vial
Moisture		≤5 mg/vial
General inspection	Verify description, appearance, and container integrity	
Physical appearance	Clear, colorless to slightly yellow	White to off-white cake or powder
Solubility		2 mg/ml soluble to clear, essentially colorless solution
pH	4.5–7.0	4.5–5.5
Content uniformity		≤6.0% RSD (n = 10, per USP)
Bioburden	<10 organisms/mg	
Particulates		≥10 μm: ≤6,000/container ≥25 μm: ≤600/container (per USP)
Sterility		No growth (per USP/CFR)

[a]HPLC, high-performance liquid chromatography; RP, reversed phase; IE, ion exchange; IU, international units; RS, related substances; EU, endotoxin units, USP, U.S. Pharmacopeia; CFR, Code of Federal Regulations. Data from J. Cohen and M. Busch, "Setting biopharmaceutical specifications," *BioPharm.*, vol. 11, p. 38, August, 1998.

The specification usually evolves as the process is developed and the product's properties are learned. It is always best to start with broad specifications that are narrowed as the product is developed for market. Products intended for parenteral human use, however, always entail certain specifications, such as sterility. Safety specifications are of the utmost importance and must be well thought out from the onset of process development.

2.3 ASSAY ATTRIBUTES

Analytical methods can be characterized by a set of measurable attributes. Techniques used to measure these attributes give insight into the quality of the results obtained by using the assay. The effectiveness of a method for measuring attributes depends on its precision, accuracy, specificity, linearity, range, and robustness. Not all attributes are appropriate to all methods, as the following subsections explain.

2.3.1 Precision

Precision is a measure of the reproducibility of an assay. Precision is expressed as a relative standard deviation (RSD), defined as the standard deviation divided by the average, also known as the coefficient of variation (CV). Typically, this is converted to a percentage. The precision tells the likelihood that a repeat test will give the same result. Assays that give precision within ±2% are normally acceptable. Assays for which the RSD is greater than 5% are generally unacceptable for anything but estimates, which sometimes are good enough.

Precision is usually measured by performing replicate analyses on a reference standard or other well-characterized material. Ideally, all external factors that can add to the variability of the assay are minimized or reduced. The sample and all reagents used in its preparation should have good stability and should give a result that is typical of the results expected in practice. Demonstrating that a purity assay can give a result of 100% pure on 100% pure material is not very interesting. Demonstrating the ability to reproduce a purity number like 97.3% is much more challenging.

One measure of precision is the estimated standard deviation s of a finite set of experimental data (generally < 30) [1]:

$$s = \sqrt{\frac{\sum_{i=1}^{n}(x_i - \bar{x})^2}{n-1}} \quad (2.3.1)$$

where $\bar{x}$ is the mean of n measurements, and x_i is an individual measurement. The standard deviation is an estimate of the probable error of a single measurement. At least three replicates must be made before a meaningful standard deviation can be determined. The standard deviation is an estimate of the true variability of the assay, based on a limited sample (the true variability requires infinite replicates to measure); however, the true value is approached asymptotically as replicates are added. The standard deviation is within 90% of the true variability after ten measurements.

The standard deviation of the mean of a series of n measurements is less than that for a single measurement and has been shown to be given by [1]

$$\text{Standard deviation of the mean} = s_{mean} = \frac{s}{\sqrt{n}} \quad (2.3.2)$$

This means that the arithmetical mean derived from n measurements is $\sqrt{n}$ times more reliable than a single measurement. The standard deviation of the mean is usually referred to as the *standard error*.

2.3.2 Accuracy

Accuracy is a measure of the closeness of the assay result to the "true value." Accuracy is often measured on the basis of the recovery of a spike of pure product added into the sample. Spiking the sample with a known amount of standard allows the analyst to determine the amount of an unknown quantity that is likely to be measured by the assay. The spiked standard should be of known content and purity, because the exact quantity of standard introduced into the sample matrix provides the basis for the assay. Accuracies within 1% are exceptional; assays outside 5% are typically unacceptable.

Accuracy experiments are typically some of the first executed in the qualifying of an assay. Quite often, accuracy is more dependent on the sample preparation and storage conditions than on the analytical method itself. For instance, product material may bind nonspecifically to beakers and plastic pipette tips. When nonspecific binding is found, a variety of different materials, or pretreatments for materials, may be used to increase accuracy. Without good recovery of the analyte (i.e., the substance being analyzed), precision and other attributes are difficult to measure or interpret. A 60% spike recovery will be difficult to reproduce with regularity, for example, while 100% recoveries are very reliable. Therefore, determining and increasing spike recovery at an early stage in assay development and making the determination across the range of concentrations anticipated for the method is desirable.

2.3.3 Specificity

The ability of the method to distinguish between the analyte and similar components is referred to as the method's specificity. No assay is specific for the target molecule against all possible contaminants, so specificity must be defined with respect to the intent of the method. For instance, an assay designed to quantitatively resolve two related chemical impurities should not also quantitate DNA.

Specificity always means that no other molecules in the sample matrix interfere with the quantitation of the target molecules. The application of this definition varies from assay to assay. For instance, when trying to measure very small amounts of a chemically unrelated contaminant such as endotoxin in a protein product, specificity is the lack of inhibition or enhancement of the endotoxin signal. In the measurement of closely related contaminants, such as the quantity of a des-Met protein variant (a protein without an N-terminal methionine, a common impurity in recombinant protein preparations) in a protein product (or other deletion or misincorporation products) by HPLC, any such contaminants must be sufficiently resolved from the product to be accurately quantitated. No single HPLC technique is specific for all

possible product-related impurities that may be found in a protein manufacturing process. For this reason, HPLC techniques are almost always used in pairs called orthogonal methods, so that a broader range of contaminants can be detected.

Identity methods usually require a particular result. Consider the example of a protein product. If N-terminal amino acid sequencing is used to characterize the protein, it will be specific for the protein to the extent that any contaminants with different residues among, for example, the first 20 amino acids, will give failing results. However, N-terminal sequencing does not distinguish contaminants with residue substitutions beyond the point where the sequencing ends. Other identity methods are tryptic (or other enzymatic) maps, specific precipitation or colorimetric assays (such as the enzymatic cleavage of a specific substrate to a pigment product), elemental analysis, total amino acid content, and HPLC retention time. Demonstrating specificity in identity assays consists primarily of demonstrating a lack of competing activities or similar responses at similar concentrations from contaminating substances.

For purity assays, the specificity is usually demonstrated through resolution of known contaminants. For instance, in HPLC or capillary electrophoresis (CE), contaminants are resolved according to a molecular property. Usually, these contaminants are collected and identified, or identified by using a "hyphenated" detection method, such as mass spectrometry (MS) attached to an HPLC or CE (LC-MS, CE-MS). Samples containing impurities are often created through "accelerated stability" or stress conditions, such as exposure to high or low pH, exposure to high temperature, exposure to intense light, and exposure to oxidizing substances, such as peroxides. Purity methods that do not detect any contaminants in samples that have been exposed to extreme conditions are suspected of not being very specific. Of course, the material being stressed may be impervious to degradation under these conditions, but this is rare for any molecule with any amount of complex structural components.

2.3.4 Linearity, Limit of Detection, and Limit of Quantitation

The linearity of a method is its ability to produce a response proportional to the concentration of the analyte. Linearity is assessed by creating a standard curve for the analyte(s) by a linear least-squares fit of the response against the concentration (or amount). The coefficient of determination (reported as r^2) is the measure of the linearity and is defined as follows [2]:

$$r^2 = 1 - \frac{SSE}{SST} = 1 - \frac{\sum_{i=1}^{n} (y_i - \hat{y}_i)^2}{\sum_{i=1}^{n} (y_i - \bar{y})^2} \quad (2.3.3)$$

where SSE is the sum of squared deviations about the least squares line, SST is the total sum of squared deviations about the sample mean $\bar{y}$ of the measured values, n is the number of measured values, y_i is the measured value i, and $\hat{y}_i$ is the model of

the measured value i. The sum of squared deviations, *SSE,* can be interpreted as a measure of how much variation in y remains unexplained by the model—i.e., how much variation cannot be attributed to a linear relationship. The ratio *SSE/SST* is the proportion of the total variation that cannot be explained by the linear regression, so $1 - SSE/SST$ is the proportion of variation in y that *can* be explained by the linear regression and is therefore equal to the coefficient of determination r^2. This coefficient varies over the range $0 \leq r^2 \leq 1$. The higher the value of r^2, the more successful the linear regression is in explaining the variation in y. For example, if r^2 is 0.98, then 98% of the variability in the data is accounted for by the model.

Linearity is important because responses from assays for any given analyte amount assayed may not always be identical. It is therefore important to have confidence that the response given is proportional to the actual result sought. Assays become nonlinear at both high and low concentrations, where detectors become saturated (high) or nonspecific responses or noise become a significant proportion of the response (low). It is always important to be making measurements that are bracketed by concentrations on the standard curve, to be assured that results reported are not within these regions of saturation or noise. Extrapolated results are not acceptable.

In purity assays, the linearity of the response of the contaminants is also of interest. Quite often, the response factor (slope of the regression, absorbance, etc.) for the contaminants is not the same as for the main analyte, although it is often assumed to be the same. Authentic samples of impurities are required to prove their amounts in purity assays.

When a standard curve is constructed via regression, a slope, intercept, and r^2 result. The slope is the response factor or signal. The intercept should be zero. If the intercept is not zero, there may be some competing activity or background in the sample (see Section 2.3.3), or noise may be present. The limit of quantitation (LOQ) and limit of detection (LOD) are precision measurements made at the lower extreme of the linearity curve. One method for determining LOQ and LOD is to determine the noise inherent in the system and then set responses that are multiples of the noise for the limits. The noise inherent in the system may sometimes be assessed by analysis of "blank" samples. Sometimes it is specified by the instrument being used. Frequently, LOD is three times the noise, and LOQ is ten times the noise. Another way is to measure precision with small amounts of analyte, and set LOQ as the concentration above which variability is less than 10% RSD and LOD as the concentration above which precision variability is less than 25% RSD. The rationale for setting these limits is based on the intent of the assay and on the way the assay results are used.

2.3.5 Range

The range of an assay refers to the upper and lower limits within which the assay can produce accurate and precise results. "Range" refers not only to the concentration or the amount of the analyte, but also to the range of solution properties associated with the sample, such as pH, temperature, and "matrix" composition (the matrix is

the composition of the sample excluding the analyte, for example, the buffer, cell culture medium, or solvents that might be present). It is a considerable amount of work to investigate every permutation of the assay range, especially if interacting factors are considered. The analytical chemist is usually judicious in selecting the factors that may have the largest impact on the assay result. Factorial design experiments, in which important variables (factors) are varied simultaneously at a limited number of levels, can be used to determine the suitable ranges of the variables to use for an assay [3].

The assay range is reported in the units that describe the sample attributes for which the assay is valid (e.g., pH 6.5–7.5). It is understood that accuracy and precision of the result do not vary across the assay range. Sometimes a secondary range may be listed, for which precision and accuracy are somewhat less, but still high enough for assay results to be useful.

2.3.6 Robustness

While "range" refers to the sample attributes that are acceptable for analysis, "robustness" refers to the assay conditions. In an HPLC method, for instance, flow rate, temperature, pH of the buffers, and solvent content of the buffers may be varied to determine method limits. The method is robust within the limits determined in the test. If the limits determined in robustness testing are not easily achieved routinely in the laboratory, further method development may be required. For example, additional analytical development would be needed when an HPLC buffer pH of 5.5 gives a different result from pH 5.6 and pH 5.7. Again, it is unrealistic to suppose that every factor will be tested and the impact on the result determined. However, critical parameters, or those that are inherently hard to control, need to be examined. Interacting factors will play a role, although the precise role is rarely measured. Statistical design of experiment methodologies is often useful to assess range and robustness.

2.4 ANALYSIS OF BIOLOGICAL ACTIVITY

Most bioproducts are useful on the basis of their biological activity. It is important, therefore, that the biological activity of the desired bioproduct be preserved during the process of bioseparation. It follows that an assay for biological activity, sometimes called potency, is an essential component of any work on the development of such a process. There are three major types of biological activity assay: animal model assays, cell-line-derived bioassays, and *in vitro* biochemical assays.

2.4.1 Animal Model Assays

Animal model assays, which have a relatively long history of use, probably give the most thorough indication of biological activity. Tests in animals should give the most direct evidence that the desired biological outcome results from the administration of

the biomolecule. It should also give the most direct evidence of possible side effects associated with the therapy, either from direct action of the biomolecule, or from impurities. When the precise mechanism of action of the biomolecule is not known, an animal test might be required, as a derivative assay may measure a biological response, but not the response, or set of responses, that would be required for the *in vivo* effect. These assays, however, have several major disadvantages including a long analysis time (several days to weeks), poor precision, and the need for a large number of animals and for appropriate animal facilities and handlers [4]. Sometimes animal model assays must be used because no cell-line-derived or *in vitro* biochemical assay has been developed. One recombinant protein that is assayed by an animal model assay is methionyl–human growth hormone (hGH). In this assay, hypophysectomized female rats are monitored for weight gain over an 11-day period after daily injections with two doses of methionyl-hGH, and the relative biological activity of the test material is obtained by comparing its activity with that of a reference standard material [5].

2.4.2 Cell-Line-Derived Bioassays

Cell-line-derived bioassays are easier to perform than animal model assays; they also give faster results (1 to 3 days) and are much less expensive and wasteful [4]. Cell-line-derived assays give information on the effect of the bioproduct in a living system, but they are also imprecise because of the variances of living cells. They can be automated, however, and therefore can be repeated enough times to give relatively reproducible results. Two general categories of cell-line-derived bioassays are cell-bound receptor systems and cell-culture-based assays.

Cell-bound receptor systems are used to assay bioproducts, such as proteins, that bind to receptors in a quantifiable and reproducible fashion [6]. It may be necessary to express the receptor on the cell surface for the proper folding of the receptor and thus product binding. An example of this type of assay is the use of human placental cells as a source of human insulin–like growth factor I receptors [7]. These cells can be bound to a solid support and a radiolabeled product used to set up a competitive binding assay. Sometimes, the cell membranes containing the receptor can be purified and used in place of the cells, although this may lead to additional nonspecific reactions with the disrupted, denatured, and hydrophobic cell membranes.

Cell-culture-based assays can be used when there is a cellular response to the bioproduct, which ideally should be linear and directly related to the desired biological activity [6]. This type of assay has been used, for example, to measure the activity of nerve growth factor (NGF): when NGF is added to a pheochromocytoma cell line (PC12 cells), the cells stop dividing, sprout neurites, and become electrically excitable [8]. Most cell-culture-based biological assays, however, are based on general effects such as inhibition or enhancement of cell growth. Tests of inhibition

of cell growth are routinely used to test the biological activity of antibiotics. One commonly used assay of this type is the dilution test, in which the cells containing the antibiotic are incubated for a fixed period of time, typically 16 to 20 hours, and the minimum concentration of antibiotic that causes inhibition of visible cell growth (minimal inhibitory concentration, MIC) is determined [9]. Another type of cell-culture inhibition assay for antibiotics is the turbidometric assay, which can be completed in less time than the dilution test and is capable of excellent precision [10]. The antibiotic causes cell death and therefore leads to a less turbid suspension. The lower the antibiotic activity, the higher the turbidity. The turbidity of the cells is measured as absorbance on a spectrophotometer, and the antibiotic concentration is determined from a standard curve.

2.4.3 *In vitro* Biochemical Assays

In comparison to assays using animals or cells, *in vitro* biochemical assays are simple, fast, precise, and accurate, and thus are usually preferred for measuring biological activity in process development work when they are available. However, they are furthest removed from any actual *in vivo* activity that might be desired in the molecule, so they should be used on more mature products, where the inference of *in vivo* activity from the *in vitro* result is more firmly established. In the case where the biomolecule is being produced for an *in vitro* application, such as an industrial enzyme, in vitro biochemical analysis is entirely appropriate. The most prevalent type of biochemical assay is the one that measures enzymatic activity. The result of a test of enzyme activity is the number of *units of activity,* where one unit (U) is defined as the enzyme activity that causes 1 micromole (μmol) of substrate to react in 1 minute at specified conditions [11].

There are two general classes of techniques for measuring enzyme activity, stopped methods and continuous methods [12]. In the stopped method, the enzyme is incubated with its substrates for a fixed amount of time, and then the reaction is stopped. The product formed is measured, and the units of activity are then calculated, assuming that the reaction rate is linear from time zero. This assumption of linearity can be checked by carrying out a series of incubations at different times. In the continuous method, multiple readings of the amount of product formed are taken over a period of time, usually on the order of minutes, and the activity is calculated from the slope of the plot of reading versus time. One commonly used variation of the continuous method relies on the principle of coupling: a product that cannot be observed directly is converted, either chemically or enzymatically, to form a compound that can be observed.

Other biochemical assays are based on mimicking the bioproduct's action *in vivo*. The activity of the recombinant tissue plasminogen activator (rt-PA), for example, can be measured with an *in vitro* clot lysis assay that can be performed within hours. The rt-PA is added to a synthetic fibrin clot in the presence of plasminogen, and the

rt-PA converts the plasminogen to the active enzyme plasmin, which then lyses the clot. The assay is followed spectrophotometrically or visually by monitoring the release of trapped air bubbles. This assay is reported to have an accuracy of 99% and a relative standard deviation of 5% [13].

EXAMPLE 2.1

Coupled Enzyme Assay for Alcohol Oxidase For the determination of the enzymatic activity of alcohol oxidase (AO) from yeast, the following coupled reactions are utilized [14]:

$$\text{methanol} + O_2 \xrightarrow{\text{AO}} \text{formaldehyde} + H_2O_2$$
$$H_2O_2 + DH_2 \xrightarrow{\text{HP}} 2H_2O + D$$

where DH_2 is a dye precursor, D is the dye, and HP is the enzyme horseradish peroxidase. The dye is monitored by means of a spectrophotometer at a wavelength of 405 nm. To prepare the standard curve for the assay, the absorbance readings shown in Table E2.1 were taken at various concentrations of H_2O_2 in the reaction mix with no AO or methanol added, using a light path length of 10 mm:

TABLE E2.1

H_2O_2 concentration (μmol/liter)	$A_{405\ nm}$
7.1	0.25
9.6	0.36
12.3	0.44
15.1	0.57
18.0	0.66

A sample of clarified yeast cell lysate (i.e., cells lysed, and cell debris removed to give a clarified solution) assayed for AO activity by this method gave a rate of change of A_{405} of 0.082/min in the assay after a dilution of the sample of 1:40,000. Calculate the AO concentration in units per milliliter, where 1 unit (U) is equal to the amount of enzyme producing 1 μmol of H_2O_2 per minute under the conditions of the assay.

Solution

We first plot A_{405} versus the concentration, c, of H_2O_2 and find that the data are well fitted by a straight line (Figure E2.1), with the result

$$\Delta A_{405} = 0.0377 \Delta c$$

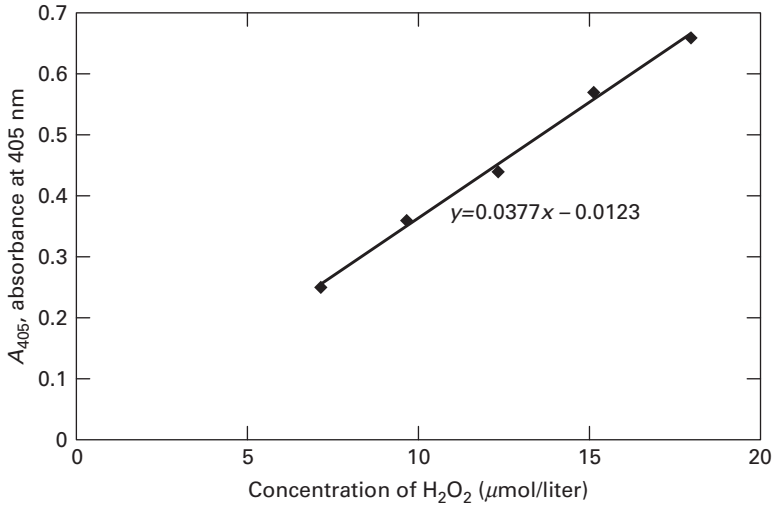

FIGURE E2.1 Standard curve for the coupled enzyme assay for alcohol oxidase.

From the ΔA_{405}/min value for the clarified yeast cell lysate,

$$\frac{\Delta c}{\Delta t} = \frac{\frac{\Delta A}{\Delta t}}{0.0377\,\frac{\text{liter}}{\mu\text{mol}}} = \frac{0.082\,\text{min}^{-1}}{0.0377\,\frac{\text{liter}}{\mu\text{mol}}} = 2.18\,\frac{\mu\text{mol}}{\text{liter min}} = 2.18\,\frac{\text{U}}{\text{liter}}$$

Since the sample was diluted 1:40,000 before assaying,

$$\text{Alcohol oxidase concentration in clarifield cell lysate} = 40{,}000\left(2.18\times10^{-3}\,\frac{U}{ml}\right)$$
$$= 87.2\,\frac{U}{ml}$$

2.5 ANALYSIS OF PURITY

Determinations of purity are inherently defined by the specificity and sensitivity of the methods used to detect the impurities that are present. Impurities can be classified according to whether they are intrinsic to the desired bioproduct (e.g., proteolytically cleaved material from a protein product) or extrinsic to the product (e.g., components of the cell growth medium). In pharmaceutical terminology, these are referred to as "product-related impurities" and "process-related impurities," respectively. A further distinction is made within product-related impurities between active and inactive impurities. Active product-related impurities are called "product-related substances," and it is expected that their activity will be demonstrated. It is important that intrinsic purity be evaluated by methods that are orthogonal (i.e., independent of

each other), through methods based on different physiochemical properties [6]. Purity assays also give information about the extent and completeness of the biochemical reaction or reactions leading to the formation of the product, the side products that may have been formed, the efficiency of the purification process, and whatever contamination may have been formed or picked up through downstream processing. The various assays for purity are discussed in this section, with an emphasis on the ones that are the most powerful, such as electrophoretic and HPLC assays.

2.5.1 Electrophoretic Analysis

Electrophoresis is a separation technique often applied to the analysis of biological or other polymeric samples. This technique is among the most powerful for estimating purity because of its simplicity, speed, and high resolution, and also because there is only a small probability that any of the components being analyzed will be lost during the process of analysis [4].

Electrophoresis has frequent application to analysis of proteins and DNA fragment mixtures and has been increasingly applied to the analysis of nonbiological and nonaqueous samples. The high resolution of electrophoresis has made it an important tool in the advancement of biotechnology. Variations of this methodology are being used for DNA sequencing and fingerprinting, for isolating active biological factors associated with diseases such as cystic fibrosis, sickle cell anemia, myelomas, and leukemia, and for establishing immunological reactions between individual compounds. Electrophoresis is an effective analytical tool because the electric field does not affect a molecule's structure, and it is highly sensitive to small differences in molecular charge, size, and sometimes shape.

The term electrophoresis refers to the movement of a molecule or particle through a stationary fluid under the influence of an electric field (*phorein*: Greek, "to carry"). The study of electrophoresis has included the movement of colloids, fibers, clay particles, latex spheres, and bubbles. While the application of greatest interest for the purpose of this text is the separation of proteins and nucleic acids, the theory is best described in consideration of a distinct particle. The application is extended to these biomacromolecules in that they have colloidal properties, such as a surface charge, an interior with a polarity distinctly different from that of their exterior, and a distinct density (see Chapter 5, Sedimentation). The fundamental principles behind electrophoresis, the commonly used modes of operation, the matrices employed, and the techniques for detection are discussed in detail in the subsections that follow.

Principles

The fundamental principle behind electrophoresis is the existence of charge separation between the surface of a particle and the fluid immediately surrounding it. An

applied electric field acts on the resulting charge density, causing the particle to migrate and the fluid around the particle to flow. The electric field exerts a force on the particle's charge or surface potential. This force results in a velocity for the particle that is proportional to the particle's surface potential. Two particles with different velocities will come to rest in different locations after a fixed time in an electric field. The particle velocity is related to the field strength by

$$v = UE = U\left(\frac{V}{L}\right) \tag{2.5.1}$$

where v is the particle velocity, E is the field strength or voltage gradient (voltage V per length L between the electrodes in the electrophoresis system), and U is the apparent electrophoretic mobility. U has a linear dependence on the dielectric constant of the liquid and an inverse linear dependence on the liquid viscosity [see Equation (3.4.4) in Chapter 3]. There are two contributions to this apparent electrophoretic mobility [15]:

$$U = U_{el} + U_o \tag{2.5.2}$$

where U_{el} is the electrophoretic mobility of the charged particle and U_o is the contribution from electroosmotic flow.

Electroosmosis is the flow of liquid in a channel to which an electric field has been applied. For instance, when a capillary connects two reservoirs containing an electrolytic fluid (such as salt water) and an electric field is applied between the reservoirs, salt water will flow, typically from the anodic chamber to the cathodic chamber. This is because the SiO^- charge on the glass capillary attracts a positive countercharge that is mobile and flows toward the cathode in an electric field. This occurs until hydrostatic head is built up in the cathodic reservoir, causing a counterbalancing flow through the middle of the capillary. Electroosmotic flow is generally minimized in polymer networks such as gels (where the effective liquid viscosity is very large or the effective capillary diameter is very small) but is important in open channels such as capillaries and tubes.

A schematic of a typical gel electrophoresis apparatus is shown in Figure 2.1. The design of analytical gel electrophoresis equipment is influenced by the generation of heat and electrolysis gases, as discussed next.

Generation of Heat in Electrophoresis Instrumentation

One of the considerations in designing electrophoresis equipment is the dissipation of heat generated by the electric field. The rate of change in temperature in an insulated electrophoretic medium is given by

$$\frac{dT}{dt} = \frac{P}{C_p M_e} = \frac{VI}{C_p M_e} \tag{2.5.3}$$

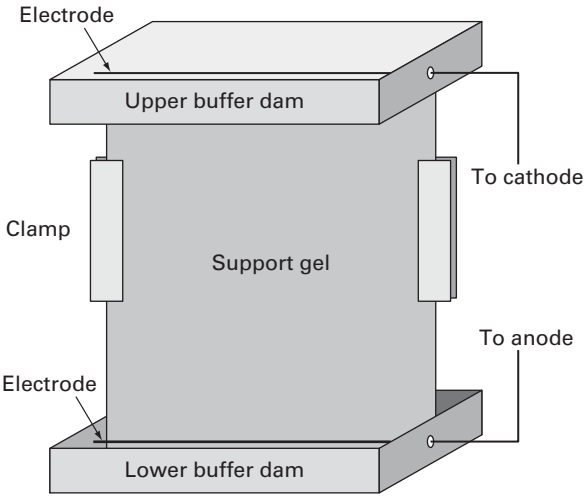

FIGURE 2.1 Typical gel electrophoresis apparatus. Samples are loaded in wells at the top of the gel, which is supported on both sides by glass plates (not shown), and components contained in the samples are separated as they travel downward toward the anode.

and the rate of heat generation per unit volume is

$$S = \rho C_p \frac{dT}{dt} \tag{2.5.4}$$

where P is the power, C_p is the heat capacity of the medium, M_e is the mass of the electrophoretic medium, V is the voltage, I is the current, and ρ is the density of the medium. From Ohm's law ($V = IR$, where R is the electrical resistance), it is seen that the temperature change increases as the square of the current. Electrophoresis is thus most conveniently conducted in highly resistive media (low salt concentrations). The addition of polymer matrices, such as gels, also serves to increase the resistivity of the media by increasing the viscosity that is resisting the movement of charge, and creating a more tortuous path through which the charge must migrate.

Heating in electrophoresis causes changes in the viscosity and density of the electrophoretic medium. High temperatures can also damage electrophoretic equipment by warping cooling blocks, melting plastic, or cracking glass plates. When fluids heat unevenly, the hot portion of the fluid rises with respect to cooler portions because of the difference in density. This convection distorts zones and thereby decreases resolution in electrophoretic separations. The ability to remove heat from electrophoretic systems ultimately determines the voltage that can be applied, and the speed and resolution that can be achieved.

Heat is dissipated from electrophoresis equipment by maximizing the surface-to-volume ratio. Most electrophoresis is conducted in thin gels (0.5–1.5 mm) or in capillaries with channels up to 100 μm in diameter. The narrow cross section also reduces the total current, although the current density (A/cm^2) remains independent

of scale. The removal of heat from the gel is a typical transport process obeying energy balances and Fourier's law of heat conduction, which states

$$q_x = -k\frac{dT}{dx} \tag{2.5.5}$$

where q_x is the heat flux in the x direction (heat flow per unit area) and k is the thermal conductivity.

EXAMPLE 2.2

Estimation of the Maximum Temperature in an Electrophoresis Gel

A vertical gel electrophoresis system consists of a gel supported on both sides by glass plates, each surrounded by a fluid stream at the same constant temperature on both sides. Develop an expression for the maximum temperature within the gel as a function of the thermal conductivity and thickness of the gel and the glass, the heat transfer coefficient at the outer surface of the glass, and the rate of heat generation per unit volume in the gel.

Solution

A schematic diagram of the cross section of the gel and the glass plates (Figure E2.2) also shows the temperature profile and the thermal conductivities k^{01} for the gel and k^{02} for the glass. We let S be the heat per unit volume per unit time generated uniformly by the electric current in the gel. We begin by making a

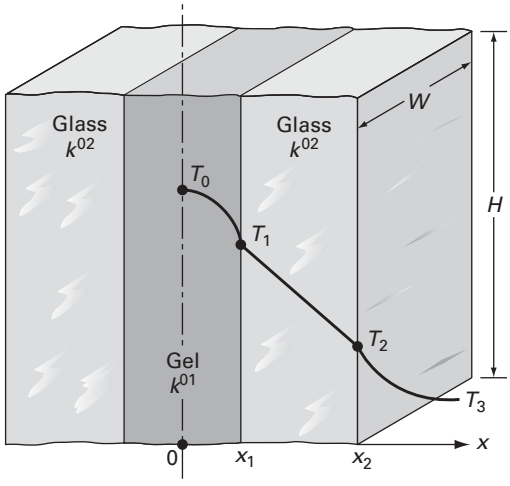

FIGURE E2.2 Schematic cross-sectional diagram of a vertical electrophoresis system. The glass plates are surrounded on each side by a fluid stream at the same constant temperature, T_3.

steady-state thermal energy balance over a thin slab of gel thickness Δx, width W, and height H:

$$q_x^{01}\Big|_x WH - q_x^{01}\Big|_{x+\Delta x} WH + SWH\Delta x = 0$$

where q_x^{01} is the heat flow per unit area (heat flux) in the x direction. After dividing by $WH\,\Delta x$ and taking the limit as x approaches zero, we obtain

$$\frac{dq_x^{01}}{dx} = S$$

Integration gives

$$q_x^{01} = Sx + C$$

where C is a constant of integration. From Figure E2.2, we see that the symmetry of the system gives the boundary condition

$$\text{at } x = 0, \qquad \frac{dT}{dx} = 0$$

From Fourier's law of heat conduction,

$$q_x = -k\frac{dT}{dx}$$

so that we have the boundary condition

$$\text{at } x = 0, \qquad q_x^{01} = 0$$

This gives $C = 0$, so that

$$q_x^{01} = Sx$$

At $x \geq x_1$, the heat flux becomes a constant because there is no heat generation in the glass support plates, which gives the additional boundary condition

$$\text{at } x = x_1, \qquad q_x^{01} = q_x^{02} = q_1 \,(\text{a constant})$$

From the equation for q_x^{01}, this boundary condition gives

$$q_1 = Sx_1$$

Writing Fourier's law of heat conduction for the gel and for the glass, we have

$$-k^{01}\frac{dT^{01}}{dx}=q_x^{01}=Sx$$
$$-k^{02}\frac{dT^{02}}{dx}=q_x^{02}=q_1$$

Integration of these equations gives

$$T_0-T_1=\frac{Sx_1^2}{2k^{01}}$$
$$T_1-T_2=\frac{q_1(x_2-x_1)}{k^{02}}$$

Finally, heat is rejected at the outer surface of the glass, and the heat transfer coefficient h is defined as

$$T_2-T_3=\frac{q_1}{h}$$

Addition of the previous three equations gives

$$T_0-T_3=\frac{Sx_1^2}{2k^{01}}+\frac{q_1(x_2-x_1)}{k^{02}}+\frac{q_1}{h}$$

Substitution for q_1 and solving for T_0 yields

$$T_0=T_3+Sx_1\left(\frac{x_1}{2k^{01}}+\frac{x_2-x_1}{k^{02}}+\frac{1}{h}\right)$$

Thus, as we would expect, an increase in the maximum temperature in the gel is caused by increasing the rate of heat generation per unit volume (S, due to current density), increasing the gel thickness ($\Delta x = 2x_1$) or the glass plate thickness ($x_2 - x_1$), and decreasing either of the thermal conductivities (k's) or the heat transfer coefficient h at the surface of the glass plates.

Electrolysis Reactions

The electrodes in electrophoresis equipment are typically constructed from platinum wire, and small ions generally carry the current in the electrophoretic medium. At the interface between the electrodes and the electrophoretic medium, electrolysis reactions occur. For aqueous systems, the following reactions are expected:

$$\text{Cathode} \qquad 2H_2O+2e^-\rightarrow 2OH^-+H_2$$
$$\text{Anode} \qquad H_2O\rightarrow 2H^++\tfrac{1}{2}O_2+2e^-$$

Electrode chambers are usually open to the atmosphere to permit venting of electrolysis gases. The reactions at the electrodes produce acid (anode) and base (cathode), thus requiring electrophoresis systems to be well buffered. Electrophoresis systems sometimes mix the buffers from the individual electrode reservoirs to equalize the pH.

Modes of Electrophoretic Separation

Electrophoresis can be performed several different ways, of which the most commonly used for bioproducts are denaturing gel electrophoresis (better known as SDS-PAGE: see the next subsection), native gel electrophoresis, capillary electrophoresis, and isoelectric focusing. The first three methods take place in a constant electric field at constant pH and separate according to actual mobility. Isoelectric focusing uses an electric field with a pH gradient and allows components to move until they have zero net charge. Mobility-based electrophoresis using either denaturing or native gels is by far the most common method for the analysis of proteins and DNA. Gel electrophoresis for analysis requires only microgram quantities of protein, usually only a small fraction of what is available.

Denaturing Gel Electrophoresis (SDS-PAGE) The use of sodium dodecyl sulfate (SDS) with polyacrylamide gel electrophoresis (PAGE) was first described in the late 1960s. The SDS is an ionic surfactant that solubilizes and denatures (unfolds) proteins. Dodecyl sulfate binds a protein through hydrophobic interactions with side chains, and disrupts side chain interactions that cause proteins to fold and interact with other subunits. Nonreduced proteins bind approximately 0.9 to 1.0 g of SDS per gram of protein, or about one dodecyl sulfate molecule for every two amino acid residues.

The SDS-PAGE technique allows separation of molecules according to size or molecular weight. When SDS-treated samples migrate into a gel and are electrophoresed, the principal difference between sample components is molecular size or length, since the ratio of charge to size is virtually the same for all proteins with bound SDS. Smaller molecules travel through the matrix more quickly than those that are larger. The rate at which molecules migrate through a polyacrylamide gel is inversely linear with the logarithm of their molecular size. Thus, denatured samples can be analyzed alongside denatured standards of known molecular weight to estimate the molecular weight of the analyte.

The typical SDS-PAGE results obtained with a gel electrophoresis apparatus presented in Figure 2.2 are for proteins denatured by SDS and stained (left) and also blotted and probed with an antibody, called a "Western blot" (right; see Blotting Techniques later in this chapter). Each band on the gel represents a highly enriched substance that has been separated from the other bands based on slightly different charge or size/shape properties. As shown, several samples are typically analyzed side by side on a gel. Bands that migrate the same distance in different sample mixtures probably have similar mass and charge characteristics. Standards having known mobility or molecular mass are run concurrently with samples whose components are to be identified (column m in Figure 2.2a).

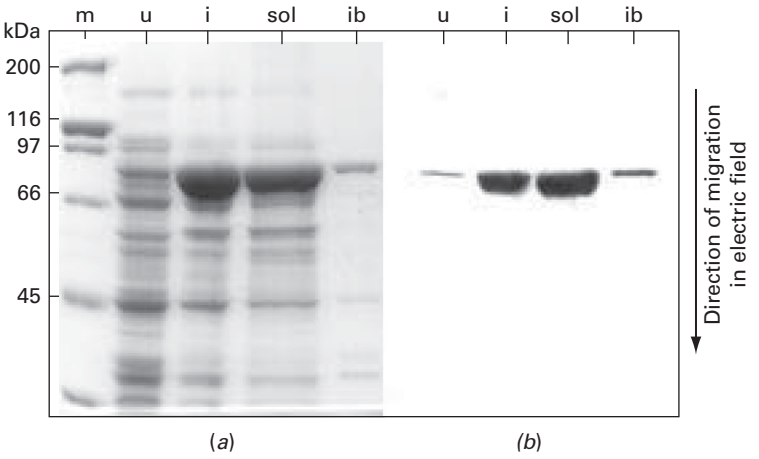

FIGURE 2.2 SDS-PAGE (denaturing gel electrophoresis) and Western blot results for human interleukin-3 (hIL-3) expressed as a C-terminal fusion to *E. coli* NusA protein. (*a*) Sodium dodecyl sulfate polyacrylamide gel electrophoresis (SDS-PAGE) results with Coomassie blue staining. (*b*) Western blot results obtained by using rabbit anti-hIL-3 polyclonal antibody and visualized by means of chemiluminescence. Fusion proteins were expressed at 37°C in *E. coli* by induction of the *tac* promoter. Equal portions of cell lysate, soluble fraction, and insoluble fraction were loaded. Key: m, markers; u, uninduced whole cell lysate; i, induced whole cell lysate; sol, soluble fraction; ib, inclusion body fraction. *(From G. D. Davis and R. G. Harrison, "New fusion protein systems designed to give soluble expression in* Escherichia coli,*"* Biotechnol. Bioeng., *vol. 65, p. 382, 1999. Copyright © 1999. Reprinted by permission of Wiley-Liss, Inc., a subsidiary of John Wiley & Sons, Inc.)*

Other dissociating agents may be used to further break down a protein. Urea is often used to disrupt hydrogen bonds. When urea is the only dissociating agent added (no SDS), a protein's intrinsic charge is not affected and separation based on size and charge may be achieved. If a protein contains internal disulfide bonds, a thiol reagent such as β -mercaptoethanol can be used to reduce the sample and break the disulfide bonds. Proteins having reduced disulfide bonds bind approximately 1.4 g of SDS per gram of protein, versus about 1 g per gram when not reduced. Sometimes, protein subunits are covalently attached by disulfide bonds. An important example of this is antibody molecules. A reducing agent dissociates the light chain from the heavy chain, so the purity of each can be verified. Typically, both reduced and nonreduced samples are run in efforts to evaluate internal disulfide bond content.

Native Gel Electrophoresis In this type of electrophoresis, a buffer is used that allows the components separated to be in their native form. When this procedure is used for proteins, a pH in the range of 8 to 9 is desirable so that most proteins will be negatively charged and thus move toward the anode. In this pH range, proteins that are either uncharged or positively charged will either stay in the starting well or move toward the cathode. If the proteins of interest are basic, a lower pH can be used, with the cathode at the bottom of the gel [12].

Native gel electrophoresis and SDS electrophoresis are good ways to determine whether a protein of interest forms subunits and, if so, the number of subunits per

molecule. The electrophoresis is run under both native and denaturing conditions and the results are compared. An immunoblot may have to also be run to positively identify the protein of interest under both sets of conditions (see the immunoblot in Figure 2.2b and Blotting Techniques, later).

Capillary Electrophoresis Capillary electrophoresis is a highly automated, commercially available technique that bears a strong resemblance to analytical chromatography. First widely used as a support medium for electrophoresis in the early 1980s, capillaries have a small cross-sectional area that minimizes power consumption, while their high surface-to-volume ratio allows efficient dissipation of heat. In practice, electric fields in excess of 300 V cm^{-1} can be utilized without encountering detrimental thermal effects. Capillary electrophoresis separations are rapid (minutes) and produce a chart recording rather than a stained gel for archiving. A typical capillary "electropherogram" is shown in Figure 2.3.

Clearance of sample components from a capillary is a problem that must be considered carefully. Usually, capillary electrophoresis is conducted in a fused-silica capillary that is coated on its inner surface. The capillaries can be open or filled with a gel (see later: Support Media). Capillaries are too expensive to discard after each use, as is done with standard gels. Therefore, the entire sample must be cleared from

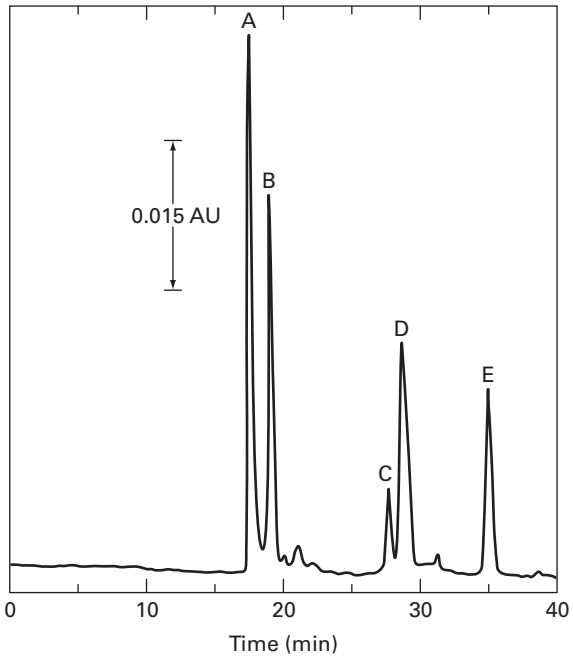

FIGURE 2.3 Separation of proteins by open tubular capillary electrophoresis, carried out in a 75 cm × 75 μm surface modified capillary at an applied voltage of 75 kV. Peak identities: A, egg white lysozyme; B, horse heart cytochrome c; C, bovine pancreatic ribonuclease a; D, bovine pancreatic α-chymotrypsinogen; E, equine myoglobin. *(Data from Y. Walbrooehl and J. W. Jorgenson, "On-column UV absorption detector for open tubular capillary zone electrophoresis,"* J. Chromatog., *vol. 315, p. 135, 1984.)*

the capillary before the capillary is used for another sample, much as in analytical chromatography.

The small quantity of material loaded into the capillary requires that high-sensitivity detection be employed with all capillary electrophoresis instruments. Typical sample volumes range from 5 to 50 nanoliters, less than 1% of the volume typically loaded onto conventional polyacrylamide or agarose gels. For trace analysis, a small number of molecules will be present in the capillary after loading. Detection of these small amounts of material necessitates very sensitive detectors.

Isoelectric Focusing Isoelectric focusing is a technique used for protein separation that operates by driving proteins to the pH equal to their isoelectric points, where the net charge on the molecule is zero. Resolution depends on the slope of a pH gradient that can be achieved in a gel or capillary.

Ampholytes. An ampholyte is a molecule that can be positively or negatively charged depending on the pH. All amino acids and proteins are ampholytes (or amphoteric). Not only does the sign of the charge of an ampholyte change with pH, but the magnitude of the charge can also vary. The charge on a protein, for example, may vary from +10 or more at low pH, to −10 or more at high pH.

A special class of ampholytes has been synthesized for isoelectric focusing. These ampholytes have an amino end and a carboxyl end that are separated by varying numbers of methylene groups. The farther apart the amino and carboxyl groups, the less they affect the ionization of each other; thus a different isoelectric point is established for each molecular species. These ampholytes, which may be added to an electrophoretic medium, migrate according to their charge under the influence of the applied electric field. When they reach a zone in which the local pH is the same as that ampholyte's isoelectric point, migration stops. The ampholyte molecules buffer themselves and establish the local pH as they migrate through the gel. As the ampholytes reach an isoelectric pH, they establish a spatially distributed and natural pH gradient in the electrophoretic medium.

Isoelectric Focusing Technique. Isoelectric focusing (IEF) is an electrophoretic technique in which amphoteric samples (such as proteins) are separated according to their isoelectric points along a continuous pH gradient. IEF analyses are carried out in various matrices: polyacrylamide, agarose, and capillaries. The agarose or polyacrylamide gels that are used must be prepared with carrier ampholytes bracketing a specific pH range. After some time, the ampholytes separate, and there is a pH gradient that covers the range of all the ampholytes' isoelectric points. A specific class of commercial ampholytes, called Immobilines®, can be added to the matrix, electrophoresed into a gradient, and covalently incorporated into the gel matrix.

Because protein samples are themselves ampholytes, when samples are loaded onto the gel and a current is applied, the compounds migrate through the gel until they come to their isoelectric point, or pI, where they reach a steady state. This technique measures an intrinsic physicochemical parameter of the protein, the pI, and therefore does not depend on the mode of sample application. In practice, IEF has the highest sample load capacity of any electrophoretic technique.

In slab gels, isoelectric focusing typically requires approximately 3 to 30 hours to complete because sample compounds move increasingly slowly as they approach the pH that corresponds to their isoelectric point. This time can be shortened to approximately 30 minutes in capillaries because of the higher electric field employed. Because the gradient ampholytes and the samples stop where they have no mobility, the resistivity of the system increases dramatically toward the end of the experiment, and the current decreases dramatically. For this reason, isoelectric focusing is usually run in constant voltage mode and has the most stringent requirements for cooling of any electrophoretic technique. A plot of current versus time can be used to determine when the system is focused, since the final steady state current is only a few microamperes. Another option with many power supplies is to run at constant power. This ensures that the heat load will remain constant, even as the current decreases and the voltage increases.

Electrophoretic Instruments

Most electrophoresis equipment shares the basic design shown in Figure 2.1. Electrophoresis equipment typically has two buffer reservoirs, one anodic and one cathodic. The equipment includes an electrophoretic medium (e.g., a gel, paper, or capillary) connecting the two reservoirs, to which a sample is applied. A direct current power supply connects two electrodes suspended in the buffer reservoirs. When an electric potential is applied between the two electrode reservoirs, the sample components migrate through the medium. At completion of an electrophoretic separation, the sample components have been either resolved into several zones along the length of the medium or eluted from the medium into the anodic buffer. Instruments for preparative electrophoresis without support media are discussed in Section 2.7.1.

Support Media

The conduction of electric current through an electrophoresis system causes the system temperature to increase if the heat is not dissipated at a rate equal to the rate of its generation. Increases in system temperature will increase the electrophoretic mobility of molecules because the viscosity of the matrix decreases with increasing temperature. Additionally, the formation of thermal gradients will result either in convection or a distribution of electrophoretic mobilities for a unique compound, and ultimately in zone spreading. To minimize the influence of convection on the electrophoretic separation, anticonvective support media such as paper or polymer gels are commonly employed.

Separation on paper or polymer gels is influenced not only by electrophoretic mobility, but also by sieving of the molecules as they pass through the network of pores and fibers. The finer the weave of this matrix, the more slowly a molecule travels through it. Therefore, molecular size, as well as charge, can influence the rate of migration in these media.

Paper Electrophoresis Paper was one of the first matrices used for electrophoresis. In paper electrophoresis, the sample is applied directly to a zone on the dry paper,

which is then moistened with a buffer solution before application of an electric field. Dyes are combined with samples and standards to help visualize the progress of the electrophoresis. The movement of samples on paper is best when the current flow is parallel to the fiber axis in the paper.

Some advantages of paper are that it is readily available and easy to handle, requires no preparation, and allows the rapid development of new methodologies. Besides being easy to obtain, paper does not contain many of the bound charges that can interfere with the separation. A disadvantage of paper electrophoresis is that the porosity of commercial paper is not controlled, and therefore the technique is not very sensitive, nor is it easily reproducible.

Polyacrylamide Gels Polyacrylamide gel electrophoresis is one of the most commonly used electrophoretic methods. Analytical uses of this technique center on protein and nucleic acid characterization (e.g., purity, size, or molecular weight, and composition). Acrylamide is a neurotoxin, however, and the reagents must be combined extremely carefully. An additional drawback is that the gels are not as pliable as most agarose gels.

Polyacrylamide gels are synthesized through the polymerization of acrylamide monomer, $CH_2{=}CHCONH_2$, and a bifunctional, cross-linking comonomer. Typically, the cross-linking comonomer is *N, N′*-methylenebisacrylamide (bisacrylamide), $(CH_2{=}CHCONH)_2CH_2$, although other compounds such as ethylenediacrylate (EDA) or *N,N′*-diallyltartar diamide (DATD) are sometimes used. The sieving properties of the gel are defined by the network of pores established during the polymerization. As the acrylamide concentration of the gel increases, the effective pore size decreases. By convention, a gel is characterized by two parameters, *%T* and *%C*, where *%T* is the mass percentage of total monomer (acrylamide plus comonomer in grams per 100 ml), and *%C* is the proportion by mass of monomer (per 100 g of acrylamide) that is the cross-linking agent. Gels typically have *%T* values between 3 and 30%.

The most commonly used combination of chemicals to produce a polyacrylamide gel is acrylamide, bisacrylamide, buffer, ammonium persulfate, and tetramethylenediamine (TEMED). TEMED and ammonium persulfate are catalysts for the polymerization reaction. The TEMED causes the persulfate to produce free radicals, initiating polymerization. After the gel has been poured into a prepared form (usually between two vertical, parallel glass plates that are sealed on the bottom and sides, see Figure 2.1), a "comb" can be inserted into the top portion of the gel before polymerization is complete. This comb sets small indentations (wells) into the gel that can be used to apply samples. If the comb is used, samples are typically mixed with a dense liquid such as glycerol to prevent the sample from dispersing into the reservoir buffer. Samples then migrate straight down the gel and appear as columns, or lanes, of separated components at the end of the experiment (see Figure 2.2).

"Precast" gels are widely available and quite often are used preferentially to casting and polymerizing gels in the lab. Gels that are formed with a gradient, particularly in *%T*, can be purchased for protein analysis. A gradient gel is useful, because it

increases the area on the gel where high molecular weight proteins may be resolved and it causes significant sharpening of protein bands during migration.

Agarose Gels Agarose is a polymer extracted from red seaweed. When agar is extracted from the seaweed, it is in two components, agaropectin and agarose. The agarose portion is nearly uncharged, making it desirable for use as an electrophoresis matrix. To prepare an agarose gel, a combination of agarose and buffer is heated until the solid is dissolved. The solution is cooled and then poured into a gel-casting apparatus and allowed to gel. The advantages of agarose electrophoresis are that it requires no additives or cross-linkers for polymerization, it is not hazardous, low-concentration gels are relatively sturdy, and it is inexpensive. Agarose gels have large pore sizes compared to polyacrylamide gels. Agarose is commonly used for the separation of large molecules such as DNA fragments.

Capillaries The fused silica capillaries used in capillary electrophoresis are flexible due to an outer polyimide coating and are available in inner diameters ranging from 10 to 300 μm. Fused silica is transparent to UV light, which enables the capillary to serve as its own detection flow cell. Electrostatic interactions with the capillary surface can develop, however, when charged species are being separated. One popular strategy to overcome this problem is to chemically modify the inner capillary surface to produce a nonionic, hydrophilic coating, resulting in the shielding of the silanol functionalities. Surface coatings can reduce or possibly eliminate electroosmosis. In the absence of electroosmosis, movement is solely dependent on the electrophoretic mobilities of the components being analyzed [see Equations (2.5.1) and (2.5.2)], thus eliminating an additional source of variation [15].

Besides the use of open capillaries in capillary electrophoresis, capillaries have been filled with gels to increase resolving power. Placing gels inside capillaries serves mainly to create an anticonvective medium for the minimization of band dispersion [15]. Cross-linked polyacrylamide gels have been widely used as sieving networks for capillary electrophoresis, and linear polyacrylamide, dextrans, polyethylene glycol, polyethylene oxide, and methylcellulose have been used also.

Table 2.2 summarizes the advantages and disadvantages of different electrophoresis matrices.

Detection Techniques

There are many techniques for detecting separated sample components, including chemical stains, photographic media, and immunochemical reactions, and many instrumental techniques. Each detection technique also gives different information about the identity, quantity, and physical properties of the molecules in the mixture. Detection is often a key part of the electrophoretic analysis and usually yields basic information about the mixture being studied.

Most sample components analyzed with electrophoretic techniques are invisible to the naked eye. Thus methods have been developed to visualize and quantify separated compounds. These techniques most commonly involve chemically fixing and then staining the compounds in the gel. Other detection techniques can sometimes provide increased selectivity or sensitivity.

TABLE 2.2 Comparison of Electrophoresis Matrices

Matrix	Advantages	Disadvantages
Paper	Contains a low level of bound charge	Porosity not controlled
	Readily available	Low sensitivity
	Easy to handle	Low reproducibility
	Requires no preparation	
Polyacrylamide	Commonly used	Acrylamide is a neurotoxin
	Useful for proteins and nucleic acids	Gels less pliable
Agarose	No additives required	Gels have short shelf life
	Inexpensive	
	Not hazardous	
	Sturdy	
	Used commonly for DNA	
Capillaries	Reusable	Require sensitive detector
	High resolving power	Relatively expensive equipment
	Permit rapid analyses, record data	Longer development cycle
	Consumes a small amount of sample	
	Easily automated	

Chemical Staining The size and type of the compound as well as the electrophoretic matrix dictate and often limit the variety of stains that can be used to help visualize electrophoretic banding patterns. Molecules can be lost during the staining process, so most staining procedures incorporate a "fixing" step, such as a soak in dilute acetic acid for 1 hour, either before or in conjunction with staining. Once fixed, molecules can be stained without loss of the separated components.

Two of the more sensitive and more-frequently used protein stains are Coomassie brilliant blue (R250 and G250) and silver stain. The Coomassie stains are appropriate for both agarose and polyacrylamide gels. The silver stain is approximately 100 times more sensitive than Coomassie, but its use is more complex and often requires more troubleshooting to obtain the desired results. Coomassie stain gives an intensity that is more proportional to the protein concentration than silver stain, although there are other stains, such as amido black, with more linearity but less sensitivity than Coomassie stains.

To quantitate stained sample components, the gel is scanned with a densitometer. These scans can be compared with equivalent scans of quantitative standards to generate a calibration curve.

Fluorescence Fluorescence detection, which provides much better detection limits than simple chemical stains, typically involves the covalent binding of a fluorescent residue to the analyte, but any type of specific interaction can be assayed. If the staining process can be performed prior to the electrophoretic analysis, the electrophoretic process can often be followed visually, and the background signal caused by dye trapping in the electrophoretic matrix will be minimized.

Fluorescamine is a popular reagent for labeling of proteins. At room temperature and alkaline pH, fluorescamine can react with primary amines (found on lysine, arginine, and the N-terminus) on the protein to generate a fluorescent derivative. Fluorescamine may alter the charge-to-mass ratio of the analytes, and it may be used to label samples before electrophoresis or to stain the gel afterward, depending on the importance of maintaining the ratio of charge to mass. The reagent ethidium bromide is commonly used to visualize DNA. The ethidium is incorporated into the structure of DNA. Once incorporated, the fluorescence quantum efficiency of ethidium is dramatically enhanced, and the bands can be easily visualized under a UV lamp.

Radioactivity Another method of visualizing and identifying separation products on a gel is through radioactivity. If a sample is radioactive, the bands that separate during electrophoresis are subsequently radioactive. When the separation is complete, the electrophoretic matrix (e.g., gel or blotting membrane) may be placed against x-ray film until the radiation makes a mirror image of the banding pattern on the film. When this film is developed, the resulting autoradiograph displays the bands.

Immunoelectrophoretic Techniques The technique of gel electrophoresis has been successfully combined with immunological techniques to further evaluate molecules. A frequently used method of immunoelectrophoresis is a technique known as "crossed immunoelectrophoresis." A sample is first run longitudinally through an agarose gel for a predetermined time. Second, a longitudinal strip of the gel area in which the sample was electrophoresed is typically cut out and placed into a similarly sized area of an antibody-containing gel. As an electrical current is applied to the second gel system, each band of the sample in question electrophoreses sideways through the second gel and forms an antigen-antibody precipitin pattern.

Both agarose and polyacrylamide gel systems have been used for direct immunofixation. In these gels, samples are electrophoresed and then immunofixed either by using strips of cellulose acetate soaked in an antibody or by placing the antibody directly over the sample area of the gel. In a related technique, the proteins on the gel are transferred to a membrane and then are probed with an antibody in the method known as Western blotting, described shortly.

On-Column/End-Column Detection Capillary electrophoresis (CE) can be used with minute amounts of sample contained in small volumes of liquid. To monitor the zones formed by the analysis requires detection methods that are extremely sensitive and do not give rise to extracolumn band broadening or dilution. Most detection methods employed with CE are capillary adaptations of detectors commonly employed with analytical liquid chromatography. By monitoring the zones directly in the capillary, distortion of the sample zone is minimized and detection sensitivity is maximized.

Absorbance is the most popular detection method employed with CE. Nearly every commercial CE instrument comes equipped with an absorbance detector. For detection by absorbance, the concentration sensitivity for CE tends to be less than for

HPLC because capillary width, the cell path length in CE, is usually smaller than in a conventional HPLC flow cell [16].

Enhanced detection sensitivity is achieved with on-column fluorescence and electrochemical detectors. With fluorescence detection, the small dimensions of the capillary help confine the sample to a small volume. Focusing the excitation beam into the small volume increases the irradiance of the fluorophore and the fluorescence signal. Electrochemical detectors are usually formed by inserting a microelectrode into the capillary, or by butting the electrode up against the capillary outlet. The small dimensions of the capillary ensure that the maximum distance the analyte must travel to reach the surface of the electrode is small, and therefore the electrochemical conversion efficiency is high.

The coupling of CE to mass spectrometry is developing rapidly because of the wealth of chemical information that can be obtained. Most often this coupling is through an online electrospray ionization interface. The primary difficulty of using mass spectrometry as the primary detector for capillary electrophoresis is the relative incompatibility of the common electrophoresis buffer salts and solvents with the electrospray interface.

The two most common modes of capillary electrophoresis are zone electrophoresis and isoelectric focusing. Capillary zone electrophoresis (CZE) is used similarly to native gel electrophoresis, where the charge properties of the analyte dominate the separation. In some cases, electroosmotic flow is used to transport analytes down the capillary, so both positively charged and negatively charged analytes have a net positive velocity. Electroosmosis can be used in an open capillary where there is no need to balance the flow at the capillary wall with a reverse flow through the center of the capillary. The electroosmotic flow is also used in capillary isoelectric focusing (cIEF). A pH gradient is formed in the carrier liquid in which analytes focus to their isoelectric points, and electroosmotic flow carries the focused analytes through the detector.

Specialized Techniques

Two-Dimensional Electrophoresis Two-dimensional (2D) electrophoresis is unique, offering an analytical method that is both reproducible and sensitive. It is referred to as 2D because it employs two different methods of electrophoresis (typically IEF and SDS-PAGE), in two different directions, to separate the sample components. The combination of the two methods gives better resolution of the compounds than could be achieved with either method alone. For example, each method alone may separate up to 100 components of a sample, whereas together they may separate up to 10,000 components. A 2D analytical technique using IEF and SDS-PAGE to separate total protein results in a gel having bands or spots in an apparently random pattern. Each spot represents a unique component present in the sample. The sample spots are lined up on the gel in order of molecular weight in one direction (typically vertical), and isoelectric point in the other (horizontal). Two-dimensional gel electrophoresis is a powerful technique for analyzing very complex samples, such as tissue

homogenates, but is not usually applied to purified samples. Only one sample can be analyzed at a time on each gel in 2D gel electrophoresis.

Pulsed-Field Gel Electrophoresis Pulsed-field gel electrophoresis was developed to separate large pieces of DNA in agarose gels. DNA had previously been separated by conventional gel electrophoretic techniques. The resolving power of this technique is inversely proportional to the log of the DNA molecular size, as discussed earlier for SDS-PAGE. Thus as the molecular weight of the DNA increases, the spatial resolution decreases. In pulsed-field electrophoresis, the direction of the field is intermittently changed—forward or backward, from side to side, or in some other sequence of directions. This causes DNA chain molecules to reorient in the electric field and entangles the DNA in the polymer matrix. Molecules that are small relative to the space between polymer strands in the matrix exhibit no significant difference in their electrophoretic mobility because they can completely reorient in the alternating field without entangling in the matrix. However, the redirection of the electric field causes molecules larger than the entanglement length to travel in a zigzag pattern, putting kinks in the molecule. The longer the molecule, the more kinks it develops, and the more slowly it travels through the gel. Pulsed field techniques significantly enhance resolution of megabase-sized strands of DNA.

Blotting Techniques Problems encountered when one is using techniques such as direct immunofixation or application of a ligand to analyze resolved components of a sample mixture on a gel can be circumvented by using blotting techniques followed by staining or autoradiography. It is the inability of some compounds, such as antibodies or ligands, to enter a specific gel matrix that necessitated the development of various blotting techniques. The nucleic acid and protein blotting techniques are useful because they combine electrophoretic analyses and sensitive immunological or hybridization detection tools. These techniques involve the transfer of nucleic acids or proteins, immediately after separation by electrophoresis, from the gel matrix to another matrix. Typically, the other matrix is nitrocellulose paper, nylon, or other high-affinity membrane. The mode of transfer is electrotransfer for proteins and capillary transfer for nucleic acids. On nitrocellulose paper or nylon, nucleic acids and proteins are more accessible than in the original gel matrix. This second matrix is then treated with a ligand to identify a specific component of a sample. Table 2.3 summarizes the common electrophoresis blotting techniques. A "Western blot" is shown in Figure 2.2b.

2.5.2 High-Performance Liquid Chromatography (HPLC)

The principles of analytical HPLC, a frequently used method for determination of purity, are identical to those used in large-scale liquid chromatography, so they will not be reviewed here (see Chapter 7). The basic differences between analytical HPLC and large-scale or preparative LC are the size of the stationary phase particles and the sample size. The size of the particles used in HPLC is typically in the range of 1 to 10 μm, much smaller than used in preparative and large-scale conventional LC.

TABLE 2.3 Blotting Techniques Commonly Used with Electrophoresis

Technique	Analyte	Membrane	Probe	Detection
Southern blot	DNA	Nitrocellulose	Radiolabeled or nonradiolabeled complementary RNA or DNA	Autoradiography, fluorescence, chemiluminescence, or colorimetry
Northern blot	RNA	Nitrocellulose	Radiolabeled or nonradiolabeled complementary RNA or DNA	Autoradiography, fluorescence, chemiluminescence, or colorimetry
Western blot	Proteins	Nitrocellulose or nylon	Whole antisera or antibodies	Autoradiography, fluorescence, chemiluminescence, or colorimetry

While large-scale LC employs sample volumes up to and beyond one column volume, HPLC sample injections range from 0.4 to 4.5% of a column volume. Clearly, in analytical HPLC, a small fraction of the capacity of the bed is used. With this limitation on the amount of material loaded onto the column, "baseline" resolution of contaminants is more likely. Other differences include higher linear velocities and higher pressures in general.

HPLC is a powerful method for the quantitation of impurities. It resolves impurities from the product in a chemistry-specific manner by taking advantage of the binding mechanism inherent between the molecule and the stationary packing. Impurities are usually related to the product, sometimes varying by one amino acid residue, by a stereochemical shift, or by a modification to a residue, such as a methylated histidine. Impurities as low as 0.05% of the total product amount can be detected reliably and can be quantitated at 0.1%. As mentioned earlier, the absolute amount of a contaminant can be known only if its response in the detection method (such as UV) is known, and this can usually be known only by isolating enough of the contaminant to characterize it.

An HPLC chromatogram that indicates the power of this technique is shown in Figure 2.4, which illustrates the separation of hemoglobin (Hb) variants by means of a cation exchange packing. Hemoglobins S and A_0 differ by only a single amino acid substitution in two of the four subunits. The only difference between Hb A_0 and Hb A_{1c} is that the N-terminal valine of two of the chains of Hb A_{1c} is bound covalently to glucose. The resolution of Hb A_{1c} and Hb F requires ammonium sulfate in the mobile phase, which indicates that this separation may be based on a mixed ion exchange and hydrophobic interaction mechanism [17]. This example illustrates the point that even though HPLC is a powerful method, more than one HPLC technique may be required to completely resolve the components in a given sample.

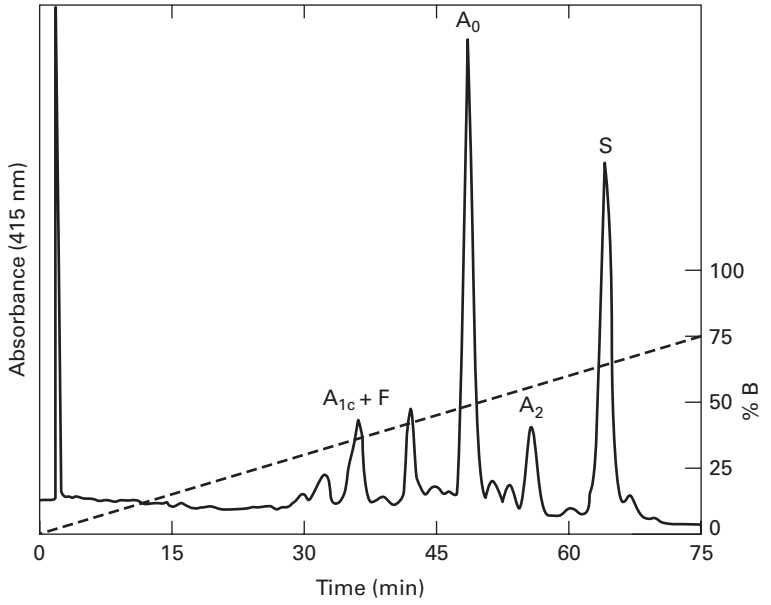

FIGURE 2.4 Separation of hemoglobin variants by ion exchange HPLC. The column was a SynChropak model CM300 (6.5 μm spherical particles with carboxymethyl groups), with 250 × 4.6 mm i.d.; buffer, 0.03 M bis-Tris/0.0015 M KCN (pH 6.4); 100 min linear gradient (shown as a straight line) from 0 to 0.15 M sodium acetate (*B*); flow rate, 1 ml/min. *(Data from F. E. Regnier and K. M. Gooding, "Proteins," in* Chromatography, Part B: Applications, *5th ed., p. B151, E. Heftmann, ed., Elsevier, Amsterdam, 1992.)*

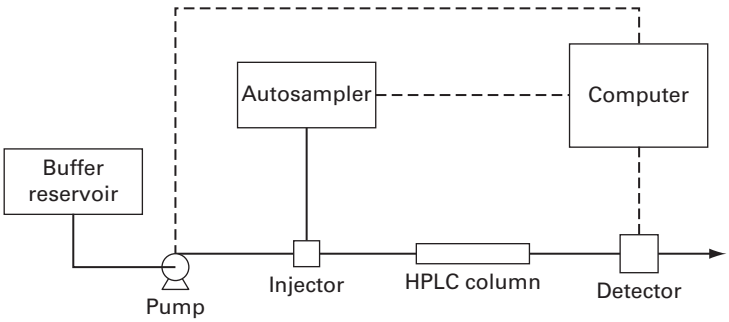

FIGURE 2.5 Schematic diagram of HPLC equipment. Solid lines represent fluid flows, and dashed lines represent paths of signals to or from the computer.

A simple schematic of HPLC equipment is shown in Figure 2.5. A temperature-controlled autosampler holds samples. A robotic arm locates sample vials and extracts a sample of a specified volume with a needle. Then microswitched valves transfer the amount drawn from the vial to the injector. The sample is delivered to the column, along with the solvent or buffer used to develop the chromatography, by a high-pressure pump upstream of the injector. The buffer or solvent is usually degassed by vacuum or sparging with helium. The sample and buffer enter the column, where adsorption/desorption phenomena occur (see Chapter 7).

The separands elute sequentially from the column and pass through one or more detectors. Detectors range from UV to mass spectrometry devices, depending on the type of information required. All the HPLC components are computer controlled. Computers are required for the large amount of data generated by the detectors, especially when a mass spectrometer or a diode array detector is used, since these detectors generate thousands of data points per second. Computers allow archiving of data for subsequent analysis. Analysis options include peak integration by a variety of methods, peak tangent skimming and dropping to baseline being the two most popular. The height equivalent of a theoretical plate (HETP), resolution, skewness, and capacity factor can all be calculated automatically.

2.5.3 Mass Spectrometry

Mass spectrometry is another powerful technique that is now very useful for the analysis of bioproducts and impurities. The result of a mass spectrometry analysis is the molecular weight of the molecule. Two methods for introducing samples to mass spectrometry, electrospray ionization (ESI) and matrix-assisted laser desorption/ionization (MALDI), extend the application of mass spectrometry to the analysis of proteins and biopolymers. These methods have the accuracy, sensitivity, and resolving power to detect posttranslational modifications of proteins and peptides [18, 19].

Because ESI mass spectrometry is highly accurate (±0.01%) and because it can be easily interfaced with liquid chromatography, it is the method of choice for peptides and proteins having a molecular weight below 70,000 Da [20]. Since this accuracy level translates to an error of ±0.5 Da for a 5000 Da peptide and ±5 Da for a 50,000 Da protein, it is clear that this is a highly useful method for determining whether any modifications have been made to a bioproduct. For a recombinant protein of known theoretical amino acid sequence, for example, this method can easily determine whether any amino acids have been cleaved from either terminus and, if so, which amino acids have likely been cleaved.

Of the various ionization techniques for mass spectrometry, electrospray is the most diverse. ESI can produce singly or multiply charged gaseous ions directly from an aqueous or aqueous/organic solvent system, and it can generate ions from almost every type of charged compound whether it is low or high mass, positively or negatively charged. The sample to be analyzed should be as homogeneous and salt free as possible to maximize sensitivity [20].

An important use of mass spectrometry for the analysis of proteins and peptides is the determination of their amino acid sequence [21, 22]. For proteins, it is necessary to first do a digestion with a proteolytic enzyme. Trypsin is a proteolytic enzyme that is commonly used for this digestion; it cleaves amide bonds at the C-terminal side of lysine and arginine, except when those bonds are to proline. The peptide fragments are analyzed by the mass spectrometer; and if the protein sequence is contained in a standard database, it may then be possible to identify the protein by a procedure known as mass fingerprinting, or mass mapping. To carry out a *de novo*

sequencing, it is then necessary to break up the enzymatic peptide fragments, usually by collisions with gas molecules. The masses of the ions produced by collisions are measured by mass spectrometry. Both stages of mass analysis are carried out in a tandem mass spectrometer. This method is capable of sequencing proteins and peptides that have been separated in SDS-PAGE electrophoresis gels, as well as those purified by other methods [21].

2.5.4 Coupling of HPLC with Mass Spectrometry

The ability of the electrospray ionization/mass spectrometry (ESI-MS) technique to analyze compounds from aqueous and aqueous/organic solutions has established ESI-MS as a convenient mass detector for HPLC. It is possible to directly couple reversed-phase HPLC with ESI-MS, since the solvents and volatile buffer salts commonly used in this type of chromatography can be employed over the whole concentration range [19]. Using volatile buffer salts, such as ammonium, acetate, and trifluoroacetate, and not phosphate, chloride, and sulfate, is critical in this application. Common effluent from ion exchange HPLC would usually need to be desalted before analysis by ESI-MS. An example of the use of reversed-phase HPLC coupled to ESI-MS is the analysis of a recombinant antimicrobial peptide that was released along with other peptides after the digestion of a fusion protein with cyanogen bromide, which cleaves at methionine residues [23]. This method identified a variant of the antimicrobial peptide that is consistent with a cyanide group added to a histidine residue (molecular weight 25 Da higher than the theoretical value).

2.5.5 Ultraviolet Absorbance

Measurement of the absorbance of ultraviolet (UV) light is a simple, fast, and widely used technique in biotechnology. Molecules absorb light according to the chemical bonds present in the molecule. Typical wavelengths used for detecting molecules with specific bond content are shown in Table 2.4. The amino acids tyrosine and tryptophan have absorbance maxima near 280 nm, so measuring the absorbance at this wavelength has proved convenient for monitoring proteins. Since the content of tyrosine and tryptophan in proteins varies greatly, the amount of absorbance by proteins at 280 nm has a corresponding significant variation, which is accounted for by a change in the molar absorptivity (defined shortly). For small polypeptides having few or no aromatic amino acids, it is common to monitor the absorbance of the peptide bond, having a maximum near 192 nm. Because of the absorbance by oxygen near this wavelength, measurements for polypeptides must be made away from the peak, and the wavelength 205 nm is typically used [12].

A solution absorbs light according to the Beer–Lambert law:

$$\text{absorbance} = \log_{10}\left(\frac{\text{incident light}}{\text{transmitted light}}\right) = \varepsilon cL \tag{2.5.6}$$

TABLE 2.4 UV Wavelengths Corresponding to Chemical Structures

Chemical structure	Wavelength (nm)
CONH (peptide bond)	192
$CH_3CH{=}CHCHO$	217
C_6H_6 (benzene)	260
$CH_3(CH{=}CH)_2CHO$	270
$C_{10}H_8$ (naphthalene)	280
$CH_3(CH{=}CH)_3CHO$	312
$CH_3(CH{=}CH)_4CHO$	343
$CH_3(CH{=}CH)_5CHO$	370
$C_{14}H_{10}$ (anthracene)	375

where ε is the molar absorptivity for the molecule (also called the molar extinction coefficient), c is its concentration, and L is the distance (path length) through which the light passes. The molar absorptivity is dependent on both the molecule and the wavelength of the light. Frequently, the molar absorptivity is measured at an absorbance maximum for the molecule. This assures the maximum sensitivity for the assay, both for LOD and LOQ (see Section 2.3.4), and for quantitation within the standard curve. Frequently, a UV absorbance result is compared against a standard curve, rather than depending on a precisely measured molar absorptivity, so that the calibration of the spectrophotometer and the upper limit of linearity can be ascertained each time the method is used.

EXAMPLE 2.3

Determination of Molar Absorptivity For the standard curve data for the assay of alcohol oxidase given in Example 2.1, determine the average value of the molar absorptivity.

Solution

From Equation (2.5.6), the molar adsorptivity is given as

$$\varepsilon = \frac{\text{absorbance}}{cL}$$

Using the path length (L) of 10 mm, we can calculate ε using the above equation at each H_2O_2 concentration given for the standard curve determination (Table E2.3).

The average ε for the five concentrations is 0.00366 liter μmol^{-1} mm^{-1}, which is very close to the literature value of 0.00368 liter μmol^{-1} mm^{-1} [14].

TABLE E2.3

H_2O_2 concentration (μmol/liter)	$A_{405\ nm}$	ε (liter μmol^{-1} mm^{-1})
7.1	0.25	0.00352
9.6	0.36	0.00375
12.3	0.44	0.00358
15.1	0.57	0.00377
18.0	0.66	0.00367

2.5.6 CHNO/Amino Acid Analysis (AAA)

Sometimes, the best way to know the content of a purified molecule is to directly measure its constituent atoms or signature molecules. This is the case with CHNO (carbon, hydrogen, nitrogen, oxygen) analysis and amino acid analysis (AAA). These methods are typically applied to a dried preparation of a purified molecule, with AAA being applied exclusively to proteins and peptides.

CHNO are measured from a dry powder by a single method or by a combination. It is very typical to do flame ionization/atomic absorption. In this way, the ratio of each of these elements can be determined and compared with the expected ratio in the molecule (including the expected salt form, and water of hydration). The limiting element can then be used, along with the dry weight, to determine the exact amount of the target molecule. This correlation technique can be applied to other atomic species as well, for instance, iron quantification in an iron-containing protein, such as hemoglobin.

EXAMPLE 2.4

Calculations Based on CHNO Analysis

You have 10 g of a protein powder. The protein has a molecular weight of 5533 and the chemical formula $C_{242}H_{397}N_{68}O_{78}$. You perform CHNO and find the following mass percentages:

C	50.11%
H	7.45%
N	16.40%
O	26.04%

What are the mass fractions of protein and water in the powder?

Solution

The formula represented by the mass fractions is $C_{3.56}H_{6.31}N_1O_{1.39}$. The formula for the protein, normalized to nitrogen content is $C_{3.56}H_{5.84}N_1O_{1.15}$. There is an

excess of 0.24 mol of oxygen, and 0.47 mol of hydrogen, confirming the formula of the excess mass as H_2O. There are x grams of protein with 397(100)/5533 = 7.2 wt% hydrogen, and $(10 - x)$ grams of water with 2(100)/18 = 11.1 wt% hydrogen. There is 0.745 g of hydrogen in the powder, so we can write a mass balance on hydrogen as

$$0.072x + 0.111(10 - x) = 0.745$$

Solving for x gives 9.36 g of protein. Therefore,
Mass fraction of protein = 0.936
Mass fraction of water = 0.064

The problem could also be solved based on doing a mass balance for oxygen instead of hydrogen.

Amino acid analysis is similar. The standard hydrolysis procedure uses 6 N HCl at 110°C for 24 h. These conditions, however, destroy 50 to 100% of cysteine/cystine and tryptophan and convert asparagine and glutamine to aspartic acid and glutamic acid, respectively. An alternative hydrolysis method has been developed that preserves tryptophan, and special pretreatments before the acid hydrolysis allow for the quantitative determination of asparagine and glutamine [24].

2.5.7 Protein Assays

Protein assays are also used to determine content in a powder or solution. Protein assays are less specific than CHNO or amino acid analysis because they are based on assumptions about the composition and structure of proteins, or the specific binding of some residues and their general prevalence in proteins. For instance, the Kjeldahl assay measures total nitrogen. The assumption is made that there are approximately 1.1 mol of nitrogen per amino acid residue.

The Bradford [25] or Coomassie blue assay depends on the binding of the Coomassie dye to protein. The reaction is based on the shift of the absorbance maximum of the dye from 465 nm to 595 nm, which occurs upon binding of dye to protein. The absorbance at 595 nm is usually compared against a standard protein, such as bovine serum albumin (BSA) or ovalbumin. This method has the advantage of being more rapid (requires 10 minutes) than either the Lowry or the bicinchoninic acid assay.

The Lowry [26] method relies on the reaction between cupric ions in alkaline tartrate solution and peptide bonds. The solution of copper in tartrate buffer is called "Biuret reagent." Addition of a phenolic reagent (Folin-Ciocalteu phenol reagent) causes a purple color, which is measured spectrophotometrically at a convenient wavelength between 550 and 750 nm. The absorbance is proportional to protein concentration and is compared to a standard, typically BSA.

The bicinchoninic acid assay [27] works based on the reaction between copper ions and the peptide bond as well. In this case, copper is reduced from Cu(II) to Cu(I). Bicinchoninic acid is a chromophoric scavenger of Cu(I), forming a purple complex that is measurable at 562 nm versus a protein standard.

2.5.8 Enzyme-Linked Immunosorbent Assay

Enzyme-linked immunosorbent assays (ELISAs) are used when specific molecules need to be detected at low concentrations (Figure 2.6) [28]. The simplest type of ELISA is where the antigen is first adsorbed to the surface of the plate, and then unadsorbed antigen is washed off (Figure 2.6a). The plate is incubated with the antibody, which has been conjugated with an enzyme, and then washed to remove excess antibody. A substrate for the enzyme is added, and the color of the enzymatic reaction product is quantified by measuring light absorbance in the visible range. A calibration curve can be constructed by plotting the absorbance measured versus the antigen concentration.

A commonly used ELISA is the sandwich ELISA (Figure 2.6b). In this system the plate is first incubated with the antibody, and unadsorbed antibody is washed off. The antigen is added, and after incubation and washing to remove unbound antigen,

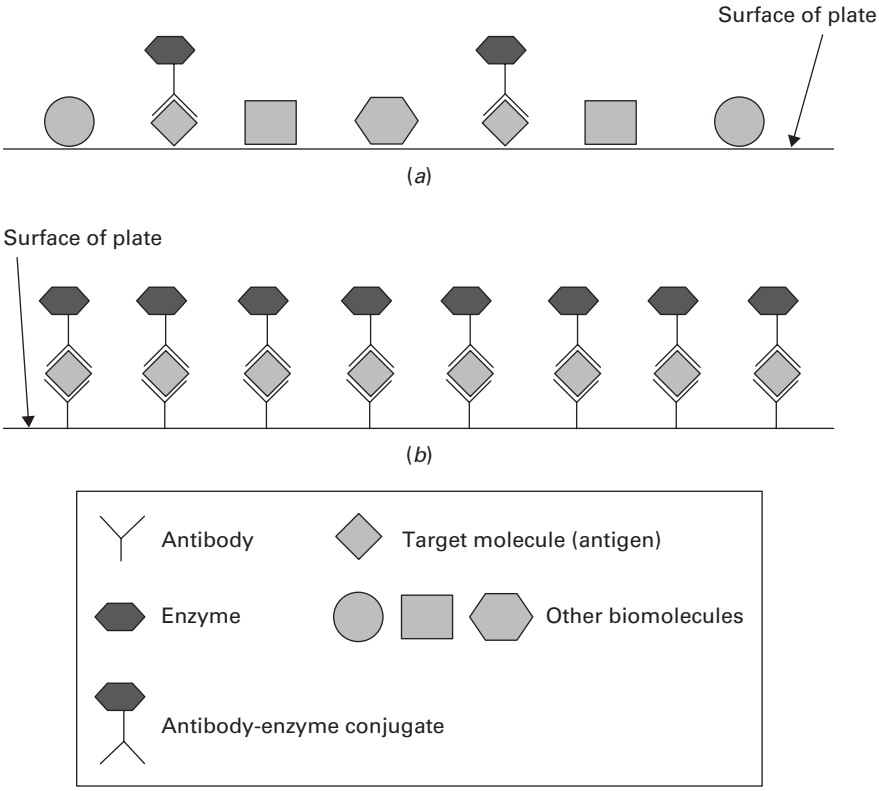

FIGURE 2.6 Schematics of (*a*) the simplest type of ELISA assay, and (*b*) a sandwich ELISA assay.

the antibody-enzyme complex is then added. After further incubation, the plate is washed and treated with the substrate for the enzyme.

A variation in the ELISA, called an indirect ELISA, is to replace the antibody-enzyme complex with the antibody and then bind an anti-species antibody to the first antibody. If, for example, the detecting antibodies were produced in goats, the enzyme-labeled antibodies would have to be anti-goat IgG's. The first antibody and the anti-species antibody are often referred to as the primary and secondary antibody, respectively. This system has the advantage that any number of antibodies can be examined for binding to a given antigen using a single anti-species conjugate.

A problem that can develop for an ELISA is weak attachment of the antibody or antigen to the surface of the plate, which leads to detachment during the incubation and washing steps [29]. This problem can be overcome by either (1) binding the antibody or antigen to the plate covalently, or (2) using a plate coated with the protein streptavidin and using an antibody or antigen labeled with biotin in order for a streptavidin-biotin complex to form. The binding of streptavidin to biotin is very strong, with a dissociation constant of approximately 10^{-15} M [30]. The addition of biotin to a protein is a gentle reaction that typically does not cause the biological activity to be reduced. Plates with streptavidin bound are available commercially.

Another problem that can occur is binding of the conjugated antibody to sites on the plate other than to the antigen, termed nonspecific binding. To reduce the amount of nonspecific binding, "blocking agents" such as other proteins are often included in the solution with the conjugated antibody.

An important application of the ELISA in bioseparations process development is for the quantitation of the level of host-cell proteins, which requires that large numbers of proteins be detected at part-per-million sensitivity [6]. In this case, the antibody attached to the surface must be polyclonal, that is, raised in an animal after injection of the target antigens, not made in cell culture by a hybridoma.* The immunogens are usually derived from a fermentation of the host cell with a transfected plasmid that is identical to the production plasmid except that it lacks the target gene. This cell is cultured as usual, with induction and feeding steps as prescribed, and purification is performed using the same process as before. This enriches the host-cell proteins that are likely to be produced and then copurified along with the product. Wider cuts are usually made in the chromatography steps, to give a wider range of protein contaminants for the immunization step. The proteins collected are injected into a rabbit or goat, serum is collected after several days, and the immunoglobulins are separated from other blood components. The antibodies are further purified to eliminate any reactivity with the product protein by passing the antibody preparation over a column where the product protein has been bound to the resin.

* Polyclonal means that there is a mixture of antibodies that have been raised against several antigens or against only one antigen. A monoclonal antibody is a single molecule specific for a certain region, called an epitope, of a single antigen. An antigen typically has more than one epitope.

This is important, as the actual samples tested will have large amounts of product protein. The technique does not distinguish between individual contaminants, although the antibodies can be used in Western blots (Section 2.5.1) to determine the exact protein contaminants for which the assay is specific. This is sometimes done in a 2D gel format so that all the host-cell contaminating proteins are well resolved from each other.

2.5.9 Gas Chromatography

Gas chromatography is used to separate and quantify volatile organic compounds. The principles are identical to those in liquid chromatography, with an inert carrier transporting solutes as they adsorb into and desorb from a stationary adsorbent phase. In the case of gas chromatography, the column is generally a coated capillary ranging in length from 30 to 100 m. The carrier is usually helium or another inert gas. The detectors used are usually flame ionization detection (FID) or thermal conductivity detection (TCD). Mass spectroscopy is a common add-on detector, especially when the contaminating species are unknown before the analysis is undertaken. Various injectors are available for the processing of solid, liquid, and gas samples. Liquid samples are injected directly and allowed to evaporate in the oven before being carried downstream into the capillary column. Gas samples can be introduced through a gastight syringe, a pressurized vessel, or through a headspace sampler. Solid samples can be processed with a headspace sampler (where a volatile substance is expected to evolve from the solid sample), or with a thermal desorption unit, when higher temperatures are required, or decomposition of the sample is sought.

Many standard methods are available for gas chromatography, for most common solvents, pesticides, carcinogens, preservatives, monomers, and surfactants. Gas chromatography is commonly used to detect residual solvents in pharmaceuticals and biologicals. There are amino acid derivatization methods that allow chiral separations by gas chromatography. The technique may also be used to assess degree of polymerization and polymer purity when a formulation requires an excipient for stability or bioavailability.

2.5.10 DNA Hybridization

DNA hybridization is used to detect small amounts of DNA in a purified product. Of primary concern is DNA from the host recombinant organism. DNA probes that are sequence specific for the host cell, and primarily for the plasmid that carries the product gene, are synthesized with a radioactive or nonradioactive label. The DNA in the sample is adsorbed to a nitrocellulose filter. The sample is then hybridized in the presence of the probes through a series of annealing steps. The amount of DNA in the sample can then be measured by detecting the label on the probe (autoradiography, fluorescence, chemiluminescence, or colorimetry). Detection limits are commonly in the picogram range.

DNA hybridization techniques can also be performed on samples that have been amplified through the polymerase chain reaction (PCR). This technique, which is used more commonly to amplify a gene that is responsible for an interesting activity in a cell homogenate, is applied in this analytical setting only when required detection limits are lower than stated earlier. A DNA fragment serves as a probe, and DNA polymerase with guanine (G), cytosine (C), adenine (A), and thymine (T) serves to make extra copies of the DNA of interest. This technique can be used to amplify the number of copies of DNA by hundreds- to millions-fold.

There are many other techniques for quantifying the amount of DNA in a sample. DNA hybridization techniques require some knowledge of a DNA sequence that might be contained in the sample. Another technique uses a single-stranded DNA-binding protein (SSB) purified from *E. coli* for capture of DNA, and an antibody to single-stranded DNA to quantify DNA, much like an ELISA assay [31]. In this case, the reporting enzyme conjugated to the antibody is urease, and the quantitation is done by following pH change. Using this technique, it is not necessary to have the SSB-DNA-antibody complex on a surface where an absorbance can be read. Instead, the complex is captured on a membrane, and the change in pH is measured.

2.5.11 ICP/MS (AES)

Inductively coupled plasma (ICP) coupled with mass spectrometry (MS) or atomic emission spectroscopy (AES) is used primarily to measure metallic elements in a sample. Inductively coupled plasma is a high-energy method for burning a sample and volatilizing the ash in a highly dispersed fashion. The resulting "gas" can be analyzed by mass spectrometry or atomic emission spectroscopy to determine its identity and concentration (in reference to standards). Heavy metal content is important for pharmaceuticals, especially those that will be administered chronically or for long periods of time. Metals can contaminate a product from contact with various metal surfaces (especially low-grade steels), but also from contact with resins and filter materials. Metals are also found in excipients and buffering agents, and they may be concentrated over time by various large-scale separation methodologies.

2.5.12 Dry Weight

Dry weight is the least specific of the assays used in biotechnology. However, it has some purposes, especially with crude materials. Before any initial purification, whether it be from a fermentor or a synthetic peptide reactor, a dry weight is often the most informative assay to monitor the behavior of the reaction step and to predict the performance of the first purification step. Dry weight is a simple assay conceptually, but in fact it requires relatively large sample amounts and careful control of sample containers and drying conditions for accuracy and precision.

2.6 MICROBIOLOGY ASSAYS

Microbiology assays are conducted to determine the safety of the product for human consumption. The history of pharmaceuticals shows that the two most dangerous things in a product are likely to be either the product itself (consider thalidomide, Phen-Fen, chemotherapeutics) or bacterial contamination (consider *Salmonella* sp., *E. coli*, HIV in transfusion blood). Therefore, basic microbiological, and more recently, viral screens have been required for pharmaceutical and food products.

2.6.1 Sterility

Sterility tests are performed on a select sampling of a batch of sterile product. They consist simply of injecting an amount of the product into a sterile growth-supporting broth, either casein soy digest or thioglycolate medium (usually both). If, after 14 days, the broth is cloudy, the product is not sterile and must be destroyed. Along with this test, the broths are tested with control bacteria to ensure that they support growth (i.e., are growth promoting), and samples of the product are tested to make sure they do not inhibit the growth of bacteria themselves (called "bacteriostasis/fungistasis testing"). These three tests, taken together, can be used to demonstrate that certain units from the batch are sterile. Unfortunately, those units have been destroyed in the testing. There are no tests that demonstrate, with complete assurance, that the entire batch is sterile and safe for human use.

Therefore surrogate tests are performed on the process of manufacturing the pharmaceutical. Sterile broth is used in a process simulation, instead of the product, to demonstrate that as the entire batch is processed, contamination is not observed in any unit (again by incubating and observing lack of cloudiness). Bacterial spikes in the form of spore strips are used to challenge sterilization steps, such as autoclaving and irradiating, to demonstrate many orders of magnitude of colony reduction through these processes. These tests form a package of data that give a high level of sterility assurance for the whole batch without having to test every unit in every batch.

2.6.2 Bioburden

Bioburden testing is the process of determining how much bacterial contamination is present in a sample. Prior to a sterilizing step, the probability of finding bacteria or mold in an in-process product sample is relatively high, especially in a process that uses bacteria or mold for production of the bioproduct. To determine the bioburden, a sample is filtered on a 0.2 μm porosity filter. The filter is then incubated on an agar plate for 24 to 48 hours, and the colonies are counted. The result is a number of "colony-forming units" that were present in the sample prior to filtration. The bioburden value is often used to set the logarithm reduction required from the sterilization step.

2.6.3 Endotoxin

Endotoxin is a lipopolysaccharide that forms some of the cell wall of Gram-negative bacteria. It is pathogenic in humans, causing illness and death in sufficiently high doses. A product that shows no bioburden and is sterile can still contain endotoxin from prior contamination. Endotoxin tests are designed to detect this possibility.

Early endotoxin tests employed rabbits. Rabbits were injected with product, and their temperatures monitored for several days. Rabbits that maintained a normal temperature indicated an endotoxin-free preparation. This test was costly and time-consuming, however, and a new test was developed that used the blood from horseshoe crabs. Called the LAL test, for *Limulus* amoebocyte lysate, this blood forms a clot when exposed to endotoxin. Horseshoe crab blood goes much further than a colony of rabbits, and the test takes only 30 minutes. More recently, an artificial substrate has been developed that is cleaved in the presence of endotoxin and produces a color. This chromogenic assay is the most convenient, and it gives a direct measure of the concentration of endotoxin. Since endotoxin is not a single chemical with a defined molecular weight, it is measured in units, which are described by any one of the three tests just described.

2.6.4 Virus, Mycoplasma, and Phage

A more recent concern in pharmaceutical preparations is viruses, once limited primarily to the blood fractionation industry. However a wider variety of opportunities for viral contamination, not the least of which is cell culture, has become available for production of bioactive products in the last several decades. Viruses that infect cell cultures may also be a source of human infection, an occurrence that is relatively rare between species. It is also presumed that a culture infected with a virus may actually be infected with many viruses, and the absence of a human pathogen is nearly impossible to prove when an unexpected viral contamination has occurred. Furthermore, less is known about the prevention and cure of viral infections, making them more dreaded than bacterial infections.

Viruses are hard to detect. In general, viruses must be found through incubation with human cells that are susceptible to viruses. If the virus is lytic—that is, if it lyses its host to release daughter virus particles—the presence of viral contamination is easily detected. A confluent cell layer is treated with the sample and checked after a day for "plaques," which are areas devoid of cells that indicate the presence of virus. Specific viruses can be identified by several immunological tests and nucleic acid probes [32]. Immunological tests commonly used are ELISAs (Figure 2.6) that detect virus particles and fluorescent antibody methods that use antibodies made against viral antigens. When nucleic acid probes are used, it is sometimes necessary to amplify the target viral DNA by means of the polymerase chain reaction.

To ensure a virus-free product requires much the same assurance as sterility. Steps in the purification process are challenged to determine their "viral clearance."

In general, three qualified viral clearance steps are incorporated into any process that has as the product source human blood, bodily fluid, or mammalian cells.

Mycoplasma are a species of bacteria that lack a cell wall and are typically smaller than bacteria, generally around 0.1 μm in diameter. Some mycoplasma are pathogenic to humans. A mycoplasma infection is generally difficult to detect, as mycoplasma generally do not alter the metabolism of cell cultures, so telltale signs like increased oxygen demand or rapid production of acid that accompany other bacterial infections are not present in mycoplasma infections. There are tests for mycoplasma that typically involve incubation of samples with "indicator" cells. These tests are specified by regulatory agencies around the world and are only recently being harmonized. There is also some effort to use PCR and other DNA based techniques to detect mycoplasma in samples. These techniques appear to be limited by the amount of sample that it is possible to process, and therefore the limit of detection is fairly high.

Phages, a virus of bacteria, pose little threat to humans but can destroy a recombinant production area. When phages have infected manufacturing, they must be detected and eliminated. Phages are detected in the same manner as viruses (i.e., by using bacterial host cells), with lytic phages being more readily detected than nonlytic ones.

2.7 BENCH SCALE PREPARATIVE SEPARATIONS

2.7.1 Preparative Electrophoresis

Electrophoresis as an analytical method was described in Section 2.5.1 of this chapter. In addition there are occasions when electrophoresis at the bench scale is useful in the preparative separation of sufficient quantities of biomolecules (or bioparticles, including cells) for further study. Electrokinetic separations in free solution (no carrier substance such as gel or particulate media as described in the earlier subsection, Support Media) are constrained by the onset of natural convection resulting from the Joule heating of solutions by the electric current caused by the movement of ions in the electric field (see Example 2.2 and the subsection Generation of Heat in Electrophoresis Instrumentation). To date, preparative electrophoresis has not been utilized in the purification of significant commercial products. As a result, very few successful commercial separators exist, and in some cases, users are required to develop their own apparatus. Two electrokinetic approaches in free solution are available: electrophoresis (a strictly rate-based separation) and isoelectric focusing (equilibrium-based) [33]. The stabilization of current-carrying solutions against natural convection is accomplished in one of three ways: rotation on an axis perpendicular to the gravity vector, upward or downward flow parallel to the gravity vector, or electrophoresis in a vertical density gradient. The formation of density gradients is described in detail in Chapter 5 Sedimentation, Section 5.3.1. The four highest capacity unit operations will be presented in this section: (1) free-flow electrophoresis

(FFE), (2) density-gradient electrophoresis (DGE), (3) recycling free-flow isoelectric focusing (RIEF) and (4) rotating isoelectric focusing (Rotofor^{TM}). The steps of operation consist of carrier fluid loading, sample loading, electric field application, resolution of separands, and collection of separands. In each case, a separation is concluded with the collection of fractions, either in flow or as a final step after separation. Therefore, the best fractional separation possible is governed by the number of fractions collected. Figure 2.7 gives schematics of each of these four unit operations.

Free-Flow Electrophoresis

In free-flow electrophoresis, a sample to be separated is continuously injected into a thin rectangular channel through which a carrier fluid flows, with an electric field that is perpendicular to the flow (Figure 2.7a). This results in differential deflection of charged solutes and particles, leading to separation by differences in electrophoretic mobility. Application of the electric field is initiated before sample loading and is achieved via two electrode compartments separated from the flow chamber by semipermeable membranes at the two vertical edges of the thin chamber. Each electrode

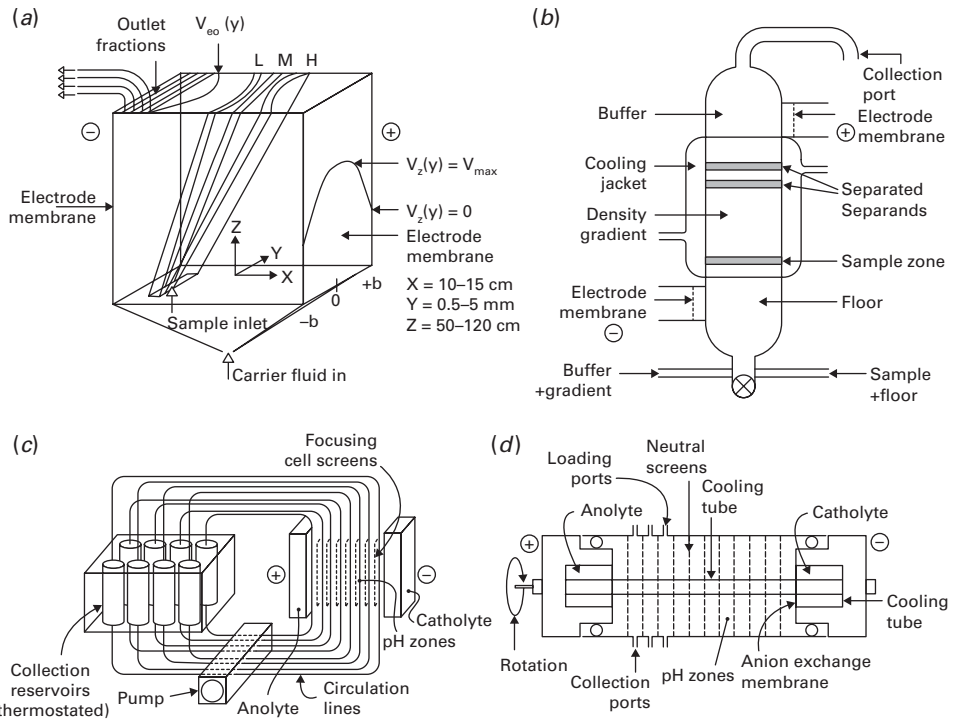

FIGURE 2.7 .Schematic drawings of four methods of preparative electrokinetic separation. *(a)* Free-flow electrophoresis (FFE), *(b)* density-gradient electrophoresis (DGE), *(c)* recycling free-flow isoelectric focusing (RIEF) and *(d)* rotating isoelectric focusing (Rotofor^{TM}). In *(a)*, separand concentration trajectories are denoted for low- (L), medium- (M), and high- (H) mobility separands.

compartment contains a single metal wire electrode and an electrolyte solution consisting of a nontoxic buffer and dissolved KCl or NaCl at an ionic strength higher than that of the carrier buffer. To maximize field strength (hence separand migration velocity) and minimize current density (hence heating and natural convection), the carrier buffer must have the lowest ionic strength possible that is compatible with separand solubility and stability (separands could be living cells). An upward flowing buffer stream becomes warmer as it rises and is more stable against natural convection than is a downward flowing stream. Heating of the stream follows Equation (2.5.4). Cooling of the stream resembles that shown in Figure E2.2 for gel slabs; a thermostated water jacket is in contact with the front and back planes, which are usually made of glass or polycarbonate.

In the example shown in Figure 2.7a, the flow is from bottom to top, but downward and horizontal configurations exist. Carrier fluid exits in thin outgoing channels at the opposite end of the chamber. The vertical flow is laminar, resulting in a parabolic velocity distribution in the *y*-*z* plane using the axes specified by the diagram. Thus

$$\upsilon_z(y) = \upsilon_{max}\left(1 - \frac{y^2}{b^2}\right) \tag{2.7.1}$$

where y is the distance from the center of the chamber in the y direction, and b is the chamber half-thickness. This velocity profile means that separands near the front and back chamber walls move vertically the most slowly, spend more time in the electric field, and are therefore carried farther horizontally in the field than their identical counterparts flowing faster at the center of the chamber. The time required for a volume element to reach the outlet is

$$t(y) = \frac{L}{\upsilon_z(y)} \tag{2.7.2}$$

where L is the distance from the inlet to the outlet.

The electric field also causes laminar electroosmotic flow at the chamber walls [Equation (2.5.2)] in the x direction (toward the negative electrode) with the result [34]

$$\upsilon_x(y) = \frac{1}{2}U_o E\left(\frac{3y^2}{b^2} - 1\right) \tag{2.7.3}$$

where U_o = electroosmotic mobility of the chamber walls due to their zeta (surface) potential (see Section 2.5.1)

E = applied electric field strength (voltage per length) given by $E = I/k_e A$

k_e = solution electrical conductivity in Siemens/meter

Fluid velocity at the front and back walls is thus $U_o E$, in the opposite direction from that of typical separands. This means separand molecules near the wall

will migrate more slowly toward their complementary electrode than will those at the center of the chamber. This relationship between laminar flow (y-z profile) and electroosmotic flow (y-x profile) leads to an exact balancing of the two migrations for certain separands and gives a flat profile of the separand concentration across the thin chamber, as shown by the letter "M" on the diagram in Figure 2.7a. "L" and "H" correspond to lower- and higher-mobility separands, respectively. Separands are resolved on the basis of distance migrated, X, in the x direction according to a variant of Equation (2.5.2), namely

$$X = \left[U_{el} t(y) + \frac{1}{2} U_o \left(\frac{3y^2}{b^2} - 1 \right) t(y) \right] E \tag{2.7.4}$$

Thus, owing to the two laminar flow profiles, the velocity in the x direction of a separand depends on its y position between the front and back walls.

In free-flow electrophoresis, the sample solution is injected into one of the inflowing channels or directly into a sample port in the chamber. There are limits on the concentration of sample based on solution density. A sample that is too dense will not rise with upward flow, and a sample that is too light will rise to the top of the chamber before significant separation can occur, and vice versa for downward flow. Ideally the carrier buffer and sample solution should have the same density and very similar conductivities. Collection of separands occurs at the top (or receiving end) of the chamber, which is perforated by 12 to 198 collection ports ("outlet fractions" in the diagram), each of which is connected by fine tubing to a collection vessel. The process is continuous, so carrier buffer is flowing out of outlets continuously during a separation. Separands exit according to their mobility. Separation may be quantified by identifying and measuring the concentration of each separand using one of the methods described in this chapter and plotting concentration versus outlet number. The result is a series of non-Gaussian peaks like those in Figure 2.4. Yield may be low in this separation method, since separand distributed in the tails of the parabolic profiles might not be collected.

Free-flow electrophoresis has been used for both analytical and preparative applications, and gram amounts per hour of pure substances have been produced [35]. Separations at the laboratory scale have been performed for proteins, subcellular particles, viruses, and bacteria [36].

Density Gradient Electrophoresis

Density-gradient electrophoresis (DGE) takes advantage of differences in the electrophoretic mobility and buoyancy of particles. In this type of electrophoresis, separands move through a density gradient in a static liquid (Figure 2.7b). Separation of particulate separands is slowed due to increased upward buoyant force.

The forces acting on a particle in density-gradient electrophoresis are the electric field, the gravitational field, and the buoyant force. Balancing these forces leads to a

particle velocity for particles migrating upward toward the anode (positively charged electrode) as [37]

$$\upsilon = U_{el}E - \frac{2}{9}\frac{a^2 g\left(\rho - \rho_o\right)}{\mu} \quad (2.7.5)$$

for a column of cross-sectional area A, where the second term is the sedimentation velocity for spheres of density ρ and radius a in a fluid of density ρ_o and viscosity μ under the influence of gravity. This velocity will not be constant as a function of the distance migrated in the z direction (upward) because ρ_o changes with z. When the viscosity does not remain constant, the term involving electrophoretic mobility in Equation (2.7.5) for velocity will change according to the factor $\mu_r/\mu(z)$, where μ_r is the viscosity at which the mobility U_{el} of the separand is known (often for pure water) and $\mu(z)$ is the viscosity at distance z in the density gradient [37]. Further correction may be required if there is a conductivity gradient. If the sample contains a high content of high molecular weight solutes, droplets may sediment out of the bottom of the separand band [38].

Carrier buffer is loaded (typically) from the bottom of a cylindrical column by a density-gradient maker (Figure 5.1) with low density followed by high density. The sample is loaded in a solution having higher density than the bottom of the density gradient, and it is followed by a very dense fluid that forms a "floor" under the fluids above it in the column. The electric field is applied after loading the sample. The DGE column has two side-arm electrode vessels (not shown in Figure 2.7b), each separated from the column by a semipermeable membrane and containing a metal electrode and a high-conductivity electrolyte solution. The lower electrode must support or balance the fluid in the DGE column. A DC power supply provides current. The result of applying an electric field to a column of suitable geometry (>1 cm diameter) results in negligible electroosmotic flow relative to the electrophoretic velocity of the separands. However, Joule heating of the fluid is inevitable and is counteracted by thermostating the column with a water jacket; additional thermostating can be achieved using a central cooling tube so that upward migration occurs in a thin (<1 cm) annulus. The density gradient counteracts the thermal convection due to Joule heating. The separands should be allowed to migrate upward a few (4–8) cm to assure adequate separation.

For collection of separands, the contents of the column are either drained slowly out the bottom or pumped out the top of the column, and fractions are collected into individual containers exactly as in preparative chromatography. Small fraction sizes result in potentially high resolution as there are no flowing influences on the precision of separand position upon separation. The smallest fraction size is one drop, or approximately 0.05 ml. The resolution of DGE is based on the number and size of fractions collected. Purity can be very high depending on fraction volume, and capacity/throughput is on the order of milligrams per hour. This low-cost method has been used to separate proteins and subcellular organelles [39].

Recycling Isoelectric Focusing

The isoelectric focusing principle was described in Section 2.5.1. In recycling isoelectric focusing (RIEF, Figure 2.7c), electrophoretic separation takes place as separands in a solution containing ampholytes flow through compartments in a focusing cell across which an electric field is applied [40]. Some number of compartments (12 to 40; 8 are shown in the illustration) are separated by screens (such as 100 μm nylon mesh) through which separands migrate freely. Separands and ampholytes pass repeatedly from compartment to compartment and back to a reservoir associated with each compartment by electrophoresis until they become neutral at their isoelectric pH in one of the compartments. At this point electrophoretic migration ceases, a steady state has been reached, and then each of the reservoirs is drained for sample collection. The number of fractions equals the number of reservoirs.

A separation begins with the loading of carrier fluid, in which a solution of ampholytes (explained in Section 2.5, subsection Isoelectric Focusing) that will form a pH gradient over the desired pH range is used to fill the entire system. It is necessary to adjust flows to be the same in and out of all of the reservoirs; flow balancing is very important. A small volume of the sample containing separands is added before or after the initiation of flow and application of the electric field. It can be added to one or more reservoirs, but it is prudent to add the sample into the reservoir that is most likely to receive the focused separand of interest.

The electric field is applied across the compartmented cell only, and the initial current is typically several mA. However, as each ampholyte and each separand is arrested in its isoelectric compartment, there are fewer and fewer ions carrying current. At this point, the current drops into the μA range, and the voltage may rise to several hundred volts. For this reason, the power supply is usually operated in constant power (versus constant current) mode. While the electric current and pumps are on, fluid is circulated out of the reservoirs through the compartments of the electrophoresis cell and back to the reservoirs. During the few seconds that a given volume element passes through its compartment, ampholytes and separands pass into or out of this volume element according to the sign of their charges and their electrophoretic mobilities. Eventually the fluid in each compartment is at a different pH resulting in a pH gradient across the separation cell. Each separand migrates to the compartment in the cell that is at its isoelectric pH, where $U_{el} = 0$, and therefore is found in the corresponding reservoir having that pH. At the end of the focusing period, the fluid contained in each reservoir is drained into a separate container, its pH is measured, and the contents are assayed for separands. A broad range of pH's, for example pH 2 to 10, will result in low resolution and purity; each reservoir could contain several separands. A narrow range of pH's, for example pH 4.2 to 4.8, will result in high resolution and purity, but the pH range must be selected to include the isoelectric pH of the separand of interest. RIEF is a relatively high-capacity method, and reservoir volumes of several hundred ml can be used, although the volume of the separation cell may be just a few ml. RIEF systems are able to process about 1 gram of protein per hour and require sample volumes of more than 150 ml [41].

Rotating Isoelectric Focusing (Rotofor™)

The mixing effects of natural convection due to temperature and concentration gradients can be counteracted by rotation of the separation vessel at a carefully chosen velocity, resulting in a constantly changing gravity vector, hence rotating isoelectric focusing [42]. The Rotofor™ cell, or cylindrical focusing chamber (Figure 2.7d), has an internal ceramic cooling tube and can handle sample volumes as large as 60 ml and up to 1 gram of protein. The rotation rate of the chamber is typically 1 rpm. Monofilament polyester membranes divide this chamber into some 20 or so compartments with cathode and anode at opposite ends. The catholyte is typically 0.1 M NaOH, and anolyte is typically 0.1 M H_3PO_4. These are loaded into their respective electrode compartments at the ends of the focusing chamber. The focusing chamber is filled with ampholyte solution with the sample mixed in using several of the loading ports. After filling without bubbles, the filling ports are sealed, and rotation is begun. The ampholytes and sample molecules will focus simultaneously. Cooling water is flowed through the central cooling tube, rotation is initiated, then power is switched on in constant-power mode (about 15 W) using a power supply capable of up to 3000 V. The voltage rises to a constant value within 2 hours, during which ampholytes and separands migrate to their respective compartments. After focusing, the solution in each compartment is rapidly drained through the collection ports without mixing. A harvesting apparatus may be supplied for this purpose. Rotofor™ has been produced by Bio-Rad Laboratories (Hercules, CA).

Other Free-Fluid Electrophoresis Methods

In addition to the four free-fluid electrokinetic separations presented in this section, others exist. The names given them by their developers reflect their features. For example, recycling free-flow focusing is a shear-stabilized combination of RIEF and FFE and collects up to 48 isoelectric fractions from a combination of a thin rapid-flow electrophoresis chamber and multiple heat exchanger reservoirs; compared to the RIEF system, this system does not use screens to separate compartments and allows faster recirculation and higher power that lead to faster focusing [43]. A horizontally flowing density gradient is used in stable-flow free boundary separation, a gravitationally stabilized continuous separation process based on either electrophoresis or isoelectric focusing. In this method, some 12 or so layers are pumped horizontally through a rectangular chamber, each layer denser than the one above it. A vertical electric field is applied, and separands migrate in and out of flow streams upward or downward according to their mobility—similar to FFE but with horizontal flow and vertical deflection [44]. Vortex stabilization has been introduced into preparative free-flow electrophoresis in an annular separator that can also be applied to isoelectric focusing [45].

2.7.2 Magnetic Bioseparations

Magnetic capture is a powerful, highly selective method for collecting separands present in low abundance in a highly mixed suspension or solution [46]. Once a

separand has reacted with magnetic beads by extensive mixing resulting in affinity adsorption, the beads are captured and held by a magnetic force so that all other components can be rinsed away, much as in a centrifugation wash step, but much more rapid, efficient, gentle, and selective. Since the introduction of magnetite-containing polymer microspheres in the 1970's, many applications of them have emerged for a wide variety of bench scale bioseparations. The general principle is not unlike that of affinity chromatography, in which ligand molecules are affixed, usually by covalent reactions, to polymer microspheres (or nanoparticles) that contain iron oxide (from 3 to 80% by mass). Examples of ligand molecules include nucleic acids, glycoconjugates, avidin and, most often, antibodies. Magnetic reagents have been manufactured for several purposes, and their sizes now range from some 20 nm up to 10 μm in diameter. While most are spherical, some may be irregular in shape, especially if the iron oxide content is high.

Physical Principles of Magnetic Separations

It is desirable that as much of the iron oxide as possible be in the form of magnetite, Fe_3O_4, a ferrite with an inverse-spinel crystal structure, which provides unpaired electrons whose orbits can be oriented in a magnetic field resulting in magnetization. This condition is referred to as *paramagnetism*, in which the material is magnetic if, and only if, it is in a magnetic field. This is important because materials that retain their magnetism after the magnetic field is removed are likely to aggregate and become difficult to handle. Paramagnetic materials do not exhibit remanent magnetization like ferromagnetic materials such as iron, cobalt, and permanent-magnet ceramics, which exhibit the familiar hysteresis curve of magnetization.

When a magnetizing field H (measured in amperes per meter, A m^{-1}) returns to zero, ferromagnets are still magnetic, but paramagnetic materials are not. The magnetization M is proportional to H so that

$$M = \chi H \tag{2.7.6}$$

where the constant of proportionality is the volume magnetic susceptibility χ. Magnetic flux density B is usually expressed in SI units of Tesla (T, 1T = 1 $NA^{-1}m^{-1}$) and is related to the applied field by the magnetic permeability, which in free space is $\mu_o = 4\pi \times 10^{-7}$ T m A^{-1}, a universal constant that can be expressed in the more convenient units of Newtons per squared ampere (N A^{-2}):

$$B = \mu_0 H \tag{2.7.7}$$

Tiny particles (ca. 20 nm) of paramagnetic material are single-domain magnets and are said to be superparamagnetic owing to their high magnetic susceptibility χ. Larger particles in the range of 50–300 nm, composed of clusters of single-domain magnetic particles, have been shown to have superparamagnetic properties [47].

In the presence of a large magnet having magnetizing field H (A m^{-1}), a small particle of volume V and susceptibility $\Delta\chi$ above that of the surrounding fluid will experience magnetization $M = \Delta\chi H$ (A m^{-1}) and a force F_m (in Newtons) that is proportional to the gradient of the flux density produced by the external magnet ∇B (T m^{-1}) at the instantaneous location of the particle, given by [48]

$$F_m = V\Delta\chi H \bullet \nabla B \tag{2.7.8}$$

but since $B = \mu_o H$, the force can be expressed in terms of the strength of the permanent magnet as

$$F_m = V\Delta\chi \frac{B}{\mu_o} \bullet \nabla B \tag{2.7.9}$$

The features of this relationship are used to understand the equipment required to perform magnetic separations using magnetic reagents. The inducing field H plays the role of magnetizing the paramagnetic reagent by orienting unpaired electron spins so that the reagent will be attracted toward the magnetizing source by the gradient ∇B. In one dimension, this gradient can be expressed as dB/dx using x as the distance from the pole face of the external magnet (permanent or electromagnet). Both B and dB/dx decrease rapidly with increasing x, so magnetic particles to be captured must always somehow be brought to the very near vicinity of the closest magnetic pole face (see Figure 2.8a).

Magnetic Reagents and Applications

The volume of available commercial magnetic particles is a deliberate variable that may vary by more than 10^6-fold (4.0 μm versus 40 nm diameter, for example). The quality of magnetic material incorporated into the bead determines $\Delta\chi$, which is the *relative* susceptibility of the average bead material, that is, its susceptibility minus that of the surrounding fluid. Parenthetically, a solution containing a high concentration of paramagnetic solutes (ions) could diminish or even reverse this value. Considering the manner in which beads are manufactured, there are four features of magnetic reagents to consider besides bead diameter: the magnetically susceptible material, the structural bead material (nonsusceptible), the conjugation site on the bead material, and the biospecific ligand (see Figure 2.8b). Table 2.5 is a list of each of these choices, and the listed components can be combined in all possible permutations.

It will be seen in Section 3.4 of this book (Flocculation) that a colloidal suspension must consist of charged particles to remain a stable colloid and not flocculate or precipitate. If magnetic reagent particles do not carry sufficient surface charge, they must be stabilized in suspension by the addition of a surfactant. Thus it is necessary to determine from the vendor of each product whether the product is electrokinetically stabilized or detergent stabilized. In the former case, the nonsusceptible material will be carboxylated or sulfonated on its outer surface.

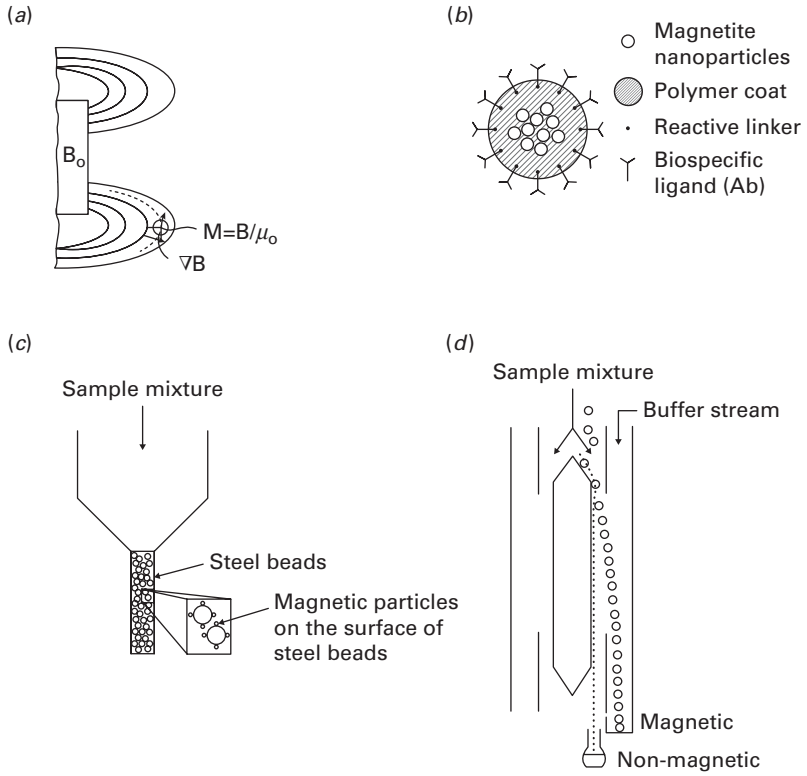

FIGURE 2.8 Magnetic separations. *(a)* The role of magnetic flux density B and gradient ∇B in applying ponderomotive (motion-causing) force to a magnetically susceptible particle (represented as a circle with an arrow passing through it). The arrow through the particle represents the polarization of the magnetization M. *(b)* The general configuration of a magnetic reagent nanoparticle or microparticle showing susceptible core, nonsusceptible material coat, linker reactive molecule, and external ligand for reacting with separands with high specificity. *(c)* Operation of a column-based (equilibrium) separator showing packed column of steel beads or susceptible metal wool to which magnetic reagents adsorb and from which they are desorbed for batch collection by removing the magnetic field. *(d)* Operation of a flow-based (rate) cylindrical separator having a core and inlet and outlet splitters showing removal of magnetic reagents from an inner to an outer parallel annular flow for continuous collection of separands.

TABLE 2.5 Examples of susceptible materials, nonsusceptible materials, reactive linkers, and biospecific ligands used in magnetic reagents

Susceptible materials	**Non-susceptible materials**	**Reactive linkers**	**Biospecific ligands**
Magnetite (Fe_3O_4)	Polystryene	Carboxyl	Biotin (or streptavidin)
Maghemite (γ-Fe_2O_3)	Silica	Amino	Antibodies
	Alginate	Epoxy	Glycoconjugates
	Agarose	Tosyl	Complementary nucleic acids

Applications include bench scale protein and nucleic-acid purification, protein and nucleic acid diagnostics (bead-based assays), and magnetic cell sorting. Bench scale purification is typically achieved using biospecific affinity ligands in much the same way as affinity chromatography, which is described in Sections 7.7.6 and 7.7.7. As in chromatography, magnetic purification can also be used as a concentration step. A typical procedure consists of coupling the biospecific ligand to the surface of magnetic beads that may be activated by tosylate, bisepoxirane, or cyanogen bromide. Unreacted antibody (or another ligand) is washed away by magnetically aggregating the paramagnetic particles. Magnetic separation has unique advantages in cell purification; it may be used to remove, select, or enrich specific subsets in cell mixtures for application to regenerative medicine and rare-cell analysis. In the case of selected cells to be retained, chemical and enzymatic methods are available for the removal of magnetic reagents from cells after separation.

Magnetic Separators

Magnetic separation devices fall into three broad categories: tube and magnet equilibrium separators, high-gradient batch column separators, and flowing continuous separators. Tube and magnet equilibrium separators are the most widely used, but they take on many forms. Table 2.6 is a partial list of separator types that are commercially available.

Different methods of magnetic field gradient formation are utilized by the different magnets used in the different devices. (1) The simpler tube-and-magnet types (i.e., Robosep, Dynal) expose the suspension of magnetic reagent (beads, ferrofluid) to one pole of a dipole magnet, which forms flux lines as shown in Figure 2.8a. (2) When steel spheres or wires are placed in a column served by dipole magnets, flux lines enter the spheres essentially perpendicular to the sphere surface creating intensely converging field lines and therefore a high flux gradient leading to the term high-gradient magnetic separation (HGMS) as in Figure 2.8c [49]. (3) Three forms of Halbach magnet assemblies have been used and are available for larger-volume separations. A Halbach array is a special arrangement of multiple permanent magnets that augments the magnetic field on one side of the array while cancelling the field to near zero on the other side—the principle of the common "refrigerator magnet," in which magnetization of small rectangular or triangular magnets is up-right-down-left-up repetitively, giving repeated flux lines like those in Figure 2.8a on the lower side and a near-zero field on the upper side, as in an Opticell and a large-scale Dynal (Life Technologies) application. A Halbach quadrupole assembly forms a central bore within which the channel of the quadrupole magnetic separator (Figure 2.8d) is held. A Halbach cylinder with multiple converging fields is used in Sepmag, for example, and, when the sample is stirred, particles will be drawn to the walls of a vessel more than 10 cm in diameter.

Magnetic Separation Procedures and Protocols

There are many ready-made magnetic reagents precoated with biospecific ligands that are commercially available. If desired reagents are unavailable, they can be synthesized by the user. Vendors of magnetic beads provide chemically activated

TABLE 2.6 Representative list of magnetic separators. Example vendors are shown in parentheses.

Separator Type	Description
Test tube and bar magnet	Any test tube and magnet in any laboratory
Robosep	Automated addition and decanting of reagents and removal of magnetic field (Stem Cell Technologies)
Dynal	Permanent magnet encompasses single tube which is manually manipulated (Life Technologies)
Multiwell plate	Single flat "refrigerator" magnet holds separands in wells of 96-well plate (Alpaqua)
V-bottom multiwell plate	Each well hangs into the field of an O-ring magnet forming a ring of beads so wash fluids can be removed from the center (Perkin Elmer)
Opticell	Flat "refrigerator" magnet holds separands in a thin (4 mm) transparent chamber normally used in specialized cell culture (Nunc)
High-gradient batch separation column	Sample is fed to a column packed with steel beads or steel or nickel wool, adsorbed and eluted (Miltenyi Biotec)
Multistage separator	Multistaged collector sorts separands according to susceptibility (Techshot)
Flowing dipole separator	Sample continuously flows in a flat sheet between angled opposing magnetic poles like continuous-flow electrophoresis (Figure 2.7a)
Flowing quadrupole separator	Sample continuously flows through the bore of a quadrupole magnetic assembly (IKOTECH)
Sepmag	Large-volume sample stirred within a large-diameter bore of a cylindrical magnet array (Sepmag)

surfaces and instructions for the conjugation of user-supplied biospecific ligands. It is easy to remove unreacted biospecific ligand and (if used) linker compounds by holding the beads in place with a magnet while the reactant solution is decanted and the beads are rinsed with a final buffer before resuspending. To purify a separand, beads are added to the mixed sample solution and held—often at 4°C to preserve specificity—with gentle agitation while separand molecules or cells collide with the bead surfaces and react. Adequate agitation is required for this reaction, since magnetic beads can be considered non-Brownian and all reagents must be transported to them by diffusion and mixing (see Section 8.3 of this book for mixing issues).

2.8 SUMMARY

Analytical methods are vital to the specification of a product through assays of biological activity, purity, and sterility. The efficient development of bioseparation processes depends on the availability of suitable analytical methods.

- Specifications required by regulatory agencies include biological activity, purity, composition, physical characteristics, and safety features.

- Assay attributes consist of precision, the reproducibility of a numerical value of a measurement; accuracy, the closeness of a numerical measurement to its real or universal value; specificity, the extent to which an assay represents the amount of target product and not something else; linearity, the dependence of the assay measurement on the first power of the quantity being measured; limits of detection, the minimum amount of an analyte that can be measured; range, the limits over which the attributes have acceptable values; and robustness, the insensitivity of the attributes to varying conditions, especially those that may be difficult to control.
- Laboratory methods for assaying biological activity include animal model assays, cell-line-derived bioassays, and *in vitro* biochemical assays.
- There are two general classes of techniques for measuring enzyme activity, stopped methods and continuous methods. Product formation in these assays is typically followed spectrophotometrically.
- Purity assays should be sensitive to impurities present in small quantities. The most powerful assays for purity are electrophoretic analysis, high-performance liquid chromatography (HPLC), and mass spectrometry (MS). MS with electrospray ionization (ESI) has high accuracy (±0.01%) for determining molecular weight, which enables the detection of posttranslational modifications of proteins and peptides.
- The velocity of a charged particle undergoing electrophoresis is

$$\upsilon = UE$$

  where υ is the particle velocity, E is the field strength (voltage per length), and U is the apparent electrophoretic mobility. There are two contributions to this apparent electrophoretic mobility,

$$U = U_{el} + U_o$$

  where U_{el} is the electrophoretic mobility of the charged particle and U_o and is the contribution from electroosmotic flow.
- The most commonly used electrophoretic techniques for bioproducts are denaturing gel electrophoresis (better known as SDS-PAGE), native gel electrophoresis, capillary electrophoresis, and isoelectric focusing. Blotting methods add to the analytical specificity of electrophoretic methods.
- Microbiology assays are used to determine sterility. Sterility tests must be performed by adding sample to a nutrient medium with positive controls consisting of the same nutrient medium spiked with bacteria and negative controls showing that the medium does not inhibit growth.
- Endotoxin testing requires a biological assay, typically the *Limulus* amoebocyte lysate (LAL) assay. Viruses are usually assayed in human cells *in vitro*.

- Bench scale purification methods include electrophoresis and magnetic bioseparations. Each method is dependent on the application of an external physical force that acts differentially on different separands.
- Free electrophoresis methods include free-flow electrophoresis, density-gradient electrophoresis, recycling isoelectric focusing and rotationally stabilized isoelectric focusing.
- Most magnetic separations exploit the fact that paramagnetic materials are only magnetized in the presence of the magnetic field, in which the magnetic force is proportional to the product of the magnetic field and its gradient. Magnetic separation methods require a paramagnetic reagent, and they include tube-and-magnet, high-gradient magnetic capture, and flowing separations.

NOMENCLATURE

a	radius (cm)
A	absorbance (dimensionless)
b	half thickness of a free-flow electrophoresis channel (cm)
B	magnetic flux density (Tesla) (T) (also in N A^{-1} m^{-1})
∇B	gradient of magnetic flux density (T m^{-1})
c	concentration of analyte (M, or g $liter^{-1}$)
C_p	heat capacity (J g^{-1} K^{-1})
E	applied field strength (V cm^{-1})
F_m	force exerted by a magnetic field and gradient on a particle (N)
h	convective heat transfer coefficient (kcal m^{-2} h^{-1} $°C^{-1}$)
H	height of gel (cm)
H	strength of applied magnetic field (A m^{-1})
∇H	magnetic field gradient, the driving force for magnetized particles (A m^{-2})
I	current (A)
k	thermal conductivity (kcal m^{-1} h^{-1} K^{-1})
k_e	solution electrical conductivity (Siemens/meter) (S m^{-1})
L	path length in an optical cell (cm)
L	distance between inlet and outlet in free flow electrophoresis system (cm)
M	magnetization of a material due to an applied magnetic field (A m^{-1})
M_e	mass of electrophoretic medium (g)
n	total number of measurements in a sample
P	power (J s^{-1})
q	heat flux (kcal m^{-2} h^{-1})
r^2	coefficient of determination
R	electrical resistance (ohms)

S rate of heat generated per volume by electric current in an electrophoresis gel (kcal h^{-1} cm^{-3})
SSE sum of squared deviations about the least squares line (units vary)
SST sum of squared deviations about the sample mean $\overline{x}$ (units vary)
t time (s)
T temperature (K)
U apparent electrophoretic mobility (cm^2 s^{-1} V^{-1})
U_{el} electrophoretic mobility of a charged particle (cm^2 s^{-1} V^{-1})
U_o contribution to electrophoretic mobility from electroosmotic flow (cm^2 s^{-1} V^{-1})
v velocity (cm s^{-1})
V voltage (V)
W width of gel (cm)
X distance (cm)
x_i individual measurement, where $i = 1, 2, \ldots, n$ (units vary)
$\overline{x}$ mean of measurements of x (units vary)
y_i individual measurement, where $i = 1, 2, \ldots, n$ (units vary)
$\overline{y}$ mean of measurements (units vary)
$\hat{y}$ model value of measured value i (units vary) $\overline{y}$

Greek Letters

ε molar absorptivity (liter $\mu$$mol^{-1}$ mm^{-1})
μ viscosity of fluid (g cm^{-1} s^{-1})
μ_o $4\pi \times 10^{-7}$ T m A^{-1}, the magnetic permeability of free space (also in N A^{-2})
ρ density (g cm^{-3})
σ standard deviation (units vary)
χ magnetic susceptibility (dimensionless)

PROBLEMS

2.1 Generation of a Specification and Validation Plan Specifications have been developed for a recombinant protein made from *E. coli* (see Table P2.1). The product has three disulfide bridges, is formed in inclusion bodies, and is purified through three chromatography steps, one of which is affinity chromatography. For each specification, check the assay attributes that apply from the indicated attributes.

TABLE P2.1 Recombinant Protein from *E. coli* with Three Disulfide Bonds, from Inclusion Body, with Affinity Purification

Specification	Precision	Accuracy	Specificity	Linearity	Range	Robustness
Purity by reversed phase, >98.0%, should detect misfolded protein, oxidized product, aggregates, some misincorporations and deletions						
Purity by size exclusion chromatography, >99.0%, for aggregates						
Purity by ion exchange chromatography, >98.0%, orthogonal purity method, should detect deamidations and other degadation products, fragments						
Identity by tryptic map						
Leached antibody from affinity step by ELISA, <10 ppm (depends on toxicity profile)						
E. coli proteins by ELISA, <100 ppm						
Host DNA, <100 ppb by autoradiograph from hybridized strands						
Bioassay, activity between 75 and 125% of standard reference material						
Product content, typically by HPLC, to be within 2.5% of the specified formula						
Endotoxin <1 endotoxin unit/mg (depends on dose, validation specified by the USP)						
Bioburden <100 colony-forming units/g (validation specified by the USP)						
pH, within 0.2 unit of formula (calibrated assay)						
Appearance, a transparent to opalescent solution essentially free of particulate						

2.2 Bioassays Discuss the relative importance of the bioassay during the different phases of research and development of a new bioactive molecule, including discovery research, laboratory process development, and large-scale process development.

2.3 Enzymatic Activity Assay for L-Alanine Dehydrogenase L-Alanine dehydrogenase can be assayed by using the following reaction:

$$L-\text{Alanine} + \text{NAD}^+ + \text{H}_2\text{O} \underset{}{\overset{L\text{-alanine dehydrogenase}}{\rightleftharpoons}} \text{pyruvate} + \text{NADH} + \text{NH}_4^+$$

For this assay, a sample containing this enzyme was diluted 1:1000 and added to a solution containing L-alanine, NAD, and carbonate buffer at pH 10.0 and 25°C. Absorbance readings versus time were taken using a path length of 10 mm and wavelength of 340 nm, as shown in Table P2.3.

TABLE P2.3

Time (min)	A_{340}
2.0	0.27
2.5	0.33
3.0	0.40
3.5	0.47
4.0	0.53
4.5	0.60
5.0	0.67

From these data and the molar absorptivity for NADH ($\varepsilon = 6.2 \times 10^2$ liter mol^{-1} mm^{-1} at 25°C and 340 nm), calculate the enzyme concentration in units per milliliter. (*Note:* NADH absorbs at 340 nm, but NAD^+ does not.) If the purified enzyme has a specific activity of 30 U/mg and the enzyme solution that was assayed has a protein concentration of 1.1 mg/ml, what is the purity of the enzyme in the sample and what is its specific activity? (Data from H. U. Bergmeyer and M. Grassl, "Handling of reagents," in *Methods of Enzymatic Analysis,* vol. II, H. U. Bergmeyer, ed., p. 102, Verlag Chemie, Weinheim, 1983.)

2.4 Troubleshooting Purity Methods A recombinant protein produced in a production scale process typically has a level of host-cell protein (HCP) by ELISA of 30 ppm. The most recent batch showed a shift in HCP to 80 ppm. What steps can you take to confirm this result?

2.5 Operating Problems During the Electrophoresis of Proteins For the following problems that can occur in the analysis of proteins by gel electrophoresis, what do you think is the cause of the problem, and how do you think the problem can be solved?

(a) "Smile effect"—band pattern curves upward at both sides of the gel
(b) Lateral band spreading
(c) Skewed or distorted bands
(d) Vertical streaking of protein bands

2.6 Protein Charge During Gel Electrophoresis A solution of 0.1% sodium dodecyl sulfate (SDS) binds so strongly to polypeptide chains that one detergent molecule is sufficient to saturate two amino acid residues (R. Scopes, *Protein Purification,* 3rd ed.,

p. 297, Springer-Verlag, New York, 1994). For a protein with a molecular weight of 60,000 in 0.1% SDS, estimate the effect on the electrical charge per protein molecule.

2.7 Problem in the Determination of Molecular Weight by Gel Electrophoresis A purified recombinant protein is analyzed for molecular weight by SDS-PAGE at pH 8.5. From the protein sequence deduced from the gene that was expressed in bacteria, the protein is expected to have a molecular weight of 44,000. However, the molecular weight of the protein is found by SDS-PAGE to be 52,000. Explain the reason or reasons for this difference in molecular weight. What calculation could you make to help explain this discrepancy?

2.8 Temperature in a Vertical Electrophoresis Gel You are designing a mini–vertical gel electrophoresis system to separate proteins. The gel is 7 cm high, 8 cm wide, and 0.075 cm thick, and runs at 200 V and 60 mA. The glass support plates on either side of the gel are each 0.200 cm thick. To finalize the design, you need to decide whether the system should be placed in an air bath or a water bath. Estimate the maximum temperature in the gel for both cases using thermal conductivities and heat transfer coefficients found in the literature. Which bath do you recommend be used?

2.9 Density Gradient Electrophoresis In a density-gradient electrophoresis separation, two separands of similar mobilities are to be separated from one another. Separand A has $U_{el} = 1.4 \times 10^{-4}$ $cm^2V^{-1}s^{-1}$ and separand B has $U_{el} = 1.6 \times 10^{-4}$ $cm^2V^{-1}s^{-1}$. Assuming that the velocity of each separand is constant over the distance migrated, how long must a field of 10 Vcm^{-1} be applied to separate their migration distances by 1.0 cm, and how far will each separand have migrated?

2.10 Magnetic Force Units Demonstrate, using the units given in Section 2.7.2, that the unit of force calculated using Equation (2.7.9) is in Newtons.

2.11 Comparison of Magnetic Force on Spherical Particles Given the following plot of *B* versus distance from a magnet pole face (Figure P2.11), calculate the forces experienced by a 20 nm spherical particle and a 4.5 μm diameter spherical particle at a distance of 1 mm and at 1.0 cm (four calculations). The volumetric susceptibility of the material of both spheres is 0.01. The volumetric susceptibility of the surrounding aqueous medium is -1 x 10^{-5}.

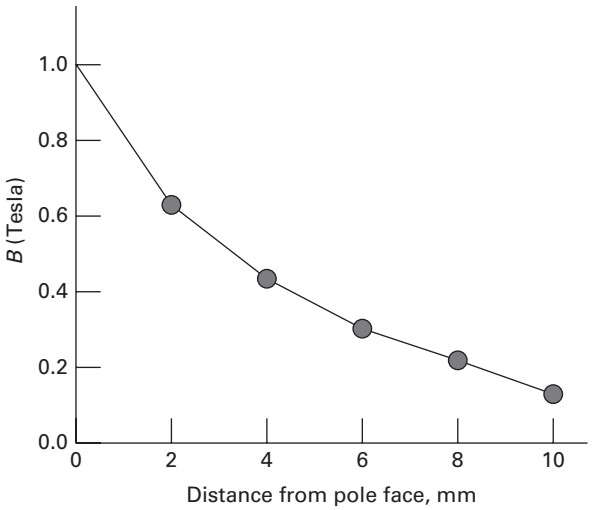

FIGURE P2.11 *B* versus distance from the pole face of a magnet.

REFERENCES

1. Christian, G. D. (2004). *Analytical Chemistry*, 6th ed., Wiley, Hoboken, NJ.
2. DeVore, J. L. (2000). *Probability and Statistics for Engineering and the Sciences*, 5th ed., Duxbury, Pacific Grove, CA.
3. Kellner, R., Mermet, J.-M., Otto, M., Valcarcel, M., and Widmer, H. M., eds. (2004). *Analytical Chemistry: A Modern Approach to Analytical Science*, 2nd ed., Wiley-VCH, Weinheim.
4. Garnick, R. L., Solli, N. J., and Papa, P. A. (1988). The role of quality control in biotechnology: An analytical perspective. *Anal. Chem*., vol. 60, p. 2546.
5. Wilhelmi, A. E. (1973). Bioassay. In *Peptide Hormones, Part II*, S. A. Berson and R. Yalow, eds., Elsevier, New York, p. 296.
6. Anicetti, V., and Hancock, W. S. (1994). Analytical considerations in the development of protein purification processes. In *Protein Purification Process Engineering*, R. G. Harrison, ed., Dekker, New York, p. 11.
7. Marshall, R. N., Underwood, L. E., Voina, S. J., Fouschee, D. B., and Van Wyk, J. J. (1974). Characterization of the insulin and somatomedin-C receptors in human placental cell membranes. *J. Clin Endocrinol. Metab*., vol. 39, p. 283.
8. Karey, K. P., Riss, T. L., Burleigh, B. D., Parker, D., and Sirbasku, D. A. (1988). Human recombinant insulin–like growth factor I. II. Binding characterization and radioreceptor assay development using BALB/c 3T3 mouse embryo fibroblasts. *In Vitro Cell. Develop. Biol*., vol. 24, p. 1107.
9. Jones, R. N., Barry, A. L., Gavan, T. L., and Washington, J. A. (1985). Susceptibility tests: Microdilution and macrodilution broth procedures. In *Manual of Clinical Microbiology*, 4th ed., E. H. Lennette, ed., American Society for Microbiology, Washington, DC, p. 972.
10. Platt, T. B. (1986). Microbiological assay of antibiotics in body fluids and tissues. In *Modern Analysis of Antibiotics*, A. Aszalos, ed., Dekker, New York, p. 341.
11. Bergmeyer, H. U. (1974). Determination of enzyme activities. In *Methods of Enzymatic Analysis*, Vol. 1, H. U. Bergmeyer, ed., Verlag Chemie, Weinheim, p. 121.
12. Scopes, R. K. (1994). *Protein Purification*, 3rd ed., Springer-Verlag, New York.
13. Carlson, R., Garnick, R. L., Jones, A. J. S., and Meunier, A. M. (1988). The determination of recombinant human tissue–type plasminogen activator activity by turbidimetry using a microcentrifugal analyzer. *Anal. Biochem*., vol. 168, p. 428.
14. Bergmeyer, H. U., and Grassl, M. (1983). Handling of reagents. In *Methods of Enzymatic Analysis*, vol. II, H. U. Bergmeyer, ed., Verlag Chemie, Weinheim, p. 102.
15. Rabel, S. R., and Stobaugh, J. F. (1997). Capillary electrophoresis. In *Chromatographic Analysis of Pharmaceuticals*, 2nd ed., J. A. Adamovics, ed., Dekker, New York, p. 209.
16. Li, S. F. Y. (1992). *Capillary Electrophoresis*, Elsevier, Amsterdam.
17. Regnier, F. E., and Gooding, K. M. (1992). Proteins. In *Chromatography, Part B: Applications*, 5th ed., E. Heftmann, ed., Elsevier, Amsterdam, p. B151.
18. Bahr, U., Karas, M., and Hillenkamp, F. (1994). Analysis of biopolymers by matrix-assisted laser desorption/ionizatin (MALDI) mass spectrometry. In *Microcharacterization of Proteins*, R. Kellner, F. Lottspeich, and H. E. Meyer, eds., VCH, Weinheim, p. 149.
19. Metzger, J. W., and Eckerskorn, C. (1994). Electrospray mass spectrometry. In *Microcharacterization of Proteins*, R. Kellner, F. Lottspeich, and H. E. Meyer, eds., VCH, Weinheim, p. 167.
20. Siuzdak, G. (1996). *Mass Spectrometry for Biotechnology*, Academic Press, San Diego, CA.
21. Kinter, M., and Sherman, N. E. (2000). *Protein Sequencing and Identification using Tandem Mass Spectrometry*, Wiley-Interscience, New York.
22. Standing, K. G. (2008). Mass spectrometry of proteins and peptides. In *Molecular Biomethods Handbook*, 2nd ed., J. M. Walker and R. Rapley, eds., Humana Press, Totawa, NJ, p. 411.

23. Haught, C., Davis, G. D., Subramanian, R., Jackson, K. W., and Harrison, R. G. (1998). Recombinant production and purification of novel antisense antimicrobial peptide in *Escherichia coli*. *Biotechnol. Bioeng*., vol. 57, p. 55.
24. Kellner, R., Meyer, H. E., and Lottspeich, F. (1994). Amino acid analysis. In *Microcharacterization of Proteins*, R. Kellner, F. Lottspeich, and H. E. Meyer, eds., VCH, Weinheim, p. 93.
25. Bradford, M. M. (1976). A rapid and sensitive method for the quantitation of microgram quantities of protein utilizing the principle of protein-dye binding. *Anal. Biochem*., vol. 72, p. 248.
26. Lowry, O. H., Rosebrough, N. J., Farr, A. L., and Randall, R. J. (1951). Protein measurement with the Folin phenol reagent. *J. Biol. Chem*., vol. 193, p. 265.
27. Smith, P. K., Krohn, R. I., Hermanson, G. T., Mallia, A. K., Gartner, F. H., Provenzano, M. D., Fujimoto, E. K., Goeke, N. M., Olson, B. J., and Klenk, D. C. (1985). Measurement of protein using bicinchoninic acid. *Anal. Biochem*., vol. 150, p. 76.
28. Crowther, J. R. (2009). *Methods in Molecular Biology. The ELISA Guidebook*, vol. 516, Humana Press, New York.
29. Wild, D., and Kusnezow, W. (2005). Separations systems. In *The Immunoassay Handbook*, 3rd ed., D. Wild, ed., Elsevier, Amsterdam, p. 177.
30. Kricka, L. J., and Wild, D. (2005). Signal generation and detection systems (excluding homogeneous assays). In *The Immunoassay Handbook*, 3rd ed., D. Wild, ed., Elsevier, Amsterdam, p. 192.
31. Kung, V. T., Panfili, P. R., Sheldon, E. L., King, R. S., Nagainis, P. A., Gomez, B., Ross, D. A., Briggs, J., and Zuk, R. F. (1990). Picogram quantitation of total DNA using DNA-binding proteins in a silicon sensor-based system. *Anal. Biochem*., vol. 187, p. 220.
32. Brock, T. D., Madigan, M. T., Martinko, J. M., and Parker, J. (1994). *Biology of Microorganisms*, 7th ed., Prentice Hall, Englewood Cliffs, NJ.
33. Todd, P. (1991). A comparison of methods of cell electrophoresis. In: *Cell Separation Science and Technology*. ACS Symposium Series. S. Kompala and P. Todd, eds., American Chemical Society, Washington, p. 216.
34. Ivory, C. F. (1980). Continuous flow electrophoresis. The crescent phenomena revisited. I. Isothermal effects. *J. Chromatography*, vol. 195, p. 165.
35. Krivankova, L., and Bocek, P. (1998). Continuous free-flow electrophoresis. *Electrophoresis*, vol. 19, p. 1064.
36. Wagner, H. (1989) Free-flow electrophoresis. *Nature*, Vol. 341, p. 669.
37. Boltz, R. C., Todd, P. (1979). Density gradient electrophoresis of cells in a vertical column. In: *Electrokinetic Separation Methods*, P. G. Righetti, C. J. van Oss, and J. Vanderhoff, eds., Elsevier/North-Holland Biomedical Press, Amsterdam, p. 229.
38. Mason, D. W. (1976). A diffusion driven instability in systems that separate particles by velocity sedimentation. *Biophys. J*., vol.16, p. 407.
39. Tulp, A., Verwoerd, D., Benham, A., and Neefjes (1997). High resolution density gradient electrophoresis of proteins and subcellular organalles. *Electrophoresis*, vol. 18, p. 2509.
40. Bier, M., Egen, N. B., Allgyer, T. T., Twitty, G. E., and Mosher, R. A. (1979). New developments in isoelectric focusing. In: *Peptides*, E. Gross and J. Meienhofer, eds., Pierce Chemical Co., Rockford, IL, p.79.
41. Thormann, W. (1998). Large-scale electrophoretic processes. In *Protein Purification: Principles, High-Resolution Methods, and Applications*, 2nd ed., J.C. Janson and L. Ryden, eds., Wiley-VCH, Weinheim, p. 651.
42. Egen, N. B., Thormann, W., Twitty, and G. E., Bier, M. (1984). A new preparative isoelectric focusing apparatus. In: *Electrophoresis '83*. H. Hirai, ed., Walter deGruyter, Berlin, p. 547.
43. Bier, M., Twitty, G. E., and Sloan, J. E. (1989). Recycling isoelectric focusing and isotachophoresis, *J. Chromatog.*, vol. 470, p. 369.
44. Mel, H. C. (1964). Stable-flow free boundary migration and fractionation of cell mixtures: I. Apparatus and hydrodynamic principles, *J. Theoret. Biol.*, vol. 6, p. 159.

45. Tracy, N., and Ivory, C. F. (2004). Preparative focusing of proteins using binary buffers in a vortex-stabilized, free-flow apparatus. *Electrophoresis*, vol. 25, p. 1748.
46. Zborowski, M., and Chalmers, J. J., eds. (2008) *Magnetic Cell Separation*, Elsevier B. V., Amsterdam.
47. Xuan, S., Wang, Y.X., Yu, J.C., and Leung, K.C. (2009). Tuning the grain size and particle size of superparamagentic Fe_3O_4 microparticles, *Chem. Mater*., vol. 21, p. 5079.
48. Moeser, G.D., Roach, K.A., Green, W.H., and Hatton, T.A. (2004). High-gradient magnetic separation of coated magnetic nanoparticles. *AIChE J*., vol. 50, p. 2835.
49. Miltenyi, S., Muller, W., Weichel, W., and Radbruch, A. (1990). High gradient magnetic cell separation with MACS. *Cytometry*, vol. 11, p. 231.

/// 3 /// CELL LYSIS AND FLOCCULATION

If a product is synthesized intracellularly and not secreted by the producing cell, or if the product is to be extracted from plant, animal, or fungal tissue, it is necessary to remove the product from the cell or tissue by force. The choice of procedure is highly dependent on the nature of the product and the nature of the cell or tissue. It was seen in Chapter 1 that bioproducts represent a wide variety of chemical species. In this chapter, we also see that the sources of bioproducts—cells and tissues—are widely varied. For this reason, there exists a wide variety of methods for breaking, or *lysing,* cells and tissues, broadly classified as "chemical" and "physical" methods.

Once cells have been suspended and/or broken open, the resulting suspension of solids must be separated from the liquid in which it is suspended. This separation process, filtration and/or sedimentation (the subjects of the next two chapters), is enhanced by having larger particles. Larger particles can be achieved by *flocculation,* a process whereby particles are aggregated into clusters, or *flocs*.

In recent years, it has become desirable to isolate specific cell types from mixtures of suspended cells and to deliver the resulting cell subpopulation(s) to a process for which they, and only they, are required. Most examples come from *in vivo* sources such as blood and dispersed tissue cells. This aspect of cell processing, namely, cell purification, places special demands on separation processes that are capable of handling particulate matter under conditions that allow cells to remain alive.

This chapter presents two major elements of cell processing: the science and engineering of cell rupture by physical and chemical methods and the flocculation of cells and subcellular particles in aqueous suspension. First, however, it is helpful to develop a broad appreciation for the variety and compositions of cells that are likely to be encountered in downstream bioprocessing.

3.1 INSTRUCTIONAL OBJECTIVES

After completing this chapter, the reader should be able to do the following:

- Recognize two classes of cells and the structures of cells that cause cell lysis to be necessary for the recovery of bioproducts.

- Choose between chemical and mechanical cell lysis methods and, within these categories, choose appropriate chemical or mechanical methods for general classes of applications.
- Describe the role of electrokinetic phenomena in the flocculation of cells and insoluble particles.
- Identify mechanisms of flocculation.
- Apply, in general terms, the Schulze–Hardy rule to flocculation problems.

3.2 SOME ELEMENTS OF CELL STRUCTURE

Initial guidance for the selection of a cell disruption method depends completely on the cell type. Once cell structure is understood, the procedure required to open the cell and otherwise process it follows a fairly logical route.

3.2.1 Prokaryotic Cells

Prokaryotic cells (cells that do not contain a membrane-enclosed nucleus) are classified as either Eubacteria (commonly called bacteria) or Archaea. Each of these groups has its own industrial potential. For example, Archaea are now looked upon as a source of industrial enzymes that are stable over a wide range of temperatures, pH values, and ionic strengths. Eubacteria, especially *Escherichia coli,* are the workhorses of genetic engineering and prokaryotic biotechnology. The envelope of the "generic" bacterial cell is extremely resistant to fracture.

Typically the bacterial cell envelope consists of an inner plasma membrane that separates all contents of the cell from the outside world, a peptidoglycan (peptides linked to oligosaccharides or polysaccharides) cell wall, and an outer membrane. Bacterial cells with a very thick cell wall stain with crystal violet (Gram stain) and are called "Gram positive," while those with thin cell walls stain very weakly—"Gram negative" (see Figure 3.1). The space between the plasma membrane and the peptidoglycan in Gram-negative bacteria is called the "periplasm"; proteins can be secreted across the plasma membrane into the periplasm in these bacteria. In addition, some Eubacteria have an outer capsule composed of mucopolysaccharide (see Figure 1.21). *Pneumococci* are spherical bacteria, some species of which cause diseases; their capsular polysaccharide ("PCP") is used as a vaccine against pathogenic species, and *Pseudomonas* species are known for their ability to form biofilms on this basis.

Most biological membranes are phospholipid bilayers. Figure 3.2a is a sketch of the shape of a phospholipid molecule, and Figure 3.2b indicates how millions of such molecules form a bimolecular layer between the inside and outside of the cell. Membrane stiffness is conferred by cholesterol and other steroids that partition into the nonpolar layer, while flexibility is conferred by amphiphilic proteins (i.e., proteins that have both hydrophilic and hydrophobic regions on their surface) that partition into the membrane and, in most cases, are exposed to the aqueous phase on both sides, as indicated by the blob in Figure 3.2b.

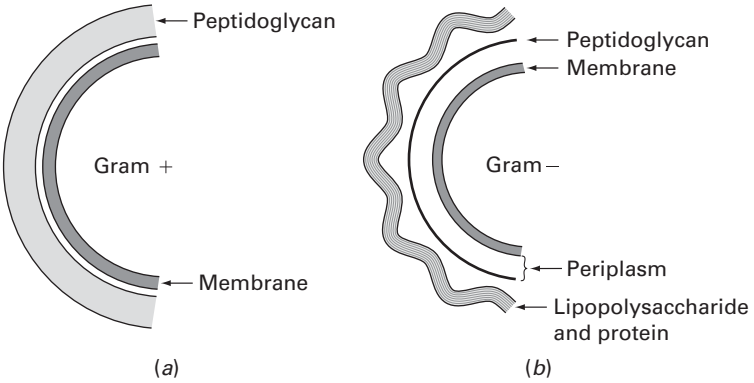

FIGURE 3.1 Diagrammatic representations of the structural features of the surfaces of (*a*) Gram-positive and (*b*) Gram-negative bacteria. The membrane is also called the plasma membrane or the cytoplasmic membrane.

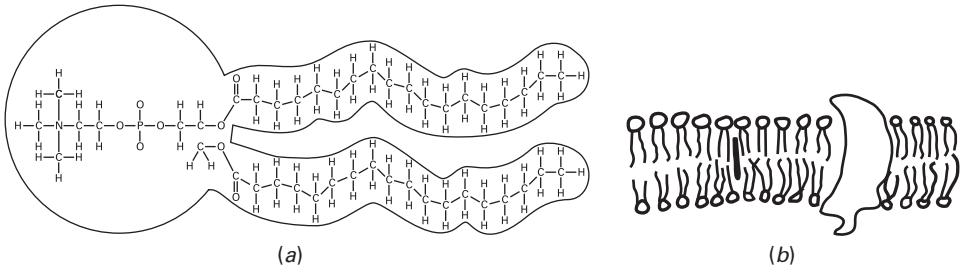

FIGURE 3.2 (*a*) Phospholipid molecule and its outline. (*b*) Cell plasma membrane formed by phospholipids with their polar head groups in contact with aqueous phases. The molecules are about 2.5 nm long. Vertical bar represents a cholesterol molecule, and the large, irregular blob represents a protein molecule that is in contact with both the cytoplasm and the extracellular milieu.

The bacterial cell wall protects the plasma membrane and the cytoplasm from osmotic stress. The iso-osmotic external concentration for most cells is 0.3 osmolar (osM). (Osmolarity refers to the molar concentration of all species in solution, including ionized species.) Higher concentrations outside the cell draw out water and cause the cytoplasm to shrink—"plasmolysis." The cell wall is rigid, so the cytoplasm collapses within the plasma membrane while the wall does not. Concentrations of salts and neutral solutes lower than 0.3 osM outside the cell force water into the cell—"turgor." Too much turgor can break the cell wall (lysis), a situation that can aid in cell disruption for retained bioproducts.

3.2.2 Eukaryotic Cells

Eukaryotic cells (cells with nuclei and internal organelles) are considerably more complicated than prokaryotic cells, and bioproducts may have to be released from intracellular particles that are themselves coated with membranes and/or consist of large macromolecular aggregates. The eukaryotes include fungi (yeasts are most

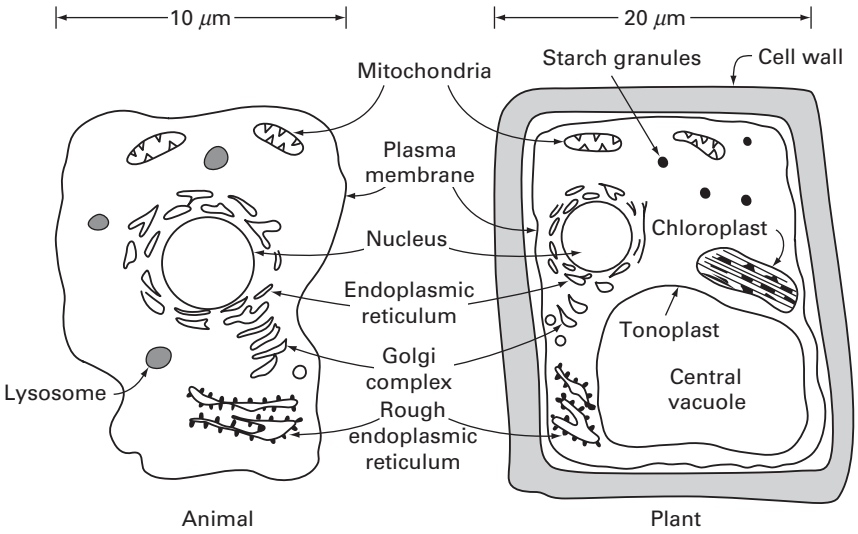

FIGURE 3.3 Eukaryotic cells. Simplified diagrammatic representation of an animal cell and a plant cell. The lysates of such cells contain the internal structures (organelles) shown.

interesting in bioprocessing, as are antibiotic-producing molds such as *Penicillium*), and, of course, the higher plants and animals, the cells of which are today grown routinely in culture as if they were microorganisms. Cell biologists recognize all cell membranes (including those of bacteria) as a separate, immiscible, liquid phase relative to the rest of the cell. The eukaryotic cell must thus be viewed as a multiphasic system. The complexity of generic animal and plant cells is indicated in Figure 3.3. Note that animal cells do not have a cell wall, while the cell wall in plants is very thick. The cell membrane of animal cells is easily broken, whereas the cell wall of plants is strong and relatively difficult to break.

It should be mentioned that the living cell is an effective chemical processor and an inspiration to the development of separation methods. Many things that a cell does can be imitated on the laboratory scale. The way solutes and particles get through cell membranes, for example, has stimulated an entire field of research in micellar extraction, liquid film membranes, and organic solvent enzymology.

3.3 CELL LYSIS

There are two principal means of lysing cells to obtain their contents: chemical cell lysis and physical destruction via mechanical force. Changes in osmotic pressure, as just mentioned, involve modification of a chemical potential that actually results in a mechanical force. Surfactants and enzymes added to a cell suspension act by dissolving a portion of the cell membrane and/or cell wall. Because chemical lysis conditions are detrimental to some bioproducts, it is sometimes necessary to use pure physical force methods, with high shear at high pressure being most popular. The various cell lysis methods are categorized in Table 3.1.

TABLE 3.1 Cell Disintegration Techniques[a]

Method	Technique	Principle	Stress	Cost	Examples
Chemical	Osmotic shock	Osmotic rupture of membrane	Gentle	Cheap	Rupture of red blood cells
	Enzyme digestion	Cell wall digested causing rupture	Gentle	Expensive	*M. lysodeikticus* treated with egg lysozyme
	Solubilization	Detergents solubilize membrane	Gentle	Moderate	Bile salts acting on *E. coli*
	Lipid dissolution	Organic solvent dissolves in membrane, destabilizes	Moderate	Cheap	Toluene disruption of yeast
	Alkali treatment	Saponification of lipids dissolves membranes	Harsh	Cheap	Nucleic acid extractions
Mechanical	Homogenization (blade or pestle type)	Cells chopped in blender or sheared	Moderate	Moderate	Animal tissues
	Grinding	Cells ruptured by grinding with abrasives	Moderate	Cheap	Yeast enzymes
	Ultrasonication	Cells broken by sonic cavitation	Harsh	Expensive	Cell suspensions on small scale
	Pressure cell	Cells broken by shear when forced through small hole	Harsh	Moderate	Large-scale treatment of cell suspensions
	Ball mill	Cells crushed between glass or steel balls or beads	Harsh	Cheap	Large-scale treatment of cell suspensions and plant tissues

[a] See references [1] and [2].

3.3.1 Osmotic and Chemical Cell Lysis

Every cell membrane maintains a substantial osmotic gradient; however, a drastic reduction in extracellular concentration of solutes, say from 0.15 M to 0.001 M, will tend to burst cells that do not have walls, such as animal cells and protoplasts [i.e., cells that normally have walls but have had them removed as a result of enzymatic digestion (lysozyme) or antibiotics (penicillin)]. If the transmembrane osmotic pressure is due to solute concentration inside the cell and out, then the van't Hoff law can be used to estimate this pressure, which applies to ideal, dilute solutions:

$$\pi = RT(c_i - c_o) \tag{3.3.1}$$

where π = osmotic transmembrane pressure
R = gas constant
T = absolute temperature (K)
$c_i - c_o$ = difference between total solute molarity inside and outside the cell, respectively

Most animal cells are quickly lysed by a rapid transition to distilled water.

Bacterial and plant cells are protected against osmotic lysis by cell walls, as noted earlier. The weakening or partial destruction of these walls can be achieved with chemical agents. These may consist of detergents, chelators, enzymes, solvents, and so on. These are summarized in the upper portion of Table 3.1.

Enzymes and Antibiotics

In the case of bacteria, the enzyme lysozyme (15 kDa), readily available in crude form from hen egg whites and relatively expensive to purchase, can be incubated at a fraction of a milligram per milliliter, in the broth, resulting in sufficient digestion of the cell wall to allow osmotic rupture of the resulting bacterial protoplast. One must be very cautious in the choice of hydrolytic enzymes for cell lysis. Proteases should not be used if the desired bioproduct is a protein. Even a label on a bottle that says polysaccharidase or nuclease does not mean that there is no protease activity inside. Hydrolase preparations, especially from animal sources, tend to be mixtures. Antibiotics that are specific for prokaryotic cell wall synthesis, such as penicillin, can be used to produce protoplasts. Simply incubating a bacterial culture for a few hours in a solution of this type of antibiotic above its minimal inhibitory concentration (MIC) will result in a few cell divisions without cell wall synthesis, and the culture will consist primarily of protoplasts.

Detergents

Nonionic detergents are able to break plasma membranes and are commonly used to lyse cultured animal cells [3]. Nonionic detergents are used because they are far less denaturing for proteins and other biological compounds than are ionic detergents.

Some nonionic detergents that are commonly used are Triton X-100 (polyoxyethylene [9-10] *p-t*-octylphenol), octyl-β-glucoside, and Tween 20 (PEG-20 sorbitan monolaurate). Many proteins are still active in 1% to 3% Triton X-100. Different proteins react differently to different detergents, so finding the best detergent is usually a trial-and-error procedure. In one published procedure to lyse cultured animal cells, 0.1% to 0.3% Triton X-100 is added to a cell suspension of 10^7 to 10^8 cells/ml [3]. The addition of glycerol to the cell extract can help to stabilize proteins (0.2 vol of 50% glycerol).

Solvents

Solvents have been used to lyse cells, especially eukaryotes. A variety of methods with toluene have been used to lyse yeast cells, but some have not been completely successful with all commercial yeasts [2]. Acetone is often used early in the preparations of biochemicals from animal tissue homogenates. It dissolves cell membranes as well as excess fat, and at appropriate concentrations may aid in precipitating the product, if that is desirable (see Chapter 8, Precipitation). A bioproduct that is extracted from cells with acetone and then precipitates is called an "acetone powder" after drying. When the precipitation is carried out below 0°C, proteins retain their native conformation, and powder precipitates can be stored before being used. Proteins can be resolubilized by mixing the acetone powder in an appropriate buffer that is warm [2].

3.3.2 Mechanical Methods of Lysis

Forces for lysing cells mechanically are developed by compression and shear. These are summarized in the lower portion of Table 3.1. Sonication, ball milling, pestle homogenization, and reciprocating milling are used. In the case of bench scale homogenizers, a tightly fitting pestle (10–100 μm gap) is reciprocated and/or rotated in a glass or steel cylinder. The Waring blender of household kitchen fame is also a popular bench scale homogenizer and has been scaled up for industrial applications (VirTis). At higher scale, shearing devices that pass particle suspensions through small orifices at high pressures (up to 200 MPa) are used, as are bead mills and ball mills. Manual (e.g., the French press) and motor-driven unit operations are used. In some motor-driven units, the operation is very similar to that of an automobile engine, with the pressure provided intermittently by a reciprocating piston and the sample introduced synchronously under the control of a cam-driven valve. Figure 3.4 is a gallery of these unit operations. Correlations for the scaling of their operation are given in the next sections, which deal with two broad classes of cell homogenizers: high-pressure shear homogenizers and bead mills.

High-Pressure Cell Homogenizers

The Manton-Gaulin valve-type homogenizer (Figure 3.5) is among the most popular in biotechnology operations. Various designs of valves used in this homogenizer are

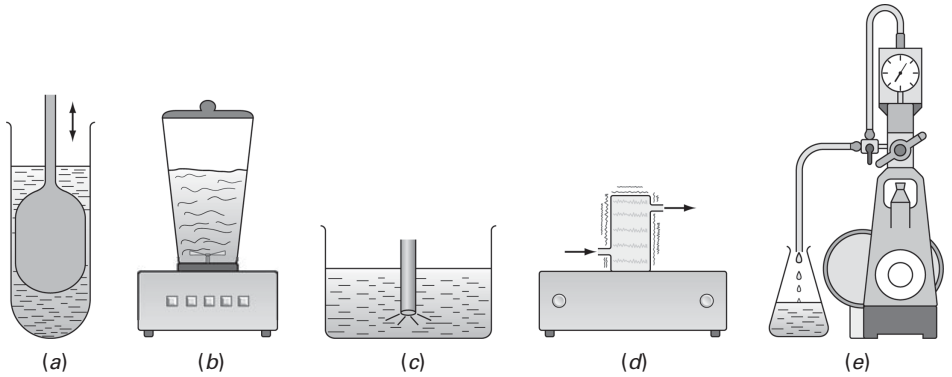

FIGURE 3.4 Equipment used for breaking cells. (*a*) Hand-operated or motor-driven pestle homogenizer. (*b*) Waring (blade) blender. (*c*) Ultrasonic probe. (*d*) Vibrating glass bead mill. (*e*) Manton-Gaulin pressure-shear cell disintegrator.

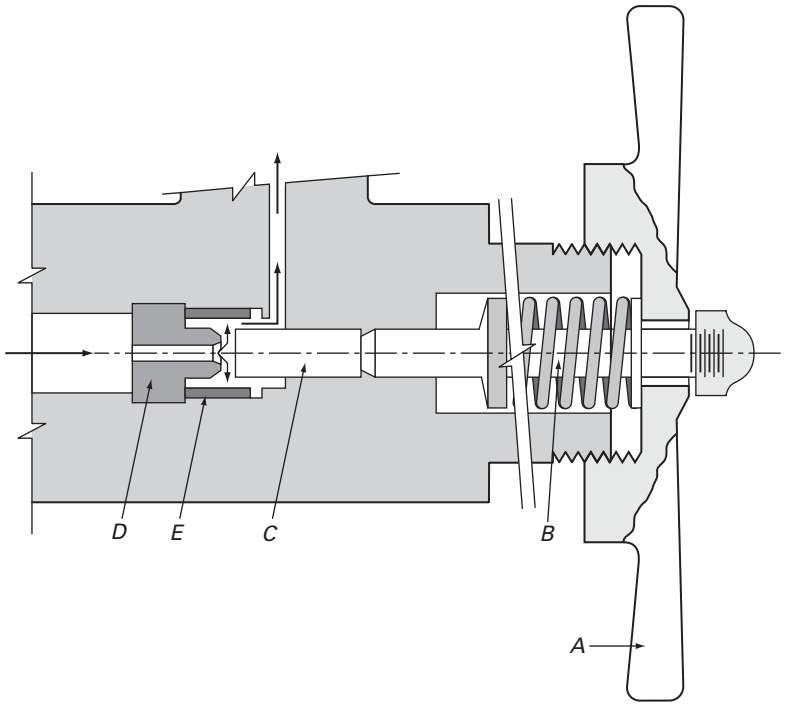

FIGURE 3.5 Details of a high-pressure (Manton-Gaulin) homogenizer valve: A, handwheel for adjusting pressure; B, spring-driven valve rod; C, valve (see Figure 3.6); D valve seat (also see Fig. 3.6); and E, impact ring of hard material. The ring E is sometimes eroded by the impact of cells and debris, which can be abrasive. (*Schematic based on a design by Manton-Gaulin APV.*)

shown in Figure 3.6. Sample feed enters the valve chamber in pulsatile flow; at each pulse, the valve closes and compresses the cell suspension against an impact ring of hard material serving as the inner wall for the chamber. The valve opens and the lysate escapes, and the cycle is repeated. After N passes through the valve, the extent of disruption is determined on the basis of the amount of soluble protein released.

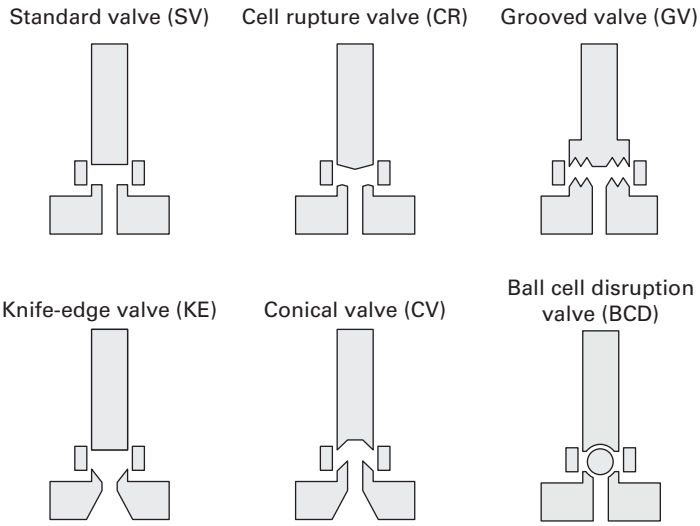

FIGURE 3.6 Configurations of high-pressure homogenizer valves used in Manton-Gaulin homogenizers (Figure 3.5).

The extent of disruption, symbolized by R, usually depends on a power function of the applied pressure and on the number of passes through the chamber [4]:

$$\ln(1-R) = -kN P^a \quad (3.3.2)$$

where P is the pressure. The value of a for bacteria and yeast ranges from 0.9 to 2.9 depending on species and culture conditions [5], while k depends on temperature [4].

The commercial high-pressure homogenizer made by Microfluidics operates on a different principle. The sample stream is focused at high velocity into two channels that are each 100 μm in diameter. These two streams collide head-on, then turn 90° to exit as one stream. The shear and collisions result in cell breakage and the release of soluble protein. For *E. coli* bacteria, the extent of disruption for this homogenizer could be correlated to the number of passes and the pressure, as follows [6]:

$$\ln(1-R) = -kN^b P^a \quad (3.3.3)$$

The value of b varies over the range 0.3 to 0.9, depending on the cell type (i.e., recombinant or native), concentration, and specific growth rate. The parameters k and a depend on the type of cells, ranging over 0.3–63 $\times 10^{-3}$ MPa^{-a} and 0.6 to 1.8, respectively.

Bead Mills

Classical bead mills, such as those used for producing fine powders of minerals, clays, and pigments, have been adapted to the disruption of cells. The unit consists of a horizontal or vertical cylinder filled to some level with (usually) glass beads that

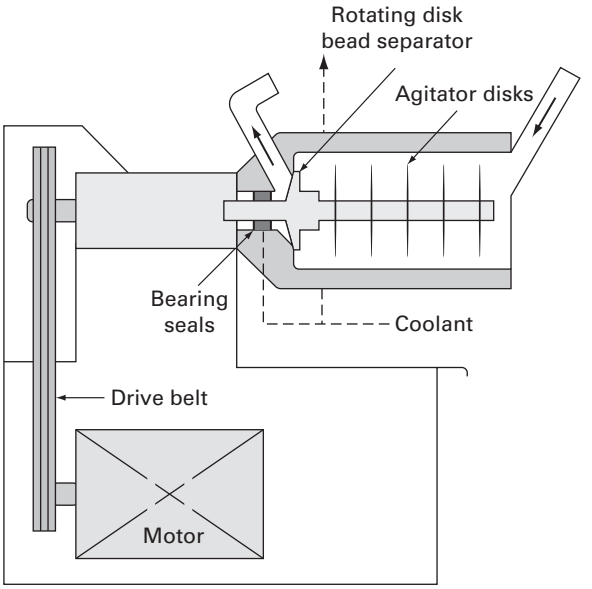

FIGURE 3.7 Schematic diagram of a typical bead mill, showing rotating agitator disks, sample inlet and outlet above the chamber, and rotating disk for the retention of beads.

are tumbled by rotating agitator disks of various shapes. A generalized bead mill configuration is shown in Figure 3.7.

The governing correlation for a bead mill operated in batch mode is [7]:

$$\ln(1-R) = -kt \tag{3.3.4}$$

where t is the processing time for a batch. It is obvious that this unit can be operated in continuous mode, in which case the correlation is [7]:

$$\frac{1}{1-R} = 1 + \left(\frac{kt}{j}\right)^{j} \tag{3.3.5}$$

where t is the mean residence time (volume of liquid in the mill divided by the flow rate), and j is equivalent to a number of continuous stirred tank reactors (CSTRs) in series and need not be an integer. The parameter j must be determined experimentally from residence time distribution studies. The most important factors that affect the cell disruption achieved in bead mills are chamber design, agitator speed, agitator design, bead size, bead loading, cell concentration, feed rate, and temperature; therefore, the application of Equations (3.3.4) and (3.3.5) will depend on these variables [5].

3.4 FLOCCULATION

After cells have been lysed or bioparticles have been dispersed, it is often useful to hasten the subsequent filtration or sedimentation step by flocculation, that is, by

reversibly increasing the size of the particles to be separated. Flocculation occurs as the result of adding a suitable chemical called a "flocculant" or by the selection of naturally flocculating cells for fermentation, as in the case of lager yeast. Flocculants can act by forming interparticle molecular "bridges" between particles, in which case the flocculants are usually polymers or oligomers; they can also act by reducing the repulsive forces between cells, usually by reducing the strength of the electrostatic field.

Flocculation is the attachment of suspended particles to one another when van der Waals interactions (attractive forces between nonpolar particles) are not counteracted by electrostatic repulsion (colloid instability). Flocculation is therefore related to the electrokinetic properties of particles and molecules. *Practically all bioparticles suspended in aqueous solutions are negatively charged.* A suspension of particles that do not aggregate is called a "stable" colloidal suspension. The transition to an "unstable" suspension requires the reduction of the surface charge of the particles. The electrokinetic properties of particles and molecules and how they can be manipulated to bring about flocculation are discussed in this section.

3.4.1 The Electric Double Layer

The electric double layer (cloud of ions of both signs) that surrounds all charged molecules and particles in solution influences several properties of significance in bioseparations:

Precipitation (salting out)

Flocculation (aggregation of particles)

Electrophoresis (electrophoretic mobility)

Colloid stability (particles remain in suspension)

Phase partitioning (charge dependence)

All these processes may be considered simultaneously, in view of Figure 3.8, in which negative (typical of biological particles and molecules) particles approach one another in an electrolyte solution. Attracting forces such as London and van der Waals forces are opposed by the interaction of like charges distributed over each particle. If the charge on the particle can be reduced, then a closer approach is possible, allowing the formation of London, van der Waals, and even hydrogen bonds. The formation of such bonds can be understood in terms of the total potential energy diagram (Figure 3.9), in which the electrostatic repulsion curve $\psi_E(r)$ and the attractive potential curve $\psi_L(r)$ sum to values less than zero. Particles attracted to each other at the "secondary minimum" (in Figure 3.9) are still approximately $4/\kappa$ apart, where κ is the *Debye-Hückel constant*.

Figure 3.10 shows the details of the distribution of dissolved ions around a positively charged, suspended spherical particle. The particle itself is considered to have

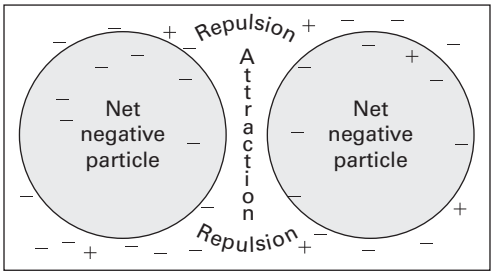

FIGURE 3.8 Forces between two like-charged particles, suspended in electrolyte solution, as they approach each other.

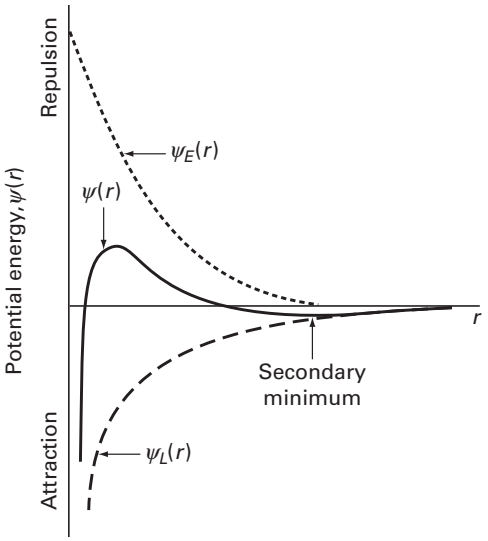

FIGURE 3.9 Potential energy between two like-charged particles separated by distance *r*, where $\psi_E(r)$ is the repulsive double-layer (electrostatic) potential, and the attractive potential curve $\psi_L(r)$ is due to London and van der Waals forces. The solid curve $\psi(r)$ is their sum. Where the two sum to values less than zero at the "secondary minimum," weak, reversible coagulation occurs. $\psi_E(r)$ is responsive to a dc electric field leading to electrophoresis or electroosmosis.

a net excess of fixed positive charges. An *electric double layer* is created around the particle surface consisting of two regions: an inner region that includes adsorbed ions (the fixed part of the double layer) and a diffuse region in which ion diffusion is weakly affected by the electrostatic potential $\psi_E(r)$, which eventually falls to zero, defining the outer boundary of the double layer. The plane that goes through the fixed layer at about one hydrated ion radius from the solid surface is called the Stern plane (see Figure 3.10). The surface of shear indicated in Figure 3.10 is the outer limit of a thin boundary layer of stagnant fluid that surrounds the particle.

There are various theories describing the electric double layer. The Gouy-Chapman theory, one of the first, states that the electrical potential as a function of the distance *r* from a surface with a uniformly distributed charge is given by [8]

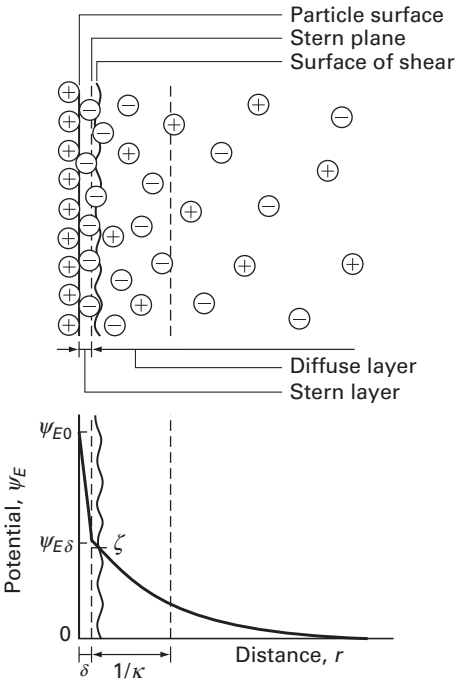

FIGURE 3.10 Schematic representation of the electric double layer of a model spherical colloidal particle, showing the change in the electric potential ψ_E with the distance r from the surface; ζ is the zeta potential, $1/\kappa$ is the Debye radius, and δ is the distance of the Stern plane from the solid surface (about equal to a hydrated ion radius).

$$\psi_E(r) = \psi_{EO} \exp(-\kappa r) \tag{3.4.1}$$

where ψ_{E0} is the potential at the surface, and κ is the Debye–Hückel constant. According to the theory, this equation is valid at small values of the potential. Equation (3.4.1) shows that the electric potential decreases by e (2.718) times at a distance of the order of $1/\kappa$. The quantity $1/\kappa$ is called the radius of the ionic atmosphere, or the *Debye radius* or *length,* and depends on the concentration of dissolved ions according to the equation [8]:

$$r_{DR} = \frac{1}{\kappa} = \left(\frac{\varepsilon RT}{8\pi F^2 \sum c_i z_i^2} \right)^{1/2} \tag{3.4.2}$$

where ε = absolute dielectric constant of the liquid
R = gas constant
T = absolute temperature
F = Faraday number
c_i = bulk concentration of different ions
z_i = valence of different ions

It should be noted that

$$\sum c_i z_i^2 = 2I \tag{3.4.3}$$

where I is the ionic strength of the solution. The Debye radius, r_{DR}, is typically less than 1 nm for most bioprocessing situations (see Example 3.1).

EXAMPLE 3.1

Dependence of the Debye Radius on the Type of Electrolyte Compare the Debye radius in a solution at 25°C of 0.01 M aluminum acetate to that in a solution of sodium chloride at the same temperature and molarity.

Solution

We use Equation (3.4.2) to calculate the Debye radius for each salt solution. We can calculate ε from

$$\varepsilon = \varepsilon_r \varepsilon_o$$

where ε_r = relative dielectric constant of liquid
ε_0 = permittivity of free space (vacuum)

At 25°C for water, $\varepsilon_r = 78.3$. For 0.01 M $Al(C_2H_3O_2)_3$,

$$\sum c_i z_i^2 = 2I = 0.01(3)^2 + 3(0.01)(1)^2 = 0.12\,\text{M} = 0.12\times10^3\,\frac{\text{mol}}{\text{m}^3}$$

From Equation (3.4.2),

$$r_{DR} = \left(\frac{\varepsilon RT}{8\pi F^2 \sum c_i z_i^2}\right)^{1/2} = \left[\frac{78.3\left(8.85\times10^{-12}\,\frac{C^2}{\text{Jm}}\right)\left(8.31\frac{\text{J}}{\text{mol K}}\right)(298\,\text{K})}{8\pi\left(9.65\times10^4\,\frac{\text{C}}{\text{mol}}\right)^2\left(0.12\times10^3\,\frac{\text{mol}}{\text{m}^3}\right)}\right]^{1/2}$$
$$= 2.47\times10^{-10}\,\text{m} = 0.247\,\text{nm}$$

For 0.01 M NaCl,

$$\sum c_i z_i^2 = 0.01(1)^2 + 0.01(1)^2 = 0.02\,\text{M} = 0.02\times10^3\,\frac{\text{mol}}{\text{m}^3}$$

Substituting this result into Equation (3.4.2) gives

$$r_{DR} = 0.605\,\text{nm}$$

Thus, we have the prediction that the Debye radius will be reduced by more than half when aluminum acetate is used instead of sodium chloride.

Conceptually, the effect of ionic strength on the double layer can be seen in Figure 3.11, in which the vertical dashed line shows the position of the Stern plane, and the potential curves intersect this line at near to the *zeta potential* ζ, which is the potential at the shear plane (see Figure 3.10). The zeta potential, the potential that is measured in an electrophoresis experiment, is the potential that determines the electrophoretic mobility in mobility equations, such as [8, 9]:

$$U_{el} = \frac{\varepsilon\zeta}{4\pi\mu} \quad (3.4.4)$$

where U_{el} is the electrophoretic mobility and μ is the viscosity of the liquid. See Equation (2.5.1) for the relationship of electrophoretic mobility to particle velocity and electric field strength.

3.4.2 Forces between Particles and Flocculation by Electrolytes

As two particles approach each other, they interact via repulsive (electrokinetic and lubrication) forces and attractive (van der Waals) forces (Figures 3.8 and 3.9). To cause particle aggregation or flocculation to occur is to manipulate these forces. The typical objective is to reduce the electrical repulsion force as much as possible to allow

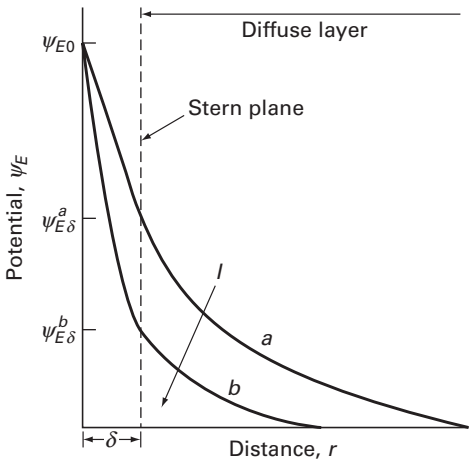

FIGURE 3.11 The Stern model of the electric double layer showing compression of the double layer due to increasing ionic strength *I* from curve *a* to curve *b*.

particles to approach close enough to one another to allow the attractive van der Waals force to exceed the repulsive electrical force. This is accomplished in the paradigm of DLVO theory, named after two research groups who studied this problem (Deryagin and Landau of Russia and Verwey and Overbeek of The Netherlands). Figure 3.9 shows a negative (attractive) potential at two locations, at the distance of closest approach and at a "secondary minimum," which is at a distance of around $4/\kappa$. Most flocculations are due to attachments between particles in the secondary minimum. If the diffuse double layer extends too far from the particle surface, then van der Waals attraction is impossible. Therefore, from the preceding sections, it should be clear that high ionic strength (small $1/\kappa$) will favor particle-particle attachments in the secondary minimum of the potential energy diagram. A useful outcome of the DLVO theory is the following prediction of the critical flocculation concentration of an indifferent electrolyte (an electrolyte that does not chemically adsorb into the Stern layer) [10]:

$$(c_i)_{\text{flocc}} = \frac{9.85\times10^4\,\varepsilon^3 k^5 T^5 \gamma^4}{\mathcal{N} e^6 A^2 z^6} \tag{3.4.5}$$

where $(c_i)_{\text{flocc}}$ = lowest molar concentration of the electrolyte that causes particles to coagulate
ε = absolute dielectric constant of the liquid
k = Boltzmann constant
γ = constant that limits to 1.0 at high potentials and to $ze\psi_{E\delta}/4kT$ at low potentials
$\mathcal{N}$ = Avogadro's number
e = electron charge
A = effective Hamaker constant
z = counterion charge number

The Hamaker constant was originally defined in a theoretical expression for the energy of attraction E_a between spherical particles *in vacuo* as a function of distance between the particles. For equal-sized particles at small interparticle separations, the following relationship was developed [10]:

$$E_a = -\frac{Aa}{12d} \tag{3.4.6}$$

where a is the particle radius and d is the shortest distance between particles.

The presence of a liquid dispersion medium, rather than a vacuum, between the particles lowers the van der Waals interaction energy, and the constant A in Equation (3.4.6) must be replaced by an effective Hamaker constant. The Hamaker constant, however, does not vary greatly from one material to another; for example, this

constant has been measured to be 4.3×10^{-20} J for water, 7.8 to 9.8×10^{-20} J for polystyrene, and 8.6×10^{-20} J for natural rubber [11].

The equation for the critical flocculation concentration [Equation (3.4.5)] reveals a number of insights into the requirements for flocculation:

1. The DLVO theory predicts that the flocculation concentrations of indifferent electrolytes depend on z^{-6}. Thus, at the critical coagulation concentration of an indifferent electrolyte, ions having charge numbers 1, 2, and 3 should be in the ratio $1/1^6$,$1/2^6$, and $1/3^6$, which is 1: 0.016: 0.0013, the theoretical counterpart to the empirical Schulze-Hardy rule (see below).
2. For a typical experimental critical coagulation concentration at 25°C of 0.1 M for $z = 1$ and taking 75 mV as a typical value for $\psi_{E\delta}$, the effective Hamaker constant, A, is calculated [10] to be 8×10^{-20} J. This is consistent with direct measurements of A for various materials.
3. Critical flocculation concentrations of electrolytes for particles of a given material should be proportional to ε^3 and independent of particle size.
4. Flocculation concentration is extremely sensitive to temperature (proportional to T^5), indicating the wisdom of carrying out flocculation reactions at low temperature.
5. The critical flocculation concentration does not depend on the concentration of the particles being flocculated [10].

EXAMPLE 3.2

Sensitivity of Critical Flocculation Concentration to Temperature and Counterion Charge Number For the flocculation of bacterial cells, how would the critical flocculation concentration of an indifferent electrolyte be expected to change if the temperature were lowered from 37°C to 4°C? How would this concentration be expected to change if Al^{3+} counterion were used for flocculation instead of Cu^{2+} counterion?

Solution

From Equation (3.4.5), it is seen that $(c_i)_{\text{flocc}}$ depends on temperature to the fifth power. Therefore,

$$\frac{(c_i)_{\text{flocc},4°\text{C}}}{(c_i)_{\text{flocc},37°\text{C}}} = \frac{(277\,\text{K})^5}{(310\,\text{K})^5} = 0.57$$

It can also be seen that $(c_i)_{\text{flocc}}$ depends on the counterion charge to the −6th power, so that

$$\frac{(c_i)_{\text{flocc},\text{Al}^{3+}}}{(c_i)_{\text{flocc},\text{Cu}^{2+}}} = \frac{(3)^{-6}}{(2)^{-6}} = 0.088$$

Thus, the change in the electrolyte counterion charge would result in a much larger effect on the critical flocculation concentration than the change in temperature.

3.4.3 The Schulze-Hardy Rule

From the first insight enumerated in Section 3.4.2, the dependence of flocculation concentration on z^{-6}, it should be obvious that whenever possible, trivalent electrolyte ions should be used for flocculation. Since most bioparticles are negative, aluminum salts are one logical choice. This theoretical prediction is empirically manifested in the Schulze-Hardy rule, which confirms that the critical electrolyte concentrations are roughly in the ratio 1000:10:1 for monovalent, divalent, and trivalent ions. An example of an experimental test of this theory is shown in Figure 3.12.

Following the foregoing paradigm, flocculation tests are carried out to experimentally determine critical flocculation concentrations. First a series of about six small

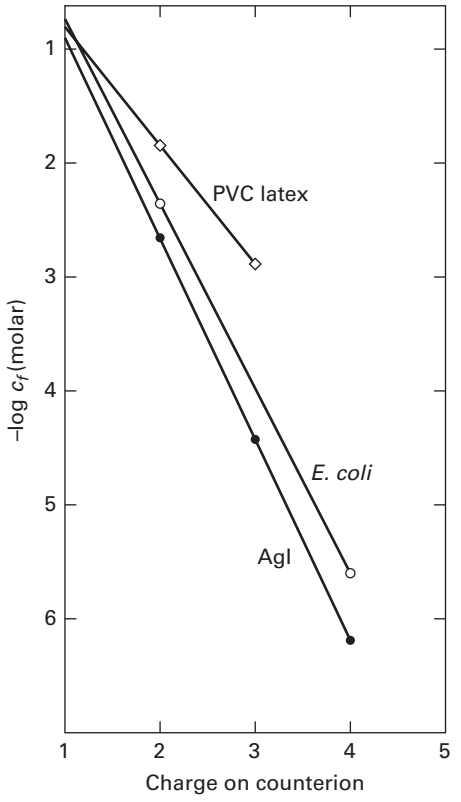

FIGURE 3.12 Experimental test of DLVO theory and the Schulze-Hardy rule, showing the approximate inverse sixth-power dependence of critical concentration for flocculation (c_f) on ion charge. Three different colloids were flocculated: poly(vinyl chloride) latex particles, *Escherichia coli* bacterial cells, and silver iodide colloidal particles. *(Data from W. Stumm and C. R. O'Melia, "Stoichiometry of coagulation,"* J. Am. Water Works Assoc., *vol. 60, p. 514, 1968.)*

test tubes of the suspended solids to be flocculated is prepared. To each is added a measured identical volume of electrolyte solution at a different concentration for each tube. These concentrations, allowing for dilution, are calculated to span the expected critical concentration for flocculation. After the tubes have been allowed to stand for a few minutes, a critical concentration is noted on the basis of the tubes in which flocculation occurred and those in which it did not. Then the flocculation test is completed by setting up a new set of tubes and adding a narrower range of electrolyte concentrations. After a longer standing time, such as 2 h, the suspensions are reagitated to break up large flocs and remix small flocs, thereby creating conditions that approach equilibrium. After another 0.5 to 1.0 h, the samples are observed once again, and the minimum concentration of electrolyte that made a visible change in the appearance of the suspensions is noted and called the critical concentration for flocculation. This concentration is then incorporated into a unit operation.

3.4.4 Flocculation Rate

Besides the critical flocculation concentration of the electrolyte, the rate at which flocculation occurs is of interest, particularly for processes that are going to be scaled up. The theory describing the rate of flocculation was developed by Smoluchowski both for the case of small particles (0.1–10 μm) growing by diffusion of particles and for larger particles that grow by particles colliding and sticking together. Both these cases are described in detail in Chapter 8, Precipitation (Sections 8.3.3 and 8.3.4).

3.4.5 Polymeric Flocculants

Polyionic polymers can be used as electrolytes in flocculation. They have the added advantage that, when they partition into the double layer, they confer a positive charge on the hydrodynamic unit, and this charge extends beyond the Debye radius, causing the particle to become electrostatically attractive to the double layers of colliding particles. Halverson and Panzer [12] have identified five mechanisms of charge-dependent flocculation:

1. Double-layer compression
2. Specific-ion adsorption
3. Sweep-flocculation enmeshment
4. Polymer charge patch formation
5. Polymer bridging

The first three mechanisms can occur regardless of whether the flocculant is a mineral ion or a polymer. A single cationic polymer molecule can neutralize several charged sites on the particle surface; furthermore, single polymer molecules can be electrostatically attracted to more than one particle simultaneously. This behavior, shown diagrammatically in Figure 3.13, is commonly called “bridging.” Figure 3.13

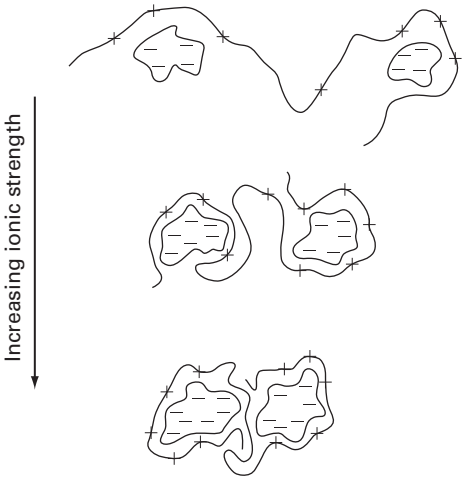

FIGURE 3.13 Flocculation by charge neutralization and bridging. A cationic polymer is used to collect particles with a net negative charge (characteristic of most bioparticles).

also shows the advantage of choosing a polymer whose charge is opposite to that of the particle.

Polymeric flocculants typically have a high molecular weight and are expensive as process chemicals go (approximately $10/kg). However, they are effective in the parts-per-million concentration range, so the total final cost may not be a serious issue. Polymer flocs usually are stronger than flocs formed by the addition of indifferent inorganic electrolytes. Some flocculating agents may have some toxicity, and this property must always be considered. Both synthetic and natural ionic polymers are available. Synthetic polymers include acrylamide-acrylic acid copolymer (anionic), polyacrylic acid (anionic), alkyl polyamines (cationic), and aminoacrylate-acrylamide copolymer (cationic). Natural ionic polymers include alginates and carboxymethylcellulose (anionic) and tannins, albumins, and diethylaminoethyl cellulose (cationic).

Several neutral polymers are also good flocculants. These include poly(ethylene oxide) [aka poly(ethylene glycol)] and polyacrylamide (synthetic), as well as guar gum and its derivatives, locust bean gum, and dextrans (natural). These apparently act by partitioning into the glycocalyx (polysaccharide-containing cell coat) of intact cells owing to strong hydrogen bonding via the hydroxyl groups of the sugars on both the cells and the polymers. Their effectiveness depends on molecular weight, charge, solubility, and so on, and their interactions with cells and particles depend, therefore, on pH, ionic strength, temperature, and dry solids concentration. Unless a great deal is known about the suspended material of interest or extensive experience has been published, the choice of flocculating conditions usually depends on educated trial and error. Typically, the engineer chooses a series of flocculants and tests them at different concentrations and ionic strengths, noting the time to observed flocculation, the clarity of the supernatant after centrifugation, and the quality of the flocculated precipitate.

Real-world tests with undiluted broth must be performed to find both the optimum polymer dose and ionic strength. The optimum final dose will probably be close to that found in this procedure. The flocculant dose for a given dry weight of whole cells (in any volume) should be approximately constant and less than that for a given dry weight suspension of lysate, which may vary according to the degree and mode of lysis.

3.5 SUMMARY

This chapter presents two major elements of cell processing—cell lysis and flocculation. Cell lysis is the process of breaking cell membranes and walls to release the cell contents. Flocculation is the process in which cells and subcellular particles are aggregated into flocs.

- Cells are classified as prokaryotic (no nucleus, such as bacteria) and eukaryotic (fungi, including yeast, and all higher organisms). Cells that do not secrete their products of interest must be subjected to lysis.
- Most prokaryotic cells and all plant and fungal cells possess cell walls that must be ruptured or digested before cells can be lysed and most bioproducts extracted. Animal cells lack cell walls and can be lysed by more benign means such as osmotic shock.
- Mechanical methods of cell lysis include applications of shear through ultrasound, high-speed homogenizers, high-pressure cells, and grinders, such as bead mills. Nonmechanical methods of cell lysis include osmotic shock, detergents, and enzymes.
- Electrokinetic phenomena are important in the flocculation of cells and insoluble particles. Like particles repel each other only when their distance of close approach is of the order of the electric double-layer thickness, or Debye radius, which decreases with increasing ionic strength, which depends, in turn, on z^2, the square of the charge of dissolved ions. In most bioprocessing solutions, the Debye radius is less than 1 nm. The critical concentration of ions to induce flocculation depends on z^{-6}, according to DLVO theory.
- Above the critical ion concentration, particles approach closely enough to adhere by van der Waals forces. The Schulze-Hardy rule, on the basis of the preceding insight, predicts that required ion concentrations for flocculation are roughly in the ratio 1000:10:1 for monovalent, divalent, and trivalent ions, respectively.
- Ionic polymers induce flocculation by a combination of five mechanisms. Neutral polymers typically form hydrogen bonds with cell surface polysaccharides.

NOMENCLATURE

a constant power of pressure in equations for extent of cell disruption in high-pressure homogenizers [Equations (3.3.2) and (3.3.3)] (dimensionless)

a particle radius (cm)

A effective Hamaker constant (J)
b constant power of pressure for extent of cell disruption in a Microfluidics high-pressure homogenizer [Equation (3.3.3)] (dimensionless)
c concentration of solute (M, or g liter^{-1})
d shortest distance between particles [Equation (3.4.6)] (cm)
e electron charge (C)
E_a energy of attraction between spherical particles in vacuo (J)
F Faraday number (9.6485×10^4 C mol^{-1})
I ionic strength (M)
j constant in equation for extent of cell disruption in a bead mill and equivalent to the number of continuous stirred tank reactors in series [Equation (3.3.5)] (dimensionless)
k constant in equations for extent of cell disruption in homogenizers [Pa^{-a} in Equation (3.3.3); s^{-1} in Equations (3.3.4) and (3.3.5)]
k Boltzmann constant (1.3807×10^{-23} J K^{-1})
N number of passes of fluid through homogenizer (dimensionless)
$\mathcal{N}$ Avogadro's number (6.022×10^{23} molecules mol^{-1})
P pressure (Pa)
r distance from surface of spherical particle (nm)
R gas constant (8.3145 J mol^{-1} K^{-1})*
R extent of cell disruption (dimensionless)
t time (s)
T temperature (K)
U_{el} electrophoretic mobility (cm^2 s^{-1} V^{-1})
z valence of ion (dimensionless)

Greek Letters

γ constant in equation for critical flocculation concentration [Equation (3.4.5)] (dimensionless)
δ distance from Stern plane to solid surface (nm)
ε absolute dielectric constant of liquid (C^2 J^{-1} m^{-1})
ε_0 permittivity of free space (vacuum) (= 8.8542×10^{-12} C^2 J^{-1} m^{-1})
ε_r relative dielectric constant of liquid (dimensionless)
ζ zeta potential (J C^{-1}, or V)
κ Debye-Hückel constant (nm^{-1})
μ liquid viscosity (g cm^{-1} s^{-1})
π osmotic pressure (Pa)
ψ total potential (J C^{-1}, or V)
ψ_E electrical potential (J C^{-1}, or V)
ψ_L attractive potential (J C^{-1}, or V)

* Other values of the gas constant R with different units are given in Appendix A.

PROBLEMS

3.1 Osmotic Cell Disruption Use the van't Hoff relationship to estimate the osmotic pressure drop across the membrane of a cell undergoing rupture in a 0.01 M salt solution, assuming the internal salt concentration is 0.2 M and that all salts are fully dissociated. Would you call this a negligible, ordinary, or large pressure drop? Why?

3.2 Osmotic Disruption of Blood Cells It is customary to prepare hemoglobin by the osmotic lysis of red blood cells. What is the van't Hoff pressure drop across the membrane of a red blood cell that is isotonic (0.30 osM) on the inside and submerged in a 0.01% NaCl solution? What is the expected outcome of this situation?

3.3 Breakage of Yeast Cells in a Valve-Type Homogenizer For the breakage of *Candida utilis* yeast cells in a valve-type continuous homogenizer, it is known that the constants in Equation (3.3.2) are $k = 5.91 \times 10^{-4}$ MPa^{-a} and $a = 1.77$ for the operating pressure range of 50 MPa < P < 125 MPa. It is desired that the extent of disruption be ≥0.9. Plot how the number of passes varies with operating pressure over the pressure range of 50 to 125 MPa. What pressure range would you probably want to operate in? (Data from C. R. Engler and W. R. Campbell, "Disruption of *Candida utilis* cells in high pressure flow devices," *Biotechnol, Bioeng.,* vol. 23, p. 765, 1981.)

3.4 Estimation of the Debye Radius and the Electro-static Potential Estimate the Debye radius for particles in a solution of 50 mM NaCl at 4°C. If the surface electrostatic potential of particles in this solution is 10 mV, estimate the electrostatic potential 1 nm from the surface. How significant is the electrostatic potential at this distance from the surface?

3.5 Flocculant Choice In a suspension of lysate consisting of a variety of anionic particles, you find that 0.22 M KCl produces the required clarification. However, a downstream adsorption process requires <0.01 M salt, so this will not work. Knowing the Schulze-Hardy rule, you resort to $Al(NO_3)_3$ as flocculant. What concentration of this salt do you expect to need? Will this concentration fulfill the downstream requirement?

3.6 Ionic Versus Polymeric Flocculant You find that you are able to flocculate yeast cell debris in 1 M NaCl in a 100 liter tank at 20°C. The use of this much salt is unsatisfactory for the next downstream step. You then find that a company markets a bridging cationic polymer for $15/kg and that this polymer (molecular weight 9000) is at least the equivalent on a molar basis of a tetravalent indifferent cation. Furthermore, this polymer can be cleared by a downstream cation exchange adsorption step that is part of the process anyway. What will it cost you to use this polymer, per tank, and how difficult would it be to convince your supervisor to pay for it? What would be the cost savings of chilling the tank to 4°C?

REFERENCES

1. Belter, P. A., Cussler, E. L., and Hu, W.-S. (1988). *Bioseparations*, Wiley, New York.
2. Scopes, R. K. (1994). *Protein Purification*, 3rd ed., Springer-Verlag, New York.
3. Bollag, D. M., Rozycki, M. D., and Edelstein, S. J. (1996). *Protein Methods*, 2nd ed., Wiley-Liss, New York.

4. Hetherington, P. J., Follows, M., Dunnill, P., and Lilly, M. D. (1971). Release of protein from bakers' yeast (*Saccharomyces cerevisiae*) by disruption in an industrial homogenizer. *Trans. Inst. Chem. Eng*., vol. 49, p. 142.
5. Engler, C. R. (1994). Cell breakage. In *Protein Purification Process Engineering*, R. G. Harrison, ed., Dekker, New York, p. 37.
6. Sauer, T., Robinson, C. W., and Glick, B. R. (1989). Disruption of native and recombinant *Escherichia coli* in a high-pressure homogenizer. *Biotechnol. Bioeng*., vol. 33, p. 1330.
7. Limon-Lason, J., Hoare, M., Orsborn, C. B., Doyle, D. J., and Dunnill, P. (1979). Reactor properties of a high-speed bead mill for microbial cell rupture. *Biotechnol. Bioeng*., vol. 21, p. 745.
8. Voyutsky, S. (1978). *Colloid Chemistry*, Mir Publishers, Moscow.
9. Tanford, C. (1961). *Physical Chemistry of Macromolecules*, Wiley, New York.
10. Shaw, D. J. (1980). *Introduction to Colloid and Surface Chemistry*, 3rd ed., Butterworths, London.
11. Hiemenz, P. C., and Rajagopalan, R. (1997). *Principles of Surface and Colloid Chemistry*, 3rd ed., Dekker, New York.
12. Halverson, F., and Panzer, H. P. (1980). Flocculating agents. In *Kirk-Othmer Encyclopedia of Chemical Technology*, vol. 10, 3rd ed. Wiley, New York, p. 489.

/// 4 /// FILTRATION

Filtration is an operation that has found an important place in the processing of biotechnology products. In general, filtration is used to separate particulate or solute components in a fluid suspension or solution according to size by flowing under a pressure differential through a porous medium. There are two broad categories of filtration, which differ according to the direction of the fluid feed in relation to the filter medium. In *conventional* or *dead-end filtration,* the fluid flows perpendicular to the medium, which generally results in a cake of solids depositing on the filter medium. In *crossflow filtration* (which is also called *tangential flow filtration*), the fluid flows parallel to the medium to minimize buildup of solids on the medium. Conventional and crossflow filtration are illustrated schematically in Figure 4.1.

Conventional filtration is typically used when a product has been secreted from cells, and the cells must be removed to obtain the product that is dissolved in the liquid. Antibiotics and steroids are often processed by using conventional filtration to remove the cells. Conventional filtration is also commonly used for sterile filtration in biopharmaceutical production. Crossflow filtration has been used in a wide variety of applications, including the separation of cells from a product that has been secreted, the concentration of cells, the removal of cell debris from cells that have been lysed, the concentration of protein solutions, the exchange or removal of a salt or salts in a protein solution, and the removal of viruses from protein solutions.

Filtration often occurs in the early stages of bioproduct purification, in keeping with the process design heuristic "remove the most plentiful impurities first" (see Chapter 12, Bioprocess Design and Economics). At the start of purification, the desired bioproduct is usually present in a large volume of aqueous solution, and it is desirable to reduce the volume as soon as possible to reduce the scale and thus the cost of subsequent processing operations. Filtration, along with sedimentation and extraction (see Chapters 5 and 6), is an effective means of accomplishing volume reduction.

In this chapter, conventional and crossflow filtration are first described mathematically as a basis for understanding how these filters perform. Next, filter media

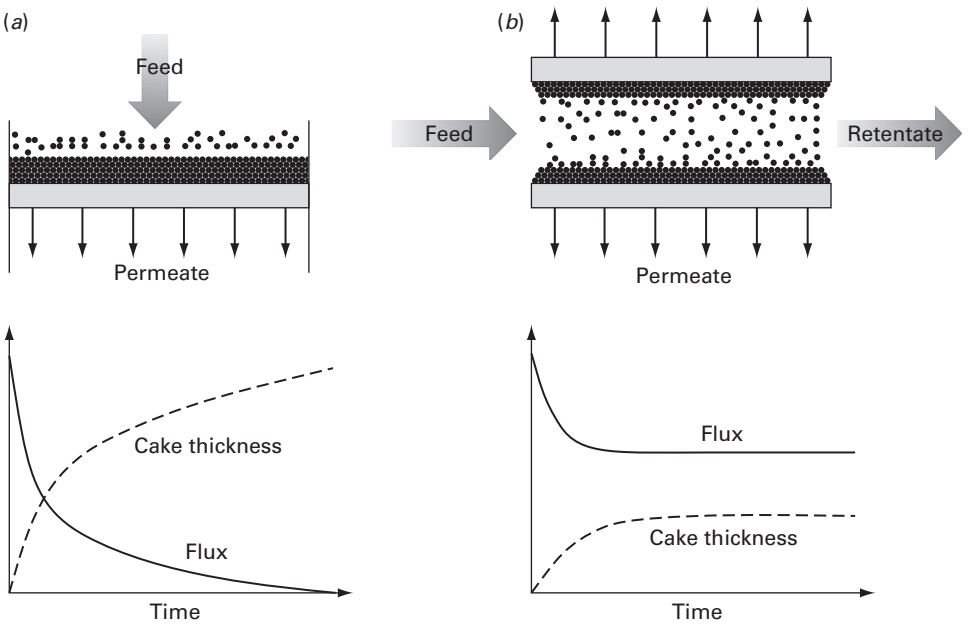

FIGURE 4.1 Schematic diagrams for (*a*) dead-end or conventional filtration and (*b*) crossflow filtration. For dead-end filtration, the thickness of the solids buildup increases and the permeate flux decreases with time, ultimately reaching zero. In crossflow filtration, the feed can contain either a soluble or a solid solute, which becomes concentrated at the membrane surface; the permeate flux reaches a constant value at steady state.

and equipment of various types are described, and mechanisms of membrane fouling are presented. The chapter concludes with a discussion of the scale-up and design of the various filtration systems.

4.1 INSTRUCTIONAL OBJECTIVES

After completing this chapter, the reader should be able to do the following:

- Calculate solvent fluxes and filtration times for conventional filtration using Darcy's law.
- Use washing theory to calculate the removal of solutes from a filter cake.
- Estimate the extent of concentration polarization in crossflow filtration.
- Select filtration media and equipment to meet bioproduct processing requirements.
- Explain and identify the mechanisms of membrane fouling.
- Select filtration unit operations to meet product requirements, consistent with product properties.
- Perform scaling calculations on conventional and crossflow filters.
- Perform process calculations for the four basic modes of operations for crossflow filters.

4.2 FILTRATION PRINCIPLES

The theory of filtration has been extensively developed. The goal of this section is to describe the fundamental filtration theory that is important to an understanding of how conventional and crossflow filters operate, which can then be used as a basis for design and scale-up of the unit operations.

4.2.1 Conventional Filtration

When a slurry containing suspended solids flows towards and through a filter medium by the application of a pressure gradient across that medium, the solids begin to build up on the filter medium as shown in Figure 4.1a. The accumulation of solids on the filter medium is called a cake. If the solids load in the slurry is high, the cake quickly comes to dominate the performance of the filtration. Darcy's law describes the flow of liquid through a porous bed of solids and can be written as follows:

$$\frac{1}{A}\frac{dV}{dt}=\frac{\Delta p}{\mu_0 R} \tag{4.2.1}$$

where V is the volume of filtrate, t is time, A is the filtration cross-sectional area, Δp is the pressure drop through the cake and filter medium, μ_0 is the viscosity of the filtrate, and R is the resistance of the cake and the filter medium. These resistances can be treated separately; thus, for R_m as the resistance of the filter medium and R_c as the resistance of the cake solids,

$$R=R_m+R_c \tag{4.2.2}$$

It is convenient to write the cake resistance R_c in terms of a specific cake resistance α as follows:

$$R_c=\alpha\rho_c\left(\frac{V}{A}\right) \tag{4.2.3}$$

where ρ_c is the mass of dry cake solids per volume of filtrate. Thus, the resistance increases with the volume filtered. Combining Equations (4.2.1), (4.2.2), and (4.2.3), we obtain

$$\frac{1}{A}\frac{dV}{dt}=\frac{\Delta p}{\mu_0[\alpha\rho_c(V/A)+R_m]} \tag{4.2.4}$$

For the case of zero filtrate at time zero, integration of this equation yields

$$\frac{t}{V/A}=\frac{\mu_0\alpha\rho_c}{2\Delta p}\left(\frac{V}{A}\right)+\frac{\mu_0 R_m}{\Delta p} \tag{4.2.5}$$

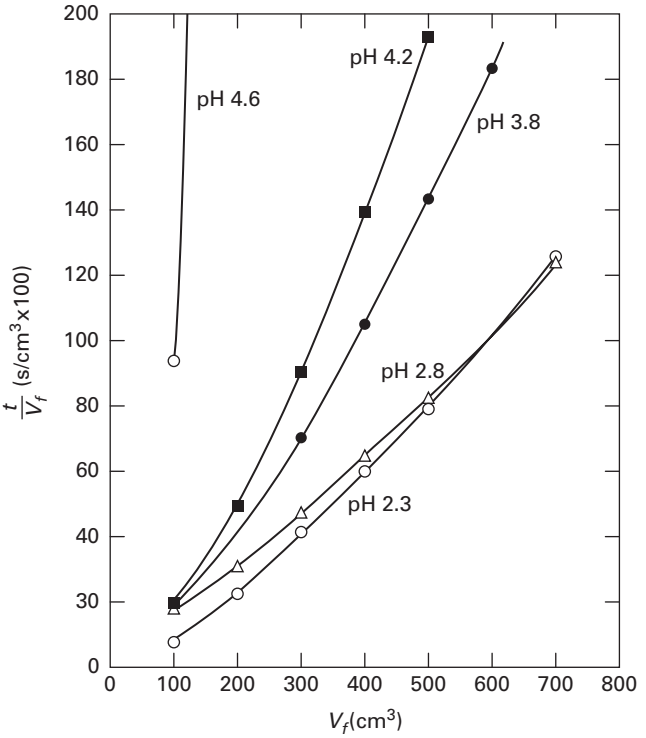

FIGURE 4.2 Filtration data for *Streptomyces griseus* broth with Δp = 2.0 bar. The filter medium was cotton cloth, and a diatomaceous earth filter aid was added to the broth. *(Data from S. Shirato and S. Esumi, "Filtration of a culture broth of* Streptomyces griseus*"* J. Ferment. Technol. (Japan), *vol. 41, p. 87, 1963.)*

This is a convenient form of the integrated equation, since a plot of $t/(V/A)$ versus V/A should give a straight line. Filtration data plotted in this manner for *Streptomyces griseus* fermentation broth are shown in Figure 4.2. One noteworthy feature of the plots in Figure 4.2 is that most of the lines connecting the data at given pH values are not perfectly straight. Of the variables constituting the slope in Equation (4.2.5), the only one that could change appreciably with Δp is α, the specific cake resistance. The slopes are increasing with the volume filtered, indicating that α is increasing. This implies that α is a function of V/A. At constant pressure, α can increase as the cake is compressed. Cakes are typically compressible when cells and other biological materials are being filtered. For soft or amorphous solids, at constant pressure, some consolidation is expected as the filtration volume increases, leading to the dependence of α on V/A.

EXAMPLE 4.1

Batch Filtration A Büchner funnel 8 cm in diameter is available for testing the filtration of a cell culture suspension, which has a viscosity of 3.0 cp. The data in

Table E4.1 were obtained with a vacuum pressure of 600 mm Hg applied to the Büchner funnel.

The cell solids on the filter at the end of filtration were dried and found to weigh 14.0 g. Determine the specific cake resistance α and the medium resistance R_m. Then estimate how long it would take to obtain 10,000 liters of filtrate from this cell broth on a filter with a surface area of 10 m^2 and vacuum pressure of 500 mm Hg.

TABLE E4.1

Time (s)	Volume of filtrate (ml)
26	100
96	200
197	300
342	400
537	500
692	600
989	690 (end)

Solution

According to Equation (4.2.5), we can plot $t/(V/A)$ versus V/A and obtain α from the slope and R_m from the intercept. We see that the data are reasonably close to a straight line. A linear regression of the data in this plot gives the following results (Figure E4.1):

$$\text{Slope} = 4.81 \frac{\text{s}}{\text{cm}^2}$$

$$\text{Intercept} = 4.26 \frac{\text{s}}{\text{cm}}$$

From these values, we can calculate α and R_m:

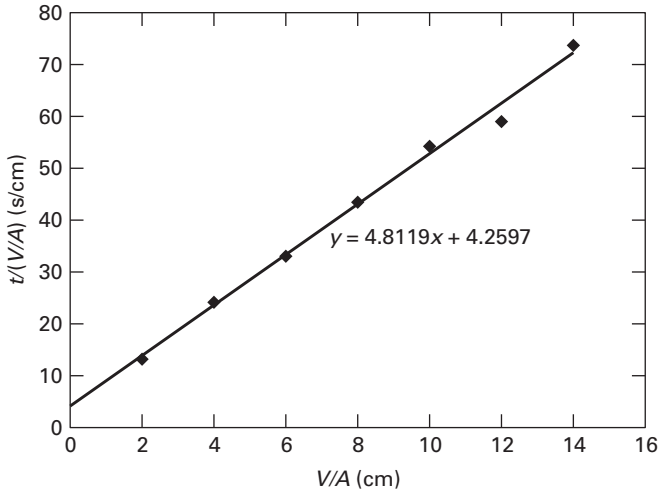

FIGURE E4.1 Plot of batch filtration data for the determination of α and R_m.

$$\begin{aligned}
\alpha &= (\text{slope})\left(\frac{2\Delta p}{\mu_0 \rho_c}\right) \\
&= \left(4.81\frac{\text{s}}{\text{cm}^2}\right)\left(\frac{2 \times 600\,\text{mm Hg} \times \dfrac{1.33 \times 10^3\,\text{g}}{\text{cm s}^2\,\text{mm Hg}}}{\dfrac{0.03\,\text{g}}{\text{cm s}} \times \dfrac{14\,\text{g}}{690\,\text{ml}}}\right) \\
&= 1.26 \times 10^{10}\,\frac{\text{cm}}{\text{g}} \\
R_m &= (\text{Intercept})\left(\frac{\Delta p}{\mu_0}\right) \\
&= \left(4.26\frac{\text{s}}{\text{cm}}\right) \times \left(\frac{600\,\text{mm Hg} \times \dfrac{1.33 \times 10^3\,\text{g}}{\text{cm s}^2\,\text{mm Hg}}}{\dfrac{0.03\,\text{g}}{\text{cm s}}}\right) \\
&= 1.13 \times 10^8\,\text{cm}^{-1}
\end{aligned}$$

This is a typical value of R_m for a large-pore (micrometer-sized) filter.

To determine the time required to obtain 10,000 liters of filtrate using a filter with an area of 10 m^2, we must make the assumption that α does not change at the new pressure drop of 500 mm Hg. We use Equation (4.2.5) and solve for time:

$$t = \frac{\mu_0 V}{\Delta p A}\left(\frac{\alpha \rho_c V}{2A} + R_m\right)$$

We calculate the two components of this equation as follows:

$$\frac{\mu_0 V}{\Delta p A} = \frac{\dfrac{0.03\,\text{g}}{\text{cm s}} \times 10^4\,\text{liters} \times \dfrac{1\,\text{m}^3}{10^3\,\text{liter}} \times \dfrac{100\,\text{cm}}{1\,\text{m}} \times \dfrac{1\,\text{h}}{3600\,\text{s}}}{500\,\text{mm Hg} \times \dfrac{1.33 \times 10^3\,\text{g}}{\text{cm s}^2\,\text{mm Hg}} \times 10\,\text{m}^2} = 1.25 \times 10^{-9}\,\text{cm h}$$

$$\begin{aligned}
\frac{\alpha \rho_C V}{2A} + R_m &= \frac{1.26 \times 10^{10}\,\dfrac{\text{cm}}{\text{g}} \times \dfrac{14\,\text{g}}{0.69\,\text{liter}} \times 10^4\,\text{liters}}{2 \times 10\,\text{m}^2\left(\dfrac{100\,\text{cm}}{\text{m}}\right)^2} + 1.36 \times 10^8\,\text{cm}^{-1} \\
&= 12.8 \times 10^9\,\text{cm}^{-1} + 0.14 \times 10^9\,\text{cm}^{-1} = 12.9 \times 10^9\,\text{cm}^{-1}
\end{aligned}$$

and finally

$$t = (1.25\times10^{-9}\ \text{cm h})(12.9\times10^{9}\ \text{cm}^{-1}) = 16.1\ \text{h}$$

Thus, this filter is probably undersized for the volume to be filtered. In addition, from this calculation we see that at the end of the filtration,

$$\frac{R_m}{R_c + R_m} = \frac{0.14}{2(12.8) + 0.14} = 0.005$$

Therefore, the filter medium is contributing very little of the resistance to filtration, a typical situation in a lengthy dead-end filtration. Also, it should be noted that 10 m^2 is a large surface area for a filter. To accommodate areas this large (and larger), filters are typically three dimensional, that is, through the use of filter press or filter leaf systems in which multiple filters are stacked atop one another, the surface area is contained in an efficient volume for manufacturing (see Section 4.3.1).

The specific resistance of the cake is directly affected by Δp_c, the pressure drop across the cake. Studies have shown that the relationship between specific resistance and pressure drop commonly takes the form [1]:

$$\alpha = \alpha'(\Delta p_c)^s \tag{4.2.6}$$

where α' and s are empirical constants. The power s has been called the "cake compressibility factor" and has been found to range from zero for incompressible cakes such as sand and diatomite (see Section 4.3.1, Conventional Filtration) to near unity for highly compressible cakes.

For products that are recovered in the filtrate, it is often necessary to wash the filter cake with water or a salt solution to maximize the removal of dissolved product from the cake. Frequently, the wash must be done with more than the volume of liquid in the cake to obtain the recovery desired. This is because some of the product is in stagnant zones of the cake, and transfer into the wash liquid from these zones occurs by diffusion, which takes place at a slower rate than the convective flow of wash through the cake. Data for the washing of filter cakes have been correlated by Choudhury and Dahlstrom [2] using the following equation:

$$R' = \left(1 - \frac{E}{100}\right)^n \tag{4.2.7}$$

where R' is the weight fraction of solute remaining in the cake after washing (on the basis that $R' = 1.0$ prior to washing), E is the percentage wash efficiency, and n is the volume of wash liquid per volume of liquid in the unwashed cake. The percentage

wash efficiency E is therefore 100% minus the percentage solute remaining in the cake after 1.0 volume of wash liquid per volume of liquid in the unwashed cake (or $n = 1.0$). Choudhury and Dahlstrom found the wash efficiency E to vary from a minimum of 35% to a maximum of 86%, with the lower values applying to cakes through which the wash liquid flows relatively rapidly.

Assuming that the liquid viscosity and the pressure drop through the bed of solids are the same during washing as during the filtration of the solids, the washing rate per cross-sectional area can be found from the filtrate flow rate per unit area given in Equation (4.2.4) at the end of the filtration. Thus, for negligible filter medium resistance for filtrate volume V_f at the end of time t_f to form the cake, this yields

$$\text{(4.2.8) Washing rate per cross-sectional area} = \left(\frac{1}{A}\frac{dV}{dt}\right)_{V=V_f} = \frac{\Delta p}{\mu_0 \alpha \rho_c (V_f/A)}$$

If V_w is the volume of wash liquid applied in time t_w, then

$$\text{(4.2.9)} \quad V_w = t_w \left(\frac{dV}{dt}\right)_{V=V_f}$$

Using the definition of $(dV/dt)_{V=V_f}$ from Equation (4.2.8), we obtain

$$\text{(4.2.10)} \quad \frac{V_w}{A} = t_w \left(\frac{1}{A}\frac{dV}{dt}\right)_{V=V_f} = \frac{t_w \Delta p}{\mu_0 \alpha \rho_c (V_f/A)}$$

At the end of the filtration, the integrated form of the filtration equation [Equation (4.2.5)], with R_m neglected, can be written

$$\text{(4.2.11)} \quad \frac{V_f}{A} = \left(\frac{2\Delta p\, t_f}{\mu_0 \alpha \rho_c}\right)^{1/2}$$

Substituting this expression for V_f/A in Equation (4.2.10) and simplifying gives

$$\text{(4.2.12)} \quad \frac{V_w}{A} = \left(\frac{\Delta p}{2\mu_0 \alpha \rho_c t_f}\right)^{1/2} t_w$$

From Equations (4.2.11) and (4.2.12), the ratio of t_w to t_f is

$$\text{(4.2.13)} \quad \frac{t_w}{t_f} = \frac{2V_w}{V_f}$$

It is helpful to write t_w/t_f in terms of n, the ratio of the volume V_w of wash liquid to the volume V_r of residual liquid in the cake:

$$\frac{t_w}{t_f} = 2\frac{V_w}{V_r}\frac{V_r}{V_f} = 2nf \tag{4.2.14}$$

where f is the ratio of V_r to the volume V_f of filtrate at the end of filtration. The ratio f can be determined by a material balance. Thus, for a given cake formation time t_f, a plot of wash time t_w versus the wash ratio n will be a straight line.

4.2.2 Crossflow Filtration

As illustrated in Figure 4.1b, the fluid in crossflow filtration flows parallel to the membrane surface, resulting in constant permeate flux at steady state. Crossflow filtration can be divided into two categories depending on whether the component being filtered is soluble or insoluble. When dissolved species such as proteins are being filtered, ultrafiltration membranes are generally used. The ultrafiltration membrane is selected so that the species of interest will not pass through these membranes. The retained species is carried to the surface of the membrane by the convective flow of fluid, and the concentration of the species builds up next to the membrane surface. The concentration of the species can be so high that it precipitates on the membrane surface, further impeding the flow of fluid through the membrane. The resulting layer of solids on the membrane surface has been called a "gel layer." In addition, even without precipitation, the increased osmolarity near the membrane surface creates a solvent gradient that opposes the applied transmembrane pressure Δp. On the other hand, when suspended particles are present, these particles are carried to the membrane surface and may form a cake at the surface. In this situation, microfiltration membranes are generally utilized. These membranes let dissolved components pass through but retain particles above a certain size. There are instances, such as in the crossflow filtration of cells that have been ruptured, where the layer at the membrane surface contains both suspended particles and precipitated solutes. More complete information about ultrafiltration and microfiltration membranes is given in Section 4.3.

Dissolved Species

In crossflow filtration, a solution under pressure flows across the surface of a membrane. As a result of this pressure, fluid is forced through the membrane. This flow toward the surface of the membrane causes species dissolved in the solution also to be carried toward the membrane's surface. For a solute that is rejected by the membrane, there will be a concentration gradient of this solute across a stagnant boundary

layer next to the surface of the membrane, as indicated in Figure 4.3. The elevation of the solute concentration at the membrane surface (c_w) compared to that in the bulk solution (c_b) is known as *concentration polarization.*

At steady state, the rate of convective mass transfer of solute toward the membrane surface must be equal to the rate of mass transfer of solute by diffusion away from the membrane surface, which is described by [3]:

$$J c = -\mathscr{D}\frac{dc}{dx} \tag{4.2.15}$$

where J is the transmembrane fluid flux, c is the concentration of the solute, and $\mathscr{D}$ is the diffusion coefficient of the solute. For a boundary layer thickness of δ, the solution of Equation (4.2.15) is

$$J = \frac{\mathscr{D}}{\delta}\ln\frac{c_w}{c_b} \tag{4.2.16}$$

which can be also written as

$$\frac{c_w}{c_b} = \exp\left(\frac{J\delta}{\mathscr{D}}\right) \tag{4.2.17}$$

The term $\mathscr{D}/\delta$ can also be defined as a mass transfer coefficient k. The ratio c_w/c_b is sometimes called the *polarization modulus* and indicates the extent of concentration polarization. From Equation (4.2.17), it can be seen that the polarization modulus is

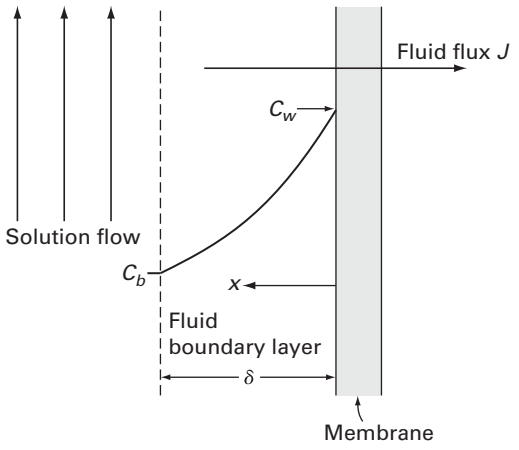

FIGURE 4.3 Schematic representation of the boundary layer in crossflow filtration with a dissolved solute in the feed. A solution flows parallel to the membrane surface, and fluid flows through the membrane under the influence of pressure. A fluid boundary layer forms next to the membrane surface, creating a gradient in the concentration c of solute.

particularly sensitive to changes in J, δ, and $\mathscr{D}$ because of the exponential functionality involved. For high molecular weight solutes (small $\mathscr{D}$) and membranes with high solvent permeability (high J), concentration polarization can become severe, with $c_w/c_b > 10$. At high concentration polarization levels, the solubility of the solute can be exceeded, resulting in the precipitation of the solute and the formation of a solids or gel layer on the membrane surface.

Experimental data have been obtained to support this simple model of concentration polarization. Figure 4.4 shows data for the ultrafiltration of the protein casein and dextran with a molecular weight of 110,000. For both species, a plot of ultrafiltration flux versus log of bulk concentration gives a straight line for bulk concentration varying by an order of magnitude. Estimates of the concentration of solute at the membrane surface can be obtained from the intercept of the straight line in Figure 4.4 at zero flux. These estimates of c_w appear to be physically reasonable.

Correlations have been developed for the mass transfer coefficient k. For laminar flow, boundary layer theory has been applied to yield analytical solutions (known as the Leveque or Graetz solutions) for k [4]:

$$k = 0.816\left(\gamma_w \frac{\mathscr{D}^2}{L}\right)^{\frac{1}{3}} \quad (4.2.18)$$

where γ_w is the fluid shear rate at the membrane surface and L is the length of the flow channel over the membrane. The constant 0.816 is applicable for the

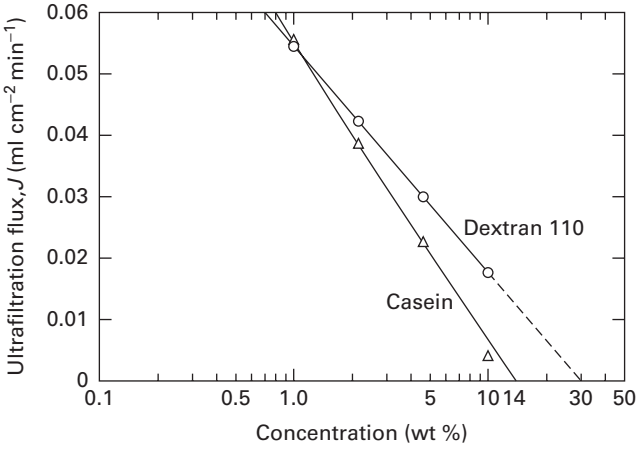

FIGURE 4.4 Decline in ultrafiltration flux with increasing concentration for solutions of casein and Dextran (MW 110,000). Data were obtained in thin-channel recirculating flow cells. *(Data from W. F. Blatt, A. Dravid, A. S. Michaels, and L. Nelsen, "Solute polarization and cake formation in membrane ultrafiltration: Causes, consequences, and control techniques," in* Membrane Science and Technology, *J. E. Flinn, ed., p. 63, Plenum Press, New York, 1970.)*

gel-polarized condition of concentration polarization where the solute concentration at the wall is constant. For a rectangular slit of height $2h$ and bulk stream velocity u_b,

$$\gamma_w = \frac{3u_b}{h} \tag{4.2.19}$$

and the equation for a circular tube of diameter D is

$$\gamma_w = \frac{8u_b}{D} \tag{4.2.20}$$

For turbulent flow, empirical correlations have been developed for the mass transfer coefficient. These correlations are based upon dimensional analysis of the equations of change for forced convection mass transfer in a closed channel, which gives [5]:

$$\mathrm{Sh} = \frac{kD_h}{\mathscr{D}} = f\left(\mathrm{Re}, Sc, L/D_h\right) \tag{4.2.21}$$

where Re $= D_h u_b \rho/\mu$ = Reynolds number
Sc $= \mu/\rho\mathscr{D}$ = Schmidt number
D_h = equivalent diameter of the channel
= 4 (cross-sectional area/wetted perimeter)
u_b = bulk stream velocity
ρ = density of fluid
μ = viscosity of fluid

A typical correlation that has been developed for this Sherwood number is [6]:

$$\mathrm{Sh} = 0.082\,\mathrm{Re}^{0.69}\mathrm{Sc}^{0.33} \tag{4.2.22}$$

Note that the L/D_h term in the generalized dimensionless analysis solution is left out of the empirical correlation in Equation (4.2.22).

EXAMPLE 4.2

Concentration Polarization in Ultrafiltration Equipment is available for ultrafiltration of a protein solution at constant volume to remove low molecular weight species (achieved by the addition of water or buffer to the feed in an operation called diafiltration—see Example 4.6). The flow channels for this system

are tubes 0.1 cm in diameter and 100 cm long. The protein has a diffusion coefficient of 9×10^{-7} cm^2/s. The solution has a viscosity of 1.2 cp and a density of 1.1 g/cm^3. The system is capable of operating at a bulk stream velocity of 300 cm/s. At this velocity, determine the polarization modulus for a transmembrane flux of 45 liters m^{-2} h^{-1}.

Solution

We see from Equation (4.2.17) that we can determine c_w/c_b if we know $J\,\delta/\mathscr{D} = J/k$, where J is as given in the problem statement. We can determine k from either Equation (4.2.18) or Equations (4.2.21) and (4.2.22), depending on whether the flow is laminar or turbulent. We first need to calculate the Reynolds number to characterize the flow regime:

$$\mathrm{Re} = \frac{D_h u_b \rho}{\mu} = \frac{0.1\,\mathrm{cm} \times \dfrac{300\,\mathrm{cm}}{\mathrm{s}} \times 1.1 \dfrac{\mathrm{g}}{\mathrm{cm}^3}}{\dfrac{0.012\,\mathrm{g}}{\mathrm{cm\,s}}} = 2750$$

In the calculation of the Reynolds number, we see that the equivalent diameter of the channel, D_h, is the same as the diameter of the tubes. The flow is turbulent, since the Reynolds number is greater than 2000. For turbulent flow, we need to know Sc, the Schmidt number:

$$\mathrm{Sc} = \frac{\mu}{\rho \mathscr{D}} \frac{\dfrac{0.012\,\mathrm{g}}{\mathrm{cm\,s}}}{1.1 \dfrac{\mathrm{g}}{\mathrm{cm}^3} \times 9 \times 10^{-7} \dfrac{\mathrm{cm}^2}{\mathrm{s}}} = 1.21 \times 10^4$$

From Equations (4.2.21) and (4.2.22),

$$k = \frac{\mathscr{D}\,\mathrm{Sh}}{D_h}$$

$$= \frac{\mathscr{D}}{D_h}(0.082)\,\mathrm{Re}^{0.69}\,Sc^{0.33}$$

$$= \left(\frac{9 \times 10^{-7} \dfrac{\mathrm{cm}^2}{\mathrm{s}}}{0.1\,\mathrm{cm}} \right) (0.082)(2750)^{0.69}\,(12{,}100)^{0.33} = 3.88 \times 10^{-3} \frac{\mathrm{cm}}{\mathrm{s}}$$

From Equation (4.2.17), the polarization modulus can be estimated:

$$\frac{c_w}{c_b} = \exp\left(\frac{J\delta}{\mathscr{D}}\right) = \exp\left(\frac{J}{k}\right)$$

$$= \exp\left(\frac{45\dfrac{\text{liters}}{\text{m}^2\text{h}} \times \dfrac{10^3\text{cm}^3}{\text{liter}} \times \dfrac{1\text{m}^2}{10^4\,\text{cm}^2} \times \dfrac{1\text{h}}{3600\text{s}}}{3.88 \times 10^{-3}\,\dfrac{\text{cm}}{\text{s}}}\right) = 1.38$$

Thus, the concentration polarization is not severe.

Concentration polarization at the surface of the membrane can become great enough that it creates a significant resistance to fluid flow. This effect on the transmembrane fluid flux J can be modeled by using Darcy's law [Equation (4.2.1)] with the flow resistance made up of the sum of the membrane resistance R_m and the resistance R_p of the polarized boundary layer and any gel layer next to the surface of the membrane. For membranes, a correction needs to be made for the osmotic pressure $\Delta\pi$ of the solute that is being filtered, which results in the following equation:

$$J = \frac{\Delta p - \sigma\,\Delta\pi}{\mu_0\,(R_m + R_p)} \tag{4.2.23}$$

where Δp is the pressure difference between the bulk fluid and the permeate, μ_0 is the viscosity of the permeate, and σ is the reflection coefficient for the solute. A reflection coefficient of 1.0 indicates no passage of solute through the membrane, while a coefficient of zero indicates free passage of the solute with the solvent through the membrane. For an ideal dilute solution,

$$\Delta\pi = RTc_w \tag{4.2.24}$$

where R is the ideal gas constant, T is the absolute temperature, and c_w is the solute concentration at the surface of the membrane.

Data for J versus Δp for the ultrafiltration of serum albumin in a stirred filtration cell are shown in Figure 4.5 as a function of both cell stirrer speed and protein concentration. At high values of Δp for 3.9 and 6.5% protein concentrations, the ultrafiltration flux J is constant with increasing Δp. Constant flux as Δp increases can be interpreted as a condition in which the solute concentration at the membrane surface c_w has reached a solubility limit; this behavior is supported by Equation (4.2.16), where J becomes constant when c_w reaches a constant.

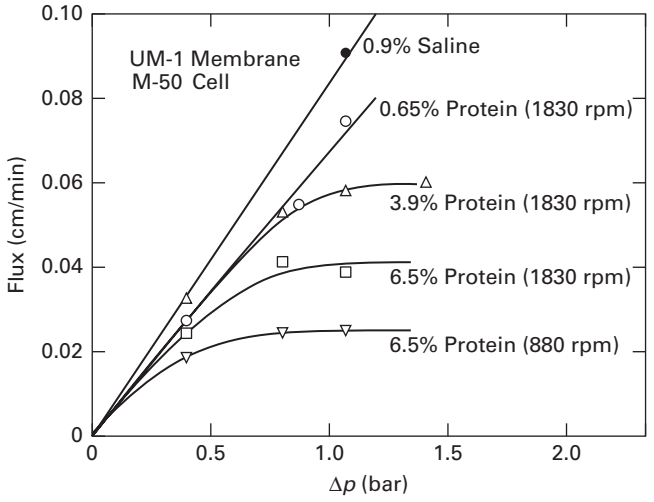

FIGURE 4.5 Ultrafiltration flux as a function of pressure drop in a stirred cell with varying protein concentration and stirring rate. *(Data from E. S. Perry, ed.,* Progress in Separation and Purification, *vol. 1, p. 318, Wiley, New York, 1968.)*

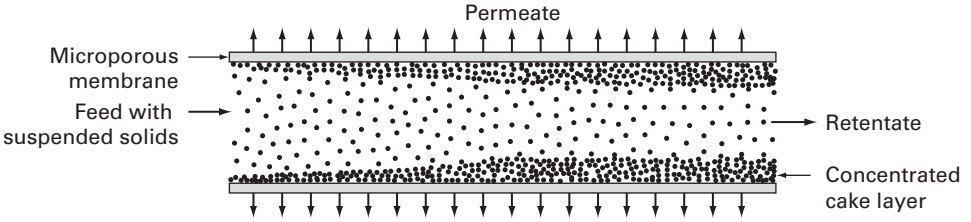

FIGURE 4.6 Illustration of the buildup of a cake layer at the membrane surface in crossflow filtration with suspended solids in the feed.

Suspended Particles

In the crossflow filtration of mixtures with suspended particles, the fluid flux toward the membrane carries particles to the membrane surface, where they are rejected and form a cake layer that is analogous to the gel layer in the ultrafiltration of dissolved species. As indicated in Figure 4.6 for crossflow filtration with microporous filtration membranes, the cake layer initially grows with time, thus reducing the permeate flux and constricting the channel. At steady state conditions, the layer reaches a constant thickness, which is relatively thin if the shear exerted by the fluid flowing tangentially to the membrane surface is high enough.

The theory for the crossflow filtration of dissolved species has been found to hold only for very small suspended particles up to approximately 1 μm in size [7]. Beyond this size, experimental membrane flux values are often one to two orders of magnitude higher than those obtained from the Leveque or Graetz theory given by Equation (4.2.18) [8]. Two different theories have been developed to more accurately predict membrane fluxes for particles larger than 1 μm, depending on the size of

the particles: a shear-induced diffusion theory for small particles and an inertial lift theory for larger particles.

The shear-induced diffusion theory was developed by Zydney and Colton [9], who proposed that the concentration polarization model could be applied to the crossflow filtration of suspended particles if the Brownian diffusivity was replaced by a shear-induced hydrodynamic diffusivity. In shear-induced hydrodynamic diffusion, the particles are randomly displaced from the streamlines in a shear flow and collide with other particles. In their model, Zydney and Colton employed an approximate relationship for the shear-induced diffusion $\mathscr{D}_s$ of spherical particles measured by Eckstein et al. [10] for $0.2 < \varphi < 0.45$

$$\mathscr{D}_s = 0.3\gamma_w a^2 \tag{4.2.25}$$

where φ is the particle volume fraction in the bulk suspension, a is the particle radius, and γ_w is the fluid shear rate at the membrane surface. Substituting for the diffusivity in the equation for the laminar flow mass transfer coefficient in the concentration polarization model [Equation (4.2.18)], we obtain

$$k = 0.366\gamma_w \left(\frac{a^4}{L}\right)^{1/3} \tag{4.2.26}$$

where L is the tube or channel length. Comparing this equation for k with the one for dissolved species in laminar flow, we see that the mass transfer coefficient is much more strongly dependent on the shear rate at the wall. Shear-induced diffusion has been found to dominate for particles up to 30 to 40 μm in size, while inertial lift dominates for larger particles [7].

Inertial lift arises when the Reynolds number based on the particle size is not negligible. Inertial lift produces a velocity that carries particles away from the membrane surface. For fast laminar flow of dilute suspensions with thin fouling layers, the steady state transmembrane flux predicted by the inertial lift theory is [7]:

$$J = \frac{0.036\rho_0 a^3 \gamma_w^2}{\mu_0} \tag{4.2.27}$$

where ρ_0 and μ_0 are the density and viscosity, respectively, of the permeate. Thus, for transport by inertial lift, the flux is strongly dependent on the particle size and shear rate at the membrane surface and not dependent at all on the length of the filter or on the concentration of particles in the bulk suspension.

EXAMPLE 4.3

Comparison of Mass Transfer Coefficient Calculated by Boundary Layer Theory Versus by Shear-Induced Diffusion Theory Cells that are 5 μm in diameter

are being concentrated by crossflow filtration using hollow fibers that are 1.1 mm in diameter (inside) and 20 cm long. The velocity of the fluid in the hollow fibers is 100 cm/s. The fluid can be assumed to have the same density and viscosity as water. The temperature is 4°C.

Compare the mass transfer coefficient k calculated using boundary layer theory with that using shear-induced diffusion theory.

Solution

Boundary layer theory

We first calculate the Reynolds number in order to determine the flow regime. At 4°C for water, $\rho = 1.00$ g/cm^3 and $\mu = 1.56$ cp from a handbook of physical properties. Therefore,

$$\mathrm{Re} = \frac{D\,u_b\rho}{\mu} = \frac{0.11\,\mathrm{cm} \times \dfrac{100\,\mathrm{cm}}{\mathrm{s}} \times 1.00\,\dfrac{\mathrm{g}}{\mathrm{cm}^3}}{\dfrac{0.0156\,\mathrm{g}}{\mathrm{cm\,s}}} = 705$$

The upper limit of the Reynolds number for laminar flow in tubes is about 2100. Therefore, the flow is laminar in our case. For laminar flow in tubes, we can calculate k using Equations (4.2.18) and (4.2.20). Equation (4.2.18) requires the diffusion coefficient for the cells, which can be estimated from the Stokes-Einstein equation for spheres, Equation (1.8.9):

$$\mathscr{D} = \frac{kT}{6\pi\mu a} = \frac{\left(1.38\times10^{-23}\,\dfrac{\mathrm{J}}{\mathrm{K}}\right)(277\,\mathrm{K})\left(\dfrac{10^7\,\mathrm{g\,cm^2\,s^{-3}}}{\mathrm{J\,s^{-1}}}\right)}{6\pi\left(0.0156\,\dfrac{\mathrm{g}}{\mathrm{cm\,s}}\right)(2.5\times10^{-4}\,\mathrm{cm})} = 5.20\times10^{-10}\,\mathrm{cm^2\,s^{-1}}$$

From Equations (4.2.20) and (4.2.18), respectively,

$$\gamma_w = \frac{8u_b}{D} = \frac{8\times100\,\dfrac{\mathrm{cm}}{\mathrm{s}}}{0.11\,\mathrm{cm}} = 7273\,\mathrm{s^{-1}}$$

$$k = 0.816\left(\gamma_w\,\frac{\mathscr{D}^3}{L}\right)^{1/3} = 0.816\left(\frac{7273\,\dfrac{1}{\mathrm{s}}\times\left(5.20\times10^{-10}\,\dfrac{\mathrm{cm^2}}{\mathrm{s}}\right)^2}{20\,cm}\right)^{1/3} = 3.77\times10^{-6}\,\mathrm{cm\,s^{-1}}$$

Shear-induced diffusion

For laminar flow with shear-induced diffusion, Equation (4.2.26) applies:

$$k = 0.366\gamma_w\left(\frac{a^4}{L}\right)^{1/3} = 0.366\left(7273\frac{1}{\text{s}}\right)\left(\frac{\left(2.5\times10^{-4}\right)^4\ \text{cm}^4}{20\ \text{cm}}\right)^{1/3} = 1.54\times10^{-2}\ \text{cm s}^{-1}$$

Therefore, k is more than 4000 times greater when calculated using shear-induced diffusion theory than when calculated using Fickian diffusion theory.

4.3 FILTER MEDIA AND EQUIPMENT

In the development of a filtration process, much effort is often devoted to the evaluation of the filter media and equipment that are available. The filter media and equipment selected can have a large impact on the process economics, both in terms of the capital outlay required and the operating expenses. Filter media and equipment considerations are discussed in this section for both conventional and crossflow filtration.

4.3.1 Conventional Filtration

Filter Media

There are many different filter media [11, 12], so the choice of the type to use can be difficult. The choice, however, is heavily governed by the type of filtration equipment being used. The filter media most commonly used in the conventional filtration of biotechnology products are woven fabrics, metal fabrics or screens, and rigid porous media. Sterile filtration in biopharmaceutical production is usually carried out in the conventional mode, and the medium is either a membrane filter or a depth filter, depending on whether a liquid solution or air is being filtered.

Woven fabrics are available in a wide variety of materials. The chemical resistance of the fabric is a primary consideration for the filtration of biotechnology products. There should be minimal or no leaching of components from the fabric during filtration, and the fabric should be able to withstand any chemicals used during cleaning. For filtration involving a filter cake, woven fabrics are the most common type of filter medium. The minimum size of particles trapped in woven fabrics is 10 μm.

Metal fabrics or screens are available in several types of weave in nickel, copper, brass, aluminum, steel, stainless steel, Monel, and other alloys. Metal media are especially desirable when good resistance to leaching and corrosion is required. The smallest size of particles trapped in woven wire media is 5 μm.

Rigid porous media are available in sheets and tubes. A wide variety of materials is available for rigid porous media, including sintered stainless steel and other metals, silica, porcelain and other ceramics, and some plastics.

For the sterile filtration of solutions, an asymmetric membrane filter (see Section 4.3.2) is used in cartridge style. Typically, these membranes are made of cellulose esters or other polymers and have pore sizes of 0.22 or 0.45 μm. In the sterile filtration of air, two types of filters are typically found. High-efficiency particulate air (HEPA) filters are large, high-throughput ventilation filters used to reduce the particulate load in a room. HEPA filters are typically depth-type filters that can collect microbes and other airborne particulates at high flow rates. Depth filters consist of compacted beds of pads of fibrous material such as glass wool. The other type of filter for the sterile filtration of air is a vent filter, installed on all equipment that needs to be filled or drained, such as product tanks. Vent filters are typically hydrophobic asymmetric membrane filters, rated at 0.22 μm.

Filter Aids

It is possible to significantly improve the filtration operation by adding a powdered solid, called a filter aid, to a feed that is to be filtered. The filter aid can be either added directly to the feed or applied to the filtration equipment. The objectives of the first approach, the admixture of the filter aid powder to the suspension, are to keep the pores in the filter cake open, to make the cake less compressible, and to provide faster filtration. In the second approach, the filter medium is precoated with a layer of the filter aid. Rotary vacuum filters can be operated with "precoat" (see the next section).

A successful filter aid must be highly permeable. Other important properties of filter aids that should be considered are surface properties, chemical resistance, and compatibility with the product.

Two of the most widely used types of filter aid are diatomite (kieselguhr or diatomaceous earth) and perlite. Diatomite is the skeletal remain of diatoms, which are a type of algae. The skeletal structure of diatomite particles gives them a high intrinsic permeability. Diatomite consists mostly of silica and thus is insoluble in both strong acids and strong alkalies. Perlite, a glassy volcanic material consisting mainly of aluminum silicate with some combined water, expands on heating during processing to give highly porous particles. Perlite is sometimes used for rough filtrations where high flow rates are desirable and less significance is given to filtrate clarity.

Equipment

A large variety of conventional filtration equipment is available. This equipment can be classified according to the driving force for filtration, whether by pressure, vacuum, or gravity. Conventional filtration equipment may be designed for batch, semicontinuous, and continuous operation.

One of the most common types of batch filter is the plate-and-frame filter press (Figure 4.7). This filter consists of a varying number of filter chambers with either

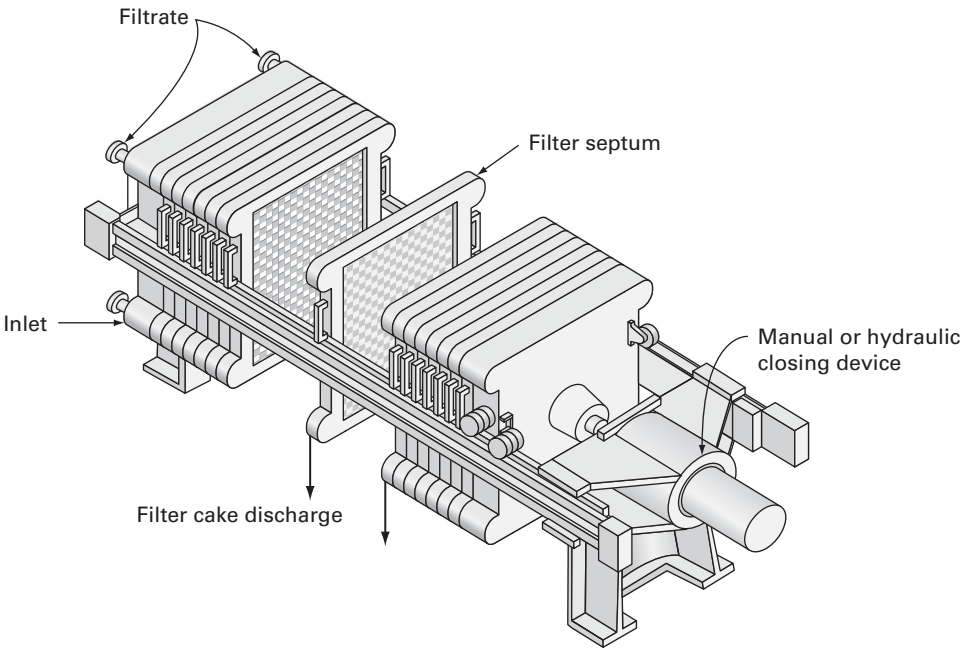

FIGURE 4.7 Plate-and-frame filter press.

medium-covered recessed filter plates, or medium-covered plates alternated with frames that provide space for the cake. The chambers are closed and tightened by a hydraulic ram or screw that pushes the plates and frames together. The feed to be filtered enters the filter press under pressure and fills each chamber simultaneously. The liquid passes through the filter medium, and the solids are retained on the medium. The clear filtrate is taken off at a discharge outlet. Mechanized systems are available for opening and closing of the filter press at the end and commencement of each filtration cycle. Because the filter cake is open to the atmosphere at the end of each cycle, this filter should not be used when the filter cake poses a biohazard.

Other types of batch filter are the horizontal or vertical leaf filter, plate filter, tray filter, tube or candle filter, and Nutsche filter. These devices are similar in that they are all pressure filters, with the filter medium being enclosed within a pressure vessel. Because these filters are enclosed, they are advantageous when one is working with materials that must be contained. A vertical leaf filter is shown as an example in Figure 4.8. The filter leaves are covered with the filter medium on either side, and the filtrate passing into the inside of each filter leaf flows into a filtrate manifold. The Nutsche filter, consisting of one horizontal medium-covered filter plate dividing half of a tank, is the simplest type of pressure filter.

The most common type of semicontinuous or continuous filter for biotechnology products is the rotary vacuum filter. The operation of a rotary vacuum filter is

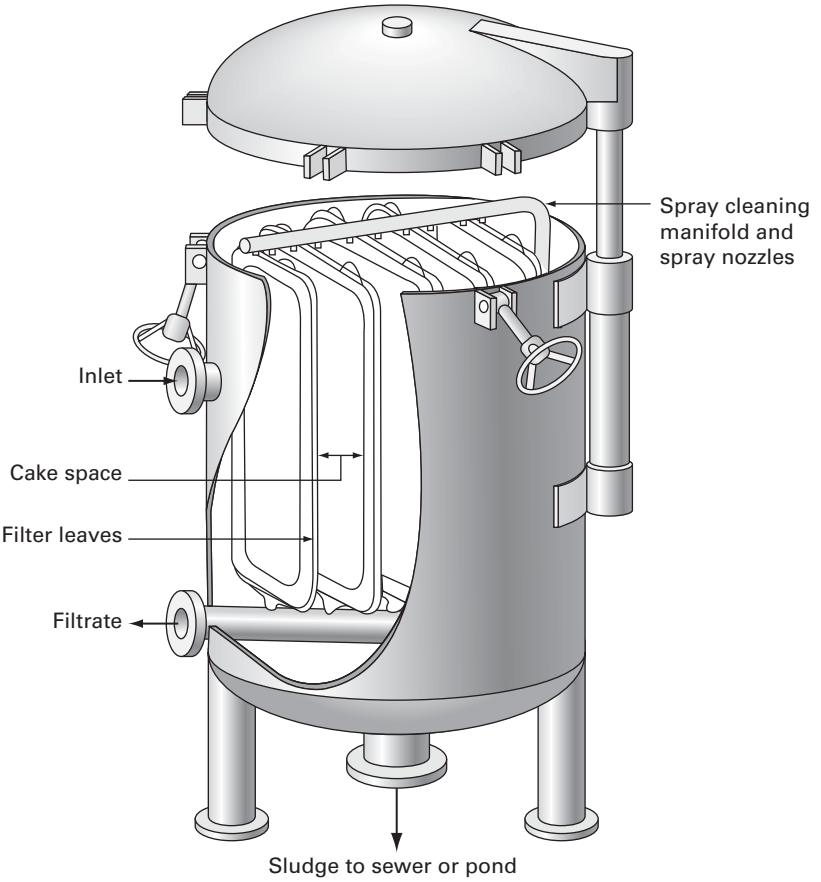

FIGURE 4.8 Vertical leaf filter.

illustrated in Figure 4.9. The drum rotates slowly about its horizontal axis and is partially submerged in a slurry reservoir. The surface of the drum is covered with the filter medium, and a vacuum is maintained below the medium on the inside of the drum. Liquid is sucked through the filter medium, and solids in the feed are retained on the medium. Filtration is followed by washing and dewatering. Several different types of cake discharge can be used: simple knife discharge, advancing knife discharge (with precoat filtration), belt or string discharge, and roller discharge. Because the feeds for biotechnology applications tend to be slimy and nongranular, precoat filtration is commonly used during rotary vacuum filtration. In precoat filtration, the filter medium is coated with a thick layer of diatomaceous earth or other type of filter aid. The solids being filtered penetrate a small distance into the precoat. The knife is adjusted to remove all the feed solids on the filter, including any precoat penetrated with feed solids to give a fresh surface of precoat. When the thickness of the precoat becomes small, a fresh batch of precoat is applied to the drum.

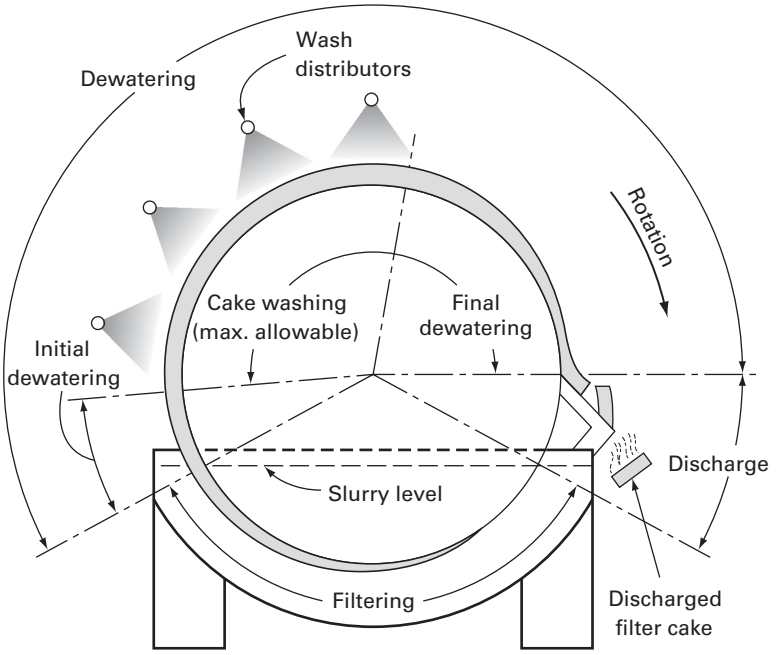

FIGURE 4.9 Rotary vacuum filter.

4.3.2 Crossflow Filtration

Filter Media (Membranes)

Filter media for crossflow filtration are generally referred to as membranes. There are two general categories of membranes: ultrafiltration membranes and microporous membranes. The separation between ultrafiltration (UF) and microfiltration (MF) is based on the pore size of the membrane, with membranes having pores 0.1 μm and larger considered to be microporous. The pore sizes of UF membranes are in the range of 0.001 to 0.1 μm [13], although these membranes are usually classified by their molecular weight cutoff (MWCO), which is the molecular weight of a globular solute at which the solute is rejected by the membrane. Typically, a 90% rejection level is used for establishing the MWCO. Ultrafiltration membranes can be obtained down to a MWCO level of 1000 Daltons (Da) and up to as high as 1,000,000 Da. There is also a category of membranes called reverse osmosis (RO) or hyperfiltration membranes that pass only water and a very low flux of solutes. A very good RO membrane rejects 99.7% or more of sodium chloride [11].

Three basic structures are commonly used for membranes: homogeneous, asymmetric, and composite. These three types are illustrated in Figure 4.10. The homogeneous structure has no significant variation in pore diameter from the feed side to the filtrate side. In the asymmetric structure, there is a thin layer on the feed side of the filter that has very small pores. Below this layer is a much thicker layer that has much larger pores and serves as structural support for the membrane. The composite membrane is similar to the asymmetric membrane in having a thin layer containing

FIGURE 4.10 Three commonly used membrane structures: (*a*) homogeneous: uniform pore profile through filter; (*b*) asymmetric: finer filtering surface faces feed suspension; and (*c*) composite: two types of materials used.

very small pores next to the filtering surface; however, the thin and thick layers of this membrane are made of two different types of material.

Backflushing composite filters is generally not recommended. The major element in pressure drop across the filter is due to the thin layer with very small pores, and so significantly more mechanical force is applied to the area of the thin layer, compared to the support layer. When operated in the intended direction, the thin layer is forced towards the support layer. But when operated in the opposite direction, the thin layer is forced away from the support layer, which can lead to delamination.

Filtration membranes are made from a wide variety of polymers and inorganic materials. The polymers that are used include cellulose acetate, polyamide, polyether, polycarbonate, polyester, polypropylene, polyethylene, regenerated cellulose, poly(vinyl chloride), poly(vinylidene fluoride) (PVDF), poly(tetrafluoroethylene) (PTFE), acrylonitrile copolymers, and polyethersulfones. The inorganic materials used include ceramics, zirconium oxide, borosilicate glass, stainless steel, and silver.

Equipment

Crossflow filtration membranes are available in a variety of configurations. The membranes are housed in a physical unit called a *module*. The membrane module must satisfy a number of mechanical, hydrodynamic, and economic requirements, the most important of which are the following [13]:

Mechanical: obtain effective (physical) separation of the feed and permeate streams; provide the necessary physical support for the membrane (including the ability of the module to endure the required pressure drops and any backflushing).

Hydrodynamic: minimize pressure drops through the module (to reduce pumping costs); optimize solute mass transfer (reduce concentration polarization); minimize particulate plugging or fouling; avoid dead spots (for sanitary design); allow for or promote turbulence (for sanitary design and to reduce boundary layer thickness).

Economic: maximize membrane packing density (ratio of membrane area to module volume); minimize manufacturing costs; permit easy access for cleaning and/or membrane replacement; provide sufficient chemical resistance and operational lifetime; incorporate modularity of design for easy scaleup, staging, or cascading.

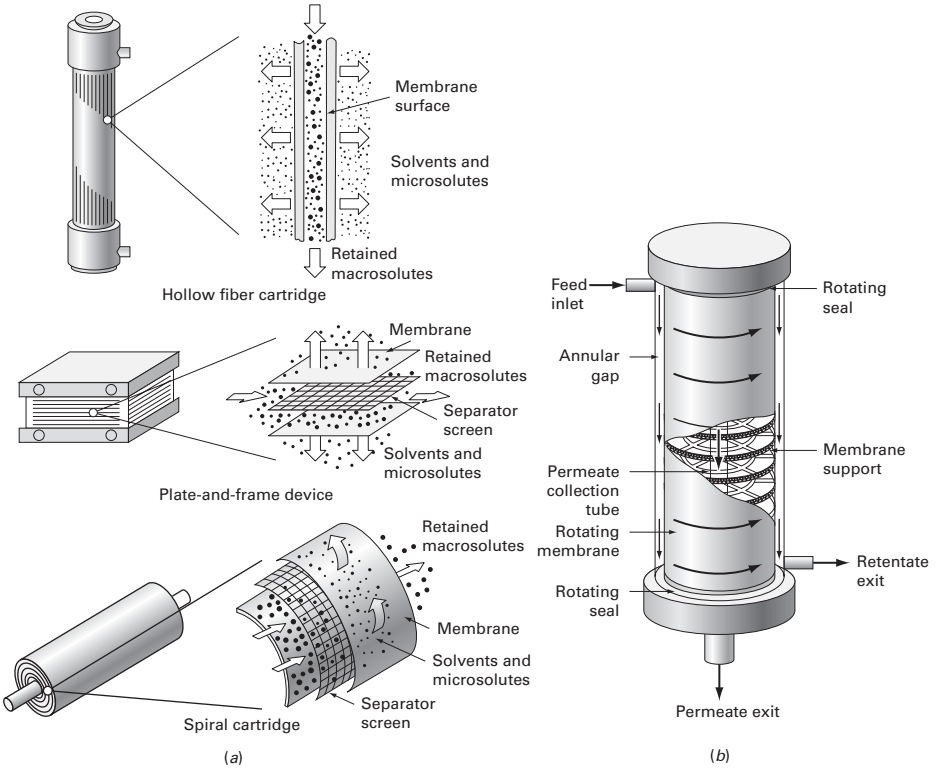

FIGURE 4.11 Schematic representations of filter modules. (*a*) Hollow-fiber, plate-and-frame, and spiral-wound membrane modules. (*b*) A rotating cylinder module.

Several of these criteria are in mutual opposition: for example, modules with high membrane packing density tend to be highly susceptible to plugging with particulates. Therefore, the choice of a particular module involves balancing these criteria to arrive at the most economic system for each particular application.

There are five types of module configuration for crossflow filtration (Figure 4.11): hollow fiber, tubular, flat plate, spiral wound, and rotating. The tubular module has the same general configuration as the hollow-fiber module, but the tubes have much larger diameters than the fibers. Some key characteristics of these modules are compared in Table 4.1.

Hollow-fiber modules consist of an array of narrow-bore, self-supporting fibers that generally have an asymmetric membrane structure. The dense skin layer is usually on the lumen side of the fiber, but it can be placed on the outside. The feed flows through the lumen of the fibers when the dense skin layer is on the lumen side, and the flow is typically laminar, although hollow-fiber systems by some manufacturers can be operated in turbulent flow. Since the hollow fibers are self-supporting, they can be cleaned by backflushing, that is, by reversing the direction of the permeate flow. One disadvantage of hollow-fiber modules is that the entire module usually needs to be replaced upon the rupture of even a single fiber. Also, to avoid plugging of the small-diameter fibers, feed streams generally need to be prefiltered.

TABLE 4.1 Comparison of Key Characteristics of Crossflow Membrane Modules[a]

Module type	Channel spacing (cm)	Packing density (m^2/m^3)	Energy costs	Particulate plugging	Ease of cleaning
Hollow fiber	0.02–0.25	1200	Low	High	Fair
Tubular	1.0–2.5	60	High	Low	Excellent
Flat plate	0.03–0.25	300	Moderate	Moderate	Good
Spiral wound	0.03–0.1	600	Low	Very high	Poor–fair
Rotating	0.05–0.1	10	Very high	Moderate	Fair

[a]See reference [13].

Except for some inorganic membranes, tubular membranes are not self-supporting and are usually cast in place within a porous support tube made of fiberglass, ceramic, plastic, or stainless steel. The feed flows through the inside of the tubes, while the permeate flows radially outward across the membrane and support tube. Inorganic membranes are usually constructed in a honeycomb monolith unit in which the membranes are arranged in a parallel array. Tubular systems are typically operated in the turbulent flow regime. Because of the large diameter of the tubes in these systems, the pumping costs are relatively high compared to other module configurations operated in turbulent flow. In addition, large diameter tubes decrease the filter surface area to module volume ratio, leading to bigger equipment footprints. The chief advantages of tubular modules are that they are highly resistant to plugging by particulates, and they can be cleaned by backflushing. The diameter of the tubes can be selected to avoid prefiltration of the feed.

Most flat-plate systems are in a rectangular configuration. The flow channels can be open or can have separator screens to improve the mass transfer characteristics. Units with open channels are usually operated in laminar flow, while those with separator screens are often operated with flow in the turbulent regime. One disadvantage of these modules is that backflushing is often impractical because the membranes are effectively supported only on one side.

Spiral-wound modules are constructed from flat sheet membranes separated by spacer screens. The feed solution is fed into one end of the module and flows through the separator screens along the surface of the membranes. The retentate is then collected on the other end of the module. The permeate spirals radially inward, eventually to be collected through a central tube. The flow in these systems tends to be turbulent. The main disadvantage of spiral-wound modules is that they are susceptible to fouling by particulates because of the narrow and irregular flow through the spacers.

One effective rotating-type module is the rotating cylinder device originally proposed by Hallstrom and Lopez-Leiva [14]. The feed flows into a thin annular region between two concentric cylinders (Fig. 4.11b). Either cylinder or both can be porous and can have a membrane bound to the surface. With the membrane on the inner cylinder, permeate is collected in the central chamber. When the membrane is on the

outer cylinder, permeate is collected in a separate annular permeate region adjacent to the outer porous cylinder. The inner cylinder is rotated at high speed (typically > 3000 rpm) to induce the formation of Taylor vortices, which effectively mix the fluid near the surface of the membrane and thereby increase the mass transfer coefficient for the solutes/particles in the feed. The vortices also help reduce the thickness of the cake or gel layer at the membrane surface. One advantage of this system is that the rate of mass transfer is determined almost entirely by the rate of rotation of the inner cylinder, which effectively decouples the mass transfer characteristics from the feed flow rate. As a result, the rotating devices can be operated at very low flow rates and with minimal pumping costs. Since, however, the energy requirements for rotating the device are usually very high, capital costs are high, and scaleup is very difficult, these systems have been limited to small-scale operation.

4.4 MEMBRANE FOULING

Fouling of membranes results from physical and/or chemical interactions between the membrane and various components that are present in the process stream. Fouling leads to a decline in the permeate flux and a change in the membrane selectivity. Because of the high affinity of proteins for solid surfaces, proteins are the leading contributor to fouling in bioseparations by UF and MF. The flux decrease caused by proteins can be attributed to one or more of the following processes [7]:

- Protein adsorption, which involves the interaction of the proteins and the membrane and occurs with no convective flow through the membrane
- Protein deposition, which is the addition of more protein that is associated with the membrane, over and above the protein that would be adsorbed in a nonflowing system
- Protein accumulation on the membrane surface exposed to the flowing process stream as a result of concentration polarization, which can lead to formation of a gel layer

This last effect is governed by the mass transfer coefficient [see Equations (4.2.18) and (4.2.22)], and thus can be minimized by increasing the fluid shear rate at the filtering surface of the membrane. These three processes can lead to pores in membranes that are constricted and even completely blocked, as illustrated in Figure 4.12.

Protein adsorption studies have been performed for both MF and UF membranes to determine the extent to which the pores are constricted by adsorbed protein. To eliminate concentration polarization effects, these studies were done in the absence of flow. The work with MF membranes and a variety of proteins showed that there was approximately monolayer adsorption throughout the internal pores [7]. Protein adsorption was reduced on the more hydrophilic membranes such as the hydrophilic PVDF type, with only a fraction of monolayer adsorption. A study of the adsorption

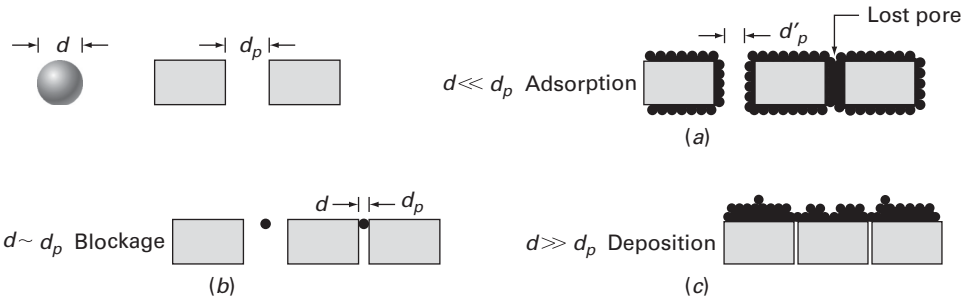

FIGURE 4.12 Mechanisms of membrane fouling. (*a*) Pore narrowing and constriction. (*b*) Pore plugging. (*c*) Solute deposition and formation of a gel or cake layer. Dimensions: *d*, protein or particle diameter; d_p, clean pore diameter; and d'_p, effective pore diameter in the presence of adsorbed proteins or particles.

of bovine serum albumin (molecular weight 69,000 Da) on UF membranes indicated the following extents of protein coverage within the ultrathin skin portion of the membrane: monolayer adsorption for the 300,000 Da MWCO membrane, only about half a monolayer for the 100,000 Da MWCO membrane, and no measurable protein adsorption for the 50,000 Da MWCO membrane [15]. Thus, protein fouling within the membrane can be completely eliminated by making the pore size small enough.

To account for fouling caused by irreversible adsorption and deposition of proteins and other biological molecules to the membrane surface, it is useful to write Darcy's law (Equation 4.2.23) for the transmembrane flux in terms of the clean membrane resistance (R_m), the resistance due to concentration polarization and a gel layer on the membrane surface (R_p), and the resistance caused by irreversible fouling (R_{if}) [16]:

$$J = \frac{\Delta p - \sigma \Delta \pi}{\mu_0 (R_m + R_p + R_{if})} \tag{4.4.1}$$

In this model, irreversible fouling is considered the fouling that can only be removed by cleaning agents such as acids, bases, enzymes, surfactants, and disinfectants; and the resistance caused by concentration polarization and any gel layer is that which can be removed by physical means, such as circulation of feed through the system at zero transmembrane pressure and relatively high shear rate, or by backflushing using negative transmembrane pressure to remove foulants from the membrane surface [13]. A comprehensive review of methods to control fouling in microfiltration and ultrafiltration membranes has been given by Hilal et al. [17].

A study of protein ultrafiltration by Rajabzadeh et al. has given insight into the relative contributions of the three resistances in Equation (4.4.1). Soy protein extract was ultrafiltered using polysulfone hollow fibers with a molecular weight cutoff of 100 kDa, and the three resistances were measured after a short (2 minutes)

filtration period [16]. As shown in Figure 4.13, the resistance R_p from concentration polarization and a gel layer increased with average transmembrane pressure (TMP, or average Δp) and was greater than the membrane and irreversible fouling resistances (R_m and R_{if}). Increasing TMP causes J to increase, thus causing greater convection of proteins to the membrane surface, leading to more concentration polarization. Computational fluid dynamics modeling was used to estimate R_p and R_{if} as a function of volume concentration ratio (VCR) and membrane length (Figure 4.14), where

$$VCR = \frac{V_{feed}}{V_{feed} - V_{permeate}} \quad (4.4.2)$$

Both R_p and R_{if} increased as the concentration progressed (i.e., as VCR increased). The transmembrane flux was both measured and modeled as a function of VCR, as shown in Figure 4.15. The decrease in flux with VCR is consistent with the increase in both R_p and R_{if} with VCR. The model showed that increasing the axial velocity caused an increase in permeate flux J, but the increase is relatively small.

4.5 SCALE-UP AND DESIGN OF FILTRATION SYSTEMS

Experimental testing is generally needed in the scale-up and design of conventional and crossflow filtration systems. This is especially true for bioprocesses because of the unique features of each bioprocess that is being considered. For example, in the filtration of ruptured cells, there can be great differences in the filtration characteristics of ruptured cells of different types; these differences can even exist for cells of the same class (e.g., yeasts). Some of the more common small-scale tests are described, as well as considerations in the design of filtration systems.

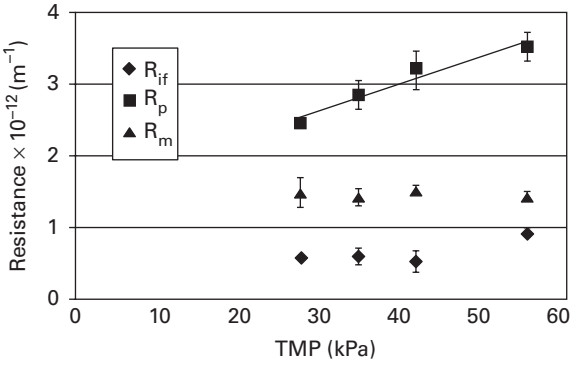

FIGURE 4.13 Effect of transmembrane pressure (TMP) on resistances in the ultrafiltration of soy protein extract at an axial velocity of 1 m s^{-1} using polysulfone hollow fibers with a molecular cutoff of 100 kDa. R_{if}, irreversible fouling resistance; R_p, concentration polarization and gel layer resistance; and R_m, membrane resistance. *(Data from A. Rajabzadeh, C. Moresoli, and B. Marcos, "Fouling behavior of electroacidified soy protein extracts during cross-flow ultrafiltration using dynamic reversible-irreversible fouling resistance and CFD modeling,"* J. Membr. Sci.*, vol. 361. p. 191, 2010.)*

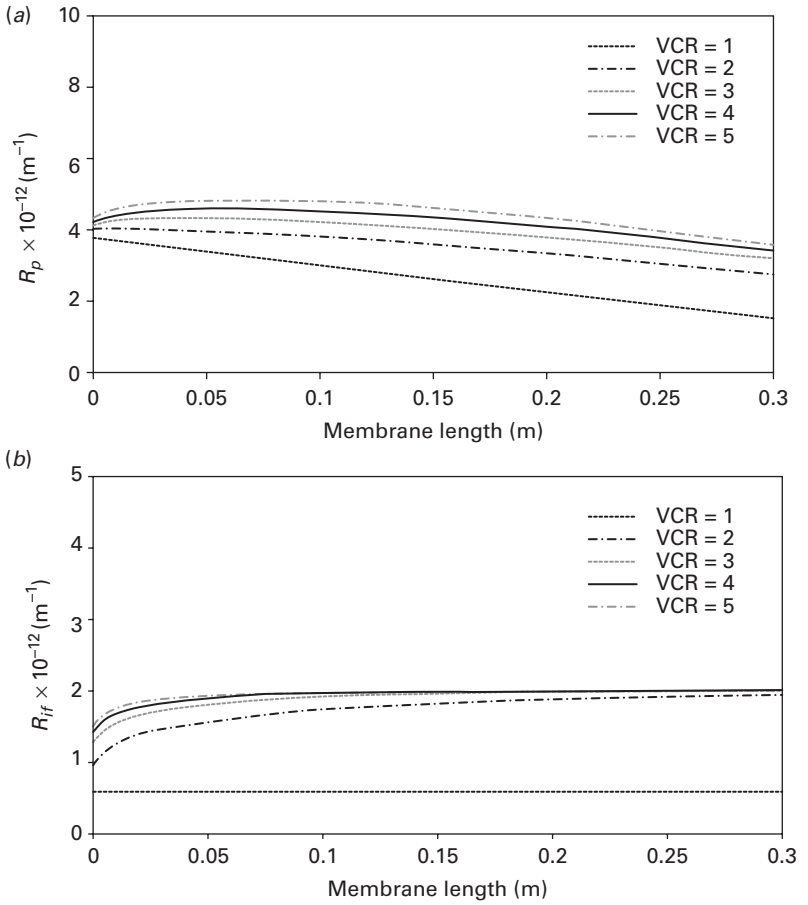

FIGURE 4.14 Computational fluid mechanics modeling results for the effect of membrane length and volume concentration ratio (VCR) on estimated concentration polarization resistance (*a*) and irreversible fouling resistance (*b*) for the ultrafiltration of soy protein extract at an axial velocity of 1 m s^{-1} and TMP of 34.5 kPa using polysulfone hollow fibers with a molecular cutoff of 100 kDa. *(Data from A. Rajabzadeh, C. Moresoli, and B. Marcos, "Fouling behavior of electroacidified soy protein extracts during cross-flow ultrafiltration using dynamic reversible-irreversible fouling resistance and CFD modeling,"* J. Membr. Sci.*, vol. 361. p. 191, 2010.)*

4.5.1 Conventional Filtration

Small-scale testing procedures are described for the two basic types of conventional filtration, vacuum filtration and pressure filtration. A large majority of all continuous filters use vacuum as the driving force for filtration. Occasionally, however, an enclosed pressure filter is needed in a bioprocess because of the presence of biohazards. The design of sterile filtration systems is also discussed.

Vacuum and Pressure Filtration

To develop data for scaling up the rotary vacuum filter (Figure 4.9), tests with a filter leaf are usually performed. The objective is to simulate the operation of a large-scale rotary vacuum filter (see the stages of operation indicated in Figure 4.9). A laboratory

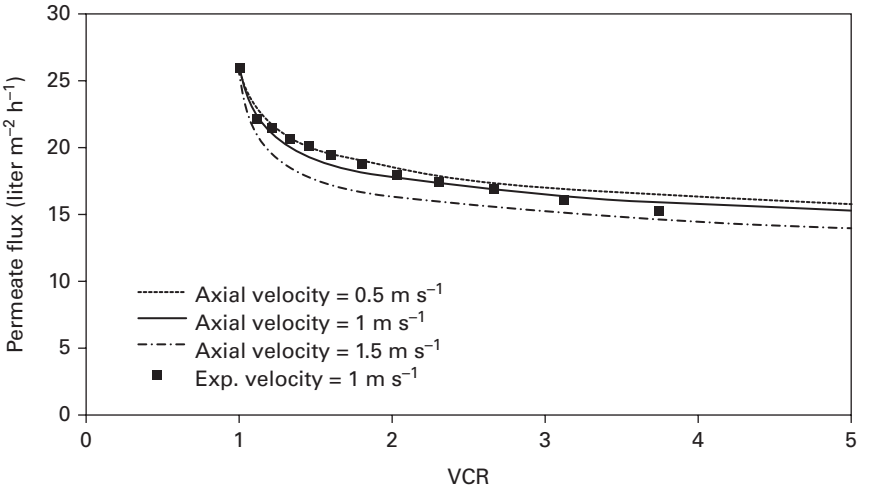

FIGURE 4.15 Comparison of model and experimental results for the effect of volume concentration ratio (VCR) and axial velocity on permeate flux for the ultrafiltration of soy protein extract at a TMP of 34.5 kPa using polysulfone hollow fibers with a molecular cutoff of 100 kDa. *(Data from A. Rajabzadeh, C. Moresoli, and B. Marcos, "Fouling behavior of electroacidified soy protein extracts during cross-flow ultrafiltration using dynamic reversible-irreversible fouling resistance and CFD modeling,"* J. Membr. Sci.*, vol. 361. p. 191, 2010.)*

system for doing vacuum filter leaf tests with a precoat is shown schematically in Figure 4.16; filter leaves that do not use a precoat are similar. To do a filter leaf test with the leaf shown in Figure 4.16, the leaf should first be precoated with a filter aid. The precoat is trimmed off until it is flat with the top of the cake ring of the leaf. The leaf is then submerged in the broth being filtered for the amount of time that the rotating drum will be submerged. To simulate the washing segment of the rotating drum, the leaf is submerged in water or other wash liquid for the amount of time of washing for the rotating drum. The leaf is removed from the wash liquid, and air is allowed to be pulled through the cake to dewater it. The cake ring is then screwed down to expose precoat that has not been penetrated by the broth solids, and the solids above the top of the ring are cut off with a knife. The leaf now has a fresh surface of precoat and is ready for another cycle of filtration, washing, and dewatering. This procedure can be repeated for as many cycles as desired. The volume of filtrate and weight of the cake can be measured, and analyses can be performed on the filtrate and cake. For example, if it were desired to recover a protein in the filtrate, the cake solids and the filtrate (plus wash) should be analyzed for the protein.

EXAMPLE 4.4

Rotary Vacuum Filtration It is desired to filter a cell broth at a rate of 2000 liters/h on a rotary vacuum filter (see Figure 4.9) at a vacuum pressure of 70 kPa. The cycle time for the drum will be 60 s, and the cake formation time (filtering time) will be 15 s. The broth to be filtered has a viscosity of 2.0 cp and a cake solids (dry basis) per

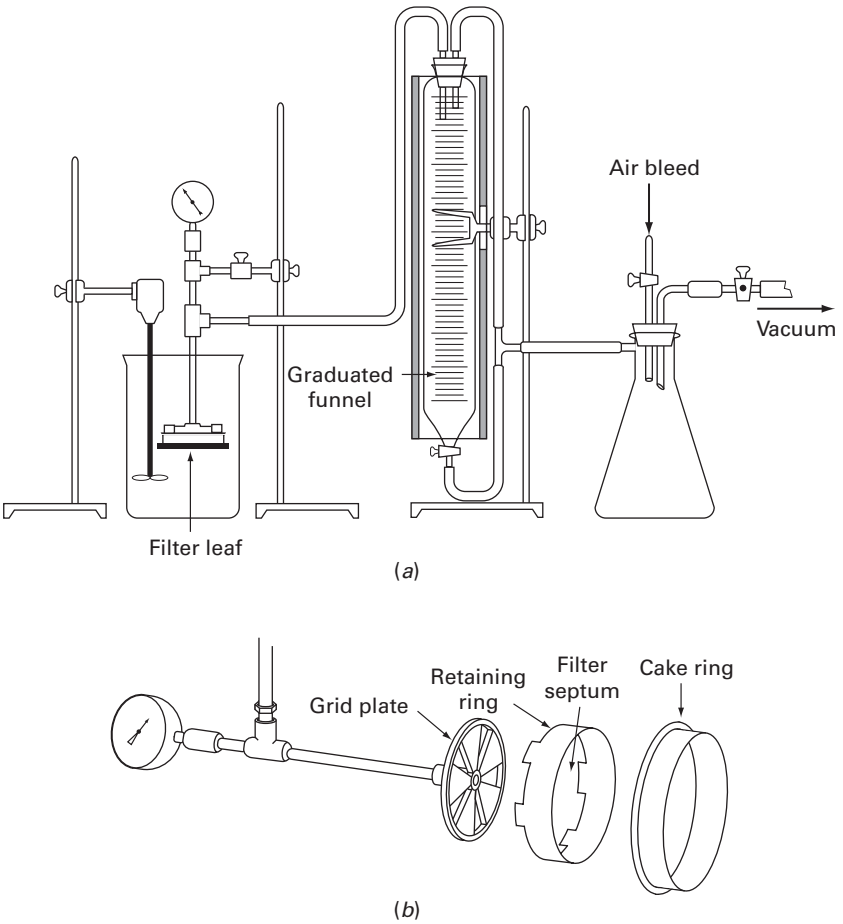

FIGURE 4.16 (*a*) Filter leaf apparatus, and (*b*) detail of a precoat filter leaf.

volume of filtrate of 10 g/liter. From laboratory tests, the specific cake resistance has been determined to be 9×10^{10} cm/g. Determine the area of the filter that is required. The resistance of the filter medium can be neglected.

Solution

We can use the integrated form of the filtration equation, Equation (4.2.5), with $R_m = 0$:

$$\frac{t}{V/A} = \frac{\mu_0 \alpha \rho_c}{2\Delta p}\left(\frac{V}{A}\right)$$

We solve for A^2 to obtain

$$A^2 = \frac{\mu_0 \alpha \rho_c V^2}{2\Delta p\, t}$$

In applying this equation, it is helpful to focus on the area of the drum that is submerged, which is where the cake is being formed and where filtrate is being obtained. Thus, A is the area of that part of the drum that is submerged. We can calculate the volume of filtrate that needs to be collected during the cake formation time of 15 s:

$$V_{15s} = \frac{2000\,\text{liters}}{\text{h}} \times 15\,\text{s} \times \frac{1\,\text{h}}{3600\,\text{s}} = 8.33\,\text{liters}$$

We use this volume of filtrate with $t = 15$ s in the equation for A^2 to obtain

$$A^2 = \frac{\frac{0.02\,\text{g}}{\text{cm s}} \times 9 \times 10^{10}\,\frac{\text{cm}}{\text{g}} \times 10\,\frac{\text{g}}{\text{liter}} \times (8.33\,\text{liters})^2 \times \frac{\text{cm s}^2\,\text{kPa}}{10^4\,g} \times \frac{10^3\,\text{cm}^3}{\text{liter}} \times \left(\frac{\text{m}}{10^2\,\text{cm}}\right)^4}{2 \times 70\,\text{kPa} \times 15\,\text{s}}$$

$$= 0.595\,\text{m}^4$$

$$A = 0.771\,\text{m}^2$$

The area A' of the entire rotary vacuum filter can be calculated from the cake formation time and the total cycle time as

$$A' = \left(\frac{60\text{ s}}{15\text{ s}}\right) \times 0.771\,\text{m}^2 = 3.08\,\text{m}^2$$

This is a medium-sized rotary vacuum filter, with possible dimensions of 1.0 m diameter by 1.0 m long.

EXAMPLE 4.5

Washing of a Rotary Vacuum Filter Cake For the filtration in Example 4.4, it is desired to wash a product antibiotic out of the cake so that only 5% of the antibiotic in the cake is left after washing. We expect the washing efficiency to be 50%. The filter cake can be assumed to contain 70 wt% water. Estimate the washing time per cycle that would be required.

Solution

From Equation (4.2.7) for the washing efficiency of a filter cake

$$R' = \left(1 - \frac{E}{100}\right)^n$$

where R' is the weight fraction of solute remaining in the cake after washing (on the basis of $R' = 1.0$ before washing), E is the percentage wash efficiency, and n is

the volume of wash liquid per volume of liquid in the unwashed cake. Substituting $R' = 0.05$ and $E = 50\%$ into this equation gives

$$n = 4.32$$

From Equation (4.2.14), the relationship between the washing time t_w and the cake formation time t_f is given by

$$t_w = 2n\,f\,t_f$$

where f is the ratio of volume V_r of residual liquid in the cake to the volume of filtrate V_f after time t_f. Thus, we need to estimate the volume of residual liquid in the filter cake to determine t_w. At the end of the 15 s cake formation time,

$$\text{Weight of dry cake solids filtered} = 10\frac{\text{g}}{\text{liter}} \times 8.33\,\text{liters} = 83.3\,\text{g}$$

Since the filter cake contains 70 wt% water, we find

$$\text{Weight of water in the filter cake} = \frac{70}{30} \times 83.3 = 194\,\text{g}$$

Thus,

$$f = \frac{V_r}{V_f} = \frac{0.194}{8.33} = 0.0233$$

$$t_w = 2n\,f\,t_f = 2(4.32)(0.0233)(15\,\text{s}) = 3.0\,\text{s}$$

From this result, the estimated washing time is 20% of the cake formation time.

For small-scale tests of pressure filtration, a bomb filter may be used (Figure 4.17). The bomb filter contains a filter leaf, typically 2 in. by 2 in., that is covered with an appropriate filter medium. Enough slurry is placed in the bomb to cover the filter leaf. Air may be sparged into the slurry to provide gentle agitation. After the filtration has been started at a given pressure, the filtrate volume is recorded as a function of time. After a given time for filtration of the slurry, the cake can be washed with a wash liquid and dewatered by flowing air through the cake. Analyses can be performed on the cake and filtrate plus wash.

The data obtained from small-scale filtration tests can be used to calculate the filtration rate and area of the large-scale unit. For units in which the filter medium is continuously washed, it is recommended that filtration rates calculated from small-scale filtration data be multiplied by a factor of 0.9 [11]. For units in which the filter medium is not continuously washed, this factor should be reduced to 0.8.

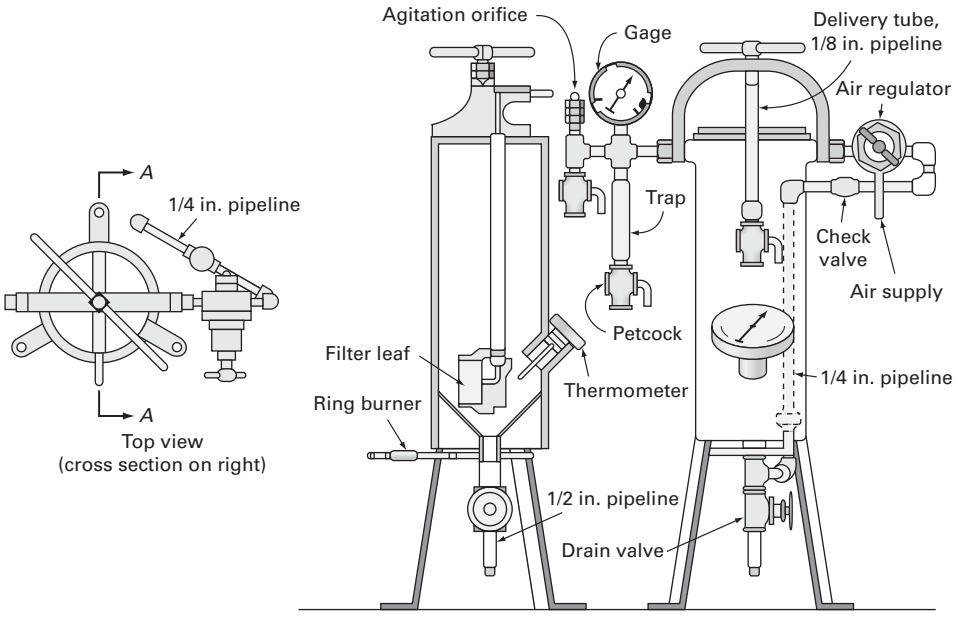

FIGURE 4.17 Bomb filter for small-scale pressure filtration tests.

Before scaling up the filtration area, the relationship between the nominal filtration area and the active filtration area should be determined. The nominal filtration area is based on the overall dimensions of the filtering surface. The active filtration area may be less than the nominal area because part of the filtration surface may be blinded by mechanical dividers or by painting.

Considerations for the Design of Sterile Filters

Sterile filtration is an important application of conventional filters in the pharmaceutical industry, where many products are sold in sterile form. It is sometimes desirable that other processing steps besides the final one be carried out under sterile conditions, which requires the filtration of both liquids and air.

Liquid Sterile Filtration

In typical sterile liquid filtration applications, there is no appreciable filter load, no cake buildup, and no contribution to filtration resistance from the filtrate that is reliable or reproducible. Further, there is no opportunity to add filter aids to form a cake, since this is usually the last step in a clean process.

Sizing of the filter is almost always based on the maximum allowable load in the solution to be filtered, and the desired sterility assurance limit. The sterility assurance limit is the calculated probability of a single unit of product containing a single microorganism. This is expected to be a maximum of 10^{-3} for aseptic processes, and one usually designs in an extra order of magnitude at least. One determines the maximum load on the filter by knowing the bioburden or viral load specification of the purified pool from the preceding step, or by knowing the acceptable microbial or viral levels in the raw materials that make up that pool. The retentive requirement

for the filter is then divided by the retention capability (per area) of the filter to be used. The resulting filter area is the minimum required to meet the sterility goal of fewer than one unit dose contaminated with one organism per thousand doses manufactured. The next step is to ensure that the filter is large enough to allow reasonable processing times. Typically, one does not want to filter for more than one shift (8 h). At 24 h, questions will be raised about "grow-through" (where retained microbes will have colonized the filter and "grown through" to the other side). The filtration time for the filter sized is determined by finding the clean water flow rate for the filter, either through laboratory experiment or through the vendor's published materials, and adjusting for the viscosity of the solution to be filtered relative to water (a correction for the effect of temperature on viscosity may be necessary). Once the flow rate is known, the time to filter a given size batch can be determined. The area of the filter can be adjusted up to reduce the filtration time, but cannot be adjusted down without jeopardizing the sterility assurance.

For the ultimate filtration step, in which the product is rendered sterile, a depth filter is often added upstream of the membrane filter. This protects the sterile filter from fouling during use. It is very risky to replace a sterile filter once in place, with all the connections downstream sterilized. Depth filters with high "dirt loads" can keep particulate matter from reaching the membrane surface, keeping it clean for the removal of microbes. Two sterile filters are sometimes used in series, for added sterility assurance. This gives very high probability that dosage units will not be contaminated, but the arrangement sometimes becomes difficult to manage in other respects. For instance, multiple sterility-assurance tests must be performed, a requirement that adds manipulations and increases chances for breeches in sterility.

Filters used for the purpose of sterilizing pharmaceutical products must be tested to ensure that they have been properly installed and have no defects that could allow sterility to be compromised. The two most common tests for a sterile filter for an aqueous product are the "bubble point" and the "pressure hold" or "diffusion" test. In both tests, a wetted, sterilized filter is pressurized with air or nitrogen. In the bubble point test, this pressure is increased until the lowest pressure is found at which air passes freely through the filter. It is assumed that this is the pressure required to overcome the surface tension and viscosity of water in the largest membrane pore (where the forces are the weakest). As the pore size of the membrane decreases, the bubble point increases. This test will also detect a sliced or unseated O-ring or other seal failure. The pressure hold test pressurizes a wetted filter to a pressure lower than the bubble point and measures either the total flow of gas through the membrane (by diffusion) or the rate of pressure decay. Both should be low, and both should meet the manufacturer's specifications for an intact, properly installed sterile filter.

Compatibility and extractable tests need to be performed on each filter type, in addition to testing each installed filter for sterility assurance. Compatibility means that the filter does not adsorb an active ingredient or any other type of active excipient, such as an antibiotic or preservative. Such adsorption to the filter medium can change the strength (or biological potency) of the solution after the filtration step.

Extractables are chemicals that can leach out of the filter medium, such as monomers from the membrane or support medium, filter coatings or mold-release agents, and storage solutions, such as ethanol. These chemicals would be considered impurities in the final product and should be removed. When the filter is used in the final sterilization step, impurities leaching into the product cannot be allowed. Compatibility and extractables should be tested in a sample of the product solution. When this is not possible, because product or excipients would interfere with the analysis of the impurities, a placebo or similar solution should be used.

Viral filtration is an emerging technology in the manufacture of biopharmaceuticals, specifically those manufactured from mammalian cell culture. Viral filters have pore sizes on the order of 10 nm, so that they exclude virus particles as small as 20 nm. These filters are qualified in viral clearance studies, in which high titers of model viruses are spiked into a sample product stream, and their recovery measured downstream of the filter. Clearance is typically measured in logs, and 5 logs are typical removal rates for viral filters. The sizing of viral filters is typically based on amount of protein filtered per unit area. Many virus filters are constructed using hollow fibers and require using the crossflow mode. For these filters, R_m is very high, but the pressure the filter can support is very low, sometimes only around 1 atm. For this reason, virus filtration can take extremely long times. The technology is still not standardized and several platforms exist. More research is needed in the application and scale-up of virus filters.

Air Sterile Filtration

Air filters are also sized based on the anticipated flow rate. Airflows are specified with one or more of the following criteria: pressure differential between areas, air changes per hour, or linear flow rate. Pressure differentials are usually measured between rooms, or between rooms and corridors. These are specified when it is important for air to flow from a "cleaner" area to a "dirtier" area when doors, windows, or pass-throughs are opened between them. Pressure differentials are typically 50 to 150 Pa (= 0.5–1.5 cm of water, or 0.4–1.1 mm Hg (torr)). Air changes per hour are often specified for rooms based on hazardous materials or operations the room is designed for. Air changeover is the airflow rate divided by the volume of the room. Air changeovers are different from "makeup rate," which is the fraction of fresh air injected in the room's air handler.

Clean rooms often have very high changeover rates but low makeup rates. Rooms handling solvents or hazardous materials have high makeup rates (also called "once-through air") but low air cleanliness requirements. The changeover rate varies with the hazard of the material. Linear flow rate is usually specified in hoods and smaller spaces. Linear flow rates of 5 to 20 ft/s (= 1.5–6.1 m/s) are found in laminar flow hoods, in aseptic areas where pharmaceuticals are sterile processed, and in clean rooms where microelectronics are manufactured. Linear flow rates are established to prevent airborne microbes and particulate matter from settling in or on the materials being processed. The flow rate required for the

room or area being ventilated can be determined by one or more of the specifications just cited.

The air quality of a room or area is typically classified according to the number of airborne particles that can be measured in a cubic meter. Increasingly, rooms are being classified according to the International Organization for Standardization (ISO), which has published a series of documents numbered 14644 (volumes 1–5). These standards classify clean room space as 1 (cleanest) through 9 (dirtiest), with each classification allowing approximately one log more particles in a cubic meter of air than the previous. For biotechnology and pharmaceuticals, the most commonly used grades are ISO Class 5 (similar to the military standard Class 100) to ISO Class 8 (similar to the military standard class 100,000). ISO Class 5 is used for aseptic processing where products may be briefly exposed to the environment, and ISO Class 8 is used for areas containing primarily closed operations. High-efficiency particulate air (HEPA) filters are routinely tested for integrity by spraying a polyalphaolefin (PAO) aerosol on the feed side of the filters. The typical specification for a PAO test is a 10^3 reduction in aerosol particles.

Vent filters filter air on tanks and drainable equipment. Vent filters typically follow the same specification as the liquid filters used in the process. Vent filters are also sized based on the maximum airflow rate anticipated. The maximum flow rate is often encountered when the tanks are being filled or cleaned. Vent filters must allow flow in both directions, which is a unique requirement among filters discussed in this chapter.

Integrity testing of vent filters is an evolving technology. These filters are typically hydrophobic, so bubble points and pressure holds are not appropriate. The PAO tests will not work because vent filters are typically membrane filters (which are the most compact), while HEPA filters are depth filters. Testing bubble points in solvents is feasible, and often performed, but is considered a destructive form of measurement.

4.5.2 Crossflow Filtration

As for conventional filtration, scale-up of crossflow filtration requires data from laboratory or pilot scale units. There are, however, more different types of designs possible for crossflow filtration compared to conventional filtration because of the various modes of operation that can be used for crossflow filtration and because there is often a choice between batch and continuous operation for crossflow filtration.

Crossflow filtration modules are available from manufacturers for carrying out laboratory or pilot plant tests. The size of a plant unit can be determined by a direct scale-up of the filtration area based on the feed or permeate flow rate. For this scale-up, however, it is important that the following variables be kept constant [18]:

- Inlet and outlet pressures
- Crossflow (or tangential) velocity

- Flow channel sizes (height and width)
- Feed stream properties—test slurries should be representative of the actual process streams
- Membrane type and configuration—test data from one design cannot directly be used to design another geometry

Maintaining the inlet and outlet pressures, the crossflow velocity, and the flow channel size means that the length of the flow path is constant as well. It is also important to make an assessment of the rate of fouling of the membranes. Tests should be performed for several cycles of operation to estimate the fouling rate and to determine how fouling can be kept to a minimum.

There are four basic modes of operation of crossflow filtration (Figure 4.18): batch concentration, diafiltration, purification, and complete recycle. In the batch concentration mode, the retained stream containing the product suspended particles or dissolved macromolecules is reduced in volume. In diafiltration, the volume of the retained stream is maintained constant by the continuous addition of water or buffer, which results in the removal of low molecular weight solutes into the permeate. Diafiltration is commonly used when salt removal or exchange is desired. In the purification mode, a low molecular weight product passes into the permeate and is thus separated from higher molecular weight impurities; or, the product can be retained and impurities removed in the filtrate. In the complete recycle mode, both the retained stream and the permeate are returned to the feed tank. Systems may be operated in complete recycle at start-up to reach

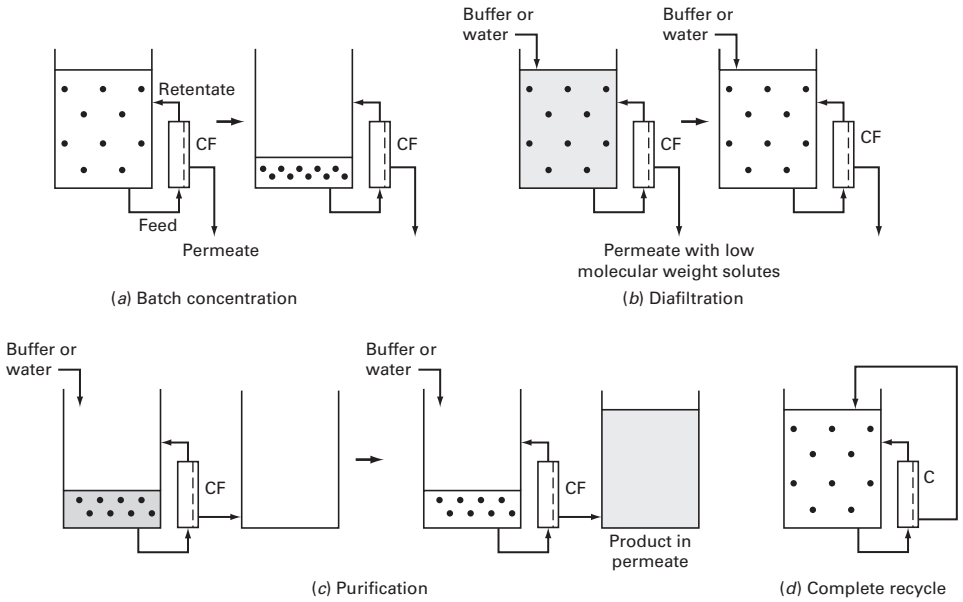

FIGURE 4.18 The four basic modes of operation of crossflow filtration (CF = crossflow filter): before the arrow, start of the operation; after the arrow, end of the operation.

steady state, saturate the membranes, test for leaks and blockage, and adjust the feed rate.

Diafiltration is similar to dialysis in that salts are exchanged or removed in both modes. Dialysis is a laboratory method that involves placing the feed in a bag made with an ultrafiltration membrane. The bag is placed in a large volume of the new solvent desired, and the new solvent is mixed until the system comes to equilibrium or near equilibrium. Complete equilibrium takes 3 to 5 h, while 90% equilibrium can be reached in 2 to 3 h [19]. For a complete change of solvent, it is necessary to do the dialysis at least twice. It is frequently the job of the engineer to scale up a dialysis done in the laboratory to a diafiltration in the pilot plant or plant. For scaling and planning, it is customary to perform material balances on solids mass and liquid volume around any component of the operation.

EXAMPLE 4.6

Diafiltration Mode in Crossflow Filtration It is desired to use a crossflow filtration system to desalt 1000 liters of a protein solution containing NaCl. The system is capable of operating at a transmembrane flux of 30 liters m^{-2} h^{-1}. To remove 99.99% of the salt, determine the time required and the volume of water required using a crossflow filtration unit with a membrane area of 100 m^2.

Solution

We operate the system in the diafiltration mode, which means that the volume of the solution being desalted is maintained constant. A material balance on the salt in the retained volume gives

$$V\frac{dc_s}{dt} = -QC_s(1 - r_s)$$

where V = volume of solution being desalted
c_s = concentration of salt in volume V
r_s = fraction of salt rejected by the membrane
Q = filtration rate (volume/time)

For this case we assume that there is no rejection of salt by the membrane, so that $r_s = 0$. Integrating the differential equation with the initial time equal to zero gives

$$\ln\frac{c_s}{c_{s0}} = -\frac{Qt}{V}$$

where c_{s0} = initial salt concentration. Solving for t, we obtain

$$t = -\frac{V \ln \dfrac{c_s}{c_{s0}}}{Q} = -\frac{(1000\,\text{liters})(\ln 0.0001)}{\left(30\dfrac{\text{liters}}{\text{m}^2\,\text{h}}\right)(100\,\text{m}^2)} = 3.07\,\text{h}$$

$$\text{Volume of water required} = (3.07\,\text{h})\left(30\frac{\text{liters}}{\text{m}^2\,\text{h}}\right)(100\,\text{m}^2) = 9210\,\text{liters}$$

Thus, a relatively large volume of wastewater will be generated by this process.

In designing a diafiltration process, a decision must be made about the concentration of retained product at which to operate. As this concentration is increased, the filtration flux will decrease according to Equation (4.2.16), and the total volume of filtrate will decrease for the removal of a given percentage of a low molecular weight solute. This leads to an optimum concentration to minimize the time required, which can be determined mathematically if the relation between filtrate flux and concentration in the bulk fluid (c_b) is known [20].

The basic components in the design of a crossflow filtration system are shown in Figure 4.19. A pump flows the feed through the filtration module to give a permeate and a retentate or retained stream. The pump needs to be sized to provide the desired flow velocity and pressure. The transmembrane pressure is controlled by a back-pressure valve on the retentate stream exiting from the filtration module. Thus the transmembrane pressure drop is estimated by

$$\Delta p_{TM} = \frac{1}{2}\left(p_i + p_o\right) - p_p \tag{4.5.1}$$

where p_i and p_o are the retentate pressures in and out of the module, respectively, and p_p is the pressure of the outlet permeate. In designing a crossflow filtration system, it is important to minimize the occurrence of gas-liquid interfaces, since bioproduct denaturation, especially of proteins, can occur at these interfaces in the presence of mechanical shear and turbulent flow (see Section 1.4.7).

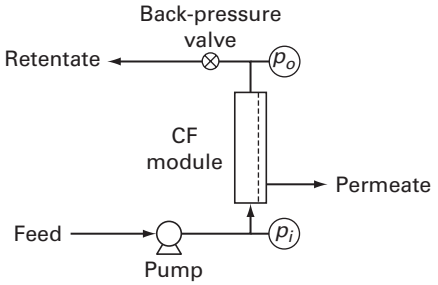

FIGURE 4.19 Basic components of a crossflow filtration system.

Crossflow filtration systems may be designed to operate in the batch or the continuous mode (Figure 4.20). In a batch system, feed is pumped through the filtration module and then back to the feed tank. In a variation of this mode (called semibatch) for diafiltration, fluid is continuously added to the feed tank to keep the feed volume constant (Figure 4.18b).

In the continuous mode of operation, also sometimes called the "feed-and-bleed" mode, or "retentate bleed" mode, feed is added to a recirculation loop by the feed pump, and concentrate exiting in the retained stream is withdrawn from the system so that the concentration factor (i.e., concentration in the retentate divided by the concentration in the feed) is at the desired value. When steady state has been achieved, the concentrate will be at its maximum concentration, which means that the filtration flux will be at a minimum throughout the run [20]. It is generally more economical to use a multistage system in a continuous process (Figure 4.21). As more stages are added, the average filtration flux approaches that for a batch system, and thus the total filtration area decreases as more stages are added. This is illustrated in Table 4.2, where batch ultrafiltration operation is compared with continuous operation using one, two, three, and five stages.

Because of the economic advantages of continuous operation and reduced tankage, this scheme is preferable to batch operation for most large-scale ultrafiltration operations [11]. Another advantage of continuous operation is that it permits the minimization of the residence time of the product in the crossflow filtration unit, which is important for products that are sensitive to heat or shear. Dairy and food

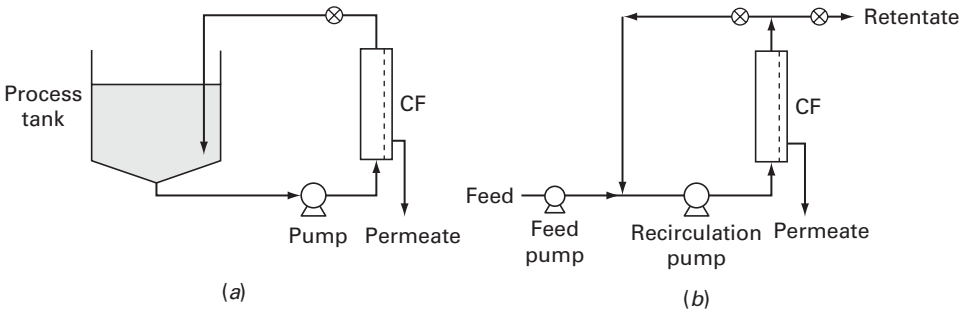

FIGURE 4.20 Comparison of (*a*) batch and (*b*) single-stage continuous (feed-and-bleed) crossflow filtration systems.

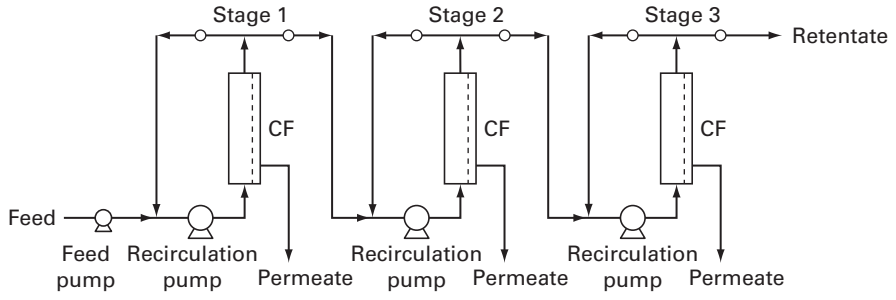

FIGURE 4.21 Multistage crossflow filtration system using the retentate bleed mode.

TABLE 4.2 Comparison of Batch and Continuous Ultrafiltration Systems[a]

System[b]	Flux (liters m^{-2} h^{-1})	Total area (m^2)
Batch	33.1 (average)	136
Continuous		
One-stage	8.1	555
Two-stage	31.1	243
	8.1	
Three-stage	38.7	194
	23.4	
	8.1	
Five-stage	44.7	165
	35.6	
	26.4	
	17.3	
	8.1	

[a] See reference [20].

[b] System design for 10× concentration factor and feed rate of 5000 liters/h. Flux from $J = 20 \ln(30/c_b)$.

proteins are generally processed continuously, while most pharmaceutical and biological products are processed using batch operation [20].

4.6 SUMMARY

Filtration separates particulate or solute components in a fluid suspension or solution according to size by flowing under a pressure differential through a porous medium. The two broad categories of filtration are conventional (or dead-end) filtration and crossflow filtration. Fluid flows perpendicular to the filter medium in conventional filtration and parallel to the membrane in crossflow filtration.

- Filtration can be used to accomplish a number of objectives, including the removal of cells or cell debris, the concentration of cells or protein solutions, and the removal or exchange of salts.
- The calculation of solvent fluxes and filtration times for conventional filtration is accomplished using various forms of Darcy's law, which states in general that the flux of filtrate is equal to pressure drop divided by viscosity and resistance, $J = \Delta p/\mu_0 R$, where R is a combination of the resistance R_m of the filter medium and the resistance R_c of the cake solids.
- The time to wash a filter cake to remove all but a desired minimal level of solute can be estimated on the basis of the washing efficiency (E), the filtration time and volume of filtrate before washing, and the volume of residual liquid in the cake.

- At steady state during the crossflow filtration of a stream containing a dissolved solute, the fluid flux of permeate through the membrane is given by

$$J = \left(\frac{\mathscr{D}}{\delta}\right) \ln\left(\frac{c_w}{c_b}\right)$$

where $\mathscr{D}$ is the solute diffusion coefficient, δ is the mass transfer boundary layer thickness next to the membrane, and c_w and c_b are the solute concentrations at the wall and in the bulk fluid, respectively. The term $\mathscr{D}/\delta$ is a mass transfer coefficient that can be predicted for both laminar and turbulent flow.

- For suspended particles greater than 1 μm in crossflow filtration, the boundary layer analysis for dissolved solutes gives low predictions of the fluid flux, and a shear-induced diffusion theory and an inertial lift theory have been used to predict fluxes for this situation, depending on the particle size.
- A variety of filter media, membranes, and equipment is available for conventional and crossflow filtration.
- Fouling of membranes adds another resistance to the transmembrane flux in crossflow filtration. Membrane fouling by proteins can be attributed to one or more of the following processes: (1) protein adsorption, which involves the interaction of the proteins and the membrane and occurs with no convective flow through the membrane, (2) protein deposition, which is the addition of more membrane-associated protein over and above the protein that would be adsorbed in a nonflowing system, and (3) protein accumulation on the membrane surface exposed to the flowing process stream as a result of concentration polarization, producing a solids or gel layer on the membrane surface.
- The scale-up of a conventional filtration can be performed with values of the specific cake resistance α and medium resistance R_m determined in laboratory filter leaf tests, assuming that feed stream properties are constant and that α does not change with a change in pressure drop upon scale-up. A crossflow filter can be scaled up directly based on membrane area, provided pressures, crossflow velocity, flow channel sizes, feed stream properties, and membrane type and configuration are held constant.
- There are numerous special considerations for the design and operation of sterile filters for liquids and air.
- There are four basic modes of operation of crossflow filtration: batch concentration, diafiltration, purification, and complete recycle. A multistage continuous process is generally more economical than a batch process in large-scale operations.

NOMENCLATURE

a	radius of spherical particles (cm)
A	filter cross-sectional area (cm^2)
c	concentration of solute (M, or g $liter^{-1}$)
D	diameter of tube (cm)
D_h	equivalent diameter of channel (cm)
$\mathscr{D}$	diffusion coefficient of solute ($cm^2\ s^{-1}$)
$\mathscr{D}_s$	shear-induced diffusion coefficient for a suspended particle ($cm^2\ s^{-1}$)
E	washing efficiency for a filter cake (%)
f	ratio of volume of residual liquid in filter cake to volume of filtrate at end of filtration (dimensionless)
h	half-height of rectangular flow channel (cm)
J	transmembrane fluid flux (liter $m^{-2}\ h^{-1}$)
k	mass transfer coefficient (= $\mathscr{D}/\delta$) (cm s^{-1})
L	length of flow channel over membrane (cm)
n	volume of wash liquid per volume of liquid in unwashed filter cake (dimensionless)
p	pressure (kPa)
R	overall resistance to filtration (cm^{-1})
R	gas constant (0.082058 liter atm $mol^{-1}\ K^{-1}$)
R_c	resistance of filter cake (cm^{-1})
R_{if}	resistance from irreversible membrane fouling (cm^{-1})
R_m	resistance of filter medium or membrane (cm^{-1})
R_p	resistance from concentration polarization and a gel layer (cm^{-1})
R'	weight fraction of solute remaining in the cake after washing (on the basis that $R' = 1.0$ before washing)
Re	Reynolds number (= $D_h u_b \rho/\mu$) (dimensionless)
Sc	Schmidt number (= μ/ρD) (dimensionless)
Sh	Sherwood number (= $kD_h/\mathscr{D}$) (dimensionless)
t	time (s)
T	temperature (K)
TMP	Average transmembrane pressure, or average pressure drop (mm Hg)
u_b	bulk fluid velocity (cm s^{-1})
V	volume of filtrate (conventional filtration) or volume of retentate (diafiltration) (liters)
VCR	volume concentration ratio (dimensionless)

Greek Letters

α	specific cake resistance (cm g^{-1})
α'	resistance parameter for a compressible cake (cm $g^{-1}\ Pa^{-s}$)
γ_w	shear rate at membrane surface (s^{-1})

δ boundary layer thickness (cm)
Δp pressure drop (mm Hg)
$\Delta \pi$ osmotic pressure (mm Hg)
Θ angle of drum rotation of rotary vacuum filter after entering broth (rad)
μ viscosity of fluid (g cm^{-1} s^{-1})
μ_0 viscosity of filtrate or permeate (g cm^{-1} s^{-1})
ρ density of fluid (g cm^{-3})
ρ_c mass of dry cake solids per volume of filtrate (g $liter^{-1}$)
σ membrane reflection coefficient for a solute (dimensionless)
φ particle volume fraction in bulk suspension (dimensionless)
ω rate of drum rotation of rotary vacuum filter (rpm)

PROBLEMS

4.1 Conventional Batch Filtration In a laboratory test of the filtration of a cell culture, the following equation was obtained to describe the filtration:

$$\frac{t}{V/A} = K_1\left(\frac{V}{A}\right) + K_2$$

where $K_1 = 0.18$ min/cm^2 and $K_2 = 0.017$ min/cm.The cell slurry has a viscosity of 2 cp, and the filter cake solids (dry basis) per volume of filtrate was 13 g/liter. The pressure drop for the filtration was 610 mm Hg (0°C). Determine the specific cake resistance α and the medium resistance R_m. Evaluate the relative significance of the medium resistance after 5 min of filtration.

4.2 Batch Filtration with Change in Pressure In a filtration of suspended cells under full vacuum using a 20 cm Büchner funnel, you collect data for the volume of filtrate as a function of time (see Table P4.2). The concentration of cells was 100 g/liter (mass of dry cake solids per volume of filtrate), and the viscosity of the filtrate was 1.0 cp.

TABLE P4.2

Time (min)	Volume filtered (liters)
0	0
20	4
30	5
40	6.5
50	7
60	7.5
70	7.8

(a) What is the resistance of the filter medium?
(b) What is the specific resistance of the cake layer?

(c) Being disappointed in the amount of time required, you decide to give the vacuum filter a boost by pressurizing the funnel to 1 atm gage pressure. The result is the same. Concerned that you may have done the wrong thing, you then remove the funnel pressure and reduce the vacuum in the flask to 0.5 atm. The result is the same. Determine the dependence of the specific resistance of the cake layer as a function of the pressure drop. Comment on what is happening in the filtration.

(d) What is the most effective change you can make to decrease the time required to filter a given volume?

4.3 Filtration on a Filter with Uniform Cylindrical Pores A depth filter has a membrane resistance of $R_m = 10^{12}$ cm^{-1} and retains all particles greater than 0.4 μm in diameter. Design a filter having uniform straight cylindrical pores with identical performance (including identical flux) to that of this depth filter using a polycarbonate film 200 μm thick.

(a) How many pores per square centimeter must the filter with straight cylindrical pores have?

(b) Is a filter with straight cylindrical pores feasible in this situation?

Hint: Assume that the flow rate Q through each pore can be described by the Hagen–Poiseuille equation for laminar flow

$$Q = \frac{\pi\left(\frac{D}{2}\right)^4 \Delta p}{8\mu L}$$

where D and L are the pore diameter and the length, respectively.

4.4 Scale-up of a Rotary Vacuum Filter A rotary vacuum filter is available with an area of 200 m^2 and vacuum pressure of 75 kPa. Filter leaf tests have been performed on a cell broth with a viscosity of 5 cp. The leaf tests gave a specific cake resistance of 1×10^{11} cm/g and a medium resistance of 1×10^8 cm^{-1}. The cake solids (dry basis) per volume of filtrate was 15 g/liter. It is desired to operate the large filter with a cycle time of 45 s and a cake formation time of 10 s. What is the filtration rate expected for the rotary vacuum filter? How significant is the medium resistance?

4.5 Accumulated Cake Solids and Cake Thickness for a Rotary Vacuum Filter For filtration with a rotary vacuum filter, the following variables are known: filtrate viscosity (μ_0), pressure drop (Δp), specific cake resistance (α), mass of cake solids on a dry basis per volume of filtrate (ρ_c), and rate of drum rotation in revolutions/time (ω).

(a) It is desired to know the mass X of accumulated cake solids on the dry basis per unit area of the filter. For the case of negligible medium resistance, determine X as a function of the foregoing variables and Θ, the angle that the drum has rotated from a given point after entering the broth.

(b) It is necessary that the thickness of the cake be limited to a value h. Determine h in terms of the same variables in part (a), the bulk density of the cake (ρ_b), and the weight fraction of water in the cake (x_w).

4.6 Continuous Crossflow Filtration System Operating at Steady State It is desired to concentrate a cell slurry continuously at a flow rate Q_f and cell concentration x_f to a concentration x_r in a steady state operation with a crossflow microfilter. The process variables are shown in the system diagram (Figure P4.6). The concentration of cells in the permeate is zero. If the dependence of the permeate rate Q_p on cell concentration x entering the pump is known, describe how you would determine the recycle ratio R and concentration x.

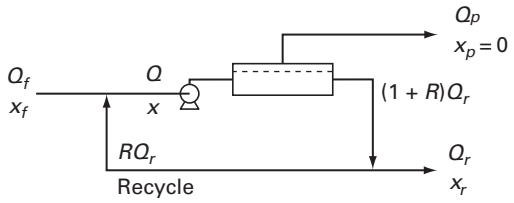

FIGURE P4.6 Process flow diagram for continuous operation of a crossflow filter. Flow rate is denoted by Q and cell concentration by x.

4.7 Crossflow Filtration Operating in Complete Recycle Mode A crossflow filtration unit is operated in the complete recycle mode.

(a) Sketch the flow diagram for the system, defining flow stream parameters for all flow streams. Write a material balance around the tank.

(b) The membrane has a molecular weight cutoff (MWCO) of 50,000 Da. (MWCO refers to the molecular weight of globular solute at which the solute is 90% rejected by the membrane.) Your product is a globular molecule with a molecular weight of 50,000 Da. Write a relationship that gives the mass of product per unit time returning to the tank through the permeate return line in terms of the starting concentration of product and the volumetric flow rates.

(c) What are the reasons for operating in the complete recycle mode?

4.8 Concentration Polarization during Ultrafiltration A system is available for the ultrafiltration of protein solutions. On Monday, you filter a globular protein with 12,000 Da molecular weight, and it is fully retained. On Tuesday, you filter a 120,000 Da molecular weight globular protein at the same molar concentration and using the same membrane. The transmembrane flux was the same on both days. Assuming identical boundary layer thicknesses for both filtrations, in which case will the polarization modulus c_w/c_b be greater? What is the relationship between the polarization moduli for the two cases?

4.9 Concentration and Diafiltration with an Ultrafiltration System A 2000-liter volume of a 30 g/liter protein solution needs to be concentrated to 200 g/liter. Also, the initial salt concentration must be reduced one hundredfold. The relationship between the permeation rate and the bulk protein concentration has been determined experimentally as follows:

$$Q = 500 \ln\left(\frac{270}{c_b}\right)$$

where Q = permeation rate (liters/h)
c_b = bulk protein concentration (g/liter)
Determine the operation batch volume that will give the minimum time for diafiltration. Then determine the times required for (a) concentration to the volume at which diafiltration is to be carried out, (b) diafiltration, and (c) concentration to the final concentration desired.

4.10 Time Required for Ultrafiltration A protein solution at a concentration of 0.5 g/liter and volume of 1000 liters must be concentrated on a crossflow ultrafilter to a concentration of 10 g/liter. The ultrafilter has an area of 100 m^2 and operates at 5°C with an inlet feed pressure of 16.0 bar, outlet feed pressure of 14.0 bar, and back pressure on the permeate of 1.4 bar. The protein has a molecular weight of 20,000 Da and will not pass through the ultrafiltration membranes. The feed has a viscosity of 1.2 cp. The membrane resistance (R_m) of the ultrafilter has been determined to be 2×10^{13} cm^{-1}. The Reynolds number for flow within the ultrafilter is large enough to render concentration polarization negligible. Determine the time required to perform the ultrafiltration.

4.11 Concentration at the Membrane Surface of a Crossflow Filter You operate a crossflow filter at a very low Δp and low flux until the transmembrane solvent flow becomes zero as a result of concentration polarization. Show how you would determine the concentration of solute c_w right at the membrane surface on the feed (retentate) side. Assume that c_w is not high enough to form a precipitate or gel layer.

4.12 Scale-up of Batch Filtration of Protein Precipitate A small test filtration of a protein precipitate in an aqueous suspension uses a conventional filter with an area of 89 cm^2 at a pressure drop of 0.4 atm to give data for the filtrate volume as a function of time (see Table P4.12). We would like to filter a much larger batch of the precipitate at the same temperature containing 1000 liters of solvent by using a filter of 1.3 m^2 area having the same filter medium as for the small-scale filtration. However, this larger batch has a concentration of 0.28 g/100 cm^3 of solvent, less than in our test filtration, which is 0.34 g/100 cm^3 of solvent. How long will it take to filter this new batch at the same pressure drop? What is the error in the calculated time if the resistance of the filter medium is neglected?

TABLE P4.12

Time (s)	Filtrate volume (liters)
10	0.489
20	0.703
30	0.864
40	0.995
50	1.120

4.13 Explanation of Flux Reduction in Microfiltration of an Enzyme A microfiltration membrane system is being used to process a cell lysate (i.e. cells broken) in the continuous mode so that a low molecular weight enzyme is obtained in the filtrate. The filtrate flux across the microfiltration membrane is less than when the membrane was tested using a buffer solution as feed before the cell lysate was processed. Explain how

you could determine if the flux reduction is due to concentration polarization on the membrane surface and/or to fouling within the membrane.

4.14 Crossflow Filtration of Suspended Particles Crossflow filtration is being perfomed at bulk velocity u_b in tubes of diameter D in a solution containing suspended biological particles of radius a. The flow regime is laminar. The diffusion coefficient in free solution of the biological molecule that makes up the particles is $\mathscr{D}$.

(a) Determine the ratio of the mass transfer coefficient k for the filtration of the particles to the mass transfer coefficient for the filtration of the dissolved biological molecule as a function of u_b, a, D, and $\mathscr{D}$, assuming the particles are in the 1 to 30 μm size range.

(b) For the conditions given in Example 4.2 for the ultrafiltration of a protein (except u_b = 210 cm/s), calculate the value of the ratio in part (a).

4.15 Estimation of Boundary Layer Thickness during Crossflow Filtration Data have been obtained for the concentration of a protein by ultrafiltration (see Table P4.15). The diffusion coefficient of the protein is 8 x 10^{-7} cm^2 s^{-1}. Estimate the thickness of the boundary layer next to the membrane.

TABLE P4.15

Protein concentration (wt. %)	Ultrafiltration flux (ml cm^{-2} min^{-1})
1.0	0.054
2.0	0.039
4.0	0.025
6.0	0.016
10.0	0.006

4.16 Initial Irreversible Fouling and Concentration Polarization Resistance in Ultrafiltration An ultrafiltration system is operated to concentrate a protein solution containing a buffer. The average pressure drop across the membrane is 30 kPa, and the fluid viscosity is 1.5 x 10^{-6} kPa s. With clean membranes, the transmembrane flux using buffer in the system is 110 liters m^{-2} h^{-1} for this pressure drop. After 2 min of operation with the protein solution, the transmembrane flux is 15 liters m^{-2} h^{-1}. At this point, the system is operated with the buffer only in the backflushing mode with negative transmembrane pressure until a constant transmembrane flux is reached. Then, the system is operated with the buffer in the normal mode (positive transmembrane pressure), and the steady-state transmembrane flux is 35 liters m^{-2} h^{-1} at a pressure drop of 30 kPa. It has been determined that the flux due to the osmotic pressure difference is negligible. Estimate the irreversible fouling resistance (R_{if}) and resistance due to concentration polarization and a gel layer (R_p) for the membrane after 2 min of operation with the protein solution.

REFERENCES

1. Grace, H. P. (1953). Resistance and compressibility of filter cakes. *Chem. Eng. Prog*., vol. 49, p. 303.
2. Choudhury, A. P. R., and Dahlstrom, D. A. (1957). Prediction of cake-washing results with continuous filtration equipment. *AIChE J*., vol. 3, p. 433.
3. Michaels, A. S. (1968). New separation technique for the CPI. *Chem. Eng. Prog*., vol. 64, p. 31.
4. Blatt, W. F., Dravid, A., Michaels, A. S., and Nelsen, L. (1970). Solute polarization and cake formation in membrane filtration: Causes, consequences, and control techniques. In *Membrane Science and Technology*, J. E. Flinn, ed., Plenum Press, New York, p. 47.
5. Bird, R. B., Stewart, W. E., and Lightfoot, E. N. (2002). *Transport Phenomena*, 2nd ed., Wiley, New York.
6. Calderbank, P. H., and Moo-Young, M. B. (1961). The continuous phase heat and mass-transfer properties of dispersions. *Chem. Eng. Sci*., vol. 16, p. 39.
7. Belfort, G., Davis, R. H., and Zydney, A. J. (1994). The behavior of suspensions and macromolecular solutions in crossflow microfiltration. *J. Membrane Sci*., vol. 96, p. 1.
8. Porter, M. C. (1972). Concentration polarization with membrane filtration. *Ind. Eng. Chem. Prod. Res. Dev*., vol. 11, p. 234.
9. Zydney, A. L., and Colton, C. K. (1986). A concentration polarization model for the filtrate flux in cross-flow microfiltration of particulate suspensions. *Chem. Eng. Commun*., vol. 47, p. 1.
10. Eckstein, E. C., Bailey, P. G., and Shapiro, A. H. (1977). Self-diffusion of particles in shear flow of a suspension. *J. Fluid Mech*., vol. 79, p. 191.
11. Perry, R. H., Green, D. W., and Maloney, J. O., eds. (1997). Liquid-solid operations and equipment (Section 18) and Membrane separation processes (Section 22). In *Perry's Chemical Engineers' Handbook*, 7th ed., McGraw-Hill, New York.
12. Rushton, A. (1996). Filter media. In *Solid–Liquid Filtration and Separation Technology*, A. Rushton, A. S. Ward, and R. G. Holdich, eds., VCH Publishers, Weinheim, Germany, p. 107.
13. Zeman, L. J., and Zydney, A. L. (1996). *Microfiltration and Ultrafiltration*, Dekker, New York.
14. Hallstrom, B., and Lopez-Leiva, M. (1978). Description of a rotating ultrafiltration module. *Desalination*, vol. 24, p. 273.
15. Robertson, B. C., and Zydney, A. L. (1990). Protein adsorption in asymmetric ultrafiltration membranes with highly constricted pores. *J. Colloid Interface Sci*., vol. 134, p. 563.
16. Rajabzadeh, A. R., Moresoli, C., and Marcos, B. (2010). Fouling behavior of electroacidified soy protein extacts during cross-flow ultrafiltration using dynamic reversible-irreversible fouling resistances and CFD modeling. *J. Membr. Sci*., vol. 361, p. 191.
17. Hilal, N., Ogunbiyi, O. O., Miles, N. J., and Nigmatullin, R. (2005). Methods employed for control of fouling in MF and UF membranes: a comprehensive review. *Sep. Sci. Tech*., vol. 40, p. 1957.
18. Datar, R. V., and Rosen, C.-G. (1993). Cell and cell debris removal: Centrifugation and cross-flow filtration. In *Biotechnology*, vol. 3, *Bioprocessing*, H.-J. Rehm and G. Reed, eds., VCH Publishers, Weinheim, p. 486.
19. Scopes, R. K. (1994). *Protein Purification*, 3rd ed., Springer-Verlag, New York.
20. Tutunjian, R. S. (1985). Ultrafiltration processes in biotechnology. In *Comprehensive Biotechnology*, vol. 2, *The Principles of Biotechnology: Engineering Considerations*, M. Moo-Young, ed., Pergamon Press, Oxford, p. 411.

/// 5 /// SEDIMENTATION

Sedimentation is the movement of particles or macromolecules in an inertial field. Its applications in separation technology are extremely widespread. Extremes of applications range from the settling due to gravity of tons of solid waste and bacteria in wastewater treatment plants to the centrifugation of a few microliters of blood to determine packed blood cell volume ("hematocrit") in the clinical laboratory. Accelerations range from $1 \times g$ in flocculation tanks to $100{,}000 \times g$ in ultracentrifuges for measuring the sedimentation rates of macromolecules. In bioprocessing, the most frequent applications of sedimentation include the clarification of broths and lysates, the collection of cells and inclusion bodies, and the separation of fluids having different densities.

Unit operations in sedimentation include settling tanks and tubular centrifuges for batch processing, continuous centrifuges such as disk centrifuges, and less frequently used unit operations such as field-flow fractionators and inclined settlers. Bench scale centrifuges that accommodate small samples can be found in most research laboratories and are frequently applied to the processing of bench scale cell cultures and enzyme preparations. Certain high-speed ultracentrifuges are used as analytical tools for the estimation of molecular weights and diffusion coefficients.

The chapter begins with a description of the basic principles of sedimentation, followed by methods of characterizing laboratory and larger-scale centrifuges. Two important production centrifuges, the tubular bowl centrifuge and the disk-stack centrifuge, are analyzed in detail to give the basis for scale-up. Ultracentrifuges, important for analytical and preparative work, are then analyzed. The effect of flocculation of particles on sedimentation is presented, and sedimentation of particles at low accelerations is discussed. The chapter concludes with a description of centrifugal elutriation.

5.1 INSTRUCTIONAL OBJECTIVES

After completing this chapter, the reader should be able to do the following:

- Determine the velocity of a sedimenting particle and calculate sedimentation times, equivalent times, and sedimentation coefficients in gravitational and centrifugal fields.

- Perform engineering analyses and scaling calculations on tubular bowl and disk-stack centrifuges.
- Choose the appropriate centrifuge for particular liquid-solid separations.
- Calculate molecular weight from ultracentrifuge data.
- Explain the behavior of sedimenting flocs.
- Discern the relative importance of diffusion in a sedimentation operation.
- Explain how inclined sedimentation, field-flow fractionation, and centrifugal elutriation work.

5.2 SEDIMENTATION PRINCIPLES

The most frequently encountered inertial fields are gravitational acceleration, $g = 9.8$ m/s^2, or centrifugal acceleration, $\omega^2 R$, where R is the distance of the particle from the center of rotation, and ω is angular velocity (rad/s). The same theory can be used to describe sedimentation in both types of inertial fields.

5.2.1 Equation of Motion

Analysis begins with the equation of motion of a particle of radius a and density ρ having mass $m = (4/3)\pi a^3 \rho$ in an inertial field moving radially at a distance R from the center of rotation (Figure 5.1)

Assuming the particle is spherical,

$$m\frac{dv}{dt} = F_{iR} + F_{bR} + F_{dR} = \left(\frac{4}{3}\right)\pi a^3 \rho \omega^2 R - \left(\frac{4}{3}\right)\pi a^3 \rho_0 \omega^2 R - 6\pi \mu a \upsilon \tag{5.2.1}$$

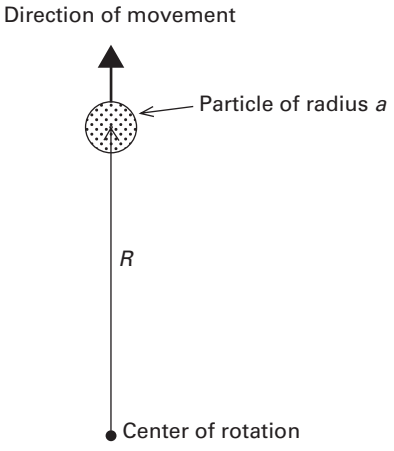

FIGURE 5.1 Particle moving radially under the influence of an inertial field at distance R from the center of rotation.

where subscripts designate forces in the R direction, due to i, inertial acceleration, b, buoyancy due to the density of the medium ρ_0 through which the particle sediments, and d, the Stokes drag force, which under conditions of creeping flow is proportional to the velocity v and viscosity μ [1]. Solving Equation (5.2.1) for velocity in a centrifugal field at steady state (all forces balanced, so $dv/dt = 0$) gives

$$\upsilon = \frac{2a^2(\rho - \rho_0)\omega^2 R}{9\mu} \tag{5.2.2}$$

commonly called the "centrifuge equation." If particles are allowed to sediment only in the presence of gravity, then the inertial acceleration is $g = 9.8$ m/s^2, and $\omega^2 R$ in Equation (5.2.2) is replaced by g. If, however, the particle is moving outwardly from the center of rotation in a centrifuge, R is not constant and is related to the velocity by $v = dR/dt$, which gives from Equation (5.2.2) after rearrangement,

$$\frac{dR}{R} = \frac{\left[2a^2(\rho - \rho_0)\omega^2\right]dt}{9\mu} \tag{5.2.3}$$

with the following initial condition:

$$at\ t = 0, \quad R = R_0 \tag{5.2.4}$$

This equation can be integrated to give

$$\ln\left(\frac{R}{R_0}\right) = \frac{2a^2(\rho - \rho_0)\omega^2 t}{9\mu} \tag{5.2.5}$$

This is a useful equation that relates time to the distance traveled by the particle.

5.2.2 Sensitivities

Creeping flow conditions are usually satisfied in sedimentation. Calculating the Reynolds number for spherical particles

$$\mathrm{Re} = \frac{2a\upsilon\rho}{\mu} \tag{5.2.6}$$

Creeping flow occurs at Reynolds numbers less than about 0.1 [1]. Table 5.1 shows the sedimentation velocities for important bioparticles and biomolecules calculated from Equation (5.2.2) with $\rho_0 = 1.0$ g/cm^3, $\mu = 0.01$ g cm^{-1} s^{-1} (poise), and representative values of ρ and a. The sedimentation velocity and Reynolds number results shown in Table 5.1 for yeast cells and bacterial cells at gravitation acceleration can be multiplied by a centrifuge's centrifugal acceleration to give the corresponding

TABLE 5.1 Calculated Settling Velocities and Reynolds Number for Example Bioproducts (Assumes $\rho_0 = 1.0$ g/cm^3 and $\mu = 1.0$ cp)

Bioparticle or biomolecule	Sedimentation Radius, a (μm)	Density, ρ (g/cm^3)	Dimensionless acceleration ($G = \omega^2 R/g$)	Sedimentation velocity, v (cm/h)	Reynolds number, Re
Yeast cell	2.5	1.1	1	0.5	7×10^{-6}
Bacteria cell	0.5	1.1	1	0.02	6×10^{-8}
Protein	0.005	1.3	10^4	0.06	2×10^{-9}

values for operation in the centrifuge; for example, at a dimensionless acceleration of 10,000, the Reynolds number for yeast cells is 0.07, which means that the flow is still creeping.

It is clear from Table 5.1 that gravitational sedimentation is too slow to be practical for bacteria, and conventional centrifugation is too slow for protein macromolecules. In the case of true particles, flocculation (see Section 5.6) is often used to increase the Stokes radius a, while ultracentrifugation (see Section 5.5) is used in macromolecular separations.

When particle density and solvent density are equal, the sedimentation velocity v is zero, and the process is called *isopycnic* or *equilibrium* sedimentation. This fact is exploited in the determination of molecular densities and in the separation of living cells. A density gradient or a density shelf is employed in such cases. Densities of representative cells, organelles, and biomolecules measured by this method are given in Table 5.2 [2–5]. The density of *Amoeba proteus* cells is low because these cells contain fat vacuoles of low density and have no cell wall.

An example of a density shelf used for the separation of cells is the preparation of lymphocytes by sedimentation. The goal of this separation is to remove erythrocytes from a leukocyte population on the basis of a density shelf. By combining Ficoll, a high molecular weight polymer, and Hypaque, a heavily iodinated benzoic acid derivative, in appropriate proportions in aqueous buffers, it is possible to achieve a density around 1.07 g/cm^3 in isotonic solutions. At this density most white blood cell subpopulations will float and nearly all red blood cells will sediment.

When the concentration of sedimenting particles increases, the sedimentation velocity has been found to decrease, a phenomenon known as "hindered settling." This effect has been quantified by the following expression for particles of any shape [6]:

$$v_c = v(1-\varphi)^n \tag{5.2.7}$$

where v_c is the sedimentation velocity of particles in a concentrated suspension, v is the velocity of individual particles [Equation (5.2.2)], φ is the volume fraction of the particles, and n is a function only of the shape of the particle and of the Reynolds number. For spherical particles with Re < 0.2 (usually satisfied during sedimentation), the exponent n has been found to be 4.65. Equation (5.2.7) may also be applied

TABLE 5.2 Measured Values of the Density of Representative Cells, Organelles, and Biomolecules

Cell, organelle, or biomolecule	Density, ρ (g/cm^3)	Ref.
Escherichia coli	1.09[a]	2
Bacillus subtilis	1.12	3
Arthrobacter sp.	1.17	4
Saccharomyces pombe	1.09	2
Saccharomyces cerevisiae	1.11[a]	2
Amoeba proteus	1.02	2
Murine B cells	1.06[a]	2
Chinese hamster ovary (CHO) cells	1.06	2
Peroxisomes	1.26[a]	5
Mitochondria	1.20[a]	5
Plasma membranes	1.15[a]	5
Proteins	1.30[a]	5
Ribosomes	1.57[a]	5
DNA	1.68[a]	5
RNA	2.00[a]	5

[a]Average value.

TABLE 5.3 Effect of Particle Volume Fraction φ on the Particle Sedimentation Velocity for Spherical Particles

φ	v_c/v
0.01	0.95
0.05	0.79
0.10	0.61
0.20	0.35

to particles of any size in a polydisperse system, using the volume fraction for all the particles in the calculation [7].

The magnitude of the hindered settling effect for spherical particles as a function of the particle volume fraction φ can be seen in Table 5.3. Note that hindered settling can be significant for particle concentrations of a few percent or greater.

5.3 METHODS FOR ANALYSIS OF SEDIMENTATION

While the fundamental principles of sedimentation are important to a basic understanding of this subject, other less theoretical methods have been developed for the actual practice of sedimentation. Equilibrium sedimentation, the sedimentation coefficient, equivalent sedimentation time, and sigma analysis are some of the more important of these methods.

5.3.1 Equilibrium Sedimentation

Some products can be isolated on the basis of their density. In ultracentrifugation this is true of nucleic acids, and isopycnic (same-density) sedimentation was the method originally used to demonstrate the semiconservative replication of DNA [8]. When $\rho = \rho_0$ in Equation (5.2.2), then $v = 0$ and all inertial motion stops; therefore, if the density of the solution is known at the location where motion stops, the density of the solute or suspended particle is known. In most applications inertial motion is arrested in a density gradient, so that the density of the medium increases below the arrest point, and the buoyant force [Equation (5.2.1)] is greater than the inertial force, which causes the particle to return to its isopycnic level. Centrifugation can therefore be used analytically to determine particle or macromolecule density, as discussed earlier.

In practice, there are at least three routes to the establishment of conditions for isopycnic sedimentation—the creation of a region in the sedimentation vessel where $\rho_0 \geq \rho$. One method is to layer solutions of decreasing density, starting at the bottom of the vessel and proceeding until the vessel is filled. The resulting gradient is like a staircase until diffusion smooths it out. Another is to centrifuge at extremely high speed, resulting in isothermal stratification of a density-forming solute, such as CsCl. Such a gradient is not necessarily linear. The most widely used method of forming a density gradient is the gradient mixing method, in which two cylindrical containers, one containing a concentrated solution and the other containing a dilute solution and a stirring apparatus, are linked as in Figure 5.2 to produce an outflow with a linear salt gradient. For these gradient mixers, the time-dependent solute concentration is as follows [9]:

$$c(t) = \frac{c_{1,0} + Q(c_2 - c_{1,0})}{2V_0} t \tag{5.3.1}$$

where Q is the outflow rate due to pumping or gravity feed, V_0 is the initial volume in each cylinder, $c_{1,0}$ is the initial concentration of solute in the mixed chamber, and c_2

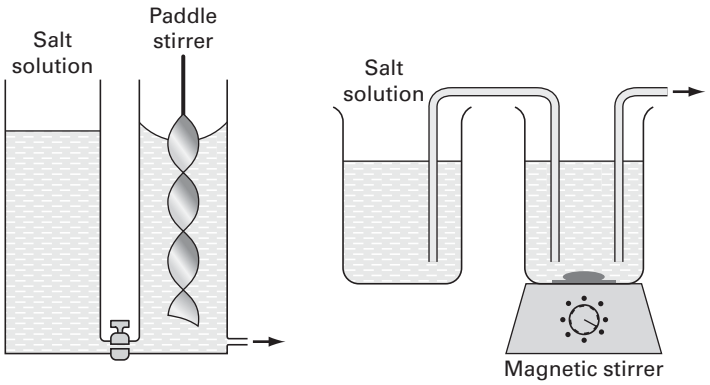

FIGURE 5.2 Two types of a linear gradient mixer.

is the concentration of solute in the nonmixed chamber (constant). By programming Q, one can set up a variety of salt gradients.

5.3.2 Sedimentation Coefficient

When a body force is applied, velocity through a viscous medium is usually proportional to the accelerating field (examples are electric, magnetic, and inertial). In the case of sedimentation, the resulting constant, a property of both the particle and the medium, is the *sedimentation coefficient,* which is defined as

$$s \equiv \frac{\upsilon}{\omega^2 R} \tag{5.3.2}$$

Comparing this equation with Equation (5.2.2), we see that

$$s = \frac{2a^2(\rho - \rho_0)}{9\mu} \tag{5.3.3}$$

which defines s in terms of only properties of the particle and the medium. This coefficient is usually expressed at 20°C and under conditions (viscosity and density) of pure water as

$$s_{20,w}(s)$$

The sedimentation coefficient is often expressed in svedberg units, where 10^{-13} s = 1 svedberg unit (S), named after the inventor of the ultracentrifuge, Theodor Svedberg.

EXAMPLE 5.1

Application of the Sedimentation Coefficient In 1974 D. E. Koppel measured the sedimentation coefficient ($s_{20,w}$) for the smaller ribosomes from *Escherichia coli* at 70 S (Koppel, D. E., *Biochemistry, 13,* 2712, 1974). Estimate how long it would take to completely clarify a suspension of these ribosomes in a high-speed centrifuge operating at 10,000 rpm with a tube containing the ribosome suspension in which the maximum distance of travel of particles radially outward is 1 cm and the initial distance from the center of rotation to the particles nearest the center of rotation is 4 cm.

Solution

We can write Equation (5.3.2) as

$$s = \frac{dR}{dt}\frac{1}{\omega^2 R}$$

or

$$\omega^2 s\, dt = \frac{dR}{R}$$

We integrate this equation with the following initial condition:

at $t = 0$, $R = R_0$ (distance from center of rotation to the particles nearest the center of rotation)

to give

$$\omega^2 st = \ln \frac{R}{R_0}$$

To determine the maximum time required, we evaluate R at the maximum travel of the cells measured from the center of rotation (5 cm):

$$t = \frac{\ln\left(\dfrac{R}{R_0}\right)}{\omega^2 s} = \frac{\ln(5/4)\dfrac{1\,\text{h}}{3600\,\text{s}}}{\left(10{,}000\dfrac{\text{rev}}{\text{min}} \times \dfrac{2\pi\,\text{rad}}{\text{rev}} \times \dfrac{1\,\text{min}}{60\,\text{s}}\right)^2 (70 \times 10^{-13}\,\text{s})} = 8.1\,\text{h}$$

This should not be an unreasonable amount of time to centrifuge the ribosomes. However, since the time varies inversely with the square of the rotation speed, the time can be reduced to 2 h by doubling the speed.

5.3.3 Equivalent Time

To assess the approximate properties of a particle type to be separated, it is sometimes convenient to calculate an "equivalent time." To do this, we first define a dimensionless acceleration, G, the ratio of the centrifugal to gravitational acceleration for a particular centrifuge:

$$G \equiv \frac{\omega^2 R}{g} \tag{5.3.4}$$

where R is usually defined as the radius of the centrifuge bowl. Thus, this dimensionless unit is measured in "g's"—multiples of the earth's gravitational acceleration. A rough approximation of the difficulty of a given separation by centrifugation is the product of the dimensionless acceleration and the time required for the separation. This product is called the equivalent time for the separation, and is written as

$$\text{Equivalent time} \equiv Gt = \frac{\omega^2 R}{g} t \tag{5.3.5}$$

Typical values of equivalent time are as follows: 0.3×10^6 s for eukaryotic cells, 9×10^6 s for protein precipitates, 18×10^6 s for bacteria, and 1100×10^6 s for ribosomes [10].

The equivalent time for the centrifugation of cells or biological particles of unknown sedimentation properties may be estimated in a laboratory centrifuge. Samples are centrifuged for various times until a constant volume of packed cells is reached. The equivalent time Gt is calculated as the product of the G for the particular centrifuge and the time required to reach constant packed-cell volume. A centrifuge that has commonly been used for this determination is the Gyro-Tester (Alfa Laval, Inc.).

One approach to scale-up of a centrifugal operation is to assume constant equivalent time:

$$(Gt)_1 = (Gt)_2 \tag{5.3.6}$$

where the subscripts refer to centrifuges 1 and 2, respectively.

EXAMPLE 5.2

Scale-up Based on Equivalent Time If bacterial cell debris has $Gt = 54 \times 10^6$ s [10], how large must the centrifuge bowl be, and what centrifuge speed is needed to effect a full sedimentation in a reasonable amount of time?

SOLUTION

Assume that a reasonable amount of time is about 2 h. From Equation (5.3.5) for Gt, we can estimate the centrifuge speed ω if we know the centrifuge bowl size and the time of centrifuging. It is reasonable to have a centrifuge that is 10 cm in diameter. Solving Equation (5.3.5) for ω using these values gives

$$\omega = \left(\frac{Gtg}{Rt}\right)^{1/2} = \left(\frac{54\times10^6\,\text{s}\times 9.81\frac{\text{m}}{\text{s}^2}}{0.05\,\text{m}\times 2(3600)\,\text{s}}\right)^{1/2} = 1213\frac{\text{rad}}{\text{s}}\times\frac{1\,\text{rev}}{2\pi\,\text{rad}}\times\frac{60\,\text{s}}{\text{min}} = 11{,}590\,\text{rpm}$$

This speed can be achieved in a production tubular bowl centrifuge (see later: Table 5.5).

5.3.4 Sigma Analysis

The more commonly used analysis in industry is "sigma analysis," which uses the operation constant Σ to characterize a centrifuge into which feed flows at volumetric

flow rate Q. Since the engineer often needs to determine Q on scale-up, a convenient relationship is

$$Q = \{\upsilon_g\}[\Sigma] \tag{5.3.7}$$

where v_g is the sedimentation velocity at $1 \times g$, namely,

$$\upsilon_g = 2a^2 \frac{(\rho - \rho_0)g}{9\mu} \tag{5.3.8}$$

and Σ represents the geometry and speed of the centrifuge, as derived in the discussion of individual centrifuges in the next section; Σ can also be thought of as the cross-sectional area equivalent of the centrifuge, with units of length squared. Therefore, in Equation (5.3.7) the accolades { } indicate properties of the particle to be separated and of the fluid in which separation is occurring, and the square brackets [] indicate properties of the centrifuge.

The sedimentation velocity at $1 \times g$ can be estimated directly by using Equation (5.3.8) if relevant properties of the system are known, or it can be measured in the laboratory. Combining Equations (5.3.8) and (5.2.5), we obtain

$$\upsilon_g = \frac{g \ln\left(\frac{R}{R_0}\right)}{\omega^2 t} \tag{5.3.9}$$

This is a useful equation for determining v_g in the laboratory. Parameters in Equation (5.3.9) can be measured as follows. The minimum time t to clarify the sample in a laboratory centrifuge at speed ω is determined; R and R_0 are the distances from the center of rotation to the top of the packed solids and to the top of the liquid in the centrifuge tube, respectively. Since the sample cannot be observed directly when the centrifuge is being operated, a series of experiments would be required to determine the time for centrifuging at which R is constant.

5.4 PRODUCTION CENTRIFUGES: COMPARISON AND ENGINEERING ANALYSIS

The common types of production centrifuges are illustrated in Figure 5.3, and a comparison of the advantages and disadvantages of the different centrifuge designs is given in Table 5.4 [11]. In the tubular centrifuge, solids deposit on the wall of the bowl, and feed continues until the bowl is almost full, at which time the operation is stopped and the solids removed. This type of centrifuge works well for particles of relatively low sedimentation coefficient that must be recovered, such as protein precipitates. The disk centrifuges have a relatively high sedimentation area for their volume and allow for continuous or intermittent solids discharge; they

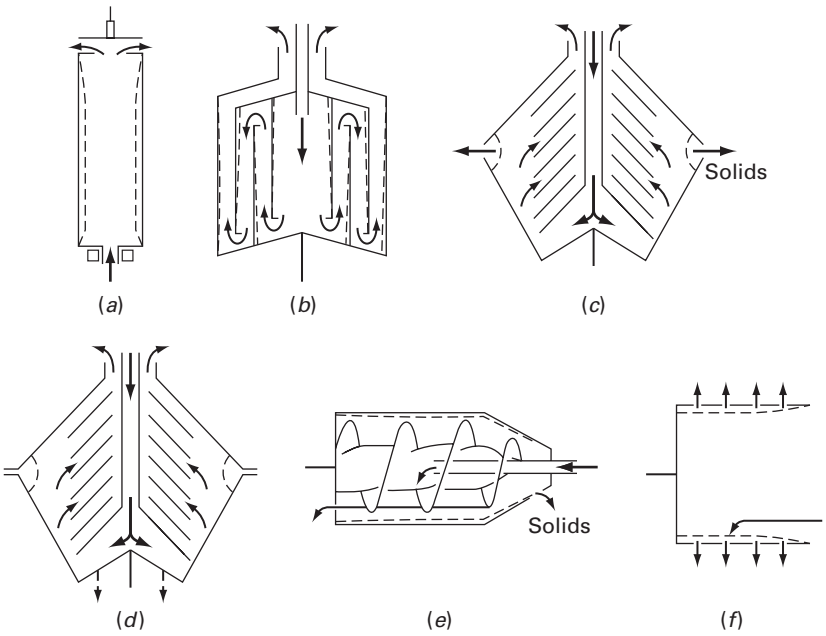

FIGURE 5.3 Common types of production centrifuges: (*a*) tubular bowl, (*b*) multichamber, (*c*) disk, nozzle, (*d*) disk, intermittent discharge, (*e*) scroll, and (*f*) basket. Arrows indicate the path of the liquid phase; dashed lines show where the solids accumulate.

have been successfully used for the centrifugation of cells and cell lysates, where the entire process often must be contained to avoid the escape of aerosols. The scroll (or decanter) and basket centrifuges are typically used for particles that sediment relatively rapidly and can be washed well as packed solids, such as antibiotic crystals.

Of all the centrifuges, the tubular and the disk types are probably the most likely to be found in a bioseparation process involving the recovery of a protein produced by cells. The capabilities of tubular and disk centrifuges are given in Table 5.5 [12]. Note that there is generally a reduction in the maximum *g*-force (dimensionless acceleration) as the diameter of the bowl increases. The tubular bowl and disk centrifuges are analyzed to develop the Σ value that can be used in scaleup.

5.4.1 Tubular Bowl Centrifuge

The tubular bowl centrifuge allows fluid to enter at one end of a rotating cylinder and exit at the opposite end, while particles move toward the wall of the cylinder and captured both at the wall and by a weir at the exit, as indicated in Figure 5.4. The liquid enters the bowl through an opening in the center of the lower bowl head. The liquid is pushed by centrifugal force toward the periphery of the rotating bowl. Clarified liquid overflows a ring weir in the upper bowl head, the radius

TABLE 5.4 Comparison of Production Centrifuges[a]

System	Advantages	Disadvantages
Tubular bowl	(a) High centrifugal force	(a) Limited solids capacity
	(b) Good dewatering	(b) Foaming unless special skimming or centripetal pump used
	(c) Easy to clean	
	(d) Simple dismantling of bowl	(c) Recovery of solids difficult
Chamber bowl	(a) Clarification efficiency remains constant until sludge space full	(a) No solids discharge
	(b) Large solids holding capacity	(b) Cleaning more difficult than tubular bowl
	(c) Good dewatering	(c) Solids recovery difficult
	(d) Bowl cooling possible	
Disk centrifuge	(a) Solids discharge possible	(a) Poor dewatering
	(b) Liquid discharge under pressure eliminates foaming	(b) Difficult to clean
	(c) Bowl cooling possible	
Scroll or decanter centrifuge	(a) Continuous solids discharge	(a) Low centrifugal force
	(b) High feed solids concentration	(b) Turbulence created by scroll
Basket centrifuge	(a) Solids can be washed well	(a) Not suitable for soft biological solids
	(b) Good dewatering	(b) No solids discharge
	(c) Large solids holding capacity	(c) Recovery of solids difficult

[a] See reference [11].

TABLE 5.5 Capabilities of Tubular and Disk Centrifuges[a]

Type	Bowl diameter (mm)	Speed (rpm)	Maximum dimensionless acceleration (G), $\omega^2 R/g$	Throughput (liters/min)
Tubular bowl	44	50,000	61,400	0.2–1.0
	105	15,000	13,200	0.4–38
	127	15,000	16,000	0.8–75
Disk with nozzle	254	10,000	14,200	40–150
discharge	406	6,250	8,850	100–570
	686	4,200	6,760	150–1500
	762	3,300	4,630	150–1500

[a] See reference [12].

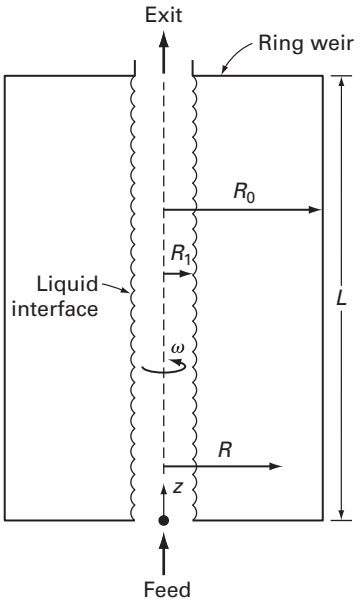

FIGURE 5.4 Cross section of a tubular centrifuge in operation.

of which establishes the depth of the pool of liquid around the periphery of the rotating bowl.

As in most engineering calculations, we wish to determine the flow rate Q. The equations of motion that give the trajectory of sedimented particles are, first, in the radial direction from Equation (5.2.2)

$$\frac{dR}{dt} = \frac{2a^2(\rho - \rho_0)\omega^2 R}{9\mu} \tag{5.4.1}$$

then in the axial direction, due only to pumped flow, Q

$$\frac{dz}{dt} = \frac{Q}{A} = \frac{Q}{\pi(R_0^2 - R_1^2)} \tag{5.4.2}$$

where A is the cross-sectional area for liquid flow in the centrifuge. These equations of motion are combined to give the trajectory equation

$$\frac{\dfrac{dR}{dt}}{\dfrac{dz}{dt}} = \frac{dR}{dz} \tag{5.4.3}$$

Substituting Equations (5.4.1) and (5.4.2) into this ratio, integrating dR between R_0 and R_1, and integrating dz between 0 and L and solving for Q gives

$$Q = \left\{\frac{2a^2(\rho - \rho_0)}{9\mu}\right\}\left[\frac{\pi L(R_0^2 - R_1^2)\omega^2}{\ln\left(\frac{R_0}{R_1}\right)}\right] \quad (5.4.4)$$

In view of Equations (5.3.7) and (5.3.8), the first factor in Equation (5.4.4) can be multiplied by g while the second is divided by g to give, again, Equation (5.3.7) for Σ analysis:

$$Q = \{v_g\}[\Sigma] \quad (5.4.5)$$

where, for a tubular bowl centrifuge,

$$\Sigma = \frac{\pi L(R_0^2 - R_1^2)\omega^2}{g \ln\left(\frac{R_0}{R_1}\right)} \quad (5.4.6)$$

In practice, one uses a benchtop centrifuge to determine v_g and chooses a centrifuge with throughput in the desired range. The centrifuge manufacturer supplies Σ for the selected centrifuge, and the flow rate is determined from Equation (5.4.5). Alternatively, if the flow rate is constrained by some other factor, a custom centrifuge with a specific Σ can be constructed. This is also true for the continuous disk-stack centrifuge, which is the subject of the next section.

A tubular bowl centrifuge operates in the batch mode. The bowl begins spinning, either dry or full of water, which will be displaced by the solids suspension. The solids suspension is fed from the bottom of the bowl, as previously described, typically through a jet that sprays the suspension onto the wall of the bowl. If the bowl begins empty, the suspension distributes rapidly up the length of the bowl in a thin film. As the suspension is fed, the liquid layer grows from the wall toward the center of the bowl, until the thickness of the liquid layer is equal to the weir at the top of the bowl. At this point, clarified liquid begins to exit the centrifuge at the rate of the feed. The residence time of fluid in the bowl is

$$\tau = \frac{\pi L(R_0^2 - R_1^2)}{Q} \quad (5.4.7)$$

As solids build up on the wall of the bowl, the inner radius of the bowl is effectively decreased, reducing the residence time in the bowl, but also reducing the sedimentation distance and the maximum sedimentation velocity [see Equation (5.2.2)]. Referring to Equation (5.4.6), it can be seen that Σ decreases with time during tubular bowl operation, as R_0 approaches R_1. Therefore, in order to continue to capture particles in the tubular bowl, the flow rate has to be decreased as operation proceeds.

Practically, this is not done—the centrifuge is fed until particles break through, and then the operation is discontinued and the bowl emptied of solids. Typically, the solids occupy no more than 80% of the bowl volume.

There are now commercial tubular bowl centrifuges which have mechanical means to discharge solids. This feature makes operation of the tubular bowl centrifuge more convenient and likely reduces downtime. However, the centrifuge still has to be stopped, solids discharged and then restarted, which reduces the efficiency overall.

Typically, tubular bowl centrifuges can concentrate solids to essentially 100% wet weight, or the weight you would measure by centrifuging a sample in the laboratory and decanting the supernatant. The solids are not required to flow in order to operate the equipment; in fact, a "tight pellet" is preferred. This is an advantage of a tubular bowl centrifuge over a disk centrifuge.

EXAMPLE 5.3

Complete Recovery of Bacterial Cells in a Tubular Bowl Centrifuge It is desired to achieve complete recovery of bacterial cells from a fermentation broth with a pilot plant scale tubular centrifuge. It has been determined that the cells are approximately spherical with a radius of 0.5 μm and have a density of 1.10 g/cm^3. The speed of the centrifuge is 5000 rpm, the bowl diameter is 10 cm, the bowl length is 100 cm, and the outlet opening of the bowl has a diameter of 4 cm. Estimate the maximum flow rate of the fermentation broth that can be attained.

SOLUTION

The flow rate can be estimated from Equation (5.4.5) by determining the settling velocity under gravity (v_g) and the Σ factor for the centrifuge. We can estimate v_g from Equation (5.3.8) and assuming the viscosity μ is the same as for water (1.0 cp):

$$v_g = \frac{2a^2(\rho-\rho_0)\mathrm{g}}{9\mu} = \frac{2(0.5\times10^{-6}\,\mathrm{m})^2\times(1.10-1.00)\dfrac{\mathrm{g}}{\mathrm{cm}^3}\times9.81\dfrac{\mathrm{m}}{\mathrm{s}^2}\times\dfrac{10^6\,\mathrm{cm}^3}{\mathrm{m}^3}}{9\left(0.01\dfrac{\mathrm{g}}{\mathrm{cm\,s}}\right)}$$

$$= 5.45\times10^{-6}\,\mathrm{cm/s}$$

For complete recovery of the cells, we can use Equation (5.4.6) to estimate Σ:

$$\Sigma = \frac{\pi L\left(R_0^2-R_1^2\right)\omega^2}{g\ln\left(\dfrac{R_0}{R_1}\right)} = \frac{\pi(100\,\mathrm{cm})\times(5^2-2^2)\,\mathrm{cm}^2\times\left(5000\dfrac{\mathrm{rev}}{\mathrm{min}}\times\dfrac{2\pi\,\mathrm{rad}}{\mathrm{rev}}\right)^2}{9.81\dfrac{\mathrm{m}}{\mathrm{s}^2}\times\ln(5/2)\times\dfrac{100\,\mathrm{cm}}{\mathrm{m}}\times\left(\dfrac{60\,\mathrm{s}}{\mathrm{min}}\right)^2}$$

$$= 2.01\times10^6\,\mathrm{cm}^2$$

From Equation (5.4.5):

$$Q = v_g \Sigma = (5.45 \times 10^{-6}\, cm/s) \times (2.01 \times 10^{6}\, cm^2) \times \frac{liter}{10^3\, cm^3} \times \frac{60\, s}{\min} = 0.66 \frac{liter}{\min}$$

5.4.2 Disk Centrifuge

A disk centrifuge is a system of rapidly rotating concentric inverted cones placed close together to minimize the time to capture dense particles or liquids at relatively high dimensionless accelerations. In this configuration (Figure 5.5), the feed suspension enters on the axis of rotation and is forced to the bottom of the rotating bowl. Pressure forces the suspension upward. The heavier fluid is forced through holes at the end of each disk channel until it reaches the outer periphery of the bowl. The lighter fluid flows up the disk channels and out of the centrifuge. The heavier sediment flows out through a nozzle if it is open; otherwise it collects on the outer wall of the bowl. Depending on whether the nozzle is open or closed, this centrifuge is operating in continuous or batch mode, respectively. The bowl can be designed to open intermittently at the periphery in the semicontinuous mode.

To determine the maximum feed rate Q, a simplified diagram of a single zone between two disks is used, as shown in Figure 5.6. For convenience, x-y coordinates are placed in a vertical plane that intersects the rotor axis with the x axis parallel to the disk surface. Equations of motion of a suspended particle are then determined with the constraint that every particle must sediment from the lower to the upper wall of a pair of disks. Thus, a suitable relationship must be obtained between v_0, the flow

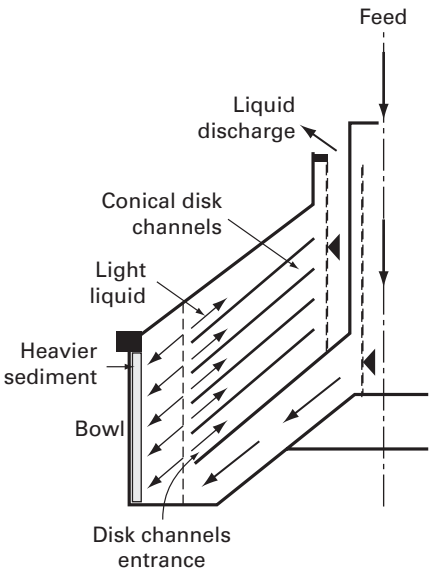

FIGURE 5.5 Cross-sectional diagram of a disk centrifuge, showing the path of the liquid flow and the collection of solids at the periphery.

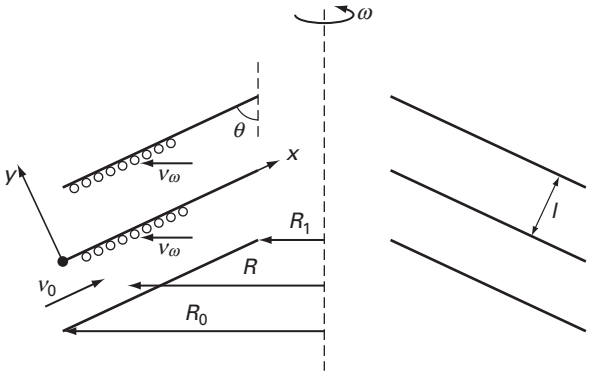

FIGURE 5.6 Diagram of the zone between two disks and the definition of variables for a disk centrifuge.

velocity, and v_ω, the sedimentation velocity of the particles. The following assumptions simplify the analysis:

1. Typically, v_0, the flow velocity, is much greater than v_ω.
2. $v_0 = Q/A$, where A decreases as particles move toward the center.
3. The fluid velocity v_0 is a function of y and goes to zero at the surface of the disks.

The equation of motion in the x direction is

$$\frac{dx}{dt} = v_0 - v_\omega \sin\theta \tag{5.4.8}$$

This is simplified by the assumption that v_0 is much greater than $v_\omega \sin\theta$. The average value of v_0, denoted $\langle v_0 \rangle$, is given by the flow rate Q divided by the cross-sectional area A perpendicular to the flow for n disks:

$$\langle v_0 \rangle = \frac{Q}{A} = \frac{Q}{n(2\pi R l)} \tag{5.4.9}$$

where the R is the radial distance from the center of rotation, which is varying, and l is the spacing between disks, which is fixed. The local value of v_0 can be found by multiplying $\langle v_0 \rangle$ by a function $f(y)$ that gives the velocity variation between the disks:

$$v_0 = \frac{Q}{n(2\pi R l)} f(y) \tag{5.4.10}$$

Integrating v_0 across the space between the disks gives the average value of v_0:

$$\frac{\int_0^l v_0(y)dy}{l} = \frac{Q}{n(2\pi Rl)} \tag{5.4.11}$$

From Equations (5.4.10) and (5.4.11), it is easily deduced that

$$\frac{\int_0^l f(y)dy}{l} = 1 \tag{5.4.12}$$

From Equations (5.4.8) and (5.4.10), neglecting v_ω sin θ in comparison to v_0, we have

$$\frac{dx}{dt} = \frac{Q}{n(2\pi Rl)} f(y) \tag{5.4.13}$$

The equation of motion in the y direction is centrifugal particle motion:

$$\frac{dy}{dt} = v_\omega \cos\theta = \frac{2a^2(\rho - \rho_0)\omega^2 R}{9\mu} \cos\theta \tag{5.4.14}$$

where the centrifugal velocity v_ω is obtained from Equation (5.2.2). The slope of the trajectory of particles moving between any pair of disks is determined by combining the equations of motion in the x and y directions:

$$\frac{dy}{dx} = \frac{\frac{dy}{dt}}{\frac{dx}{dt}} = \frac{4n\pi a^2(\rho - \rho_0)\omega^2 R^2 l \cos\theta}{9\mu Q f(y)} \tag{5.4.15}$$

Since $dx = -dR/\sin\theta$, Equation (5.4.15) can be rearranged to give

$$\frac{Q f(y)dy}{l} = -\frac{4n\pi a^2(\rho - \rho_0)\omega^2 R^2 \cot\theta}{9\mu} dR \tag{5.4.16}$$

For the boundary conditions of integration, we focus on the particles that are the most difficult to capture: such a particle entering at $y = 0$ and $R = R_0$ would exit at $y = l$ and $R = R_1$ (see Figure 5.6). After integration of Equation (5.4.16) and using the result of Equation (5.4.12), the result can be rearranged after multiplying and dividing by g to yield

$$Q = \left\{\frac{2a^2(\rho - \rho_0)g}{9\mu}\right\}\left[\frac{2n\pi\omega^2(R_0^3 - R_1^3)\cot\theta}{3g}\right] = \{v_g\}[\Sigma] \tag{5.4.17}$$

Therefore, in a sensitivity analysis it is seen that the Σ factor depends on the cube of the bowl radius, the cotangent of the disk acute angle, the number of disks in the stack, and, as in the tubular centrifuge, the square of the rotor speed. The disk acute angle θ made by the conical disks is typically between 35° and 50° [13].

There are three types of disk centrifuges, depending on the mode of discharging the solids. In the batch mode, solids accumulate at the periphery of the bowl until the bowl is nearly full, which is evidenced by turbidity of the liquid flowing out of the centrifuge. At this point, the centrifuge needs to be shut off and the solids removed manually. The solids content of the feed needs to be low (0 to 1 vol. %) in order that the downtime for solids removal does not become excessive. In the semicontinuous mode, the bowl is opened intermittently to allow solids to discharge through ports at the periphery. The solids content of the feed can be in the range of 0 to 10 vol. % for the intermittent discharge, and the solids exiting can be nonflowable. For continuous operation, nozzles are placed at the periphery of the centrifuge, and the solids content of the feed is in the range of 6 to 25% vol. %. The solids exiting from the nozzles are flowable. Nozzles are distributed around the periphery of the centrifuge and typically range from 12 to 24, depend on the size of the centrifuge [13].

The time between discharges in the semi-continuous mode of operation of a disk centrifuge with volumetric feed rate Q can be estimated from [13]:

$$t_d = \frac{V_s \varphi_e}{Q \varphi_f} \tag{5.4.18}$$

where V_s is the solids holdup volume of the bowl (which typically is 40 to 50% of the entire bowl volume) and φ_e and φ_f are the volume fractions of solids in the exiting sediment and feed, respectively.

5.5 ULTRACENTRIFUGATION

Ultracentrifuges operate over a range of inertial accelerations of 50,000 to 100,000 × g. These accelerations are so great that it is possible to sediment very small particles and even macromolecules in solution by an ultracentrifuge. In *analytical* ultracentrifugation [14], a sample volume of less than 1.0 ml is centrifuged in an optical cell while the concentration is monitored optically as a function of distance from the center of rotation. In *preparative* centrifugation, samples of up to 50 ml are centrifuged in a batch operation and collected, usually as a function of final distance from the center of rotation. This collection is usually accomplished by carefully puncturing the bottom of the centrifuge tube and collecting the outflow in a series of tubes.

5.5.1 Determination of Molecular Weight

One of the most important uses of ultracentrifugation has been the determination of molecular weights by the combined measurement of sedimentation and diffusion coefficients—the "sedimentation-diffusion molecular weight." Proteins are the most common macromolecular compounds that are homogeneous with respect to molecular weight, and it is for these compounds that the sedimentation-diffusion method has been mainly used. The molecular weights of proteins, as well as for viruses, obtained by this method have been found to be in excellent agreement with those obtained by other methods [15]. Today, protein and nucleic acid molecular weights are commonly determined by mass spectroscopy, electrophoresis, or chromatography (see Chapter 2).

The development of the dependence of molecular weight on the sedimentation and diffusion coefficients starts with the equation of motion for a sedimenting molecule at steady state [Equation (5.2.1)], which can be written as follows:

$$V(\rho - \rho_0)\omega^2 R - 6\pi\mu a v = 0 \tag{5.5.1}$$

where V is the volume of a single molecule. If we let $V = m\bar{V} = m/\rho$, where $\bar{V}$ is the molecule's specific volume and m is the mass of a single molecule, then Equation (5.5.1) can be rearranged to give

$$m = \frac{6\pi\mu a v}{(1 - \bar{V}\rho_0)\omega^2 R} \tag{5.5.2}$$

Viscosity can be related to the diffusion coefficient by the Stokes-Einstein equation:

$$\mathscr{D} \frac{\mu}{kT} = \frac{1}{6\pi a} \tag{5.5.3}$$

where k is Boltzmann's constant. Substituting the Stokes-Einstein equation into Equation (5.5.2) and making use of the definition of the sedimentation coefficient s [Equation (5.3.2)] and of Boltzmann's constant (= $R/\mathscr{N}$, where R is the universal gas constant and $\mathscr{N}$ is Avogadro's number) leads to

$$M = \frac{sRT}{\mathscr{D}\left(1 - \bar{V}\rho_0\right)} \tag{5.5.4}$$

where M is the molecular weight and here R is the gas constant. The partial specific volume $\bar{V}$ can be easily determined as the slope of a plot of the specific volume of the solution versus the weight fraction of the substance (see, e.g., the determination of M of chymotrypsinogen by Schwert [16]). For accurate determinations of M using this method, it is necessary that s and $\mathscr{D}$ be extrapolated to zero concentration. The diffusion coefficient of the macromolecule can be measured from concentration profiles at equilibrium during sedimentation with a density gradient, or more commonly, in a separate procedure such as by the free-diffusion method [15].

5.6 FLOCCULATION AND SEDIMENTATION

After cells have been lysed or bioparticles have been dispersed, it is often useful to hasten the subsequent sedimentation or filtration step by reversibly increasing the size of the particles to be separated. To this end, flocculation is used, and it occurs as the result of adding a suitable chemical called a "flocculant" or by the selection of naturally flocculating cells for fermentation, as in the case of lager yeast. Flocculants can act by forming interparticle molecular "bridges" between particles, in which case the flocculants are usually polymers or oligomers; they can also act by reducing the repulsive forces between cells, usually by reducing the strength of the electrostatic field (for details see Chapter 3, Section 3.4).

Centrifugation is frequently used after the addition of a flocculant to uncleared broth or cell lysates. While the resulting aggregates are often treated as Stokes spheres, they are actually open structures in which internal convection may occur. Various theories of sedimentation of flocs have therefore been proposed, in view of the importance of this motion in the water-processing (sewage treatment) industry [17].

Chapter 3 introduces the subject of flocculation but not the collection of the flocs that are produced. In process engineering, the sedimentation of flocs is usually treated empirically. Nevertheless, a number of formal treatments of this problem have been carried out. In the standard Equation (5.2.2) for the sedimentation of spheres, empirical adjustments for sedimentation velocity of flocs can be made on the basis of the reduction of density by the void volume fraction ε of the floc and the reduction of the drag force by the drag reduction factor Ω, which is also a function of the void volume fraction ε and the floc radius a. The resulting Stokes sedimentation velocity of spherical flocs composed of particles of density ρ is then

$$\upsilon = \frac{2a^2(1-\varepsilon)(\rho-\rho_0)\omega^2 R}{9\mu\Omega(\varepsilon,a)} \tag{5.6.1}$$

To estimate the drag force reduction due to liquid flow through the void volume of the floc, a dimensionless, normalized diameter $\beta \equiv a / k_f^{1/2}$ is defined, in which k_f is the permeability of the floc for the fluid in which it is settling. The drag force reduction factor has been related to the void volume fraction and the floc radius by a variety of closely related functions, the most widely used of which seems to be [18]:

$$\Omega(\varepsilon,a) = \frac{2\beta^2\left(1-\dfrac{\tanh\beta}{\beta}\right)}{2\beta^2+3\left(1-\dfrac{\tanh\beta}{\beta}\right)} \tag{5.6.2}$$

The determination of β requires knowing the floc permeability k_f, which can be calculated by using the following form of the Carman-Kozeny equation:

$$k_f = \frac{\varepsilon^2}{KS^2(1-\varepsilon)^2} \tag{5.6.3}$$

where Kozeny's constant K = 4.8 [19], and S is Carman's specific surface area, defined as the area of nonporous materials exposed to the liquid per unit volume, as determined from the geometry of the individual particles that form the aggregate.

In addition to the collective behavior of particles in flocs, particles do not behave totally independently when they are suspended at high concentration, such as at the outer rim of a centrifuge or the bottom of a settling tank.

5.7 SEDIMENTATION AT LOW ACCELERATIONS

At low g forces, the sedimentation rate slows down and can sometimes be similar to the rate of transport by diffusion, which is not affected by inertial forces. Here, we examine ways to compare sedimentation and diffusion rates. The case of isothermal settling is evaluated, which can lead to exponential distributions of concentration as a function of height for small particles. Inclined sedimentation and field-flow fractionation, two operations that separate suspended particles on the basis of inertial motion at 1 × g, are also described.

5.7.1 Diffusion, Brownian Motion

Einstein described diffusion as the consequence of a "random walk" by particles due to their thermal energy kT (k = Boltzmann's constant). The surprisingly simple result was

$$\left\langle x^2 \right\rangle = 2\mathscr{D}t \tag{5.7.1}$$

where $\langle x^2 \rangle$ is the mean square distance traveled by a particle having diffusion coefficient $\mathscr{D}$ in time t. Using the Stokes-Einstein equation [Equation (5.5.3)] for spherical particles of radius a undergoing Brownian movement in a fluid of viscosity μ, we can relate the diffusion coefficient to the thermal energy kT as follows:

$$\mathscr{D} = \frac{kT}{6\pi\mu a} \tag{5.7.2}$$

In a concentration gradient, the net unidirectional flux of particles is proportional to $\mathscr{D}$ and the gradient, dc/dx, of the particle concentration c. Diffusion is not affected by gravity. Diffusion and sedimentation velocities, however, are sometimes similar, and their sum results in gradual settling.

5.7.2 Isothermal Settling

If the temperature T does not change over the height h of an ensemble of particles, then the mean kinetic energy, which is proportional to kT, of all particles is the same at all heights. The potential energy of a particle of mass m is usually expressed as mgh; but if the particles are subject to buoyant forces in the fluid, the potential energy becomes $V(\rho - \rho_0)gh$ for particle volume V. From the Boltzmann distribution rule, the concentration of particles at height h at equilibrium is therefore

$$c(h) = c(0)\exp\left[\frac{-V(\rho-\rho_0)gh}{kT}\right] \tag{5.7.3}$$

This means that concentration is an exponential function of height under isothermal conditions and that large, dense particles with potential energy much greater than kT (from mammalian cells to marbles) will be concentrated at $h = 0$ and that small particles (mainly molecules) will have $c(h) \approx$ constant. However, submicrometer organic particles and certain macromolecules have values of V and ρ that lead to measurable exponential distributions of $c(h)$.

5.7.3 Convective Motion and Péclet Analysis

One way to determine whether $c(h)$ will be distributed as in Equation (5.7.3) is to estimate the value of the Péclet number, Pe, commonly used in the dimensionless analysis of fluid motion relative to diffusive transport. The Péclet number is a ratio of the sedimentation velocity to the characteristic rate of diffusive transport over distance L:

$$\mathrm{Pe} = \frac{\upsilon}{\mathscr{D}/L} \tag{5.7.4}$$

If Pe < 0.1, diffusion is dominant; and $c(h)$ is approximately constant or distributed. In this case, Equation (5.7.3) should be used. If Pe > 10, sedimentation dominates, and the concentration will eventually be high at $h = 0$ and 0 elsewhere.

5.7.4 Inclined Sedimentation

Rapid removal of high-density solids can be achieved at $1 \times g$ by using inclined sedimentation. An inclined settler is shown in Figure 5.7; the dimensions and the flow rates are labeled. In a typical application, feed containing suspended particles is pumped into the settler near or at its lower end at flow rate Q_f, particle-free overflow exits the upper end at flow rate Q_o, and particle-rich suspension leaves in the underflow at rate Q_u. This is an excellent method for harvesting supernatants continuously or batchwise from particle (cell)-laden broth. The material balance relationships are

$$Q_f = Q_u + Q_o \tag{5.7.5}$$

$$c_f Q_f = c_u Q_u + c_o Q_o \quad (5.7.6)$$

where the c's designate particle concentrations. It is often desirable that $c_o = 0$. To achieve this, Q_o must equal the volumetric clearing rate $S(\upsilon)$. This volumetric clearing rate S is equal to the vertical settling velocity υ_g of the cells multiplied by the horizontal projected area of the upward-facing surfaces of the channel onto which the cells may settle, which is given by the following equation [20]:

$$S = \upsilon_g w (L \sin\theta + b \cos\theta) \quad (5.7.7)$$

where θ is the angle of inclination of the plates from the vertical, and b, w, and L are the height, width, and length of the rectangular settler, respectively (Figure 5.7).

Inclined settlers are designed so that the path to the completion of sedimentation of a particle is extremely short, only a few millimeters, before the sedimented particles begin to be convected toward the underflow. If the particulate fraction is desired, it can be batch concentrated by continuous recycle of the underflow back to the tank while the overflow bleeds off the supernatant. By the use of appropriate settings, governed and predicted by the foregoing equations, it is also possible to remove small particles in the overflow while retaining larger ones in the underflow, thereby effecting a binary particle classification by size [20].

An important application of inclined settlers is in the removal of unproductive or parasitic cells from bioreactors or cell culture systems; this method was used to remove nonviable hybridoma cells from a cell culture, which resulted in high viable cell concentrations and high monoclonal antibody productivity over a 2-week culture period [20].

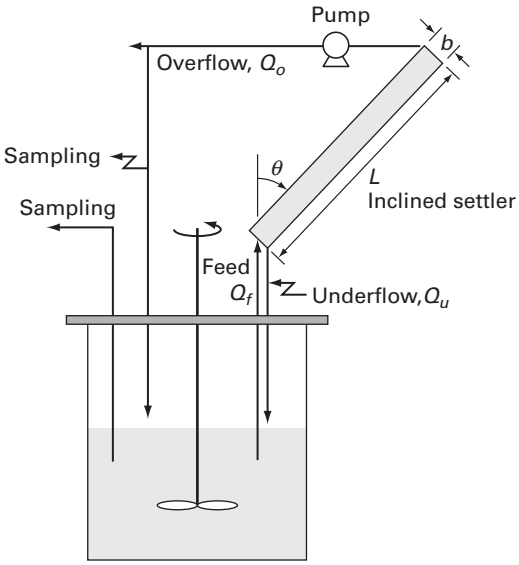

FIGURE 5.7 Diagram of an inclined settler system indicating variables used in the mass balance [Equation (5.7.5)] and volumetric clearing rate [Equation (5.7.7)].

Since inclined settlers can be scaled up directly by increasing the area for settling, they potentially could be used at larger than laboratory scale. These settlers operate at much higher capacities than vertical settlers because cells need to settle only a distance of order b (see Figure 5.7) in an inclined settler, compared with a distance of order L in a vertical settler.

5.7.5 Field-Flow Fractionation

Field-flow fractionation (FFF) is designed to separate particles of different sizes on the basis of the hydrodynamics of a very thin, flat, horizontal channel through which a sample suspension is pumped and subjected to the laminar flow velocity gradient in the channel as shown in Figure 5.8. In the case of sedimentation, the driving force toward the lower channel wall is gravity or centrifugal sedimentation. In the latter case, the channel is "wrapped" around the perimeter of a rotating centrifuge. Steep velocity gradients occur at the upper and lower walls of the channel, and these result in a distribution of larger particles toward the center and smaller particles toward the lower wall. The separation of particles by this phenomenon is called "steric" FFF. As particle transport proceeds along the lower wall, the particles bunch up according to their velocity; thus the lower wall is called an "accumulation wall." For continuous operation, a horizontal splitter at the outlet permits the collection of large particles in an upper outlet and small particles in a lower outlet. The governing equation for field-flow fractionation is

$$R = \frac{6\gamma a}{b} \tag{5.7.8}$$

where R is the retention ratio, defined as the ratio of the particle velocity to the mean fluid velocity, a is the particle radius, b is the channel height, and γ is the "steric factor" that determines the particle net velocity and is approximately equal to $(1 + \delta/a)$, where δ is the distance between the particle and the accumulation wall, as noted in

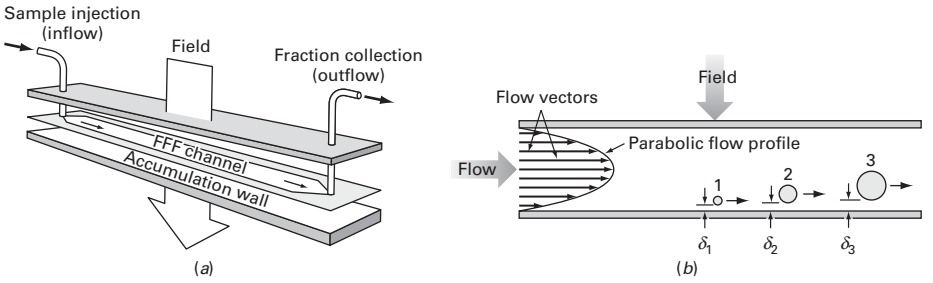

FIGURE 5.8 (*a*) Exploded view of a field-flow fractionation (FFF) channel. The "field" is the driving force for separation, expected to act differentially on particles of different types. The field could be gravitational, electrical, thermal, adsorptive, or steric, to name a few. (*b*) The principle of steric FFF. Larger particles protrude into the higher-velocity region of laminar flow, hence are carried farther in a specific amount of time than their smaller counterparts.

Figure 5.8. This technique has been shown to separate two cell-sized latex populations having sphere diameters of 10 and 15 μm, and also to separate white and red blood cells [21].

5.8 CENTRIFUGAL ELUTRIATION

Centrifugal elutriation is similar to inclined sedimentation and field-flow fractionation in that sedimentation takes place in the presence of fluid flow. In centrifugal elutriation, also called counterstreaming centrifugation, the effective length of a sedimentation path is greatly extended by continuously pumping a counterstreaming fluid in the opposite direction to that of sedimentation. To accomplish this, "elutriation rotors" have been designed. Such rotors perform functions similar to those of the tubular bowl and disk-stack centrifuges. The sample suspension is held in the rotor chamber, and the particles remain there as long as the two opposing forces are in balance. By incremental increases in the flow rate of the fluid or by decreases in the centrifugal force, distinct populations of particles (including cells) with relatively homogeneous sizes can be eluted out of the rotor sequentially. The objective of elutriation is thus to collect particles of a specified volume by modifying the velocity of the eluent fluid or the angular velocity of the rotor [22]. Both these variables must be controlled with extreme care if precision of separation is to be achieved. The volume and radius of the largest particle that can escape against the counterflow and be collected in the effluent can be determined from the equation of motion for a spherical particle in an inertial field [Equation (5.2.1)], using the velocity v_0 for the eluting fluid [22]:

$$V = \frac{9\pi\sqrt{2}\left[\dfrac{v_0\mu}{R(\rho-\rho_0)}\right]^{3/2}}{\omega^3} \tag{5.8.1}$$

$$a = \frac{3\left[\dfrac{v_0\mu}{2R(\rho-\rho_0)}\right]^{1/2}}{\omega} \tag{5.8.2}$$

where V and a are the volume and radius of the particle, respectively. The capacity of centrifugal elutriation in the batch mode is about 10^8 particles of about 10 μm diameter.

5.9 SUMMARY

Sedimentation is the movement of particles or macromolecules in an inertial field. Inertial accelerations vary from 1 × g in flocculation tanks to 100,000 × g in ultracentrifuges.

- Sedimentation, like filtration, is used in early stages in downstream bioprocessing mainly for liquid–solid separations. Particles can be separated at large scale in continuous centrifuges, and macromolecules can be separated, either for analysis or collection, at small scale by ultracentrifugation at very high speeds.
- The sedimentation velocity v of a particle depends on the square of its radius a and linearly on the difference between its density ρ and that of the suspending solvent ρ_0:

$$v = \frac{2a^2(\rho - \rho_0)\omega^2 R}{9\mu}$$

  where ω is angular velocity (rad/s), R is the distance of the particle from the center of rotation, and μ is fluid viscosity. The term $\omega^2 R$ is the centrifugal acceleration.
- Corrections related to sedimentation calculations are required when particle concentrations are high enough to hinder settling. Functions of concentration are available for this correction.
- The sedimentation coefficient s, a property of both the particle and the medium, is defined as

$$s \equiv \frac{v}{\omega^2 R}$$

  which leads to

$$s = \frac{2a^2(\rho - \rho_0)}{9\mu}$$

- Equivalent time is the product Gt, where G is defined as

$$G \equiv \frac{\omega^2 R}{g}$$

  One approach to scale-up of centrifugation is to assume constant equivalent time.
- Engineering analyses and scaling calculations on large-scale centrifuges are often performed by means of "sigma analysis," which uses the operation constant Σ to characterize a centrifuge into which feed flows at volumetric flow rate Q. Since the engineer often needs to estimate Q, a convenient relationship is

$$Q = \{v_g\}[\Sigma]$$

where v_g is the sedimentation velocity at $1 \times g$,

$$v_g = \frac{2a^2(\rho - \rho_0)g}{9\mu}$$

and Σ represents the geometry and speed of the centrifuge.

- The appropriate centrifuge for a particular liquid-solid separation is chosen on the basis of the objectives of the operation, the solids content and flow rate of the feed stream, and the maximum acceleration at which the device can operate.
- The molecular weight of a macromolecule such as a protein can be determined from ultracentrifuge data, which measure the sedimentation and diffusion coefficients.
- After flocculation, loosely structured, porous particles form, and these sediment more rapidly than their solid counterparts having the same size. Correction factors allow the calculation of the velocity of flocculated particles.
- Diffusion occurs in sedimentation operations, and its significance, specifically at low accelerations, can be ascertained by calculating the Péclet number.
- Two useful sedimentation operations at $1 \times g$ are inclined sedimentation and field-flow fractionation.
- In centrifugal elutriation, a counterstreaming fluid is continuously pumped in the opposite direction to that of sedimentation. This greatly extends the sedimentation path and allows distinct populations of particles (including cells) with relatively homogeneous size to be eluted out of the centrifuge rotor sequentially.

NOMENCLATURE

a	radius of particle (μm)
A	cross-sectional area (cm^2)
b	height (cm)
c	concentration (M, or g liter^{-1})
$\mathscr{D}$	diffusion coefficient (cm^2 s^{-1})
g	gravitational acceleration (9.8066 m s^{-2})
G	multiple of gravitational acceleration (= $\omega^2 R/g$) (dimensionless)
h	height (cm)
F_x	force in x direction (N)
k	Boltzmann's constant (1.3807×10^{-23} J K^{-1})
k_f	floc permeability (cm^2)
K	Kozeny's constant (= 4.8) (dimensionless)
m	mass of particle or molecule (g)
M	molecular weight (Daltons)

n exponent in Equation (5.2.7) (dimensionless)
n number of disks in a disk centrifige (dimensionless)
$\mathscr{N}$ Avogadro's number (6.0221×10^{23} molecules mol^{-1})
l spacing between disks in a centrifuge (cm)
L distance (cm)
L length of an inclined settler (cm)
Pe Péclet number ($= vL/\mathscr{D}$) (dimensionless)
Q flow rate ($cm^3\ s^{-1}$)
R distance from center of rotation (cm)
R retention ratio in field-flow fractionation (= ratio of particle velocity to the mean fluid velocity) (dimensionless)
R gas law constant (8.3145 J mol^{-1} K^{-1})
Re Reynolds number ($2av\rho/\mu$) (dimensionless)
s sedimentation coefficient [Equation (5.3.2)] (s)
S volumetric clearing rate in an inclined settler ($cm^3\ s^{-1}$)
t time (s)
t_d time between discharges of a solids-ejecting disk centrifuge (s)
T temperature (K)
v sedimentation velocity (cm s^{-1})
v_c sedimentation velocity in a concentrated suspension (cm s^{-1})
v_g sedimentation velocity at $1 \times g$ (cm s^{-1})
v_ω sedimentation velocity at ω angular velocity (cm s^{-1})
v_0 fluid velocity (cm s^{-1})
V volume of a molecule or particle (cm^3)
V_0 volume of cylinder in a gradient mixer [Equation (5.3.1)] (cm^3)
V_s volume of solid holdup in the bowl of a disk centrifuge (cm^3)
$\bar{V}$ specific volume of a molecule ($cm^3\ g^{-1}$)
w width of an inclined settler (cm)

Greek Letters

β normalized diameter of a floc $(= a / k_f^{1/2})$ (dimensionless)
γ steric factor in field-flow fractionation $(\cong 1 + \delta / a)$ (dimensionless)
δ distance between particle and accumulation wall in field-flow fractionation (cm)
ε void fraction of particles in a floc (dimensionless)
θ centrifuge disk acute angle (Figure 5.6) (degrees)
θ angle of inclination of an inclined settler from vertical (degrees)
μ viscosity of fluid (g cm^{-1} s^{-1} = poise)
ρ density of particle or molecule (g cm^{-3})
ρ_0 density of medium (g cm^{-3})
Σ operation constant of a centrifuge (cm^2)
τ residence time of fluid in the centrifuge bowl (s)
φ volume fraction of particles (dimensionless)

φ_e volume fraction of solids in the exiting sediment (dimensionless)
φ_f volume fraction of solids in the feed (dimensionless)
ω angular velocity (rad s^{-1})
Ω drag reduction factor [Equation (5.6.2)] (dimensionless)

PROBLEMS

5.1 Sedimentation versus Filtration Four particulate materials, A, B, C, and D, are suspended in water (density = 1.00 g/cm^3) and have the properties given in Table P5.1. Choose between sedimentation and filtration for the separation of the following pairs of particles from one another in mixed suspensions in water. Explain your answer in each case.

(a) A from B
(b) B from C
(c) C from D

TABLE P5.1

Particle name	Density (g/cm^3)	Radius (μm)
A	1.05	10
B	1.05	12
C	1.01	50
D	1.04	25

5.2 Strategies for Product Separation Yeast cells (a = 3 μm) in a fermentor secrete a low molecular weight product at a concentration that produces uniform rod-shaped crystals 2 × 6 μm at about 20 times the number concentration (particles/ml) as the cells. Using concise statements, design two possible strategies that take advantage of the particulate nature of the product to separate the product from the broth and from the cells. What additional information about the product crystals would be useful?

5.3 Isopycnic Sedimentation You wish to capture 3 μm particles in a linear density gradient having a density of 1.12 g/cm^3 at the bottom and 1.00 at the top. You layer a thin particle suspension on the top of the 6 cm column of fluid with a viscosity of 1.0 cp and allow particles to settle at 1 g.

(a) How long must you wait for the particles you want (density = 1.07 g/cm^3) to sediment to within 0.1 cm of their isopycnic level? Is it possible to determine the time required for particles to sediment to *exactly* their isopycnic level?
(b) If instead of 1 g you use a centrifuge running at 800 rpm, and the top of the fluid is 5 cm from the center of rotation, how long must you centrifuge for the particles to move to within 0.1 cm of their isopycnic level?

5.4 Time Required for Sedimentation by Gravity A certain reagent is added to a suspension of cells 4 μm in diameter. These cells have a density of 1.08 g/cm^3, and they are suspended in liquid with a density of 1.00 g/cm^3 and viscosity of 1.0 cp. This reagent causes about half of the cells to form fairly solid aggregates, all of which are 90 μm

in diameter and have density midway between that of the liquid and the cells. How much time is required for all the aggregates to sediment to within 1 cm of the bottom of a vessel filled with suspension that is 0.5 m high? Approximately what fraction of the single cells would have sedimented to this depth in the same amount of time? How much time is required for all the single cells to sediment to within 1 cm of the bottom of the vessel?

5.5 Time Required for Sedimentation in a Centrifuge Using the results of Problem 5.4, determine the diameter and speed of a centrifuge required to reduce the total sedimentation time for the aggregates by a factor of ten, assuming you will use containers that are 20 cm high in the centrifuge. Also assume that the center of rotation is 3 cm from the tops of the containers. How much time must the same centrifuge be operated to also sediment all the single cells? For simplicity, assume a swinging-bucket type of centrifuge, in which the axis of the cylindrical vessel is horizontal, hence parallel to the direction of sedimentation.

5.6 Determination of Sigma for a New Pilot Scale Centrifuge You test a new pilot scale centrifuge by doing a breakthrough experiment using yeast as test particles. The yeast were previously found to sediment at 100 μm/s in a laboratory centrifuge operated at an acceleration of 500 × g. The breakthrough flow rate is found to be 10 liters/min. What is the sigma (Σ) of this new centrifuge?

5.7 Bench Scale Tests for a Tubular Bowl Centrifuge You can bench-test a tubular bowl separation by first characterizing the product in a test-tube centrifugation. Without actually knowing the size and density of the particles in the suspension, derive an expression for the angular velocity required to capture the solids at a given volumetric flow rate Q in terms of the geometry of the tubular bowl and the quantities you would measure in the test tube centrifugation.

5.8 Recovery of *E. coli* in a Tubular Bowl Centrifuge You are using a tubular bowl centrifuge to recover *E. coli* cells containing an important bioproduct from a fermentation broth. In a preliminary run you find that 50% of the cells are recovered at a flow rate of 5 liters/min and rotation speed of 6000 rpm.

(a) To increase the yield to 95% using the same centrifuge, what must the flow rate be?

(b) How much does the sedimentation velocity change if you double the rotation speed?

5.9 Scale-up of a Disk Centrifuge Based on Laboratory Data Determine the maximum flow rate for the clarification of a suspension of lysed *Escherichia coli* cells by a plant scale disk centrifuge based on laboratory data. The plant centrifuge has a bowl diameter of 25.4 cm and capabilities shown in Table 5.5. For this centrifuge, you also know that $\theta = 42^{\circ}$, $R_1 = 8$ cm, $R_0 = 20$ cm, and number of disks = 100 (see Figure 5.6).

In a laboratory centrifuge, you determined that it took a minimum of 17 min to clarify the cell lysate at 12,000 rpm. The top of the culture being centrifuged was 32 mm from the center of rotation, and the top of the packed solids was 79 mm from the center of rotation after 17 min.

5.10 Determination of Molecular Weight by Ultracentrifugation A new biopharmaceutical "X" has been discovered. Only crude extracts are available, and the material is known to be a macromolecule. You are given a preparative ultracentrifuge and asked to estimate the molecular weight of the macromolecule. You then do two experiments.

In the first one, you set up a linear sucrose density gradient and layer a crude sample of X on top of it, using a 5 cm long centrifuge tube (completely filled) and centrifuge to equilibrium for 3 days (72 h) at 25,000 rpm. In the second experiment, you place the sample in its dilute buffer (viscosity the same as water) directly into *two* of the same plastic ultracentrifuge tubes and run the centrifuge for 24 h at 25,000 rpm, at which time you stop and remove fractions from one of the two tubes. After an additional 72 h at 25,000 rpm, you stop the centrifuge and remove fractions from the remaining tube. In all three cases, you collect 20 fractions, and each fraction corresponds to a 2.5 mm layer, so fraction 1 came from the bottom of the tube and fraction 20 came from the top. Assume that the top of each centrifuge tube is 3 cm from the center of rotation.

The company biologist then takes the three sets of 20 fractions and tests them on cell cultures. The biologist returns data to you in terms of biological activity units in each fraction, on a scale that is known to be linear with product mass. You then plot the data from the three centrifuge tubes (Figure P5.10).

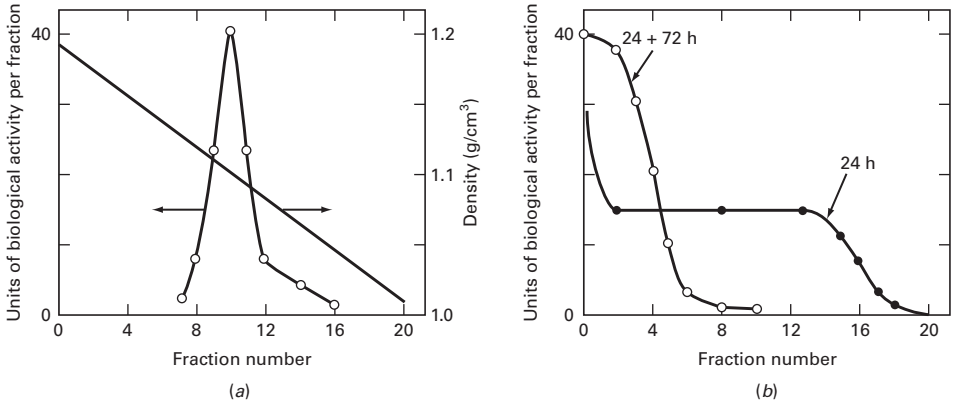

FIGURE P5.10 Ultracentrifugation results. (*a*) First experiment: crude extract layered on the top of a tube with a linear sucrose density gradient and centrifuged to equilibrium for 72 h. (*b*) Second experiment: crude extract in its dilute buffer in each of two of the same plastic tubes with one tube centrifuged for 24 h and the other tube for 72 h. Centrifuge speed 25,000 rpm. Fractions, each corresponding to a 2.5 mm layer in the tube, are numbered from the bottom to the top of each tube.

(a) From the appropriate equations for ultracentrifugation, use the data to estimate the molecular weight of product X. (*Hint:* Use widths of profiles to estimate diffusivity.)

(b) Make a sketch of the method for collecting fractions.

(c) After you completed your material balance calculations on the tubes, which were 8 mm in diameter, the biologist told you that each tube originally contained 20 units of biological activity. Speculate about why the material balance did not close.

5.11 Isothermal Settling Based on the data in Table 5.1, estimate the reduced concentration profile, $c(h)/c(0)$, for the isothermal settling at 1 g of a protein with a sedimentation radius of 0.005 μm at ambient temperature up to a height of 100 cm. Recalculate the profile for a protein with a sedimentation radius of 0.002 μm. Also calculate the molecular weight of each protein. Explain the meaning of the concentration profiles.

5.12 Cost of Centrifugation In a bioprocess for the production of foreveron (a hypothetical youth-giving protein made by Kindergen, Inc.), a centrifuge is used to remove the cells from the culture broth. The centrifuge operates continuously at 20 kW and processes 20 liters of feed culture broth per hour, discharging a liquid supernatant phase containing 92 vol% of the feed liquid and no cells. The cell paste output has a density of 1.08 g/cm^3. The feed is processed batchwise in 40 liters of feed per batch. It takes a busy technician ($20/h) 15 min to start the feed flow and 15 min to collect each batch and deliver the supernatant and sediment to the next steps. Kindergen paid $50,000 for the centrifuge, which has a useful life of 10 years, buys a service contract for $5000/year, and replaces the rotor every year for $10,000. The centrifuge is used only for foreveron processing at two batches per day, 300 days a year.

Calculate the cost of the centrifugal processing per kilogram of cell paste produced. What contributes the most to the cost of centrifuging?

5.13 Estimation of Flow Rate for Centrifugation of Yeast Cells A maximum flow rate of 50 liters/min was achieved for the centrifugation of bacteria cells in a tubular centrifuge. The cells were 2.0 μm in diameter and had a density of 1.08 g/cm^3. The medium had a density of 1.01 g/cm^3 and viscosity of 1.2 cp.

It is desired to centrifuge yeast cells in this same centrifuge. The yeast cells have a diameter of 5.0 μm and a density of 1.10 g/cm^3. The medium has a density of 1.02 g/cm^3 and a viscosity of 1.3 cp. Estimate the maximum flow rate that can be used to centrifuge the yeast cells.

5.14 Determination of Sigma from Laboratory Data In a laboratory centrifuge, it was found that it took 300 s to centrifuge cells at 2000 rpm to a constant height of packed cells. The top of the cell suspension and the top of the packed cells were 5 cm and 9 cm, respectively, from the center of rotation of the centrifuge. For processing these cells in a tubular bowl centrifuge at a flow rate of 20 liters/min, what should the value of Σ be?

REFERENCES

1. Bird, R. B., Stewart, W. E., and Lightfoot, E. N. (2002). *Transport Phenomena*, 2nd ed., Wiley, New York.
2. Kubitschek, H. E. (1987). Buoyant density variation during the cell cycle in microorganisms. *Crit. Rev. Microbiol*., vol. 14, p. 73.
3. Hart, A., and Edwards, C. (1987). Buoyant density fluctuations during the cell cycle of *Bacillus subtilis*. *Arch. Microbiol*., vol. 147, p. 68.
4. Illmer, P. (2001). How big is a bacterium? Approximation to a correct total cell density of *Arthrobacter* sp. *FEMS Microbiol. Lett*., vol. 196, p. 85.
5. Sheeler, P. (1981). *Centrifugation in Biology and Medicine*, Wiley-Interscience, New York.
6. Richardson, J. F., and Zaki, W. N. (1954). Sedimentation and fluidisation: Part I. *Trans. Inst. Chem. Eng*., vol. 32, p. 36.
7. Richardson, J. F., and Shabi, F. A. (1960). The determination of concentration distribution in a sedimenting suspension using radioactive solids. *Trans. Inst. Chem. Eng*., vol. 38, p. 33.
8. Meselson, M., and Stahl, F. W. (1957). The replication of DNA in *E. coli*. *Proc. Natl. Acad. Sci. USA*, vol. 44, p. 671.
9. Ladisch, M. R. (2001). *Bioseparations Engineering*, Wiley, New York.
10. Belter, P. A., Cussler, E. L., and Hu, W.-S. (1988). *Bioseparations*, Wiley, New York.

11. Bell, D. J., Hoare, M., and Dunnill, P. (1983). The formation of protein precipitates and their centrifugal recovery. In *Advances in Biochemical Engineering/Biotechnology*, vol. 26, A. Fiechter, ed., Springer-Verlag, Berlin, p. 1.
12. Perry, R. H., Green, D. W., and Maloney, J. D., eds. (1997). Liquid-solids operations and equipment (Section 18). *Perry's Chemical Engineers' Handbook*, McGraw-Hill, New York.
13. Leung, W. W. (2007). *Centrifugal Separations in Biotechnology*, Academic Press, Amsterdam.
14. Schachman, H. K. (1959). *Ultracentrifucation in Biochemistry*, Academic Press, New York.
15. Tanford, C. (1961). *Physical Chemistry of Macromolecules*, Wiley, New York.
16. Schwert, G. W. (1951). The molecular size and shape of the pancreatic proteases. II. Chymotrypsinogen. *J. Biol. Chem*., vol. 190, p. 799.
17. Li, D., and Ganczarczyk, J. (1992). Advective transport in activated sludge flocs. *Water Environ. Res*., vol. 64, p. 236.
18. Neale, G., Epstein, N., and Nader, W. (1973). Creeping flow relative to permeable spheres. *Chem. Eng. Sci*., vol. 28, p. 1865.
19. Adler, P. M. (1986). Transport processes in fractals. VI. Stokes flow through Sierpinski carpets. *Phys. Fluids*, vol. 29, p. 15.
20. Davis, R. H., Lee, C.-Y., Batt, B. C., and Kompala, D. S. (1991). Cell separations using differential sedimentation in inclined settlers. In *Cell Separation Science and Technology*, D. S. Kompala and P. Todd, eds., ACS Symposium Series 464, American Chemical Society, Washington, DC, p. 113.
21. Giddings, J. C., Barman, B. N., and Liu, M.-K. (1991). Separation of cells by field-flow fractionation. In *Cell Separation Science and Technology*, D. S. Kompala and P. Todd, eds., ACS Symposium Series 464, American Chemical Society, Washington, DC, p. 128.
22. Keng, P. C. (1991). High-capacity separation of homogeneous cell subpopulations by centrifugal elutriation. In *Cell Separation Science and Technology*, D. S. Kompala and P. Todd, eds., ACS Symposium Series 464, American Chemical Society, Washington, DC, p. 103.

/// 6 /// EXTRACTION

Extraction is a process in which two phases come into contact with the objective of transferring a solute or particle from one phase to the other. For the separation and purification of biological products, the phases are most commonly immiscible liquids, and the solute is in soluble form. In certain instances, however, one phase is a liquid and the other phase is a solid; the extraction of caffeine from coffee beans is one example. Although most extractions in biotechnology involve the transfer of soluble bioproducts, organelles and cells have at times been transferred between phases. An organic solvent is often used as the extracting liquid when the solute to be extracted is stable in the organic solvent, typical examples being low molecular weight antibiotics. It is usually not feasible to extract proteins with organic solvents, since proteins are often denatured or degraded as a result of contact with the organic solvent. Proteins can often be successfully extracted by means of two immiscible liquid phases that consist of solutions of two water-soluble but incompatible polymers, or one polymer plus a high concentration of certain salts.

Extraction usually comes early in the purification process for a bioproduct and typically would precede a high-resolution step such as chromatography. Extraction is often advantageous because it can bring about a significant reduction in volume and/or can separate the desired product from cells or cell debris. It is desirable to reduce the volume as soon as possible in the process, since large volumes typically lead to large costs.

The extractions of interest in the purification of biotechnological and pharmaceutical products are mainly liquid-to-liquid, and this is the emphasis in this chapter. The basic definitions and principles of extraction are developed first, followed by an explanation of scale-up and design procedures for the extractors most commonly used for bioproducts.

6.1 INSTRUCTIONAL OBJECTIVES

After completing this chapter, the reader should be able to do the following:

- Define and use key constants such as the partition coefficient, solvent-to-feed ratio, and extraction factor.

- Explain the factors that affect the partitioning of biomolecules.
- Construct a phase diagram for aqueous two-phase systems and understand their applications to the extraction of proteins.
- Calculate solute concentrations in multistage countercurrent extraction cascades.
- Draw equilibrium and operating lines, and use them to calculate equilibrium stages in countercurrent extraction.
- Perform scaling calculations for reciprocating-plate and centrifugal extractors.

6.2 EXTRACTION PRINCIPLES

Separation of biomolecules in liquid-liquid extraction depends on the partitioning of the biomolecules between the liquid phases. Design of the extraction process depends on the miscibility of the two liquid phases in each other, and the rate of equilibration of the biomolecules between the two phases. Aqueous two-phase extraction is a nondenaturing and nondegrading technique that can be used for a number of biomolecules such as proteins, viruses, cells, and cell organelles; therefore, the analysis of partitioning in aqueous two-phase extraction is emphasized. Both graphical and analytical approaches to extractor stage calculations are discussed.

6.2.1 Phase Separation and Partitioning Equilibria

In a single-stage extraction process, one feed stream contacts one extraction solvent stream, and the mixture divides into equilibrium extract and raffinate phases, as shown schematically in Figure 6.1. The distribution of a solute at equilibrium between two liquid phases is defined by the *partition* or *distribution coefficient* as

$$K = \frac{y}{x} \tag{6.2.1}$$

where y and x are the concentrations of the solute in the extract and raffinate phases, respectively. Thus, for the lowest volume of extraction solvent, it is desirable to have K as large as possible. Partition coefficients near unity would require large volumes and many serial extractions for full recovery. Partition coefficients near zero would indicate no extraction at all.

The partition coefficient can depend on many parameters, such as the size of the molecule being extracted, pH, types of solvent, temperature, and concentration and

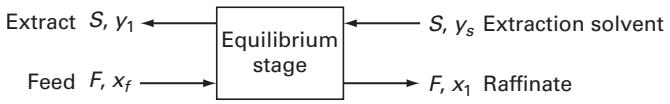

FIGURE 6.1 Flow diagram of one equilibrium stage, showing stream variables. The two phases are assumed to be immiscible.

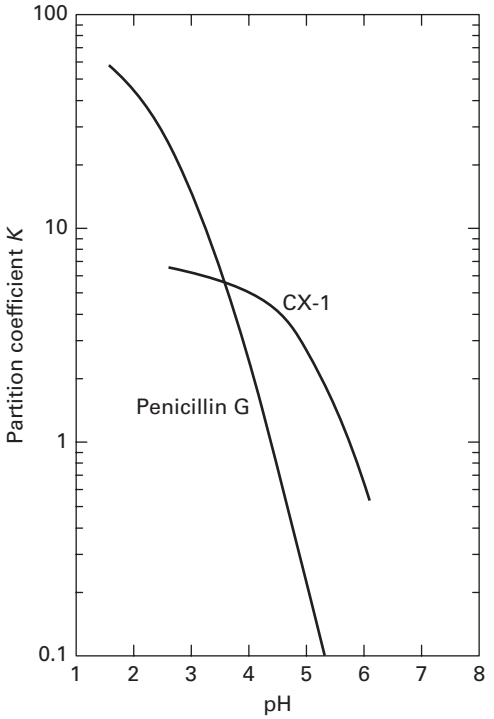

FIGURE 6.2 Dependence of the partition coefficient on pH for penicillin G and acidic impurity CX-1: an organic solvent was used for extraction from filtered fermentation broth. *(Data from M. Souders, G. J. Pierotti, and C. L. Dunn, "The recovery of penicillin by extraction with a pH gradient,"* Chem. Eng. Prog. Symp. Ser. *100, vol. 66, p. 39, 1970.)*

molecular weight of polymers (or salt) in the phases. The literature contains partition coefficients for many biological molecules, especially amino acids and antibiotics, but caution must be exercised if conditions other than those reported are used. An example of the effect of pH on the partition coefficient is shown in Figure 6.2 for the antibiotic penicillin G and an acidic impurity. It can be seen that below pH 4 the extraction of penicillin G into the solvent phase is favored over that of the acidic impurity CX-1.

Models developed to describe the partitioning of biomolecules are useful not only in extending existing partitioning data to new conditions, but also in obtaining reasonable first estimates of partition coefficients. One of the simplest models to describe partitioning between phases is the one developed by Brønsted [1]:

$$K = \exp\left(\frac{M\lambda}{kT}\right) \tag{6.2.2}$$

where M is the molecular weight of the molecule being partitioned, k is the Boltzmann constant, T is absolute temperature, and λ is a constant (lumped parameter) that includes characteristics of both the phase system and the partitioning substance. It

can be observed that for the partitioning of penicillin G (Figure 6.2) the Brönsted model corresponds to a steadily decreasing λ from pH 2 to 5.

Aqueous *two-phase extraction systems* are made by combining two water-soluble polymers or a polymer and a salt in water, above a "critical concentration." These systems separate into two immiscible liquid phases, one of them enriched in one polymer and the other enriched in the other polymer or salt. Soluble or particulate separands, added to the system, partition themselves between the two phases. Aqueous two-phase extraction has become recognized as a nondenaturing and nondegrading technique for the separation of a number of biological entities such as proteins, enzymes, viruses, cells, and cell organelles. This method also has been useful for the removal of undesirable contaminating by-products such as nucleic acids and polysaccharides.

Each two-phase aqueous system can be characterized by a phase diagram, an example of which is shown in Figure 6.3. At concentrations of poly(ethylene glycol) (PEG) and dextran below the curve in Figure 6.3, there is only one liquid phase. On the curve, there are two liquid phases, and tie lines connect the compositions of the phases that are in equilibrium. As observed in Figure 6.3, the phase enriched in PEG can contain almost no dextran. The most common systems use dextran and PEG, or PEG and potassium phosphate, although purified dextran is expensive and alternatives to it have been used [2]. The PEG-rich phase is less dense than either the dextran-rich or salt-rich phase and thus is the lighter or top phase. Typical concentrations of PEG-dextran systems are 10% (w/w) PEG and 15% dextran, or with salt-rich bottom phases, 15% PEG and 15% salt [3].

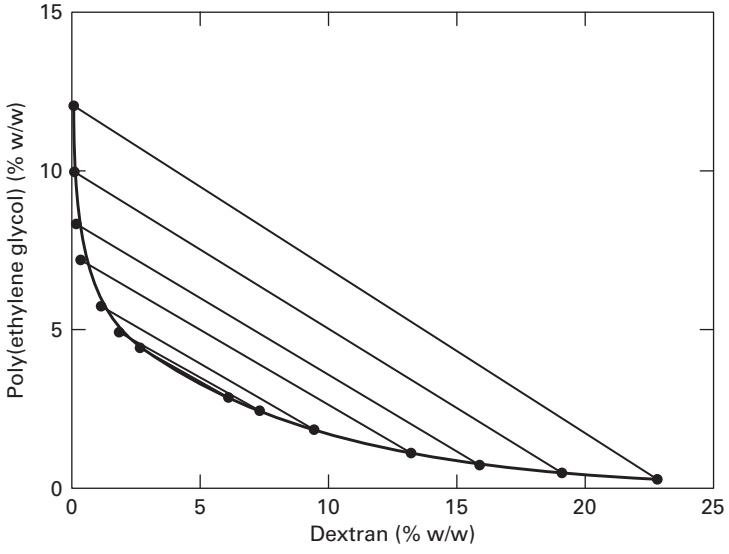

FIGURE 6.3 Phase diagram for a PEG 6000–dextran D48 system at 20°C. *(Data from P.-Å. Albertsson,* Partition of Cell Particles and Macromolecules, *3rd ed., Wiley, New York, 1986.)*

TABLE 6.1 Factors That Affect Protein Partitioning in Two-Phase Aqueous Systems[a]

Protein molecular weight
Protein charge, surface properties
Polymer(s) molecular weight
Phase composition, tie-line length
Salt effects
Affinity ligands attached to polymers

[a] See reference [3].

In general for aqueous two-phase extraction, contaminants such as cells and cell debris partition to the bottom phase or interface. For proteins, the partitioning is affected by many parameters, which are given in Table 6.1. These parameters are difficult to separate and analyze individually, which means that an a priori prediction of partition coefficients is very difficult.

Models have been developed to explain several molecular level mechanisms influencing the partition of proteins in aqueous two-phase extraction. These models can be categorized into three types: lattice models, virial expansions, and scaling-thermodynamic approaches. These models tend to be complicated, requiring the independent measurement of several parameters. An example of these models is the virial expansion model developed by King et al. [4]. For a solution with two polymers that is very dilute in protein, such that the concentration of either polymer is much greater than the protein concentration, the protein partition coefficient K_p is given by

$$\ln K_p = \ln \frac{y_p}{x_p} = a_{1p}(x_1 - y_1) + a_{2p}(x_2 - y_2) + \frac{z_p F(\phi_x - \phi_y)}{RT} \tag{6.2.3}$$

where y_p, x_p = concentration of protein in light and heavy phase, respectively
y_1, x_1 = concentration of polymer 1 in light and heavy phase, respectively
y_2, x_2 = concentration of polymer 2 in light and heavy phase, respectively
a_{1p} = second virial coefficient for interaction between protein and polymer 1
a_{2p} = second virial coefficient for interaction between protein and polymer 2
φ_y, φ_x = electrical potential for light and heavy phase, respectively, relative to some reference
z_p = net surface charge of protein
F = Faraday number
R = gas constant

The virial coefficients can be measured for each type of polymer and salt by membrane osmometry or by low-angle laser light scattering. The electrical potentials can be determined as a function of the type of salt and tie-line length. Data are also necessary for the protein surface charge as a function of pH. The use of these methods gave good agreement between predicted and experimentally measured partition coefficients for albumin, α-chymotrypsin, and lysozyme in PEG-dextran systems [4].

The influence of protein size on the phase partitioning has been shown by correlating the partition coefficient with molecular weight for a number of proteins. As indicated in Figure 6.4, partitioning of the protein to the top phase is weakly favored at lower molecular weights, while bottom phase partitioning is strongly favored for the largest proteins. For all these data, the pH of the solution was at the protein's isoelectric point (pI) to minimize any effects of protein charge.

Other factors that can have a large effect on protein partitioning are the type and concentration of the salt in the system and the charge on the protein. For example, Figure 6.5 shows that the partition coefficient for ovalbumin can vary widely depending on the pH, which means that this is an electrostatic effect. This is further supported by the observation that all the curves in Figure 6.5 intersect at the isoelectric pH of the protein, where there is zero net charge on the molecule. It is also seen that

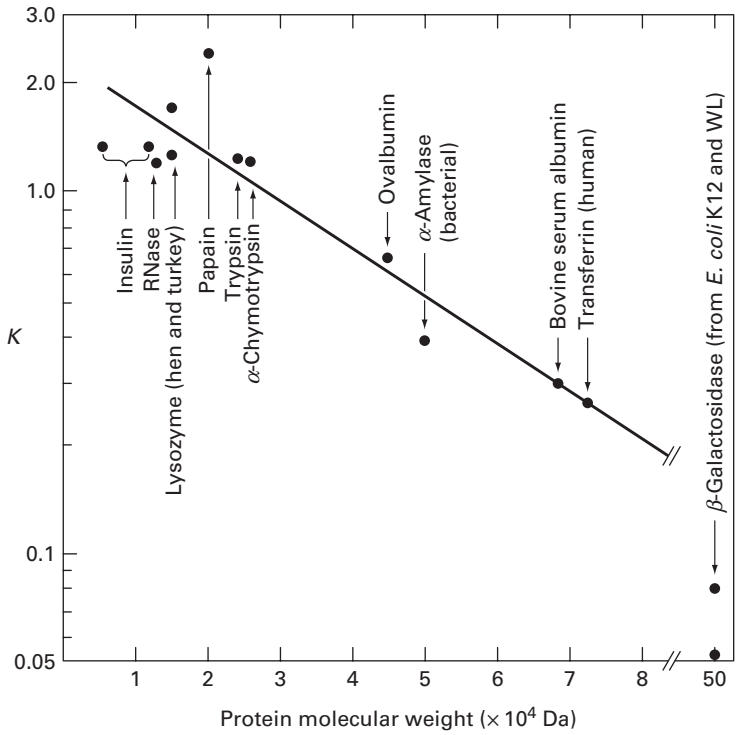

FIGURE 6.4 Effect of protein molecular weight on partitioning in a PEG 6000–dextran 500 system with pH at the isoelectric point (pI) for all proteins. *(Data from S. Saskawa and H. Walter, "Partition behavior of native proteins in aqueous dextran–poly(ethylene glycol)-phase systems,"* Biochemistry, *vol. 11, p. 2760, 1972.)*

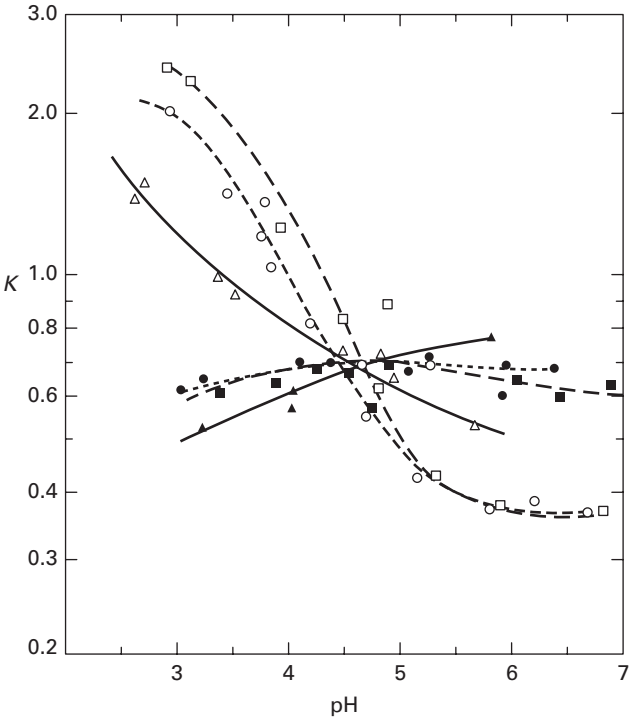

FIGURE 6.5 Dependence of ovalbumin partitioning on solution pH and salt type in a PEG 6000–dextran 500 system. Open symbols denote chloride salts, solid symbols, sulfates (squares, potassium; circles, sodium; triangles, lithium). *(Data from H. Walter, S. Sasakawa, and P.-Å. Albertsson, "Cross-partition of proteins: Effect of ionic composition and concentration,"* Biochemistry, *vol. 1 1, p. 3880, 1972.)*

the partition coefficient is greatly affected by whether chloride or sulfate salts are used. Thus, the effect of any change in the salt type in an aqueous two-phase system should be checked experimentally.

The selectivity of the extraction for the protein of interest may be enhanced by the coupling of a biospecific ligand to one of the polymers. PEG is a polymer often selected for conjugation because chemical techniques for modifying PEG are simple, highly efficient, and well known. By coupling a biospecific ligand to PEG and using conditions that favor the partition of contaminants to the bottom phase, the partition coefficient of a desired protein may be greatly increased. The most common strategy is to attach the ligand to the PEG polymer by derivatization of the free hydroxyls at each end of the polymer chain. Reactive intermediates have been formed by conversion of the PEG terminal hydroxyl to halides, sulfonate esters, or epoxide derivatives, which couple to a ligand to form a polymer with a protein binding site on each end [5]. Ligands from the reactive dyes, including Cibacron blue, Procion red, and Procion yellow, have been used for the affinity separation of many proteins. The dye functions as a competitive inhibitor for the substrate, coenzyme, or effector of a variety of proteins, often with an affinity greater than that shown by the competitive

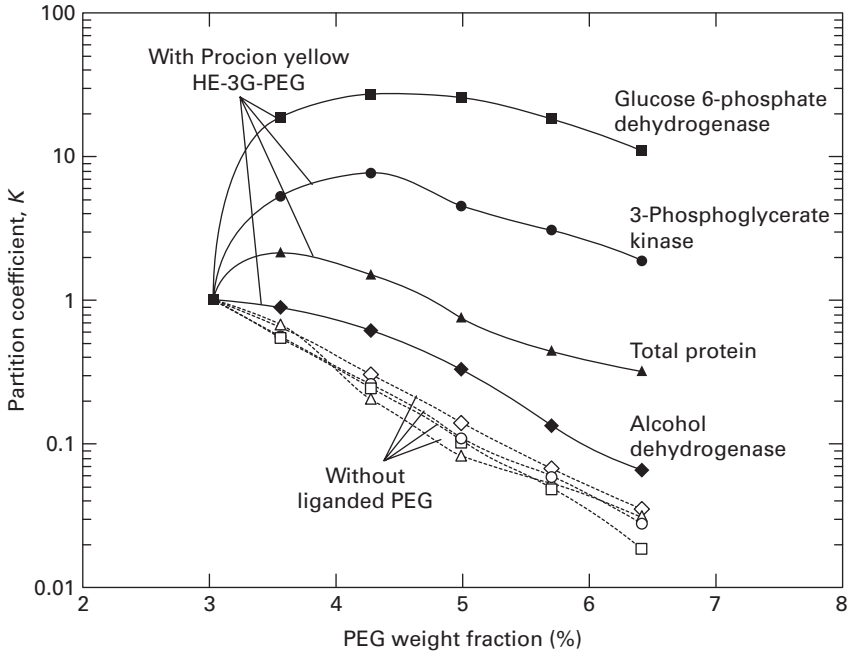

FIGURE 6.6 Affinity partitioning of enzymes in a PEG 6000–dextran 500 system with and without Procion yellow–PEG. *(Data from G. Johansson and M. Andersson, "Parameters determining affinity partitioning of yeast enzymes using polymer-bound triazine dye ligands,"* J. Chromatogr.*, vol. 303, p. 39, 1984.)*

molecule [6]. The improvement in the partition coefficient for three enzymes when Procion yellow was attached to PEG in the PEG-dextran aqueous two-phase extraction system is shown in Figure 6.6.

After binding of the protein to the ligand-polymer, it is necessary to recover the protein in free form. This has been performed by adding salt to the top phase, rich in ligand-polymer, yielding two phases and consequent partitioning of the protein to the resulting bottom phase [7]. In another approach, a soluble effector was added to a new two-phase system to compete with the bound ligand for the protein's binding site, causing the protein to be released from the ligand-polymer and shift to the bottom phase [8].

6.2.2 Countercurrent Stage Calculations

To achieve high bioproduct recovery in extraction, it is frequently necessary to use more than one extraction stage. Extraction processes are usually set up where the extraction solvent and the feed run countercurrent to each other. Countercurrent flow is preferable to cocurrent flow because the solute concentration difference between the raffinate and extraction phases, the driving force for the process, is greater in the countercurrent case. Countercurrent extraction is analyzed both graphically and analytically for equilibrium in each stage of contacting. This analysis is helpful in determining the balance between the number of stages and the ratio of the extraction

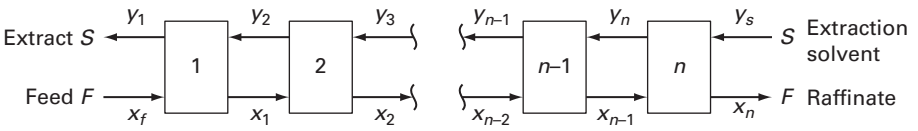

FIGURE 6.7 Countercurrent extraction cascade with n equilibrium stages, showing stream variables.

solvent flow rate to the feed flow rate. This analysis can also be used to determine the extraction efficiency of pilot plant and plant scale extractors.

A countercurrent extraction cascade is shown schematically in Figure 6.7 for n stages, each like that shown in Figure 6.1. The streams leaving each stage are in equilibrium and are numbered according to the stage they are leaving. Feed enters at stage 1 and leaves at stage n, while the extraction solvent is flowing in the opposite direction. Once the feed has entered the cascade, it is called the "raffinate." For these calculations, we make three key assumptions:

1. The two solvents are immiscible or are already in phase equilibrium (i.e., no solvent or polymer is exchanged between phases).
2. The solute concentrations are sufficiently low that the flow rates of the raffinate and extract are constant.
3. Equilibrium is achieved in each stage.

The first assumption depends on the solvents that are chosen. Usually, the extraction solvent is selected to minimize its solubility in the raffinate; otherwise, the loss of extraction solvent in the raffinate can be so great that it must be recovered for the process to be economically viable. The second assumption typically holds for the extraction of bioproducts. Concentrations of bioproducts in fermentation broths are typically less than 10 g/liter (or 1%) and often are less than 1 g/liter (0.1%), which means that the error caused by the second assumption is usually less than the error in the assay of the bioproduct. Should deviations from the second assumption become significant, then F and S should be the flow rates of pure solvent and the concentrations should be ratios of solute to pure solvent.

A material balance on the solute around the feed end of the cascade down to stage $n-1$ is

$$x_f F + y_n S = x_{n-1} F + y_1 S \tag{6.2.4}$$

where F is the flow rate of feed or raffinate phase, S is the flow rate of extract phase, and the concentrations are defined as in Figure 6.7. This equation can be written in terms of y_n as

$$y_n = \frac{F}{S} x_{n-1} + \frac{y_1 S - x_f F}{S} \tag{6.2.5}$$

From Equation (6.2.5) it is seen that y_n and x_{n-1} are concentrations of passing streams on a line of slope *F/S*, which is called the *operating line*. The calculation of the number of stages required to reduce the concentration of solute in the feed stream to x_n can be carried out graphically on a McCabe-Thiele-type diagram with y plotted versus x as shown in Figure 6.8. The cascade operating line of slope *F/S* intersects the x axis at point (x_n, y_s). In drawing point (x_n, y_s), it is assumed here that $y_s = 0$ (since extraction solvent is usually solute free). The *equilibrium curve,* not necessarily a straight line [i.e., the partition coefficient, defined by Equation (6.2.1), may not be constant for the range of concentrations that apply], originates at $x = y = 0$. The stepping off of equilibrium stages starts on the operating line where the feed enters and the extract exits the cascade (x_f, y_1). The concentrations x_1 and y_1 are in equilibrium and are thus on the equilibrium curve. One equilibrium stage is graphed as the horizontal line drawn from (x_f, y_1) that intersects the equilibrium curve at (x_1, y_1); a vertical line is drawn from (x_1, y_1) that intersects the operating line at (x_1, y_2). This procedure is continued until y_s is reached.

For isothermal, dilute solutions, the partition coefficient K is often constant. For this situation, an analytical solution can be developed for the concentration of solute in the raffinate as a function of the concentration in the feed and other process variables. It is convenient to define an *extraction factor E* as the slope of the equilibrium line divided by the slope of the operating line:

$$E = \frac{K}{F/S} = \frac{KS}{F} \tag{6.2.6}$$

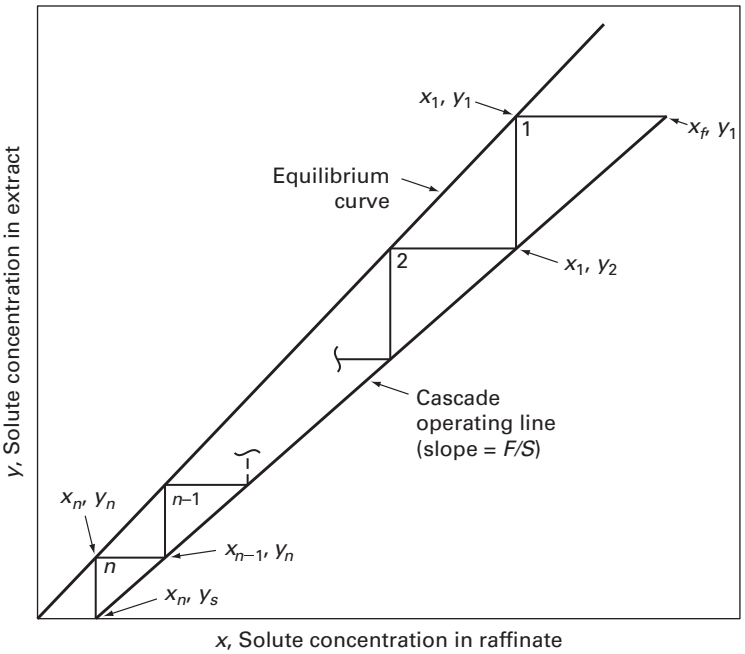

FIGURE 6.8 Graphical calculation of equilibrium stages for countercurrent extraction.

A material balance on the solute for the *n*th stage, assuming no solute in the entering extraction solvent ($y_s = 0$), gives

$$x_{n-1}F = x_nF + y_nS \tag{6.2.7}$$

Using the definitions of K and E leads to

$$x_{n-1} = (E+1)x_n \tag{6.2.8}$$

A material balance on the solute for the $(n-1)$th stage results in

$$x_{n-2} = (E^2 + E + 1)x_n \tag{6.2.9}$$

Continuing this procedure until stage 1 gives

$$x_f = (E^n + E^{n-1} + \cdots + E^2 + E + 1)x_n \tag{6.2.10}$$

which is mathematically equivalent to

$$x_f = \left(\frac{E^{n+1}-1}{E-1}\right)x_n \tag{6.2.11}$$

or

$$x_n = \left(\frac{E-1}{E^{n+1}-1}\right)x_f \tag{6.2.12}$$

This equation can be rearranged to give the more commonly used form

$$n = \frac{\ln\left[\frac{x_f}{x_n}(E-1)+1\right]}{\ln E} - 1 \tag{6.2.13}$$

As the number of stages becomes large ($n \to \infty$), we see from Equation (6.2.11) that

$$x_n \to \frac{x_f}{E^n} \to 0 \tag{6.2.14}$$

which we know by intuition—we can extract almost all the solute with a very large number of stages.

For the special case of the extraction factor $E = 1.0$, we can see from Equation (6.2.10) that

$$x_n = \frac{x_f}{n+1} \tag{6.2.15}$$

For values of $E < 1.0$ and a large number of extraction stages ($n \to \infty$), it is clear from Equation (6.2.12) that

$$x_n \to (1-E)x_f \tag{6.2.16}$$

EXAMPLE 6.1

Separation of a Bioproduct and an Impurity by Countercurrent Extraction
A countercurrent extractor with four equilibrium stages is available for separating a desired bioproduct from a contaminating impurity, which is 10% of the weight of the bioproduct in a feed stream. For the extraction solvent being used, which is immiscible with the feed stream, the bioproduct has a partition coefficient K of 10, while the impurity has $K = 1$. For an S/F ratio of 0.2, what will be the ratio of impurity to bioproduct in the extract phase at the outlet of the extractor?

Solution
We can use Equation (6.2.12) to calculate the ratio of bioproduct or impurity in the outlet raffinate to that in the inlet feed:

$$\text{Bioproduct:} \quad E = \frac{KS}{F} = 10(0.2) = 2.0$$

$$\frac{x_n}{x_f} = \frac{E-1}{E^{n+1}-1} = \frac{2-1}{2^{4+1}-1} = 0.0323$$

$$\text{Impurity:} \quad E = 1.0(0.2) = 0.2$$

$$\frac{x_n}{x_f} = \frac{0.2-1}{0.2^{4+1}-1} = 0.800$$

To calculate the ratio of impurity to bioproduct in the outlet extract, we use 100 g of bio-product in the feed as a basis:

$$\text{Ratio of impurity to bioproduct in the extract} = \frac{10 - 0.8(10)}{100 - 0.0323(100)} = 0.021$$

EXAMPLE 6.2

Effect of Solvent Rate in Countercurrent Staged Extraction of an Antibiotic
An antibiotic has been found to have a partition coefficient K of 8.4 at pH 10.0 in a system with aqueous and butyl acetate phases. The pK_a of the antibiotic is 8.5, due to a single tertiary amine group on the molecule. It is desired to recover 95% of this

antibiotic by countercurrent staged extraction with butyl acetate from an aqueous phase feed at a pH of 10.0. The flow rate of the feed is 200 liters/min.

Determine the dependence of the number of ideal stages on the flow rate of the extract phase. In what flow rate range would there likely be an economic optimum? Why is it desirable to do the extraction at a pH of 10.0?

Solution

To solve this problem, we need an expression relating the number of ideal countercurrent stages n to the flow rate of extraction solvent S. Substituting into Equation (6.2.13) for E gives

$$n = \frac{\ln\left[\dfrac{x_f}{x_n}\left(\dfrac{KS}{F} - 1\right) + 1\right]}{\ln\left(\dfrac{KS}{F}\right)} - 1$$

The above equation assumes that water and butyl acetate are immiscible. Since the solubility of water in butyl acetate is less than 1%, this is a good assumption. For this problem we know that the ratio $x_n / x_f = 0.05$. By substituting the values for x_n / x_f, K, and F, and various values of S in this equation, we obtain a plot of n versus S (Figure E6.2).

The determination of an exact economic optimum would involve calculating the total annualized cost as a function of the extract flow rate, which would require

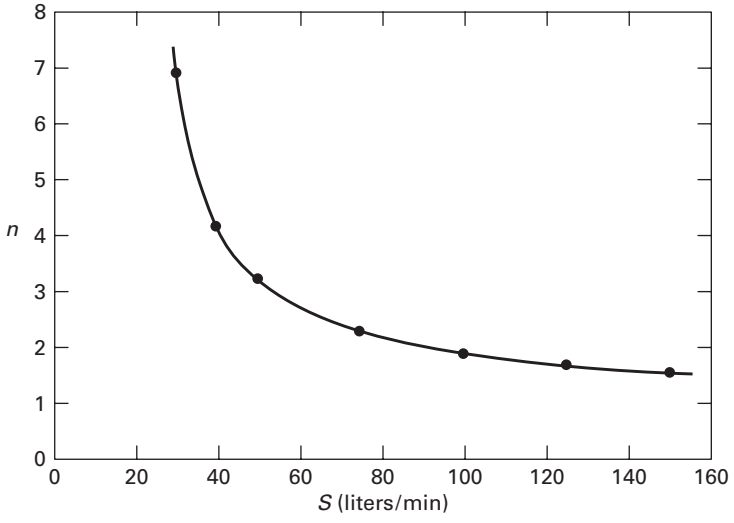

FIGURE E6.2 Dependence of the number n of theoretical extraction stages on the flow rate S of the butyl acetate extract phase.

putting the equipment costs on an annualized basis. Nevertheless, the range of the extraction solvent flow rate where an economic optimum lies can be estimated from the n versus S curve. From this plot, below an extract flow rate of 30 liters/min, the number of ideal stages appears to increase exponentially; while above a flow rate of about 80 liters/min, the change in the number of stages with the flow rate becomes relatively small. Thus, the economic optimum will likely be in the butyl acetate flow rate range of 30 to 80 liters/min.

Above its pK_a of 8.5, the tertiary amine becomes progressively more unprotonated, while below this pK_a the reverse is true. At a pH of 10.0, this amine is essentially unprotonated, and the antibiotic is thus more readily extracted into the more hydrophobic butyl acetate phase than if it were protonated.

6.3 SCALE-UP AND DESIGN OF EXTRACTORS

Although many different types of extractors are used at large scale in the chemical industry, only a few are used in the biotechnology field. By far the most commonly used extractors in biotechnology are the mechanically agitated extraction columns and the centrifugal extractors [9]. Of the mechanically agitated extraction columns, the reciprocating-plate extraction columns have been the most widely used. Centrifugal extractors have been widely used in the recovery of antibiotics, and probably the most widely used extractor of this type is the Podbielniak centrifugal extractor. A summary of the general features of these two extractors is given in Table 6.2. Both these extractors will be discussed in detail.

Two concepts that are useful in scaleup and design are *overall stage efficiency* and *height equivalent to a theoretical stage* (HETS). The column may be treated as a stack of stages, in which the product is at equilibrium between the two phases in each stage as in Figure 6.7. These variables are

$$\text{Percent stage efficiency} = \frac{\text{number of theoretical stages}}{\text{number of actual stages}} \times 100 \tag{6.3.1}$$

TABLE 6.2 Summary of Features of Two Extractors Commonly Used in Biotechnology[a]

Types of extractor	General features
Reciprocating-plate column	High throughput, low HETS; great versatility and flexibility; simplicity in construction; handles liquids containing suspended solids and mixtures with emulsifying tendencies
Centrifugal extractor	Short contacting time for unstable material; limited space required; handles easily emulsified material and systems with little liquid density differences

[a] See reference [10].

$$\text{HETS} = \frac{\text{height of extractor}}{\text{number of theoretical stages}} \tag{6.3.2}$$

The number of theoretical stages is defined by Equation (6.2.13). Design goals are to maximize stage efficiency and minimize HETS.

6.3.1 Reciprocating-Plate Extraction Columns

The most important feature for biotechnology applications of reciprocating-plate extraction columns is their ability to handle liquids with suspended solids and mixtures that emulsify easily. In these columns, first developed by Karr [11], interdispersion is achieved by reciprocating or vibrating plates. The column consists of a stack of perforated plates, which are reciprocated vertically by means of a reciprocating drive mechanism located at the top of the column (Figure 6.9). The amplitude of reciprocation is variable and generally in the range 3 to 50 mm; the reciprocation frequency is variable up to 1000 strokes/min (SPM).

Research studies on the hydrodynamics and axial mixing in reciprocating-plate extraction columns have shown that the presence of many closely spaced plates leads to conditions that closely approximate uniform isotropic turbulence [12]. The more uniform distribution of energy dissipation in these columns gives high turbulence of interdispersing phases and low axial mixing, and thus gives high mass transfer rates and low HETS. Thus commercial columns are designed with optimal plate spacing built in.

This column obeys the relationship for the number of theoretical stages in a countercurrent staged extractor [Equation (6.2.13)] and is further scaled on the basis of column diameter D and rate of reciprocation of the plates, SPM. Based on performance data obtained for columns having diameters of 25, 76, 305, and 914 mm (1, 3, 12, and 36 in.), the following equations have been developed for the scale-up of reciprocating-plate extractors [13]:

$$\frac{(\text{HETS})_2}{(\text{HETS})_1} = \left(\frac{D_2}{D_1}\right)^{0.38} \tag{6.3.3}$$

$$\frac{(\text{SPM})_2}{(\text{SPM})_1} = \left(\frac{D_1}{D_2}\right)^{0.14} \tag{6.3.4}$$

where subscripts 1 and 2 refer to the small- and large-scale columns, respectively. A successful design of a large-scale reciprocating-plate extractor can be achieved after optimization experiments have been performed on the pilot plant scale. The following procedures are recommended for the scale-up:

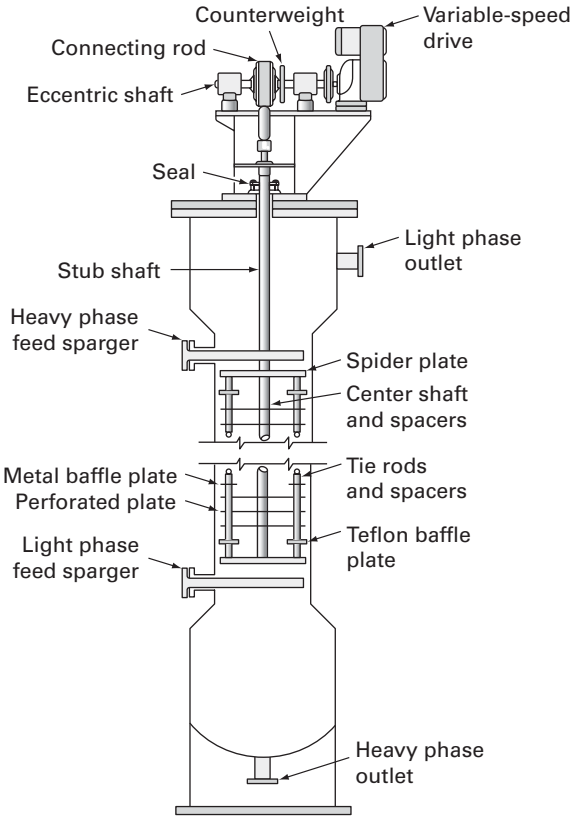

FIGURE 6.9 Schematic diagram of a 900 mm (36 in.) diameter reciprocating-plate extraction column. *(Drawing based on a design by Glitsch Process Systems Inc.)*

1. Data such as x_n / x_f at specified S and F are obtained in a column of 25, 51, or 76 mm (1, 2, or 3 in.) diameter.
2. The optimum performance of the pilot column is determined. The criterion for optimum performance is maximum volumetric efficiency in a column having optimal plate spacing.
3. When scaling up from the pilot scale data, the following parameters are held constant: solvent-to-feed ratio S/F, throughput per column cross-sectional area $(S + F)/A$, plate spacing, and stroke length.
4. The expected minimum HETS in the large-diameter column is calculated from Equation (6.3.3). The height of the extractor is calculated from Equation (6.3.2), with the number of theoretical stages estimated from Equation (6.2.13), which is based on the three assumptions introduced in Section 6.2.2.
5. The corresponding reciprocating speed required is calculated from Equation (6.3.4).
6. Suitable baffle plates in design and spacing are provided.

Column volumetric efficiency is defined as

$$\text{Volumetric efficiency} = \frac{\text{total volumetric throughput/column cross-sectional area}}{\text{HETS}} \tag{6.3.5}$$

where total volumetric throughput is defined as the sum of the feed flow rate and the solvent flow rate, $S + F$. This procedure has been used to successfully scale up columns to a diameter of 1.5 m (5 ft) [12] and to a plate stack height of 12.2 m (40 ft) [13].

EXAMPLE 6.3

Scale-up of a Reciprocating-Plate Extraction Column The operation of a pilot scale reciprocating-plate extraction column has been optimized for the extraction of an antibiotic from whole fermentation broth using amyl acetate as solvent. The antibiotic has a partition coefficient K of 7.5. The optimal operating conditions are as follows: solvent flow rate of 105 ml/min, flow rate of fermentation broth of 70 ml/min, and ratio of antibiotic in raffinate to antibiotic in feed of 0.07. The column was 2.54 cm in diameter, and the height of the extractor (height of the reciprocating plates) was 1.83 m. The agitator speed was 280 strokes/min. What column size and agitator speed are required to give a ratio of antibiotic in the raffinate to antibiotic in the feed of 0.03 and to handle fermentation broth at a rate of 150,000 liters every 12 h? (*Note:* 150,000 liters is a typical volume for a plant antibiotic fermentor.)

Solution

Our first objective is to find the HETS for the optimal pilot plant run. We know for the pilot run that

$$\frac{x_f}{x_n} = \frac{1}{0.07} = 14.29$$

$$\frac{S}{F} = \frac{105}{70} = 1.5$$

We let subscripts 1 and 2 denote the pilot plant and plant scales, respectively. Since the solubility of amyl acetate in water is well below 1%, we make the assumption of immiscible phases. Thus, we can use Equation (6.2.13) to determine the number of theoretical stages

$$n_1 = \frac{\ln\left[\dfrac{x_f}{x_n}\left(\dfrac{KS}{F} - 1\right) + 1\right]}{\ln\left(\dfrac{KS}{F}\right)} - 1 = \frac{\ln[14.29(7.5 \times 1.5 - 1) + 1]}{\ln(7.5 \times 1.5)} - 1 = 1.06$$

and from Equation (6.3.2)

$$(\text{HETS})_1 = \frac{\text{height of plates}}{n_1} = \frac{1.83}{1.06} = 1.73\,\text{m}$$

For the large-scale unit, we can first find the diameter by maintaining a constant total throughput per unit cross-sectional area. For the pilot unit

$$\frac{\text{Total throughput}}{\text{Cross-sectional area}} = \frac{70+105}{\pi\,(2.54)^2/4} = 34.6\,\frac{\text{ml}}{\text{min cm}^2}$$

Maintaining *S/F* constant at large scale gives

$$(\text{Total throughput})_{\text{large scale}} = \frac{(105/70)(150{,}000)+150{,}000}{12}\,\frac{\text{liters}}{\text{h}} \times \frac{1\text{ h}}{60\text{ min}}$$
$$= 520.8\,\frac{\text{liters}}{\text{min}}$$

We can now solve for the diameter of the large column:

$$D = \left(\frac{4 \times 520{,}800}{34.6\pi}\right)^{1/2} = 136.3\text{ cm}$$

The HETS for the large-scale column can be found by using Equation (6.3.3):

$$(\text{HETS})_2 = (\text{HETS})_1\left(\frac{D_2}{D_1}\right)^{0.38} = (1.73)\left(\frac{138.5}{2.54}\right)^{0.38} = 7.91\,\text{m}$$

To find the height of the large-scale column, we need to use the desired concentration of antibiotic in the raffinate to calculate the number of theoretical stages for this column:

$$n_2 = \frac{\ln[(1/0.03)(7.5 \times 1.5 - 1) + 1]}{\ln(7.5 \times 1.5)} - 1 = 1.41$$

From Equation (6.3.2)

$$(\text{Height of plates})_{\text{large column}} = n_2(\text{HETS})_2 = 1.41(7.91) = 11.2\,\text{m}$$

The agitator speed at large scale can be found by using Equation (6.3.4):

$$(SPM)_2 = (SPM)_1\left(\frac{D_1}{D_2}\right)^{0.14} = (280)\left(\frac{2.54}{138.5}\right)^{0.14} = 160\text{ strokes/min}$$

Thus, the large-scale column is not wider or higher than the largest columns of these types that have been built.

6.3.2 Centrifugal Extractors

Centrifugal extractors were first developed for biotechnology processing, and that is still their main application. These extractors are the most popular in antibiotics production, where the large volumes of fermentation broth that must be processed are easily emulsified. Key advantages of centrifugal extractors are their ability to avoid emulsions and to separate liquid phases with small density differences (as small as 0.01 g/cm^3).

Centrifugal extractors consist of several concentric perforated cylinders that rotate around a shaft. The principle of this design is to feed the heavy phase near the axis of the rotating cylinder, while the light phase is fed close to the periphery. Figure 6.10 is a cross-sectional diagram of the widely used Podbielniak centrifugal extractor that indicates the flows of the heavy and light phases. The centrifugal force applied causes the two phases to move radially in a countercurrent mode, such that the heavy phase moves to the periphery and the light phase to the axis of rotation. The capabilities of the various sizes of Podbielniak centrifugal extractors for the extraction of fermentation broth are given in Table 6.3.

The scale-up of Podbielniak centrifugal extractors uses the concept of *equivalent time, Gt*, discussed earlier for centrifuges [see Equation (5.3.5)]. First, optimum performance of the pilot centrifugal extractor is determined. The ratio of feed volume to solvent volume is kept constant upon scaleup. The contact time *t* for the feed stream in the centrifuge is calculated for the large-scale extractor, assuming that *Gt* is constant in the scale-up. The feed rate at large scale is calculated from this contact time [14].

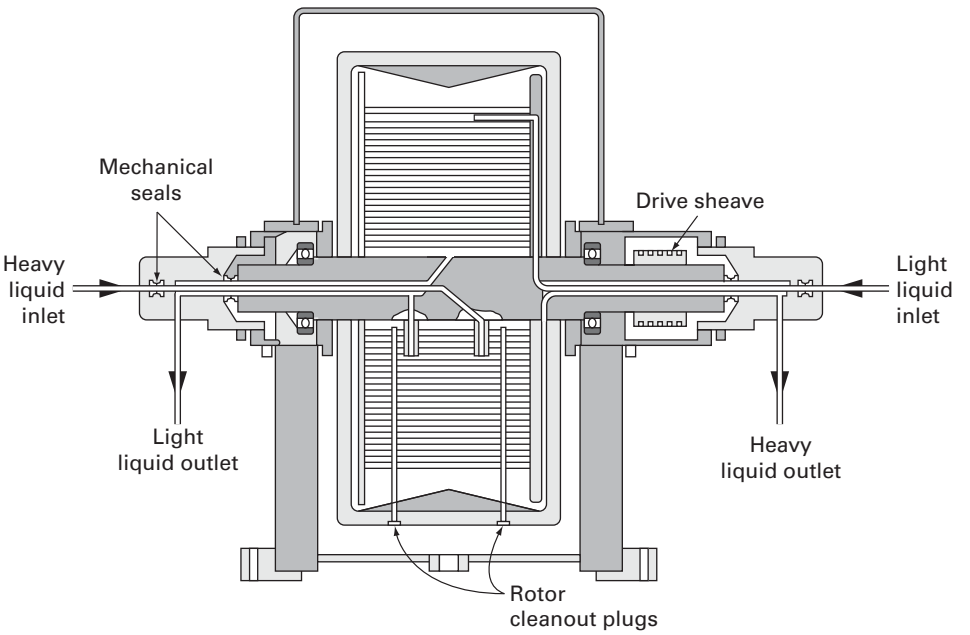

FIGURE 6.10 Cross-sectional diagram of a Podbielniak centrifugal extractor.

TABLE 6.3 Capabilities of Podbielniak Centrifugal Extractors for Fermentation Broth Extraction

Capacity (m^3/h)[a]	Maximum speed (rpm)	Maximum centrifugal force × *g* (*G*, dimensionless acceleration)
0.05	10,000	11,400
6.0	3,200	3,600
15.0	2,100	2,300
30.0	2,100	2,300

[a] Sum of feed and solvent flow rates.

Source: B&P Process Equipment and Systems, 2000.

EXAMPLE 6.4

Increase in Feed Rate to a Podbielniak Centrifugal Extractor A Podbielniak centrifugal extractor with a capacity of 30.0 m^3/h (see Table 6.3) is operating at a speed of 1500 rpm, feed rate of 300 liters/min, and solvent rate of 60 liters/min for the extraction of a bioproduct in the feed. Changes in the process upstream of the extractor require that the feed rate be raised to 400 liters/min. What changes in the operating variables should be made to maintain the same recovery of the bioproduct? Can these changes be made within the capabilities of this extractor?

Solution

Following the guidelines for scaling up centrifugal extractors, the equivalent time (Gt) is kept constant in order to achieve the same recovery when the flow rates are changed.

$$G_1 t_1 = G_2 t_2$$

where subscripts 1 and 2 refer to current and new operating conditions, respectively. We also maintain the solvent-to-feed ratio (S/F) constant, which is equivalent to keeping the extraction factor E (= KS/F) constant since the partition coefficient K has not changed (same feed and extract system). Using the definition of G (Equation 5.3.4) and writing t's in terms of feed flow rates and volume V occupied by the feed in the extractor gives

$$G \equiv \frac{\omega^2 R}{g}$$

$$\frac{\omega_1^2 R}{g}\frac{V}{F_1} = \frac{\omega_2^2 R}{g}\frac{V}{F_2}$$

which reduces to

$$\frac{\omega_1^2}{F_1} = \frac{\omega_2^2}{F_2}$$

so that

$$\omega_2 = \omega_1 \left(\frac{F_2}{F} \right)^{1/2} = 1500\,\text{rpm} \left(\frac{400}{300} \right)^{1/2} = 1732\,\text{rpm}$$

This speed is still below the maximum speed for this centrifuge (see Table 6.3). The new solvent rate is

$$S_2 = F_2 \left(\frac{S_1}{F_1} \right) = 400 \left(\frac{60}{300} \right) = 80\,\text{liters min}^{-1}$$

At the new flow rates,

$$S_2 + F_2 = 80 + 400 = 480 \frac{\text{liters}}{\text{min}} \times \frac{1\,\text{m}^3}{10^3\,\text{liters}} \times \frac{60\,\text{min}}{\text{h}} = 28.8\,\text{m}^3\text{h}^{-1}$$

Therefore, at the new flow rates the sum of S and F is within the capacity for this extractor.

6.4 SUMMARY

In extraction, two phases come into contact with the goal of transferring a solute or particle from one phase to the other. Liquid-liquid extraction is the type of extraction that is most commonly used for bioproducts. Liquid-liquid extraction aids in product isolation and can be used for partial purification of solutes when used in the multistage mode.

- The key physical constants used in extraction are the partition coefficient $K = y/x$, the ratio of the concentration of a solute in the extract phase to that in the raffinate phase at equilibrium; the solvent-to-feed ratio S/F, the extract phase volume or flow rate divided by the feed phase volume or flow rate; and the extraction factor $E = KS/F$.
- Chemical conditions and properties have predictable effects on the partition coefficient. Both pH and the type of salt or salts present generally have a strong effect on K.
- An equilibrium phase diagram for aqueous two-phase systems consists of a plot of the concentration of a polymer enriched in one of the phases against the concentration of another polymer or salt enriched in the other phase. Points formed by phases in equilibrium on the equilibrium (binodal) curve are connected by tie lines.

- The extraction of enzymes by affinity partitioning consists of coupling one of the polymers, usually poly(ethylene glycol) (PEG), to an affinity ligand to which the target protein will bind.
- In an n-stage countercurrent extraction cascade, the fraction of solute extracted is calculated from the relationship

$$\frac{x_n}{x_f} = \frac{E-1}{E^{n+1}-1}$$

  where n is the number of theoretical stages, x_f is the feed concentration, and x_n is the concentration in the exit raffinate.
- An equilibrium line is constructed as a plot of y versus x, and an operating line is constructed by plotting the material balance on the same axes. The combined plot is known as a McCabe-Thiele diagram and is used to calculate the number of equilibrium stages required by starting at $x = x_f$ and reducing x by graphing steps between the two plots until the desired x_n is reached.
- A reciprocating-plate extractor consists of a vertical column through which phases flow counter to each other and in which interdispersion of phases is driven by reciprocating plates. Scaling rules for column height and speed of the reciprocating perforated plates are based on a power of the ratio of the large-scale diameter to the small-scale diameter.
- Centrifugal (Podbielniak) extractors effect phase separation by applying a centrifugal force field as the phases flow countercurrent to each other through perforated cylinders to effect contacting. Scaling rules are those applied to centrifugation.

NOMENCLATURE

a_{ij}	second virial coefficient for interaction between protein i and polymer j (liter mol^{-1})
A	cross-sectional area (cm^2)
D	column diameter (cm)
E	extraction factor (= KS/F)
F	feed flow rate (= raffinate flow rate when solvents are immiscible and solute concentrations are low) (liter h^{-1})
F	Faraday number (9.6485×10^4 C mol^{-1})
g	gravitational acceleration (= 9.8066 m s^{-2})
G	multiple of gravitational acceleration (= $\omega^2 R/g$) (dimensionless)
HETS	height equivalent to a theoretical stage [Equation (6.3.2)] (cm)
k	Boltzmann's constant ($= 1.3807 \times 10^{-23}$ J K^{-1})
K	partition or distribution coefficient (= y/x)
M	molecular weight (Daltons)

R gas constant (8.3145 J mol^{-1} K^{-1})
S extraction solvent flow rate (= extract flow rate when solvents are immiscible and solute concentrations are low) (liter h^{-1})
SPM rate of reciprocation of plates (strokes min^{-1})
t time (h)
x concentration of solute in raffinate phase or heavy phase (M, or g $liter^{-1}$)
y concentration of solute in extract phase or light phase (M, or g $liter^{-1}$)
z_p net surface charge of protein

Greek Letters

λ lumped parameter in equation for partition coefficient K [Equation (6.2.2)]
φ electrical potential (mV)

PROBLEMS

6.1 Two-Stage Countercurrent Extraction In a two-stage countercurrent extraction of a pharmaceutical product, what is the relationship between the feed concentration and the final raffinate concentration in terms of the extraction factor E if both stages are at equilibrium? For a partition coefficient K of 5.0 and a solvent-to-feed ratio (S/F) of 0.5, what will be the ratio of the raffinate concentration to the feed concentration?

6.2 Purification Factor for Extraction of an Enzyme You are preparing an industrial enzyme, alcohol dehydrogenase, from yeast using two-phase aqueous extraction. The crude, clarified extract contains only proteins and has a specific activity of 200 units/g protein. After a single stage of affinity extraction using a Cibacron dye–PEG complex, the extract contains 400,000 units of enzyme activity and 20 g of protein. What is the purification factor for this step?

6.3 Extraction Conditions for Various Bioproducts For the following bioproducts, outline how extraction can be used in the purification process using information obtained from work reported in the literature:

(a) Magnamycin, a macrolide antibiotic from *Streptomyces halstedii*
(b) Glumamycin, a peptide antibiotic from *Streptomyces zaomyceticus*
(c) β-Galactosidase, an enzyme from *Escherichia coli*
(d) Pullulanase, an enzyme from *Klebsiella pneumoniae*

Give as much information as possible about what the process conditions should be (solvents, pH, concentration, etc.).

6.4 Required Solvent-to-Feed Ratio in Countercurrent Extraction In a countercurrent, equilibrium staged extractor with four equilibrium stages, determine the necessary ratio of extract to feed (S/F) to purify bioproduct A to 90% purity from contaminant B. The feed contains two components, 60% A and 40% B, and the partition coefficients are $K_A = 13.0$ and $K_B = 1.0$.

6.5 Purification of an Antibiotic by Countercurrent Extraction A countercurrent extraction unit with three equilibrium stages is used for the separation of a desired antibiotic (partition coefficient = 6.0) from a major contaminant (partition coefficient = 1.0)

in an aqueous feed stream. The feed (or raffinate) and extract phase flow rates are equal. What fraction of each is discarded from the raffinate? Assuming that the feed contains only these two components at an antibiotic-to-contaminant ratio of 3:1, what is the purity of the antibiotic in the exit extract from stage 3? What do you conclude about the effectiveness of this extraction as a means of purification of the antibiotic?

6.6 Mixer-Settler Extraction System You are assigned the task of extracting zithramycin with a yield of at least 90% from a clarified fungal fermentation broth, using a four-stage mixer-settler extraction unit in the pilot plant. (One mixer-settler constitutes one equilibrium stage in the countercurrent extraction cascade shown in Figure 6.7.) The *n*-butanol extraction solvent flows at 20 liters/h, while the clarified broth flows at 30 liters/h. The partition coefficient of zithramycin is adjustable by changing the pH. What minimum value of the partition coefficient should you use for the successful completion of your assigned task?

6.7 Graphical Equilibrium Stage Calculations for Extraction of a Peptide The equilibrium partitioning of a peptide between an aqueous feed phase and an organic solvent extract phase has been found to be nonlinear and can be represented by the following equation:

$$y = 1.47 \ln x + 3.96$$

where y and x are concentrations of the peptide in the extract and aqueous feed (or raffinate) phases, respectively, in grams per liter. It is desired to extract 95% of the peptide from a feed stream having a peptide concentration of 4.0 g/liter. For a feed stream at a flow rate of 5.0 liters/min and an extract stream at a flow rate of 3.3 liters/min, graphically estimate how many equilibrium stages will be required for countercurrent flow of the phases. What is the concentration of the peptide in the exit extract stream? As the concentration of the peptide in the raffinate decreases, does the partitioning of the peptide into the extract become more or less favorable?

6.8 Scale-up of a Podbielniak Centrifugal Extractor Pilot plant tests with a Podbielniak centrifugal extractor indicated that excellent recovery (>95%) of a desired bioproduct could be obtained from filtered fermentation broth by extraction with an immiscible organic solvent. The flow rates were the following:

$$\text{Filtered broth (aqueous) flow rate} = 500 \text{ ml/min (continuous phase)}$$
$$\text{Organic solvent flow rate} = 125 \text{ ml/min (dispersed phase)}$$

The pilot plant extractor delivers a centrifugal force of 11,400 × *g*, and the rotating cylinder inside the extractor has a diameter of 20 cm and is 2.5 cm wide.

You have been asked to scale up this extraction by using a larger Podbielniak extractor, which delivers 2300 × *g* and has a rotating cylinder with a diameter of 91 cm and a width of 91 cm. What flow rates should be used in the larger extractor to achieve the same recovery of bioproduct?

6.9 Scale-up of Pilot Plant Tests of a Reciprocating-Plate Extraction Column The pilot plant data in Table P6.9 are for the extraction of an antibiotic from whole

TABLE P6.9

Run number	Flow rates (ml/min)		Antibiotic concentration in raffinate (mg/liter)
	Broth	Chloroform	
1	45	135	2
2	67.5	135	3
3	125	135	30
4	80	120	5
5	100	150	7
6	120	180	9
7	150	225	25

fermentation broth using the solvent chloroform in a reciprocating-plate extraction column. The concentration of the antibiotic was 1.4 g/liter in the broth. The column had a diameter of 2.54 cm, and the height of the plates was 3.05 m. The partition coefficient K for the antibiotic is known to be 2.68.

For each pilot run, determine the diameter and height of the plates for the plant column that would be required for processing 50,000 liters of broth in 12 h to give an exit raffinate concentration of antibiotic of 10 mg/liter, assuming a concentration of antibiotic in the feed broth of 1.0 g/liter (a spreadsheet is convenient for these calculations). Without doing a complete economic analysis, in your judgment which scaled-up pilot run appears to be optimum? (Data from A. E. Karr, W. Gebert, and M. Wang, *Can. J. Chem. Eng.,* vol. 58, p. 249, 1980.)

REFERENCES

1. Brønsted, J. N. Z. (1931). Molecular magnitude and phase distribution. I. *Z. Phys. Chem*., Abt. A, vol. 155, p. 257.
2. Diamond, A. D., and Hsu, J. T. (1992). Aqueous two-phase systems for biomolecule separation. *Adv. Biochem. Eng. Biotechnol*., vol. 47, p. 89.
3. Kelley, B. D., and Hatton, T. A. (1993). Protein purification by liquid-liquid extraction. In *Biotechnology*, vol. 3, *Bioprocessing*, G. Stephanopoulos, ed., VCH Publishers, Weinheim, p. 593.
4. King, R. S., Blanch, H. W., and Prausnitz, J. M. (1988). Molecular thermodynamics of aqueous two-phase systems for bioseparations. *AIChE J*., vol. 34, p. 1585.
5. Harris, J. M., and Yalpani, M. (1985). Polymer-ligands used in affinity partitioning and their synthesis. In *Partition in Aqueous Two-Phase Systems. Theory, Methods, Uses, and Applications*, H. Walter, D. E. Brooks, and D. Fisher, eds., Academic Press, Orlando, FL, p. 589.
6. Stellwagen, E. (1990). Chromatography on immobilized reactive dyes. In *Guide to Protein Purification*, M. P. Deutscher, ed., Academic Press, San Diego, CA, p. 343.
7. Cordes, A., and Kula, M.-R. (1986). Process design for large-scale purification of formate dehydrogenase from *Candida boidinii* by affinity partition. *J. Chromatog*., vol. 376, p. 375.
8. Kopperschlager, G., and Birkenmeier, G. (1990). Affinity partitioning and extraction of proteins, *Bioseparations*, vol. 1, p. 235.
9. Schugerl, K. (1994). *Solvent Extraction in Biotechnology*, Springer-Verlag, Berlin.

10. Lo, T. C., and Baird, M. H. I. (1997). Extraction, liquid-liquid. In *Encyclopedia of Separation Technology*, vol. 1, D. M. Ruthven, ed., Wiley, New York, p. 760.
11. Karr, A. E. (1959). Performance of a reciprocating plate column. *AIChE J*., vol. 5, p. 446.
12. Lo, T. C. (1997). Commercial liquid-liquid extraction equipment. In *Handbook of Separation Techniques for Chemical Engineers*, 3rd ed., P. A. Schweitzer, ed., McGraw-Hill, New York, p. I–449.
13. Karr, A. E. (1980). Design, scale-up, and applications of the reciprocating plate extraction column. *Sep. Sci. Technol*., vol. 15, p. 877.
14. Creegan, R. (2000). B&P process equipment and systems. *Personal communication*.

/// 7 /// LIQUID CHROMATOGRAPHY AND ADSORPTION

Liquid chromatography and adsorption processes are based on the differential affinity of various soluble molecules for specific types of solids. In these processes, equilibrium is approached between a solid phase, often called the resin, or *stationary phase,* and the soluble molecules in a liquid phase. The solid phase is "stationary" because it is often packed in a fixed column. Since the liquid phase is often flowing past the solid phase, it is referred to as the *mobile phase*.

Chromatography and adsorption are related unit operations. In chromatography, typically multiple solutes are separated from each other, with the target product solute being one of many that might be recovered at the end of the process step. In adsorption, there are typically only three groups of solutes: those that do not adsorb to the stationary phase (sometimes called "flow through"); secondly, those that adsorb and then are subsequently recovered by an elution step; and thirdly, those solutes that are nearly irreversibly bound and can only be removed from the adsorbent by regenerating the adsorbent, which usually results in the chemical destruction of these solutes. The word "adsorption" is used both to describe the physical adherence of a solute to a stationary phase, and as the name of the unit operation described above. Adsorption is a subset of the "sorption" phenomena, absorption (transfer of a solute from one phase into another) and ion exchange (exchange of a counter-ion between two opposing co-ions) being the other two sorption phenomena. The unit operations chromatography and adsorption can rely on any of these three sorption processes individually or in combination.

In chromatography and adsorption, a mixture of solutes in a feed solution is introduced at the inlet of a column containing the stationary phase and separated into zones of individual solutes over the length of the column. The solutes are carried by the convective action of an elution solvent that is continuously fed to the column after the feed solution has been introduced. Figure 7.1 shows the method of separating solutes known as *elution chromatography.* By contrast, in an adsorption process, the stationary phase is generally saturated with the target solute before the introduction of an elution solvent that causes the solute to transfer into the mobile

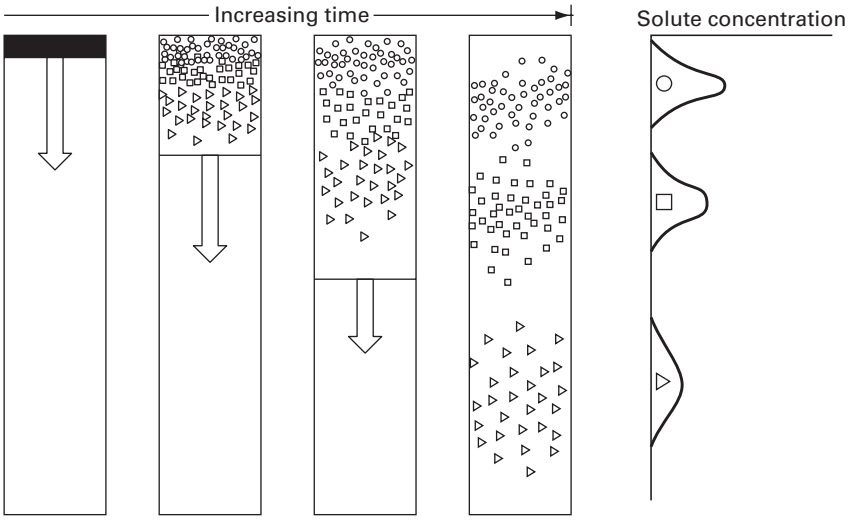

FIGURE 7.1 Schematic illustration of elution chromatography. Three solutes, fed to a column containing a stationary phase, separate in the column as the elution solvent flows through the column. The three solutes separate as a result of differing affinities for the stationary phase.

phase; this type of operation is sometimes referred to as *on-off chromatography* [1]. Chromatography is usually performed downflow through a stationary phase in a fixed bed, although in some instances the column is operated upflow during the feed step to allow the bed to expand with minimal mixing of the adsorbent phase, which can accommodate whole cells and cell fragments in the feed [2].

Besides the traditional elution mode for chromatography, other modes of chromatography are sometimes used, including the *frontal mode* and the *displacement mode*. In frontal chromatography, the target solute does not adsorb to the column, while some impurities are strongly retained by the stationary phase. The feed continues until the front of adsorbed impurities approaches the column outlet. An example of frontal chromatography is the use of an anion exchanger to adsorb contaminating DNA from a protein product stream. The protein is rendered positively charged by adjusting the pH of the feed solution to a value below the isoelectric point of the protein. The positively charged protein does not bind to the anion exchange resin, while DNA is adsorbed because it is negatively charged at almost all pH values. This technique allows processing of large amounts of material with a relatively small column, because contaminants are usually present in small amounts relative to the product.

In displacement chromatography, the column is loaded with the target solute to a significant fraction of its capacity and then is eluted by continuously introducing an even more strongly adsorbing substance, known as the displacer. For sufficiently long columns, the solutes in the feed become distributed in a pattern of adjacent pure solute bands, where each upstream solute acts as a displacer for each immediately adjacent downstream solute [3].

Liquid chromatography is a commonly used separation process for biologics and fine and specialty chemicals, while adsorption is widely used for high-throughput processes for small biomolecules such as antibiotics, sugars, amino acids and other commodities. As a unit operation, chromatography is a specialized version of adsorption-based separations, and many of the concepts taught in this chapter apply to both.

Adsorption is based on a variety of chemistries, some highly customized. At equilibrium, the individual components in the mixture to be separated are distributed between the stationary and mobile phases. This equilibrium can be modified by standard thermodynamic manipulations, such as temperature or composition (chemical activity) of the mobile phase. The most common thermodynamic variable to be modified is the composition of the mobile phase. Salt concentration, organic solvent concentration, and pH are common mobile phase thermodynamic characteristics that can be modified easily.

As in all separation operations, transport processes play a major role. Transport of chemical species from the mobile phase to the stationary phase takes place through a mass transfer layer at the surface of the particle, and solutes diffuse through pores in the resin to an adsorption site. The kinetics of the adsorption reaction can sometimes affect the separation. Axial and radial mixing can also be important factors in the separation, especially if the resin bed has not been well packed. Finally, the peripherals to the chromatography or adsorption column, such as the pumps, detectors, injectors, and filters, potentially add dead space and mixing volumes that affect the ultimate quality of the separation.

Adsorption equilibrium is described first in this chapter, followed by the dynamics of adsorption and chromatography. Both fixed-bed adsorbers and agitated-bed adsorbers are included. Two newer types of chromatography, membrane chromatography and simulated moving bed chromatography, are discussed. Various adsorbent types are discussed, as well as particle size, pressure drop, and equipment considerations. Scale-up applied to both adsorption and chromatography concludes the chapter.

7.1 INSTRUCTIONAL OBJECTIVES

After completing this chapter, the reader should be able to do the following:

- Write, plot, and use equations for adsorption isotherms.
- Derive the mass balance for fixed-bed adsorption and understand how it can be solved when simplifying assumptions are made.
- Calculate the shock wave velocity of a solute front when local equilibrium and negligible dispersion are assumed.
- Derive the mass balance for a series of agitated-bed adsorber columns.
- Assess chromatographic performance by elution peak analysis and moment analysis.

- Predict the chromatographic separation of solutes under assumptions of a linear isotherm, local equilibrium, and negligible dispersion.
- Explain the origins of band spreading in chromatography and its application to column optimization.
- Use computer simulation to predict the chromatographic separation of solutes taking into account axial dispersion, external mass transfer, intraparticle diffusion, and nonlinear equilibrium.
- Explain the principles and advantages of membrane chromatography and simulated moving bed chromatography.
- Select resins based on the adsorption chemistry of the separands.
- Use particle size and pressure drop in the scaling of adsorption and chromatography.
- Use the length of unused bed (LUB) method to scale up a fixed-bed adsorber.
- Use constant resolution scaling rules for elution chromatography.
- Choose equipment for chromatographic separations including columns, packing procedures, pumps, and gradient makers.

7.2 ADSORPTION EQUILIBRIUM

Chromatography and adsorption work by the differential adsorption of species to a resin surface, or ligands, from a complex chemical mixture. The adsorption of a chemical species can be represented by the equilibrium reaction

$$\text{(7.2.1)} \quad C + S \xleftrightarrow{K_{eq}} CS$$

where C is the dissolved chemical species, S is an adsorption site, CS is the chemical bound to the site, and K_{eq} is the equilibrium constant governing the reaction. The equilibrium constant for this adsorption is

$$\text{(7.2.2)} \quad K_{eq} = \frac{[CS]}{[C][S]}$$

Consider the three assumptions inherent in this representation of the adsorption reaction. First, it is completely reversible, and the chemical's interaction with the adsorption site causes no alteration in its solution properties or solution state. Second, chemicals bind to sites in a one-to-one fashion, and they bind only to sites. In other words, the binding is "specific," and there is no "nonspecific" binding, or interaction between molecules and the surface. Third, there is only one mode of binding to the site; all binding is equal and is described by a single value for K_{eq}. Despite these limiting assumptions, this "site model" of adsorption still serves as a very accurate description of adsorption in liquid chromatography.

In many cases, the concentration of adsorption sites is very much larger than the concentration of dissolved chemical species ([S] >> [C]), and the equilibrium expression becomes

$$K_{eq} = \frac{[CS]}{[C]} \quad (7.2.3)$$

or,

$$[CS] = K_{eq}[C] \quad (7.2.4)$$

This representation is particularly common in analytical liquid chromatography, where sample volumes are very small and solutes typically dilute. This is known as *linear equilibrium,* because the concentration of the adsorbed species can be expressed as a multiple of the concentration of the dissolved species. There is no limitation to binding set by the inherent ability of the resin to bind the chemical. In other words, it is implied that no saturation limit of the resin will be reached.

Chromatography in the linear limit is very suitable for analytical chromatography because it emphasizes the difference in K_{eq} between species in order to separate them; these differences can be very small for very similar molecules. The purpose of analytical chromatography is to detect and if possible to measure the concentrations of the various components of a mixture. To achieve this goal, "baseline resolution" (zero concentration between eluted separands) is critical, since determining the concentrations of two species that are not completely separated is less accurate. It is also critical that the concentrations of the various solutes do not affect their retention time, which is the case in linear equilibrium.

The linear isotherm approximation is less useful for preparative or industrial scale adsorption and chromatography. The most efficient operation uses all the adsorption sites available. In this case, the concentration of the empty adsorption sites available cannot be ignored. The concentration of unoccupied sites is not readily measurable, but the total number of sites is, so

$$S_{tot} = [CS] + [S] \quad (7.2.5)$$

where S_{tot} is the total site concentration. Combining the general expression for K_{eq}, Equation (7.2.2), with Equation (7.2.5) for S_{tot} gives

$$[CS] = \frac{K_{eq} S_{tot}[C]}{1 + K_{eq}[C]} \quad (7.2.6)$$

the well-known *Langmuir isotherm*. In the limit where $K_{eq}[C]$ is small in comparison to one, the denominator of Equation (7.2.6) goes to one, and the form of the linear adsorption equation is recovered [Equation (7.2.4)]. When $K_{eq}[C]$ is large in comparison to one, [CS] is equal to S_{tot}; that is, the adsorption sites are saturated. The Langmuir isotherm [a plot of Equation (7.2.6)] is "concave downward," having a linear slope in the low-concentration limit and a plateau as the resin becomes saturated (Figure 7.2). Equilibrium isotherms that are concave downward are considered to be favorable for adsorption. The Langmuir isotherm has often been used to correlate equilibrium adsorption data for proteins [4].

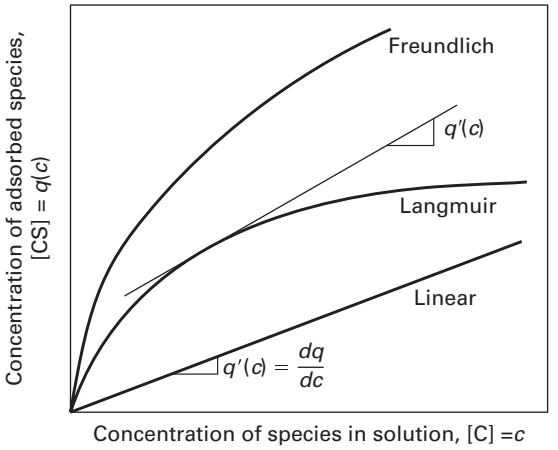

FIGURE 7.2 Shapes of different equilibrium adsorption isotherms.

The consequences of the Langmuir isotherm for preparative and industrial chromatography are many. The adsorption of various species from a complex mixture is now seen as influenced not only by the equilibrium constants (K_{eq}'s), which are species specific, but also by the total binding capacity of the resin (S_{tot}), which is more specific to the resin than to the chemical species. This potentially decreases the differences between species in their chromatographic behavior at high concentrations. Baseline resolution of species is no longer generally attainable, and the concept of resolution begins to lose value in these applications. The goal of large-scale chromatographic separation is also different. Here, we are trying to purify one or possibly two major components. Purification is usually defined as a limit of particular contaminants, for example removal of DNA to less than 10 ppm. Measurement of contaminants is no longer the goal, and separation of contaminants from each other is also not important.

Another equilibrium isotherm that has proven useful is the empirical *Freundlich isotherm* [5]:

$$[\mathrm{CS}] = K_{eq}[\mathrm{C}]^{1/n} \qquad n > 1 \tag{7.2.7}$$

With $n > 1$, this isotherm is also concave downward (Figure 7.2). This isotherm can be explained as a result of energetic heterogeneity of the surface of the adsorbent. An expression of the Freundlich form results when a set of Langmuir isotherms (with different K_{eq} values) is superimposed. The Freundlich isotherm has been used to describe the adsorption of a wide range of antibiotics, steroids, and hormones [4]. Thermodynamics such as described above typically dominate preparative and industrial chromatography and adsorption. Some implications of the isotherms will be discussed below, in section 7.3 for adsorption and section 7.4.3 for chromatography.

7.3 ADSORPTION COLUMN DYNAMICS

A basic understanding of the dynamic behavior of adsorption processes is essential for the design and optimization of large-scale processes. The most important types of adsorbers for biotechnology are fixed-bed columns and agitated-bed columns. The dynamics of each of these systems are analyzed.

7.3.1 Fixed-Bed Adsorption

The development of a mass balance is the starting point for analyzing fixed-bed adsorption. Simplifications of this mass balance lead to analytical solutions that give insight into the separation process.

Mass Balance for Fixed-Bed Adsorption

To understand the dynamics of a fixed-bed adsorption column, a mass balance is performed by considering a disk of cross-sectional area equivalent to that of the column (A), but differential in thickness (Δx), as shown in Figure 7.3. A species to be separated (called the separand) flows in and out of the disk by convection and the combined effects of molecular diffusion and mechanical dispersion. The rate of convection into the disk is the interstitial velocity, that is, the velocity of fluid between the resin particles, or in the "void fraction," ε. This convection rate is the superficial velocity (the flow rate divided by the cross section of the column) divided by the void fraction ($= Q/\varepsilon A$). Within the volume of the disk, separand may accumulate within both the mobile and stationary phases. The mass balance for separand i can be written as follows:

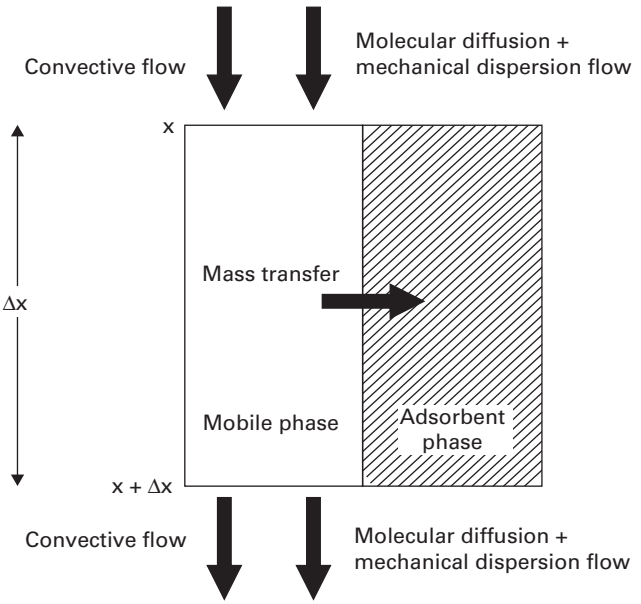

FIGURE 7.3 Schematic representation of adsorption in a column of differential thickness Δx.

(7.3.1) (Rate of separand in) − (rate of separand out) = (rate of accumulation of separand)

$$A\varepsilon\,\Delta t\left(\frac{\upsilon}{\varepsilon}c_i-\mathscr{D}_{\text{eff}}\frac{\partial c_i}{\partial x}\right)\Bigg|_{x,t}-A\varepsilon\,\Delta t\left(\frac{\upsilon}{\varepsilon}c_i-\mathscr{D}_{\text{eff}}\frac{\partial c_i}{\partial x}\right)\Bigg|_{x+\Delta x,t}$$
$$=A\varepsilon\,\Delta x(c_i|_{t+\Delta t}-c_i|_t)+A(1-\varepsilon)\,\Delta x(q_i|_{t+\Delta t}-q_i|_t) \tag{7.3.2}$$

where c_i = concentration of separand i in the mobile phase = $[C]_i$
q_i = concentration of separand i in the stationary phase averaged over an adsorbent particle = $[CS]_i$
ε = void fraction (mobile phase volume/total column volume), commonly 0.3 to 0.4 in fixed beds
υ = mobile phase superficial velocity (flow rate divided by the empty column cross-sectional area, Q/A; also called the "linear velocity")
$\mathscr{D}_{\text{eff}}$ = effective dispersivity of the separand in the column
t = time
x = longitudinal distance in the column; x = 0 at column inlet

Dividing by $A\varepsilon\Delta x\Delta t$, and taking the limit as Δx and Δt go to zero, this mass balance becomes

$$\mathscr{D}_{\text{eff}}\frac{\partial^2 c_i}{\partial x^2}-\frac{\upsilon}{\varepsilon}\frac{\partial c_i}{\partial x}=\frac{\partial c_i}{\partial t}+\frac{1-\varepsilon}{\varepsilon}\frac{\partial q_i}{\partial t} \tag{7.3.3}$$

The right-hand side of this equation represents the rate of accumulation of separand in any section of the column and recognizes that adsorption is an inherently unsteady state operation. The left-hand side of the equation represents the "in minus out" terms of the mass balance; separand moves through the column via the convection of the mobile phase (second term), or by diffusion or mechanical dispersion down a concentration gradient (first term). The term involving $\partial q_i/\partial t$ represents the rate of accumulation in the resin for the separand i. This accumulation can be represented in general as

$$\frac{\partial q_i}{\partial t}=f(c_i,c_j,\ldots,q_i,q_j,\ldots) \tag{7.3.4}$$

where the subscripts represent separands $i, j, \ldots$. This rate expression may be a linear driving force expression of the form

$$\frac{\partial q_i}{\partial t}=K_a(c_i-c_i^*) \tag{7.3.5}$$

where K_a is an overall mass transfer coefficient that includes both internal and external mass transfer resistance, and c_i^* is the liquid phase concentration that would exist at equilibrium with q_i.

Assumption of Local Equilibrium and Negligible Dispersion

Since the overall pattern of mass transfer is governed by the form of the equilibrium relationship, the main features of the dynamic behavior can be understood without doing detailed calculations [5]. Thus, this first analysis of the mass balance for adsorption will assume equilibrium locally and ignore the dispersion term for simplicity. This allows us to focus on the velocity, u_i, at which a solute traverses the column. Using an equilibrium isotherm relationship in the form $q_i = f(c_i)$ (Figure 7.2), Equation (7.3.3) becomes

$$\frac{\partial c_i}{\partial t} + \frac{\upsilon}{\varepsilon + (1-\varepsilon) q_i'(c_i)} \frac{\partial c_i}{\partial x} = 0 \tag{7.3.6}$$

where $q_i'(c_i)$ is the slope of the equilibrium isotherm at concentration c_i. If we let

$$u_i = \frac{\upsilon}{\varepsilon + (1-\varepsilon) q_i'(c_i)} \tag{7.3.7}$$

then Equation (7.3.6) becomes

$$\frac{\partial c_i}{\partial t} + u_i \frac{\partial c_i}{\partial x} = 0 \tag{7.3.8}$$

We see that Equation (7.3.8) is identical in form to the equation of continuity for solute i moving at velocity u_i through a column with no packing [6]. Thus, the expression for u_i given by Equation (7.3.7) is the *effective velocity* of component i through the packed bed. When the equilibrium is linear for the solute, $q_i'(c_i)$ is equal to $K_{\text{eq},i}$, so that the effective solute velocity is independent of the concentration and is inversely proportional to $K_{\text{eq},i}$.

For preparative and industrial scale adsorption processes, where it is desired to use high adsorbent loadings, the equilibrium is nonlinear and generally the Langmuir isotherm is applicable. From Figure 7.2 for the Langmuir isotherm, it can be seen that $q_i'(c_i)$ decreases with concentration; according to Equation (7.3.7), a decrease in $q_i'(c_i)$ causes u_i to increase. This would result in the physically unreasonable overhanging concentration profiles shown in Figure 7.4. However, for the solute at the front that advances through the fixed bed, the concentration change is not continuous, and finite differences rather than differentials must be used for the change in q_i with c_i, as follows:

$$u_{i,\text{sh}} = \frac{\upsilon}{\varepsilon + (1-\varepsilon) \dfrac{\Delta q_i}{\Delta c_i}} \tag{7.3.9}$$

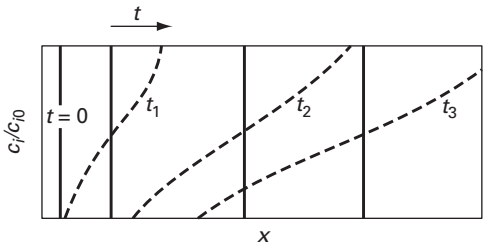

FIGURE 7.4 Shapes of shock wave concentration profiles (solid lines) and physically unreasonable overhanging concentration profiles for a favorable equilibrium isotherm (dashed lines): c_i, mobile phase concentration of solute; c_{i0}, solute concentration in feed to the adsorber.

The resulting $u_{i,\mathrm{sh}}$ of the solute front is called the *shock wave velocity*, as the mathematics describing this phenomenon are similar to those describing acoustic waves and ocean waves. The calculation of the shock wave velocity is illustrated later (see Example 7.3).

In real systems, solute dispersion in the column makes perfect step changes in concentration impossible. However, when the equilibrium isotherm is favorable (i.e., concave downward, as for the Langmuir isotherm and the Freundlich isotherm), which is often the case for biological solutes, a solute wave front is *self-sharpening*. This can be explained from an examination of the effect of a favorable isotherm on the solute velocity u_i determined by Equation (7.3.7): low concentrations ahead of the wave result in higher $q_i'(c_i)$ and thus lower u_i, while high concentration within the wave give lower $q_i'(c_i)$ and therefore higher u_i. These effects both work to sharpen the front. On the other hand, low concentrations that trail the front also give higher $q_i'(c_i)$ and thus lower u_i resulting in a broadening tail behind the sharp front. These effects are illustrated later in Example 7.4.

Assumption of a Linear Equilibrium Isotherm and Negligible Dispersion

If the equilibrium isotherm is linear and dispersion is neglected, an analytical solution of the mass balance for adsorption [Equation (7.3.3)] can be obtained. Although numerical solutions of this mass balance can be obtained, analytical solutions are valuable because they provide greater insight into the behavior of the system. The following equations describe adsorption assuming a linear adsorption isotherm, a linear driving force for the mass transfer rate, and negligible dispersion, respectively:

$$q_i = K_{eq,i} c_i \tag{7.3.10}$$

$$\frac{\partial q_i}{\partial t} = K_a (c_i - c_i^*) \tag{7.3.5}$$

$$\frac{\partial c_i}{\partial t} + \frac{1-\varepsilon}{\varepsilon}\frac{\partial q_i}{\partial t} + \frac{\upsilon}{\varepsilon}\frac{\partial c_i}{\partial x} = 0 \tag{7.3.11}$$

The initial and boundary conditions for a column initially free of solute subjected to a step change in the solute concentration at the inlet at time zero are as follows:

$$(7.3.12)\quad t < 0 \quad q_i(0,x) = c_i(0,x) = 0$$

$$(7.3.13)\quad t \geq 0 \quad c_i(t,0) = c_{i0}$$

For the solution of these equations, it is convenient to write Equations (7.3.11) and (7.3.5) in terms of dimensionless variables:

$$(7.3.14)\quad \frac{\partial \varphi}{\partial \xi} + \frac{\partial \psi}{\partial \tau} = 0$$

$$(7.3.15)\quad \frac{\partial \psi}{\partial \tau} = \varphi - \psi$$

where $\varphi = c_i / c_{i0}$
$\psi = q_i / q_{i0}$
$q_{i0} = K_{\mathrm{eq},i}\, c_{io}$
$\xi = (k\, K_{\mathrm{eq},i}\, x / \upsilon)(1 - \varepsilon)$
$k = K_a / K_{\mathrm{eq},i}$
$\tau = k(t - x\, \varepsilon/\upsilon)$

Equations (7.3.14) and (7.3.15) are exactly analogous to those used to describe heat transfer in a packed bed, and using classical methods the following solution was obtained [7]:

$$(7.3.16)\quad \frac{c_i}{c_{i0}} = e^{-\xi} \int_0^{\tau} e^{-u} I_0(2\sqrt{\xi u})\, du + e^{-(\tau+\xi)} I_0(2\sqrt{\tau\xi})$$

where the Bessel function is given by

$$(7.3.17)\quad I_0(2\sqrt{\tau\xi}) = \sum_0^{\infty} \frac{(\tau\xi)^n}{(n!)^2} = 1 + \tau\xi + \frac{\tau^2\xi^2}{4} + \frac{\tau^3\xi^3}{36} +$$

The numerical evaluation requires tedious graphical integrations. Representative results of breakthrough curves using the results of graphical integrations [8] are shown in Figure 7.5.

Analytical solutions of the mass transfer equations for adsorption have been obtained with more realistic models, including intraparticle diffusion with and without external film resistance, but the solutions for the breakthrough curve are too cumbersome to be of much practical value [9].

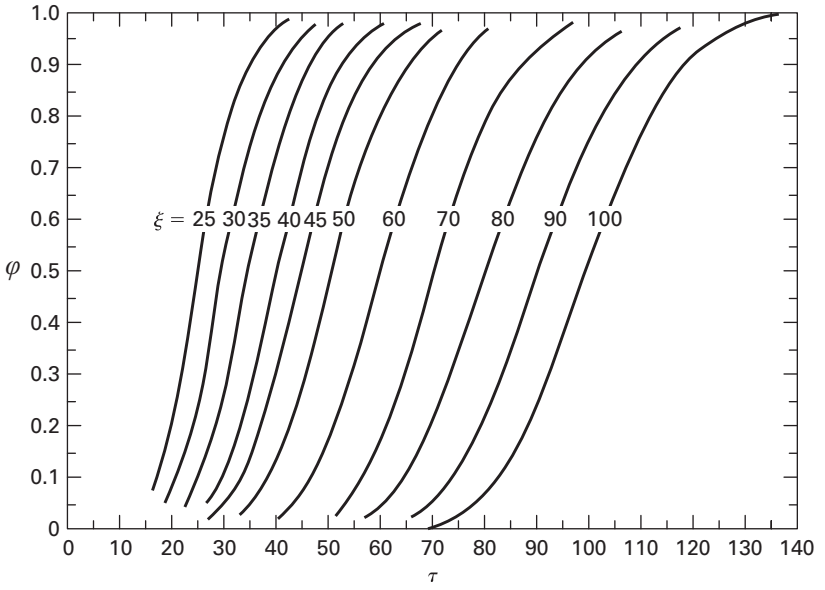

FIGURE 7.5 Adsorption breakthrough curves based on an analytical solution of the mass balance assuming a linear adsorption isotherm, a linear driving force for the mass transfer rate, and negligible dispersion. *(Data from C. C. Furnas, "Heat transfer from a gas stream to a bed of broken solids,"* Trans. AIChE, *vol. 24, p. 155, 1930.)*

EXAMPLE 7.1

Determination of the Mass Transfer Coefficient from Adsorption Breakthrough Data A solution containing a biological compound was fed at a superficial velocity of 20 cm/h to a fixed-bed column containing an adsorbent until breakthrough (when $c_i/c_{i0} = 0.1$) was obtained 9.5 h from the start of feeding. The feed concentration was low enough that the equilibrium isotherm was linear, found previously in equilibrium experiments to be

$$q_i = 40c_i^*$$

where q_i and c_i^* have units of milligrams per milliliter. The column was 10 cm long, and the void fraction of the packing was 0.34. From this information, estimate the mass transfer coefficient K_a, assuming a linear driving force for the mass transfer rate,

$$\frac{\partial q_i}{\partial t} = K_a(c_i - c_i^*)$$

Solution

We can solve this problem using the analytical solution of the breakthrough curve in graphical form (Figure 7.5) for the equations that describe mass transfer in adsorption, assuming a linear equilibrium isotherm, a linear driving force for the mass

transfer rate, and negligible dispersion. At the column outlet, the parameters in the graphical solution shown in Figure 7.5 are as follows, using the definitions for the variables in Equations (7.3.14) and (7.3.15):

$$\varphi = \frac{c_i}{c_{i0}} = 0.1$$

$$\xi = \frac{K_a x}{\upsilon}(1-\varepsilon) = \frac{K_a \times 10\,\text{cm}}{20\dfrac{\text{cm}}{\text{h}}}(0.66) = 0.33\,K_a$$

$$\tau = \frac{K_a}{K_{\text{eq}}}\left(t - \frac{x\varepsilon}{\upsilon}\right) = \frac{K_a}{40}\left(9.5\,\text{h} - \frac{10\,\text{cm}\times 0.34}{20\dfrac{\text{cm}}{\text{h}}}\right) = 0.233K_a$$

where K_a has units of hours^{-1}. We can rewrite these in terms of K_a as

$$K_a = 3.03\xi = 4.29\tau$$

Finding K_a is a trial-and-error solution. We select values of τ and ξ that give $\varphi = 0.1$ in Figure 7.5 and calculate K_a using each of the two foregoing equations. This is continued until the same K_a is obtained for each equation. This procedure leads to

$$K_a \cong 105\,\text{h}^{-1}$$

This value of K_a could now be used to predict breakthrough for other superficial velocities and column lengths.

Constant Pattern Behavior

In preparative and industrial adsorption processes, high feed concentrations, resistance to mass transfer, and axial mixing in the column lead to departures from ideal situations where a linear isotherm, local equilibrium, and negligible dispersion can be assumed. In the case of a favorable equilibrium isotherm (i.e., isotherms that are concave downward, which is the case for the Langmuir isotherm that can often be used for the adsorption of proteins), the concentration profile in the column develops in the initial region; and at some point from the column entrance, the profile propagates without further change in shape—thus the term "constant pattern." This occurs because the dispersion in the column resulting from longitudinal dispersion and mass transfer resistance is opposed by the self-sharpening effect discussed earlier. When the equilibrium isotherm is highly favorable, the distance required to approach the constant pattern limit may be very small, a few centimeters to up to a meter [5]. The constant pattern approximation provides the basis for a very useful and widely

utilized method for scale-up design using the concept of the length of unused bed (LUB) (see Section 7.10.1).

7.3.2 Agitated-Bed Adsorption

Agitated-bed adsorption processes have been developed to allow removal of a product secreted by the cells without first having to remove the cells. In this type of process, cell culture broth is passed through a series of agitated columns containing an adsorbent, as shown in Figure 7.6. Each column has screens at the inlet and outlet that are designed to retain the adsorbent within the column but allow the broth to pass through. When the concentration of the product in the effluent of the last column in the series reaches a certain value, the flow is stopped, and the lead column is taken out of the train. Periodic countercurrent operation is obtained by advancing each of the remaining columns in the train, placing a regenerated column of adsorbent in the last position, and starting the feed flow again. The lead column taken out of the train is washed with the adsorbent agitated to remove the broth solids, and the product is eluted from the adsorbent, usually in the fixed-bed mode.

This process has advantages over filtration, in that there is no filter aid to dispose of and it is not necessary to wash a filter cake containing the cells, so losses of the product are often less. The equipment for this process is less expensive and easier to maintain than that used for centrifugation. The disadvantage is that expensive solid adsorbents are more easily fouled by the dirtier feed stream and so require harsher or more expensive regeneration procedures and more frequent replacement, compared to adsorbents utilized with streams with fewer impurities. Also, resin attrition can be an issue.

A useful mathematical model for this process has been developed [10]. The continuity equation for the nth column in the train can be written for separand i as

$$\text{(Rate of separand in)} - \text{(rate of separand out)} = \text{(rate of accumulation of separand)} \tag{7.3.18}$$

$$Qc_{i,n-1} - Qc_{i,n} = V_L \frac{dc_{i,n}}{dt} + V_R \frac{dq_{i,n}}{dt} \tag{7.3.19}$$

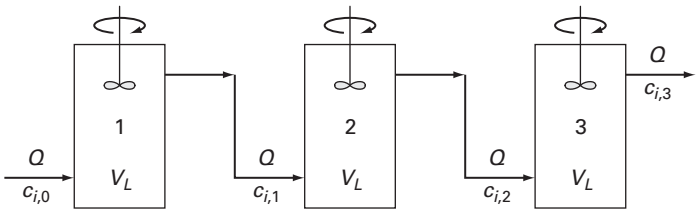

FIGURE 7.6 Train of agitated-bed adsorption columns for the processing of cell culture broth.

where Q = volumetric flow rate

$c_{i,n-1}$, $c_{i,n}$ = separand concentration in feed to and effluent from column n, respectively

V_L = liquid volume in column

V_R = volume of adsorbent in column

$q_{i,n}$ = separand concentration in adsorbent phase of column n averaged over an adsorbent particle

t = time

The rate of mass transfer of separand to the adsorbent phase is described by a linear driving force expression similar to Equation (7.3.5):

$$\frac{dq_{i,n}}{dt} = K_a(c_{i,n} - c^*_{i,n}) \tag{7.3.20}$$

where $c^*_{i,n}$ is the separand concentration in the bulk liquid when it is at equilibrium with $q_{i,n}$, and K_a is an overall mass transfer coefficient that can be correlated to experimental data as

$$K_a = A\exp\left(-B\frac{q_i}{q_{i,\text{sat}}}\right) + D\exp\left(-E\frac{q_i}{q_{i,\text{sat}}}\right) \tag{7.3.21}$$

Here A, B, D, and E are constants, and $q_{i,\text{sat}}$ is the adsorbent phase concentration that is in equilibrium with the separand concentration c_{i0} in the feed to the train of mixed columns. In the use of this model for the recovery of an antibiotic, equilibrium was modeled by the Freundlich isotherm written in the form

$$c'^*_{i,n} = bq^a_{i,n} \tag{7.3.22}$$

where a and b are constants.

Equations (7.3.19) to (7.3.22) constitute a set of mathematical relationships that govern the performance of each column in the train. These simultaneous equations can be solved by the Runge-Kutta numerical method [11] to predict the effluent and adsorbent concentrations as a function of time. Excellent agreement between predicted and experimental adsorption data for the recovery of the antibiotic novobiocin in a three-stage train has been obtained using this method [10].

7.4 CHROMATOGRAPHY COLUMN DYNAMICS

There are many methods of analysis for the dynamics of chromatography unit operations, too many to cover in detail in this textbook. To speak the language of chromatographers, the most relevant method to know is theoretical plate analysis. To be conversant with engineering methods of analysis, the application of mass balances,

rate equations, and equilibria (Section 1.8 in Chapter 1) are the most relevant. A brief treatment of each of these methods is given here.

7.4.1 Plate Models

Plate models seek to explain the band broadening observed in chromatography by approximating a chromatograph as a series of well-mixed tanks at equilibrium. The terminology comes from analysis of distillation, where plates are sometimes used to hold vapor and liquid in contact to approach equilibrium at various temperatures and compositions. Just as distillation is often performed in a packed column but the concept of a "theoretical equilibrium plate" remains, so has it also come to symbolize resolving power of a chromatography column. A resemblance to the analysis of multistage extraction (Section 6.2) should be noted.

The original analogy was drawn by Martin and Synge [12] in 1941. By dividing the column into a series of imaginary well-mixed tanks at equilibrium and computing the mass balance around each, they deduced when the number of tanks became large, and the initial condition was a solute at a finite concentration in the first tank, that the concentration profile could be described by a Gaussian curve. Properties of a Gaussian curve are shown in Figure 7.7. The number N of theoretical tanks can be found through the properties of the Gaussian curve. The volume of the theoretical

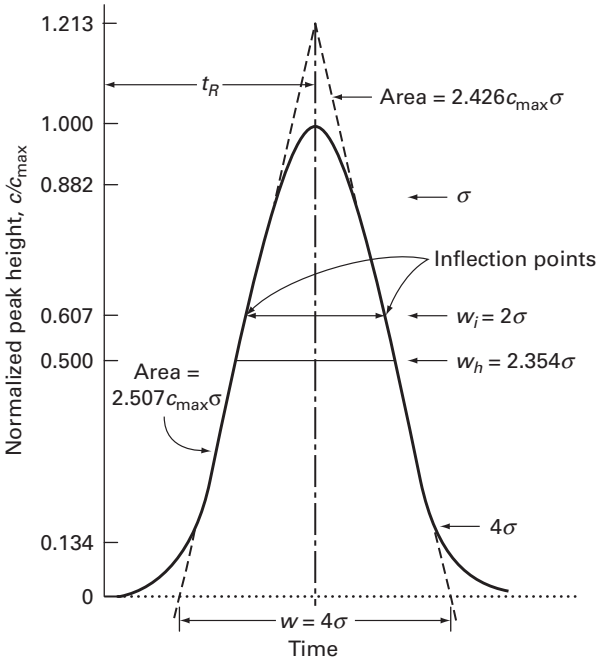

FIGURE 7.7 Properties of a Gaussian peak c_{max}, maximum peak height; σ, standard deviation; w_i, peak width at inflection points; w_h, peak width at half-height; w, peak width at base (base intercept); t_R, average retention time. *(Data from C. Horvath and W. R. Melander, "Theory of chromatography," Fundamentals and Applications of Chromatographic and Electrophoretic Methods, Part A, E. Heftmann, ed., p. A41, Elsevier Scientific, Amsterdam, Netherlands, 1983.)*

tanks (also called plates) is found by dividing the column volume by the number of tanks, and H, the height of the equivalent theoretical plate (HETP), can be expressed as

$$H = \frac{L}{N} \tag{7.4.1}$$

where L is the length of the column. For Gaussian peaks, the plate count can be expressed as the squared retention time divided by the variance of the peak [13]:

$$N = \frac{t_R^2}{\sigma^2} = \frac{t_R^2}{(w/4)^2} \tag{7.4.2}$$

where w is the peak width at the base (the base intercept as shown in Figure 7.7). The determination of the number of theoretical plates is a primary method by which scientists compare the performance of different columns, packed by different methods or with different resins.

Peak width is used in the definition of *resolution,* R_s, which is a measure of the extent of separation of two peaks in a chromatogram (the graphical representation of the concentration of solutes at the column exit plotted against time, as in Figure 2.4):

$$R_s = \frac{t_{R_2} - t_{R_1}}{\frac{1}{2}(w_2 + w_1)} \tag{7.4.3}$$

where t_{R_1}, t_{R_2} = average retention time for separands 1 and 2, respectively
w_1, w_2 = peak width (time) for separands 1 and 2, respectively

Thus, resolution is increased by increasing the difference in the retention times and by decreasing the peak widths.

A low concentration of a moderately bound solute should be used to evaluate a column HETP. Linear response is desired from a molecule that will bind and release from the resin, so that kinetics and mass transfer are measured, as well as mechanical mixing that may be present in the column hydrodynamics. To be certain the solute is in the linear binding range, a variety of concentrations may be tried at first, to measure the effect of concentration on retention time and peak shape. Very often, a water-soluble aromatic compound like benzoic acid is used. A popular series of solutes are the "parabens," methyl parabenzoic acid, ethyl paraben, and propyl paraben. HETP should also be measured under isocratic conditions (i.e., constant eluent buffer composition) to avoid influencing retention time and peak shape with a peak-sharpening gradient.

The undeniable simplicity of this plate model for evaluating the inherent separating power of a chromatography column accounts for its wide use in the field. Its primary use is in comparing multiple packings of the same column geometry with the same resin. Its applicability to the actual separation under study is always under debate, especially when the separation is at high solute concentration and large total solute load, and is eluted with a gradient.

7.4.2 Moment Analysis

HETP tests are useful for assessing column packing, but there are even more generalized tools that are becoming more accessible with increases in computing power and data storage. One of these tools is moment analysis, also called transition analysis. Moment analysis is another way to assess the concentration variance being generated in a chromatographic separation that is more generalized than HETP, and more likely to identify problems that are hidden in the shoulders and tails of chromatography peaks.

To demonstrate the value of moment analysis, it is important first to illustrate the weaknesses of the HETP test. Practically, the HETP test is easily applied to analytical chromatography but less easily applied to manufacturing scale chromatography. The test is best when a peak with a normal distribution can be generated with a test solution on a column. This requires a chemical that will bind and release from the resin. Preferably, the chemical will be detectable at low concentrations and already be present in the process, or have no effect on the product or resin if traces remain on the column after cleaning. This chemical must be introduced as a pulse at the inlet of the column and generally at very small volumes relative to the column load. This may require extra piping, or some operational practices that risk introducing air onto the column. Secondly, the math that transforms the shape of the peak into a comparative number assumes that the peak is normally distributed, or Gaussian. Deviations from Gaussian peak shape may not be detected with the HETP math.

Moment analysis does not have these limitations. Moment analysis can be applied to a step change at the column inlet during normal column operation, for example, the introduction of an equilibration solution, a load solution, or a regeneration solution. The step change need not be of low concentration, as long as it is relatively consistent from analysis to analysis. The math does not require a Gaussian or any other type of distribution for the curve and is capable of detecting changes in the column response to the step change, as long as the step size in the numerical integration is sufficiently small.

Moment analysis as applied to chromatography has been described in great detail by Kucera [14]. "Moments" describe the distribution of concentration of an eluting solute with respect to time, distance, or volume. Because there are often delays in liquid chromatographic operations, and it is very inconvenient to actually measure concentration as a function of distance inside a chromatography column, moments are often determined as a function of volume. The equation for a moment resulting from a step change at the column inlet is [15]

$$\mu_k = \int_0^{V_F} V^k \frac{dc}{dV} dV \tag{7.4.4}$$

where μ_k is the k^{th} moment, c is solute concentration, V is the volume of mobile phase eluted from the column outlet since the time of the step change at the column inlet,

and V_F is the total volume to be integrated. The choice of V_F is somewhat arbitrary, but is more convenient if it encompasses only one step change.

There is no limit to the number of moments that can be calculated, but generally the first three are found to be the most useful. The zeroth moment (μ_0) describes the average retention time of the transition. With a Gaussian distribution, for a pulse input this would be the peak maximum; for a step change, this would correspond to the inflection point, where the maximum in the first derivative with respect to concentration is reached. With a non-Gaussian distribution, for example a skewed peak, the zeroth moment shows the "center of gravity" of the distribution, for example, to the right or left of the peak maximum in a peak that is fronting or tailing.

The first moment (μ_1) describes the variance of the transition or peak. In general, the width of the elution zone is described from minimum to maximum, or baseline to baseline. This is similar to what is measured by the HETP, except that the HETP assumes that the width of the peak is evenly distributed around the maximum, while the moment, again, is calculated as the "center of gravity" of the distribution.

The second moment (μ_2) describes the skewness of the transition or peak. If the second moment is positive, the leading edge of the peak is sharp and the trailing edge is diffuse. The higher-order moments give more information on the broadening and asymmetry of the peak or transition but will not be discussed further in this chapter.

The first three moments, shown below, are the ones most often used for comparisons.

$$\mu_0 = \int_0^{V_F} \frac{dc}{dV} dV \tag{7.4.5}$$

$$\mu_1 = \int_0^{V_F} V \frac{dc}{dV} dV \tag{7.4.6}$$

$$\mu_2 = \int_0^{V_F} V^2 \frac{dc}{dV} dV \tag{7.4.7}$$

Calculating the moments from real chromatography data is best done numerically, using the trapezoidal rule, for example, for small steps in V. The step size must be small, and increasingly smaller for higher-order moments.

In applying moment analysis to monitor the performance of chromatography columns, it is convenient to calculate the "non-Gaussian" HETP, which is found from [16]

$$\mathrm{HETP_N} = \frac{L\sigma^2}{\left(\frac{\mu_1}{\mu_0}\right)^2} \tag{7.4.8}$$

where L is the column length, and σ is the variance, which can be approximated from the moments as

$$\sigma^2 = \frac{\mu_2}{\mu_0} - \left(\frac{\mu_1}{\mu_0}\right)^2 \quad (7.4.9)$$

Using these equations, it is possible to obtain values for HETP for any transition during chromatography operations.

Moment analysis is advantageous in that it can be performed on existing process data without having to do a separate test in which a special chemical is introduced into the column. It has proven to be superior to the Gaussian method of HETP determination in being able to detect integrity breaches in production scale protein chromatography columns [16].

7.4.3 Chromatography Column Mass Balance with Negligible Dispersion

Chromatography separates solutes based on their differential binding to the resin. As the solute is carried by the mobile phase through the resin, each solute partitions between the mobile and stationary phases. The solutes that partition more strongly are retarded more with respect to the flowing fluid, and they exit the column later (see Figure 7.1). Solutes that do not partition to the stationary phase at all exit the column in the "void volume," which represents the mobile phase volume in the interstices of the packed resin.

How the binding of solutes to resins at equilibrium translates into an elution time difference for the solutes is found in the mass balance. The mass balance for chromatography is identical to that for adsorption, Equation (7.3.3). The first analysis of this mass balance for chromatography will ignore the dispersion term for simplicity. This allows us to focus on the peak position, or the rate at which a solute traverses the column. By assuming local equilibrium and neglecting dispersion, we find that the effective velocity of a solute moving through the packed column is the same as that previously found in general for adsorption [Equation (7.3.7)]; this equation is useful for predicting the separation of different solutes, as is illustrated in Example 7.2.

EXAMPLE 7.2

Chromatographic Separation of Two Solutes Two solutes have linear equilibrium constants of $K_{eq,1} = 7.5$ and $K_{eq,2} = 7.8$, respectively. For a flow rate of 1.5 liter/min, in a column 63 cm in diameter, with a void fraction of 0.33, and local equilibrium, what column length is required to separate the two solutes by 5 min?

Solution

The effective velocity of solute i for negligible dispersion is given by Equation (7.3.7) as

$$u_i = \frac{\upsilon}{\varepsilon + (1-\varepsilon)q_i'(c_i)}$$

For linear equilibrium,

$$q_i = K_{\text{eq},i}c_i$$

$$q_i'(c_i) = K_{\text{eq},i}$$

The superficial velocity is

$$\upsilon = \frac{1500\dfrac{\text{cm}^3}{\text{min}}}{\pi(31.5)^2\,\text{cm}^2} = 0.481\frac{\text{cm}}{\text{min}}$$

For solute 1, the effective velocity is therefore

$$u_1 = \frac{0.481\dfrac{\text{cm}}{\text{min}}}{0.33 + (1-0.33)(7.5)} = 0.08982\frac{\text{cm}}{\text{min}}$$

This same equation gives 0.08657 cm/min for solute 2. Translating solute velocities into elution times for a constant distance traveled (L),

$$5\,\text{min} = L\left(\frac{1}{u_2} - \frac{1}{u_1}\right)$$

Solving for L gives

$$L = 12.0\,\text{cm}$$

Note that four significant figures are used to calculate u_1 and u_2 to avoid error in calculating L.

Equilibrium relations are usually more complicated than the linear case. For the nonlinear Langmuir equilibrium isotherm [Equation (7.2.6)], we obtain for the first derivative of q_i with respect to c_i,

$$q_i'(c_i) = \frac{K_{\text{eq},i}S_{\text{tot}}}{1 + K_{\text{eq},i}c_i} - \frac{K_{\text{eq},i}^2 S_{\text{tot}}c_i}{(1 + K_{\text{eq},i}c_i)^2} \quad (7.4.10)$$

As the concentration becomes higher, the value of the derivative becomes smaller and the solute velocity is higher. This makes sense, because to have a high mobile phase concentration, the stationary phase concentration must be near saturation, thus leaving no sites on the resin for the solute in the mobile phase to bind to. This holds true as long as the change in concentration is continuous. However, when a pulse injection is made, the resin immediately preceding the solute front is devoid of bound solute. In this case, the concentration change is not continuous but is a step change, and finite differences must be used for q and c, giving Equation (7.3.9) for the effective velocity of the solute. This velocity is called a shock wave velocity, as discussed for adsorption in Section 7.3.

EXAMPLE 7.3

Calculation of the Shock Wave Velocity for a Nonlinear Isotherm Solute 1 has a Langmuir isotherm characterized by an S_{tot} of 120 μg/ml, and a K_{eq} of 7.5 ml/mg. Calculate the shock wave velocity for an injection of 1 mg/ml, and column conditions identical to those of Example 7.2.

Solution

To use Equation (7.3.9) for the shock wave velocity, we need to know Δq. For the Langmuir isotherm [Equation (7.2.6)], the resin concentration q = [CS] in equilibrium with concentration [C] = 1 mg/ml in the mobile phase is

$$[\mathrm{CS}] = \frac{K_{eq} S_{tot}[\mathrm{C}]}{1 + K_{eq}[\mathrm{C}]} = \frac{\left(7.5\frac{\mathrm{ml}}{\mathrm{mg}}\right)\left(0.120\frac{\mathrm{mg}}{\mathrm{ml}}\right)\left(1\frac{\mathrm{mg}}{\mathrm{ml}}\right)}{1 + \left(7.5\frac{\mathrm{ml}}{\mathrm{mg}}\right)\left(1\frac{\mathrm{mg}}{\mathrm{ml}}\right)} = 0.106\frac{\mathrm{mg}}{\mathrm{ml}}$$

Since the column initially has no solute,

$$\frac{\Delta q_1}{\Delta c_1} = \frac{(0.106 - 0)\frac{\mathrm{mg}}{\mathrm{ml}}}{(1 - 0)\frac{\mathrm{mg}}{\mathrm{ml}}} = 0.106$$

From Equation (7.3.9), we obtain

$$u_{i,sh} = \left(\frac{\upsilon}{\varepsilon + (1 - \varepsilon)\frac{\Delta q_1}{\Delta c_1}}\right) = \frac{0.481\frac{\mathrm{cm}}{\mathrm{min}}}{0.33 + (1 - \varepsilon)(0.106)} = 1.20\frac{\mathrm{cm}}{\mathrm{min}}$$

This is over 10 times the solute velocity for the linear isotherm case given in Example 7.2. This is because the concentration of the solute is limited to 0.120 mg/ml on the stationary phase. For the linear case where the stationary phase concentration is assumed to be unlimited, a 1 mg/ml injection would lead to a 7.5 mg/ml concentration in the stationary phase.

The leading edge of a solute front derived from a Langmuir isotherm is a self-sharpening shock wave, which leads to the constant pattern behavior discussed earlier. The trailing edge, on the other hand, is a continuous diffuse wave. The trailing edge has a continuous concentration from the injection concentration to zero. To predict the elution profile of a peak, both the leading shock wave and the trailing diffuse wave must be calculated. This is done by solving Equation (7.3.7) for the trailing edge with respect to a range of mobile phase concentrations between the injection concentration and zero, and Equation (7.3.9) with respect to the shock front (as in Example 7.3). This is shown in Example 7.4.

EXAMPLE 7.4

Calculation of the Elution Profile For an injection volume of 5 liters, and other conditions as stated in Examples 7.2 and 7.3, calculate the elution profile for solute 1.

Solution

As determined in Example 7.3, the velocity of the shock front is 1.20 cm/min. The diffuse wave velocity is determined by selecting concentrations between 0 and the injection concentration of 1 mg/ml, and determining the velocity of each of these concentrations trailing the shock front. For example, at a solute concentration of 0.4 mg/ml, we can calculate dq_1/dc_1 from Equation (7.4.10):

$$\frac{dq_1}{dc_1} = \frac{K_{\text{eq},1}S_{\text{tot}}}{1+K_{\text{eq},1}c_1} - \frac{K_{\text{eq},1}^2 S_{\text{tot}} c_1}{(1+K_{\text{eq},1}c_1)^2} = \frac{7.5(0.120)}{1+7.5(0.4)} - \frac{(7.5)^2(0.120)(0.4)}{[1+7.5(0.4)]^2} = 0.056$$

We can use Equation (7.3.7) to calculate the solute velocity:

$$u_1 = \left(\frac{\upsilon}{\varepsilon + (1-\varepsilon)\dfrac{dq_1}{dc_1}} \right) = \frac{0.481}{0.33+(1-0.33)(0.056)} = 1.31\frac{\text{cm}}{\text{min}}$$

For a flow rate of 1.5 liters/min, and an injection volume of 5 liters, the diffuse wave trails the shock by 3 min and 20 s [5 liters/(1.5 liters/min)]. Table E7.4 gives the solute velocities for various concentrations.

As can be seen, concentrations above 0.23 mg/ml run faster than the shock front. Since nothing can pass the shock front, these concentrations do not appear in the thermodynamic diffuse wave. They do, however, represent concentrations on the isotherm where the first derivative is less than the slope of the chord that connects the shock concentrations. Concentrations of 0.23 mg/ml and less run behind the shock front, and thus constitute the diffuse wave. The shock front elutes from the 12.0 cm bed in 10.0 min. The diffuse wave is delayed by 3.33 min, as mentioned earlier, and then starts at approximately 0.23 mg/ml. The diffuse wave decreases in concentration to 0.1 mg/ml at 16.5 min, to 0.01 mg/ml at 24.8 min, to 0.005 mg/ml at 25.6 min, and to 0.001 mg/ml at 26.4 min. A representative graph is shown in Figure E7.4.

TABLE E7.4 Diffuse Wave Concentrations Following the Shock Wave for Example 7.3

Solute concentration, c_1 (mg/ml)	Isotherm derivative, dq_1/dc_1	Solute velocity, u_1 (cm/min)
0.8	0.018	1.40
0.6	0.030	1.37
0.5	0.040	1.35
0.4	0.056	1.31
0.23	0.121	1.17
0.1	0.294	0.91
0.01	0.779	0.56
0.005	0.836	0.54
0.001	0.887	0.52

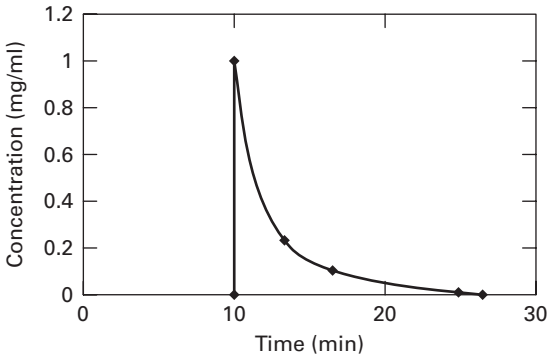

FIGURE E7.4 The elution profile calculated for a Langmuir isotherm. Conditions are given in the examples in the text.

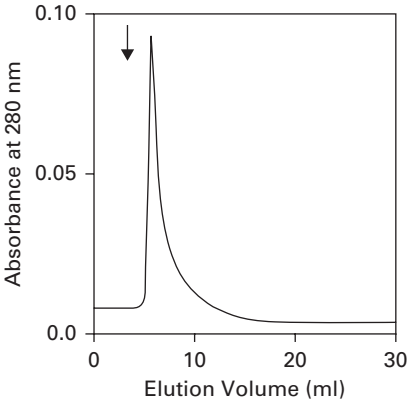

FIGURE 7.8 Elution profile for the chromatography to purify the L-asparaginase-atrial natriuretic peptide fusion protein on a column of L-asparagine agarose (1 cm x 4.5 cm) after loading clarified cell lysate and washing. The column was washed with sodium phosphate buffer immediately preceding elution with 0.2 M sodium chloride in sodium phosphate butter (10 mM, pH 7.5). The arrow indicates the start of the elution. *(Data from N. T. Ma, Y. F. Wang, B. A. Roe, and R. G. Harrison, "Purification of an L-asparaginase—atrial natriuretic peptide fusion protein expressed in* Escherichia coli*," Biotechnol. Bioeng., vol. 47, p. 483, 1995.)*

The Langmuir isotherm and other concave downward equilibrium conditions are very common for large-scale liquid chromatography. Analytical chromatography does not generally deal with concentrations large enough to generate a Langmuir isotherm. Ion exchange binding is related to, but not exactly the same as, the Langmuir isotherm. Concave upward isotherms result in peaks that have self-sharpening trailing edges and diffuse leading fronts. Most concave upwards isotherms result from multilayer binding in which the binding becomes more energetically favorable as the layers build up. This is most typical in gas adsorption/desorption applications and is rarely, if ever, found in the liquid chromatography of bioactive molecules.

An example of a chromatography to purify a protein where an elution profile similar to that in Figure E7.4 was obtained is shown in Figure 7.8. Analysis by SDS-PAGE of the peak eluted indicated elution to near homogeneity [17]. As in Example 7.4, elution is in the isocratic mode, in this case using 0.2 M sodium chloride. The shock front is sharp, as in Figure E7.4, and there is a trailing diffuse wave. Therefore, this elution profile in Figure 7.8 is consistent with a Langmuir isotherm.

7.4.4 Dispersion Effects in Chromatography

So far, we have discussed chromatography and adsorption from a purely thermodynamic point of view. Mass transfer and diffusion also play an important role in the development and scale-up of these separation techniques. Diffusion takes place longitudinally in the mobile phase, and also within the pores of the stationary phase. Mass transfer takes place between the mobile and stationary phases. Slow diffusion and mass transfer always decrease the efficiency of the separation, and steps should be taken where possible to increase the rates of each.

Longitudinal dispersion is represented in the complete mass balance for adsorption, Equation (7.3.3). The effective dispersivity $\mathscr{D}_{\text{eff}}$ is a combination of the molecular or binary diffusivity in the mobile phase $\mathscr{D}_{\text{m}}$ and a dispersion coefficient E, which accounts for additional solute transport caused by back-mixing and nonuniformity of the convective velocity profile [18]:

$$\mathscr{D}_{\text{eff}} = \mathscr{D}_{\text{m}} + E \tag{7.4.11}$$

For a chromatography process in which the feed solution contains a concentration pulse of the separand, the mass balance including the dispersivity term [Equation (7.3.3)] has been solved by Lapidus and Amundson [19], assuming a linear isotherm, local equilibrium, and a semi-infinite column to give an analytical solution:

$$\begin{aligned} c_i(x,t) &= c_{i0}H(x,t) - c_{i0}H(x,t-\bar{t}) \qquad && \bar{t} < t < \infty \\ &= c_{i0}H(x,t) && t < \bar{t} \end{aligned} \tag{7.4.12}$$

where the dispersion function is

$$\begin{aligned} H(x,t) = \frac{1}{2}\Bigg[& 1 + \operatorname{erf}\left(\sqrt{\frac{u^2 t}{4\gamma \mathscr{D}_{\text{eff}}}} - x\sqrt{\frac{\gamma}{4t\mathscr{D}_{\text{eff}}}} \right) \\ & + e^{ux/\mathscr{D}_{\text{eff}}} \operatorname{erfc}\left(\sqrt{\frac{u^2 t}{4\gamma \mathscr{D}_{\text{eff}}}} - x\sqrt{\frac{\gamma}{4t\mathscr{D}_{\text{eff}}}} \right) \Bigg] \end{aligned} \tag{7.4.13}$$

in which u is the velocity of fluid through the interstices of the bed (= υ/ε), $\gamma = K_{\text{eq}}(1 - \varepsilon)/\varepsilon$, and erf and erfc are the error function and complementary error function, respectively. It is also assumed that the adsorbent is initially free of the separand (clean column) and that the feed concentration is c_{i0} from zero time to time $\bar{t}$, after which it changes back to zero. In this solution, band broadening is dependent on the value of $\mathscr{D}_{\text{eff}}$. When this equation is used to fit real liquid chromatographic data, $\mathscr{D}_{\text{eff}}$ is found to be on the order of 10^{-3} cm^2/s, whereas for pure diffusion of a macromolecule in liquid, $\mathscr{D}_{\text{m}}$ is on the order of 10^{-6} to 10^{-7} cm^2/s. This would lead one to believe that dispersion effects such as back mixing and flow nonuniformity are approximately 1000 times more important than longitudinal molecular diffusivity in determining band broadening in chromatography. However, the effects of mass transfer to the resin boundary, the diffusion of molecules within the resin, and kinetics of binding are also contributing to the band broadening. With the exception of poorly packed columns and poorly designed peripherals, mass transfer and intraresin diffusion are the controlling factors in band broadening in fixed-bed operations, and these are addressed by decreasing resin particle size. Further effects of particle size, and methods for understanding them, are discussed below.

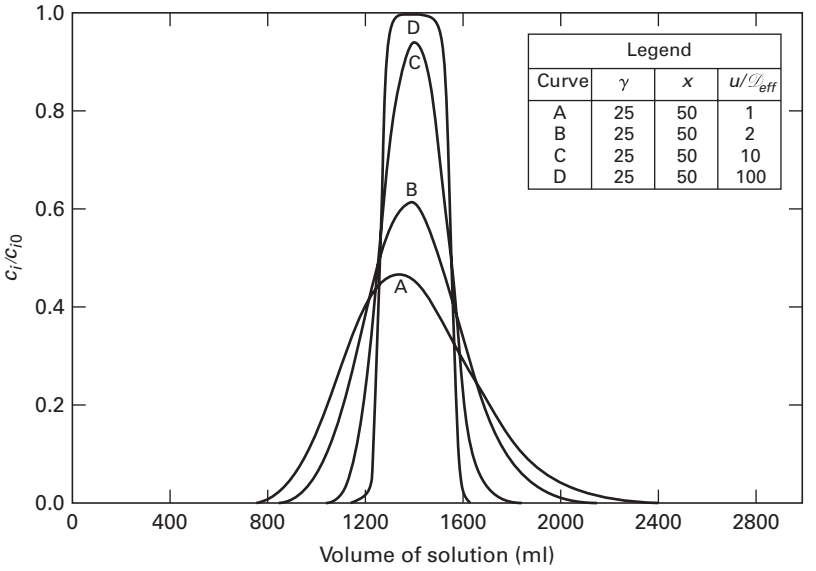

FIGURE 7.9 Prediction of chromatographic peaks from an analytical solution of the mass balance assuming a linear isotherm, local equilibrium, and a semi-infinite column. In this case, initial adsorbate concentration is zero, and feed solution has a pulse in concentration of c_{i0} of duration equivalent to 300 ml of feed. *(Data from L. Lapidus and N. R. Amundson, "Mathematics of adsorption in beds. VI. The effect of longitudinal diffusion in ion exchange and chromatographic columns,"* J. Phys. Chem., *vol. 56, p. 984, 1952.)*

An application of Equations (7.4.12) and (7.4.13) is shown in Figure 7.9, which shows the effect of dispersion with respect to mobile phase velocity for a simulated pulse feed. As the dispersivity increases ($u/\mathscr{D}_{\text{eff}}$ decreases) two orders of magnitude from curve D to curve A, the band widens by a factor of four, and the maximum concentration decreases to less than 50% of the feed concentration.

In addition to the effect of convective axial dispersion, models have been developed that also consider the effects of intraparticle diffusion and fluid-phase mass transfer [20, 21]. The starting point for the formulation of these models is the complete mass balance for adsorption, Equation (7.3.3), and the following equations, which assume a linear equilibrium isotherm and spherical symmetry:

Intraparticle diffusion:

$$\frac{\partial q_{i,p}}{\partial t} = \frac{\mathscr{D}_{\text{p}}}{r^2}\frac{\partial}{\partial r}\left(r^2\frac{\partial q_{i,p}}{\partial r}\right) - \frac{\partial q_{i,s}}{\partial t} \tag{7.4.14}$$

Fluid-phase mass transfer:

$$\frac{\partial q_{i,s}}{\partial t} = k_a\left(q_{i,p} - \frac{q_{i,s}}{K_{\text{eq}}}\right) \tag{7.4.15}$$

with the matching condition of flux continuity at the particle surface

$$-\mathscr{D}_{\mathrm{p}} \frac{\partial q_{i,p}}{\partial r} = k_c \left(\frac{q_{i,p}}{\varepsilon^*} - c_i \right) \tag{7.4.16}$$

where r = distance from center of spherical resin particle
$q_{i,p}$ = concentration of separand i in the pore fluid based on a unit volume of stationary phase (i.e., the solid matrix and the pore space)
$q_{i,s}$ = concentration of separand i adsorbed on the internal surfaces of the stationary phase based on a unit volume of stationary phase
c_i = concentration of solute i in the mobile phase
$\mathscr{D}_{\mathrm{p}}$ = effective separand diffusivity in the pore fluid
k_a = forward rate constant of adsorption
k_c = fluid-phase mass transfer coefficient
ε^* = effective volume fraction of the stationary phase that is accessible to the separand

For the case of isocratic elution, where the concentration of the elution solvent is constant, a lumped-parameter type of solution in a simple form was obtained by Athalye et al. [20]. Their solution relied on using empirical correlations to predict the height equivalent of a theoretical plate (HETP) for the column. The performance of chromatography columns can be predicted using this model based on independent estimates of transport parameters. The general solution of Rasmuson and Neretnieks [21] involves a special numerical integration method, to which the interested reader is referred. The procedure for calculating HETP depends on the approach of van Deemter et al. [22], which is now presented.

While chromatography and adsorption can be modeled accurately, and elution profiles solved exactly on high-speed computers by means of finite element analysis, the most practical rule of thumb for estimating the impact of mass transfer and diffusion effects is the van Deemter equation. Van Deemter et al. [22] determined empirically that the bandwidth [measured as the height equivalent of a theoretical plate, or HETP—see Equations (7.4.1) and (7.4.2)] can be related to the linear velocity in the column by the following expression:

$$H = A + \frac{B}{u} + Cu \tag{7.4.17}$$

The HETP (H) has dimensions of length, and is usually reported in centimeters. The factor A is primarily due to dead volume and other sources of mechanical mixing and is thought to be proportional to resin particle size. Molecular diffusion in the mobile phase is represented by B ($\mathrm{cm^2\ s^{-1}}$). If the flow rate is on the order of the liquid phase diffusivity of the solute, the peak broadens. This is almost never the case

in liquid chromatography, but this case is relevant for gas chromatography. Finally, mass transfer and intraparticle diffusion are represented by C (s), which is thought to be proportional to the square of the effective liquid film thickness at the surface of the resin particle, divided by the effective diffusivity within the particle. Liquid chromatography is dominated by this mass transfer term. The van Deemter equation is also important because it shows the efficiency of the separation, represented by the value of H, as a function of the productivity of the column, represented by the value for u. Note that the optimum balance of peak broadening and chromatography cycle time may not be at the minimum point on the van Deemter curve.

The van Deemter equation can be normalized as

$$H^* = a + \frac{b}{u^*} + cu^* \tag{7.4.18}$$

where $H^* = H/d_p$ and $u^* = ud_p/\mathscr{D}_m$, d_p is the stationary phase particle diameter, and $\mathscr{D}_m$ is the diffusivity of the solute of interest [23]. The reduced velocity u^* is also the Péclet number for chromatography. The reduced plate height, H^*, is rarely below 2, that is, two particle diameters in a chromatography bed constitute a mixing zone. A typical van Deemter plot is shown in Figure 7.10.

When normalized in this manner, the data for many chromatographic applications fall very close to one another [23]. Giddings has given rules of thumb for parameter estimation for *a, b*, and *c* [24]. While these rules of thumb are valuable for estimation of peak broadening in the design stage, data for individual applications should always be acquired.

The most efficient separation is achieved with the lowest possible plate height. The definition of efficient separation that is meant here is the separation with the least energy lost to entropy (or thermodynamically speaking, most reversible). More theoretical plates are contained in a given column length when the plate height is minimized. In liquid chromatography, u^* is typically a large number, as diffusivities are on the order of 10^{-5} to 10^{-7} cm^2/s, while linear velocities are typically on the

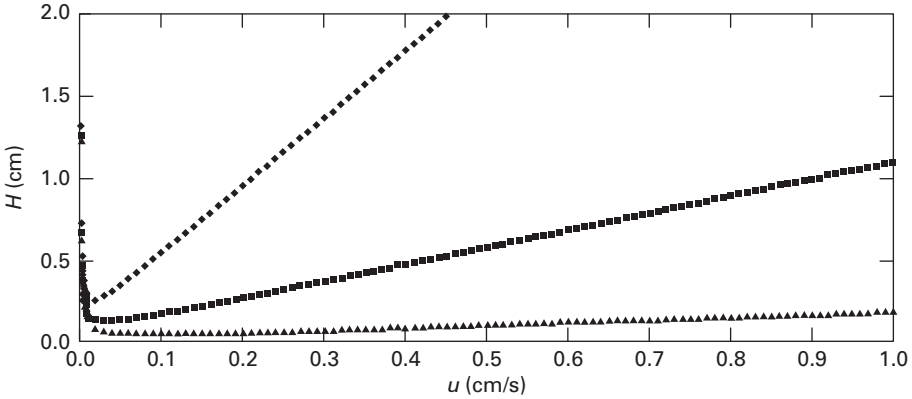

FIGURE 7.10 Typical van Deemter plot for three particle diameters: 50 μm (♦), 25 μm (■), 10 μm(▲).

order of 10^{-2} cm/s, and the smallest resin diameter is 10^{-4} cm, so in the best case, u^* is 0.1. If *a, b*, and *c* are of the same order of magnitude (*b* is commonly smallest), then no term in the van Deemter equation dominates. Resins smaller than 1 μm are not commonly available for large-scale operation, since the practical limit of resin containment seems to have been reached at this particle size. Larger particle resins are often chosen because they are considerably cheaper, in which case u^* approaches 100 and the cu^* term in the van Deemter equation dominates the plate height. Clearly, small stationary phase particle diameter (1 μm) is desirable for efficient separations.

A comparison of separation efficiency to process cost has been developed for large-scale chromatography for biotechnological applications that gave an optimum particle diameter of 30 μm [25]. This work indicated that particle diameters in the range of 20 to 40 μm make good targets for scaleup of chromatographic processes. Comparisons of this type are subject to the economics of each particular case and become dated as prices change and new technologies become available.

The van Deemter equation has been recast into dimensionless transport parameters by Athalye et al. [20] as follows:

$$\frac{H}{d_p} = \frac{2}{\mathrm{Pe}_g} + \frac{(1-x)^2}{3(1-\varepsilon)}(\mathrm{Re\,Sc})\left(\frac{1}{\mathrm{Nu}} + \frac{m}{10} + \frac{m'}{\mathrm{Da}}\right) \tag{7.4.19}$$

where Pe_g = dispersion Péclet number = $d_p u / \mathscr{D}_{\mathrm{eff}}$

$x = \varepsilon/[\varepsilon + (1-\varepsilon)\varepsilon^*(1 + K_{\mathrm{eq}})]$, or the fraction of separand in the mobile phase at long times

Re Sc = (Reynolds number)(Schmidt number) = $(d_p u \varepsilon\rho/\mu)(\mu/\rho\mathscr{D}_{\mathrm{m}}) = d_p u \varepsilon / \mathscr{D}_{\mathrm{m}}$, reduced velocity or diffusion Péclet number

$\mathscr{D}_{\mathrm{m}}$ = separand diffusivity in unbounded solution

Nu = Nusselt number = $d_p k_c / \mathscr{D}_{\mathrm{m}}$

$m = \mathscr{D}_{\mathrm{m}} / \varepsilon^* \mathscr{D}_p$

$m' = \frac{3}{2} m([K_{\mathrm{eq}} / (1 + K_{\mathrm{eq}})])^2$

$\mathrm{Da} = \text{Damköhler number} = d_p^2 k_a / 4\mathscr{D}_p$

The physical significance of each term in Equation (7.4.19) is as follows:

Pe_g term:	convective axial dispersion
Nu term:	fluid-phase mass transfer resistance
m term:	intraparticle diffusion resistance
m′ term:	sorption kinetics resistance

Equation (7.4.19) is valuable because it enables the quantification of each contribution to the plate height, hence a conceptually useful sensitivity analysis.

7.4.5 Computer Simulation of Chromatography Considering Axial Dispersion, Fluid-Phase Mass Transfer, Intraparticle Diffusion, and Nonlinear Equilibrium

When it is desired to consider axial dispersion, fluid-phase mass transfer between mobile and stationary phases, intraparticle diffusion, and nonlinear equilibrium in the mathematical modeling of chromatography, it is necessary to resort to computer simulation to deal with the complexity of the mathematics involved. Computer simulation models addressing these phenomena are called general multicomponent rate models. These models consist of a coupled partial differential equation system with two sets of mass balance equations, one for the bulk fluid and the other for the particle phase for each component. One such model that is available (free on the internet for academic users) has been developed by Gu [26] (other computer simulation models are available commercially). This is a powerful model that uses the method of orthogonal collocation for the particle phase equations and the finite element method for the bulk fluid phase equations, leading to an ordinary differential equation system.

The assumptions used in this general multicomponent rate model are as follows:

1. The chromatographic process is isothermal.
2. The adsorbent particles in the column are spherical and monodisperse (i.e., have the same radius, r_p).
3. Concentration gradients in the radial direction in the column are negligible.
4. There is no convective flow in the pores of the particles.
5. An instantaneous local equilibrium exists between the surface of the pores and the stagnant fluid inside the pores.
6. The film mass transfer mechanism can be used to describe the interfacial mass transfer between the bulk fluid and the particle phases.
7. The diffusional and mass transfer parameters are constant and independent of the mixing effects of the components involved.

The partial differential equations for the bulk fluid and particle phases, respectively, used in this model are

$$\mathscr{D}_{\text{eff}} \frac{\partial^2 c_i}{\partial x^2} - u\frac{\partial c_i}{\partial x} = \frac{\partial c_i}{\partial t} + \frac{3k_c(1-\varepsilon)}{\in r_p}\left(c_i - \frac{q_{i,p,r=r_p}}{\varepsilon^*}\right) \tag{7.4.20}$$

$$\frac{\partial q_{i,p}}{\partial t} = \frac{\mathscr{D}_p}{r^2}\left[\frac{\partial}{\partial r}\left(r^2\frac{\partial q_{i,p}}{\partial r}\right)\right] - \frac{\partial q_{i,s}}{\partial t} \tag{7.4.21}$$

with the initial and boundary conditions

$$t = 0,\ c_i = c_i(0,x);\ q_{i,p} = q_{i,p}(0,r,x) \tag{7.4.22}$$

$$x = 0,\ \frac{\partial c_i}{\partial x} = \frac{u}{\mathscr{D}_{\text{eff}}}\left(c_i - c_{io}(t)\right);\ x = L, \frac{\partial c_i}{\partial x} = 0 \tag{7.4.23}$$

$$r = 0,\ \frac{\partial q_{i,p}}{\partial r} = 0;\ r = r_p, \frac{\partial q_{i,p}}{\partial r} = \frac{k_c}{\varepsilon^* \mathscr{D}_p}\left(c_i - q_{i,p,r=r_p}\right) \tag{7.4.24}$$

Note that the mass balance for the mobile phase, Equation (7.4.20), is not exactly the same as the earlier one derived for adsorption and chromatography, Equation (7.3.3), with the term for mass transfer of separand to the particle expressed using Equation (7.3.5); this is because a fluid-phase mass transfer coefficient is used in Equation (7.4.20) while an overall mass transfer coefficient is used in Equation (7.3.5).

The multicomponent Langmuir isotherm for n components is given by

$$q_{i,s} = \frac{a_i q_{i,p}}{1 + \sum_{j=1}^{n} b_j q_{j,p}} \tag{7.4.25}$$

The computer simulation gives a plot of the dimensionless concentration (C_i) versus dimensionless time (τ), defined as

$$c_i = \frac{c_i}{c_{io}} \tag{7.4.26}$$

$$\tau = \frac{ut}{L} \tag{7.4.27}$$

There are several dimensionless parameters required in the computer simulation:

Pe_L Péclet number for axial dispersion, uL/E
Bi Biot number of mass transfer, $k_c r_p / \varepsilon^* \mathscr{D}_\text{p}$
k_c film mass transfer coefficient for the component, which can be determined from the correlation $\text{Sh} = k_c\, d_p / \mathscr{D}_\text{m} = 2.0 + 1.45\,\text{Sc}^{1/3}\text{Re}^{1/2}$
Re Reynolds number, $d_p u \rho / \mu$
Sc Schmidt number, $\mu / \rho \mathscr{D}_\text{m}$
η dimensionless constant, $\varepsilon^* \mathscr{D}_\text{p} L / r_p{}^2 u$
τ_{imp} dimensionless time for feed flow, $u\, t_{feed}/L$

Some of the assumptions used for this mathematical model may not hold in actual chromatography operation. For example, the equilibrium relationships may change according to the gradient in nonisocratic elution [27], and there can be radial velocity profiles in the column, particularly in preparative chromatography where columns of larger diameters are used [28].

Progress has also been made on applying computational fluid dynamics to chromatography. In one study, Pathak et al. [29] used computation to model a 1.5 m diameter column of 20 cm bed depth. They found substantial uniformity of flow across the radius of the column, with the exception of regions located very close to inlet ports. These flow inhomogeneities were more pronounced at higher flow rates but still present at low flow rates. The computational fluid dynamics simulations were followed up with dye tests to validate the model predictions. The model and dye tests showed qualitative agreement, primarily predicting flow anomalies near column ports. The computational fluid dynamics model was also used to suggest design changes to column hardware that greatly improved flow distribution, including a modified design of the head distribution plate.

7.4.6 Gradients and Modifiers

Chemical gradients are used to elute solutes that are bound tightly to the stationary phase. The constituents of the chemical gradient are chosen to compete with the target solute for binding sites on the surface of the stationary phase. This affects the binding equilibrium, such that, at different concentrations of the gradient-forming chemical, different binding profiles are given for the solute of interest.

EXAMPLE 7.5

Equilibrium for a Protein Anion in the Presence of Chloride Ion Derive the equilibrium for a monovalent protein anion on an ion exchanger in the presence of sodium chloride ion and plot isotherms for various concentrations of chloride ion.

Solution

The equilibrium is described by the following two expressions

$$P^- + S^+ \underset{}{\overset{K_{eq.1}}{\rightleftharpoons}} S \cdot P$$

$$Cl^- + S^+ \underset{}{\overset{K_{eq.2}}{\rightleftharpoons}} S \cdot Cl$$

where P^- is the protein anion, S^+ is an unoccupied binding site on the stationary phase, and sodium is a spectator counterion. The equilibrium expressions are

$$K_{eq,1} = \frac{[S \cdot P]}{[P][S]}$$

$$K_{eq,2} = \frac{[S \cdot Cl]}{[Cl][S]}$$

Mass balances on protein concentration, chloride concentration, and total sites apply.

$$S_{\text{tot}} = [\text{S}] + [\text{S} \cdot \text{P}] + [\text{S} \cdot \text{Cl}]$$

The preceding three equations can be solved for the adsorbed protein concentration to give the "multicomponent" Langmuir isotherm:

$$[S \cdot P] = \frac{K_{eq,1} S_{tot} [P]}{1 + K_{eq,1}[P] + K_{eq,2}[Cl]}$$

where $K_{\text{eq,1}}$ is the equilibrium constant for the protein measured in the presence of chloride, and $K_{\text{eq,2}}$ is the equilibrium constant for chloride measured in the presence of protein.

As can be seen from the expression derived for [S · P], as the chloride concentration is increased, the concentration of bound protein decreases. A protein that is tightly bound at low ionic strength can be eluted efficiently by an increase in the salt concentration. With $K_{\text{eq,1}} = 7.5$, $K_{\text{eq,2}} = 2.0$, and $S_{\text{tot}} = 120\ \mu$g/ml, we find the binding isotherms shown in Figure E7.5, where the increasing chloride concentration is seen to decrease binding of the protein. This is the principle of *gradient elution chromatography,* as well as of the regeneration of columns in adsorption processes. Changing the thermodynamic conditions so that the equilibrium is shifted back in favor of the unbound species effects the elution of that species and the regeneration of the resin. The thermodynamic condition may be ionic strength or pH (so as to shift a multivalent ion to a monovalent or uncharged species), temperature, or solvent composition. Slowly changing the thermodynamic conditions, in a gradient in the mobile phase, can sharpen diffuse waves, as well as cause desorption of the bound species. A step change (step gradient) can regenerate a resin or displace bound constituents.

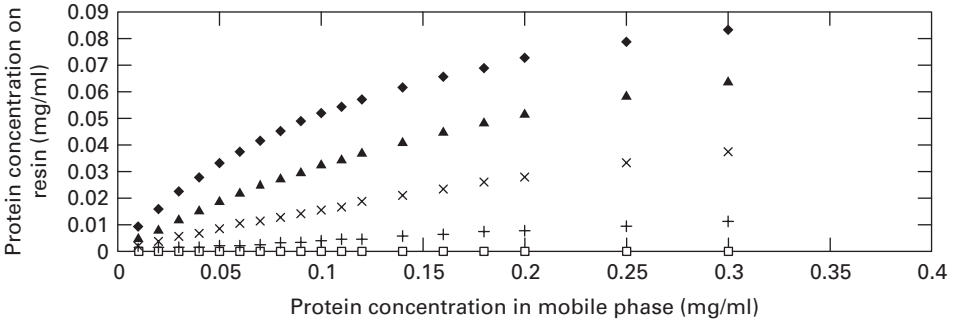

FIGURE E7.5 Effect of increasing chloride concentration on the equilibrium binding of a monovalent protein. [NaCl] = 0 (♦), 0.5 (▲), 2.0 (×), 10 (+), and 100 (□) mg/ml

The rate of change of the gradient with time is important. Most gradients are linear—their rate of change is constant. In reversed-phase chromatography, a gradient of 1%/min is often used; that is, the percentage of organic modifier is increasing smoothly by 1% per minute with a constant flow rate. Another useful but less common gradient is exponential. This provides for a shallower gradient early in the chromatography, and a rapidly increasing gradient late. An exponential gradient is useful when one is separating a wide variety of molecules that range from very loosely bound to extremely tightly bound. Yet another technique is to run a linear gradient to the point of product elution, hold an isocratic condition (i.e., constant composition of the elution solvent) through the product zone to maximize resolution, and follow by a gradient or steep step change to regeneration conditions. Obviously, countless combinations and options exist.

There are two other special cases that arise from the equilibrium isotherm derived in Example 7.5. Ignore, for a moment, the identity of chloride in the equation, for this identity was assigned merely for purpose of example. The first is the situation of very large $K_{eq,1}$. In this case, the isotherm is very steep, approximating a square wave, and the chromatographic mode is called "on–off." The isotherm remains steep until $K_{eq,2}\, c_2$ is of the order $K_{eq,1}\, c_1$, where c_1 and c_2 represent protein and salt anion concentration, respectively. Then solute 1 comes "off" the resin. Many proteins follow this case.

In the second case $K_{eq,2}$ is large, and greater than $K_{eq,1}$. In this case, solute 2 "displaces" solute 1 from the resin. Since solute 1 runs ahead of solute 2, and it has nonlinear binding itself, solute 1's leading edge is sharpened by the shock wave effect, and its trailing edge is sharpened by the displacement affected by solute 2. This is the displacement chromatography technique that was discussed earlier.

7.5 MEMBRANE CHROMATOGRAPHY

The use of filters and membranes to adsorb substances from a process stream has a long history. Indeed, the classic elementary school experiment, in which India ink is separated into a rainbow of colors as it ascends a wetted strip of filter paper, is a form of membrane chromatography, in which the pigment chemicals have differential binding affinities for the cellulose fibers that form the filter material. However, the use of membranes in chromatography received renewed interest with the development of microporous adsorptive membranes, in which the surfaces of the pores are chemically derivatized with an interactive ligand. Membrane chromatography was first performed in 1988 by Brandt et al. [30] using hollow fiber membranes functionalized either with the protein gelatin for isolating fibronectin from human plasma, or with Protein A for purifying an IgG antibody. Compared to the equivalent chromatography column packed with 100 μm adsorbent particles, the membrane chromatography column volume and fluid residence time were less by more than three orders of magnitude.

The major difference between membrane and packed bed chromatography is that in membrane chromatography the transport of solutes to their binding sites takes place predominantly by convection through the pores rather than by diffusion in the stagnant fluid inside the adsorbent particles for packed bed chromatography, thereby reducing both process time and liquid volume. Much higher flow rates can be used in membrane chromatography than in packed beds, and the binding efficiency is relatively independent of the feed flow rate over a wide range [31]. Although they have a shorter flow path, membrane chromatography systems have generally been found to achieve resolutions comparable to those with packed beds of adsorbent [32, 33]. However, membrane chromatography systems typically are used for adsorption of contaminants in a process stream, such as DNA or endotoxin, or low levels of host-cell proteins, rather than for the binding and elution of a product molecule and its closely related variants, such as those caused by oxidation or amino acid misincorporation. For example, in an antibody purification process, a final step may be the reduction of DNA, endotoxin, and certain host-cell proteins. In this case, the monoclonal antibody need not bind to the chromatography media (resin or membrane); therefore a pH may be chosen where the antibody does not bind, while the contaminants do. This is called the "flow-through mode," or frontal chromatography.

Another application where membrane chromatography is particularly suitable is for the purification of large proteins (molecular weight > 250,000) [31]. Proteins this large diffuse slowly into the pores of chromatography adsorbent media, but this is not a limitation in membrane chromatography since diffusion paths are very short.

In membrane chromatography, there is dispersion in the system due to the flow found in open pores, and the diffusion of molecules in the radial direction across the parabolic flow profile and also in the axial direction. There is some dispersion due to the kinetics of adsorption and desorption, which are a feature of conventional chromatography as well. Finally, there is dispersion due to mixing volumes upstream and downstream of the membrane for flow distribution.

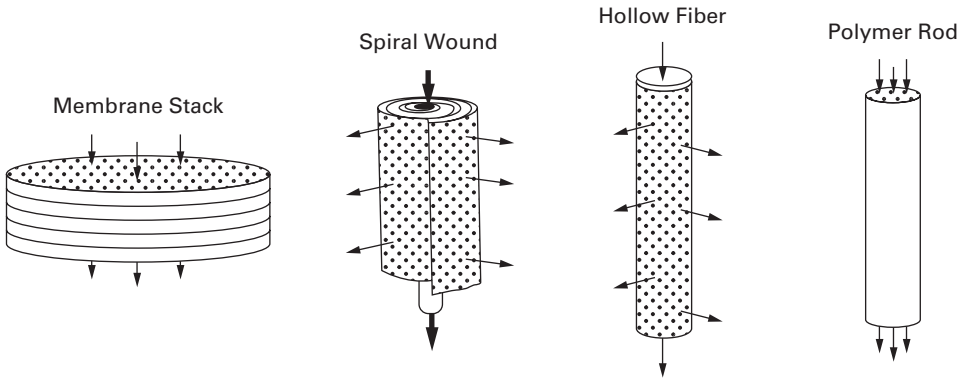

FIGURE 7.11 Various configurations used in membrane chromatography systems. The arrows represent the direction of flow, and the membrane cross-sectional area is shown by the dotted pattern.

Membranes for chromatography have been fabricated and are commercially available as thin sheets, flat disks, hollow fibers, and monolithic rods, disks, and tubes [34]. Hollow fibers are usually bundled within a shell using potting material. For large-scale production, thin membrane sheets are usually stacked or spiral wound. Various configurations of membrane systems are illustrated in Figure 7.11. The volumetric binding capacities are lower compared to conventional chromatography, and the depths are not typically high.

The case typically made for membrane chromatography is that the disposable nature of the filters and the large volumes of water required to operate a fixed column make membrane chromatography a viable alternative to column chromatography for polishing applications for removal of contaminants such as viruses, DNA, and endotoxins [35]. However, in analyses such as these, the chromatography column is sized at 100 times the size of the membrane; in other words, the chromatography column will be used at 1% of its dynamic binding capacity, where the membrane will be used at 100% dynamic binding capacity. Furthermore, the dynamic binding capacity of the chromatography resin typically exceeds that of the membrane configuration (70 mg/mL for Sepharose Q–HP [36] versus 50 mg/mL for the Sartobind Q [37], for example). The actual ligand density in the two formats is approximately 50 mM for the Sartobind Q, versus 140 mM for the Sepharose Q-HP. This demonstrates two related points. The first is that the ligand density achievable in membrane chromatography is much lower (three times in this comparison) because the surface area for adsorption is lower than in resin chromatography. The second is that because this internal surface area in resin chromatography is less accessible than for membrane chromatography, the proportion of dynamic binding capacity available to a large molecule like a protein is much smaller for resin than for membranes.

Another perceived limitation of using membranes as chromatography media is the cleanliness of the feed stream required. For the specific application of stripping extremely low-concentration contaminants from a concentrated antibody solution as the last step (with the cleanest feed stream) in the process, a high solids load could potentially foul the membrane surface and blind pores. Ultimately, only the largest pores will be left open, diffusion path lengths increase, and flow will deteriorate. However, this is typically not a problem in the polishing of antibody solutions using anion exchange, since many contaminants, including viruses, nucleic acids, and endotoxins, tend to be negatively charged at neutral pH, while antibodies are positively charged at this pH and flow through without binding [38].

Scale-up of membrane chromatography is typically achieved by increasing the diameter of the filter, conserving the interstitial velocity (u) from scale to scale. However, it is possible to scale up by maintaining L/u constant [39], and when this is done, the longer or thicker membranes would have to be able to perform with higher pressure drops and higher velocities than their scaled down counterparts.

As an example of the use of membrane chromatography, data is shown in Figure 7.12 for plate height H as function of $u/\mathscr{D}_m$ using stacked membranes with a pore size of 0.8 μm to purify plasmid DNA and other biomolecules operating in forward-flow

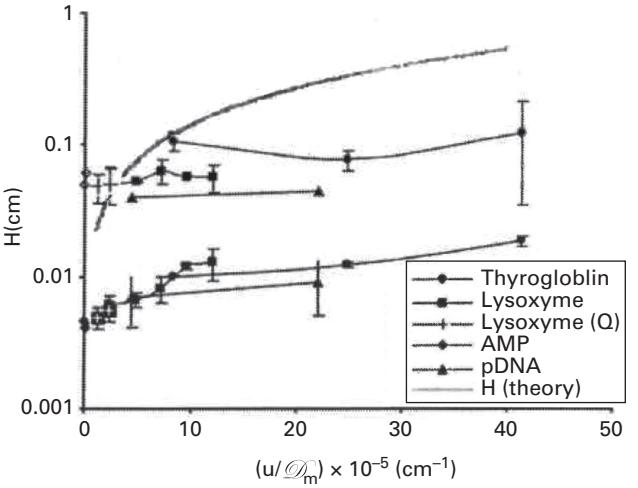

FIGURE 7.12 Plate height versus scaled velocity using membrane chromatography for forward-flow (open symbols) and reverse-flow (closed symbols) operation for various biomolecules including plasmid DNA (pDNA). Stacked polyethersulfone membranes functionalized with either a quaternary amine (Mustang-Q) or sulfonic acid (Mustang-S) with a 10 ml membrane volume were used. The theoretical prediction is for a bed packed with 15 μm particles using Equation (7.4.19). *(Data from M.A. Teeters, S.E. Conrady, B.L. Thomas, T.W. Root, and E.N. Lightfoot, Adsorptive membrane chromatography for purification of plasmid DNA," J. Chromatogr. A, vol. 989, p. 165, 2003.)*

and reverse-flow [40]. For comparison, the plate heights were calculated for a bed packed with 15 μm particles using Equation (7.4.19). The plate heights determined in the reverse-flow experiments are over an order of magnitude lower than for those predicted for 15 μm particles in a packed bed and do not increase appreciably with scaled velocity; while for the forward-flow experiments, the plate heights are similar to those for the 15 μm particles at low values of scaled velocity but also do not increase appreciably as scaled velocity increases. A significant finding from the data in Figure 7.12 is that the plate heights for the plasmid DNA were similar to those for much smaller biomolecules, confirming the absence of mass transfer limitations. The large differences in plate heights between the reverse-flow and forward-flow tests were attributed to there being more dispersion due to mixing in the flow distributors. This last finding points out the importance of optimal design of flow distribution for membrane chromatography to have maximum effectiveness [31].

EXAMPLE 7.6

Comparison of Time for Diffusion Mass Transfer in Conventional Chromatography and Membrane Chromatography. Estimate the time for diffusion mass transfer in conventional chromatography and membrane chromatography assuming a typical particle diameter for an adsorbent used in preparative chromatography of 100 μm, pore diffusion coefficient $\mathscr{D}_p$ of 3 x 10^{-7} cm^2 s^{-1} of a representative protein (bovine

hemoglobin in size exclusion media at 20°C [41]), superficial velocity of 600 cm/h in the pores in membrane chromatography (possible in membrane chromatography with no compromise in efficiency [38]), void fraction of 0.6 for the membranes, and a membrane pore size of 1 μm. Assume the fluid has the properties of water.

Solution

The time required for diffusion can be calculated using the Einstein diffusion equation (Equation 8.3.2):

$$t = \frac{\delta^2}{2\mathscr{D}_p}$$

For conventional chromatography, the diffusion length is 50 μm (half the particle diameter). The type of convective flow regime in the pores in membrane chromatography can be determined by calculating the Reynolds number in a cylindrical pore:

$$\mathrm{Re} = \frac{d_m\left(\frac{\upsilon}{\varepsilon}\right)\rho}{\mu} = \frac{1\,\mu\mathrm{m} \times \frac{600\frac{\mathrm{cm}}{h}}{0.6} \times 1.0\frac{g}{\mathrm{cm}^3} \times \frac{1\,\mathrm{cm}}{10^4\,\mu\mathrm{m}} \times \frac{1\mathrm{h}}{3600\,\mathrm{s}}}{0.01\frac{g}{\mathrm{cm\,s}}} = 0.003$$

where d_m is the diameter of a pore in the membrane, υ is the fluid superficial velocity, ε is the void fraction, and ρ and μ are the density and viscosity of the fluid, respectively. Thus, this is laminar, creeping flow since Re is less than 0.1 [6]. Since the protein is being adsorbed on the surface of the pore, there will be a radial concentration gradient from the surface to the center of the pore, and the maximum diffusion length will therefore be 0.5 μm (half the pore diameter).

Therefore, for the conventional chromatography the diffusion time from the Einstein diffusion equation is

$$t = \frac{(50\,\mu\mathrm{m})^2 \times \left(\frac{1\,\mathrm{cm}}{10^4\,\mu\mathrm{m}}\right)^2}{2 \times 3.0 \times 10^{-7}\,\frac{\mathrm{cm}^2}{\mathrm{s}}} = 42\,\mathrm{s}$$

For membrane chromatography, assuming the diffusion coefficient in the pores of the membrane is the same as in pores of the conventional chromatography adsorbent,

$$t = \frac{(0.5\,\mu\mathrm{m})^2 \times \left(\frac{1\,\mathrm{cm}}{10^4\,\mu\mathrm{m}}\right)^2}{2 \times 3.0 \times 10^{-7}\,\frac{\mathrm{cm}^2}{\mathrm{s}}} = 0.004\,\mathrm{s}$$

These calculations show that the diffusion time is four orders of magnitude less for membrane chromatography compared to conventional chromatography. A similar result was obtained by Klein [42] for the diffusion time of IgG antibody in membrane chromatography with hollow fibers compared to a fast-flow gel matrix, both using immobilized Protein A.

In summary, membrane chromatography is a technology that is growing in importance in bioseparations. There is a place for low-capacity, high-throughput adsorption media for the stripping of low-level contaminants from a process stream. The membranes are available with virtually all the same chemistries as conventional chromatography. They can be made inexpensively and fit well with disposable technologies currently in favor in the industry.

7.6 SIMULATED MOVING BED CHROMATOGRAPHY

Although chromatography is a workhorse of biochemical separations, especially for molecules that are particularly heat labile or otherwise delicate, it is inherently inefficient. Even with scaled up, overloaded, preparative, and manufacturing chromatographic modalities, the throughput is low, and only relatively small portions of the chromatography column are actually performing useful separation at any given time.

The inefficiency of chromatography is best illustrated by imagining a separation in progress. An example is shown in Figure 7.13, where solutes A and B are being separated chromatographically. Solutes A and B have a lesser and greater affinity for the stationary phase, respectively. You might notice that these are self-sharpening peaks, implying a favorable Langmuir isotherm for each. There are five "zones" in the column. Zones 1 and 5 contain no solute. Zone 1 has the elution solution, and zone 5 is still equilibrated under the loading conditions. Zones 1 and 5 are doing no useful work and are therefore inefficient. Zone 2 contains only solute B, already separated from solute A. All that happens in zone 2 is the dilution of solute B, which is counterproductive work; therefore zone 2 is not performing efficient work. Similarly, zone 4 is only accumulating solute A. Since the peak is self-sharpening, the peak is not becoming more dilute, per

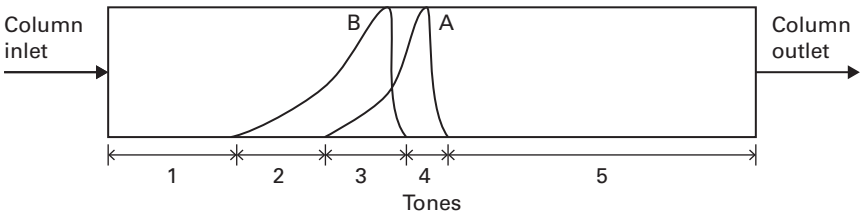

FIGURE 7.13 Example of the inefficient nature of chromatography. The internal concentration profiles of solutes A and B are shown, along with zones 1-5 in the column.

se; however as it further separates from solute B, more of the diffuse trailing edge will be incorporated into zone 4. Zone 3 contains both solute A and B, binding and desorbing and otherwise interacting with the adsorbent. This is the only zone in the column that is actually performing separation work. As the peaks progress down the column, zone 2 and 4 grow in volume, while zone 3 becomes vanishingly small, until, as the peaks elute from the column and zone 3 is completely gone by definition (because the desired resolution between solute A and B has been achieved in a properly designed column).

In order to improve the efficiency of chromatography, one idea that has been pursued is to collect solutes A and B as they are purified and to inject more mixed solutes to compensate for the volume removed. This can be accomplished using countercurrent chromatography, where the adsorbent particles flow in the opposite direction to the fluid stream at a velocity that gives propagation rates of solutes A and B in the positive and negative directions, respectively. This has been called "moving bed chromatography" and more usually, "simulated moving bed chromatography," as actually moving the solids is impractical because it causes problems with mixing and solids attrition. Components A and B can be fed continuously to the middle of the column. If this column is divided into sections, at some point purified A can be obtained at one end of the column and purified B can be obtained at the other end.

Simulated moving bed chromatography (SMB) uses several fixed-bed columns in series to simulate the movement of the solid phase by periodically shifting the points to introduce the feed and elution solvent and to remove the products. A classical simulated moving bed chromatography system is illustrated in Figure 7.14, where the column is divided into four zones with three column segments per zone. This figure illustrates the movement of the two solutes, A and B, through the zones.

To obtain pure products in the SMB system shown in Figure 7.14, the following constraints must be met [43]:

- Zone 1: the more strongly adsorbed solute (B, extract) must be completely desorbed.
- Zone 2: the less strongly adsorbed solute (A, raffinate) must be completely desorbed.
- Zone 3: the more strongly adsorbed solute (B, extract) must be completely adsorbed.
- Zone 4: the less strongly adsorbed solute (A, raffinate) must be completely adsorbed.

The use of four zones in SMB is the most widely adopted configuration [44]. Eight subsections is a typical number for a small-scale application, while large-scale systems can involve up to 24 subsections [45]. The maintenance of steady state concentration profiles for the system shown in Figure 7.14 requires controlling the various adsorption and desorption events by adjustment of the flow rates and column

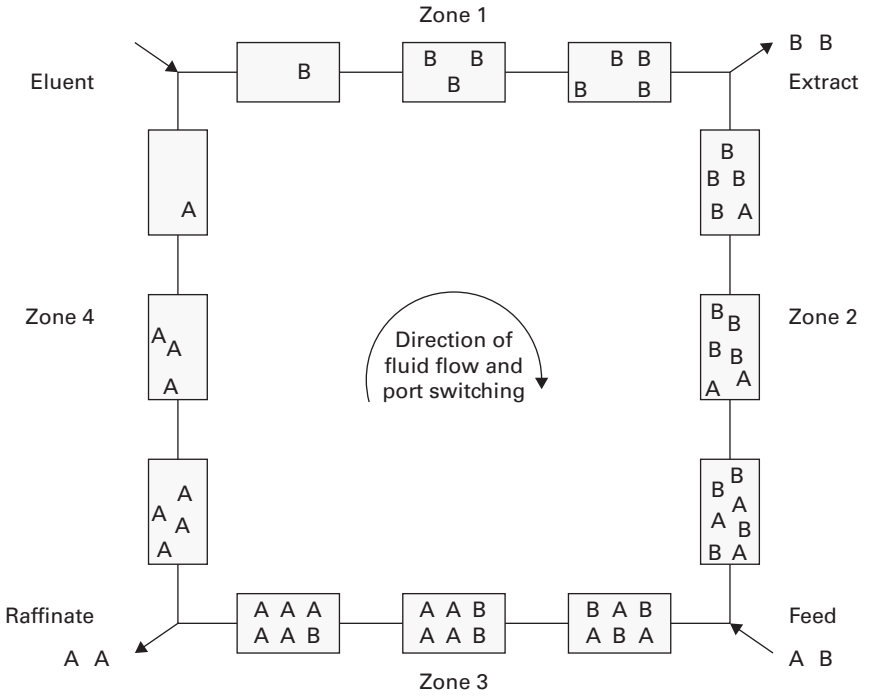

FIGURE 7.14 Principle of operation of simulated moving bed chromatography, indicating the separation of solutes A and B.

switch times. This is a complicated system, and a trial-and-error approach to optimizing system operation is not likely to succeed. Therefore, the system must be simulated to determine the optimum operating parameters.

An approach that has been used successfully in simulating SMB operation is to use a Langmuir-type isotherm equilibrium model where mass transfer resistance and dispersion are neglected, which has been called the "triangle theory" [46]. A major feature of this model is that the typical overloaded operating conditions of SMB are accounted for through the use of a two-component Langmuir isotherm, which describes nonlinear and competitive adsorption behavior. This model gives better results than those that assume linear adsorption isotherms. In the triangle theory model, the separation performance is controlled by the flow rate ratios, m_j, one for each zone of the SMB unit, defined as

$$m_j = \frac{Q_j t_s - V\varepsilon_o}{V(1-\varepsilon_o)} \quad (7.6.1)$$

where V is the column volume; t_s is the column switch time, i.e., the time between two successive switches of the inlet and outlet ports; $\varepsilon_o = \varepsilon + (1–\varepsilon)\varepsilon^*$ is the overall void fraction of the column, with ε and ε^* being the bed void volume and the porosity of the adsorbent particles, respectively; and Q_j is the volumetric flow rate

in the j^{th} zone of the SMB system. The binary Langmuir equilibrium isotherm is defined as

$$q_i = \frac{H_i c_i}{1 + K_A c_A + K_R c_R} \quad (i = A, B) \tag{7.6.2}$$

where K_i is the equilibrium constant of the i^{th} component, and H_i is the Henry constant of the i^{th} component, i.e. the slope of the single component adsorption isotherm at infinite dilution (the linear adsorption isotherm). For this model, a set of mathematical conditions are set in order to achieve complete separation. The final result is a set of algebraic expressions that are easily applied.

The topological structure of the regions of separation in the central sections of the unit (m_2 and m_3) is illustrated in Figure 7.15. The triangle-shaped region in this plot shows where pure products can be obtained. This theory can be used to explain experimental results and to design optimal operating conditions. According to Figure 7.15, for a robust design it would be desirable to operate within the triangle and not near a boundary, so that a slight disturbance would not lead to one or both of the products being less than 100% pure. Further modeling using numerical methods to take into account mass transfer resistance and dispersion has shown that the effect of these variables is relatively small when realistic values of the process parameters are used [47].

The SMB process is inherently suited to large-scale operation since it can be operated continuously; this process is advantageous in that significantly less eluent is required compared to other chromatographic separation modes [43]. SMB has been used to purify many bioproducts at large scale, mostly for small molecule products. The first large-scale SMB process was used by UCB

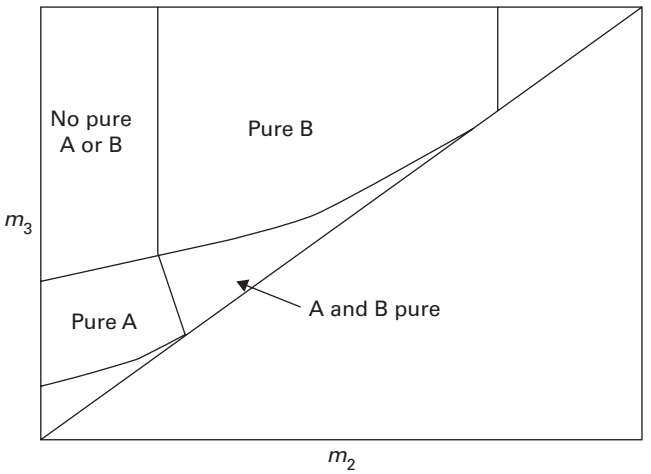

FIGURE 7.15 Regions attaining different separation regimes for components A and B in the operating plane spanned by the flow rate ratios m_2 and m_3 in the two central sections of the simulated moving bed chromatography system.

Pharma in Belgium in 1997 to separate optical isomers, and since then other large-scale SMB processes have included the separation of fructose and glucose sugars, the purification of the amino acid lysine, and the purification of the enantiamer drug Lexapro.

7.7 ADSORBENT TYPES

Many adsorbent resins have been developed for chromatographic separations. There are two basic resin materials, polymer and silica. Many types of ligand chemistries can be conjugated to either resin material. Typically, however, silica resins most commonly have hydrophobic coatings and are used for reversed-phase chromatography. Polymer resins are more often used in aqueous applications and are conjugated with ion exchange, hydrophobic interaction, or affinity-type ligands.

The selection of the resin material defines many resin physical properties. The resin provides the surface area for the adsorption, which is generally 100 to 1500 m^2/g. The surface area on the outer surface of a 10 μm diameter solid sphere is 1.7 m^2/g, so it follows that most of the surface area is in the internal porosity of the particle. Since this surface area is accessed by molecular diffusion (one class of resins, called perfusion resins, allows convection through some macro-pores), the path length for this diffusion is important. As mentioned previously, this path length is the radius of the resin particle (see Example 7.6). Therefore, both the diameter of the particle and its internal surface area are important for the resin performance.

7.7.1 Silica-Based Resins

Uncoated silica is compatible with water or organic solvent and serves as a good reversible adsorbent for hydrophilic compounds. An organic solvent is often used in the mobile phase, and water is added as the chromatography progresses. Silica is not typically stable at extremes of pH, especially basic pH (exceptions exist). Silica is available with high surface area and small particle size; being very rigid, it does not collapse under high pressures. Silica resins are thought to denature some proteins and irreversibly bind others. However, silica-based chromatography is used for the purification of many commercial biotechnology products.

Silica particles coated with long-chain alkanes are widely available. The long chain alkanes change the surface from hydrophilic to hydrophobic. Thus, this derivatized class of silica resins became known as “reserved phase.” Uncoated silica used in chromatography came to be known as “normal phase.”

Coated silica resin has a high affinity for hydrophobic molecules, which increases as the chain length of the bonded alkane increases. The bonding of organic layers to silica has become a science in its own right, and there are many varieties of the same chain length phase. Some phases are polymerized, some are

simple monolayers, and some are "end capped," which means that any uncovered surface of the silica is covered with an organic layer after the hydrophobic chain group has bonded. Each variety of resin may have different properties with respect to the mixture to be separated, and in many cases, different lots from the same supplier have different properties as well. The silica left bare around the bonded chains (in resins that are not end capped) often plays a role in the binding, and therefore the percent of the surface covered with each bonding reaction will lead to different properties for a particular resin type or manufacturer's lot. Often, these imperfections in the manufacture of reversed-phase chromatography resins are important for the separation that can be achieved, but complicate the strict interpretation of the chromatographic result and can be difficult to reproduce. Reversed-phase chromatography is a very popular laboratory analytical technique and has been scaled up for the production of small molecules and peptides. Concerns about protein denaturation have slowed its introduction into protein manufacture; however, this is changing as the high resolving power of the technique is making it more and more attractive for high value added products.

7.7.2 Polymer-Based Resins

Polymer-based resins are frequently used in industrial applications because of their high stability and low cost. The resins are manufactured by suspension polymerization, in which an emulsion of the polymer is made in an immiscible solvent, and a cross-linking agent is added. The reaction is allowed to proceed to completion, and then the particles are isolated from the suspension, washed, and frequently derivatized. Surfactants are often added in the suspension polymerization to control particle size; in general, however, polymer resins are larger (10–100 μm) than silica-based resins (1–25 μm). Polymer resins are also less rigid and not generally suitable for high-pressure (>4 bar) applications (exceptions exist).

Two synthetic polymers that are commonly used are styrene divinylbenzene and polyacrylamide. Styrene divinylbenzene is very stable at pH extremes, and it has been used primarily as a support for ion exchange chromatography. While the backbone is somewhat hydrophobic, and nonspecific binding does occur, the stability and rigidity of this polymer make it a superior support for chromatography. Polyacrylamide is used less often. It is not used as a polymer solid but as a hydrogel, and its primary use in chromatography has been as a size exclusion gel. The cross-linking in polyacrylamide can be controlled very precisely by the amount of bisacrylamide added in the suspension mixture. The analogy to protein electrophoresis gels (Chapter 2) is apparent here.

Natural polymers such as agarose and dextran are also used in hydrogel form for low-pressure chromatography resins. These polymers are naturally hydrophilic and are very compatible with proteins and other biomaterials. Agarose can be cross-linked to form a reasonably rigid bead that is capable of tolerating pressures up to 4 bar.

Dextran is less rigid and, like polyacrylamide, is used primarily in size exclusion. Dextran gels can be formed with very large pores, capable of including antibody molecules and virus particles. Both dextran and agarose have been derivatized with ion exchange groups, phenol and butyl groups, antibodies, dyes, heavy metals, and other biological epitopes that allow very specific binding behavior for the target molecule.

7.7.3 Ion Exchange Resins

Ion exchange resins are those that have been derivatized with an ionic group. The most commonly used ionic groups, listed in order of increasing p*K*, are sulfopropyl ($CH_2CH_2CH_2SO_3^-$), carboxyl (COO^-), diethylaminoethyl (DEAE) ($2C_2H_5N^+HC_2H_5$), and ammonium (Q) ($CH_2N^+[CH_3]_3$). Therefore, sulfoxyl is the most acidic, and QAE is the most basic. When the acidic ion exchangers are used at pH values above their respective p*K* values, they carry a negative charge and attract positive counterions. These are called cation exchangers. Conversely the basic ion exchangers are known as anion exchangers.

Sulfopropyl and Q are a strong acid and a strong base, respectively. Their p*K* values are close to 1 and 14, meaning they are fully ionized at all practical pH values for bioseparations. Carboxyl and DEAE are, respectively, a weak acid and base, with p*K* values closer to 4 and 10. These resins may be used with a pH gradient to ionize more or fewer of the ionic groups on the resin, thus effecting the separation. When the process calls for a pH shift, but separation of molecules along with that shift is not desirable, "strong" ion exchangers are preferred because their binding capacity is not likely to be altered.

Ion exchange resins are almost always used in aqueous mobile phases, and they are almost always polymer resins. Water is the universal solvent for salts, which dissociate poorly in most organic solvents. The ability to manipulate the pH to effect separation also favors polymer matrices as backbone material. Finally, many common biological contaminant molecules bind nearly irreversibly to ion exchangers. Therefore, to regenerate ion exchange resins, extreme pH values are often used, such as 1.0 M NaOH (pH 14), which would dissolve many common silica-based resins.

Ion exchange resins, once exclusively used to separate small ions, are now heavily used in the separation of proteins, peptides, nucleic acids, small polynucleotides, and other small molecules such as antibiotics. Proteins have distinct isoelectric points (see Chapter 1) based on the content and conformation of their charged amino acids, arginine, lysine, histidine, glutamic acid, and aspartic acid, in decreasing p*K* of the side chain group. Sometimes tyrosine deprotonates, depending on its microenvironment. Proteins have multiple charges and can be separated based on their number of charges, as well as the sign of the charge and sometimes charge heterogeneity. Nucleic acids, on the other hand, have a charge at each base, such that their charge is proportional to their mass. Since they have a negative charge at each base, they bind very well to

anion exchangers, and not at all to cation exchangers. Once bound to an anion exchange column, nucleic acids are very difficult to elute in an aqueous solution that does not simultaneously degrade them.

The selection of the buffer is an important consideration in the use of ion exchangers. It is advisable that the buffering species not interact with the adsorbent, which means that the charged form of the buffer should have the same sign as the charge on the adsorbent. It is also preferable that only simple anions be used in anion exchange (e.g., Cl^-, acetate$^-$) and only simple cations (e.g., Na^+, K^+) in cation exchange [48]. For example, when one is using DEAE–cellulose (an anion exchanger) at pH 8.0, a Tris–chloride buffer might be selected because it has $HTris^+$ (noninteractive) and Tris (neutral) buffering species and Cl^- counterion.

7.7.4 Reversed-Phase Chromatography

Reversed-phase chromatography employs a hydrophobic phase bonded to the surface of the resin. Typically, reversed-phase resins are silica based. Reversed phase is so named because the partitioning of solutes between the mobile phase and stationary phase is opposite to that observed with bare silica. In other words, hydrophobic solutes bind in higher proportions in reversed phase, while hydrophilic solutes bind in higher proportion in "normal phase." Solutes are typically introduced into reversed-phase columns in water, or with minimal amounts of organic solvent, so that most solutes partition to the stationary phase. The organic content of the mobile phase is slowly increased, typically as a percent of acetonitrile, methanol, or isopropanol, thereby decreasing the polarity of the mobile phase.

Hydrophobic phases that are bonded to silica are typically octyl (C_8), octyldecyl (C_{18}), phenyl, and methyl (C_1). The different chain lengths and densities (called "coverage" in the commercial literature) of the different bonded phases obviously lead to more or less hydrophobicity. The entire surface of the silica cannot be fully covered with a monolayer of the desired phase, however, because of steric effects. Bare silica remains exposed, and this bare silica can participate in the separation by interacting with hydrophilic molecules, or hydrophilic domains of large molecules, thereby altering the binding. The strategy employed for covering this exposed silica surface lends almost as much to the specifics of the separation achieved as the chain length of the bonded phase. Polymerized phases represent an attempt to cover the surface by polymerizing the alkyl chains together at their point of attachment to the silica. End-capped resins use a short chain length group, such as methyl or ethyl, to cover the unreacted surface sites. Resins that do not utilize either method are left so intentionally to take advantage of the "mixed-mode" separation that may result. The separation characteristics of these resins are difficult to reproduce precisely, leading to considerable variation in separation from one manufacturer's lot of resin material to another.

Ions do not partition well in hydrophobic phases. It is common, therefore, to choose a counterion for reversed-phase chromatography. For biological mixtures, the counterion is nearly always a strong acid anion, such as trifluoroacetate, acetate, or chloride. The counterion has a strong effect on the separation, by partitioning along with the co-ion of interest. The counterion can be used to make solutes more or less hydrophobic and will not affect all solutes equally.

7.7.5 Hydrophobic Interaction Chromatography

Hydrophobic interaction chromatography is often used for protein separations. It employs derivatized polymer resins, with phenyl, butyl, or octyl ligand groups, typically. Proteins adhere to the hydrophobic surface under high salt conditions and redissolve into the mobile phase as the salt concentration is reduced. Hydrophobic interaction chromatography differs from reversed phase in that the mobile phase is kept aqueous (polar), and the salt concentration is used to effect the partitioning to the surface. The mechanism of partition is related to precipitation as opposed to two-phase partitioning (reversed phase) or ionic interaction (ion exchange). This is due to the use of salts that strip proteins of their solvation water. As the concentration of "lyophilic" salts increases, the probability increases that the protein will aggregate, or nucleate on the surface of the resin [49]. Hydrophobic interaction chromatography is sensitive to pH, salt used, buffer type, and temperature. Each of these must be carefully controlled to achieve reproducible separation but also represent an opportunity for increased selectivity.

7.7.6 Affinity Chromatography

Affinity chromatography takes advantage of biological interactions to effect binding of specific solutes. Antibodies, antigens, or dyes are conjugated to polymer resins for the purpose of binding specific solutes from a mixture. For instance, an antibody could be raised against a target protein. The antibody would be conjugated to a resin, usually via cyanogen bromide activation. The antibody then captures the solute out of the mixture, and the impurities flow through the column. The solute can be recovered by changing the pH, increasing the salt concentration, or adding a displacer, that is, a molecule that also has some affinity for the antibody, or other binding agent (affinity ligand) on the stationary phase.

Other examples of specific interactions that can be used to isolate proteins are enzyme–ligand, enzyme–cofactor, receptor–agonist (antagonist). In each case, one member of any of these pairs may be immobilized to a resin to isolate the desired partner. Affinity chromatography is often coupled with cloning techniques to synthesize the target molecule with an "epitope" or recognition sequence that can be captured by the affinity ligand. Affinity chromatography is used from small-scale research (e.g., high-throughput screening) to large-scale purification.

An example of a type of affinity chromatography that has had a major impact on the purification of monoclonal antibodies is the use of immobilized protein A in process scale purification [50]. Protein A is often used as the first chromatography step in the purification, which gives a large purification factor and results in simplifying the purification process. Protein A is a polypeptide with a molecular mass of 54 kDa that is found in the cell wall of *Staphylococcus aureus.* Recombinant Protein A that lacks the membrane-binding region is used in affinity purification. One of the drawbacks of this method is that low levels of Protein A or its fragments co-elute with the antibody. However, trace amounts of this contaminant and others such as high molecular weight aggregates of the antibody and host-cell protein can be removed in one or two subsequent chromatography steps. More information about the process scale purification of monoclonal antibodies using Protein A is found in "Therapeutic Monoclonal Antibody Production" (Section 12.6.3).

7.7.7 Immobilized Metal Affinity Chromatography (IMAC)

Some proteins have high affinities for specific metals. This affinity may either be structural, as in the case of metalloproteins, which require metal centers for their biological activity, or based on the content of specific amino acid residues, such as histidine, tryptophan, and cysteine, which have increased affinity for transition metals such as nickel and copper. Techniques have been developed to immobilize metal ions with spacer arms onto polymer resins. These resins are referred to as IMAC resins, and they are used to purify proteins that have one of the two characteristics mentioned above. Genetic engineering has also been used to enable IMAC to be performed, with cloned target biomolecules being fused to polyhistidine tags (Section 1.4).

7.7.8 Size Exclusion Chromatography

Sometimes referred to as "gel filtration," size exclusion chromatography (SEC) separates solutes on the basis of their size. There is no derivatization of the polymer gel, and there is no binding between the solutes and the resin. Molecules larger than the largest pores in the gel (the exclusion limit) cannot enter the gel and are eluted first. Smaller molecules enter the gel to varying extents, depending on their size and shape, and thus are retarded on their passage through the bed. In general, SEC resins are hydrophilic polymer gels with a broad distribution of pore sizes. The pore size is dependent on the degree of polymerization of the gel. Size exclusion chromatography is a useful technique, especially for changing buffers, or for removing small molecules from protein solutions. Because of the lack of binding between the solute and the resin, however, the capacity of this technique is low. Size exclusion effects may be in action in all the above-described techniques, since all resins are macroporous.

7.8 PARTICLE SIZE AND PRESSURE DROP IN FIXED BEDS

Particle diameter dominates the pressure drop in fixed-bed columns. The pressure drop is given by the Darcy equation [6]:

$$\frac{\Delta p}{L} = \frac{\mu v}{k} \quad (7.8.1)$$

where Δp is the pressure drop over column length L, μ is the viscosity of the mobile phase, v is the superficial velocity, and k is a constant. [In writing Equation (7.8.1), the term $-\rho g$ on the left side in the complete form of the Darcy equation has been omitted because it is very small compared to $\Delta p/L$.] A further correlation, known as the Blake-Kozeny equation [6], gives k as a function of resin particle size and void fraction:

$$k = \frac{d_p^2}{150} \frac{\varepsilon^3}{(1-\varepsilon)^2} \quad (7.8.2)$$

The Darcy equation applies for rigid particles, such as silicas. For polymer resins that are compressible, k is a function of the linear velocity and column diameter, and a plot of Δp versus v would be nonlinear over a sufficiently wide range of v. Compressible gels get some of their hydrodynamic stability from the walls of the column; therefore the diameter of the column itself plays a role in the pressure drop. These factors need to be investigated for each application. As the stationary phase particle size is decreased, the pressure drop in the column increases as the inverse square. This increased pressure drop then requires additional power in pumping, as well as more specialized requirements for the construction of the column and its seals. The smallest particle sizes create inlet pressures of several hundred bars of pressure (several thousand psi) with a column length of 25 cm and a velocity v of 0.01 cm/s. Seals and columns that contain these pressures are typically of narrow bore (2.5 mm i.d.), since a small radius of curvature is more effective for holding pressure than a large radius. Large columns packed with small particles are built like pressure vessels, with large lug nuts closely spaced around the flange at the end pieces.

A further complication arising from small particles is containment. The column end pieces must contain the particles without plugging. Plugging can be caused by resin particles, fragments of particles generated through attrition, or other debris in the chromatography feed streams. Particles 1 μm in diameter must be contained by 0.25 μm frits. These frits become easy to foul. The smaller the particle size, the more finely the mobile phase must be filtered and held particle free.

The selection of the resin particle diameter is probably the most critical engineering choice to be made in chromatography design and scale-up. The resolution of the column is favored by small particle size, while the pressure drop is adversely

affected. The smaller the particle size, the shorter the column can be made, while maintaining the same separation. To retain binding capacity, the same resin volume must be used. Thus, smaller particles may be packed in short, flat beds, resembling pancakes, while larger particles can be accommodated in long tubes. As the column narrows, linear flow rates increase for the same volumetric flow, thus adversely affecting both pressure drop and resolution. As the columns get shallow and broad, mechanical seals and good flow distribution become more difficult to attain.

7.9 EQUIPMENT

Equipment for adsorption and chromatography is similar in that a fixed column or columns are generally involved. The equipment for chromatography, however, tends to be more sophisticated than that for the fixed-bed adsorption process, since the scale of operation is generally smaller and the requirement for resolution is greater. This is reflected in the fact that fixed- and agitated-bed adsorption operations tend to be near the beginning of the purification process, while chromatography is generally at or near the end of the purification. This section describes some of the special design considerations required for adsorption and chromatography equipment.

7.9.1 Columns

Adsorption

Most fixed-bed adsorbers are cylindrical, vertical vessels through which feed, eluent, and regenerant streams are passed down through the bed of resin. There are two types of system to support fixed beds of adsorbents. One is a series of grids and screens, where each higher layer screen has successively smaller openings to prevent adsorbent from passing through and each lower layer has greater strength. In the other type of support, there is a graded system of particles such as ceramic balls. To prevent movement of the adsorbent at the top of the bed, a retention screen is usually installed on the top of the adsorbent and a layer of support balls placed on the top of the screen to hold the screen in place. Because the bed tends to expand and contract during operation of the process, the retention screen must be floating and not attached to the wall of the column. For large columns, it may also be necessary to have the inlet pipe branch into several pipes that are perforated along their length to ensure even distribution of the liquid across the column's cross section [51].

Chromatography

Chromatography columns are also cylindrical, vertical vessels designed to contain resin particles between 2 and 100 μm in diameter. Fluid is typically pumped downflow through chromatography columns, since air trapped beneath a column can cause voids that are ruinous for resolution and cleaning. The frit, or in some cases netting, is critical for design of the columns. The frit is held in place by the end fittings on

the column, often between gaskets, or incorporated into gaskets. A frit is critical at both the inlet and outlet of the column. The frit serves as a filter of last resort on the column inlet and holds the resin in place in the event the column is back-flushed. Polymer-based resins also swell under different conditions of ionic strength and pH, a phenomenon the inlet frit helps to contain.

The column comes in three basic types, fixed bed height, variable bed height, and axial compression. Fixed beds are used when a process is mature and the columns can be dedicated. The fixed bed is a tube that is fixed directly to end fittings. Threaded fittings are used on the analytical and preparative scales (up to 10 cm diameter); flanged connections are used for larger diameters. Fixed beds are also used for analytical high-performance liquid chromatography (HPLC).

Variable or adjustable beds are common in pilot plants and development settings. The variable bed column is typically a tube that fits the outside diameter of the end fittings. The end fittings often consist of two flat plates sandwiching a gasket. When the end pieces are in place, the flat plates are compressed together, squeezing the gasket out against the tube. The top end piece may be placed at any level, depending on the volume of resin required for the process.

Axial compression columns are principally used for large-scale HPLC. When a rigid packing is used for chromatography, such as silica, packing efficiency is critical for high resolution. In this case, it has been found that slurry packing under high flow rate is not adequate. Axial compression columns address this by using a hydraulic piston as the inlet piece that compresses the resin along the length of the column. This not only causes the column to achieve the highest possible packing density, but also holds the resin in place as the action of the pump causes pressure pulses to wash through the column.

7.9.2 Chromatography Column Packing Procedures

Column packing is the most critical step in achieving high column performance in chromatography. There are three objectives in packing the column: to have the resin particles fully wetted, to have the particles fully disassociated from one another, and to achieve the highest possible packing density. To achieve the first objective, resin is slurry packed. This allows the resin to be in full contact with a solvent for an indefinite time prior to packing. It is critical to column capacity that the resin pores be full of solvent so that they are accessible to the process separands. Sometimes, especially at small scale, the resin is actively degassed, by sonication, vacuum, or heat. On larger scales, these methods are often impractical. In these cases, solvents such as ethanol that have high oxygen solubilities can be used to wet the particles.

Ensuring that the particles do not clump or form aggregates that can cause segregation during packing is goal number two. For this reason, solvents such as isopropanol are often added to the slurry. Isopropanol decreases the surface tension sufficiently to allow particles to disaggregate. Other agents, such as buffer salts, are sometimes used to enhance particle-particle repulsive forces. Resin disaggregation is

important, because the packing should be in a random order in the column. Any partial structuring of the resin particles will affect the positioning of adjacent particles, which can lead to channeling. Additionally, particle aggregates may act as larger particles, which will have poor mass transfer and intraparticle diffusion characteristics.

Finally, achieving the highest possible resin density is the ultimate packing goal. There are both chemical and mechanical considerations here. Chemically, particles should be in their least swollen state. If maximally swollen particles are packed, column conditions that cause the particles to subsequently contract will result in a bed that will no longer be packed efficiently, and voids will form. If particles are packed in their most contracted state, conditions that cause them to swell result in a more tightly packed column. High ionic strength is typically used to contract the particles. Attention must be paid to the strength of the seals when swellable resins are used. Resin can push through seals, crack the column, or occlude flow if allowed to swell too much. Highly swellable resins are generally avoided in large-scale processes. Mechanically, the particles should be packed quickly to deprive the slurry of the opportunity to settle and segregate according to particle size. The column should also be packed at or above the highest pressure (or flow rate) conditions expected for the column during normal processing. Finally, the inlet fitting should be placed as quickly and as evenly as possible, so that there are no biases in bed height and so that the pressure developed in the bed is captured mechanically in the seals.

Prior to the packing procedure, the resin is slurried at a packing density much lower than what will ultimately be achieved in the packed column. Therefore, a method is required for providing the extra volume to the column in which to slurry the resin. There are at least two common methods for doing this. The first is to temporarily increase the volume of the column, and the second is to use a secondary vessel. Adjustable-bed columns are easily adapted to the first method. Fixed-bed columns are often fitted with a packing extension tube to use this method. A secondary slurry vessel may also be used. This vessel is typically closed so that it can hold pressure. Then, clean solvent is pumped into the slurry vessel, displacing slurry to the column. Pumping slurries directly through a pump is not recommended because damage to both the resin and the pump may result.

Recently, large-scale columns have been fitted with retractable nozzels that can be lowered from the head plate of the column. This nozzle is lowered during column packing, and slurry is pumped through under pressure. When all the resin has been introduced, the nozzle is raised back to be flush with the head plate. These columns are called “pack in place” and have had variable results to date.

7.9.3 Detectors

Detectors are selected to match the molecule in the application. Almost any detection method can be adapted to chromatography and adsorption, from Fourier transform infrared spectroscopy to antibody conjugation techniques to mass spectroscopy. However, the most common are pH, conductivity, and light

absorbance. Conductivity and pH are monitored to check the performance of the gradient, the loading of the column, the regeneration, and reequilibration. Automated chromatography equipment relies on these measurements to proceed to the next steps. Light absorbance, primarily in the ultraviolet range (280, 254, 229, or 214 nm, depending on the application) is used to monitor the effluent for evidence of the target molecule. All three measurements are noninvasive and use well-developed technologies. Other common detection methods in use in large-scale chromatography and adsorption are refractive index, electrochemical detection, and light scattering.

Some applications are sufficiently sensitive to warrant on-line analytical detection. In these applications, a "split stream" is taken, and an analytical instrument, such as an HPLC, is injected with a sample. The purity can then be found for the sample, and a decision made to start, continue, or stop collection of the product. In these cases, the HPLC must be very fast compared with the large-scale chromatography, to permit assessment of purity of the target compound from contaminants and to allow a decision to be made before conditions have changed dramatically in the column effluent. HPLC methods can be developed that run in 1 or 2 min, when specific analytes are sought. In contrast, preparative scale chromatography cycles can last 4 to 8 h, depending on the optimization of the flow rates and elution sequence. For side stream analysis to be worthwhile, the preparative separation must give no apparent resolution of the target compound from a key contaminant that is present in levels of at least 1%. Also, there must be a requirement for purity of less than approximately 0.1% of this contaminant in the final product.

7.9.4 Chromatography System Fluidics

The fluidics of the chromatography system are always important in design and operation. Distribution of fluid across the column cross section is a key aspect in column efficiency and reproducibility. The pumps and tubing that feed the column are often part of this design.

Pumps

Pumps used in chromatography are typically positive displacement pumps. These provide reasonable pressures at reasonable cost. They have low shear, so do not pose a problem for sensitive biomolecules. Positive displacement pumps generally come in two varieties, peristaltic and rotary lobe. Peristaltic pumps use a rotating gear to compress flexible tubing through which the product stream flows. These are very familiar to biochemists and are useful for flow rates up to 10 liters/min. Rotary lobe pumps use two gears whose surfaces align such that at any rotation, they form a seal against each other, as well as against the interior of the pump housing. Rotary lobe pumps, uncommon below 1 liter/min, are almost always used at flow rates above 10 liters/min, where peristaltic pumps generally are not used.

Rotary lobe pumps must be fed with positive pressure on the inlet, since they are not self-priming in general.

Gradient Makers

Most laboratory HPLC equipment allows programmed gradients; that is, the user selects a gradient type from a menu, and the gradient is mixed from two reservoirs in a dual-chamber pump. The two reservoirs contain the leanest concentration of salt or solvent and the richest concentration. The gradient is formed by the pump(s) selecting more or less volume from each reservoir as time progresses. The gradient can also be mixed from two tanks using CSTR principles; these principles were illustrated in Figure 5.1 and Equation (5.3.1), which gives the solute concentration at the outlet of the gradient mixer for a linear gradient. A linear gradient results if the rich tank is fed into the lean tank by gravity, while the lean tank (well mixed) feeds the chromatography system. In this case, both the rich tank and the lean tank decrease in volume at half the column flow rate each. It is important that the tanks be level with each other, be at the same height, and have the same cross section. To make an exponential gradient, the volume in the lean tank should remain constant, while the rich tank feeds at the same rate as the column flow rate.

7.10 SCALE-UP

The scale-up of adsorption and chromatography processes usually involves changes in flow rates and in the dimensions of the column. A safe way to scale up is to keep the column length constant, but this is sometimes not feasible. Because the objectives of adsorption and chromatography are usually different, the scale-up of these two operations is considered separately.

7.10.1 Adsorption

The scale-up of a fixed-bed adsorption focuses on the breakthrough curve for a single column, while scale-up of an agitated-bed process is concerned with breakthrough for the last column in a series of columns. The scale-up of mixing becomes important for the mixed-bed process. Scaleup for both types of adsorption process can generally be carried out based on laboratory data.

Fixed-Bed Adsorption

Several approaches can be used to scale up fixed-bed adsorption processes [52]. Two useful approaches are discussed here: (1) the length of unused bed (LUB) concept, which allows scaleup based on data from laboratory columns, keeping the particle size and superficial velocity constant, and (2) the computer simulation method,

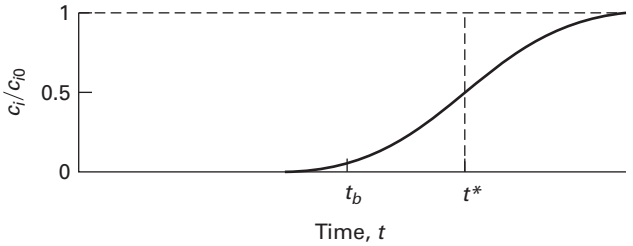

FIGURE 7.16 Breakthrough curve for a fixed-bed adsorber, showing the break-point time t_b, chosen at 5% of the solute feed concentration, and the ideal adsorption time t^*. The ratio of mobile phase concentration of solute to solute concentration in feed to the adsorber is c_i/c_{i0}.

which also requires laboratory experimental data and constant particle size but does not require the superficial velocity to be constant.

LUB Method

In discussing the LUB method of scaleup, it is necessary to define the *breakpoint time* (t_b) and the *ideal adsorption time* (t^*) on a breakthrough curve, which are indicated in Figure 7.16. The break-point time is usually taken at the relative concentration, (c_i/c_{i0}, where c_{i0} is the feed concentration) of 0.05 or 0.10 [53]. Since only the fluid last exiting the column has this concentration, the average fraction of the solute removed from the start of feeding to the break-point time is usually 0.99 or higher. The ideal adsorption time is the time for breakthrough that would occur if the solute were in perfect equilibrium with the bed of adsorbent, which would give a vertical breakthrough curve. For a symmetrical breakthrough curve, the ideal adsorption time is the time at which $c_i/c_{i0} = 0.5$. At the ideal adsorption time for a bed initially free of the solute to be adsorbed, based on a unit area of bed cross section,

$$\upsilon c_{i,0} t^* = L\rho_b q_{i,\text{sat}} \tag{7.10.1}$$

where L = bed length
$q_{i,sat}$ = average adsorbent phase concentration of solute i in equilibrium with feed concentration c_{io}, based on the adsorbent weight (weight of solute i per weight of adsorbent)
υ = superficial velocity
c_{io} = concentration of solute i in the feed
ρ_b = bulk density of the adsorbent

The ideal adsorption time is therefore given by

$$t^* = \frac{L\rho_b q_{i,\text{sat}}}{\upsilon c_{i,0}} \tag{7.10.2}$$

The amount of the solute adsorbed at the break point can be determined by integrating the breakthrough curve up to time t_b, as indicated in Figure 7.17. The width of the breakthrough curve defines the width of the *mass transfer zone* in the bed.

For adsorption where the equilibrium isotherm is favorable, which is true for the Langmuir isotherm that can often be used for protein adsorption, the concentration profile in the mass transfer zone takes on a characteristic shape that does not change as the zone propagates through the bed [5]. At the break-point time, the adsorbent between the inlet of the bed and the beginning of the mass transfer zone is completely saturated (in equilibrium with the solute in the feed). The adsorbent in the mass transfer zone goes from being completely saturated to being almost free of solute, and the adsorbent could be assumed to be on the average about half-saturated. This would be equivalent to half the adsorbent in the mass transfer zone being saturated and the other half being unused. The scale-up principle is that the length of the unused bed in the mass transfer zone does not change as the bed length is changed [54].

The length of unused bed (LUB) can be determined directly from the breakthrough curve obtained experimentally. If $q_{i,b}$ is the average adsorbent phase concentration of solute i at the breakpoint time, then the fraction of bed capacity utilized at the breakpoint time is $q_{i,b}/q_{i,sat}$. Therefore, the unused fraction of the bed is $1 - q_{i,b}/q_{i,sat}$. From Equation (7.10.1),

$$\frac{q_{i,b}}{q_{i,\mathrm{sat}}} = \frac{t_b}{t^*} \tag{7.10.3}$$

so that LUB can be written as:

$$\mathrm{LUB} = \left(1 - \frac{q_{i,t_b}}{q_{i,\mathrm{sat}}}\right) L = \left(1 - \frac{t_b}{t^*}\right) L \tag{7.10.4}$$

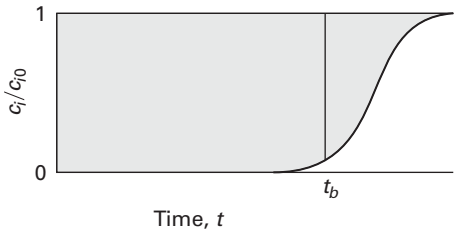

FIGURE 7.17 Integration of the breakthrough curve for a fixed-bed adsorber. The area of integration to the left of a vertical line at time t is proportional to the amount of solute adsorbed up to that time. The ratio of mobile phase concentration of solute to solute concentration in feed to the adsorber is c_i/c_{i0}.

where t_b and t^* are stoichiometric times determined by integration of the breakthrough curve:

$$t^* = \int_0^{\infty} \left(1 - \frac{c_i}{c_{i0}}\right) dt \tag{7.10.5}$$

$$t_b = \int_0^{t_b} \left(1 - \frac{c_i}{c_{i0}}\right) dt \tag{7.10.6}$$

In scale-up calculations, the length of column required can easily be found by adding the LUB to the length calculated by assuming local equilibrium, with a shock wave concentration front [5].

EXAMPLE 7.7

Scale-up of the Fixed-Bed Adsorption of a Pharmaceutical Product The breakthrough data given in Table E7.7 were obtained for the adsorption of a pharmaceutical product in a laboratory column (5 cm diameter × 15 cm high) at a feed flow rate of 400 ml/h and feed concentration of 0.75 U/liter, where U is units of biological activity of the pharmaceutical product. It is desired to scale up the process to operate in a column 30 cm high. What break-point time can be expected in the 30 cm high column?

TABLE E7.7

t (h)	c_i (U/liter)
20.5	0.01
26.7	0.20
32.0	0.39
36.0	0.53

Solution

We use the LUB method, which involves graphical integrations of the breakthrough curve to determine the amount of solute adsorbed at various times. The breakthrough curve with concentration in dimensionless form is therefore plotted, with the curve extended to $c_i/c_{i0} = 1.0$ assuming that the curve is symmetrical about $c_i/c_{i0} = 0.5$ (Figure E7.7). By doing graphical integrations of this curve, we find the following:

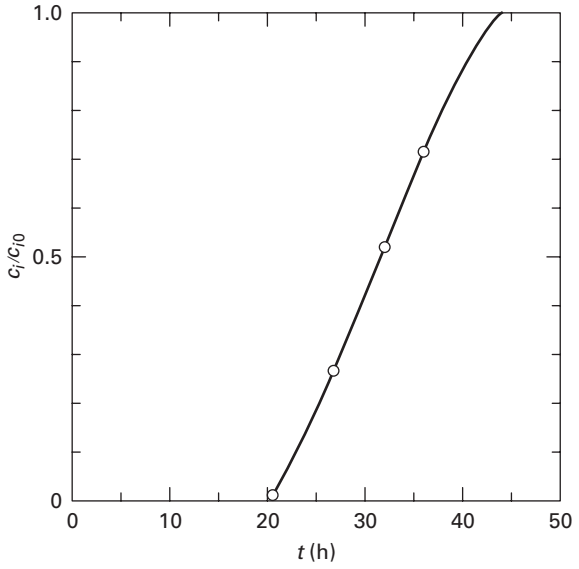

FIGURE E7.7 Breakthrough curve for the fixed-bed adsorption of a pharmaceutical product in Example 7.7.

$$\text{Total solute absorbed at saturation } (c_i/c_{i0} = 1.00) = Qc_{i0}\int_0^{31.5\,\text{h}} \left(1 - \frac{c_i}{c_{i0}}\right) dt$$
$$= Qc_{i0}(31.5\,\text{h})$$

$$\text{Total solute absorbed at break point } (c_i/c_{i0} = 0.05) = Qc_{i0}\int_0^{21.5} \left(1 - \frac{c_i}{c_{i0}}\right) dt$$
$$= Qc_{i0}(21.5\,\text{h})$$

where Q is the volumetric flow rate. Thus, t^* and t_b are 31.5 and 21.2 h, respectively, for this column. From Equation (7.10.4)

$$\frac{\text{LUB}}{L} = 1 - \frac{Qc_{i0}(21.2\,\text{h})}{Qc_{i0}(31.5\,\text{h})} = 1 - 0.673 = 0.327$$

$$\text{LUB} = 0.327(15\,\text{cm}) = 4.90\,\text{cm}$$

The adsorbent loading at saturation per total bed volume is

$$\rho_b q_{i,\text{sat}} = \frac{\upsilon c_{i0} t^*}{L} = \frac{400\dfrac{\text{cm}^3}{\text{h}} \times 0.00075\dfrac{\text{U}}{\text{cm}^3} \times 31.5\,\text{h}}{\dfrac{3.14 \times 5^2 \times \text{cm}^2 \times 15\,\text{cm}}{4}} = 0.0321\frac{\text{U}}{\text{cm}^3}$$

For the column 30 cm high, the LUB does not change, so that

$$\frac{\text{LUB}}{L} = \frac{4.90}{30} = 0.163$$

The superficial velocity stays the same and is

$$\upsilon = \frac{400 \dfrac{\text{cm}^3}{\text{h}}}{\dfrac{3.14 \times 5^2 \text{cm}^2}{4}} = 20.4 \frac{\text{cm}}{\text{h}}$$

From Equation (7.10.2),

$$t^* = \frac{L\rho_b q_{i,\text{sat}}}{\upsilon c_{i0}} = \frac{30\,\text{cm} \times 32.1 \dfrac{\text{U}}{\text{liter}}}{20.4 \dfrac{\text{cm}}{\text{h}} \times 0.75 \dfrac{\text{U}}{\text{liter}}} = 62.9\,\text{h}$$

Therefore, from Equation (7.10.4),

$$t_b = t^* \left(1 - \frac{\text{LUB}}{L}\right) = (62.9\,\text{h})(1 - 0.163) = 52.6\,\text{h}$$

Computer Simulation Method

In the design of a production scale adsorption process, it is often desirable to simulate the process on a computer based on laboratory or pilot plant data. An example of such a simulation for design and scale-up was carried out by Chen et al. [55] for the fixed-bed adsorption of a valuable pharmaceutical product. Their model neglected dispersion [Equation (7.3.11)] and used a linear driving force expression for the mass transfer rate [Equation (7.3.5)] and a combination of linear and Freundlich isotherms for the equilibrium relations. From a laboratory column, the following relationships for the mass transfer coefficient K_a were obtained:

$$K_a = 1640 - 3700 \frac{q_i}{q_{i,sat}} \quad for \frac{q_i}{q_{i,sat}} \le 0.4 \tag{7.10.7}$$

$$K_a = 264 - 260 \frac{q_i}{q_{i,sat}} \quad for 1 \ge \frac{q_i}{q_{i,sat}} > 0.4 \tag{7.10.8}$$

The laboratory column experiments indicated that pore diffusion in the adsorbent was the controlling mechanism for mass transfer. The equilibrium isotherm relationships were

$$c_i^* = 0.00006 q_i \quad \text{for } q_i \le 20 \tag{7.10.9}$$

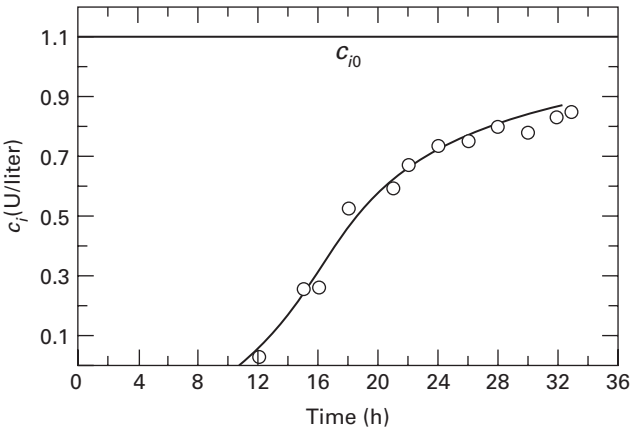

FIGURE 7.18 Comparison of model predictions (curve) and experimental data (open points) for the fixed-bed adsorption of a pharmaceutical product for a plant scale column 40 in. in diameter at a column height/column diameter ratio of 3.0. *(Data from J. W. Chen, J. A. Buege, F. L. Cunningham, and J. I. Northam, "Scale-up of a column adsorption process by computer simulation,"* Ind. Eng. Chem. Process Des. Dev.*, vol. 7, p. 1849, 1968.)*

$$c_i^* = 2.74 \times 10^{-8} q_i^{3.57} \quad \text{for } q_i > 20 \tag{7.10.10}$$

Equations (7.3.5) and (7.3.11) were solved on a computer by the method of finite differences, subject to the mass transfer and equilibrium isotherm relationships for a step change in the concentration in the feed from 0 to c_{i0} and no solute on the adsorbent at time 0. This model was used to predict the operation of 24 and 40 in. columns, and excellent agreement was obtained between the model and experimental data for c_i versus time. Model predictions and experimental data are shown in Figure 7.18. Computer simulation was used to optimize process variables such as flow rate, temperature, cycle time, concentration of product in the feed stream, and amount of adsorbent. Such a computer model of the adsorption process also enables the ready evaluation of changes in the process variables after the plant process is put into operation.

Agitated-Bed Adsorption

The scale-up of a series of agitated columns containing adsorbent (Figure 7.6), operated in the periodic countercurrent mode, follows directly from the mathematical model presented for this process [Equations (7.3.19)–(7.3.22)] [10]. Besides the increases in the flow rate and volume that occur upon scale-up, the mixing patterns may also change. A change in the mixing during scale-up was demonstrated in a mixed-bed adsorption process applied to a fermentation broth containing an antibiotic [56]. For a change in column volume by a factor of 29 from the laboratory column 2 in. in diameter to the pilot plant column with a 6 in. diameter, the mixing changed from perfect mixing in the laboratory column to mixing characterized by

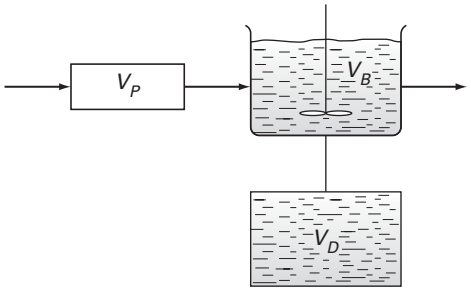

FIGURE 7.19 Mixing model based on the age distribution function determined experimentally for a pilot scale (6 in. diameter) agitated-bed adsorption column. Stagnant volume $V_D = V_L - V_B - V_P$. The total volume of liquid in the column is V_L.

the following equation in the pilot plant column, based on the following age distribution function that was determined:

$$1 - \frac{c_i}{c_{i0}} = \exp\left[-\frac{V_L}{V_B}\left(\frac{t}{\tau} - \frac{V_P}{V_L}\right)\right] \quad (7.10.11)$$

where c_{i0}, c_i = concentration of a nonadsorbing component i in the feed or effluent, respectively
V_L = total volume of liquid in the column
V_B = volume of back-mixed liquid in the column
V_P = volume of liquid in plug flow in the column
τ = column residence time (V_L/Q, where Q = feed flow rate)
t = time from the start of a step change in the concentration of the nonadsorbing component from 0 to c_{i0}

Equation (7.10.11) corresponds to a mixing model consisting of a plug flow region in series with a perfectly mixed region connected to a stagnant region (Figure 7.19) [57]. A model for nonideal mixing can be incorporated into the mathematical simulation and design of the large-scale process.

7.10.2 Chromatography

Chromatography scale-up algorithms typically account for changes in bed height and diameter, linear and volumetric flow rate, and particle size. A general approach to scale-up is based on keeping the resolution constant. Yamamoto et al. [58, 59] have developed the following proportionality for resolution, R_s, of proteins in linear gradient elution ion exchange chromatography and hydrophobic interaction chromatography:

$$R_s \propto \left(\frac{\mathscr{D}_m L}{g(V - V_0) u d_p^2}\right)^{1/2} \quad (7.10.12)$$

where $\mathscr{D}_m$ = diffusion coefficient of the protein in solution
L = column length
g = slope of the gradient (change in concentration of gradient per volume of gradient)
V = column volume
V_0 = column void volume
u = interstitial fluid velocity
d_p = particle diameter

This equation has been found to be valid over a wide range of experimental conditions [58, 59]. To remove the volume terms from the expression for resolution, we make the definitions

$$\bar{Q} = \frac{Q}{V} = \frac{\varepsilon u A}{V} \tag{7.10.13}$$

$$G = Vg \tag{7.10.14}$$

where Q is the inlet flow rate, ε is the column void fraction, and A is the column cross-sectional area. These substitutions lead to

$$R_s \propto \left(\frac{\mathscr{D}_m \varepsilon}{G(1-\varepsilon)\bar{Q} d_p^2} \right)^{1/2} \tag{7.10.15}$$

Thus, for scaleup with constant resolution from scale 1 to scale 2 for the same product and the same column void fraction, the scaleup equation is

$$G_1 \bar{Q}_1 d_{p1}^2 = G_2 \bar{Q}_2 d_{p2}^2 \tag{7.10.16}$$

Thus, as the particle size increases on scale-up, the flow rate relative to the column volume must decrease and/or the gradient slope must decrease to maintain constant resolution, which seems correct intuitively.

In practice, the gradient and the stationary phase size and chemistry are not changed upon scale-up. This is because it is easy to develop lab scale processes that use the same resin and same gradient that can be used at the commercial process scale. Therefore, in practice, only the ratio between column volume and flow rate need be addressed:

$$\frac{Q_1}{V_1} = \frac{Q_2}{V_2} \tag{7.10.17}$$

Scale-up from a well-designed process development or preparatory column is reasonably straightforward. When the bed height can be maintained on scale-up, the mobile phase linear velocity remains the same, and the column is simply scaled by

diameter. Scaling from a column 1 cm in diameter to column having a diameter of 10 cm would constitute a 100-fold increase in scale. This is the most conservative way to scale up a column but is not a necessary constraint.

EXAMPLE 7.8

Scale-up of a Protein Chromatography A column 20 cm long, with an internal diameter of 5 cm, gives sufficient purification to merit scale-up. The column produces 3.2 g of purified protein per cycle, and a cycle takes 6 h, from equilibration through regeneration. To design a throughput of 10 g/h, what are the new column's dimensions if the superficial velocity is held constant and it is assumed that the gradient and particle size are not changed on scale-up?

Solution

Equation (7.10.16) is applicable since the gradient and particle size remain the same. According to this equation, the residence time is the same at small and large scale, and therefore the cycle time is not changed. Thus, the scaled-up column must produce 6 h/cycle ×10 g/h = 60 g/cycle. Since the flow rate is proportional to the throughput of protein,

$$\frac{Q_2}{Q_1} = \frac{60\,\text{g/cycle}}{3.2\,\text{g/cycle}} = 18.75$$

From (7.10.17),

$$\frac{Q_1}{A_1 L_1} = \frac{Q_2}{A_2 L_2}$$

which leads to

$$\frac{\upsilon_1}{L_1} = \frac{\upsilon_2}{L_2}$$

Since the superficial velocity is constant,

$$L_1 = L_2$$

Therefore,

$$\frac{Q_2}{Q_1} = \frac{V_2}{V_1} = \frac{\pi\left(\frac{D_2}{2}\right)^2 L_2}{\pi\left(\frac{D_1}{2}\right)^2 L_1} = \left(\frac{D_2}{D_1}\right)^2 = 18.75$$

where D_1 and D_2 are the column diameters for columns 2 and 1, respectively. Since $D_1 = 5.0$ cm, we obtain

$$D_2 = (18.75)^{0.5} D_1 = 21.6 \text{ cm}$$

It is not always necessary to scale according to bed diameter. The flow rate may be normalized against the volume of the empty column, to give units of time^{-1}. This normalized flow rate is held constant from one scale to another, as shown in Equation (7.10.17). The case given in Example 7.8 can be shown to be a special case of this more general rule. Considerable research and practice indicates that this technique is equally effective and less restrictive compared to that just mentioned. In this case, column bed height may be increased or decreased, depending on the requirements of pressure drop and mechanical seals. A shallower bed gives a lower linear velocity and a wider diameter. A deeper bed gives a higher linear velocity (and higher pressure drop) and a proportionally narrower bed diameter. Therefore, bed height may need to be scaled on the basis of pressure drop constraints.

EXAMPLE 7.9

Scale-up of Protein Chromatography Using Standard Column Sizes Consider the case given in Example 7.8. Available standard column diameters are 20 and 25 cm. What bed depths would apply to each of these columns?

Solution

The column volumes for both columns are still 18.75 times that used in the laboratory column. Thus,

$$V_2 = 18.75 V_1 = 18.75\left(\frac{\pi D_1^2}{4} L\right) = 18.75\left(\frac{\pi 5^2}{4} \times 20\right) = 7359 \text{ cm}^3$$

For a column 20 cm in diameter,

$$L = \frac{V_2}{\pi \dfrac{D_2^2}{4}} = \frac{7359 \text{ cm}^2}{\dfrac{\pi}{4}(20 \text{ cm})^2} = 23.4 \text{ cm}$$

and for column the 25 cm in diameter,

$$L = \frac{V_2}{\pi \frac{D_2^2}{4}} = \frac{7359\,\text{cm}^2}{\frac{\pi}{4}(25\,\text{cm})^2} = 15.0\,\text{cm}$$

In both cases, the gradient is also expressed in column volumes. The total gradient volume, that is, the total volume of eluent used to go from the leanest mobile phase condition to the richest, is expressed in terms of column volumes, and this is held constant on scale-up.

EXAMPLE 7.10

Scale-up of Elution Buffer Volumes in Protein Chromatography An NaCl gradient is used to elute the product in Example 7.8. The gradient increases from 100 mM NaCl to 250 mM in 3 h. To form this gradient a 100 mM NaCl solution is combined with a 250 mM NaCl solution in a gradient mixer, in which the 100 mM NaCl solution is mixed (see Figure 5.1). The flow rate is 40 ml/min. What volumes of low-salt and high-salt eluent should be made for the scale-up column with an internal diameter of 20 cm?

Solution

The small-scale volume of each gradient buffer is 3.6 liters (40 ml/min × 180 min/2). The scale-up factor of 18.75 still applies, so that

$$\text{Volume of each buffer at large scale} = (18.75)(3.6\ \text{liters}) = 67.5\ \text{liters}$$

Suppose that in development, the product elutes in 60% of the gradient volume. The gradient may be truncated to save time and buffer volume. From Equation (7.10.14), the gradient can be adjusted according to:

$$G = \frac{c_{\text{hi}} - c_{\text{low}}}{V_g/V} = \text{constant} \qquad (7.10.18)$$

where c_{hi} and c_{low} are the concentrations of the high-strength and low-strength buffers, respectively, and V_g is total gradient volume. Keeping the gradient slope constant is essential for maintaining resolution in chromatography.

Finally, pressure drop must be considered. Pressure drop is given by Darcy's equation [Equation (7.8.1)]. As columns increase in diameter, the pressure they can hold generally decreases (or the structural mass is increased, to provide the strength to maintain a seal). This is because as the radius of curvature increases, the force against the pressure decreases, which weakens the seal (think, e.g., about the stability of large bubbles in a glass of beer, compared with the smaller ones). It is possible to design the scaled-up column from the accessible pressure drop of the column.

EXAMPLE 7.11

Consideration of Pressure Drop in Column Scaling Determine the minimum diameter possible for the columns analyzed in Example 7.9 and subject to the flow rate given in Example 7.10, when the column pressure should not exceed 300 kPa (28.8 psig), the maximum solution viscosity is 1.1 cp, and the void fraction in the column is 0.35. The resin particle size is 100 μm.

Solution

Pressure drop can be calculated using Darcy's law [Equation (7.8.1)] by knowing μ, v, k, and L. We can calculate k from the Blake-Kozeny equation (7.8.2):

$$k = \frac{(100\,\mu\text{m})^2}{150}\frac{0.35^3}{(1-0.35)^2} = 6.77\,\mu\text{m}^2$$

The column volume must be 7359 ml (from Example 7.9), and the flow rate is 40 ml/min (from Example 7.10) times the scaleup factor of 18.75 (= 750 ml/min). We calculate the pressure drop for the column 20 cm in diameter and 23.4 cm in length, which would give the higher pressure drop of the two standard column sizes (20 and 25 cm):

$$\text{Cross-sectional area} = \frac{\pi(20\,\text{cm})^2}{4} = 314\,\text{cm}^2$$

$$v = \frac{750\dfrac{\text{cm}^3}{\text{min}}}{314\,\text{cm}^2} = 2.39\frac{\text{cm}}{\text{min}}$$

From Equation (7.8.1) the pressure drop is

$$\Delta p = \frac{\mu v L}{k} = \frac{0.011\dfrac{\text{g}}{\text{cm s}} \times 2.39\dfrac{\text{cm}}{\text{min}} \times 23.4\,\text{cm} \times \dfrac{1\,\text{min}}{60\,\text{s}} \times 10^{-4}\,\dfrac{\text{kPa cm s}^2}{\text{g}}}{6.77 \times 10^{-8}\,\text{cm}^2}$$
$$= 15.1\,\text{kPa}$$

Thus, the standard 20 cm diameter column would operate at well below the maximum allowable pressure.

7.11 SUMMARY

The differential affinity of various solute molecules for solids of specific types is the basis for liquid chromatography and adsorption separation processes. Liquid chromatography is traditionally defined as the process where solutes are separated based on the speed at which they move through a column packed with adsorbent, also

called the resin or stationary phase. By contrast, in pure adsorption processes the stationary phase is generally uniformly saturated with the target solute before an eluting solvent is introduced to cause the solute to transfer into the liquid or mobile phase.

- Different adsorption equilibrium constants make it possible to separate solutes from one another; equilibrium constants are controlled by solvent composition. In the reaction C + S ↔ CS at equilibrium, the adsorption equilibrium constant is given by K_{eq} = [CS]/[C][S], where [S] is the concentration of vacant sites in the solid phase. If the total number of sites S_{tot} is not much greater than [CS], then sites are nearly saturated, and combining the site balance with the equilibrium relationship gives the Langmuir adsorption isotherm equation, which shows site saturation when [CS] is plotted versus [C]. The Langmuir isotherm is often used to describe the equilibrium data for proteins.
- A special case occurs when S_{tot} is much greater than [CS]: without saturation, the plot is a linear adsorption isotherm, or [CS] = K_{eq}[C]. The linear isotherm is applicable to analytical chromatography.
- Another equilibrium isotherm that has proven useful is the Freundlich isotherm, which states that [CS] is proportional to $[C]^{1/n}$, with $n > 1$. This isotherm has been used to describe the adsorption of a number of antibiotics, steroids, and hormones.
- As a solution containing a species to be separated, called a separand, is flowed into a packed bed, sites become occupied until they are saturated; then separand flows past this saturation zone to find new sites in a transition zone until the transition zone reaches the end of the bed, resulting in outflow of separand known as breakthrough. The analysis of breakthrough curves serves as the basis for scaling and optimizing separand isolation by packed-bed adsorption.
- The complete mass balance for the separand in a fixed-bed adsorber is given by

$$\mathscr{D}_{\text{eff}} \frac{\partial^2 c_i}{\partial x^2} - \frac{\upsilon}{\varepsilon} \frac{\partial c_i}{\partial t} = \frac{\partial c_i}{\partial t} + \frac{1-\varepsilon}{\varepsilon} \frac{\partial q_i}{\partial t}$$

  where c_i is the concentration of separand in the mobile phase, q_i is the concentration of separand in the adsorbent phase averaged over a particle, $\mathscr{D}_{\text{eff}}$ is the effective dispersivity of the separand, x is the distance from the bed inlet, υ is the superficial velocity, ε is the void fraction of the bed packing, and t is time. This mass balance also applies to chromatography.
- The mass transfer rate of separand into the adsorbent particle is often expressed in terms of a linear driving force as

$$\frac{\partial q_i}{\partial t} = K_a (c_i - c_i^*)$$

  where K_a is an overall mass transfer coefficient, and c_i^* is the liquid phase concentration at equilibrium with q_i.

- By assuming local equilibrium and negligible dispersion, the mass balance can be solved to give the effective velocity of separand i as

$$u_i = \frac{\upsilon}{\varepsilon + (1-\varepsilon)q_i'(c_i)}$$

  where $q_i'(c_i)$ is the slope of the equilibrium isotherm at concentration c_i. When the equilibrium isotherm is nonlinear and favorable (e.g., a Langmuir isotherm) and there is a discontinuous change in concentration in the bed, $q_i'(c_i)$ becomes $\Delta q_i/\Delta c_i$, where the differences are taken across the discontinuity. The resulting velocity of the solute front is called the shock wave velocity.
- The mass balance for adsorption with the linear driving force expression for the mass transfer rate, a linear equilibrium isotherm, and negligible dispersion has been solved analytically to give an expression for the breakthrough curve.
- Chromatographic performance is assessed by elution peak analysis and moment analysis. Elution peak analysis uses a plate model, in which the number of theoretical plates is proportional to $t_R^2/(w/4)^2$ where t_R is average retention time and w is peak width. The resolution of two solutes is directly proportional to the difference in average retention times and inversely proportional to the sum of the peak widths. Moment analysis can be applied using a step change in the column inlet and can be used to analyze non-Gaussian peaks, for example peaks that are skewed. Moment analysis results in a non-Gaussian number of theoretical plates and has been found to be a superior method for detecting integrity breaches in production scale chromatography columns.
- Band spreading in chromatography can be attributed to mechanical dispersion in the mobile phase, and molecular diffusion in the mobile and adsorbent phases. These factors govern the choice of particle size, pressure drop, and flow velocity. The impact of mass transfer and diffusion effects can be estimated by using the van Deemter equation.
- Chromatography can be simulated on a computer when axial dispersion, external mass transfer, intraparticle diffusion, and nonlinear equilibrium are considered.
- Equilibria for protein–salt ion exchange chromatography are calculated by using two equilibrium constants, one for protein and one for salt ion in the multicomponent Langmuir equation. This gives the protein adsorption isotherm as a function of salt concentration, which can be varied continuously in gradient elution chromatography. Gradient elution is thus distinguished from isocratic elution, in which no solute concentrations are varied.
- Membrane chromatography results in lower column volume and residence time compared to packed bed chromatography. Membrane chromatography is advantageous for the removal of contaminants such as viruses, nucleic acids, and endotoxins and for the purification of plasmid DNA and very large proteins (> 250 kDa).
- Simulated moving bed chromatography is a process in which the columns are fixed and the injection and collection points are periodically shifted. In the most widely adopted configuration, there are four chromatography zones. Simulated

moving bed chromatography has been used to purify many bioproducts at large scale, mostly for small molecule products.

- Adsorbents are selected on the basis of the adsorption chemistry of the separands, such as ion exchange, hydrophobic interaction, affinity reactions, metal affinity, and size exclusion.
- For a given mobile phase flow velocity, the required pressure drop is inversely proportional to the square of the particle diameter and directly proportional to column length and the viscosity and superficial velocity of the mobile phase (Darcy's law). Small particle size, desired for high resolution, can lead to unreasonable pressure requirements.
- Numerous design considerations are required for adsorption and chromatography equipment.
- A common method to scale up fixed-bed adsorbers is the length of unused bed (LUB) method, which is dependent on the equilibrium isotherm being favorable (concave downward) and on the particle size and superficial velocity remaining constant.
- The scale-up of a series of agitated columns containing adsorbent follows directly from the mass balance for each column, linear driving force expression for the mass transfer rate, and equilibrium isotherm, which must be solved by numerical methods. For this system, scale-up of the mixing is an important consideration.
- The constant resolution scaling rules for gradient elution chromatography, in their simplest form, specify that the product of gradient slope, normalized flow rate, and particle diameter squared should be held constant. Since normalized flow rate includes column area, an efficient way to scale up is to increase column diameter.

NOMENCLATURE

a_i	constant of i^{th} component in multicomponent Langmuir isotherm [Equation (7.4.25]
A	constant in the van Deemter equation [Equation (7.4.17)] (cm)
A	cross-sectional area of column (cm^2)
b_j	equilibrium constant of *jth* component in multicomponent Langmuir isotherm [Equation (7.4.25]
B	constant in the van Deemter equation[Equation (7.4.17)] ($cm^2\ s^{-1}$)
Bi	Biot number of mass transfer ($k_c\ r_p / \varepsilon^* \mathscr{D}_p$) (dimensionless)
c	concentration of a separand in the mobile phase (M, or g $liter^{-1}$)
c^*	equilibrium concentration of separand in the mobile phase (M, or g $liter^{-1}$)
c_0	feed concentration of a separand in the mobile phase (M, or g $liter^{-1}$)
C	chemical species in the mobile phase
C	constant in the van Deemter equation [Equation (7.4.17)] (s)
CS	chemical species adsorbed to an adsorption site
d_p	stationary phase particle diameter (cm)
D	column diameter (cm)
Da	Damköhler number ($= d_p^2 k_a / 4\mathscr{D}_p$) (dimensionless)

$\mathscr{D}_m$ molecular diffusivity of separand in unbounded solution ($cm^2\ s^{-1}$)
$\mathscr{D}_{eff}$ effective dispersivity in the column ($cm^2\ s^{-1}$)
$\mathscr{D}_p$ molecular diffusivity of separand in the pore fluid ($cm^2\ s^{-1}$)
E dispersion coefficient of separand, as a result of back-mixing in the fixed-bed and nonuniformity of the velocity ($cm^2\ s^{-1}$)
g slope of the elution gradient (M $liter^{-1}$, or g $liter^{-2}$)
g gravitational acceleration (9.0866 m sec^{-2})
G normalized slope of the gradient (M, or g $liter^{-1}$)
H height equivalent to a theoretical plate (HETP) (cm)
H_i Henry constant for component i in multicomponent Langmuir isotherm (Equation 7.6.2) (dimensionless)
$H(x, t)$ dispersion function (dimensionless)
H^* normalized height equivalent of a theoretical plate (H/d_p) (dimensionless)
I_0 Bessel function (dimensionless)
k constant in the Darcy equation [Equation (7.8.1)] (cm^2)
k $K_a/K_{eq}(s^{-1})$
k_a forward rate constant of adsorption (s^{-1})
k_c fluid-phase mass transfer coefficient (cm s^{-1})
K_a overall mass transfer coefficient (s^{-1})
K_{eq} equilibrium constant (units vary)
K_i equilibrium constant of i^{th} component in multicomponent Langmuir isotherm [Equation (7.6.2)] (M^{-1}, or g^{-1} liter)
L length of the column (cm)
m $\mathscr{D}_m / \mu^* \mathscr{D}_p$ (dimensionless)
m' $\frac{3}{2} m[K_{eq} / (1 + K_{eq})]^2$ (dimensionless)
N number of theoretical plates
Nu Nusselt number ($= d_p k_c / \mathscr{D}_m$) (dimensionless)
Δp pressure drop (kPa)
Pe_g dispersion Péclet number ($= ud_p / \mathscr{D}_{efl}$) [Equation (7.4.19)] (dimensionless)
Pe_L dispersion Péclet number ($= uL/E$) (dimensionless)
q concentration of a separand in the stationary phase averaged over an adsorbent particle (M, or g $liter^{-1}$)
q_p concentration of separand in the pore fluid based on a unit volume of stationary phase (i.e., the solid matrix and the pore space) (M, or g $liter^{-1}$)
q_s concentration of separand adsorbed on the internal surfaces of the stationary phase based on a unit volume of stationary phase (i.e., the solid matrix and the pore space) (M, or g $liter^{-1}$)
q_{sat} concentration of separand on the stationary phase at equilibrium with feed concentration c_0, averaged over an adsorbent particle (M, g $liter^{-1}$, or g g^{-1})
Q flow rate (ml min^{-1})
$\bar{Q}$ (flow rate)/(column volume) (min^{-1})

r	radial distance in the stationary phase (cm)
r_p	particle radius (cm)
R_s	chromatographic resolution (dimensionless)
Re	Reynolds number (= $d_p u\varepsilon\rho/\mu$) [Equation (7.4.19)] (dimensionless) (= $d_p u\rho/\mu$) [Section 7.4.5] (dimensionless)
Sc	Schmidt number (= $\mu/\rho\mathscr{D}_m$) (dimensionless)
Sh	Sherwood number ($k_c\, d_p/\mathscr{D}_\mathrm{m}$) (dimensionless)
S_{tot}	total concentration of adsorbent sites (mg ml^{-1})
t	time (s)
t_R	retention time (s)
t_s	column switch time in simulated moving bed chromatography (s)
t^*	ideal adsorption time, or column switch time (s)
u	velocity of fluid through the interstices of the bed (cm s^{-1})
u_i	separand i effective velocity (cm s^{-1})
$u_{i,\mathrm{sh}}$	separand i shock wave velocity (cm s^{-1})
v	mobile phase superficial velocity (cm s^{-1})
V	volume of fixed-bed column (ml)
V_B	volume of back-mixed liquid in column (ml)
V_L	liquid volume in column (ml)
V_P	volume of liquid in plug flow in column (ml)
V_R	volume of adsorbent in column (ml)
V_0	column void volume (ml)
w	peak width at base (base intercept) (s)
x	longitudinal distance in the column (cm)
x	fraction of separand in the mobile phase at long times [$\varepsilon/\varepsilon + (1 - \varepsilon)\varepsilon^*(1 + K_{\mathrm{eq}})$]

Greek Letters

γ	$1 + K_{\mathrm{eq}}(1 - \varepsilon)/\varepsilon$
ε	column void fraction (dimensionless)
ε^*	effective volume fraction of the stationary phase that is accessible to the separand (dimensionless)
ε_o	$\varepsilon + (1–\varepsilon)\varepsilon^*$
ξ	$(k\, K_{\mathrm{eq}} x/v)(1 - \varepsilon)$ (dimensionless)
η	constant for computer simulation of chromatography ($\varepsilon^*\mathscr{D}_\mathrm{p}L/r_p{}^2u$) (dimensionless)
μ	viscosity of mobile phase (g cm^{-1} s^{-1})
μ_k	k^{th} moment of the frequency distribution of solute concentration (units vary)
ρ	density of fluid (g cm^{-3})
ρ_c	bulk density of adsorbent (g cm^{-3})
σ	standard deviation for a peak (s)
τ	dimensionless time (= $k(t - x\varepsilon/v)$ [Equations (7.3.14 and 7.3.15)] (dimensionless) (= ut/L) [Equation (7.4.27)] (dimensionless)

τ column residence time (V_L/Q) (s)
φ c/c_0 (dimensionless)
ψ q/q_0 (dimensionless)

Subscripts
i, j components *i, j*
$n-1, n$ columns $n-1$, n in a series of columns

PROBLEMS

7.1 Freundlich versus Langmuir Isotherm Apply both the Freundlich isotherm and the Langmuir isotherm to the set of data shown in Table P7.1. Determine the applicable constants for the two different isotherms. Which is better, and why?

TABLE P7.1

q (mg/g)	c (mg/ml)
2.00×10^{-2}	3.20×10^{-9}
8.00×10^{-2}	3.28×10^{-6}
1.00×10^{-1}	1.00×10^{-5}
5.00×10^{-1}	3.12×10^{-2}
7.00×10^{-1}	1.68×10^{-1}
1.00	1.00

7.2 Langmuir Isotherm For the Langmuir isotherm [Equation (7.2.6)], determine the relationship between the equilibrium constant K_{eq} and the mobile phase concentration [C] when the adsorbent is half saturated.

7.3 Three Binding Solutes Derive the isotherms for three binding solutes that all compete for the same sites on the resin. If $K_{eq2} < K_{eq1} < K_{eq3}$, qualitatively describe the effects of the following situations:
(a) c_1 is very small compared to c_2 and c_3.
(b) $K_{eq3} >> K_{eq1}$
(c) c_2 is low initially, and increases throughout the elution process.

7.4 Solute Binding to Two Binding Sites Derive an isotherm for a single solute molecule that binds simultaneously to two binding sites. An example of this would be a divalent cation binding to a carboxymethyl-derivatized resin. Use this expression to generate an example isotherm.

7.5 Dispersion versus Molecular Diffusivity What is the difference between the effective dispersivity $\mathscr{D}_{eff}$ and molecular diffusivity $\mathscr{D}_m$? What are the units for each?

7.6 Prediction of the Break-Point Time in Fixed-Bed Adsorption At low concentrations, the equilibrium for the antibiotic novobiocin and Dowex 21K anion exchange resin is linear,

$$q_i = 125c_i^*$$

for q_i and c_i^* in units of milligrams per milliliter. For the range of concentrations where this isotherm is valid, the mass transfer coefficient K_a averages 82 h^{-1}. Assuming a linear isotherm, estimate the break-point time (where $c_i/c_{i0} = 0.05$) in a fixed-bed adsorber with a bed length of 20 cm and superficial velocity of 40 cm/h. (Data from P. A. Belter, F. L. Cunningham, and J. W. Chen, "Development of a recovery process for novobiocin," *Biotechnol. Bioeng.,* vol. 15, p. 533, 1973.)

7.7 Separation of Two Solutes Having Linear Equilibrium Two solutes have a linear equilibrium with the stationary phase. Their equilibrium constants are 6.5 and 6.6, respectively. The task is to separate 20 ml of the mixture on a column 5 cm in diameter. The flow rate is 10 ml/min. Determine the minimum column length required to just separate the two compounds, with $\varepsilon = 0.3$.

7.8 Calculation of the Shock Wave Velocity A solute has a Langmuir isotherm characterized by an S_{tot} of 120 μg/ml and a K_{eq} of 60 ml/mg. Calculate the shock wave velocity for an injection of 1 mg/ml and column conditions identical to those presented in Problem 7.7.

7.9 Using the LUB Method to Scale Up Fixed-Bed Adsorption Breakthrough data (see Table P7.9) have been obtained for a fixed-bed adsorption process with a weakly anionic adsorbent using a feed of filtered fermentation broth containing the antibiotic cephalosporin at a concentration of 4.3 g/liter. The bed is 1 m long × 3 cm diameter, and the superficial velocity is 2 m/h. It is desired to scale up this process to a bed length of 3 m using the same superficial velocity. Use the LUB method to estimate the break-point time, defined here as occurring when $c_i/c_{i0} = 0.1$, for the large column. (Data from P. A. Belter, E. L. Cussler, W.-S. Hu, *Bioseparations,* p. 174, Wiley-Interscience, New York, 1988.)

TABLE P7.9

t (h)	c_i (g/liter)
4.7	0.2
6.5	0.4
7.3	1.0
7.8	1.8
8.1	2.7
8.7	3.8
9.3	4.2
10.3	4.3

7.10 Removal of a Low-Level Contaminant One mode in which adsorbents are used is to strip a low-level contaminant like DNA from a product solution. No other solution components are negatively charged at the operating pH for the column.

(a) If an anion exchanger is used for this purpose, determine the total bed capacity for DNA given these parameters: bed volume = 2 liters, S_{tot} = 2 mg/ml, K_{eq} = 2 ml/mg, and DNA concentration = 5 μg/ml.
(b) Determine the bed capacity for the same conditions except that the DNA concentration is 100 μg/ml.

7.11 Chromatography Scale-up It is desired to scale up the throughput by a factor of 150 for a linear gradient ion exchange chromatography of a product protein from the laboratory to the plant. The conditions for the laboratory chromatography are the following: 1.0 cm bed diameter (ID) × 20 cm bed height, 20 μm particle size, and 30 cm/h superficial velocity. The particle size of the same type of ion exchange resin available for the plant operation is 40 μm. Two columns are available in the plant: one column 14.0 cm diameter (ID) × 50 cm high, and another column 18.0 cm diameter (ID) × 50 cm high. To keep the resolution for the chromatography constant in the plant, which column should be used? For this column, what should be the resin bed height and the superficial velocity and what do you estimate the pressure drop to be? The viscosity of the mobile phase is 1.0 cp, and the void fraction for resin in the plant column is 0.33.

7.12 Design of a Protein Purification Process (Mini-Case Study) Propose a purification process for the protein described. Assume a bacterial process. Design of the process will involve estimation of protein properties, for which a spreadsheet is provided at the textbook website (http://www.biosep.ou.edu). (Protein adapted from H. Zou, T. J. McGarry, T. Bernal, and M. W. Kirschner, "Identification of a vertebrate sister-chromatid separation inhibitor involved in transformation and tumorigenesis," *Science*, vol. 285, pp. 418–422, 1999.)

Sequence

1 MATLIYVDKENGEPGTRVVAKDGLKLGSGPSIKALDGRSQVSTPRFGKTFD

52 APPACLPKATRKALGTVNRATEKSVKT-|---------S-S---------|
KGPLKQKQPSCFSAKKMTEKTCVKAKS

106 SVPASDDAYPEIEKFFPFNPLDFESFDLPEEHQIAHLPLSGVPLMILDEER

157 ELEKLFQLGPPSPVKMPSPPWESNLLQSPSSILSTLDVELPPVCCDIDI

Research Production Process

A PCR-amplified gene was cloned into a modified pET28a vector to express recombinant protein in *E. coli*. Protein more than 90% pure was obtained by affinity purification with Ni-nitrilotriacetic acid (NTA) beads followed by Resource Q column chromatography.

In addition to the traditional process and host-cell-related impurities, the following substance related impurities are present in the process:

Impurity 1: Des-Met (N-terminal methionine deleted for the desired protein)
Impurity 2: C-terminal cleavage product (cleavage between lysine 9 and glutamic acid 10)

1 ENGEPGTRVVAKDGLKLGSGPSIKALDGRSQVSTPRFGKTFD

43 APPACLPKATRKALGTVNRATEKSVK-|---------S-S---------|
TKGPLKQKQPSCFSAKKMTEKTCVKAKS

97 SVPASDDAYPEIEKFFPFNPLDFESFDLPEEHQIAHLPLSGVPLMILDEER

148 ELEKLFQLGPPSPVKMPSPPWESNLLQSPSSILSTLDVELPPVCCDIDI

Impurity 3: N-terminal cleavage product (cleavage between lysine 9 and glutamic acid 10)
1 MATLIYVDK

Impurity 4: Misfolded isoform

1 MATLIYVDKENGEPGTRVVAKDGLKLGSGPSIKALDGRSQVSTPRFGKTFD
|----------S-S----------

52 APPACLPKATRKALGTVNRATEKSVK----------|

TKGPLKQKQPSCFSAKKMTEKTCVKAKS

106 SVPASDDAYPEIEKFFPFNPLDFESFDLPEEHQIAHLPLSGVPLMILDEER

157 ELEKLFQLGPPSPVKMPSPPWESNLLQSPSSILSTLDVELPPVCCDIDI

Impurity 5: Covalent dimer between cysteine 56 on adjacent molecules

Information about chromatography adsorbents can be found through links to various companies at the textbook website (www.biosep.ou.edu). There is also a link to a spreadsheet to approximate protein charge as a function of pH at the textbook website.

7.13 **Specification of Equipment for Chromatography Steps (Mini-Case Study)** Use the purification steps selected in Problem 7.12, to choose equipment and specify column scale for the chromatography steps, given the following considerations:

- Fermentation titer: The *E. coli* process produces 500 liters of product at a concentration of 2.5 g/liter. One fermentation cycle is 48 h, and the success rate is 90% (failure means that the entire fermentation batch had to be dumped); 50% of the recovered protein is the target product.
- There will be a need for 3000 g for clinical trial material for *E. coli* product, produced over three or more batches.
- There are 3 months available to campaign the clinical material, starting after the year end shutdown.
- Each purification step gives a yield of 90%, and there is an additional 10% penalty every third step.
- The protein degrades with the following zero-order kinetics (independent of concentration):

$$\text{rate}\,(\%\,/\,\text{day}) = -50\,e^{-1000/T} \qquad T \text{ in K}$$

The degradation product is a deamidation of asparagine 11 and must be purified away if it exceeds 0.1%.

General Plant Resources

- There is one 500-liter fermentor available.
- Fermentation products can be delivered to the first separation step free from solids.
- There are five columns available in the manufacturing area (see Table P7.13).

TABLE P7.13

Number of columns	Diameter (cm)	Minimum/maximum length (cm)	Maximum pressure (bar)
1	100	5/20	3
1	63	7/30	3
2	25	12/50	5
1	15	30/100	100

- One chromatography cycle takes 6 h starting from storage or cleaning solutions, 4.5 h when one is resuming from the elution step.
- A water for injection (WFI) still is available that produces 200 liters/h.
- There are two 4°C cold rooms.
- Two crossflow filter housings are available, one capable of holding 50 ft^2 of membrane, the other capable of holding 200 ft^2.
- Any tank you size can be made available.

Factors to Consider

- Compatibility with current processes (what's currently used in manufacturing?)
- Cleaning and storage requirements (ease of accommodation in the plant, handling issues, etc.)
- Preferred vendor (experience, reliability, delivery, price, validation package?)
- Future scalability

7.14 Specification of a Column for Protein Chromatography A protein chromatography column that processes 15 kg of protein in 60 h, is cycled every 6 h, can be loaded with 10 grams of protein per liter of column volume, has a maximum flow rate of 50 liters/min at a pressure of 4 bar, and is packed with an incompressible resin having a particle diameter of 90 μm and void fraction of 0.35. The viscosity can be assumed to be that of water.

(a) What are the dimensions required for the column?

(b) If the flow rate is 1 column volume per minute and the pressure rating is still 4 bar, what column dimensions are required? Is the resolution equivalent to that for part (a)?

(c) If the pressure rating for the column were raised to 12 bar, should the column dimensions change? Is so, what should the dimensions be? Do they make sense?

(d) What is the best way to increase the productivity of the column packing?

7.15 Estimation of the Number of Theoretical Plates for Ion Exchange Chromatography of a Protein Following a Langmuir Isotherm A 20 cm long ion exchange column is loaded with a protein solution at a concentration of 3 mg/ml and is eluted isocratically at a superficial velocity of 30 cm/h. The void fraction is 0.3. The protein has a K_{eq} (Langmuir isotherm) of 1.0 ml/mg, and the column's resin is saturated with the protein

at a resin-phase concentration of 10 mg/ml. If the protein peak has a standard deviation of 4.0 min, estimate the number of theoretical plates in the column.

7.16 Chromatographic Separation of a Protein A protein is being separated on a chromatography column. The protein has been found to obey the Langmuir isotherm, with $S_{tot} = 300\,\mu$g/ml and $K_{eq} = 10$ ml/mg. The concentration of the protein in the feed (3 liters) to the column is 2 mg/ml. The column flow rate is 2.0 liters/min. The column is 50 cm in diameter and 100 cm long. The void fraction of the chromatography bed is 0.35.

Determine (a) the time for the protein shock front to exit the column, and (b) the time when the concentration of the protein in the diffuse wave is 0.01 mg/ml at the exit of the column.

7.17 Chromatography of an Antibiotic with a Freundlich Isotherm The antibiotic cephalosporin C is being purified on a chromatography column packed with XAD-2 adsorbent beads. Adsorption experiments have shown that the equilibrium can be described by the following Freundlich isotherm:

$$q = 1.99\,c^{0.746}$$

for q and c in units of mg/ml. For an injection concentration of 0.5 mg/ml and elution superficial velocity of 30 cm/h, determine the time for the shock wave front to exit a column that is 50 cm long and has a void fraction of 0.37 (Data from N. F. Kirkby, N. K. H. Slater, K. H. Weisenberger, F. Addo-Yobo, and D. Doulia, "An HPLC technique for parameter estimation for reversed-phase chromatography: A case study on cephalosporin C," *Chem. Eng. Sci.*, vol 41, p. 2005, 1986).

7.18 Chromatography Scale-up—Pilot Plant to Plant You are designing a plant scale chromatography to purify a protein. You have pilot scale data with an adequate resolution. In this pilot data, the column has a cross-sectional area A_1 and a bed height, L_1. The pilot column data has it operating with a gradient going from $c_{low,1}$ to $c_{hi,1}$, and a total gradient volume of $V_{g,1}/V_1$ (in bed volumes). The pilot column is able to produce M_1 grams of protein per cycle. You want to scale up the column to produce M_2 grams of protein per cycle. You only have one large column available to use, with a cross-sectional area of A_2. The maximum pressure drop allowed for the large column is Δp_2. The particle diameter d_p, column void fraction ε, and solution viscosity μ are the same at the pilot plan and plant scales. It is desired to operate the large column at flow rate Q_2 at the same resolution as in the pilot scale column. The lower and upper concentrations of the gradient (c_{low} and c_{hi}) are different for the plant column. For the large column, develop expressions for the maximum allowable bed height and for the bed volumes of the gradient.

7.19 Evaluation of Chromatography Column Performance In evaluating the performance of two chromatography columns of the same length, it is found that the peak width of methyl parabenzoic acid is decreased from 13.1 s to 3.8 s, while giving the same retention time. By what factor has the number of theoretical plates changed?

7.20 Darcy's Law for Pressure Drop Calculation Two different forms of Darcy's law have been given, Equations 7.8.1 and 4.2.1. What is the relationship between k and R?

7.21 Computer Simulation of Chromatography for the Separation of Two Biological Macromolecules It is desired to simulate on a computer the separation of two

biological macromolecules on a chromatography column at 4°C in an aqueous system. Equilibrium for the two molecules follows a Langmuir binary isotherm according to Equation (7.4.25) with $n = 2$. The column conditions and physical property information are known, as follows (subscripts 1 and 2 refer to macromolecules 1 and 2):

$$d_p = 100\mu\text{m}$$
$$\upsilon = 12 \text{ cm h}^{-1}$$
$$L = 20 \text{ cm}$$
$$\mathscr{D}_{m1} = 6.0\times10^{-7}\text{cm}^2\text{s}^{-1}$$
$$\mathscr{D}_{m2} = 9.0\times10^{-7}\text{cm}^2\text{s}^{-1}$$
$$\mathscr{D}_{p1} = 3.0\times10^{-7}\text{cm}^2\text{s}^{-1}$$
$$\mathscr{D}_{p2} = 4.5\times10^{-7}\text{cm}^2\text{s}^{-1}$$
$$E_1 = E_2 = 10^{-3}\text{cm}^2\text{s}^{-1}$$
$$c_{o1}\left(\text{feed concentration of component 1}\right) = 0.1 \text{ M}$$
$$c_{o2}\left(\text{feed concentration of component 2}\right) = 0.1 \text{ M}$$
$$\varepsilon = 0.4$$
$$\varepsilon^* = 0.4$$

The Langmuir binary isotherm constants for components 1 and 2 are as follows: $a_1 = 5$, $b_1 = 6$, $a_2 = 1.2$, and $b_2 = 1.5$.

The feed time is 4 min, and then an isocratic elution is carried out.

Simulate this chromatography using the simulation software developed by T. Gu that is available through instructors for academic use (http://www.ohio.edu/people/gu/CHROM/) to make the following predictions:

(a) Predict the elution profile of macromolecules 1 and 2 and calculate the resolution, R_s.
(b) With d_p decreased to 10 μm, predict the elution profile and resolution.
(c) With υ increased to 120 cm h^{-1} and maintaining d_p at 100 μm and the same feed volume as for parts (a) and (b), predict the elution profile and resolution.

7.22 Using Moment Analysis to Evaluate Chromatography Column Performance On 2 different days 2 weeks apart for a 50 cm long ion exchange chromatography column, a step change in sodium chloride concentration is introduced at the column inlet in order to evaluate the column performance. Conductivity is measured at the column outlet as a function of the effluent volume, as shown in Table P7.22.

TABLE P7.22

	Case 1	Case 2
Volume (liters)	Conductivity (mmho/cm)	Conductivity (mmho/cm)
5	0	0
6	0	0
7	0	1.7
8	0	2.3

TABLE P7.22 (Continued)

Volume (liters)	Case 1 Conductivity (mmho/cm)	Case 2 Conductivity (mmho/cm)
9	0	2.7
10	0	2.8
11	0.6	3.4
12	2.0	4.9
13	9.2	12.7
14	18.2	24.0
15	28.9	34.2
16	39.1	41.6
17	45.0	47.3
18	50.8	51.3
19	53.8	54.0
20	55.0	55.0
21	55.0	55.0

Determine the non-Gaussian HETP for each case. How do these cases compare in terms of column efficiency? If there is a significant difference in column efficiency between the two cases, what may be a reason for the discrepancy?

REFERENCES

1. Simpson, J. M. (1994). Conventional chromatography. In *Protein Purification Process Engineering*, R. G. Harrison, ed., Dekker, New York, p. 209.
2. Shiloach, J., and Kennedy, R. M. (2000). Expanded-bed adsorption process for protein capture. In *Handbook of Separations*, S. Ahuja, ed., Academic Press, San Diego, CA, p. 431.
3. Shukla, A. A., and Cramer, S. M. (2000). Bioseparations by displacement chromatography. In *Handbook of Separations*, S. Ahuja, ed., Academic Press, San Diego, CA, p. 379.
4. Belter, P. A., Cussler, E. L., and Hu, W.-H. (1988). *Bioseparations*, Wiley-Interscience, New York.
5. Ruthven, D. M. (1991). Adsorption. In *Kirk–Othmer Encyclopedia of Chemical Technology*, vol. 1, 4th ed., J. I. Kroschwitz, ed., Wiley-Interscience, New York, p. 493.
6. Bird, R. B., Stewart, W. E., and Lightfoot, E. N. (2002). *Transport Phenomena*, 2nd ed., Wiley, New York.
7. Klinkenberg, A. (1954). Heat transfer in cross-flow heat exchangers and packed beds. *Ind. Eng. Chem*., vol. 46, p. 2285.
8. Furnas, C. C. (1930). Heat transfer from a gas stream to a bed of broken solids. *Trans. AIChE*, vol. 24, p. 142.
9. Ruthven, D. M. (1984). *Principles of Adsorption and Adsorption Processes*, Wiley-Interscience, New York.
10. Belter, P. A., Cunningham, F. L., and Chen, L. W. (1973). Development of a recovery process for novobiocin. *Biotechnol. Bioeng*., vol. 15, p. 533.
11. Chapra, S. C., and Canale, R. C. (1998). *Numerical Methods for Engineers*, 3rd ed., WCB/McGraw-Hill, Boston.

12. Martin, A. J. P., and Synge, R. L. M. (1941). A new form of chromatogram employing two liquid phases. I. A theory of chromatography. *Biochem. J*., vol. 35, p. 1358.
13. Horvath, C., and Melander, W. R. (1983). Theory of chromatography. In *Fundamentals and Applications of Chromatographic and Electrophoretic Methods, Part A*, E. Heftmann, ed., Elsevier, Amsterdam, Netherlands, p. A27.
14. Kucera, E. (1965). Contribution to the theory of chromatography: Linear nonequilibrium elution chromatography. *J. Chromatog*., vol. 19, p. 237.
15. Garcia, F. A. P., and Pires, E. M. V. (1993). Chromatography. In: *Recovery Processes for Biological Materials*, J. F. Kennedy and J. M. S. Cabral, eds., Wiley, Chichester, p. 415.
16. Larson, T. M., Davis, J., Lam, H., and Cacia, J. (2003). Use of process data to assess chromatographic performance in production-scale protein purification columns. *Biotechnol. Prog*., vol. 19, p. 485.
17. Ma, N. T., Wang, Y. F., Roe, B. A., and Harrison, R. G. (1995). Purification of an L-asparaginase—atrial natriuretic peptide fusion protein expressed in *Escherichia coli*. *Biotechnol. Bioeng*., vol. 47, p. 483.
18. Lightfoot, E. N., Sanchez-Palma, R. J., and Edwards, D. O. (1962). Chromatography and allied fixed-bed separations processes. In *Interscience Library Chemical Engineering Processing*, H. M. Schoen, ed., Interscience, New York, p. 99.
19. Lapidus, L., and Amundson, N. R. (1952). Mathematics of adsorption in beds. VI. The effect of longitudinal diffusion in ion exchange and chromatographic columns. *J. Phys. Chem*., vol. 56, p. 984.
20. Athalye, A. M., Gibbs, S. J., Lightfoot, E. N. (1992). Predictability of chromatographic separations. Study of size-exclusion media with narrow particle size distributions. *J. Chromatog*., vol. 589, p. 71.
21. Rasmuson, A., and Neretnieks, I. (1980). Exact solution of a model for diffusion in particles and longitudinal dispersion in packed beds. *AIChE J*., vol. 26, p. 686.
22. Van Deemter, J. J., Zuiderweg, F. J., and Klinkenberg, A. (1956). Longitudinal diffusion and resistance to mass transfer as causes of non-ideality in chromatography. *Chem. Eng. Sci*., vol. 5, p. 271.
23. Knox, J., and Scott, H. (1983). B and C terms in the van Deemter equation for liquid chromatography. *J. Chromatog*., vol. 282, p. 297.
24. Giddings, J. C. (1965). *Dynamics of Chromatography*, Pt. 1, *Principles and Theory*, Dekker, New York.
25. Peskin, A. P., and Rudge, S. R. (1992). Optimization of large-scale chromatography for biotechnological applications. *Applied Biochem. Biotechnol*., vol. 34/35, p. 49.
26. Gu, T. (1995). *Mathematical Modeling and Scale-up of Liquid Chromatography*. Springer, Berlin.
27. Garcia, F.A.P., Prazeres, D.M.F., and Cabral, J.M.S. (2002). Industrial biochromatography: Engineering aspects. In *Biochromatography*, M.A. Vijayalakshmi, ed., Taylor and Francis, London.
28. Nicoud, R.M., and Perrut, M. (1991). Operating modes, scale-up and optimization of chromatographic processes. In *Chromatographic and Membrane Processes in Biotechnology*, C.A. Costa and J.S. Carbral, eds., NATO ASI Series, Kluwer Academic Publishers, Dordrecht.
29. Pathak, N., Norman, C., Kundu, S., Nulu, S., and Durst, M. (2008). Modeling flow distribution in large-scale chromatographic columns with computational fluid dynamics. *BioProcess Int.*, vol. 6, p. 72.
30. Brandt, S., Goffe, R. A., Kessler, S. B., O'Connor, J. L., and Zale, S. E. (1988). Membrane-based affinity technology for commercial scale purifications. *Bio/technol.*, vol. 6, p. 779.
31. Ghosh, R. (2002). Protein separation using membrane chromatography: opportunities and challenges. *J. Chromatogr. A*, vol. 952, p. 13.
32. Yamamoto, S., and Sano, Y. (1992). Short-cut method for predicting the productivity of affinity chromatography. *J. Chromatogr*., vol. 597, p. 173.
33. Gerstner, J.A., Hamilton, R.H., and Cramer, S.M. (1992). Membrane chromatographic systems for high-throughput protein separations. *J. Chromatogr*., vol. 596, p. 173.

34. Avramescu, M. E., Borneman, Z., and Wessling, M. (2009) Membrane chromatography. In *Handbook of Membrane Separations*, A. K. Pabby, S. S. H. Rizvi, and A. M. Sastre, eds., CRC Press, Boca Raton, p. 25.
35. Fraud, N., Lim, J., Sinclair, A., and Gottschalk, U. (2010). Technical and economic benefits of membrane chromatography during polishing steps. *BioPharm Int*., vol. 23, p. 44.
36. GE Life Sciences technical literature. Available at www.gelifesciences.com.
37. Sartorius technical literature. Available at www.sartorius.com.
38. Zhou, J. X., Tressel, T., and Guhan, S. (2007). Disposable chromatography. *BioPharm Int*., vol. 20, p. 26.
39. Etzel, M.R., and Riordan, W. T. (2007). Membrane chromatography: analysis of breakthrough curves and viral clearance. In *Process Scale Bioseparations for the Biopharmaceutical Industry*, A. A. Shukla, M.R. Etzel, and S. Gadam, eds., Taylor and Francis, Boca Raton, p. 278.
40. Teeters, M. A., Conrady, S. E., Thomas, B. L., Root, T. W., and Lightfoot, E. N. (2003). Adsorptive membrane chromatography for purification of plasmid DNA. *J. Chromatogr. A*, vol. 989, p. 165.
41. Athalye, A. M., Gibbs, S. J., and Lightfoot, E. N. (1992). Predictability of chromatographic protein separations. Study of size-exclusion media with narrow particle size distributions. *J. Chromatog*., vol. 589, p. 71.
42. Klein, E. (1991). *Affinity Membranes*, Wiley, New York.
43. Imamoglu, S. (2002) Simulated moving bed chromatography (SMB) for application in bioseparation. In *Advances in Biochemical Engineering/Biotechnology*, vol. 76, T. Scheper, ed., Springer-Verlag, Berlin, p. 211.
44. Mazzotti, M., Storti, G., and Morbidelli, M. (1997), Optimal operation of simulated moving bed units for nonlinear chromatographic separations. *J. Chromatog. A*, vol. 769, p. 3.
45. Juza, M., Mazzotti, M., and Morbidelli, M. (2000), Simulated moving-bed chromatography and its application to chirotechnology. *Trends Biotechnol*., vol. 18, p. 108.
46. Migliorini, C., Mazzotti, M., and Morbidelli, M. (1998), Continuous chromatographic separation through simulated moving beds under linear and nonlinear conditions. *J. Chromatog. A*, vol. 827, p. 161.
47. Migliorini, C., Gentillini, A., Mazzotti, M., and Morbidelli, M. (1999), Design of simulated moving bed units under nonideal conditions. *Ind. Eng. Chem. Res*., vol. 38, p. 2400.
48. Scopes, R. K. (1982). *Protein Purification*, Springer-Verlag, New York.
49. Roettger, B. F., Myers, J. A., Ladisch, M. R., and Regnier, F. E. (1989). Adsorption phenomena in hydrophobic interaction chromatography. *Biotechnol. Prog*., vol. 5, p. 79.
50. Vunnum, S., Vedantham, G., and Hubbard, B. (2009). Protein A-based affinity chromatography. In *Process Scale Purification of Antibodies*, U. Bottschalk, ed., Wiley, Hoboken, NJ, p. 79.
51. Keller, G. E., Anderson, R. A., and Yon, C. M. (1987). Adsorption. In *Handbook of Separation Process Technology*, R. W. Rousseau, ed., Wiley-Interscience, New York, p. 644.
52. Thomas, W. J., and Crittenden, B. (1998). *Adsorption Technology and Design*, Butterworth-Heinemann, Oxford.
53. McCabe, W. L., Smith, J. C., and Harriott, P. (1993). *Unit Operations of Chemical Engineering*, McGraw-Hill, New York.
54. Collins, J. J. (1967). The LUB/equilibrium section concept for fixed-bed adsorption. *AIChE Symp. Ser.* 74, vol. 63, p. 31.
55. Chen, J. W., Buege, J. A., Cunningham, F. L., and Northam, J. I. (1968). Scale-up of a column adsorption process by computer simulation. *Ind. Eng. Chem. Process Des. Dev*., vol. 7, p. 1849.
56. Harrison, R. G. (1981). Antibiotic adsorption process using a non-ionic macroporous resin. *Presented at AIChE National Meeting*, Houston, 1981.
57. Levenspiel, O. (1962). *Chemical Reaction Engineering*, Wiley, New York.
58. Yamamoto, S., Nomura, M., and Sano, Y. (1987). Resolution of proteins in linear gradient elution ion-exchange and hydrophobic interaction chromatography. *J. Chromatog*., vol. 409, p. 101.
59. Yamamoto, S., Nakanishi, K., and Matsuno, R. (1988). *Ion-Exchange Chromatography of Proteins*, Dekker, New York.

/// 8 /// PRECIPITATION

Precipitation, which is the process of coming out of solution as a solid, is an important method in the purification of proteins that usually comes early in the purification process. Precipitation is frequently used in the commercial separation of proteins. The primary advantages of precipitation are that it is relatively inexpensive, can be carried out with simple equipment, can be done continuously, and leads to a form of the protein that is often stable in long-term storage. Since precipitation is quite tolerant of various impurities, including nucleic acids and lipids, it is used early in many bioseparation processes.

The goal of precipitation is often concentration to reduce volume, although significant purification can sometimes be achieved. For example, all the protein in a stream might be precipitated and redissolved in a smaller volume, or a fractional precipitation might be carried out to precipitate the protein of interest and leave many of the contaminating proteins in the mother liquor.

In this chapter the focus is first upon protein solubility, which is the basis of separations by precipitation. Then we discuss the basic concepts of particle formation and breakage and the distribution of precipitate particle sizes. The specific methods that can be used to precipitate proteins are treated next. The chapter concludes with methodology to use for the design of precipitation systems.

8.1 INSTRUCTIONAL OBJECTIVES

After completing this chapter, the reader should be able to do the following:

- Explain the various factors that influence protein solubility.
- Use the Cohn equation to predict solution equilibria (precipitation recoveries).
- Identify the distinct steps in the development of a precipitate.
- Calculate mixing times in an agitated precipitator, the kinetics of diffusion-limited growth of particles, and the kinetics of particle-particle aggregation.
- Perform particle balances as a function of particle size in a continuous-flow stirred tank reactor (CSTR).
- Explain the methods used to cause precipitation.

- Outline the advantages and disadvantages of the three basic types of precipitation reactor: the batch reactor, the CSTR, and the tubular reactor.
- Implement simple scaling rules for a precipitation reactor.

8.2 PROTEIN SOLUBILITY

Since proteins precipitate because they become insoluble, a knowledge of the factors that influence protein solubility is important in understanding why proteins precipitate. The most important factors affecting the solubility of proteins are structure and size, protein charge, and the solvent. Explanations follow for each of these factors.

8.2.1 Structure and Size

In the native state, a protein in an aqueous environment assumes a structure that minimizes the contact of the hydrophobic amino acid residues with the water solvent molecules and maximizes the contact of the polar and charged residues with the water. The major forces acting to stabilize a protein in its native state are hydrogen bonding, van der Waals interactions, and solvophobic interactions. In aqueous solution, these forces tend to push the hydrophobic residues into the interior of the protein and the polar and charged residues on the protein's surface. For example, one study of 36 globular proteins has shown that 95% of the ionizable groups are solvent accessible [1]. In other studies of 69 proteins, the average solvent-(water-) accessible atomic surface was found to be 57% nonpolar, 25% polar, and 19% charged [2, 3]. Thus, in spite of the forces operating to force hydrophobic residues to the protein's interior, the surface of proteins usually contains a significant fraction of nonpolar atoms.

The forces acting on a protein lead to the achievement of a minimum Gibbs free energy. For a protein in its native configuration, the net Gibbs free energy is on the order of only 10 to 20 kcal/mol. This is a relatively small net free energy, which means that the native structure is only marginally stable and can be destabilized by relatively small environmental changes [4].

Water molecules bind to the surface of the protein molecule because of association of charged and polar groups and immobilization by nonpolar groups. For example, a study of the hydration of human serum albumin found two layers of water around the protein [5]. In the layer next to the protein, the water molecules are almost totally oriented, with the hydrogen atoms adjacent to and facing the albumin surface, while the oxygen atoms face away from the protein surface. In the second layer of water molecules, most of the water molecules (70%) are nonoriented. These hydration layers are thought to promote solubility of the protein by maintaining a distance between the surfaces of protein molecules. This phenomenon is illustrated in Figure 8.1.

The size of a protein becomes important with respect to solubility when the protein is excluded from part of the solvent. This can happen when nonionic polymers that are added to the solution result in steric exclusion of protein molecules from the

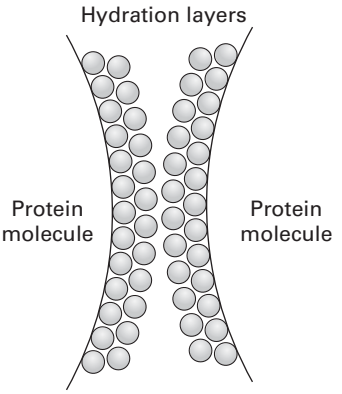

FIGURE 8.1 Schematic diagram of the limit of approach of two protein molecules to each other because of the hydration layers on the surface of each molecule.

volume of solution occupied by the polymer. Juckes [6] developed a model for this phenomenon based on the protein molecule being in the form of a solid sphere and the polymer molecule in the form of a rod, which gave the following equation for S, the solubility of the protein:

$$\ln S = \beta' - K' c_p \tag{8.2.1}$$

where

$$K' = \frac{\bar{V}}{2.303}\left(\frac{r_s + r_r}{r_s}\right)^3 \tag{8.2.2}$$

Here, r_s and r_r are the radius of the protein solute and polymer rod, respectively, $\bar{V}$ is the partial specific volume of the polymer, c_p is the polymer concentration, and β' is a constant. Based on this model, we can expect the lowest protein solubility for large proteins.

Molecular size is the predominant factor in a type of precipitation known as affinity precipitation. When affinity groups or antibodies to a specific biomolecule (antigen) are added to a solution, the antibody-antigen interaction can form large multimolecular complexes as shown in Figure 8.2. Such complexes are usually insoluble and cause selective precipitation of the antigen. The average size of the complex agglomerates is maximized when there is a stoichiometric ratio of antibody and antigen. If either is present in great excess, only bimolecular complexes will be formed; and there may be no precipitation, or low recovery, even if a precipitate is formed.

8.2.2 Charge

The net charge of a protein has a direct bearing upon the protein's solubility. The solubility of a protein increases as its net charge increases, a result of greater interaction

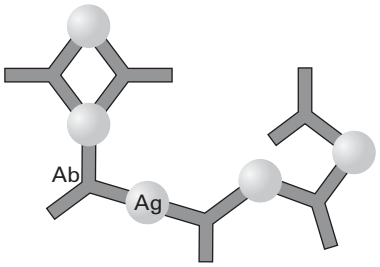

FIGURE 8.2 Schematic representation of antibody-antigen (Ab-Ag) interaction.

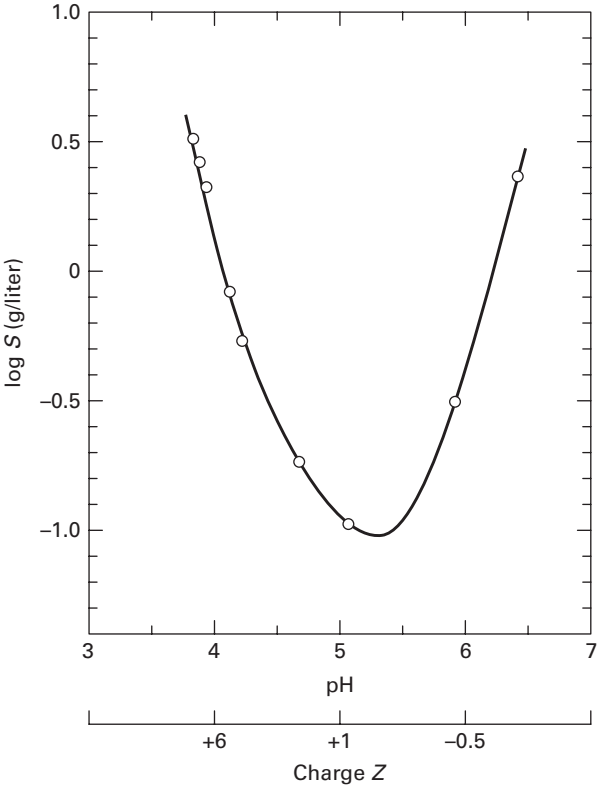

FIGURE 8.3 The solubility (S) of insulin in 0.1 N NaCl as a function of pH. The charge Z is the average protonic charge per 12,000 g of insulin at the pH values indicated. *(Data from C. Tanford,* Physical Chemistry of Macromolecules*, p. 242, Wiley, New York, 1961.)*

with dipolar water molecules. A repulsive reaction between protein molecules of like charge further increases solubility.

A simple way to vary the charge on a protein is by changing the pH of the solution. The pH of the solution in which a protein has zero net charge is called the isoelectric pH or isoelectric point. The solubility of a protein is, in general, at its minimum at the isoelectric point. A typical example is shown in Figure 8.3. Nonuniform charge distribution, however, results in a dipole moment on the molecule, which

leads to an increase in solubility and a move in the minimum solubility away from the isoelectric point. The effect of the dipole moment is discussed further in the following section.

The net charge of a protein is determined by the following factors: the total number of ionizable residues, the accessibility of the ionizable residues to the solvent, the dissociation constants (or pK_a values) of the ionizable groups, and the pH of the solution [7]. Besides the chemical makeup of the ionizable groups, factors that can influence the pK_a values are the chemical nature of the neighboring groups (e.g., inductive effects), the temperature, the chemical nature of the solvent as partially reflected by its dielectric constant, and the ionic strength of the solvent.

8.2.3 Solvent

The solvent affects the solubility of proteins primarily through two parameters, hydrophobicity and ionic strength. The first of these parameters has been well studied through observations of single-phase solutions of water and monohydric alcohols. Although these solutions can cause protein denaturation at room temperature, denaturation can be avoided at sufficiently low temperatures. Studies of monohydric alcohols have shown that denaturing efficiency is as follows:

$$\text{methanol} < \text{ethanol} < \text{propanol} < \text{butanol}$$

This led to the conclusion that the alcohols with longer alkyl chains are binding more effectively to apolar groups on the protein, weakening intraprotein hydrophobic interactions and thus leading to denaturation [8]. It is thought that when the temperature is low, the monohydric alcohols compete for the water of hydration on the protein and cause the protein molecules to approach more closely, so that van der Waals interactions lead to aggregation.

The ionic strength of the solvent can have both solubilizing and precipitating effects. The solubilizing effects are referred to as salting in, while the precipitating actions are called salting out. The salting-in effect has been observed for several proteins, including the class of proteins named euglobulins. These proteins are insoluble in the absence of salt at their isoelectric points but become soluble when salt is added. In contrast, members of another class of proteins, the albumins, are very soluble in water as well as in high concentrations of salt. It is believed that the solubilities of the euglobulins and the albumins differ because the euglobulins have a much higher dipole moment than the albumins [9].

A theoretical treatment of the interactions between ions and dipoles developed in 1943 by Kirkwood [10] accounts for salting-in effects by considering the solute size, solute shape, solute dipole moment, solvent dielectric constant, solution ionic strength, and temperature. One of Kirkwood's models was for a spherical dipolar

ion with a point dipole moment u located at the center of the sphere. The equation derived to describe the interactions is as follows:

$$\ln\left(\frac{S_p}{S_0}\right) = K_i I - K_s I \tag{8.2.3}$$

where S_p is the solubility of the dipolar ion at ionic strength I, S_0 is the solubility of the dipolar ion in the absence of salt, K_i is the salting-in constant, and K_s is the salting-out constant. Ionic strength is defined by

$$I = \frac{1}{2}\sum_i c_i z_i^2 \tag{8.2.4}$$

where c_i is the molar concentration of any ion and z_i is its charge. The salting-in and salting-out constants can be related to other variables as follows [7]:

$$K_i \propto \left(\frac{u}{\varepsilon T}\right)^2 \tag{8.2.5}$$

$$K_s \propto \left(\frac{V_e}{\varepsilon T}\right) \tag{8.2.6}$$

where ε is the dielectric constant of the solvent, T is temperature, and V_e is the excluded volume of the dipolar ion. Equations (8.2.3) and (8.2.5) confirm the observed strong relationship between the solubility of dipolar proteins and the size of their dipole moment u, as well as the greater salting-in effect observed with proteins with high dipole moments. Also, it can be seen that the salting-in term increases more than the salting-out term as the dielectric constant decreases. The dielectric constant decreases as the polarity of the solvent decreases. Therefore, the salting-in effect tends to predominate in relatively nonpolar solvents, while the salting-out effect is more dominant in aqueous solvents.

At high ionic strength, the salting-out effect becomes predominant and can be described empirically by the Cohn equation [11]:

$$\ln S = \beta - K_s' I \tag{8.2.7}$$

where S is the solubility of the protein and K_s' is a salting-out constant characteristic of the specific protein and salt that is independent of temperature and pH above the isoelectric point. The constant β, the hypothetical solubility of the protein at zero ionic strength, depends only on temperature and pH for a given protein and is a minimum at the isoelectric point. It is interesting that the Cohn equation is identical in form to the equation that describes the precipitation of proteins by the addition of nonionic polymers, Equation (8.2.1). In addition, the Kirkwood equation for the solubility of dipolar ions [Equation (8.2.3)] can be arranged to give

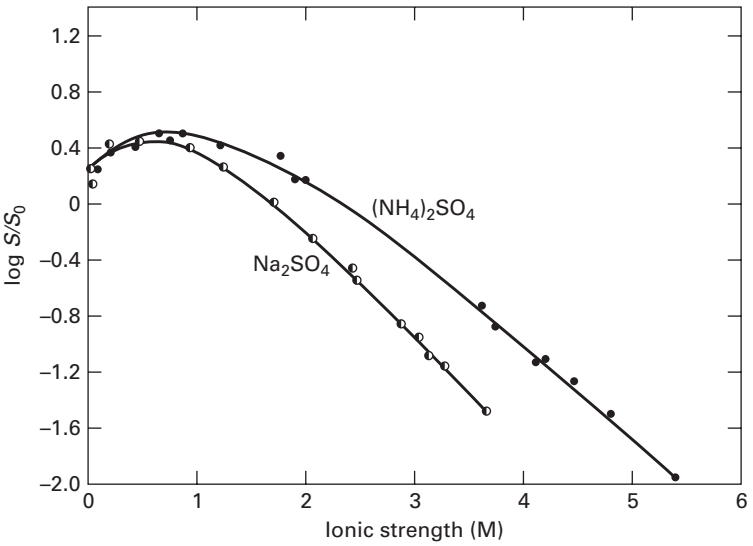

FIGURE 8.4 The effect of $(NH_4)_2SO_4$ and Na_2SO_4 on the solubility of hemoglobin: S_0 is the solubility in pure water, and S is the solubility in the salt solution. *(Data from C. Tanford,* Physical Chemistry of Macromolecules*, p. 244, Wiley, New York, 1961.)*

$$\ln S_p = \ln S_0 - \left(K_s - K_i\right) I \tag{8.2.8}$$

which is also identical in form to the Cohn equation, with

$$\beta = \ln S_0 \tag{8.2.9}$$

$$K_s' = K_s - K_i \tag{8.2.10}$$

Both salting in and salting out are illustrated in Figure 8.4 for hemoglobin with ammonium sulfate or sodium sulfate being added. From zero ionic strength, the solubility of the protein increases to a maximum as salt is added and then continuously decreases as even more salt is added.

EXAMPLE 8.1

Salting Out of a Protein with Ammonium Sulfate Data were obtained on the precipitation of a protein by the addition of ammonium sulfate. The initial concentration of the protein was 15 g/liter. At ammonium sulfate concentrations of 0.5 and 1.0 M, the concentrations of the protein remaining in the mother liquor at equilibrium were 13.5 and 5.0 g/liter, respectively. From this information, estimate the ammonium sulfate concentration to give 95% recovery of the protein as precipitate.

Solution

We can use the Cohn equation [Equation (8.2.7)], to solve this problem if we can determine the constants in the equation. Since ionic strength is directly proportional to concentration c for a given salt [Equation (8.2.4)], we can rewrite the Cohn equation as

$$\ln S = \beta - K_s'' c$$

Substituting the experimental data into this equation gives

$$\ln 13.5 = \beta - 0.5K_s''$$
$$\ln 5.0 = \beta - 1.5K_s''$$

Solving these equations for the constants yields

$$\beta = 3.60$$
$$K_s'' = 1.99\,\mathrm{M}^{-1}$$

For 95% recovery, the protein solubility in the mother liquor at equilibrium is 5% of the initial protein concentration. At this solubility, from the Cohn equation

$$c = \frac{\beta - \ln S}{K_s''} = \frac{3.60 - \ln\left(0.05 \times 15\right)}{1.99} = 1.95\,\mathrm{M}$$

8.3 PRECIPITATE FORMATION PHENOMENA

By studying the phenomena of precipitate formation, we can maximize our control over the characteristics of the final protein precipitate. Important characteristics of protein precipitates are the particle size distribution, density, and mechanical strength. Normally, it is desired to avoid having a large fraction of particles in the small size range. For proteins, particle sizes near or below 1 μm are considered to be small. Protein precipitates that consist largely of particles with small particle sizes can be difficult to filter or centrifuge. Low particle densities also can lead to filtration or centrifugation problems and can give excessive bulk volumes of the final dried precipitate. Particles with low mechanical strength can give problems with excessive attrition when the dry particles are moved. Low strength can also be interpreted as gel formation, which leads to major problems in filtration and centrifugation.

Precipitates form by a series of steps that occur in sequence, which are the following: (1) initial mixing, (2) nucleation, (3) growth governed by diffusion, and (4) growth governed by fluid motion. There is often some overlap between these

steps. The final size of the precipitate particles during step 4 is subject to the limits imposed by particle breakage during mixing. The completion of the growth by fluid motion step can be followed by an "aging" step, where the particles are mixed until reaching a stable size.

8.3.1 Initial Mixing

Initial mixing is the mixing required to achieve homogeneity after the addition of a component to cause precipitation. It is important to bring precipitant and product molecules into collision as soon as possible. This is a problem in "micromixing," which is also important in fermentation. This subject was studied by the Russian statistician Kolmogoroff in the form of the homogeneous isotropic turbulence model, which assumes that mixing between randomly dispersed eddies is instantaneous and the mixing within eddies is diffusion limited. It is therefore important to know the mean length of eddies, also known as the "Kolmogoroff length," here designated l_e. It can be calculated from [12]

$$l_e = \left(\frac{\rho \nu^3}{P/V} \right)^{1/4} \tag{8.3.1}$$

where ρ is the liquid density, ν is the liquid kinematic viscosity, and P/V is the agitator power input per unit volume of liquid.

It is necessary to mix until all molecules have diffused across all eddies. This time can be estimated from the Einstein diffusion relationship (see Section 5.7.1):

$$t = \frac{\delta^2}{2\mathscr{D}} \tag{8.3.2}$$

where δ is the diffusion distance and $\mathscr{D}$ is the diffusion coefficient for the molecule being mixed. For spherical eddies of diameter l_e, this becomes

$$t = \frac{l_e^2}{8\mathscr{D}} \tag{8.3.3}$$

Thus, precipitation is initiated in a well-stirred tank for a period of time determined on the basis of isotropic turbulence.

8.3.2 Nucleation

Nucleation is the generation of particles of ultramicroscopic size. For particles of a given solute to form, the solution must be *supersaturated* with respect to the solute. In a supersaturated solution the concentration of the solute in solution is greater than

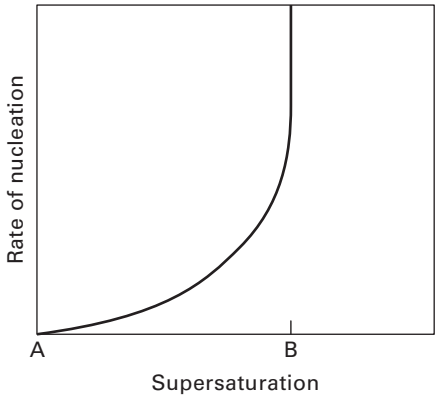

FIGURE 8.5 Nucleation rate as a function of degree of supersaturation. The normal equilibrium solubility is at A, and the supersaturation limit is at B.

the normal equilibrium solubility of the solute. The difference between the actual concentration in solution and the equilibrium solubility is called the degree of supersaturation, or just supersaturation. The rate of nucleation increases exponentially up to the maximum level of supersaturation, or supersaturation limit, which is illustrated in Figure 8.5. It should be noted that the rate of nucleation increases to a very high value at the supersaturation limit.

High supersaturations generally have negative consequences in carrying out precipitations. When the supersaturation is high, the precipitate tends to be in the form of a colloid, a gel, or a highly solvated precipitate. To obtain precipitate particles having desirable characteristics, the supersaturation should be kept relatively low.

8.3.3 Growth Governed by Diffusion

The growth of precipitate particles is limited by diffusion immediately after nucleation and until the particles grow to a limiting particle size defined by the fluid motion, which generally ranges from 0.1 to 10 μm for high-and low-shear fields, respectively [13]. In a dispersion of particles of uniform size that are growing as dissolved solute diffuses to the particles, the initial rate of decrease of particle number concentration (N) can be described by a second-order rate equation that was first derived by Smoluchowski [14]:

$$-\frac{dN}{dt} = K_A N^2 \tag{8.3.4}$$

Here N is the number of mono-sized particles at any given time t. The constant K_A is determined by the diffusivity $\mathscr{D}$ and diameter L_{mol} of the molecules that are adding to the particles as follows:

$$K_A = 8\pi \mathscr{D} L_{\text{mol}} \tag{8.3.5}$$

Integrating Equation 8.3.4 gives

$$N = \frac{1}{K_A t + 1/N_0} \tag{8.3.6}$$

For convenience, N_0 is taken as the initial number concentration of dissolved solute molecules. The Stokes-Einstein equation can be used to estimate the diameter of globular proteins, which can be modeled as spheres:

$$L_{\text{mol}} = \frac{kT}{3\pi \mathscr{D} \mu} \tag{8.3.7}$$

where k is the Boltzmann constant, T is the absolute temperature, and μ is the liquid viscosity.

Equation (8.3.6) can be rewritten as

$$\frac{N}{N_0} = \frac{1}{1 + N_0 K_A t} \tag{8.3.8}$$

With M as the molecular weight of particles at time t and M_0 as the molecular weight of the solute,

$$\frac{M}{M_0} = \frac{N_0}{N} \tag{8.3.9}$$

so that

$$M = M_0 \left(1 + K_A N_0 t\right) \tag{8.3.10}$$

This equation has been verified experimentally by measuring the molecular weight of precipitating α-casein. The data plotted in Figure 8.6 indicate good agreement with Equation (8.3.10) after an initial lag time.

EXAMPLE 8.2

Calculation of Concentration of Nuclei in a Protein Precipitation We wish to precipitate the protein α_2-macroglobulin contained in 100 liters of aqueous solution at 20°C in a tank at a concentration of 0.2 g/liter. α_2-Macroglobulin is a globular protein with a molecular weight of 820,000 and a diffusion coefficient of 2.41×10^{-7} cm^2/s at 20°C. (Data from *Handbook of Biochemistry and Molecular Biology,* vol. III, G. D. Fasman, ed., CRC Press, Cleveland, 1976.) The precipitate particles have a density of 1.3 g/cm^3. The solution is stirred with a 75 W (0.1 hp) motor. Calculate the concentration of nuclei at the end of the "initial mixing" period.

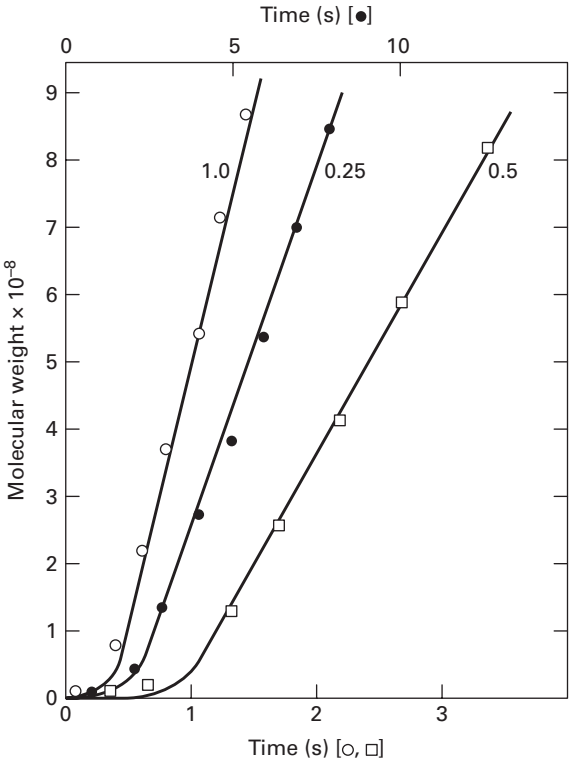

FIGURE 8.6 Molecular weight–time plots for three concentrations of α_3-casein (concentrations as indicated on graph in kilograms per cubic meter), aggregating in the presence of 0.008 M $CaCl_2$. Molecular weight was determined from light-scattering and turbidity measurements. *(Data from D. J. Bell, M. Hoare, and P. Dunnill, "The formation of protein precipitates and their centrifugal recovery,"* Adv. Biochem. Eng., *vol. 26, p. 20, Springer-Verlag, Berlin, 1983.)*

Solution

During the initial stirring, diffusion-limited molecular collisions occur, and molecules must travel by diffusion across an eddy in order to meet. The time required for this is determined by combining the Einstein diffusion equation for spherical eddies [Equation (8.3.3)] and the equation for the Kolmogoroff eddy length l_e, or the average diameter of an unstirred zone [Equation (8.3.1)]. Assume the properties of water since the solution is dilute, so that $\rho = 1.0$ g/cm^3 and v = kinematic viscosity = 0.01 cm^2/s. First, convert power per unit volume to appropriate units:

$$\frac{P}{V} = \left(\frac{75\ \text{W}}{100\ \text{liters}}\right)\left(\frac{10^7\ \text{g cm}^2\text{s}^{-3}}{\text{W}}\right)\left(\frac{1\ \text{liter}}{1000\ \text{cm}^3}\right)$$

$$= 7.5 \times 10^3\ \frac{\text{g cm}^2\text{s}^{-3}}{\text{cm}^3}$$

Therefore,

$$t = \frac{\left(\frac{\rho\nu^3}{P/V}\right)^{1/2}}{8\mathscr{D}} = \frac{\left(\frac{1.00(0.01)^3}{7.5\times10^3}\right)^{1/2}}{8\left(2.41\times10^{-7}\right)} = 6.0\,\text{s}$$

Since diffusion is limiting during this 6 s period, the number concentration of nuclei N can be determined from the integrated form of the second-order rate equation for the growth of particles limited by diffusion [Equation (8.3.6)]:

$$N = \frac{1}{K_A t + 1/N_0}$$

where $K_A = 8\pi\mathscr{D}L_{\text{mol}}$. Since globular proteins are approximately spherical, we can estimate the diameter L_{mol} of the molecule from the Stokes-Einstein equation [Equation (8.3.7)]:

$$L_{\text{mol}} = \frac{kT}{3\pi\mu\mathscr{D}} = \frac{\left(1.38\times10^{-23}\,\frac{\text{J}}{\text{K}}\right)(293\,\text{K})\left(\frac{10^7\,\text{g cm}^2\text{s}^{-3}}{\text{J s}^{-1}}\right)}{3\pi\left(0.01\frac{\text{g}}{\text{cm s}}\right)\left(2.41\times10^{-7}\,\frac{\text{cm}^2}{\text{s}}\right)} = 1.78\times10^{-6}\,\text{cm}$$

This value of L_{mol} allows us to calculate K_A:

$$K_A = 8\pi(2.41\times10^{-7}\,\text{cm}^2\text{s}^{-1})(1.78\times10^{-6}\,\text{cm}) = 1.08\times10^{-11}\,\text{cm}^3\text{s}^{-1}$$

N_0 is the number concentration of protein molecules that are dissolved before starting precipitation, so that

$$N_0 = \left(\frac{0.2\,\text{g}}{\text{liter}}\right)\left(\frac{\text{liters}}{1000\,\text{cm}^3}\right)\left(\frac{\text{mol}}{820{,}000\,\text{g}}\right)\left(6.02\times10^{23}\,\frac{\text{molecules}}{\text{mol}}\right)$$
$$= 1.47\times10^{14}\,\frac{\text{molecules}}{\text{cm}^3}$$

Substituting into Equation (8.3.6) for N, we obtain after the initial 6 s mixing period

$$N = \left[\left(1.08\times10^{-11}\,\text{cm}^3\text{s}^{-1}\right)(6.0\,\text{s}) + \left(1.47\times10^{14}\,\text{cm}^{-3}\right)^{-1}\right]^{-1}$$
$$= \left[(6480 + 0.7)\times10^{-14}\,\text{cm}^3\right]^{-1} = 1.54\times10^{10}\,\frac{\text{particles}}{\text{cm}^3}$$

In this calculation we note that the term involving N_0 is very small, and thus the initial number of molecules is not important to the calculation.

EXAMPLE 8.3

Diffusion-Limited Growth of Particles For the protein precipitation in Example 8.2, calculate the time for the particles to reach a size of 1.0 μm, assuming that growth is governed by diffusion only up to this particle size. Also calculate the number concentration of the 1.0 μm particles.

Solution

Assuming spherical particles, we can calculate the number of molecules per 1.0 μm particle from the volume per particle, the particle density, and the molecular weight of the protein. This enables us to calculate the ratio of the molecular weight of the particle to that of an individual molecule, M/M_0, and from this ratio we can calculate the time to reach this particle size by rearranging Equation (8.3.10):

$$t = \frac{\dfrac{M}{M_0} - 1}{K_A N_0}$$

$$\frac{\text{Volume}}{\text{Particle}} = \frac{\pi\left(10^{-4}\,\text{cm}\right)^3}{6} = 5.23 \times 10^{-13}\,\text{cm}^3$$

$$\frac{\text{Mass}}{\text{Particle}} = \left(5.23 \times 10^{-13}\,\text{cm}^3\right)\left(\frac{1.3\,\text{g}}{\text{cm}^3}\right) = 6.80 \times 10^{-13}\,\text{g}$$

$$\frac{\text{Molecules}}{\text{Particle}} = \left(6.80 \times 10^{-13}\,\text{g}\right)\left(\frac{\text{mol}}{820{,}000\,\text{g}}\right)\left(\frac{6.02 \times 10^{23}\,\text{molecules}}{\text{mol}}\right)$$

$$= 4.99 \times 10^5\,\text{molecules}$$

Therefore,

$$\frac{M}{M_0} = 4.99 \times 10^5$$

Substituting into the equation for time using the values of K_A and N_0 calculated in Example 8.2, we obtain

$$t = \frac{\left(4.99 \times 10^5\right) - 1}{\left(1.08 \times 10^{-11}\,\text{cm}^3\text{s}^{-1}\right)\left(1.47 \times 10^{14}\,\text{cm}^{-3}\right)\left(\dfrac{60\,\text{s}}{\text{min}}\right)} = 5.24\,\text{min}$$

We can easily calculate N from Equation (8.3.9):

$$N = \frac{N_0 M_0}{M} = \frac{1.47 \times 10^{14}}{4.99 \times 10^5} = 2.95 \times 10^8 \ \frac{\text{particles}}{\text{cm}^3}$$

8.3.4 Growth Governed by Fluid Motion

Growth of particles is governed by fluid motion after the particles have reached a critical size, typically 1 μm in diameter [12]. In this growth regime, particles tend to grow by colliding and then sticking together. This is a flocculation process, governed by the factors discussed in detail in Chapter 3. Flocculation is enhanced when electrostatic repulsion between particles is reduced in comparison to the attractive van der Waals force. This can be accomplished by raising the ionic strength and lowering the temperature, to reduce the thickness of the electrical double layer, or Debye length, around particles.

For particles of uniform size in a suspension, the initial rate of decrease of particle number concentration (N) due to collisions can be described by a second-order rate equation:

$$-\frac{dN}{dt} = \frac{2}{3} \alpha L^3 \gamma N^2 \tag{8.3.11}$$

which was also derived by Smoluchowski [14]. Here α is the collision effectiveness factor (fraction of collisions that result in permanent aggregates), L is the diameter of the particles, and γ is the shear rate (velocity gradient). Assuming that the volume fraction of the particles ($\varphi = \pi L^3 N/6$) is constant during particle growth governed by fluid motion, Equation (8.3.11) becomes

$$-\frac{dN}{dt} = \frac{4}{\pi} \alpha \phi \gamma N \tag{8.3.12}$$

Integrating Equation (8.3.12) yields

$$\frac{N}{N_0} = \exp\left(\frac{-4 \alpha \phi \gamma t}{\grave{A}} \right) \tag{8.3.13}$$

where N_0 is now the particle number concentration at the time [$t = 0$ in Equation (8.3.13)] at which particle growth starts to be governed by fluid motion. For turbulent flow, the average shear rate $\bar{\gamma}$ can be estimated by the following equation developed by Camp and Stein [15]:

$$\bar{\gamma} = \left(\frac{P/V}{\rho \nu} \right)^{1/2} \tag{8.3.14}$$

where P/V is power dissipated per unit volume, and ρ and v are the density and kinematic viscosity of the liquid, respectively.

EXAMPLE 8.4

Growth of Particles Limited by Fluid Motion Calculate the time required for the 1 μm particles in Example 8.3, to reach a size of 20 μm when growth is limited by fluid motion and assuming that the flow is turbulent.

Solution

Here we use Equation (8.3.13) for particles growing by colliding and sticking together. Solving Equation (8.3.13) for time, we obtain

$$t = \frac{\pi \ln \dfrac{N_0}{N}}{4\alpha\phi\gamma}$$

From Example 8.3, N_0 is the particle concentration of 1 μm particles (= 2.95×10^8 particles/cm^3). We can find the particle concentration N of 20 μm particles from the volume of these particles, assuming spherical particles and 100% of the protein mass is 20 μm particles, so that

$$N = \frac{\dfrac{c_{i0}}{\rho_p}}{\dfrac{\pi L^3}{6}} = \frac{\left(\dfrac{0.2\,\text{g}}{\text{liter}}\right)\left(\dfrac{\text{liters}}{10^3\,\text{cm}^3}\right)\left(\dfrac{\text{cm}^3}{1.3\,\text{g}}\right)}{\dfrac{\pi\left(2\times10^{-3}\,\text{cm}\right)^3}{6}} = 3.67\times10^4\,\frac{\text{particles}}{\text{cm}^3}$$

where c_{i0} is the feed concentration of the protein before starting the precipitation, and ρ_p is the density of protein particles. The volume fraction φ of particles is assumed to be constant, so we will calculate it for the 20 μm particles:

$$\varphi = \left[\frac{\pi(2\times10^{-3})^3}{6}\,\frac{\text{cm}^3}{\text{particle}}\right]\left[3.67\times10^4\,\frac{\text{particle}}{\text{cm}^3}\right] = 0.000154$$

The shear rate γ is estimated from the equation of Camp and Stein for the average shear rate in turbulent flow [Equation (8.3.14)], where we use the P/V calculated in Example 8.2:

$$\bar{\gamma} = \left(\frac{P/V}{\rho\nu}\right)^{1/2} = \left(\frac{7.5\times10^3}{(1.0)(0.01)}\right)^{1/2} = 866\,\text{s}^{-1}$$

Using a conservative value of the collision effectiveness factor α of 0.05 [12], we obtain

$$t = \frac{\pi \ln\left(\frac{2.95\times10^{8}}{3.67\times10^{4}}\right)}{4(0.05)(0.000154)(866)} = 1059\,\text{s} = 17.6\,\text{min}$$

8.3.5 Precipitate Breakage

When precipitate particles grow large enough by colliding and sticking together, they become susceptible to breakage during collisions. The rate of precipitate breakage has been shown to depend on the shear rate and particle concentration. In a study of soy protein precipitate particles, for example, particle breakup dominated at sizes greater than 16 μm, and breakup became negligible at low particle volume fractions (0.0002) [16].

A model that has successfully described the breakup of protein precipitates is the displacement model, which depicts the rate of aggregate size change as a function of displacement from an equilibrium aggregate diameter, L_e [17]:

$$\frac{dL}{dt} = k\left(L_e - L\right)^n \tag{8.3.15}$$

where the rate constant k would be expected to depend on the volume fraction of particles φ and the shear rate γ. This model with $n = 1$ (first order) fits data well for the mean diameter of soy protein particles at constant shear and various particle concentrations (Figure 8.7). The equilibrium diameter L_e has been shown to depend on the shear rate. For soy protein precipitate in laminar Couette shear [17],

$$\bar{L}_{e,v} \propto \gamma^{-0.14}, \quad 2000\,\text{s}^{-1} \le \gamma \le 80{,}000\,\text{s}^{-1} \tag{8.3.16}$$

and for casein precipitated by salting out in a continuous stirred tank reactor [17],

$$\bar{L}_{e,v} \propto \gamma^{-0.21}, \quad 12\,\text{s}^{-1} \le \bar{\gamma} \le 154\,\text{s}^{-1} \tag{8.3.17}$$

where $\bar{L}_{e,v}$ is the equilibrium particle size at the volume mean of the particle size distribution. Particle breakage is also discussed in the analysis of the particle size distribution in a continuous-flow stirred tank reactor (Section 8.4).

8.3.6 Precipitate Aging

As indicated in Figure 8.7, protein precipitate particles reach a stable size after a certain length of time in a shear field. The time period for reaching this stable size

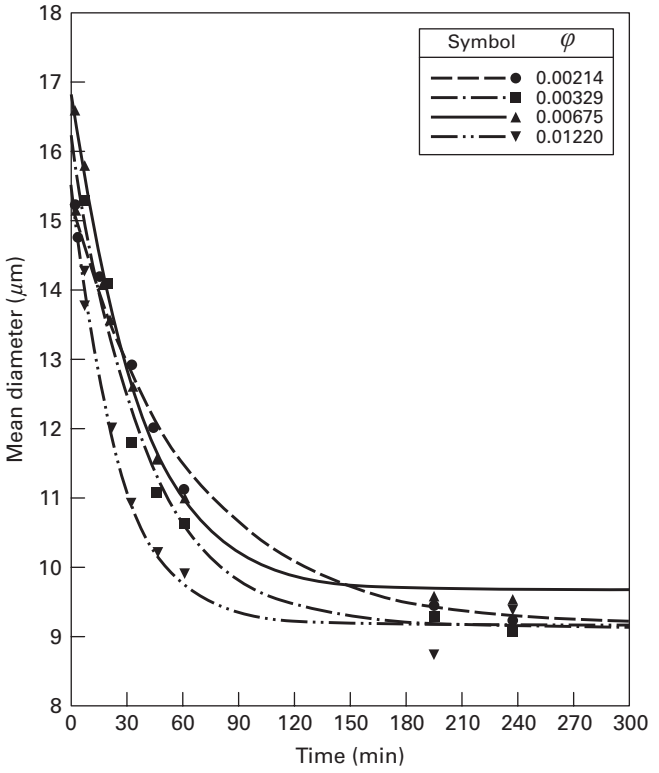

FIGURE 8.7 Volume mean aggregate diameter as a function of time for soy precipitate particles exposed to shear rate of 1340 s^{-1} at different particle volume fractions (φ). Lines are drawn for the displacement model. Points are experimental data. *(Data from D. L. Brown and C. E. Glatz, "Aggregate breakage in protein precipitation,"* Chem. Eng. Sci., *vol. 42, p. 1831, 1987.)*

is called the "aging" time. The strength of protein particles has been correlated with the product of the mean shear rate and the aging time, $\bar{\gamma}t$, which is known as the *Camp number*. As indicated in Figure 8.8 for soy protein particles, the mean particle size becomes approximately constant after reaching a Camp number of 10^5. Aging of precipitates helps the particles withstand processing in pumps and centrifuge feed zones without further size reduction.

8.4 PARTICLE SIZE DISTRIBUTION IN A CONTINUOUS-FLOW STIRRED TANK REACTOR

The equations describing precipitate formation and breakage in the preceding section are convenient to use when the size of the precipitate is changing with time. In addition to being applicable to the batch reactor, these equations can also be used to describe precipitate growth in the tubular reactor (see Section 8.6). However, for one important type of reactor—the continuous-flow stirred tank reactor (CSTR)—operation is

at steady state. Because precipitated protein leaves the CSTR at the same time the feed protein solution enters, the product stream leaving the CSTR will have a *range of particle sizes,* which does not vary with time for operation at steady state. The distribution of particle sizes can be characterized by performing a population balance for precipitate particles in the CSTR [18]. Before writing the population balance, it is first necessary to define the population density distribution function $n(L)$ and the linear growth rate G:

$$n(L) \equiv \frac{dN}{dL} \tag{8.4.1}$$

$$G \equiv \frac{dL}{dt} \tag{8.4.2}$$

Thus, if we know $n(L)$, we can take the integral of $n(L)dL$ to find the total number of particles within two given particle diameters.

Making a balance on the number ΔN of precipitate particles within a given size range ΔL gives

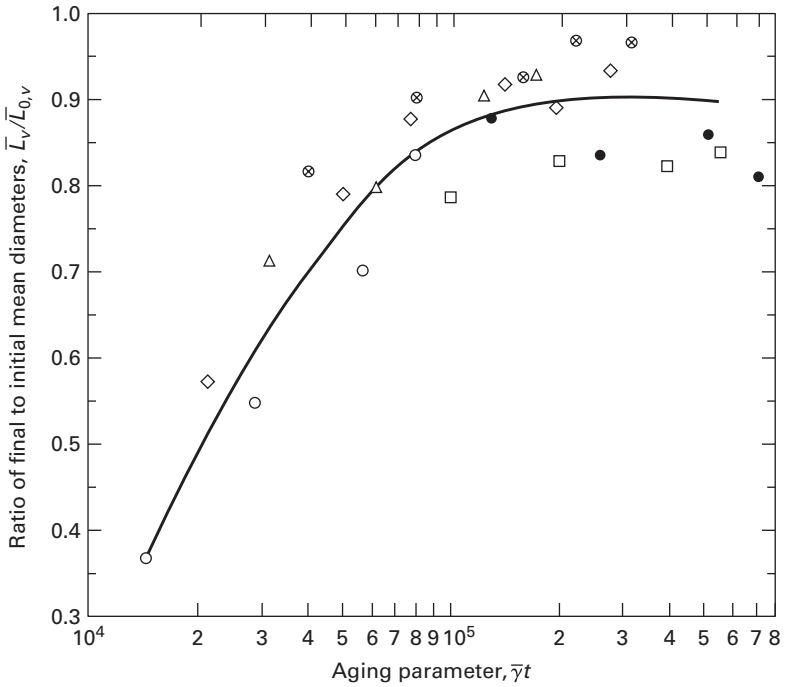

FIGURE 8.8 The effect of aging on the change in the volume mean diameter of soy protein precipitate particles exposed to capillary shear. Average capillary rate of shear, 1.7×10^4 s^{-1}; average time of exposure in capillary, 0.065 s; protein concentration, 30 kg m^{-3}; initial mean diameter $\bar{L}_{o,}$ (μm) prior to exposure to capillary shear: ○, 53.5; Δ, 23.4; ◊, 19.5; ⊗, 15.2; □, 10.2; ●, 8.8. *(Data from D. J. Bell and P. Dunnill, "Shear disruption of soya protein precipitate particles and the effect of aging in a stirred tank,"* Biotechnol. Bioeng., *vol. 24, p. 1271, 1982.)*

$$\begin{aligned}(\text{Accumulation of particles}) = &(\text{particles growing into range})\\ &-(\text{particles growing out of range})\\ &-(\text{particles of given range flowing out})\\ &-(\text{particles in range broken up})\end{aligned} \tag{8.4.3}$$

For steady state operation there is no accumulation, so that the balance on particles in the L to $L + \Delta L$ size range is

$$0 = \left(V\frac{dN}{dt}\right)_{\text{growth},L} - \left(V\frac{dN}{dt}\right)_{\text{growth},L+\Delta L} - Q\Delta N - VB\Delta L \tag{8.44}$$

where Q is the volumetric flow rate, V is the volume of the CSTR, and B is the volumetric breakage or death rate of particles in the size range L to $L + \Delta L$, such that the net rate of disappearance of particles due to breakage per volume is $B\Delta L$. Using the definitions of n and G, this equation becomes

$$(VnG)\big|_L - (VnG)\big|_{L+\Delta L} - Qn\Delta L - VB\Delta L = 0 \tag{8.4.5}$$

Dividing by ΔL and taking the limit as $\Delta L \to 0$, we obtain for constant reactor volume V

$$V\frac{d(nG)}{dL} + Qn + VB = 0 \tag{8.4.6}$$

or

$$\frac{d(nG)}{dL} + \frac{n}{\tau} + B = 0 \tag{8.4.7}$$

where τ is the mean residence time (= V/Q).

The growth of protein precipitate particles in a CSTR has been successfully described by Petenate and Glatz [19], who used the following expression for the linear growth rate:

$$G = \frac{dL}{dt} = \left(\frac{A}{4\pi}\right)\gamma\varphi_1 L = K_0 L \tag{8.4.8}$$

where A is a constant and φ_1 is the volume fraction of submicrometer-sized "primary" particles. In this model, aggregates above a critical diameter L_0 grow because small primary particles collide with aggregates and stick (see Figure 8.9). Primary particles typically have diameters of about 0.2 μm for protein precipitation in a CSTR [19].

The larger a precipitate aggregate becomes, the more susceptible it is to being broken up by the local shear stresses encountered in turbulent flow. For the conditions under which local shear stresses are dominant, the following equation for the volumetric breakage or death rate has been successfully used by Petenate and Glatz [19] to describe the breakup of protein aggregates:

$$B = K\mu\gamma^2 n L^3 = K_1 n L^3 \tag{8.4.9}$$

where K is a constant and μ is the viscosity.

A useful parameter to know for the precipitation in a CSTR is the mass-averaged particle size. For spherical particles, the total mass concentration M_T in terms of the mass-averaged diameter $\bar{L}_m$ is

$$M_T = \rho_p \pi \left(\frac{\bar{L}_m^3}{6} \right) N \tag{8.4.10}$$

where ρ_p is the density of individual particles and N is the total particle number concentration. From $n(L)$, we can determine M_T and N for spherical particles equal or greater than L_0 in size as follows:

$$M_T\big|_{L \geq L_0} = \frac{\rho_p \pi}{6} \int_{L_0}^{\infty} L^3 n(L)\, dL \tag{8.4.11}$$

$$N\big|_{L \geq L_0} = \int_{L_0}^{\infty} n(L)\, dL \tag{8.4.12}$$

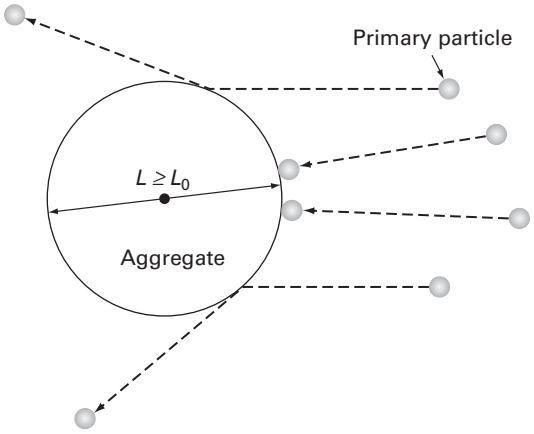

FIGURE 8.9 Schematic drawing of the growth of a precipitate aggregate by collisions of the aggregate with small primary particles: L_0 is the critical diameter above which particles grow by colliding with and sticking to small primary particles.

Combining Equations (8.4.10), (8.4.11), and (8.4.12) gives the mass-averaged particle diameter for $L \geq L_0$:

$$\bar{L}_m\big|_{L\geq L_0} = \left(\frac{\int_{L_0}^{\infty} L^3 n(L)\, dL}{\int_{L_0}^{\infty} n(L)\, dL} \right)^{1/3} \tag{8.4.13}$$

EXAMPLE 8.5

Dependence of Population Density on Particle Size and Residence Time in a CSTR For the precipitation of protein in a CSTR, determine the dependence of the population density distribution n on the particle diameter L and residence time τ. Consider both particle growth by aggregation and particle breakup.

Solution

Use the expressions for the linear growth rate and particle breakup [Equations (8.4.8) and (8.4.9)] in the population balance equation [Equation (8.4.7)]. This gives

$$\frac{d(K_0 L n)}{dL} + \frac{n}{\tau} + K_1 n L^3 = 0$$

Differentiating and rearranging, we have

$$\frac{dn}{n} = -dL \left(\frac{1 + \dfrac{1}{K_0 \tau}}{L} + \frac{K_1 L^2}{K_0} \right)$$

With lower limits of integration of n_0 (the population density function at $L = L_0$) and critical diameter L_0, we obtain

$$\frac{n}{n_0} = \left(\frac{L_0}{L} \right)^{1+1/K_0\tau} \exp\left[\frac{-K_1}{3K_0} \left(L^3 - L_0^3 \right) \right]$$

8.5 METHODS OF PRECIPITATION

Methods that have been developed to precipitate proteins are based on a knowledge of the solubility of proteins. Based on our discussion in Section 8.2, the most obvious methods that emerge are pH adjustment to the isoelectric point of the protein (called isoelectric precipitation), addition of organic solvents, salting out, and addition of nonionic polymers.

Isoelectric precipitation is based on the fact that the solubility of a given protein is generally at a minimum at the isoelectric point (pI) of the protein (see Figure 8.3). This is a convenient method to use when fractionating a protein mixture. For this situation the pH should be adjusted above the highest pI or below the lowest pI of all the proteins present. The pH is then changed to the nearest pI, where precipitate is allowed to form and is then removed. This procedure is repeated for as many proteins as one desires to precipitate. Local extremes of pH should be avoided during pH adjustment to minimize protein denaturation (see Chapter 1, Section 1.4.7). There are two advantages of isoelectric precipitation when acids are added to cause precipitation: mineral acids are cheap, and several acids (e.g., phosphoric, hydrochloric, sulfuric) are acceptable in protein food products. This method, however, will not work for all proteins; for example, gelatin, which is a very hydrophilic protein, does not precipitate at its isoelectric point in solvents having low ionic strength [12].

Several organic solvents have been used to precipitate proteins, including alcohols, acetone, and ether. Alcohols, however, have been the most widely used in industry. One of the most important processes utilizing alcohol to precipitate proteins is the Cohn process to purify therapeutic proteins from human plasma. This process uses ethanol at temperatures below 0°C to minimize denaturation by the organic solvent. The variables that are manipulated in the Cohn process are pH, ionic strength, and ethanol concentration. Ionic strength is kept low, which leads to a salting-in effect (see Section 8.2). This salting-in effect is enhanced when ethanol is added. Cohn's methods for the preparation of albumin, plasminogen, prothrombin, isoagglutinins, and γ -globulin starting with blood plasma are illustrated in Figure 8.10.

In the salting out of proteins, salt is dissolved in the solution containing the proteins. The protein solubility decreases as the salt ionic strength rises according to the Cohn equation [Equation (8.2.7)]. The most important consideration in salting out is the type of salt that is used. Salts with multiply charged anions such as sulfate, phosphate, and citrate are the most effective; while for the cation, monovalent ions should be used [20]. Following the Hofmeister or lyotropic series, the salting-out ability of the common multiply charged anions is citrate^{2-} > phosphate^{3-} > sulfate^{2-}; for the common monovalent cations the order is $NH^+_4 > K^+ > Na^+$.

The salt that has the most desirable properties in general for precipitating proteins is ammonium sulfate. The solubility of this salt is very high (approximately 4 M in pure water) and varies very little in the range of 0 to 30°C. The density of a saturated solution of ammonium sulfate is 1.235 g cm^{-3}, which is enough below the density of protein aggregates (approximately 1.29 g cm^{-3}) to allow centrifugation. Another advantage of using ammonium sulfate is that protein precipitates are often very stable for years in 2 to 3 M salt; in fact, many commercial enzymes are normally sold in ammonium sulfate solution at high molarity. Furthermore, proteolysis and bacterial action are prevented in concentrated ammonium sulfate solutions. The only disadvantage of ammonium sulfate is that it cannot be used above pH 8 because of the buffering action of ammonia. Sodium citrate is very soluble and is a good alternative to ammonium sulfate when the precipitation must be performed above pH 8 [20].

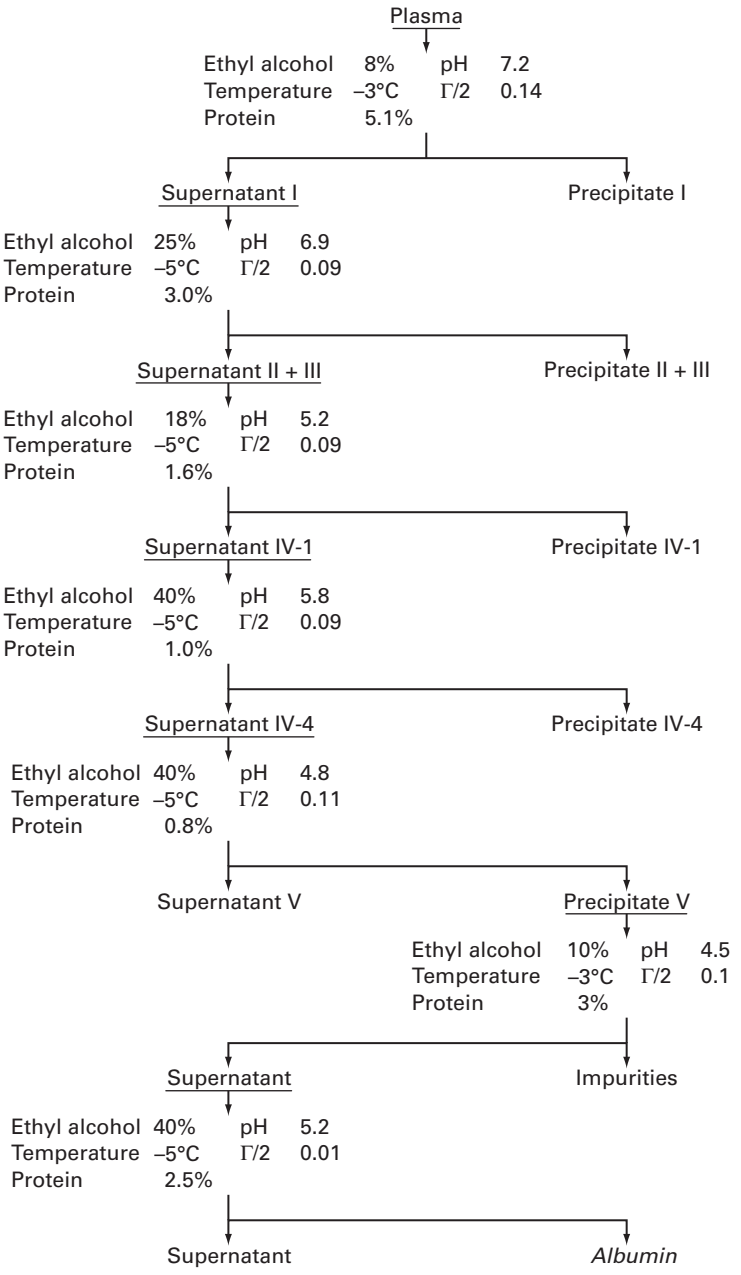

FIGURE 8.10 Cohn's method (1946) for blood protein fractionation: $\Gamma/2$ = ionic strength. *(Data from L. E. Strong, "Blood fractionation," in* Encyclopedia of Chemical Technology, *vol. 2, R. E. Kirk and D. F. Othmer, eds., p. 566, Interscience Encyclopedia, New York, 1948.)*

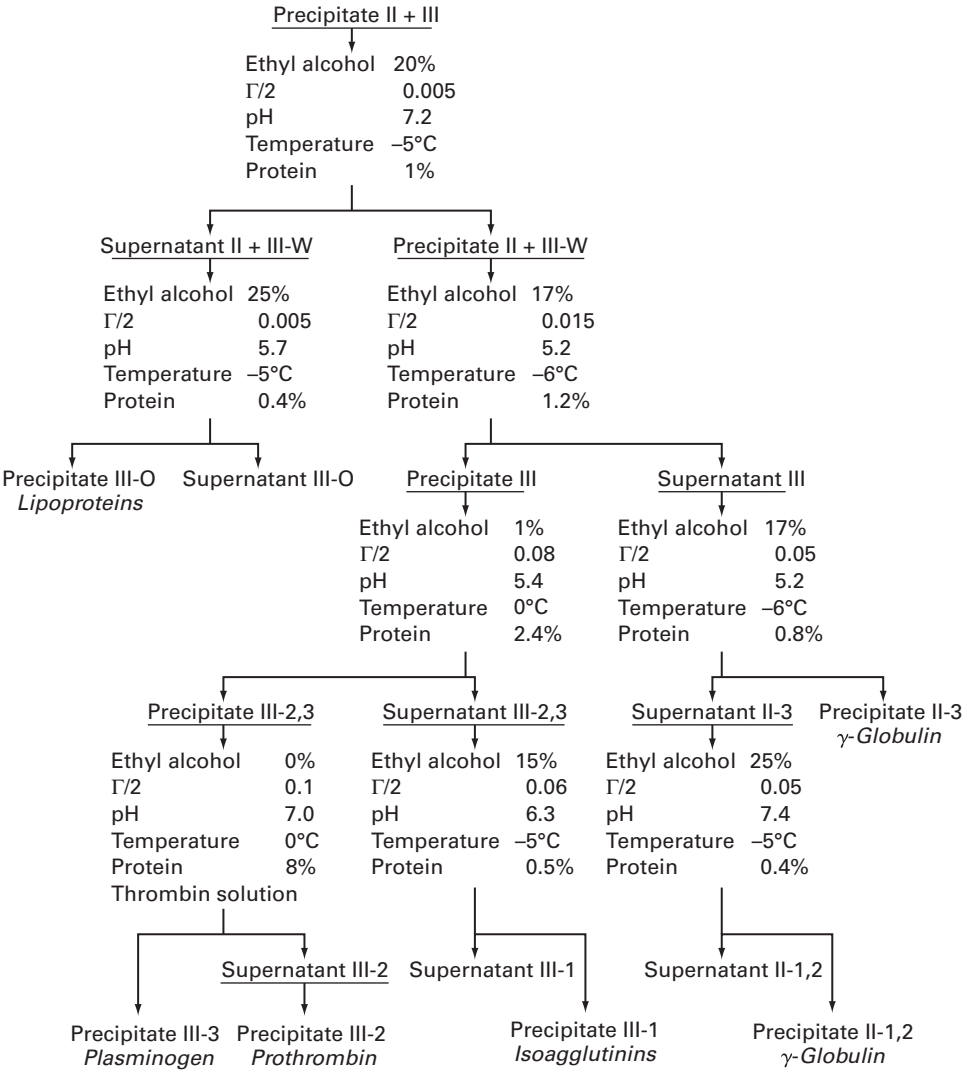

FIGURE 8.10 (Continued)

Several nonionic polymers have been used to precipitate proteins, including dextran, poly(vinyl pyrrolidone), poly(propylene glycol), and poly(ethylene glycol) (PEG). Of these polymers, by far the most extensively studied is PEG. Several guidelines have been developed for the use of PEG as a protein precipitant. Solutions of PEG up to 20% w/v can be used without viscosity becoming a problem. PEG's with molecular weights above 4000 have been found to be the most effective [20]. Protein destabilization in PEG solutions does not occur until the temperature is significantly higher than room temperature (>40°C) [7].

8.6 DESIGN OF PRECIPITATION SYSTEMS

Once a precipitating agent has been chosen for the protein of interest, it may be necessary to design a large-scale precipitation process. The safest procedure is to base the design on a laboratory or pilot plant system that has given acceptable results. Important considerations in obtaining the best possible plant design are the following: the type of precipitation reactor, processing conditions (flow rates, concentrations, etc.), and assumptions used to scale up to the plant scale. There are three basic types of precipitation reactor: the batch reactor, the continuous stirred tank reactor (CSTR), and the tubular reactor. These types are discussed and compared.

The batch reactor is the simplest of the three types and is often the one that is tried first at small scale. Batch precipitation is carried out by slowly adding the precipitating agent to a protein solution that is being mixed. Addition of the precipitating agent continues until the desired level of supersaturation is reached with respect to the protein being precipitated. At this point nucleation begins, and precipitation proceeds through the steps of particle growth and aggregation. Mixing continues until the precipitation is complete. The mixing in a batch reactor is generally turbulent. Protein particles precipitated in a batch reactor tend to be more compact and regular in shape than those precipitated in a tubular reactor, apparently because of the different shear profiles existing in the two reactors and the length of time the particles are exposed to this shear [21]. The shear field in a tubular reactor is essentially homogeneous; by contrast, in the batch reactor the precipitate particles are exposed to a very wide range of shears and to much longer times of exposure than in the tubular reactor, resulting in improved precipitate mechanical stability.

In a tubular reactor, precipitation takes place in volume elements that approach plug flow as they move through the tube. Thus, the distance–particle size distribution history of the particles in a volume element moving through a tubular reactor is comparable to the time–particle size distribution history of a stationary volume element in a batch reactor. In the tubular reactor the feed protein solution and the precipitating agent are contacted in a zone of efficient mixing at the reactor inlet. Good mixing can be accomplished, for example, by flowing the protein solution through a convergent nozzle to a biplanar grid and then introducing the precipitating agent just downstream of the biplanar grid [22]. The flow pattern in the reactor can be turbulent, a property that can be promoted by wire meshes at intervals along the reactor. In comparison to either the batch reactor or the CSTR, the tubular reactor has the advantages of short fluid residence times, an absence of moving mechanical parts, uniformity of flow conditions throughout the reactor, a simple and inexpensive design, and a relatively small holdup of fluid. For particles that grow relatively slowly, however, the length of the tubular reactor can be excessive.

In the CSTR, fresh protein feed contacts a mixed slurry containing precipitate aggregates. The mixing conditions in a CSTR are similar to those in a batch reactor. Upon entering the CSTR, fresh protein feed nucleates, the nucleate particles grow by diffusion, and the submicrometer-sized "primary" particles collide with and adhere to growing aggregates. The degree of supersaturation can be more easily controlled than in the batch or tubular reactor, which means that the formation of precipitates with undesirable properties is less likely.

A few general statements can be made regarding the processing conditions in precipitation systems. Flows are normally turbulent; flow must be high enough to avoid inadequate mixing and high supersaturation but low enough to avoid excessive particle breakage leading to particles that are smaller than desirable. For both the batch and tubular reactors, the flow regime can be changed from turbulent to laminar during the particle growth phase to avoid excessive particle breakage. The rate of addition of precipitant is especially important. This rate should be kept low enough to avoid high supersaturations that lead to colloidal, highly solvated precipitates. The concentration of the precipitant being added is also important, with lower concentrations leading to lower supersaturations [7].

The key parameter for scale-up of precipitation is mixing. One recommended approach to scale up mixing is to first consider using geometric similarity and constant power per unit volume (*P/V*) [23]. For geometric similarity all important dimensions are similar and have a common constant ratio. As seen in Figure 8.11, this method gave reasonable agreement for the d_{90} particle size (the particle size for which all particles that are larger account for 90 wt% of the total) as a function of *P/V* for the batch isoelectric precipitation of soy protein for vessels ranging in size from 0.27 to 200 liters. If the precipitate is susceptible to shear breakage, however, the assumption of constant *P/V* for scaleup may not be satisfactory. The impeller tip speed, which determines the maximum shear rate, rises when *P/V* is held constant upon scale-up of the reactor volume, as seen in Table 8.1. These results assume turbulent flow, where the power number is constant, so that

$$P \propto N_i^3 d_i^5 \tag{8.6.1}$$

Here, N_i is the impeller rotation rate, and d_i is the impeller diameter. It is also assumed that the maximum shear rate is proportional to the impeller tip velocity ($= \pi N_i d_i$) and that the volume is proportional to ${d^3}_i$. From Table 8.1 we see that even for a volume scale-up of 10,000 for constant *P/V*, the tip speed increases by less than a factor of 3. A volumetric scaleup factor of 10,000 is typical in scaling up from the lab to the plant.

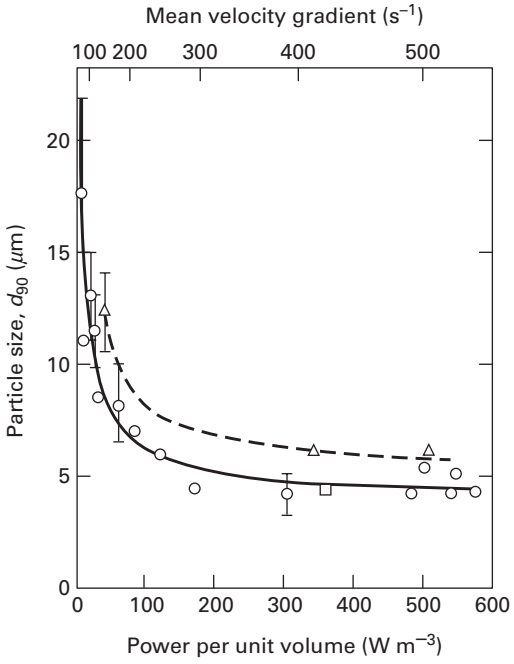

FIGURE 8.11 The relationship between aggregate size and power per unit volume for the preparation of isoelectric soy protein precipitate in batch stirred tanks: d_{90} is the particle size for which all particles that are larger account for 90 wt% of the total. Protein concentration is 30 kg m^{-3}. Vessel volumes: Δ, 0.27 liters; ○, 0.67 liters; □, 200 liters. *(Data from D. J. Bell, M. Hoare, and P. Dunnill, "The formation of protein precipitates and their centrifugal recovery,"* Adv. Biochem. Eng., *vol. 26, p. 40, Springer-Verlag, Berlin, 1983.)*

TABLE 8.1 Scaleup of Turbulent Agitation, Assuming Constant *P/V*

Volume scale-up factor	$\frac{(\text{Tip speed})_{large}}{(\text{Tip speed})_{small}}$
10	1.3
100	1.7
1000	2.2
10,000	2.8

8.7 SUMMARY

Precipitation is the process of coming out of solution as a solid. Often, the goal of precipitation is concentration to reduce volume, although significant purification can sometimes be achieved, and in certain instances precipitation has been used as the final step in the process.

- Precipitation is based on protein solubility, which depends, in turn, on the molecular properties of the protein and on the properties of the solvent. Proteins are usually least soluble near their isoelectric pH.
- The Cohn equation is an empirical relationship between protein solubility S and ionic strength I:

$$\ln S = \beta - K_s' I$$

where β is the hypothetical solubility at zero ionic strength and depends on temperature and pH (protein charge) for a given protein, while K_s' is the "salting-out" coefficient, which also accounts for "salting in" at low I. Similar correlations apply to nonionic precipitants.

- Precipitation occurs in distinct steps that can overlap in time as a precipitate develops: (1) initial mixing to achieve homogeneity, (2) nucleation, the generation of ultramicroscopic particles, (3) growth governed by diffusion of dissolved solute molecules to the particle surface, and (4) growth governed by fluid motion, in which particles grow by colliding and sticking together. Particle breakage imposes limits on the final particle size that can be attained.
- The initial mixing time required to distribute all molecules throughout a given volume depends on the diffusivity of the protein and the distance it must diffuse within mixing eddies, which is the Kolmogoroff length. This length, l_e, is calculated by using the theory of homogeneous isotropic turbulence from the equation

$$l_e = \left(\frac{\rho \nu^3}{P/V} \right)^{1/4}$$

where ρ is the liquid density, ν is the liquid kinematic viscosity, and P/V is the agitator power input per unit volume of liquid. The initial mixing time can be calculated from the Einstein diffusion equation by using the Kolmogoroff length and the diffusivity of the molecule being mixed.

- Intermediate particle growth depends on the diffusion of protein molecules to each growing particle. The loss rate of single molecules to this process follows the second-order rate law of Smoluchowski. The mass, measured in units of molecular weight, of a growing particle can be shown to increase linearly with time t:

$$M = M_0 \left(1 + K_A N_0 t\right)$$

where M_0 is the molecular weight of the solute, N_0 is the initial number concentration of dissolved solute, and K_A is a constant that depends on the solute diffusivity and molecular diameter.

- After growing particles have reached a certain size, typically 1 μm, further precipitant growth depends on the aggregation of these particles. In growth of particles governed by fluid motion, the particle number concentration N is given by the Smoluchowski second-order rate theory as

$$N = N_0 \exp\left(\frac{-4\alpha\varphi\gamma t}{\pi}\right)$$

where N_0 is the particle number concentration at time zero, when particle growth starts to be governed by fluid motion, α is the collision effectiveness factor (fraction of collisions that result in permanent aggregates), γ is the shear rate, and φ is the volume fraction of the particles. Aggregation depends on the balance of electrostatic repulsion and van der Waals attraction between particles and obeys the DLVO principles introduced in Chapter 3.

- Particle population balances are calculated for a CSTR using a material balance on a differential particle size interval. Because precipitated protein leaves the CSTR at the same time that the feed protein solution enters, the product stream leaving the CSTR will have a range of particle sizes that does not vary with time, since operation is at steady state.
- Methods to precipitate proteins include pH adjustment to the isoelectric pH of the protein (isoelectric precipitation), addition of organic solvents, salting out, and addition of nonionic polymers. An example of the use of organic solvents is Cohn's method for the fractionation of serum proteins.
- The key parameter for scale-up of precipitation is mixing, which suggests holding power input per volume constant. For turbulent mixing, power input increases as the third power of the impeller rotation rate and the fifth power of the impeller diameter.

NOMENCLATURE

A	constant in the equation for linear growth rate [Equation (8.4.8)] (dimensionless)
B	volumetric breakage rate of particles in the size range L to ΔL (number s^{-1} liter cm^{-1})
c_i	concentration of component i (M, or g $liter^{-1}$)
c_{i0}	feed concentration of component i (M, or g $liter^{-1}$)
c_p	polymer concentration (M)
d_i	impeller diameter (cm)

$\mathscr{D}$	diffusion coefficient of solute ($cm^2\ s^{-1}$)
G	particle linear growth rate ($cm\ s^{-1}$)
I	ionic strength (M)
k	Boltzmann constant ($1.3807 \times 10^{-23}\ J\ K^{-1}$)
k	constant in the displacement model for particle breakage [Equation (8.3.15)] ($cm^{1-n}\ s^{-1}$)
K	constant in the equation for the volumetric breakage rate [Equation (8.4.9)] ($s^2\ cm^{-2}\ g^{-1}$)
K_1	constant in the equation for the volumetric breakage rate [Equation (8.4.9)] ($liter^{-1}\ s^{-1}$)
K_A	rate constant for particle growth by diffusion ($liter\ s^{-1}$)
K_i	salting-in constant (M^{-1})
K_s	salting-out constant (M^{-1})
K'	constant in the Juckes equation [Equation (8.2.1)] (M^{-1}, or $liter\ g^{-1}$)
K_s'	constant in the Cohn equation [Equation (8.2.7)] (M^{-1})
l_e	mean eddy length, or Kolmogoroff length (cm)
L	particle diameter (cm)
L_e	equilibrium particle diameter (cm)
$\bar{L}_m$	mass-averaged particle diameter (cm)
L_{mol}	molecular diameter (cm)
L_0	critical particle diameter at which particles start to grow by colliding and sticking together (cm)
$\bar{V}$	volume-averaged particle diameter (cm)
M	molecular weight (Daltons)
M_0	molecular weight of solute (Daltons)
M_T	total mass concentration of particles ($g\ liter^{-1}$)
n	population density distribution function (number $liter^{-1}\ cm^{-1}$)
n	order of the displacement model for particle breakage [Equation (8.3.15)] (dimensionless)
n_0	population density distribution function at $L = L_0$ (number $liter^{-1}\ cm^{-1}$)
N	particle number concentration (number $liter^{-1}$)
N_0	particle number concentration at time zero (number $liter^{-1}$)
N_i	impeller rotation rate (revolutions s^{-1})
P/V	power input per volume of liquid ($W\ liter^{-1}$)
Q	volumetric flow rate ($liters\ s^{-1}$)
r_r, r_s	radius of polymer rod, radius of protein solute (cm)
S	protein solubility (M, or $g\ liter^{-1}$)
S_0	solubility of dipolar ion at zero ionic strength (M, or $g\ liter^{-1}$)
S_p	solubility of dipolar ion (M, or $g\ liter^{-1}$)
t	time (s)
T	temperature (K)
u	dipole moment (C cm)

V precipitation reactor volume (liters)
$\overline{V}$ partial specific volume of polymer (liters mol^{-1})
z_i charge of component i (dimensionless)
Z average protonic charge of protein

Greek Letters

α particle collision effectiveness factor (dimensionless)
β constant in the Cohn equation [Equation (8.2.7)] (dimensionless)
β' constant in the Juckes equation [Equation (8.2.1)] (dimensionless)
δ diffusion distance (cm)
$\gamma, \overline{\gamma}$ shear rate, average shear rate (s^{-1})
ε dielectric constant of solvent (dimensionless)
μ liquid viscosity (g cm^{-1} s^{-1})
ν liquid kinematic viscosity (cm^2 s^{-1})
ρ liquid density (g cm^{-3})
ρ_p density of precipitate particle (g cm^{-3})
τ mean residence time (s)
φ volume fraction of total particles (dimensionless)
φ_1 volume fraction of submicrometer-sized "primary particles" (dimensionless)

PROBLEMS

8.1 Solubility of Proteins Based on the Kirkwood theory of the interactions between ions and dipoles, answer the following:

(a) When comparing the solubilities of proteins at the same ionic strength, would you expect the solubility of a protein with a high dipole moment to be high or low?

(b) In highly polar solvents, what balance would you expect between salting in and salting out of a protein?

Use appropriate equations to justify your answers.

8.2 Precipitation of Albumin and γ-Globulin from Blood Plasma Explain the solubility principles involved in the precipitation of albumin and γ-globulin from blood plasma by the Cohn process.

8.3 Fractionation of a Protein Solution Four proteins are dissolved in solution. The constants in the Cohn equation (see Example 8.1) for the proteins are given in Table P8.3 along with the concentration of each protein in solution. Assume that the Cohn equation constants are valid when other proteins are present.

(a) Determine the maximum percentage recovery of protein 4 that can be obtained if it is desired to obtain a precipitate containing 100% protein 4.

(b) Determine the maximum percentage recovery of protein 3 that can be obtained if it is desired to obtain a mother liquor containing 99% protein 3.

TABLE P8.3

Protein	β	K_s'' (M^{-1})	Concentration (g/liter)
1	6.30	2.84	0.3
2	10.20	4.34	0.4
3	8.60	2.48	5.0
4	8.00	3.97	10.0

8.4 Mixer Power to Achieve Complete Mixing It is desired to precipitate a protein in a solution with a density of 1.02 g/cm^3 and kinematic viscosity of 0.012 cm^2/s. The diffusion coefficient of the protein has been estimated to be 1.2×10^{-7} cm^2/s. You need to select a mixer for this precipitation. To aid in this selection, plot as a straight line the dependence of the mixer power per solution volume (kW/liter) as a function of the time (s) to completely mix the solution for mixing times up to 100 s.

8.5 Kinetics of Precipitation of a Protein The data in Table P8.5 for particle number concentration N were obtained for the precipitation of a protein. Nucleation started at time zero. You also know the following information:

Protein concentration = 3.0 g/liter
Power input = 1.5 kW (2.0 hp)
Liquid volume = 1000 liters
Liquid density = 1.05 g/cm^3
Liquid viscosity = 0.012 g cm^{-1} s^{-1}
Molecular weight of protein = 200,000
Density of protein particles = 1.3 g/cm^3

The flow is turbulent.

From this information, determine:

(a) The time and particle diameter at which particle growth started to be governed by particles colliding and sticking together,
(b) The constant K_A in the equation by Smoluchowski describing particle growth by diffusion,
(c) The collision effectiveness factor α for particle growth by fluid motion

TABLE P8.5

t (min)	N (particles/cm^3)	t (min)	N (particles/cm^3)
0.5	3.72×10^9	3.5	4.51×10^8
1.0	1.86×10^9	4.0	2.29×10^8
1.5	1.24×10^9	4.5	8.49×10^7
2.0	9.28×10^8	5.0	3.14×10^7
2.5	7.42×10^8	5.5	1.16×10^7
3.0	6.19×10^8	6.0	4.31×10^6

8.6 Protein Precipitation in a CSTR For a protein precipitation in a CSTR, determine the functional dependence of the mass-averaged particle size $\bar{L}_m$ (for particles above the critical aggregate diameter L_0) on the residence time τ, parameter K_0, and L_0. Assume that particle breakage is negligible. For a value of K_0 of 0.02 min^{-1} (determined for soy protein precipitating in a CSTR by A. M. Petenate and C. E. Glatz, "Isoelectric precipitation of soy protein. II. Kinetics of protein aggregate growth and breakage," *Biotech. Bioeng.,* vol. 25, p. 3059, 1983) and L_0 of 1.0 μm, plot the dependence of $\bar{L}_m$ on τ.

8.7 Scale-up with Constant Power/Volume or Maximum Shear Rate A protein precipitation reactor with a mechanical agitator is being scaled up from volume V_1 to volume V_2 by two different methods: keeping power per unit volume (*P/V*) constant, or keeping the maximum shear rate ($\gamma_{\max}$) constant.

(a) For the scaleup keeping *P/V* constant, determine the ratio of $\gamma_{\max}$ at volume V_2 to $\gamma_{\max}$ at volume V_1 as a function of V_1 and V_2:

$$\frac{\left(\gamma_{\max}\right)_2}{\left(\gamma_{\max}\right)_1} = f\left(V_1, V_2\right)$$

(b) If constant $\gamma_{\max}$ is being used for scaleup, determine the ratio of *P/V* at volume V_2 to *P/V* at volume V_1 as a function of V_1 and V_2:

$$\frac{\left(P/V\right)_2}{\left(P/V\right)_1} = g\left(V_1, V_2\right)$$

8.8 Design of a Tubular Reactor to Precipitate a Protein A protein at a concentration of 2.0 g/liter is to be precipitated in a tubular reactor at 20°C and a rate of 1.0 kg/h. It is desired that the protein precipitate particles leaving the reactor have a diameter of 10 μm. The properties of the protein are as follows: molecular weight of 480,000, diffusion coefficient of 3.5×10^{-7} cm^2/s at 20°C, and precipitate particle density of 1.29 g/cm^3. Design a tubular reactor (i.e., specify diameter and length) to carry out the precipitation in turbulent flow at a Reynolds number of 10,000. It can be assumed that the particle collision effectiveness factor (α) is 0.05 for particle growth governed by fluid motion.

8.9 Prediction of the Solubility of Bovine Serum Albumin The solubility of bovine serum albumin has been measured to be 1.2 and 0.26 g/liter in 2.8 and 3.0 M ammonium sulfate, respectively. Estimate the solubility of bovine serum albumin in 3.5 M ammonium sulfate.

REFERENCES

1. Rashin, A., and Honig, B. (1984). On the environment of ionizable groups in globular proteins. *J. Mol. Biol*., vol. 173, p. 515.
2. Miller, S., Janin, J., Lesk, A. M., and Chothia, C. (1987). Interior and surface of monomeric proteins. *J. Mol. Biol*., vol. 196, p. 641.

3. Janin, J., Miller, S., and Chothia, C. (1988). Surface, subunit interfaces, and interior of oligomeric proteins. *J. Mol. Biol*., vol. 204, p. 155.
4. Privalov, P. L. (1989). Thermodynamic problems of protein structure. *Annu. Rev. Biophys. Biophys. Chem*., vol. 18, p. 47.
5. Van Oss, C. J., and Good, R. J. (1988). Orientation of the water molecules of hydration of human serum albumin. *J. Protein Chem*., vol. 7, p. 179.
6. Juckes, I. R. M. (1971). Fractionation of proteins and viruses with polyethylene glycol. *Biochim. Biophys. Acta*, vol. 229, p. 535.
7. Rothstein, F. (1994). Differential precipitation of proteins. In *Protein Purification Process Engineering*, R. G. Harrison, ed., Dekker, New York, p. 115.
8. Bull, H. B., and Breese, K. (1978). Interaction of alcohols with proteins. *Biopolymers*, vol. 17, p. 2121.
9. Oncley, J. L. (1943). The electric moments and the relaxation times of proteins as measured from their influence upon the dielectric constants of solutions. In *Proteins, Amino Acids, and Peptides*, E. J. Cohn and J. T. Edsall, eds., Reinhold, New York, Chap. 22, p. 543.
10. Kirkwood, J. G. (1943). The theoretical interpretation of the properties of solutions of dipolar ions. In *Proteins, Amino Acids, and Peptides*, E. J. Cohn and J. T. Edsall, eds., Reinhold, New York, Chap. 12, p. 276.
11. Cohn, E. J. (1925). The physical chemistry of proteins. *Physiol. Rev*., vol. 5, p. 349.
12. Bell, D. J., Hoare, M., and Dunnill, P. (1983). The formation of protein precipitates and their centrifugal recovery. In *Advances in Biochemical Engineering/Biotechnology*, vol. 26, A. Fiechter, ed., Springer-Verlag, Berlin, p. 1.
13. Ives, K. J. (1978). Rate theories. In *The Scientific Basis of Flocculation*, K. J. Ives, ed., Sijthoff and Noordhoff, Alphen aan den Rijn, The Netherlands, p. 37.
14. Smoluchowski, M. (1917). Mathematical theory of the kinetics of coagulation of colloidal solutions. *Z. Phys. Chem*., vol. 92, p. 129.
15. Camp, T. R., and Stein, P. C. (1943). Velocity gradients and internal work in fluid motion. *Boston Soc. Civ. Engs*., vol. 30, p. 219.
16. Brown, D. L., and Glatz, C. E. (1987). Aggregate breakage in protein precipitation. *Chem. Eng. Sci*., vol. 42, p. 1831.
17. Twineham, M., Hoare, M., and Bell, D. J. (1984). The effects of protein concentration on the break-up of protein precipitate by exposure to shear. *Chem. Eng. Sci*., vol. 39, p. 509.
18. Randolph, A. D., and Larson, M. A. (1971). *Theory of Particulate Processes*, Academic Press, New York.
19. Petenate, A., and Glatz, C. E. (1983). Isoelectric precipitation of soy protein. II. Kinetics of protein aggregate growth and breakage. *Biotechnol. Bioeng*., vol. 25, p. 3059.
20. Scopes, R. (1994). *Protein Purification*, 3rd ed., Springer-Verlag, New York.
21. Bell, D. J., and Dunnill, P. (1982). The influence of precipitation reactor configuration on the centrifugal recovery of isoelectric soya protein precipitate. *Biotechnol. Bioeng*., vol. 24, p. 2319.
22. Virkar, P. D., Hoare, M., Chan, M. Y. Y., and Dunnill, P. (1982). Kinetics of the acid precipitation of soya protein in a continuous-flow tubular reactor. *Biotechnol. Bioeng*., vol. 24, p. 871.
23. Oldshue, J. Y. (1983). *Fluid Mixing Technology*. McGraw-Hill, New York.

/// 9 /// CRYSTALLIZATION

Crystallization is the process of producing crystals from a homogeneous phase. For biochemicals, the homogeneous phase from which crystals are obtained is always a solution. Crystallization is similar to precipitation in that solid particles are obtained from a solution. However, precipitates have poorly defined morphology, while in crystals the constituent molecules are arranged in three-dimensional arrays called space lattices. In comparison to crystallization, precipitation occurs at much higher levels of supersaturation and rates of nucleation but lower solubilities. These and other differences between crystallization and precipitation are highlighted in Table 9.1. Because of these differences and because the theory of crystallization that has been developed is different from that for precipitation, crystallization is considered separately from precipitation.

Crystallization is capable of producing bioproducts at very high purity (say, 99.9%) and is considered to be both a polishing step and a purification step. Polishing refers to a process needed to put the bioproduct in its final form for use. For some bioproducts, such as antibiotics, this final form must be crystalline, and sometimes it is even necessary that a specific crystal form be obtained. In some instances, the purification that can be achieved by crystallization is so significant that other more expensive purification steps such as chromatography can be avoided.

There are actually two very different applications of crystallization in biotechnology and bioproduct engineering: crystallization for polishing and purification, and crystallization for crystallography. In the latter case, the goal is a small number of crystals with good size (0.2–0.9 mm) and internal quality. Although it has become common to crystallize proteins for characterization of their three-dimensional structure by x-ray diffraction, this is performed only at small scale in the laboratory, and the knowledge about how to crystallize proteins at large scale in a production process is less developed. However, many antibiotics and other small biomolecules are routinely crystallized in production scale processes.

This chapter is oriented toward the use of crystallization in processes that can be scaled up. The principles of crystallization are discussed first, including information about crystals, nucleation, and crystal growth. This is followed by discussions of batch crystallizers, which are widely used in the pharmaceutical industry. Strategies

TABLE 9.1 Comparison of Crystallization and Precipitation

Description	Crystallization	Precipitation
Solubility	Wide range, usually medium to high	Sparingly soluble
Relative supersaturation	Low	High
Product morphology	Well-defined	Ill-defined
Product crystal size	Large	Small
Nucleation mechanism	Secondary	Primary
Nucleation rate	Low	High
Growth rate	Wide range	Low
Controllability	Controllable	Difficult to control

Adapted from Tavare [1].

for the crystallization of proteins from solution are outlined. The chapter concludes with a discussion of crystallizer scale-up and design.

9.1 INSTRUCTIONAL OBJECTIVES

After completing this chapter, the reader should be able to do the following:

- Explain the differences between crystallization and precipitation.
- Utilize power law kinetics in the primary and secondary nucleation of crystals.
- Calculate crystal nucleation and growth rates from crystal size distribution data taken from batch experiments.
- Perform engineering analysis of a batch crystallizer.
- Outline strategies for crystallizing proteins.
- Scale up a crystallization process.

9.2 CRYSTALLIZATION PRINCIPLES

To understand crystallization, it is important to know what crystals are and how they form and grow. This understanding can then be used as a basis for the appropriate design and operation of crystallizers.

9.2.1 Crystals

When crystals are allowed to form freely, they appear as polyhedrons, or solids formed by plane faces. Although the relative sizes of the faces of the same material may differ considerably, the *angles* made by the corresponding faces of the same material do not vary—they are characteristic of that substance. These angles are the basis of the classification of seven crystal systems.

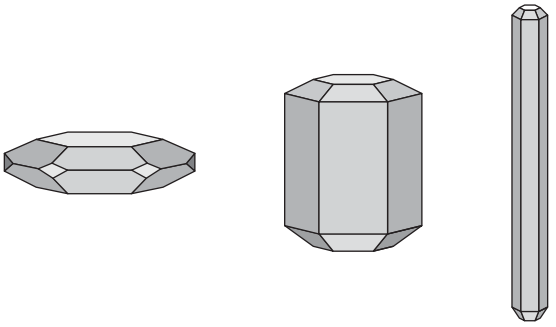

FIGURE 9.1 Crystal habit illustrated for hexagonal crystals: (*a*) tabular, (*b*) prismatic, and (*c*) acicular.

The relative sizes of the faces of a crystal in a particular system can vary considerably, resulting in a variety of crystal shapes. This variation is called a modification of *habit*. For example, if the crystals grow much more rapidly in one direction, needle-shaped crystals can result. This variation is illustrated in Figure 9.1 for hexagonal crystals. Crystal habit is influenced by the conditions of crystallization, particularly by the impurities present and by the particular solvent or solvents used. Impurities have been found to stunt the growth of a crystal in certain directions.

9.2.2 Nucleation

The generation of submicron particles in the process of nucleation is the sum of contributions by *primary nucleation* and *secondary nucleation*. Primary nucleation occurs in the absence of crystals, while secondary nucleation is attributed to the influence of existing crystals.

Primary nucleation can be either homogeneous or heterogeneous. For homogeneous nucleation, no foreign particles are present, while there are foreign particles present during heterogeneous nucleation. Primary nucleation is usually heterogeneous in actual practice. The rate of primary nucleation, either homogeneous or heterogeneous, has been modeled by the following power law expression [1]:

$$B = \frac{dN}{dt} = k_n (c - c^*)^n \tag{9.2.1}$$

where B is the number of nuclei formed per unit volume per unit time, N is the number of nuclei per unit volume, k_n is a rate constant, c is the instantaneous solute concentration, and c^* is the solute concentration at saturation. The $(c - c^*)$ term is called the *supersaturation*. The exponent n can range up to 10 but typically is in the range of 3 to 4.

Experimental data from industrial crystallizers have indicated that secondary nucleation usually predominates. Two types of secondary nucleation are shear

nucleation and contact nucleation [1]. Shear nucleation occurs as a result of fluid shear on growing crystal faces, and contact nucleation happens because of crystals colliding with each other and with the impeller and other vessel internal surfaces. The most widely used relation for the rate of secondary nucleation in crystallization is the following [1, 2]:

$$B = \frac{dN}{dt} = k_1 M_T^j (c - c^*)^b \tag{9.2.2}$$

where k_1 is a rate constant, and M_T is the suspension density. The exponent b can range up to 5 but has a most probable value of 2. The exponent j ranges up to 1.5, with 1 being the most probable value.

As in precipitation, the solution must be supersaturated in order for particles to form in crystallization, which is reflected in Equations (9.2.1) and (9.2.2). However, as indicated in the phase diagram in Figure 9.2, the supersaturation must be above a certain value before nucleation will begin. In a part of the phase diagram called the metastable region, the supersaturation is so low that nucleation will not start. Once the supersaturation has been raised enough to be in the labile region of the phase diagram, nucleation can begin. At this point, crystals begin to grow, and the supersaturation decreases. A possible way of carrying out a crystallization is indicated by the lines with arrows in Figure 9.2. If the supersaturation becomes too high, the nucleation rate will be too great, and an amorphous precipitate will result.

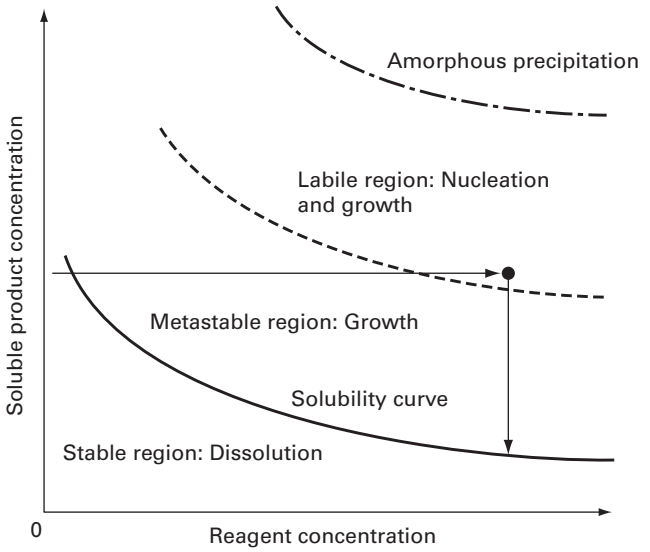

FIGURE 9.2 Typical phase diagram. The components in solution consist of the product (ordinate) and the precipitating reagent (abscissa). The lines with arrows outline one possible way of performing the crystallization.

9.2.3 Crystal Growth

Crystal growth is the postnucleation process in which molecules in solution are added to the surface of existing crystals. For engineering purposes in crystallizer design, the most useful relationship describing the rate of mass deposition R during crystal growth is [1, 2]

$$R = \frac{1}{A}\frac{dW}{dt} = k_G(c - c^*)^g \tag{9.2.3}$$

where W is the mass of crystals per volume of solvent, A is the surface area of crystals per volume of solvent, and k_G is an overall mass transfer coefficient. The order, g, of the overall growth process is usually between 0 and 2.5, with an order near unity being the most common. The overall mass transfer coefficient k_G in general depends on temperature, crystal size, hydrodynamic conditions, and the presence of impurities.

It is also sometimes convenient to express the overall linear growth rate as

$$G \equiv \frac{dL}{dt} = k_g(c - c^*)^g \tag{9.2.4}$$

where L is a characteristic single dimension of the crystal, such as length. It has been shown that geometrically similar crystals of the same material grow at the rate described by Equation (9.2.4), independent of crystal size [3]. This is known as the *delta L law*. Although a few exceptions to this law have been found (e.g., when the crystals are very large), it is reasonably accurate in numerous crystallizations of industrial importance [4].

Crystal growth is actually a process that consists of two steps in series. Solute molecules must reach the crystal surface by means of diffusion through a boundary layer. At the surface, the solute must be integrated into the crystal lattice. These two processes may be modeled as [1]

$$\text{Diffusion}: \quad R = k_d(c - c_i)^d \tag{9.2.5}$$

$$\text{Surface integration}: \quad R = k_r(c_i - c^*)^r \tag{9.2.6}$$

where c_i is the concentration at the interface between the liquid and solid phase, and k_d and k_r are mass transfer coefficients. When the exponents are unity, combining Equations (9.2.3), (9.2.5), and (9.2.6) gives

$$\frac{1}{k_G} = \frac{1}{k_d} + \frac{1}{k_r} \tag{9.2.7}$$

Thus, if surface integration is very fast compared with bulk diffusion, then $k_r >> k_d$, and $k_G \cong k_d$.

9.2.4 Crystallization Kinetics from Batch Experiments

Estimates of nucleation and growth rates during crystallization can be obtained from batch experiments by a method known as moments analysis [1]. By making a mass balance on the number of crystalline particles within a given size range between L and $L + \Delta L$, as was done for precipitate particles (Chapter 8), the population balance equation for size-independent growth in a perfectly mixed, constant-volume batch crystallizer with negligible attrition and agglomeration becomes

$$\frac{\partial n(L)}{\partial t} + G\frac{\partial n(L)}{\partial L} = 0 \tag{9.2.8}$$

The kth moment of the population density distribution in L about the origin, obtained by moment transformation of Equation (9.2.8) with respect to size, is defined as

$$\mu_k \equiv \int_0^\infty n(L)L^k dL \tag{9.2.9}$$

If the moments of the experimental population density function can be determined at two times that differ by a small time interval Δt over which the linearity of the model can be assumed, then the average values of the nucleation and growth rates can be expressed as

$$\bar{B} = \frac{\Delta\mu_0}{\Delta t} \tag{9.2.10}$$

and

$$\bar{G} = \frac{\Delta\mu_1}{\bar{\mu}_0 \Delta t} \tag{9.2.11}$$

Here, Δ represents the difference in values of a quantity at two different times and the bar an arithmetic average of the quantities. These equations are derived by moment transformation of the population balance equation with respect to size [Equation (9.2.8)]. Therefore, the average nucleation rate $\bar{B}$ and the average overall linear growth rate $\bar{G}$ may be calculated from two experimental population density plots obtained from a batch crystallization experiment at times t and $t + \Delta t$. In addition, the average size $\bar{L}$ at each time can be obtained as follows from the moments:

$$\bar{L} = \frac{\int_0^\infty n(L)\,L\,dL}{\int_0^\infty n(L)\,dL} = \frac{\mu_1}{\mu_0} \tag{9.2.12}$$

The meaning of each kth moment in the crystal population is given in Table 9.2.

TABLE 9.2 Moment Analysis of Crystal Size Distribution

Moment	*k* of moment [Equation (9.2.9)]	Meaning of moment	Mathematical definition	Average value for spherical crystals
μ_0	0	Number of crystals	$\int_0^\infty n(L)\,dL$	
μ_1	1	Size of crystals	$\int_0^\infty n(L)\,L\,dL$	$\frac{\mu_1}{\mu_0}$
μ_2	2	Area of crystals[a]	$\int_0^\infty n(L)\,L^2\,dL$	$\pi\left(\frac{\mu_2}{\mu_0}\right)$
μ_3	3	Mass of crystals[b]	$\int_0^\infty n(L)\,L^3\,dL$	$\frac{\pi\rho}{6}\left(\frac{\mu_3}{\mu_0}\right)$

[a]Multiply moment by area shape factor relating area to L^2 to obtain area of crystals per unit volume (area shape factor = π for spheres).

[b]Multiply moment by crystal density ρ and by a volume shape factor relating volume to L^3 to obtain mass of crystals per unit volume (volume shape factor = π for spheres).

Fractional moments can also be useful. For example,

$$\text{Fraction of total number of crystals between size 0 and size } L = \frac{\int_0^L n(L)dL}{\int_0^\infty n(L)LdL} \tag{9.2.13}$$

Fractional moments can also be applied to the number, area, and mass of crystals.

9.3 BATCH CRYSTALLIZERS

Batch crystallizers are extensively used in the pharmaceutical industry to produce biochemicals such as antibiotics. Often, the final step of purification of an antibiotic is crystallization. Batch crystallizers have the advantages of being flexible to operate and requiring less capital investment than continuous crystallizers. A widely employed technique for achieving supersaturation in batch crystallizers is the method of dilution, also called the "salting-out" method if the diluent contains a salt. The addition of a diluent reduces the solubility of the solute that is desired to be crystallized. For example, antibiotics have been crystallized from aqueous solution by the slow addition of a miscible organic solvent such as ethanol. Another way of

generating supersaturation in batch crystallizers is by chemical reaction to form a less soluble product; the reaction can vary from the addition or removal of a proton to the coupling of two molecules. In this section, the dilution method of batch crystallization is analyzed.

9.3.1 Analysis of Dilution Batch Crystallization

In dilution batch crystallizers, operation can be by several different modes, which include a constant diluent addition rate, a constant rate of diluent concentration change, and a constant level of supersaturation. Since the process includes the addition of a third component (the diluent), the crystallizer volume varies with time, although in some cases the diluent volume required may be relatively small, and thus the volume change may be neglected. The addition of a diluent causes the solubility of the solute being crystallized to be lowered. A commonly used expression for the dependence of the solubility of the solute upon the concentration of the diluent being added is the following [5]:

$$c^* = c_o^* \exp(-k_p c_d) \tag{9.3.1}$$

where c_d is the diluent concentration and k_p is a constant.

Since the working volume of a batch crystallizer may vary with time, it is convenient to define the population density function, $\hat{n}$, based on the total solvent volume at any time as

$$\hat{n}(L) = n(L)V \tag{9.3.2}$$

The resulting population balance equation for a perfectly mixed batch crystallizer with negligible attrition and agglomeration is [6]

$$\frac{\partial \hat{n}(L)}{\partial t} + \frac{\partial \hat{n}(L)G}{\partial L} = 0 \tag{9.3.3}$$

where G is the overall linear growth rate, previously defined by Equation (9.2.4). To simplify the solution of this equation, a new variable, y, is defined such that

$$y \equiv \int_o^t G(t)dt \tag{9.3.4}$$

so that

$$t = \int_0^y \frac{dy}{G(y)} \tag{9.3.5}$$

The variable y represents the size of a crystal at any time t, that originally nucleated at time $t = 0$. With y as a variable, the population balance for a crystal system where the growth rate is independent of size becomes

$$\frac{\partial \hat{n}}{\partial y} + \frac{\partial \hat{n}}{\partial L} = 0 \tag{9.3.6}$$

The boundary conditions ($y = 0$) for the nuclei population density can be represented by the equation [1]

$$\hat{n}(t,0) = \hat{n}^0 = \frac{\hat{B}}{G} \tag{9.3.7}$$

To average the distribution with respect to the internal coordinate properties, a transformation of the population balance equation [Equation (9.3.6)], leads to the following moment equations [6], where the hat symbol (^) represents quantities based on total solvent volume:

$$\frac{d\hat{N}}{dy} = \hat{n}(0, y) \tag{9.3.8}$$

$$\frac{d\hat{L}}{dy} = \hat{N} \tag{9.3.9}$$

$$\frac{d\hat{A}}{dy} = 2k_a\hat{L} \tag{9.3.10}$$

$$\frac{d\hat{W}}{dy} = \frac{3k_v\rho}{k_a}\hat{A} \tag{9.3.11}$$

where $\hat{N}$ = number of crystals
$\hat{L}$ = crystal size (length)
$\hat{A}$ = crystal area
$\hat{W}$ = mass of crystals
k_a, k_v = surface and volume shape factors
ρ = crystal density

These relationships can be combined to predict the time dependence of crystal size in a batch crystallization process, as in the following example.

EXAMPLE 9.1

Batch Crystallization with Constant Rate of Change of Diluent Concentration
Derive the relationship between y and t for an unseeded batch dilution crystallizer with a constant rate of change of diluent concentration, given the following information [6, 7]:

$$\text{System kinetics}: G = 10^{-6}\Delta c \text{ m/s}; B = 10^{6}\Delta c^{2} \text{ number } \left(\text{liter of solvent}\right)^{-1} \text{s}^{-1}, \text{ where } \Delta c = c - c^{*}$$

Physical parameters: $\rho = 2 \times 10^3$ kg/m^3; $k_v = 0.5$; $k_a = 3.5$; $c_0^* = 0.25$ kg of solute/liter solvent; $k_p = 10$ liters (solvent and diluent)/liter of diluent; V_0 = initial volume of solvent = 1.0 liter; $\Delta c_0 = 0.01$ kg of solute per liter of solvent; and $k_m = 10^{-6}$ liter of diluent (liter of solvent)$^{-1}$ s^{-1}, where

$$\frac{dc_d}{dt} = k_m = \text{rate of change of diluent concentration}$$

Solution
We need to determine how y depends on t in this dilution crystallizer. Assume that the nuclei population density based on the initial supersaturation level is constant throughout the volume of the batch. From Equation (9.3.7) at $t = 0$,

$$\hat{n}(0,0) = \hat{n}_0^0 = \frac{\hat{B}}{G} = \frac{10^6 \Delta c_0^2 V_0}{10^{-6}\Delta c_0} = 10^{12}\left(0.01 \frac{\text{number}}{\text{m liter}}\right)(1.0 \text{ liter}) = 10^{10} \frac{\text{number}}{\text{m}}$$

Assuming the nuclei population density to be constant at this value, after integration of Equations (9.3.8), (9.3.9), and (9.3.10) and substitution into Equation (9.3.11), we obtain

$$\frac{d\hat{W}}{dy} = k_v \rho \hat{n}_0^0 y^3 = 0.5(2\times 10^3)(10^{10})y^3 = 10^{13} y^3 \frac{\text{kg}}{\text{m}}$$

Since the change in solute concentration leads to crystal formation, we can write the mass balance for the crystallization as

$$d\hat{c} + d\hat{W} = 0$$

where $\hat{c} = Vc$ and $\hat{W} = V\,W$. From the definition of supersaturation ($\Delta\hat{c} = \hat{c} - Vc^*$), the mass balance can be rewritten as

$$\frac{d\Delta\hat{c}}{dy} + \frac{dVc^*}{dy} + \frac{d\hat{W}}{dy} = 0$$

which is called the "supersaturation balance equation."

We now evaluate the first two terms of the foregoing mass balance equation, with the objective of obtaining a term involving *dt/dy* that would allow us to determine *y* as a function of *t*. To evaluate the term dVc^*/dy, we first differentiate the solubility c^*, as given by Equation (9.3.1), with respect to *t*:

$$\frac{dc^*}{dt} = -c_0^* k_p \frac{dc_d}{dt} \exp(-k_p c_d) = -k_p c^* \frac{dc_d}{dt}$$

Substituting for dc_d/dt gives

$$\frac{dc^*}{dt} = -k_p k_m c^*$$

Assuming the initial concentration of diluent to be zero, the solution volume increases according to

$$V = \frac{V_0}{1 - k_m t}$$

Differentiating *V* with respect to time gives

$$\frac{dV}{dt} = \frac{V_0 k_m}{(1 - k_m t)^2} = \frac{V^2}{V_0} k_m$$

The term dVc^*/dt can be expanded to give

$$\frac{dV\,c^*}{dt} = V \frac{dc^*}{dt} + c^* \frac{dV}{dt}$$

Substituting for dc^*/dt and *dV/dt* yields

$$\frac{dV\,c^*}{dt} = c^* k_m V \left(\frac{V}{V_0} - k_p \right)$$

or,

$$dV\,c^* = c^* k_m V \left(\frac{V}{V_0} - k_p \right) dt$$

Next, we assume that volume and solubility changes are negligible (i.e., $V \cong V_0$ and $c^* \cong c_0^*$, and that changes in the supersaturation are negligible with respect to *y* (i.e., $d\Delta\hat{c}/dy = 0$). This last assumption is realistic because of the inherent

self-regulating character of batch crystallizers [6]. Substituting for $dV\ c^*$ in the supersaturation balance equation gives

$$[c_0^* k_m V_0 (k_p - 1)] \frac{dt}{dy} = \frac{d\hat{W}}{dy}$$

Substituting the result obtained previously for $d\hat{W}/dy$ and rearranging leads to

$$\frac{dt}{dy} = \frac{10^{13} y^3}{(0.25 \times 9) 10^{-6}} = 4.44 \times 10^{18} y^3 \frac{\text{s}}{\text{m}}$$

Integrating with $y = 0$ at $t = 0$ gives

$$y = 3.08 \times 10^{-5} t^{0.25} \text{ m}$$

This is a useful result that gives an estimate of how long the crystallization must be carried out to obtain crystals of a desired size. Note the modest time dependence of $y(t)$. Also note that this derivation is for a specific case and must be modified when different cases have different kinetic power functions.

9.4 PROCESS CRYSTALLIZATION OF PROTEINS

Because crystals of bioproducts tend to be quite pure, the use of crystallization in a purification process often results in great simplification of the process. For the purification of proteins, there are some strong reasons for utilizing crystallization in the process: (1) one or more expensive chromatography steps possibly can be eliminated; (2) in comparison to chromatography, crystallization is relatively inexpensive to carry out, since costly adsorbents are not required; and (3) proteins crystals often can be stored for long periods at low temperatures without being degraded or denatured after the addition of stabilizing agents such as ammonium sulfate, glycerol, or sucrose.

The methods that have been used to crystallize proteins include those used for precipitation: adjustment of the pH to the isoelectric point (isoelectric precipitation), the addition of organic solvents, the addition of salts (salting out), and the addition of nonionic polymers. Another crystallization method that has proven useful for proteins is the reduction of ionic strength by dialysis or diafiltration, which relies on the limited solubility of many proteins at low ionic strength (the reverse of the "salting-in" effect described in Chapter 8, Section 8.2.3).

Besides the method chosen for the protein crystallization, there are important factors to consider about how the method is performed, which include the rate of addition of the precipitation agent, the protein concentration and purity, precipitant concentration, pH, and temperature. A key strategy for crystallization is to move the

system *very slowly* to a state of minimum solubility of the desired protein until a limited degree of supersaturation is reached. High protein concentrations, in the range of 10 to 100 mg/ml, are recommended for crystallization, and seeding with small crystals of the desired protein is often beneficial [8]. While the protein purity needs to be 99% and greater for the crystallization for structural studies, it can be as low as 50-60% for large-scale crystallization of industrial enzymes such as alkaline phosphatase [9]. In a study of the effect of impurities on the crystal growth of lysozyme, this effect varied from no effect to a significant crystal face specific effect leading to growth cessation, while little effect was observed on solubility or crystal purity [10]. Growth cessation of crystal faces is frequently observed in protein crystal growth. Proteins are typically crystallized over a narrow pH range (< 1 pH unit) and at either 4°C or at ambient temperature [9]. Since the growth rate of protein crystals is slowed at low temperature, crystallization at ambient temperature is common at large scale if protein stability is not affected.

The following studies of protein crystallization illustrate the different approaches that can be taken:

- To crystallize rituximab, a chimeric murine/human monoclonal antibody, a procedure originally used at the microscale with vapor diffusion drops was scaled up. A rituximab solution was added to an equal volume of buffer containing polyethylene glycol, and the mixture was seeded with rituximab crystals made at the microscale. After overnight mixing, rituximab crystals in the form of needle clusters formed. The yield was 85%, and the biological activity of the antibody was fully retained [11].
- Alcohol oxidase, originally contained in *Pichia pastoris* yeast broth grown in a 100-liter pilot plant fermentor, was crystallized by lowering the ionic strength by diafiltration with deionized water; crystallization was preceded by lysis of the yeast cells, diafiltration with a microfilter to obtain the alcohol oxidase in the permeate, and concentration and then diafiltration with an ultrafiltrater [12]. The yield was 208 g of pure enzyme.
- Ovalbumin was crystallized in the presence of conalbumin and lysozyme by the addition of 2.5 μm seed crystals to a solution (600 ml) that had been made supersaturated by slowly adding ammonium sulfate solution [13]. The supersaturation was kept in the metastable region to avoid nucleation (see Figure 9.2). The growth rate of ovalbumin crystals was found to have a second-order dependence on the ovalbumin supersaturation, and the presence of the other two proteins did not affect the growth rate constant [k_g in Equation (9.2.4)].
- A fungal lipase was crystallized at low conductivity by slowly lowering the pH with formic acid [14]. The solution for crystallization was prepared by removing the cells by centrifugation (the lipase had been secreted from the cells), concentration by ultrafiltration, and diafiltration to lower the conductivity. An analysis of the crystal size distribution data gave a power dependency of the nucleation rate and growth rate on the lipase supersaturation of 10.8 and 6.4,

respectively. These high powers were attributed to possible underestimation of the supersaturation.

- Recombinant human insulin was commercialized by Eli Lilly in 1982, and crystallization was the final step in the purification process. The crystallization process for insulin is discussed in Chapter 12 with the other steps in the production process.

9.5 CRYSTALLIZER SCALE-UP AND DESIGN

Since the behavior of each biochemical to be crystallized is unique, the development of a large-scale crystallization process must be based on experimental data. Thus, data are taken first in the laboratory and are followed by data from pilot plant equipment, which form the basis of the scale-up calculations and plant process design.

9.5.1 Experimental Crystallization Studies as a Basis for Scale-up

Experimental work to serve as a basis for scale-up can be divided into three stages: (1) gathering basic data on solubility and metastable zone width, (2) developing the conditions in a laboratory scale batch crystallizer to obtain a product that meets required specifications at a satisfactory yield, and (3) pilot plant crystallizations that use optimal laboratory conditions as a starting point.

Data on the solubility of the solute to be crystallized should be obtained in the starting solvent as a function of temperature. These solubility data are the upper limit of the concentration of the solute at the start of the crystallization. The metastable zone width is the increase in concentration above the equilibrium solubility before primary nucleation occurs (see Figure 9.2). The metastable zone width can be determined by slowly increasing the supersaturation in a solution free of crystals until primary nucleation occurs, then noting the equilibrium solubility level at nucleation conditions [15].

A convenient size of a batch crystallizer for carrying out initial tests of crystallization is around 1 liter, assuming that enough material is available [15]. Protein equilibrium data, however, have been obtained using as little as 10 μl. A 1-liter volume is generally enough to allow for sampling during the experiment, generating of enough product slurry to obtain filtration rate data, and determining the effect of washing on crystal purity. Typically, the experiment starts with a crystal-free undersaturated solution, and for the proposed end point of the crystallization to be reached in about 2 h, supersaturation is generated by using the chosen method at an approximately linear rate. The point at which primary nucleation occurs is noted and compared with the earlier previous measurements of the metastable zone width. When crystallization has started, it is useful to measure the solution concentration as a function of time. At the end of the generation of supersaturation, the crystal slurry should be agitated for an additional hour or two, continuing to measure the solution concentration to determine the approach to equilibrium. After this holding period, the crystal slurry can be filtered to obtain filtration rate data. If there is sufficient slurry, the effect of

different types of washing on crystal purity can be determined. After drying, the crystals should be characterized for particle size distribution and examined under an optical microscope, which often gives important information about crystal structure.

Problems with the final crystals not meeting specifications or with low yield should be addressed at the laboratory scale before the scale of testing is increased. One such problem that can be difficult to solve occurs when the particle size distribution is out of range, resulting in low filtration rates of the crystal slurry. In order to change the crystal size distribution, the relative rates of nucleation and growth must be changed, which can be accomplished by adjusting the supersaturation history. In general, the nucleation rate increases more than the growth rate with increasing supersaturation, as can be seen from the exponent of the supersaturation in Equations (9.2.1) and (9.2.3). Therefore, operating at low supersaturation favors growth of large crystals, while high supersaturation close to the metastable limit tends to give many more nuclei and smaller crystals. One method that may increase crystal size is the addition of seed crystals to a just-supersaturated solution.

The production of crystals with a purity that is lower than that required is another problem that can occur in crystallization. An impurity that is the cause of the problem can be in the following locations in the crystal sample [15]:

1. Deposited on crystal surfaces due to incomplete removal of impure mother liquor
2. Trapped within voids between separate crystals in materials that agglomerate
3. Contained in inclusions of mother liquor within individual crystals
4. Distributed throughout the crystals by molecular substitution at the lattice sites

An obvious approach to eliminating the impurity from the crystal surface is to improve the solid-liquid separation and washing procedures. For crystals that agglomerate, it may be possible to reduce agglomeration by changing the crystallization conditions (such as using a different crystallization solvent). Reducing the supersaturation level to reduce both the nucleation and growth rates should help to minimize the problem of impurities in inclusions of mother liquor. The problem of the impurity being distributed throughout the crystals is difficult to solve for an individual crystallization and many require that the crystals be *recrystallized*. Recrystallization, which is widely used, is done by dissolving the crystals in fresh solvent and performing the crystallization again. Purer crystals can result if the impurity is more soluble in the solvent than the main product. Complex fractional recrystallization schemes, requiring more than one recrystallization [5], have been developed but are not used frequently at the plant scale.

Once satisfactory operating conditions have been obtained at the laboratory scale, it is often advisable to test the crystallization at the pilot plant scale. Scale-up ratios of 100 to 1000 from laboratory to pilot plant appear reasonable [1]. Common scale-up rules are outlined in the next section. The same types of measurement made in the laboratory crystallizations should also be made in the pilot plant crystallizations.

9.5.2 Scale-up and Design Calculations

The challenge in scale-up is to generate conditions at the large scale that are similar to those at the small scale. As with precipitation (Chapter 8), the key problem is in the scale-up of mixing to control the supersaturation level both locally and globally throughout the crystallizer and to ensure that the crystals are carried throughout the volume of the crystallizer under controlled conditions of frequency and intensity of crystal-crystal interactions [15]. Crystallizer scale-up ratios of 50 to 500 from pilot plant to commercial scale are reasonable [1].

As with precipitation, it is often recommended that geometric similarity and constant power per volume be used in scaleup of crystallizers [1, 16]. For turbulent flow in vessels (Reynolds number > 10,000), constant power per volume means that [17]

$$\frac{P}{V} \propto N_i^3 d_i^2 \tag{9.5.1}$$

where N_i is the impeller rotation rate and d_i is the impeller diameter. For an agitated tank, the Reynolds number is given by [17]

$$\mathrm{Re} = \left(\frac{d_i^2 N_i \rho}{\mu} \right) \tag{9.5.2}$$

where N_i is in revolutions per unit time, ρ is the fluid density, and μ is the fluid viscosity.

Two additional strategies are also sometimes used in scale-up of crystallizers [16]:

1. Maintaining constant impeller tip speed, which implies that

$$N_i d_i = \text{constant} \tag{9.5.3}$$

2. Scale-up at the minimum speed required for particle suspension, which has been shown to require [18]

$$N_i d_i^{0.85} = \text{constant} \tag{9.5.4}$$

This last criterion should give both secondary nucleation and crystal growth rates that are more or less independent of the scale of operation.

From an analysis of the data for the operation of the crystallization at the laboratory and pilot plant scales, the scale-up equation or equations that prove to be the most accurate in describing the laboratory to pilot plant scale-up should be used in the design of the plant crystallizer. However, flexibility should be designed into the plant unit so that agitation rates and flow rates can be varied, which may be necessary because of error in the scale-up to the larger scale and because of the effect that changes in the concentration of impurities in the starting solution may have on the operation.

EXAMPLE 9.2

Scale-up of Crystallization Based on Constant Power per Volume It is desired to scale-up a batch crystallization of an antibiotic based on experiments with a 1-liter crystallizer. The use of a 3 cm diameter impeller at a speed of 800 rpm led to good crystallization results. For maintaining power per volume constant upon scale-up to 300 liters, what should be the diameter and speed of the large-scale impeller? The solvent has the same density and viscosity as water.

Solution

For the scale-up, we assume geometric similarity. Thus, the volume (V) scales with the impeller diameter (d) as

$$V \propto d_i^3$$

Letting subscripts 1 and 2 denote the small and large scales, respectively,

$$\frac{V_2}{V_1} = \left(\frac{d_{i,2}}{d_{i,1}}\right)^3$$

Solving for d_2,

$$d_{i,2} = d_{i,1}\left(\frac{V_2}{V_1}\right)^{1/3} = 3\left(\frac{300}{1}\right)^{1/3} = 20.1\,\text{cm}$$

From Equation (9.5.1), for power per volume to be constant,

$$N_{i,1}^3 d_{i,1}^2 = N_{i,2}^3 d_{i,2}^2$$

This equation is valid for turbulent flow in the crystallizer. To verify that the flow is turbulent, we use Equation (9.5.2) to calculate the Reynolds number for the lab crystallizer:

$$\text{Re} = \left(\frac{d_i^2 N_i \rho}{\mu}\right)_1 = \frac{(3\,\text{cm})^2 \times 800\frac{\text{rev}}{\text{min}} \times 1.00\frac{\text{g}}{\text{cm}^3} \times \frac{1\,\text{min}}{60\,\text{s}}}{0.01\frac{\text{g}}{\text{cm s}}} = 12{,}000$$

This Reynolds number indicates that the flow is turbulent. Solving for $N_{i,2}$,

$$N_{i,2} = N_{i,1}\left(\frac{d_{i,1}}{d_{i,2}}\right)^{2/3} = 800\left(\frac{3}{20.1}\right)^{2/3} = 225\,\text{rpm}$$

Thus, the rotation rate is reduced considerably compared with the laboratory scale.

9.6 SUMMARY

The process of producing crystals from a homogeneous phase is called crystallization. Bioproducts can be obtained at very high purity (say, 99.9%) by crystallization. This process is considered to be both a polishing step and a purification step, and, in some instances, the purification that is achieved by crystallization is so significant that other more expensive purification steps such as chromatography can be avoided.

- Crystallization differs primarily from precipitation in that when a substance comes out of solution as a solid it also forms a regular lattice of molecules, or crystal.
- Crystals nucleate either by primary or secondary nucleation. Primary nucleation occurs in the absence of crystals, while secondary nucleation is attributed to the influence of existing crystals. Secondary nucleation dominates in industrial crystallizers. Two types of primary nucleation are possible: homogeneous and heterogeneous, where heterogeneous nucleation requires the presence of foreign particles for nucleation to occur and homogeneous nucleation does not.
- The rate of increase in the concentration of nuclei is proportional to a power of the supersaturation, $c - c^*$, where c^* is the concentration at equilibrium ("saturation"). The power has a most probable value of 3 to 4 for primary nucleation and 2 for secondary nucleation.
- The crystal growth rate is also proportional to a power of the supersaturation, with a power of unity being the most common.
- The differential equation for a material balance on a crystal size interval can be subjected to a moment transformation. The zeroth moment is the number of nuclei (crystals), the first moment is the linear size, the second moment is proportional to the area, and the third moment is proportional to the mass (or volume). The crystal nucleation and growth rates can be determined from the moments of the experimental population density function.
- Batch crystallizers can be analyzed by the population balance equation.
- Scale-up of crystallizers, like scale-up of precipitation units, emphasizes mixing. The mixing parameters that can be held constant are power input per volume, impeller tip speed, and agitation sufficient to keep crystals in suspension. All three of these variables cannot be held absolutely constant upon scale-up at the same time, because each depends differently on the impeller diameter. Therefore, scaling priorities are also based on experimental measurements and plant scale design for flexibility.

NOMENCLATURE

A	surface area of crystals per volume of solvent (cm^2 $liter^{-1}$)
B	nucleation rate during crystallization (number $liter^{-1}$ s^{-1})
c	concentration of solute (M, or g $liter^{-1}$)
c_d	concentration of diluent (liter $liter^{-1}$)
c_i	concentration of solute at interface between liquid and solid phases (g $liter^{-1}$)

d_i impeller diameter (cm)
G overall linear growth rate of crystals (cm s^{-1})
P/V power input per volume of liquid (W $liter^{-1}$)
k_a surface shape factor (dimensionless)
k_d mass transfer coefficient for bulk diffusion [Equation (9.2.5)] [g cm^{-2} s^{-1} $(g/liter)^{-d}$]
k_g overall mass transfer coefficient for linear crystal growth [Equation (9.2.4)] [cm s^{-1} $(g/liter)^{-g}$]
k_G overall mass transfer coefficient for crystal growth [Equation (9.2.3)] [g cm^{-2} s^{-1} $(g/liter)^{-g}$]
k_1 rate constant for secondary nucleation [Equation (9.2.2)] [number $liter^{-1}$ s^{-1} $(g/liter)^{b-j}$]
k_m rate of change of diluent concentration (liter $liter^{-1}$ s^{-1})
k_n rate constant for primary nucleation [Equation (9.2.1)] [number $liter^{-1}$ s^{-1} $(g/liter)^{-n}$]
k_p constant in equation for solubility of solute as a function of diluent concentration [Equation (9.3.1)] (liter $liter^{-1}$)
k_r mass transfer coefficient for surface integration [Equation (9.2.6)] [g cm^{-2} s^{-1} $(g/liter)^{-r}$]
k_v volume shape factor (dimensionless)
L characteristic dimension of crystal (cm, or cm $liter^{-1}$)
M_T crystal suspension density (g $liter^{-1}$)
n population density distribution function (number $liter^{-1}$ cm^{-1})
N number concentration of nuclei (number $liter^{-1}$)
N_i impeller rotation rate (revolutions s^{-1})
Re Reynolds number $d_i^2 N_i \rho / \mu$ (dimensionless)
R rate of mass deposition on crystals during growth (g cm^{-2} s^{-1})
t time (s)
V solvent volume (liter)
W mass of crystals per volume of solvent (g $liter^{-1}$)
y size of crystals at time t [Equation (9.3.4)] (cm)

Greek Letters

μ fluid viscosity (g cm^{-1} s^{-1})
μ_k kth moment of the population density distribution (units vary)
ρ crystal or fluid density (g $liter^{-1}$)

Subscripts

f final
0 initial

Superscripts

* saturation or equilibrium
^ quantities based on total solvent volume
¯ average quantities

PROBLEMS

9.1 Modeling of Crystal Growth The data in Table P9.1 have been measured for the growth of crystals of an antibiotic. From this data set, obtain an expression for the relationship between dL/dt and the supersaturation $c - c^*$.

TABLE P9.1

$c - c^*$ (g/liter)	dL/dt (μm/min)
0.20	0.21
0.35	0.45
0.67	0.90
1.25	1.80
2.05	3.30
2.75	5.00

9.2 Nucleation and Growth Rates from Crystal Size Distribution Data Crystal size distribution (CSD) data were obtained with a multichannel Coulter counter during a crystallization experiment in a batch agitated vessel with isothermal conditions. The results of two CSD samples taken at different times differing by a small time interval are shown in Table P9.2. Use the method of moments analysis to determine the average nucleation and growth rates. At each time, also determine the population average crystal size. (Data from N. S. Tavare, *Industrial Crystallization,* p. 180, Plenum Press, New York, 1995.)

TABLE P9.2

Channel number	$\overline{L}$ (μm)	ΔL (μm)	$n(L) \times 10^{-10}$ (number m^{-1} kg^{-1})	
			At $t_1 = 3600$ s	At $t_2 = 4500$ s
4	17.4	4.0	180.9	176.3
5	21.9	5.0	43.6	55.7
6	27.6	6.4	24.5	32.1
7	34.8	8.0	21.8	23.4
8	43.8	10.1	13.8	17.6
9	55.2	12.7	13.9	18.1
10	69.6	16.0	6.4	9.3
11	87.7	20.2	3.8	4.8
12	110.5	25.4	0.7	1.3
13	139.2	32.0	0.4	0.3
14	175.4	40.3	0.06	0.12
15	221.0	50.8		0.09

9.3 Batch Crystallizer with Constant Rate of Diluent Addition For a solute being crystallized by batch crystallization with a constant rate of change of diluent concentration, predict the effect on the crystal size at any given time for each of the changes in the variables given. Justify your answers based on an expression for the crystal size as a function of these variables.

(a) An increase in the nucleation rate
(b) An increase in the growth rate
(c) An increase in the supersaturation, for b [Equation (9.2.2)] greater than g [Equation (9.2.3)]
(d) An increase in k_m in the equation $dc_d/dt = k_m$, where c_d is the diluent concentration
(e) An increase in k_p [Equation (9.3.1)]

9.4 Estimate of Particle Size for an Unseeded Batch Crystallizer For an unseeded batch crystallization of a biochemical using a constant rate of diluent concentration, the following is known:

$G = 10^{-7}\,\Delta c^2$ m/s
$B = 10^6\,\Delta c^3$ number (liter of solvent)$^{-1}$ s^{-1}
$\rho = 2.5 \times 10^3$ kg/m^3
$k_v = 0.6$
$k_a = 3.0$
$c^*_0 = 0.05$ kg of solute per liter of solvent
$k_p = 5$ liters (solvent and diluent) per liter of diluent
V_0 = initial volume of solvent = 1.0 liter
$\Delta c_0 = 0.005$ kg of solute per liter of solvent
$k_m = 2 \times 10^{-5}$ liter of diluent (liter of solvent)$^{-1}$ s^{-1}, where

$$\frac{dc_d}{dt} = k_m$$

Estimate the average size of the crystals 20 min from the start of nucleation. State all the assumptions necessary for the calculation.

9.5 Comparison of Three Scale-up Methods for a Crystallization A batch crystallization of an antibiotic was performed using a volume of 750 ml in the laboratory with a 3.5 cm diameter impeller at a speed of 600 rpm, the minimum speed required to fully suspend the crystals. Estimate the size of the impeller and the impeller speed for scale-up to 250 liters for each of the following three assumptions as a basis for scale-up: (1) constant power per volume, (2) constant impeller tip speed, and (3) full suspension of crystals (at minimum speed).

9.6 Deduction of Scale-up Equations for a Crystallization The batch crystallization of a biochemical resulted in virtually identical properties when conducted either at the laboratory scale (1 liter) or the plant scale (1000 liters). The lab crystallizer had an impeller of 3 cm diameter operating at 750 rpm, while the plant crystallizer had a 30 cm impeller with a speed of 77 rpm. What scale-up equations can be used to approximately characterize the scale-up of this crystallization? What property or properties are being assumed constant upon scale-up?

9.7 Bulk Volume Too High for Crystalline Erythromycin The bulk volume of dry, crystalline erythromycin (an antibiotic) produced in a plant batch crystallizer is out of specification (too high). Erythromycin free base is crystallized by the slow addition of dilute sodium hydroxide to a solution of an erythromycin salt dissolved in water-acetone. You have been asked to study this problem in the laboratory and

recommend a solution based on your results. Outline the experiments you would conduct in the lab, the results of which would serve as a basis for recommendations for how to change the operation of the plant crystallizer.

9.8 Primary versus Secondary Nucleation Why is it generally more desirable to have secondary nucleation rather than primary nucleation in crystallization?

REFERENCES

1. Tavare, N. S. (1995). *Industrial Crystallization*, Plenum Press, New York.
2. Genck, W. J. (1997). Crystallization from solutions. In *Handbook of Separations Techniques for Chemical Engineers*, 3rd ed., P. Schweitzer, ed., McGraw-Hill, New York, p. 2.
3. McCabe, W. L. (1929). Crystal growth in aqueous solutions. *Ind. Eng. Chem*., vol. 21, p. 30.
4. Perry, R. H., Green, D. W., and Maloney, J. O., eds. (1997). Liquid-solids operations and equipment. Section 18 in *Perry's Chemical Engineers' Handbook*, McGraw-Hill, New York.
5. Mullin, J. W. (1972). *Crystallization*, 2nd ed., CRC Press, Cleveland.
6. Tavare, N. S., Garside, J., and Chivate, M. R. (1980). Analysis of batch crystallizers. *Ind. Eng. Chem. Process Des. Dev*., vol. 19, p. 653.
7. Tavare, N. S., and Chivate, M. R. (1980). CSD analysis from a batch dilution crystallizer. *J. Chem. Eng. Jpn*., vol. 13, p. 371.
8. McPherson, A. (1985). Crystallization of macromolecules: general principles. *Methods Enzymol*., vol. 114, p. 112.
9. Lee, E. K., and Kim, W. S. (2003). Protein crystallization for large-scale bioseparation. *Biotechnol. Bioprocess*., vol. 27, p. 277.
10. Judge, R. A., Forsythe, E. L., and Pusey, M. L. (1998). The effect of protein impurities on lysozyme crystal growth. *Biotechnol. Bioeng*., vol. 59, p. 776.
11. Shenoy, B., Govardhan, C. P., Yang, M. X., and Margolin A. L. (2002). Crystals of whole antibodies and fragments thereof and methods for making and using them. *PCT Int. Appl*. WO 02072636 (A3).
12. Harrison, R. G., and Nelles, L. P. (1990). Large-scale process for the purification of alcohol oxidase, U.S. Patent 4,956,290.
13. Judge, R. A., Johns, M. R., and White, E. T. (1995). Protein purification by bulk crystallization: The recovery of ovalbumin. *Biotechnol. Bioeng*., vol. 48, p. 316.
14. Jacobsen, C., Garside, J., and Hoare, M. (1998). Nucleation and growth of microbial lipase crystals from clarified concentration fermentation broths. *Biotechnol. Bioeng*., vol. 57, p. 666.
15. Price, C. J. (1997). Take some solid steps to improve crystallization. *Chem. Eng. Prog*., vol. 93, p. 34.
16. Nienow, A. W. (1976). The effect of agitation and scale-up on crystal growth rates and on secondary nucleation. *Trans. Inst. Chem. Eng*., vol. 54, p. 205.
17. Rushton, J. H., Costich, W. W., and Everett, H. J., (1950). Power characteristics of mixing impellers. Part 2. *Chem. Eng. Progr*., vol. 46, p. 467.
18. Nienow, A. W. (1968). Suspension of solid particles in turbine agitated baffled vessels. *Chem. Eng. Sci*., vol. 23, p. 1453.

/// 10 /// EVAPORATION

Evaporation is a process that involves the removal by vaporization of part of the solvent from a solution, with the objective being to concentrate the solution. In the evaporation of solutions containing biological compounds, the volatile solvent can be water or an organic solvent. Organic solvents are frequently used for antibiotics, steroids, and peptides. Often the solution is under a moderate vacuum, at pressures down to about 0.05 atm absolute [1], which is especially important for heat-sensitive biologicals where the temperature should be as low as possible to minimize degradation. The energy source for evaporation is usually steam at a low pressure, below 3 atm absolute [1].

Evaporation processes typically occur after the processes used for the removal of insolubles. They are often used to concentrate a solution just prior to the bioproduct being crystallized or precipitated. Evaporation can often be coupled with extraction: for example, a bioproduct is extracted from an aqueous stream with an organic solvent, and the extract is sent to an evaporator for concentration.

In this chapter, the basic principles of evaporation are discussed, followed by a description of the most common types of evaporators for heat sensitive biological products and a discussion of scale-up and design methods.

10.1 INSTRUCTIONAL OBJECTIVES

After completing this chapter, the reader should be able to do the following:

- Explain the different types of resistances to heat transfer in an evaporator.
- Take into account the boiling point elevation in heat transfer calculations for evaporators.
- Calculate the heat transfer resistances and residence time for the concentration of a heat-sensitive bioproduct in a falling film evaporator.
- Estimate the fouling factor in an evaporator.
- Calculate the maximum allowable vapor velocity from an evaporator.
- Select an appropriate type of evaporator to use based on the specific operational and product characteristics.

- Size evaporators based on specific operating conditions and the expected overall heat transfer coefficient.

10.2 EVAPORATION PRINCIPLES

The main principles to consider for evaporators are heat transfer and vapor-liquid separation. The theoretical basis of these principles will be discussed.

10.2.1 Heat Transfer

Evaporators are in essence heat exchangers. Thermal energy is added to vaporize the solvent, leading to feed solution concentration. The heat exchange capacity for evaporators is usually expressed in the familiar form [1]

$$Q = UA\Delta T \tag{10.2.1}$$

where Q is the heat transfer rate, U is the overall heat transfer coefficient, A is the heat transfer surface area, and ΔT is the difference between the process heating medium temperature and the temperature of the solution being vaporized.

The overall resistance to heat transfer is composed of five resistances in series, which for the commonly used tube-and-shell geometry are as follows: the process heating medium film resistance, the resistance of solid deposits due to fouling (scale, dirt, and other types of solid deposits) on the outside of the tubes, the tube wall resistance, the resistance of solid deposits on the inside of the tubes, and the resistance of the film of the solution being vaporized. These resistances are related to the overall heat transfer coefficient by the equation [1]

$$U = \frac{1}{\frac{1}{h_{fi}} + \frac{1}{h_i} + \frac{D_i X_w}{\overline{D}_L k_w} + \frac{D_i}{D_o h_o} + \frac{D_i}{D_o h_{fo}}} \tag{10.2.2}$$

where h_{fi} and h_{fo} are the heat transfer coefficients of inside and outside fouling deposits, respectively, defined as *fouling factors;* h_i and h_o are the inside and outside film heat transfer coefficients, respectively; k_w is the thermal conductivity of the tube wall; X_w is the wall thickness; and D_i, D_o, and $\overline{D}_L$ are the inside, outside, and logarithmic mean diameters of the tube, respectively. This form of the equation is written with respect to the inside area of the tubes, because evaporation unit operations that will be discussed in this chapter occur mainly on the tube side, rather than the shell side.

Each term in the denominator of the right side of Equation 10.2.2 is termed a resistance to heat transfer. In most evaporators and especially in ones that process viscous liquids, the film coefficient of the solution being evaporated controls the overall heat transfer rate. In evaporators that use steam as the heating medium, the

fouling resistance of the condensing steam is usually very low and can be neglected in evaporator calculations. The resistance of the tube wall (X_w/k_w) is also very low, except in the case of agitated-film evaporators where the wall thickness can be large enough to cause this resistance to be significant.

In determining the temperature of the solution being vaporized, it is sometimes necessary to take into account the fact that because of the presence of a nonvolatile solute or solutes, at a given pressure the boiling point of the solution will be higher than that of pure solvent. This difference in boiling points is known as the *boiling point elevation* (BPE) of the solution. The BPE is small for dilute solutions but can be appreciable for concentrated solutions of inorganic salts. For dilute solutions [2]

$$BPE = \frac{RT_b^{o2}}{\lambda_o} x_i \tag{10.2.3}$$

where x_i is the mole fraction of solute i, T_b^o is the boiling temperature of pure solvent at the relevant pressure, λ_o is the molar heat of vaporization of pure solvent, and R is the ideal gas constant. For solutions containing appreciable mass fractions of solutes with high molecular masses, such as proteins, the mole fractions are very low, and hence the BPE is negligible. Duhring's rule can be used to estimate the BPE for aqueous concentrated solutions where Equation 10.2.3 does not apply [3]. According to this empirical rule, the boiling point of a solution is a linear function of the boiling point of pure water as the latter varies with pressure. This is illustrated by the plot of the boiling temperature of the solution versus the boiling temperature of water, which gives a straight line. A plot using Duhring's rule for sodium chloride is shown in Figure 10.1, where there is a different straight line at each concentration of sodium chloride. Over a moderate range of temperatures, the lines for these plots are very nearly straight, although not always parallel [1].

The liquid head and frictional losses are two other factors that lead to the boiling point of the solution being greater than the boiling point corresponding to the pressure in the vapor space. The liquid head can be determined based on the height of the evaporator. Several correlations for predicting the pressure drop in various flow configurations in evaporators are given by Minton [4].

Correlations have been developed to predict film heat transfer coefficients for different patterns of flow [4]. For highly heat-sensitive bioproducts, one flow configuration that is often used is falling-film flow down a vertical tube. For this flow configuration, the inside and outside heat transfer coefficient can be estimated using a modified Nusselt number [1]:

$$\mathrm{Nu}' = \frac{h}{k_f}\left(\frac{\mu_f^2}{\rho_f^2 g}\right)^{1/3} \tag{10.2.4}$$

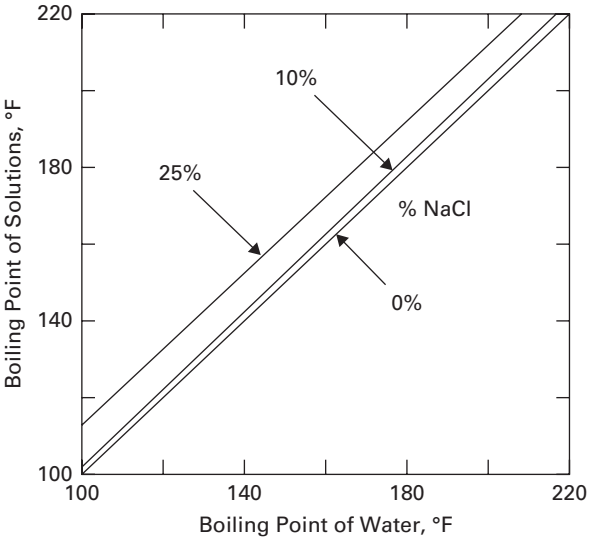

FIGURE 10.1 Illustration of Duhring's rule for sodium chloride. *(Data from A. J. Hickey and D. Ganderton, (2001).* Pharmaceutical Process Engineering*, p. 130, Dekker, New York, 2001.)*

where k_f = thermal conductivity
μ_f = viscosity
ρ_f = density
g = gravitational acceleration

and the subscripts refer to the properties of the liquid in the film

For laminar flow in the film, the correlation based on theory has been found to be [1]

$$\text{Nu}' = 1.47\text{Re}^{-1/3} \tag{10.2.5}$$

where $\text{Re} = 4\,\Gamma/\mu_f$
Γ = mass flow rate per unit of circumference of the tube

Experimental data agree with Equation 10.2.5 up to Re of about 30. In the range of $30 < \text{Re} < 1800$, waves appear on the surface of the film, resulting in an increase in the heat transfer rate. This region of flow is called the wavy-laminar region. At above Re of 1800, flow in the film becomes turbulent. The empirical equation for the wavy-laminar and turbulent regions is [1]

$$\text{Nu}' = \left(\text{Re}^{-0.44} + 5.82 \times 10^{-6}\,\text{Re}^{0.8}\text{Pr}^{1.3}\right)^{1/2} \tag{10.2.6}$$

where Pr = Prandtl number ($= C_{pf}\mu_f/k_f$)
C_{pf} = specific heat

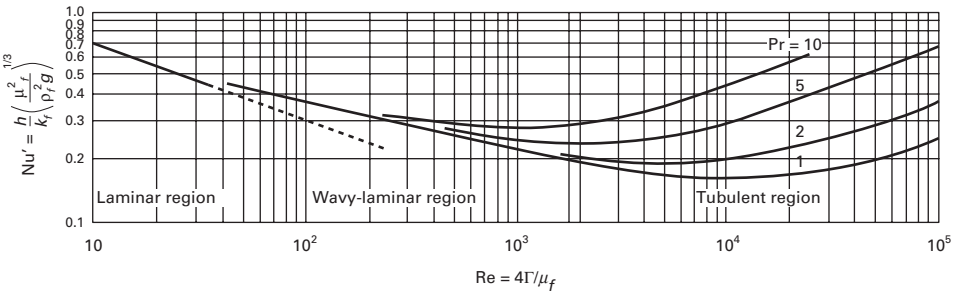

FIGURE 10.2 Correlation of the film heat transfer coefficient as a function of the Reynolds number for condensation on vertical surfaces. *(Data from W. L. McCabe, P. Harriott, and J. C. Smith,* Unit Operations of Chemical Engineering*, 7th ed., p. 394, McGraw-Hill, Boston, 2005.)*

The correlations for all three flow regions are shown graphically in Figure 10.2. These correlations were developed for condensation on vertical surfaces, but they have been found to be approximately correct for evaporation from a film flowing down a vertical surface.

In order to estimate the residence time in a falling film, it is necessary to calculate the film thickness. The following equation for the film thickness δ has been derived by a shell momentum balance on a film falling in laminar flow down a flat plate [5]:

$$\delta = \left(\frac{3\mu_f \Gamma}{\rho_f^2 g \cos\varphi} \right)^{1/3} \tag{10.2.7}$$

where φ is the angle of the surface from vertical. Film thickness measurements have shown Equation (10.2.7) to be valid up to a Reynolds number of approximately 1200 [1].

Fouling of the heat exchanger surface by the solution being vaporized depends on the specific solutes present in the solution; therefore, the fouling factor for a given solution being evaporated must be determined experimentally. In one such experimental study, the fouling factor for the evaporation of whey in a vacuum falling-film tubular evaporator was measured for a variety of process conditions [6]. The fouling heat transfer resistance factor for the whey solution was found to range up to a maximum of 1400 W m^{-2} K^{-1}, giving an overall heat transfer coefficient U that was 32% of this coefficient before fouling took place. Two conclusions of this study are that the pH strongly influenced the fouling and that evaporation should be performed at no more than 60°C to minimize the deposition of proteins.

EXAMPLE 10.1

Evaporation of a Butyl Acetate Stream Containing a Heat-Sensitive Antibiotic in a Falling-film Evaporator In a process to purify a highly heat-sensitive antibiotic produced by fermentation, an extract stream in butyl acetate needs to be concentrated by evaporation. A falling-film evaporator is available that has

stainless steel tubes with a 40 mm inside diameter, 2 mm wall thickness, and length of 4 m. Evaporation takes place at 55°C, the boiling point of butyl acetate at an absolute pressure of 52 mm Hg. Steam at 60°C is used as the heating medium. The butyl acetate extract stream flows on the inside of the tubes at 50 kg/h per tube at 55°C. Assuming that the physical properties of the butyl acetate stream are unaffected by the evaporation, determine the inside film heat transfer coefficient, the overall heat transfer coefficient, the evaporation rate per tube, and the average residence time in the evaporator.

Solution.

In solving this problem, we use the appropriate correlation for the Nusselt number for heat transfer in a falling film, either Equation 10.2.5 or 10.2.6, depending on the flow regime. The film thickness calculated from Equation 10.2.7 can be used to determine the residence time. This problem involves a trial-and-error calculation, where an overall heat transfer coefficient U is initially selected in order to be able to calculate the flow rate for the steam and the butyl acetate stream at the bottom of the evaporator. The calculation is repeated until the initial U selected and final U calculated match each other. Calculations of U are based on the inside heat transfer surface area.

In calculating the modified Nusselt number, several physical properties are needed. For most of the physical properties of butyl acetate and steam, correlations can be used to obtain estimates at the temperatures for this problem:

Butyl acetate at 55°C = 328 K:

From *Yaws' Handbook of Thermodynamic and Physical Properties of Chemical Compounds* [7] at temperatures in K,

$$\lambda_o = 57.75\left(1-\frac{T}{579.65}\right)^{0.393} = 57.75\left(1-\frac{328}{579.65}\right)^{0.393} = 41.6\,\frac{\text{kJ}}{\text{mol}}$$

$$k_f = 0.1862 - 8.7332\times10^{-5}T - 2.5688\times10^{-7}T^2 = 0.130\,\frac{\text{W}}{\text{m K}}$$

$$\mu_f = 10^{-8.3884+\frac{1.3075\times10^3}{T}+0.0177\,T-1.6145\times10^{-5}T^2} = 0.463\text{ cp}$$

$$\rho_f = \frac{0.2986}{\left(0.2603^{\left(1-\frac{T}{579.65}\right)^{0.309}}\right)} = 0.845\,\frac{\text{g}}{\text{cm}^3}$$

$$C_{pf} = 122.827 + 6.590\times10^{-1}T - 1.844\times10^{-3}T^2 + 2.6300\times10^{-6}T^3$$

$$= 233\,\frac{\text{J}}{\text{mol K}}$$

Steam condensate at 60°C = 140°F:

From the *Handbook of Chemical Engineering Calculations* [8] for temperatures in °F,

$$\lambda_o = 1087.54 - 0.4311T - 5.5440\times10^{-4}T^2$$

$$= 1087.54 - 0.4311(140) - 0.5440\times10^{-4}(140)^2$$

$$= 1016\frac{\text{Btu}}{\text{lb}} = 2363\frac{\text{J}}{\text{g}}$$

$$k_f = 0.31171 + 6.2278\times10^{-4}T - 1.1159\times10^{-6}T^2$$

$$= 0.377\frac{\text{Btu}}{\text{h ft °F}} = 0.652\frac{\text{W}}{\text{m K}}$$

$$\mu_f = -0.23535 + 208.65T^{-1} - 2074.8T^{-2}$$

$$= 1.15\frac{\text{lb}}{\text{h ft}} = 0.475\ \text{cp}$$

$$\rho_f = 62.7538 - 3.5347\times10^{-3}T - 4.8193\times10^{-5}T^2$$

$$= 61.3\ \frac{\text{lb}}{\text{ft}^3} = 0.982\ \frac{\text{g}}{\text{cm}^3}$$

From the *Chemical Engineers' Handbook* [9] at 60°C,

$$C_{pf} = 75.4\frac{\text{J}}{\text{mol K}}$$

Calculations are first performed for the butyl acetate falling film. Because the flow rate of the film changes from the top to the bottom of the tube, in calculating the inside film heat transfer coefficient we calculate Re, Pr, and Nu' at the top and bottom of the tube. At the top of the tube:

$$\Gamma = \frac{50\frac{\text{kg}}{\text{h}}\times\frac{1\text{h}}{3600\text{s}}\times\frac{10^3\text{g}}{\text{kg}}}{\pi\times0.040\text{m}} = 111\frac{\text{g}}{\text{m s}}$$

$$\text{Re} = \frac{4\Gamma}{\mu} = \frac{4\times111\frac{\text{g}}{\text{m s}}\times\frac{1\text{m}}{10^2\text{cm}}}{0.463\text{cp}\times\frac{0.01\text{g}}{\text{cp cm s}}} = 959$$

$$\mathrm{Pr} = \frac{C_p \mu}{k} = \frac{233 \dfrac{\mathrm{J}}{\mathrm{mol\,K}} \times 0.463\,\mathrm{cp} \times \dfrac{0.01\,\mathrm{g}}{\mathrm{cp\,cm\,s}} \times \dfrac{\mathrm{mol}}{116.2\,\mathrm{g}} \times \dfrac{1\,\mathrm{W\,s}}{\mathrm{J}} \times \dfrac{10^2\,\mathrm{cm}}{\mathrm{m}}}{0.130 \dfrac{\mathrm{W}}{\mathrm{m\,K}}} = 7.14$$

We use Equation 10.2.6 to calculate Nu′ since the Reynolds number indicates that flow is in the wavy-laminar region:

$$\mathrm{Nu}' = \left(\mathrm{Re}^{-0.44} + 5.82 \times 10^{-6} \mathrm{Re}^{0.8} \mathrm{Pr}^{1.3}\right)^{1/2}$$

$$= \left[(959)^{-0.44} + 5.82 \times 10^{-6} (959)^{0.8} (7.14)^{1.3}\right]^{1/2} = 0.259$$

Using these results, the internal heat transfer coefficient can be calculated using Equation 10.2.4:

$$h_i = k_f Nu' \left(\frac{\rho_f^2 g}{\mu_f^2}\right)^{1/3}$$

$$= 0.130 \frac{\mathrm{W}}{\mathrm{m\,K}} \times 0.259 \left[\frac{\left(0.845 \dfrac{\mathrm{g}}{\mathrm{cm}^3}\right)^2 \times 980.7 \dfrac{\mathrm{cm}}{\mathrm{s}^2} \times \left(\dfrac{10^2\,\mathrm{cm}}{\mathrm{m}}\right)^3}{\left(0.463\,\mathrm{cp} \times \dfrac{0.01\,\mathrm{g}}{\mathrm{cp\,cm\,s}}\right)^2}\right]^{1/3}$$

$$= 1076 \frac{\mathrm{W}}{\mathrm{m\,K}}$$

At the bottom of the tube, we can relate the overall heat transfer coefficient U to the evaporation rate w using Equation 10.2.1:

$$Q = UA\Delta T = w\lambda_o$$

or

$$w = \frac{UA\Delta T}{\lambda_o}$$

Overall heat transfer coefficients for heat exchangers in which steam is the hot fluid and a light organic is the cold fluid have been found to vary over the range 500-1000 W m^{-2} K^{-1} [10]. We initially choose U = 1000 and calculate a value of U = 892. Further iterations give an initial and final U = 888, as follows:

$$w = \frac{888\dfrac{\mathrm{W}}{\mathrm{m^2\,K}} \times \pi\left(0.040 \times 4\right)\mathrm{m^2} \times 5\mathrm{K}}{41{,}600\dfrac{\mathrm{J}}{\mathrm{mol}} \times \dfrac{\mathrm{mol}}{116.2\,\mathrm{g}} \times \dfrac{\mathrm{W\,s}}{\mathrm{J}}} = 6.23\frac{\mathrm{g}}{\mathrm{s}}$$

Therefore, at the bottom of the tube

$$\text{Product rate} = 50{,}000\frac{\mathrm{g}}{\mathrm{h}} \times \frac{1\mathrm{h}}{3600\,\mathrm{s}} - 6.23 = 13.89 - 6.23 = 7.66\frac{\mathrm{g}}{\mathrm{s}}$$

$$\Gamma = \frac{7.66}{\pi \times 0.040} = 61.0\frac{\mathrm{g}}{\mathrm{ms}}$$

$$\mathrm{Re} = \frac{4 \times 61.0}{0.438} = 527$$

$$Pr = \frac{233 \times 0.463}{0.130 \times 116.2} = 7.14$$

The value of Re indicates that the flow is still in the wavy-laminar region, so we can use Equation 10.2.6 again:

$$Nu' = \left[\left(527\right)^{-0.44} + 5.82 \times 10^{-6}\left(527\right)^{0.8}\left(7.14\right)^{1.3}\right]^{1/2} = 0.273$$

$$h_i = 0.130 \times 0.273\left[\frac{\left(0.845\right)^2 \times 980.7 \times \left(10^2\right)^3}{\left(0.463 \times 0.01\right)^2}\right]^{1/3} = 1134\frac{\mathrm{W}}{\mathrm{m^2K}}$$

Based on the h_i at the top and bottom,

$$h_{i,avg} = \frac{1076 + 1134}{2} = 1105\frac{W}{m^2K}$$

To calculate U, we also need to calculate h_o for the steam condensate film at 60°C. We first calculate the steam rate, using the outside diameter of the tubes for the calculations:

$$w = \frac{UA\Delta T}{\lambda_o} = \frac{888\dfrac{\mathrm{W}}{\mathrm{m^2K}} \times \pi\left(0.044 \times 4\right)\mathrm{m^2} \times 5\mathrm{K}}{2363\dfrac{\mathrm{J}}{\mathrm{g}} \times \dfrac{\mathrm{Ws}}{\mathrm{J}}} = 1.038\frac{\mathrm{g}}{\mathrm{s}}$$

$$\Gamma = \frac{1.038}{\pi \times 0.044} = 7.51 \frac{\text{g}}{\text{ms}}$$

$$\text{Re} = \frac{4 \times 7.52}{0.475} = 63.2$$

$$Pr = \frac{75.4 \times 0.475}{0.652 \times 18.0} = 3.05$$

Equation 10.2.6 can be used to calculate Nu′ since Re indicates the flow is in the wavy-laminar region:

$$Nu' = \left[(63.2)^{-0.44} + 5.82 \times 10^{-6} (63.2)^{0.8} (3.05)^{1.3} \right]^{1/2} = 0.402$$

$$h_o = 0.652 \times 0.402 \left[\frac{(0.982)^2 \times 980.7 \times (10^2)^3}{(0.475 \times 0.01)^2} \right]^{1/3} = 9105 \frac{\text{W}}{\text{m}^2\text{K}}$$

Now U can be calculated from Equation 10.2.2 assuming no resistance from fouling and assuming the thermal conductivity of stainless steel = 15.7 W m^{-1} K^{-1} at 58°C [11]:

$$\overline{D}_L = \frac{D_o - D_i}{\ln\left(\frac{D_o}{D_i}\right)} = \frac{44 - 40}{\ln\left(\frac{44}{40}\right)} = 42.0\,\text{mm}$$

$$U = \frac{1}{\frac{1}{1105} + \frac{0.040}{0.042}\left(\frac{0.002}{15.7}\right) + \frac{0.040}{0.044}\left(\frac{1}{9105}\right)} = 888 \frac{\text{W}}{\text{m}^2\text{K}}$$

To calculate the residence time of the butyl acetate stream in the evaporator, the film thickness is first calculated at the top and bottom using Equation 10.2.7, which is then used to calculate the fluid velocity u in the film. The tubes are assumed to be perfectly vertical, so $\cos\varphi = 1$ in Equation 10.2.7.

Top:

$$\delta = \left(\frac{3\mu_f \Gamma}{\rho_f^2 g} \right)^{\frac{1}{3}} = \left[\frac{3 \times 0.463\,\text{cp} \times 111 \frac{\text{g}}{\text{ms}} \times \frac{0.01 \frac{\text{g}}{\text{cms}}}{\text{cp}} \times \frac{1\,\text{m}}{10^2\,\text{cm}}}{\left(0.845 \frac{\text{g}}{\text{cm}^3}\right)^2 \times 980.7 \frac{\text{cm}}{\text{s}^2}} \right]^{1/3} = 0.0280\ \text{cm}$$

$$u = \frac{\text{volumetric flow rate}}{\text{cross} - \text{sectional area}} = \frac{50\dfrac{\text{kg}}{\text{h}} \times \dfrac{1\,\text{h}}{3600\,\text{s}} \times \dfrac{10^3\,\text{g}}{\text{kg}} \times \dfrac{\text{cm}^3}{0.845\,\text{g}}}{\pi(4.0\,\text{cm}) \times 0.0280\,\text{cm}} = 46.7\frac{\text{cm}}{\text{s}}$$

Bottom:

$$\delta = \left(\frac{3 \times 0.463 \times 61.0 \times 10^{-4}}{(0.845)^2 \times 980.7} \right)^{1/3} = 0.0230\,\text{cm}$$

$$u = \frac{\left(\dfrac{50 \times 10^3}{3600} \right) \times \dfrac{1}{0.845}}{\pi \times 4.0 \times 0.0230} = 56.9\frac{\text{cm}}{\text{s}}$$

The average velocity and residence time in the film therefore are

$$u_{avg} = \frac{46.7 + 56.9}{2} = 51.8\frac{\text{cm}}{\text{s}}$$

$$\tau_{\text{avg}} = \frac{4000\ \text{cm}}{51.8\dfrac{\text{cm}}{\text{s}}} = 7.7\,\text{s}$$

Thus, the residence time is very short, which is highly desirable for a heat-sensitive bioproduct.

10.2.2 Vapor-Liquid Separation

For an evaporator to operate efficiently, the vapor released from the evaporator should contain little or no liquid in the form of droplets or foam. The carryover of droplets with the vapor is called entrainment. At the outlet of the evaporation tubes, there is a volume called the vapor space where liquid/gas separation can take place. The cross-sectional area of the vapor space must be large enough so that the droplets can fall into the liquid collection zone, while the gas rises to a vapor collection zone. When the vapor and liquid are both moving up in a vertical rising-film evaporator, or horizontally in a forced-circulation evaporator, the velocity of the vapor is a key factor in the final separation of liquid and vapor phases. The maximum allowable velocity u_m of the vapor can be estimated by the Souders-Brown equation [12]:

$$u_m = K\left[\frac{(\rho_l - \rho_v)}{\rho_v} \right]^{1/2} \quad (10.2.8)$$

where ρ_l and ρ_v are the density of the liquid and vapor, respectively, and K is an experimentally determined constant having units of velocity that depends on the size distribution of the droplets and the desired level of removal of droplets from the exiting vapor. The constant K can be estimated as a function of the decontamination factor F (kg of vapor per kg of entrained liquid) as shown in Table 10.1.

For decontamination factors between 100 and 10,000, K can be estimated by the relationship [9]

$$K \cong \frac{0.245}{(F-50)^{0.4}} \tag{10.2.9}$$

Often, the vapor space is designed for a decontamination factor of approximately 200 [12].

It is generally not economical to design for the desired degree of vapor-liquid separation in the vapor space alone. One or more additional separators are frequently used to reduce entrainment of liquid drops in the vapor. These separators are designed so the vapor flow changes its direction when traveling at a high velocity [9]; a typical design that involves the use of a cyclone is shown in Figure 10.3. In falling-film evaporators, both the vapor and liquid move down (see Figure 10.4), and most of the entrainment separation occurs within the tubes [12]. Therefore, gas velocities can be higher in these evaporators to achieve the same separation.

Foaming can be a problem in the evaporation of liquid containing colloids, surface tension depressants, or finely divided solids [9]. Causes of foaming include an air leak below the liquid level or the presence of dissolved gases in the liquid [4]. Operating under a vacuum, often used in evaporation, would cause air to be drawn into the evaporator and would also cause bubbles to be created from dissolved gases. Measures taken to reduce foaming losses include the use of antifoams agents, steam jets that impinge on the foam surface, and baffles that impinge on the foam at high velocity in order to break the foam mechanically.

TABLE 10.1 Estimate of the constant K for values of the decontamination factor F in the Souders-Brown equation for maximum allowable velocity in the vapor space of an evaporator [12]

F	K (m/s)
100	0.051
200	0.033
500	0.020
1000	0.015
2000	0.011

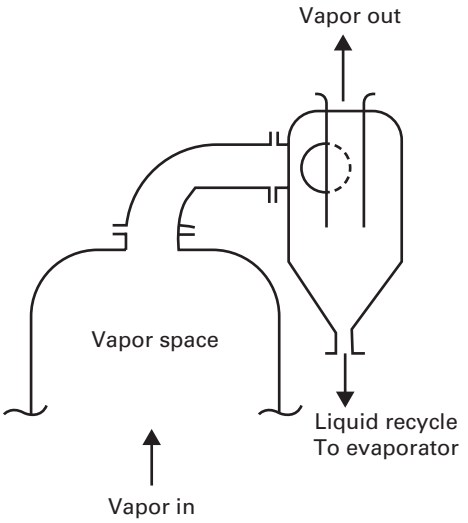

FIGURE 10.3 Example of a cyclone entrainment separator for an evaporator.

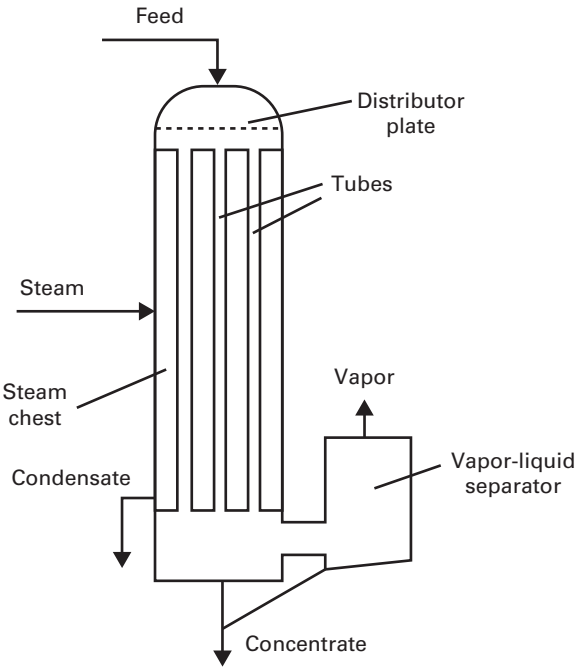

FIGURE 10.4 Falling-film evaporator with long tubes.

10.3 EVAPORATION EQUIPMENT

In selecting the type of evaporator for an application, several operational and product characteristics of the solution to be evaporated need to be considered. These include [13]:

- Heat sensitivity
- Fouling

- Foaming
- Solids
- Viscosity
- Wetting of the heat exchanger surface

Heat sensitivity is an issue for many bioproducts. Mitigation of foaming may require a special design for the vapor/liquid separation area or for reducing the vapor velocity in the tubes. Increasing the viscosity of the concentrate will reduce the overall heat transfer coefficient. Serious fouling and deposits of solids on the heat exchange surface may occur if the surface is not sufficiently wetted, which can lead to product degradation as a result of hot spots on the surface; recycling some of the concentrate may be required to avoid this problem.

A number of different types of evaporators have been developed for a variety of applications. Here, we will focus on the evaporator types that are used to concentrate liquid streams containing biological products, all of which are heat-sensitive to some degree.

Evaporators used for processing heat-sensitive bioproducts can be generally classified as long-tube vertical evaporators or agitated-film evaporators. The major types of long-tube vertical evaporators are the climbing-film evaporator, the falling-film evaporator, and the forced circulation evaporator. Evaporators can be operated in either the once-through or circulation mode. In once-through operation, the feed passes through the tubes only once, with vapor and a concentrated product leaving the unit. In the circulation mode, there is a pool of liquid within the unit, which is circulated through the tubes with incoming feed, and vapor is withdrawn. In circulating systems, even though the residence time in the heating zone is relatively short, some of the liquid is held within the evaporator for a considerable length of time. Therefore, bioproducts that are heat sensitive should be processed using the once-through mode; bioproducts that have relatively low heat sensitivity can possibly be processed in the circulation mode in evaporators, depending on the bioproduct. For some bioproducts such as food, heating damage to even a small part of a batch can lead to an unacceptable product.

The climbing-film evaporator and falling-film evaporator can be operated in both the once-through and circulation modes. The agitated-film evaporator is only operated in the once-through mode, while the forced-circulation evaporator is operated only in the circulation mode.

10.3.1 Climbing-Film Evaporators

In the climbing-film evaporator, evaporation starts at the bottom of the tubes (Figure 10.5). The vapor produced by this heating travels faster than the liquid upward through the core of the tube, which ideally leads to liquid being pulled up the tube in a thin film at the tube wall. In reality, slugs of liquid and gas bubbles also rise up the tubes. The liquid becomes more concentrated as it rises up the

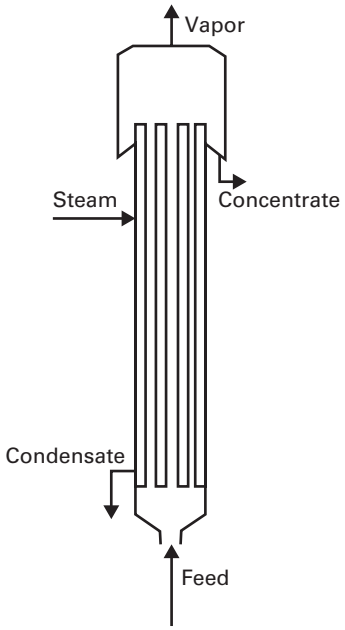

FIGURE 10.5 Climbing-film evaporator with long tubes.

tubes. The vapor-liquid mixture enters a cyclone separator at the top of the tubes, where the vapor flows overhead and the liquid exits. Climbing-film evaporators are effective in evaporating liquids that tend to foam [1, 14], but they are not suitable for processing viscous liquids [3, 15].

10.3.2 Falling-Film Evaporators

In a falling-film evaporator, feed that has been preheated is fed to the top of long tubes that are heated (Figure 10.4). The feed is distributed so that a thin film of liquid flows down the inner surface of each tube by gravity. Evaporation takes place on the surface of this falling film, and liquid and vapor are usually separated at the bottom of the tubes. For this type of evaporator to operate correctly, it is essential that the liquid be distributed evenly at the tube inlet so that the film is uniform around the circumference of the tube. Even distribution of liquid can be achieved by a perforated distribution plate, or by a spray nozzle inside each tube [1]. In this evaporator, there is not an elevation of the boiling point to consider since there is no hydrostatic head above the boiling surface. These evaporators can operate with low temperature differences between the falling liquid film and the heating medium and can handle viscous liquids [15].

10.3.3 Forced-Circulation Evaporators

Fluid is pumped through the tubes in a forced-circulation evaporator. An example of this type of evaporator is shown in Figure 10.6, where the tubes are horizontal

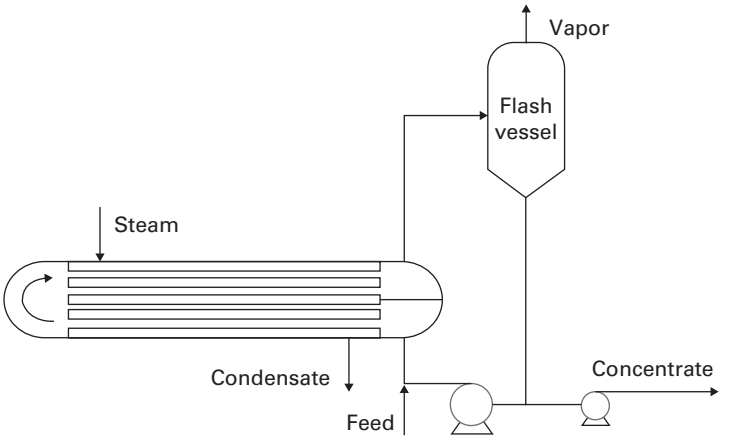

FIGURE 10.6 Forced-circulation evaporator with horizontal tubes.

and there are two passes on both the tube and shell sides. Vertical tubes can be used with a single pass exchanger. In forced-circulation evaporators, typically there is sufficient hydrostatic head on the liquid in the tubes that boiling does not take place in the tubes. The liquid in the tubes becomes superheated, and it flashes at the tube exit into vapor and a liquid spray. The vapor leaves the evaporator, while the liquid circulates back to the inlet of the pump. These evaporators have high heat transfer coefficients, and they have the advantage of being able to process viscous liquids [1, 14].

10.3.4 Agitated-Film Evaporators

As mentioned earlier, the film coefficient of the liquid being evaporated usually controls the overall heat transfer coefficient. In an agitated-film evaporator, this liquid-film coefficient can be increased greatly by the action of rotating wiper blades that spread the liquid across the surface of the tube (Figure 10.7). This evaporator is similar to the falling-film evaporator in that the liquid enters the tube at the top and concentrated liquid leaves at the bottom after entering a cyclone separator. Agitated-film evaporators operate well for extremely viscous fluids, with viscosity in the range of 1000 to 50,000 centipoise, and have much higher heat transfer coefficients than in any other type of evaporator for the same conditions [14]. Foaming and fouling are inhibited in this type of evaporator [15].

10.4 SCALE-UP AND DESIGN OF EVAPORATORS

After the selection of the type of evaporator for the desired operation, the next steps are scale-up and design. Pilot plant testing is often necessary to obtain data for scale-up and design. In some cases, it might be desirable to test more than one evaporator type. Data typically obtained include operating temperatures and pressures, feed rates, heat transfer coefficients, physical property data (including viscosities),

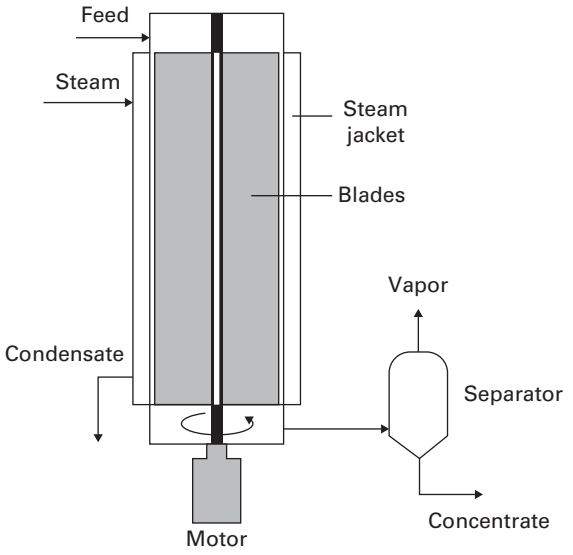

FIGURE 10.7 Agitated-film evaporator with a single tube.

and data on foaming and fouling. Most commercial equipment vendors for evaporators maintain pilot plant facilities for this testing, and they have developed process modeling software for the design of large scale evaporators. For example, to obtain scaleup data for agitated thin-film evaporators, the minimum size required is 0.10 to 0.13 m^2 of heat exchanger area, and the feed rate is about 20 to 70 kg/h [16]. However, a bench scale evaporator with a surface are of 0.023 m^2 can be used for feasibility studies using laboratory-produced quantities of material at a feed rate of 1 to 8 kg/h. In the design of evaporators, it is necessary to do calculations for each evaporator that include a material balance, enthalpy balance, and the heat transfer relationship (Equation 10.2.1) [1].

In order to reduce energy costs, the use of more than one evaporator unit in series is common in systems that require solvent evaporation rates of from thousands to hundreds of thousands of kg per hour [14]. The use of more than one evaporator in series is called a *multiple-effect* system. In a single-effect evaporator, 0.8 to 0.9 kg of water is evaporated per kg of steam used for heating [15]. The kg of solvent evaporated per kg of steam used is known as the *steam economy*. The operation of the multiple-effect evaporator system is shown schematically in Figure 10.8. The basic principle is that the heat released by condensing the vapor from the first evaporator is used for heating in the second evaporator, and so on for additional evaporators in series. This system is possible only if the evaporation temperature of the liquid in effect $i + 1$ is lower than the temperature of the vapor leaving the evaporator in effect i, which is achieved by operating effect $i + 1$ at a lower pressure than effect i. The steam economy for a double- and triple-evaporator is 1.4 to 1.8 and 2.2 to 2.7 kg of water evaporated per kg of steam used, respectively [15]. Multiple-effect systems commonly have three to

five effects. In some large plants for processing milk and fruit juice, up to seven effects are being used.

An analysis can be performed for a multiple-effect evaporator system to determine the relationship between the temperature drops and the overall heat transfer coefficients [1]. The heat transfer equation for the first effect is

$$Q_1 = U_1 A_1 \Delta T_1 \tag{10.4.1}$$

Assuming that the feed to the first effect is at its boiling point, nearly all of Q_1 is the latent heat of the vapor leaving the first effect. In steady state operation, nearly all of this heat is given up when this vapor condenses in the second effect, and therefore

$$Q_1 \cong Q_2 = U_2 A_2 \Delta T_2 \tag{10.4.2}$$

Similar expressions can be written for additional effects. For economical construction, the same evaporator areas are used in each effect, which gives

$$U_1 \Delta T_1 \cong U_2 \Delta T_2 \tag{10.4.3}$$

or

$$\frac{U_2}{U_1} \cong \frac{\Delta T_1}{\Delta T_2} \tag{10.4.4}$$

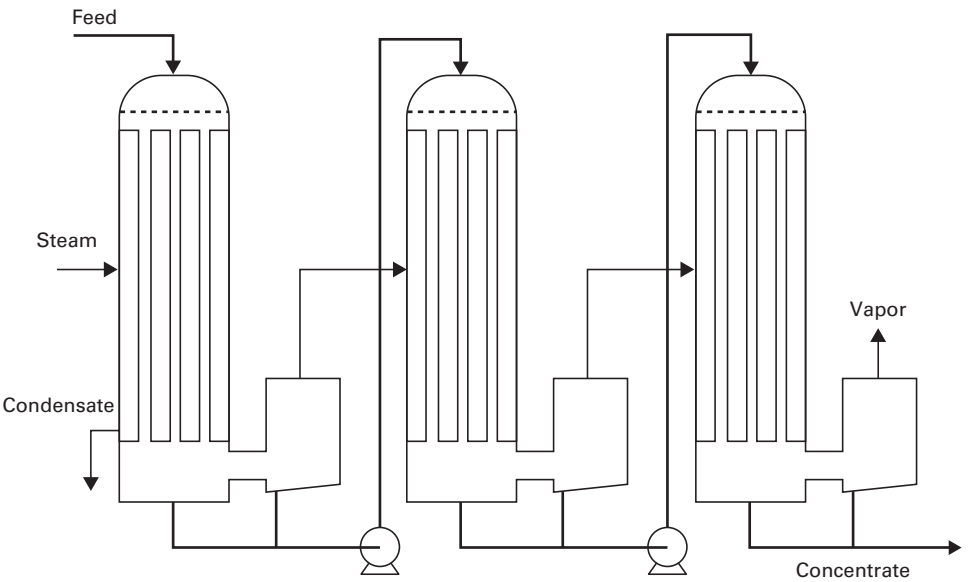

FIGURE 10.8 Multiple-effect evaporator system with three effects.

When the vapor from the evaporator is steam, another method to reduce the energy required for evaporation is by using *vapor recompression*. This involves increasing the pressure of the vapor by mechanical or thermal recompression and then using this vapor as the heating medium in the same evaporator effect, which is possible because the condensing temperature of the vapor is higher than it was before recompression. The energy savings by using multiple-effect evaporation can sometimes be achieved with a single-effect evaporator with recompression [14]. Vapor recompression can be applied to one or more effects, although mechanical compression is usually limited to a single effect system. For vacuum evaporators, thermal recompression is normally used, since the steam jets employed can handle large volumes of low-density vapor and are easier to maintain than compressors [1].

10.5 SUMMARY

In evaporation, a volatile solvent is removed from a solution containing biological compounds, with the objective of concentrating the solution. For heat-sensitive biological substances, evaporation usually is carried out under a vacuum in order to reduce the processing temperature.

- The overall heat transfer coefficient U is composed of five resistances in series, which for the commonly used tubular geometry are as follows: the process heating-medium film resistance, the fouling deposit resistance on the outside of the tubes, the tube wall resistance, the fouling deposit resistance on the inside of the tubes, and the resistance of the film of the solution being vaporized. For most evaporators, the film resistance of the solution being vaporized controls the overall heat transfer rate.
- The presence of nonvolatile solutes can cause the boiling point of the solution being evaporated to be higher than that of the pure solvent, an effect known as the boiling point elevation (BPE). Protein solutes, even at high mass fractions, have a negligible contribution to the BPE; however, the contribution from concentrated solutions of salts can be appreciable.
- Correlations have been developed to predict heat transfer coefficients in various types of evaporators. The falling-film evaporator is an evaporator type for which there are correlations of heat transfer coefficients. The thickness of the falling film can also be estimated from a correlation, and this thickness can be used to predict the residence time for the film in the evaporator.
- The maximum allowable velocity of vapor released from an evaporator for a given desired level of removal of droplets from the exiting vapor can be estimated from the Souders-Brown equation.
- A number of different types of evaporators have been developed. The evaporators that have been found to be the most useful for processing heat-sensitive bioproducts are the long-tube vertical evaporators (climbing-film, falling-film,

and forced-circulation types) and the agitated-film evaporator. Once-through operation is best for bioproducts that have relatively high heat sensitivity, while those with relatively low heat sensitivity can be processed in the circulation mode.

- To obtain data for evaporator scale-up and design, pilot plant testing is often necessary. Data typically obtained include operating temperatures and pressures, feed rates, heat transfer coefficients, physical property data (including viscosities), and data on foaming and fouling.
- A multiple-effect evaporator system is one in which more than one evaporator in series is used. These types of systems are common when thousands to hundreds of thousands of kg per hour of solvent must be evaporated. The use of a multiple-effect system can dramatically increase the steam economy (kg of solvent evaporated per kg of steam used) compared to a single-effect evaporator.

NOMENCLATURE

A	cross-sectional area (m^2)
BPE	boiling point elevation (K)
C_p	specific heat (J mol^{-1} K^{-1})
D	tube diameter (m)
g	gravitational acceleration (9.8066 m s^{-2})
h	film heat transfer coefficient (W m^{-2} K^{-1})
h_f	fouling factor in heat transfer (W m^{-2} K^{-1})
K	decontamination factor, or the weight of vapor per weight of entrained liquid [Equation 10.2.9] (dimensionless)
k	thermal conductivity (W m^{-1} K^{-1})
$\dot{m}$	mass flow rate (g s^{-1})
Nu′	modified Nusselt number $\left(= \frac{h}{k_f}\left(\frac{\mu_f^2}{\rho_f^2 g}\right)^{1/3}\right)$ (dimensionless)
Pr	Prandtl number (= $C_{pf}\mu_f/k_f$) (dimensionless)
Q	rate of heat flow (J s^{-1})
R	gas law constant (8.3145 J mol^{-1} K^{-1})
Re	Reynolds number (= 4 Γ/μ_f for flow of a film on the surface of a tube) (dimensionless)
T	temperature (K)
T_b^o	boiling temperature of pure solvent (K)
U	overall heat transfer coefficient (W m^{-2} K^{-1})
u	velocity (m s^{-1})
w	evaporation rate (kg s^{-1})
x_i	mole fraction of solute i
X_w	wall thickness of tube (m)

Greek Letters

Γ	mass rate per unit width of flowing film (g m^{-1} s^{-1})
σ	film thickness (m)
λ_o	heat of vaporization of solvent (J g^{-1}, or J mol^{-1})
μ	viscosity (cp)
ρ	density (g cm^{-3})
τ	residence time (s)
φ	angle of surface of heat exchange surface from vertical (degrees)

PROBLEMS

10.1 Estimation of the Fouling Factor A stream containing a peptide in aqueous solution is concentrated inside the tubes of a falling-film evaporator using steam as the heating source. Just after cleaning the evaporator tubes, the overall heat transfer coefficient was measured to be 2000 W m^{-2} K^{-1}. After 30 days of operation, the overall heat transfer coefficient was again measured and found to be 1500 W m^{-2} K^{-1}. Assuming the steam is not causing fouling on the outside of the tubes, what is the inside fouling factor after 30 days of operation?

10.2 Temperature Differences in a Multiple Effect Evaporator For a multiple effect evaporator with a total of n effects and equal transfer areas in the effects, develop a relationship for ΔT_i ($= T_{i-1} - T_i$) in the i^{th} effect as a function of the overall heat transfer coefficients for the effects and the overall temperature difference ($T_s - T_n$), where T_s is the temperature of the steam to the first effect and T_n is the boiling temperature of the process fluid in the last effect. State any assumptions that are made.

10.3 Maximum Allowable Velocity of Vapor from an Evaporator A bioproduct in an aqueous liquid is concentrated in a climbing film evaporator at a pressure of 150 mm Hg absolute. Estimate the maximum allowable velocity of the vapor from the evaporator for there to be only 0.0025 kg of entrained liquid in the vapor phase per kg of vapor. The vapor pressure P (psia) of water as a function of temperature T (°F) is given by [8]:

$$P = \exp\left[10.9955 - 9.6866 \ln T + 1.9779 (\ln T)^2 - 0.085738 (\ln T)^3\right]$$

The liquid density ρ_l (lb/ft^3) and vapor density ρ_v (lb/ft^3) of water as a function of temperature T (°F) are given by [8]:

$$\rho_l = 62.7538 - 3.5347 \times 10^{-3} T - 4.8193 \times 10^{-5} T^2$$

$$\rho_v = \exp\left(-9.3239 + 4.1055 \times 10^{-2} T - 7.1159 \times 10^{-5} T^2 + 5.7039 \times 10^{-8} T^3\right)$$

State any assumptions that are made.

10.4 Single-effect Falling Film Evaporator for a Peptide Solution A solution containing a peptide with a molecular weight of 8000 Daltons needs to be concentrated from

1% solids to 15% solids at a feed rate of 200 kg/h using a falling-film evaporator. The evaporator operates at a pressure of 100 mg Hg, and the heating medium is steam at 60°C. The overall heat transfer coefficient for the evaporator is 2000 W m^{-2} K^{-1}. The feed enters the evaporator at 20°C. The vapor pressure P (psia) and heat of vaporization λ_o (Btu/lb) of water as a function of temperature T (°F) are given by [8]:

$$P = \exp\left[10.9955 - 9.6866 \ln T + 1.9779 (\ln T)^2 - 0.085738 (\ln T)^3\right]$$

$$\lambda_o = 1087.54 - 0.43110 T - 5.5440 \times 10^{-4} T^2$$

The specific heat of water for the range of operation of the evaporator can be assumed to be constant at 4.18 kJ/kg-K [9]. Determine steam rate, steam economy, and the heating surface area required for this evaporator.

10.5 Double-effect Falling Film Evaporator The peptide solution in problem 10.4 is to be concentrated to the same outlet solids concentration and at the same feed rate in a double-effect falling film evaporator that has the same heat transfer area in each of the effects. However, the feed enters the first effect at its boiling point. For the first effect, the operating pressure, steam temperature, and overall heat transfer coefficient are the same as in problem 10.4. The overall heat transfer coefficient in the second effect is 1800 W m^{-2} K^{-1}. Determine the operating pressure in the second effect, heat transfer area for each evaporator, the steam rate, and the steam economy.

REFERENCES

1. McCabe, W. L., Harriott, P., and Smith, J. C. (2005). *Unit Operations of Chemical Engineering*, McGraw-Hill, MA.
2. Laidler, K. J., Meiser, J. H., and Sanctuary, B. C. (2003). *Physical Chemistry*, Houghton Mifflin, Boston.
3. Hickey, A. J., and Ganderton, D. (2001). *Pharmaceutical Process Engineering*, M. Dekker, New York.
4. Minton, P. E. (1986). *Handbook of Evaporation Technology*, Noyes Publications, Park Ridge, NJ.
5. Bird, R. B., Stewart, W. E., and Lightfoot, E. N. (2002). *Transport Phenomena*, J. Wiley, New York.
6. Kessler, H.-G. (2002). *Food and Bio Process Engineering: Dairy Technology*, Verlag A. Kessler, München.
7. Yaws, C. L. (2003). *Yaws' Handbook of Thermodynamic and Physical Properties of Chemical Compounds*, Knovel, Norwich, NY.
8. Chopey, N. P. (2004). *Handbook of Chemical Engineering Calculations*, McGraw-Hill, New York.
9. Perry, R. H., and Green, D. W. (2008). *Perry's Chemical Engineers' Handbook*, McGraw-Hill, New York.
10. Peters, M. S., Timmerhaus, K. D., and West, R. E. (2003). *Plant Design and Economics for Chemical Engineers*, McGraw-Hill, New York.
11. McAdams, W. H. (1954). *Heat Transmission*, McGraw-Hill, New York.
12. Standiford, F. C. (2000). Evaporation. In *Kirk-Othmer Encyclopedia of Chemical Technology (online)*, John Wiley & Sons, Hoboken, NJ.

13. Glover, W. B. (2004). Selecting evaporators for process applications. *Chem. Eng. Prog.*, vol. 100, p. 26.
14. Freese, H. L. (1997). Evaporation. In *Fermentation and Biochemical Engineering Handbook*, H. C. Vogel and C. L. Todaro, eds., Noyes Publications, Westwood, NJ, p. 476.
15. Brennan, J. G. (2006). Evaporation and dehydration. In *Food Processing Handbook*, J. G. Brennan, ed.,Wiley-VCH Verlag GmbH & Co. KGaA, Weinheim, p. 71.
16. Glover, W. B. (2004). Scaleup of agitated thin-film evaporators. *Chem. Eng.*, vol. 111, p. 55.

/// 11 /// DRYING

The last step in the separation process for a biological product is usually drying, which is the process of thermally removing volatile substances (often water) to yield a solid. In the step preceding drying, the desired product is generally in an aqueous solution and at the desired final level of purity. The most common reason for drying a biological product is that it is susceptible to chemical (e.g., deamidation or oxidation) and/or physical (e.g., aggregation and precipitation) degradation during storage in a liquid formulation. Another common reason for drying is for convenience in the final use of the product. For example, it is often desirable that pharmaceutical drugs be in tablet form. Additionally, drying may be necessary to remove undesirable volatile substances. Also, although many bioproducts are stable when frozen, it is more economical and convenient to store them in dry form rather than frozen.

Drying is now an established unit operation in the process industries. However, because most biological products are thermally labile, only those drying processes that minimize or eliminate thermal product degradation are actually used to dry biological products. This chapter focuses on the types of dryer that have generally found the greatest use in the drying of biological products: vacuum-shelf dryers, batch vacuum rotary dryers, freeze dryers, and spray dryers [1]. The principles discussed, however, will apply to other types of dryers as well.

We begin with the fundamental principles of drying, followed by a description of the types of dryer most used for biological products. Then we present scale-up and design methods for these dryers.

11.1 INSTRUCTIONAL OBJECTIVES

After completing this chapter, the reader should be able to do the following:

- Do drying calculations involving relative humidity using the psychrometric moisture chart and the equilibrium moisture curve for the material being dried.
- Calculate the relative amounts of bound and unbound water in wet solids before drying.

- Model heat transfer in conductive drying and calculate conductive drying times.
- Interpret drying rate curves.
- Calculate convective drying times of nonporous solids based on mass transfer.
- Distinguish and choose among vacuum-shelf dryers, vacuum rotary dryers, freeze dryers, and spray dryers.
- Scale up the four dryer types studied.

11.2 DRYING PRINCIPLES

A considerable amount of theory has been developed for drying, from simple approaches to complex theory involving the numerical solution of differential equations. We emphasize the basic theory that will illuminate underlying drying principles, along with theory that will assist in scale-up and design.

11.2.1 Water in Biological Solids and in Gases

Before considering the removal of water by drying, it is helpful to understand how water is held within biological solids and also to know how to estimate the properties of gases, especially air, containing water vapor. As for all materials, the water contained within biological solids is in two forms, *unbound or free water* and *bound water*. Unbound water is free to be in equilibrium with water in the vapor phase; thus, unbound water has the same vapor pressure as bulk water. Unbound water is mainly held in the voids of the solid. On the other hand, bound water can exist in several conditions: (1) water in fine capillaries that exerts an abnormally low vapor pressure because of the highly concave curvature of the surface, (2) water containing a high level of dissolved solids, and (3) water in physical or chemical combination with the biological solids. Solids containing bound water are called *hygroscopic;* different solids can have widely varying hygroscopic properties [2].

Equilibrium data for moist solids in contact with humid air give valuable information about the water capacity of the solids. Typically, the water content of the solid is plotted as a function of the relative humidity of air, as shown in Figure 11.1 for three bioproducts. Curves of the type shown in Figure 11.1 are nearly independent of temperature. Humidity is defined as the mass of water per mass of dry air. From the ideal gas law, the concentration of water c_w in moles per volume can be related to the humidity $\mathscr{H}$ and total pressure p as follows:

$$c_w = \frac{P_w}{RT} = \frac{\mathscr{H}(M_{air}/M_{water})}{1+\mathscr{H}(M_{air}/M_{water})}\frac{p}{RT} = \frac{\mathscr{H}(28.9/18)}{1+\mathscr{H}(28.9/18)}\frac{p}{RT} \tag{11.2.1}$$

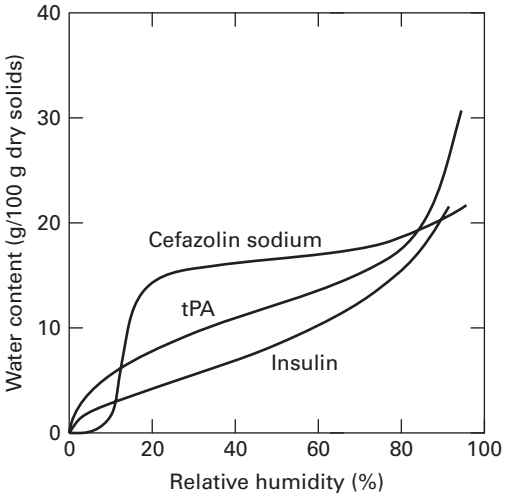

FIGURE 11.1 Equilibrium-moisture curves drawn to represent data for the antibiotic cefazolin sodium (crystalline) [3] and the proteins human tissue type plasminogen activator (tPA, lyophilized) [4] and human insulin (crystalline) [5].

Here p_w is the partial pressure of water, M is molecular weight, T is the temperature, and R is the ideal gas constant. The relative humidity R_m can be determined from p_w and the saturation vapor pressure of water p_{ws} as follows:

$$(11.2.2)\quad R_m = \frac{p_w}{p_{ws}} \times 100$$

The saturation vapor pressure of water is a function of temperature only and is known exactly when the temperature is known.

A convenient way of showing the properties of mixtures of air and water vapor mixtures is the humidity or psychrometric chart shown in Figure 11.2. Any point on this chart represents a specific mixture of air and water. The curved line denoted by 100% represents the humidity of air saturated with water as a function of temperature. Any point below the 100% or saturation curve represents air that is unsaturated with water, and a point on the dry-bulb temperature axis represents the air temperature. The web-bulb or saturation temperature lines that slant downward from the saturation curve are called adiabatic cooling lines. Thus, if an unsaturated air-water mixture at a point on one of these lines had been cooled adiabatically, the change in composition of the mixture when the temperature was lowered could be followed by moving along these lines toward the 100% saturation curve.

The wet-bulb temperature is the temperature measured by a glass thermometer covered with a wet wick and air flowing past. This results in evaporation of water in the wick and the loss of the heat of vaporization, resulting in cooling of the water. The extent of evaporation depends on the humidity of the air. Note that at less than

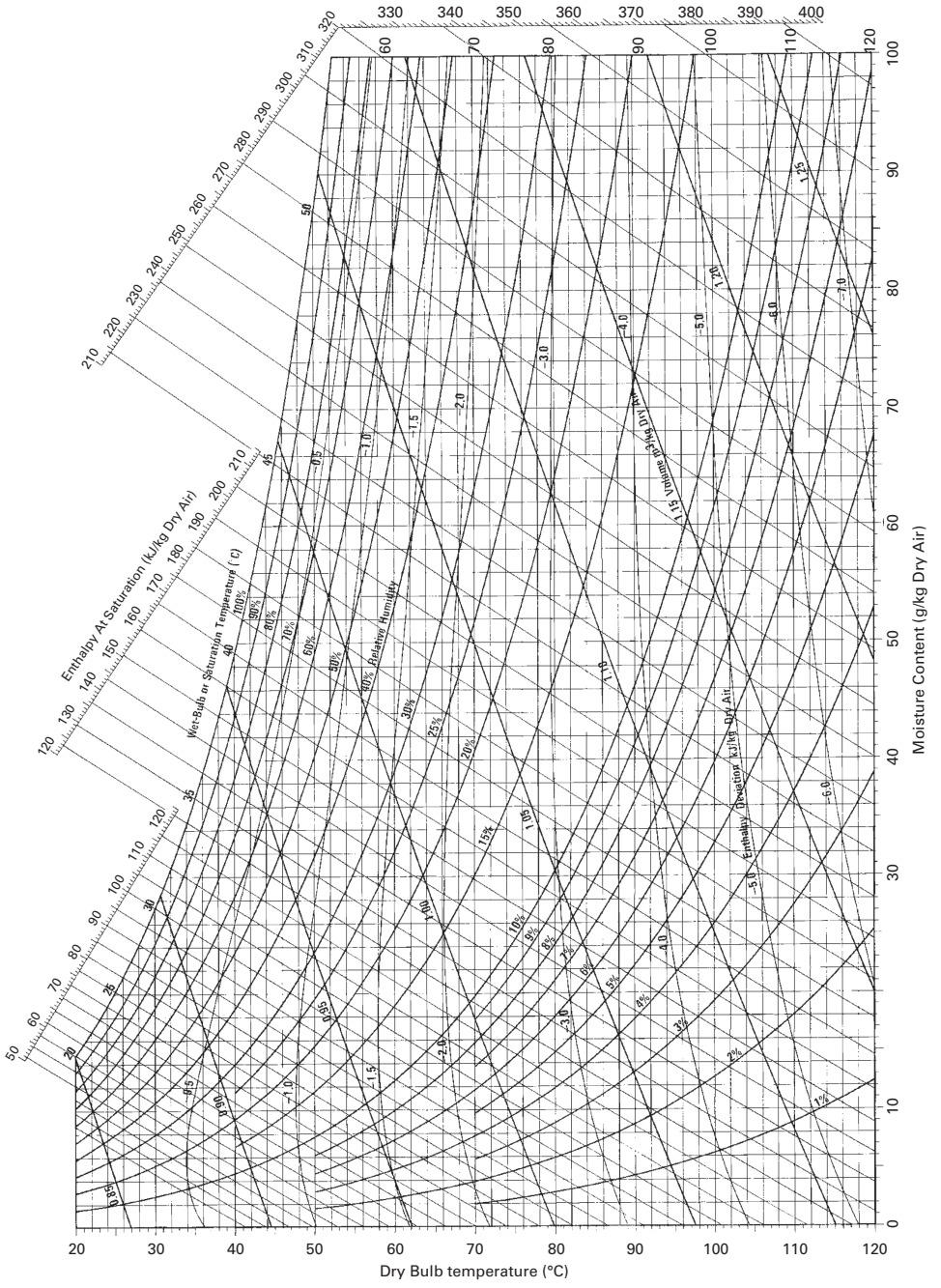

FIGURE 11.2 Properties of air and water vapor mixtures from 20 to 120°C. *(Courtesy of Carrier Corp.)*

100% humidity in Figure 11.2, the wet-bulb temperature is always less than the dry-bulb temperature, but both temperatures are identical at 100% humidity.

It can also be observed in Figure 11.2 that as the temperature is raised at constant moisture content (humidity), the relative humidity decreases. This is explained by Equation (11.2.2): while the mole fraction of water and thus the partial pressure of water (p_w) remains constant as the temperature rises, the saturation vapor pressure of water (p_{ws}) rises and thus causes R_m to decrease.

In carrying out heat calculations for dryers, the enthalpy of the drying gas must be calculated. The total enthalpy H_y at temperature T of a unit mass of gas plus water vapor is defined relative to a datum temperature T_0 as

$$H_y = C_s(T - T_0) + \mathscr{H}\lambda_0 \tag{11.2.3}$$

where C_s is the specific heat (also called the humid heat) of the gas and water vapor mixture, and λ_0 is the latent heat of the liquid at T_0 [2]. The specific heat C_s can be further defined as

$$C_s = C_{pg} + C_{pw}\mathscr{H} \tag{11.2.4}$$

where C_{pg} and C_{pw} are the specific heats of the gas and water vapor, respectively. For air and water vapor mixtures,

$$C_s\left(\frac{\text{kcal}}{\text{kg dry air} - \text{K}}\right) = 0.24 + 0.46\mathscr{H}$$

$$\lambda_0 = 597\frac{\text{kcal}}{\text{kg water at 0°C}} \quad (\text{at 0°and 760 mm Hg}) \tag{11.2.5}$$

EXAMPLE 11.1

Drying of Antibiotic Crystals Air at 1 atm and 25°C with a relative humidity of 50% is to be heated to 50°C and then to be used in drying wet crystals of the antibiotic cefazolin sodium. The wet crystals contain 30 g of water per 100 g of dry antibiotic. In the drying process, the air at 50°C and the crystals reach equilibrium with respect to the moisture. Determine the following: the percentages of bound and unbound water in the wet crystals before drying, the moisture content of the crystals after drying, and the water partial pressure at the drying temperature.

Solution

The equilibrium moisture curve for cefazolin sodium in Figure 11.1 can be extrapolated to 100% relative humidity to give a water content of 23 g/100 g dry weight. The water corresponding to concentrations lower than 23 g/100 g dry weight is bound water, because it exerts a vapor pressure less than that of liquid water at the same temperature. The balance of water contained in the crystals is therefore unbound water. Thus,

$$\text{Bound water} = 23\ \frac{\text{g}}{100\,\text{g dry weight}}$$

$$\text{Unbound water} = 30 - 23 = 7\ \frac{\text{g}}{100\,\text{g dry weight}}$$

Using Figure 11.2, we move from a temperature of 25°C and relative humidity of 50% to a temperature of 50°C, keeping the moisture content constant. By interpolation, the relative humidity of the air is read to be 13%. At this relative humidity, we see from the equilibrium moisture curve for cefazolin sodium (Figure 11.1),

$$\text{Moisture content of antibiotic after drying} = 8\ \text{g water} / 100\ \text{g dry weight}$$

It has been assumed that the equilibrium curve in Figure 11.1 is independent of temperature for the temperature range in this example. From Equation (11.2.1),

$$p_w = \frac{\mathscr{H}(28.9/18)p}{1+\mathscr{H}(28.9/18)}$$

From Figure 11.2 at 13% relative humidity and 50°C,

$$\mathscr{H} = 0.010\,\frac{\text{kg}}{\text{kg dry air}}$$

so that the water partial pressure at 50°C is

$$p_w = \frac{0.010(28.9/18)(1\,\text{atm})}{1+0.010(28.9/18)} = 0.016\,\text{atm}$$

11.2.2 Heat and Mass Transfer

Two fundamental processes take place during the drying of solids: the transfer of heat to evaporate liquid and the transfer of mass as a liquid or vapor within the solid and as a vapor from the surface of the solid. The rate of drying depends on the factors governing heat and mass transfer.

Heat Transfer

Because the drying of wet solids is by definition a thermal process, heat transfer is of primary importance in drying. Although diffusion can be important in some types of drying, drying rates are often limited by heat transfer. The principal heat transfer mechanisms are the following: *conduction* from a hot surface contacting the material, *convection* from a gas that contacts the material, *radiation* from a hot gas or hot surface, and *dielectric or microwave heating* in high-frequency electric fields that generate heat within the wet material [6]. We will focus on conductive drying and convective drying. Conductive drying dominates in vacuum-shelf dryers, batch vacuum rotary dryers, and freeze dryers, while convective drying is predominant in spray drying.

In conductive drying, heat is supplied through the surface of the dryer and flows into the solids being dried. Either the solids are contained in trays on shelves that are heated, or they are moving freely inside the dryer and come in frequent contact with the surface of the dryer, where heat is transferred by conduction to the solid particles being dried. Fourier's law of heat conduction applies in conductive drying:

$$q = -k\frac{dT}{dy} \tag{11.2.6}$$

where q is the heat flux (flow rate of heat per unit area), T is the temperature, k is the thermal conductivity of the solid, and y is measured in the direction of heat flow. For a slab held at a different temperature on each surface, this equation states that the heat flux is constant if the thermal conductivity is constant throughout the slab.

Convective drying involves the transfer of heat from a moving gas phase, providing the heat for drying to a solid phase. For this situation, the rate of heat transfer is described in terms of a heat transfer coefficient h:

$$Q = hA(T - T_s) \tag{11.2.7}$$

where Q is the rate of heat flow into the solid, A is the surface area through which heat flows, T is the gas bulk phase temperature, and T_s is the temperature at the solid surface [7]. This can be written in terms of the heat transfer rate per unit area, or heat flux q as

$$q = h(T - T_s) \tag{11.2.8}$$

In analyzing the performance of either a conductive or a convective dryer, it is sometimes convenient to describe the system by an overall heat transfer coefficient U:

$$Q = UA\Delta T \tag{11.2.9}$$

where A is the heat transfer area and ΔT is the average temperature difference [2]. The average temperature difference depends on the dryer being considered and is not always the logarithmic mean temperature difference. For some types of dryer, the area available for heat transfer is not known with certainty; and it is more convenient to use a volumetric heat transfer coefficient Ua, with a being the heat transfer area per unit dryer volume:

$$Q = UaV\Delta T \tag{11.2.10}$$

where V is the volume of the dryer. For this situation, a is unknown and the quantity Ua is either calculated or measured. For some dryers, the true average temperature difference for the whole dryer is difficult to define. Often, no general correlations are available for heat transfer coefficients, and these coefficients must be found experimentally.

EXAMPLE 11.2

Conductive Drying of Wet Solids in a Tray Wet biological solids contained in trays are being dried in a vacuum-shelf dryer. The following information is known. The shelves are maintained at temperature T_0 by circulating warm water. The wet solids have thermal conductivity k. The heat of vaporization of water is λ, and mass of water per unit volume of wet solids is ρ_0. Develop an expression for the time to dry a bed of wet solids of depth d. The solids have a porous, granular character when dry.

Solution

In this problem, heat flows by conduction through the bottom of the tray and into the solids, as shown in Figure E11.2. For granular solids, we can assume that water begins to evaporate at the top of the solids and then continues to evaporate at a boundary between the wet and dry solids that recedes into the bed at a distance y from the bottom of the bed. The water vapor is not bound to the dry solids lattice and is rapidly removed. This is the "receding front" or "shrinking core" model of drying [8, 9]. We assume that the temperature of the moving interface stays constant at the boiling point of evaporating water at temperature T_s, which is determined by the operating vacuum pressure

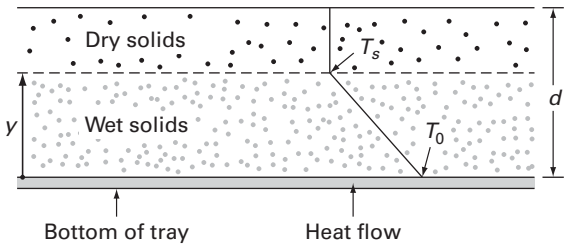

FIGURE E11.2 Schematic of conductive drying of biological solids in a tray, showing the receding boundary between the wet and dry solids.

of the dryer. If the thermal conductivity of the tray is much greater than the thermal conductivity of the solids being dried, then we can assume that the shelf temperature is the same as the solids temperature at the bottom of the tray. Applying Fourier's law of heat conduction [Equation (11.2.6)] gives

$$q = k\frac{(T_0 - T_s)}{y}$$

Thus, the heat flux increases as the drying progresses since y decreases. Relating the rate of heat conduction to the heat to vaporize water gives

$$q\,A = -\lambda\frac{d}{dt}\left(\rho_0 y\,A\right)$$

where A is the cross-sectional area. After combining with the equation for q according to Fourier's law of conduction, this equation can be integrated with the following initial condition

$$\text{At } t = 0, \qquad y = d$$

to yield

$$\frac{d^2 - y^2}{2} = \frac{k(T_0 - T_s)}{\lambda\rho_0}t$$

The drying is complete when $y = 0$, which gives time as

$$t = \frac{d^2\lambda\rho_0}{2k\left(T_0 - T_s\right)}$$

Mass Transfer

Drying can be limited by mass transfer in convective drying. In convective drying, the first water to evaporate is that next to the gas moving across the surface of the wet solids. After an initial warming-up period, the rate of movement of water to the surface is rapid enough that the surface remains saturated, and the drying rate remains constant for a period of time called the constant drying rate period. During this period, mass transfer is limited by a gas boundary layer at the surface of the solids. At a *critical moisture content* X_c, however, the internal rate of water movement is not fast enough to keep the surface saturated, and the drying rate begins to fall. In the falling drying rate period, the drying rate asymptotically approaches the *equilibrium moisture content* X_e. These drying periods are illustrated in Figure 11.3.

The drying rate curve is influenced by the type of material being dried as well as by the type of mass transfer that is controlling, as indicated in the representative

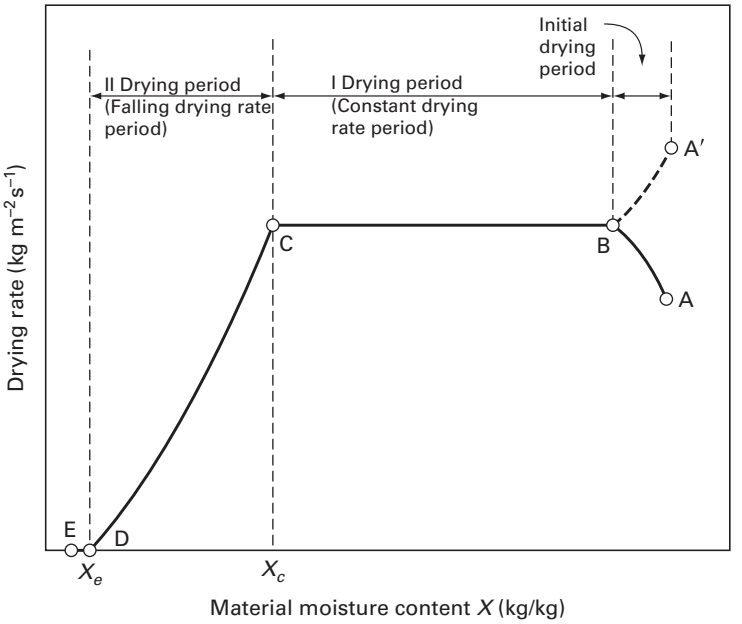

FIGURE 11.3 Drying rate curve, illustrating the periods of drying.

curves shown in Figure 11.4. Biological materials can be classified as nonhygroscopic, partially hygroscopic, or totally hygroscopic. Thus, there is no constant drying period in completely hygroscopic biological solids or in solids of any type when the mass transfer is completely controlled by internal diffusion.

The mass transfer of water being evaporated at the solid surface by gas flowing past the surface can be defined in terms of a mass transfer coefficient k_G:

$$N_w = k_G \Delta p_w \tag{11.2.11}$$

where N_w = molar flux of water, and Δp_w = difference in partial pressure of water between the surface and the bulk gas stream [7].

This equation can also be put in terms of concentrations by using Equation (11.2.1). Thus, when the partial pressure of water at the surface starts to drop, the critical moisture content X_c has been reached and the period of falling drying rate begins. During the constant drying rate period, the steady-state relationship between heat and mass transfer at the liquid surface is

$$q = \lambda N_w \tag{11.2.12}$$

where q is the heat flux and λ is the heat of vaporization of water. Combining Equations (11.2.8) and (11.2.12) leads to

$$N_w = \frac{h(T - T_s)}{\lambda} \tag{11.2.13}$$

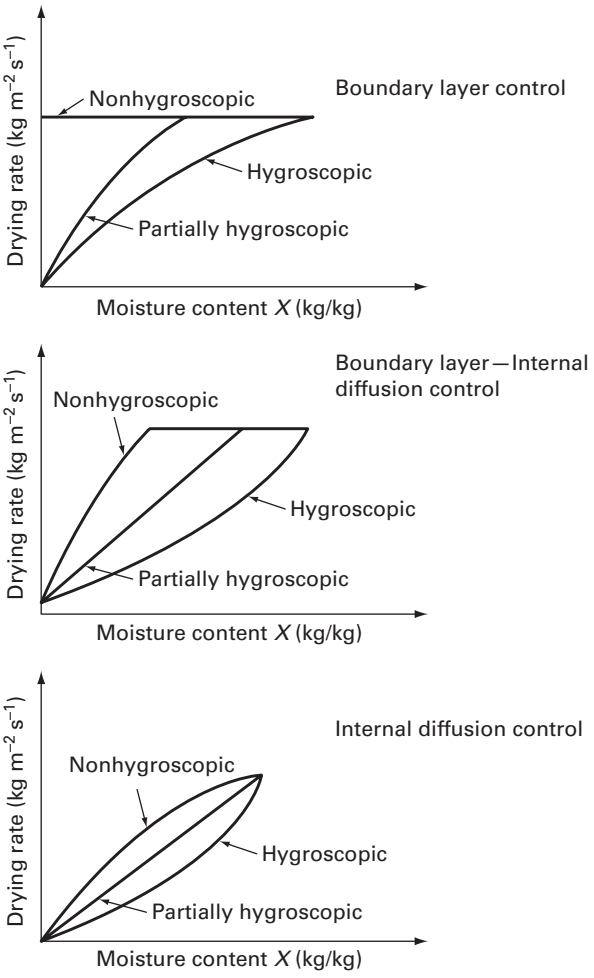

FIGURE 11.4 Drying rate curves for various types of materials and mass transfer conditions.

This equation allows us to estimate the evaporation rate if we know the heat transfer coefficient and the relevant temperatures. This heat transfer coefficient has been found to vary from 10 to 100 kcal m^{-2} h^{-1} K^{-1} for forced convection of gases [7].

The temperature at the surface of a moist solid that is undergoing drying in the constant drying rate period is usually very nearly at the *wet-bulb temperature,* which is defined as the steady state temperature of a small mass of water that is evaporating into a continuous stream of humid air [2]. The wet-bulb temperature is very nearly equal to the adiabatic saturation temperature for air-water mixtures, which is shown in Figure 11.2 on the curve denoted 100% saturation.

During the falling rate drying period, the principal mass transfer mechanisms are (1) liquid diffusion in continuous, homogeneous materials, (2) vapor diffusion in porous or granular materials, (3) capillary flow in porous or granular materials, (4) gravity flow in granular materials, and (5) flow caused by shrinkage-induced pressure gradients [6]. A bed of antibiotic crystals, for example, is granular and

porous, while a protein precipitate tends to be nonporous and colloidal. Vapor diffusion occurs in the dry solids when there is a shrinking interface between the dry solids and either wet solids (see Example 11.2) or frozen solids (where sublimation is occurring at the interface during freeze drying—see Section 11.3.3). One mechanism generally dominates at a given time in the drying cycle, although several mechanisms can occur together.

The liquid diffusion of water, either liquid or vapor, through a solid matrix undergoing drying can be described by Fick's second law of diffusion, written in terms of the moisture content X in mass of water per mass of dry solids:

$$\frac{\partial X}{\partial t} = \mathscr{D} \frac{\partial^2 X}{\partial y^2} \tag{11.2.14}$$

where t is time, $\mathscr{D}$ is the diffusion coefficient of water in the solid matrix, and y is the distance measured in the direction of diffusion. Because diffusion is much slower in the liquid phase than in the vapor phase, it is of interest to solve Fick's second law for the case of liquid diffusion in nonporous solids. An analytical solution of this equation has been obtained by making the following assumptions: (1) liquid diffusion is independent of moisture content (i.e., $\mathscr{D}$ is constant), (2) initial moisture distribution is uniform, and (3) material size, shape, and density are unchanging. For solids in the shape of a slab of thickness $2d$ with drying on both sides, with the following initial and boundary conditions:

$$\text{At } t = 0 \text{ and } -d < y < d, \quad X = X_c \tag{11.2.15}$$

$$\text{At } t > 0 \text{ and } y = \pm d, \qquad X = X_e \tag{11.2.16}$$

where X_c and X_e are the critical and equilibrium moisture contents, respectively, the solution for the average moisture content is

$$\frac{X_m - X_e}{X_c - X_e} = \frac{8}{\pi^2}\left[\sum_{n=0}^{n=\infty} \frac{1}{(2n+1)^2} \exp\left[-(2n+1)^2 \mathscr{D} t \left(\frac{\pi}{2d}\right)^2\right]\right] \tag{11.2.17}$$

where X_m is the average moisture content [9]. For long drying times when $\mathscr{D}t/d^2$ exceeds approximately 0.1,

$$\frac{X_m - X_e}{X_c - X_e} = \frac{8}{\pi^2} \exp\left[-\mathscr{D} t \left(\frac{\pi}{2d}\right)^2\right] \tag{11.2.18}$$

Differentiating Equation (11.2.18) with respect to time gives the following expression for the drying rate:

$$-\frac{dX_m}{dt}=\frac{\pi^2\mathscr{D}}{4d^2}(X_m-X_e) \tag{11.2.19}$$

Equation (11.2.18) can also be solved for t to obtain the time for the falling drying rate period:

$$t=\frac{4d^2}{\pi^2\mathscr{D}}\ln\left[\frac{8(X_c-X_e)}{\pi^2(X_m-X_e)}\right] \tag{11.2.20}$$

In actuality, the diffusion coefficient usually declines as the moisture content decreases, so an average value of $\mathscr{D}$ should be used over the range of moisture content during drying. Moisture diffusion coefficients have been measured for a large number of materials, especially foods. For example, the moisture diffusion coefficients of 24 different food materials were mostly in the range 10^{-8} to 10^{-4} cm^2/s for moisture contents ranging from 0.01 to 10 g/g (dry basis), respectively [10].

Another way to model the falling drying rate period is to assume that the rate of drying is proportional to the residual moisture content less the equilibrium moisture content, which approximates the falling rate period shown in Figure 11.3:

$$-\frac{dX_m}{dt}=K(X_m-X_e) \tag{11.2.21}$$

where K is a constant. Note that this equation has the same form as the analytical solution of the diffusion equation at long drying times [Equation (11.2.19)]. At the beginning of the falling rate period, X_m is at the critical moisture content X_c, which gives

$$-\left.\frac{dX_m}{dt}\right|_{X_c}=K(X_c-X_e) \tag{11.2.22}$$

During the constant rate drying period, from Equation (11.2.13), we have

$$N_w=\frac{h\left(T-T_s\right)}{\lambda}=\frac{\rho_s d}{M}\left(-\frac{dX_m}{dt}\right)\Bigg|_{X_c} \tag{11.2.23}$$

where ρ_s is the mass of dry solids per volume of wet solids and M is the molecular weight of water. Upon applying Equation (11.2.22), we find that Equation (11.2.23) leads to

$$K=\frac{hM\left(T-T_s\right)}{\rho_s d\lambda(X_c-X_e)} \tag{11.2.24}$$

so that during the falling drying rate period,

$$-\frac{dX_m}{dt} = \frac{hM\left(T - T_s\right)}{\rho_s d\lambda}\left(\frac{X_m - X_e}{X_c - X_e}\right) \tag{11.2.25}$$

This equation can be integrated with the following initial condition:

$$At\ t = 0, \qquad X_m = X_c \tag{11.2.26}$$

to give

$$t = \frac{\rho_s d\lambda\left(X_c - X_e\right)}{hM(T - T_s)}\ln\left(\frac{X_c - X_e}{X_m - X_e}\right) \tag{11.2.27}$$

For granular or porous solids, moisture tends to flow by the action of capillary forces rather than by diffusion. During the constant rate drying period, water evaporates out of the pores near the surface. The strength of the capillary forces in a pore increases as the curvature of the meniscus of the water in the pore increases; this curvature increases as the pore size decreases. Therefore, the small pores develop greater capillary forces than the larger ones and tend to pull water out of the large pores. The larger pores tend to empty first during the constant rate drying period, and the small pores are opened later during the falling rate period.

Shrinkage occurs when bound moisture is removed from colloidal nonporous solids. For the drying of thin layers, shrinkage does not usually cause much of a problem, but serious difficulties can result if the layer being dried becomes too thick. The outer layer next to the surface dries much more rapidly than the interior, and this can lead to cracking and warping of the outer layer. This problem is accentuated by the decrease in the diffusion coefficient of water as the moisture drops in the outer layer. For some cases, depending on the nature of the solids, the shrinkage and decline in the diffusion coefficient of water can be so great that a skin is formed on the surface that becomes impenetrable to water, and drying ceases as a result. This phenomenon is called case hardening [2].

EXAMPLE 11.3

Mass Flux During the Constant Rate Drying Period in Convective Drying Wet biological solids contained in a tray are dried by blowing air with 2% relative humidity and at 60°C and atmospheric pressure across the tray. For the constant drying rate period, estimate the temperature at the surface of the solids and the maximum molar flux of water.

Solution
From Figure 11.2, for air with 2% relative humidity and at 60°C,

$$T_{100\%} = 23°\text{C}$$

This temperature, found by moving up the adiabatic cooling curve to 100% relative humidity, is a good approximation of the surface temperature of the solids and of the wet-bulb temperature. At atmospheric pressure, we have

$$\lambda = 539.1 \frac{\text{kcal}}{\text{kg}}$$

From Equation (11.2.13),

$$N_w = \frac{h(T - T_s)}{\lambda}$$

The maximum molar flux would correspond to a forced convection heat transfer coefficient h of approximately 100 kcal m^{-2} h^{-1} K^{-1} (upper limit of the range for forced convection heat transfer coefficients of gases). Thus,

$$(N_w)_{\max} = \frac{100 \dfrac{\text{kcal}}{\text{m}^2\text{h K}} \times (60 - 23)\text{K}}{539.1 \dfrac{\text{kcal}}{\text{kg}} \times \dfrac{18\,\text{kg}}{\text{kg-mol}}} = 0.38 \frac{\text{kg-mol}}{\text{m}^2\text{h}}$$

EXAMPLE 11.4

Time to Dry Nonporous Biological Solids by Convective Drying A nonporous wet cake of biological solids that is 0.5 cm thick is to be dried by blowing dry air across the top surface. The initial moisture content is 70 wt% water, and it is desired to dry the cake to a water content of 5 wt%. The diffusion coefficient of water in the cake has been estimated to be 7×10^{-6} cm^2 s^{-1}. Estimate how long the drying will take.

Solution
Because the cake is nonporous, we assume that internal diffusion is controlling the drying. According to Figure 11.4 for drying with internal diffusion control, there will be no constant drying rate period, which means that the initial water content is equal to the critical moisture content X_c. Because the drying is by dry air, the water content

at equilibrium (X_e) is assumed to be zero. Calculating X_c and X_m on the basis of the dry mass of solids gives

$$X_c = \frac{70}{30} = 2.333 \frac{\text{g water}}{\text{g dry solids}}$$

$$X_m = \frac{5}{95} = 0.053 \frac{\text{g water}}{\text{g dry solids}}$$

We tentatively assume that $\mathscr{D}t/d^2 > 0.1$, so that we can use Equation (11.2.20) to estimate the drying time:

$$t = \frac{4d^2}{\pi^2 \mathscr{D}} \ln\left[\frac{8(X_c - X_e)}{\pi^2 (X_m - X_e)}\right]$$

$$= \frac{4(0.5)^2 \text{cm}^2}{\pi^2 \left(7 \times 10^{-6} \frac{\text{cm}^2}{\text{s}}\right)} \ln\left[\frac{8(2.3333 - 0)}{\pi^2 (0.053 - 0)}\right] \frac{1\text{h}}{3600\text{s}} = 14.4\text{h}$$

As a check, we see that

$$\frac{\mathscr{D}t}{d^2} = \frac{7 \times 10^{-6} \frac{\text{cm}^2}{\text{s}} \times 14.4(3600)\text{s}}{0.5^2 \text{cm}^2} = 1.45$$

which satisfies the assumption that $\mathscr{D}t/d^2 > 0.1$.

11.3 DRYER DESCRIPTION AND OPERATION

Several types of dryers have been used to dry biological materials. However, the great majority of dryers used for these products fall into four categories: vacuum-shelf dryers, batch vacuum rotary dryers, freeze dryers, and spray dryers. Our basic description of each of these dryers will discuss the dryer's operation, as well.

11.3.1 Vacuum-Shelf Dryers

The vacuum-shelf dryer is a relatively simple type of dryer, as shown in Figure 11.5. Trays filled with the product to be dried rest on shelves through which warm water or other suitable heat exchange medium is circulated. Heat is conducted from the shelves to the trays and into the wet solids. Vacuum is applied to the chamber containing the trays to speed up the drying and allow drying to take place at lower temperatures. The evaporating water vapor is drawn off in the vacuum system. Vacuum-shelf dryers up to several square meters of shelf area are available [11]. This type of dryer

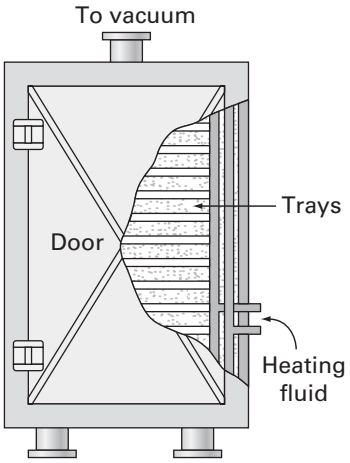

FIGURE 11.5 Vacuum-shelf dryer.

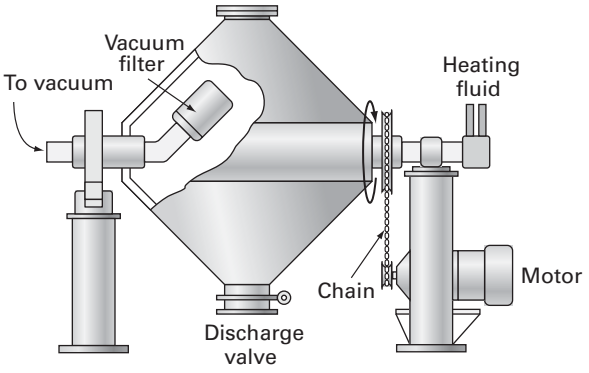

FIGURE 11.6 Batch vacuum rotary dryer. *(Based on a design by Stokes Equipment Division, Penwalt Corporation.)*

is used extensively for pharmaceutical products such as antibiotics, which are often in crystalline form and exhibit moderate to high heat sensitivity.

11.3.2 Batch Vacuum Rotary Dryers

Another type of dryer in which the heat transfer is by conduction is the batch vacuum rotary dryer, also called a vacuum tumble dryer. Heat is supplied by warm water or other heat exchange medium circulated through a jacket on the rotating double-cone drum, shown in Figure 11.6. In this dryer, the solids are continually tumbled by rotation of the drum, so that solid particles come in contact with the walls of the jacket and with each other. Vacuum is applied to the rotating drum to be able to dry at lower temperatures and to dry more rapidly. The largest dryers of this type have volumes of up to 30 to 40 m^3 [11]. This type of dryer is generally applicable for biological

products of the same type handled by the vacuum-shelf dryer, but it would not be feasible when the tumbling motion causes the particles to form larger and larger balls or when the particles stick to the metal surfaces in the drum.

11.3.3 Freeze Dryers

A freeze dryer is essentially a more sophisticated version of vacuum-shelf dryer. Freeze drying requires that both the temperature and pressure be controlled during the drying process. The product to be dried can be either in vials or in trays. The pharmaceutical freeze dryer shown schematically in Figure 11.7 can dry a liquid product contained in vials. When the vials are placed on the trays, the stoppers are closed only partially so that water vapor can escape. The hydraulic piston allows for the stoppers to be completely pushed into the top of the vials at the end of drying. A heat transfer fluid is circulated through the trays to provide temperature control of the vials.

The first step in the freeze-drying process is the cooling of the product to a sufficiently low temperature to allow complete solidification. The pressure in the chamber is then reduced to below the vapor pressure at the triple point of water so that drying can occur by sublimation. Ice, water, and water vapor exist in equilibrium at the triple point (0.01°C and 4.6 mm Hg); below the triple point, water passes directly from the solid to the vapor phase by sublimation when the temperature is raised. Thus, the temperature of the shelves is increased to provide energy for sublimation. As drying occurs, a boundary between the dry solids and frozen solution can be observed in each vial (Figure 11.8), similar to the receding front in tray drying modeled in Example 11.2. Unbound water is removed in a drying phase called *primary drying*. A higher shelf temperature and additional time are required to remove the bound water in the *secondary drying phase*. Typical plots of temperature and pressure as a function of time during the freezing, primary drying, and secondary drying phases are shown in Figure 11.9. The time to complete the drying cycle is typically 24 to 48 h [12].

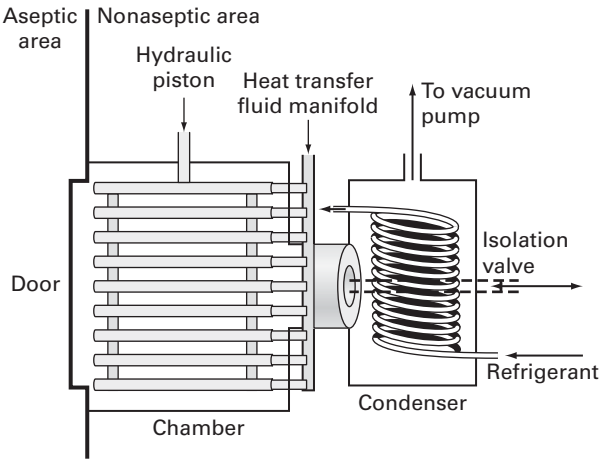

FIGURE 11.7 Pharmaceutical freeze dryer.

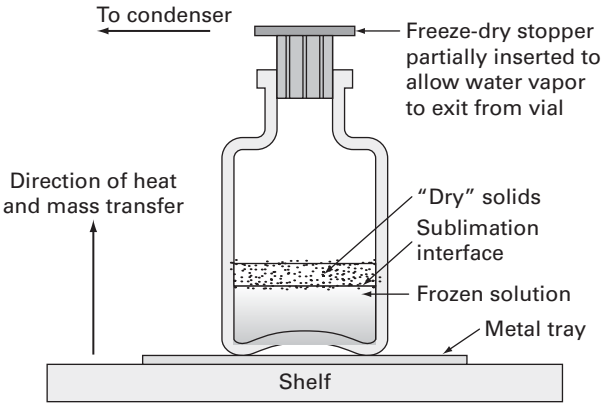

FIGURE 11.8 Schematic of freeze-drying in a vial, showing the boundary between the frozen solution and the dry solids.

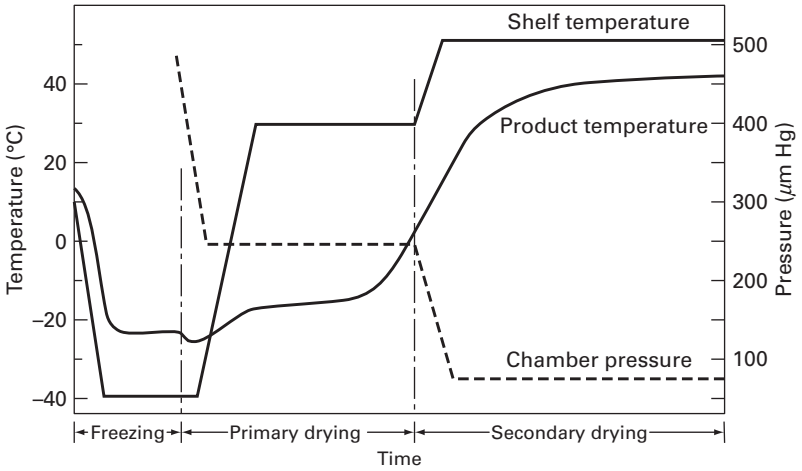

FIGURE 11.9 Process variables during the freeze-drying cycle.

During the freeze-drying process, it is important that the product not exceed either the eutectic temperature or the glass transition temperature; otherwise the product can "collapse" [13]. Collapse is the loss of either the crystalline or the amorphous structure of the product. The eutectic temperature is the temperature in crystalline systems below which no liquid exists. The glass transition temperature exists only in amorphous systems and is the temperature at which there is a change in viscosity of the system from a viscous liquid to a glass. Both the eutectic temperature and the glass transition temperature can be determined by differential thermal analysis (DTA).

Freeze drying is generally used only for biological products that have a high sensitivity to heat. Most proteins fall into this category. Because the liquid phase is not present after the product is initially frozen, reactions that can occur to the product in the liquid phase such as hydrolysis, cross-linking, oxidation, aggregation, and disulfide rearrangement are essentially eliminated [14]. Freeze drying is also

advantageous in that the dry product has a very high specific surface area, which leads to a rapid and complete redissolution [13].

11.3.4 Spray Dryers

A spray dryer transforms a feed in the liquid state into a dried particulate form by spraying the liquid into a hot gas, usually air. A schematic diagram of a spray dryer is shown in Figure 11.10. The majority of spray dryers in commercial use utilize cocurrent flow of gas and feed. Three basic unit processes are involved in spray drying: liquid atomization, gas-droplet mixing, and drying from liquid droplets. Spherical particles are produced, which are not usually obtainable by any other drying method. These particles can be either solid or hollow and range in size from 2 μm to (rarely) more than 500 μm. Drying is carried out essentially at the air wet-bulb temperature, and the time of drying is measured in seconds. Inlet gas temperatures can range from 150 to 250°C. The rapidity of drying and the relatively low temperature experienced by the solids during drying have led to the successful application of spray drying for many types of heat-sensitive products, including milk, coffee, blood, spores, and various microorganisms, and antibiotics [15].

The most important operation in the spray-drying process is atomization. The type of atomizer determines the size and size distribution of the drops and their trajectory and speed. Three general types of atomizer are available. Rotary wheel atomizers (also called centrifugal disk atomizers) and pressure nozzle single-fluid

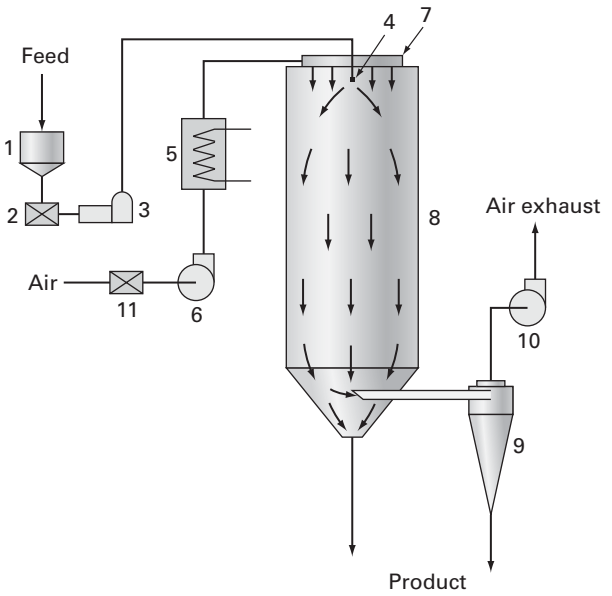

FIGURE 11.10 Spray dryer with a pressure nozzle atomizer: 1, feed tank; 2, filter; 3, pump; 4, atomizer; 5, air heater; 6, fan; 7, air disperser; 8, drying chamber; 9, cyclone; 10, exhaust fan; 11, filter.

atomizers are the most commonly used. Pneumatic two-fluid nozzles are used only rarely in specialized applications. For example, skim milk, milk, and whole eggs have been spray-dried with both rotary wheel and pressure nozzle atomizers [16].

The rotary wheel atomizer is generally preferred for high flow rate feed streams (i.e., >5 metric tons/h). The particles produced are relatively small (30–120 μm). This atomizer can handle a wide variety of streams with different physical properties, and its large flow ports result in a negligible tendency to clog [11, 16].

The pressure nozzle atomizer produces larger particles than the rotary wheel atomizer (e.g., 120–250 μm), and it is generally able to produce drops within a narrow range of diameters. This atomizer is not recommended for highly concentrated suspensions and abrasive materials which tend to clog and erode the orifice nozzle [11, 16].

11.4 SCALE-UP AND DESIGN OF DRYING SYSTEMS

It is not yet possible to design with confidence a large-scale dryer for a biological material based only on the physical properties of the material. Theory and empirical correlations are helpful in estimating dryer size and drying time and are also helpful in analyzing dryer performance and in predicting the effect of changes in operating conditions. Small-scale drying tests in the pilot plant and/or laboratory are an essential element of dryer scale-up and design. It is often possible to ship samples of the material to be dried to the drying equipment manufacturer for tests to be performed in the manufacturer's small-scale unit. If these tests are successful, then it is also a good idea to test the small-scale unit where the biological material is being produced. This will enable the testing of the drying for numerous batches of the material, which for biological materials can be significantly variable, and over a longer period of time [11].

11.4.1 Vacuum-Shelf Dryers

The scale-up and sizing of large-scale vacuum-shelf dryers is relatively straightforward. One good procedure is to test the drying in a bench or pilot scale dryer using the same depth of wet solids that would be used in the large-scale unit. The effect of changes in conditions upon scale-up can be estimated using the equation for the time of conductive drying determined in Example 11.2:

$$t = \frac{d^2 \lambda \rho_0}{2k\left(T_0 - T_s\right)} \tag{11.4.1}$$

The thermal efficiency of vacuum-shelf dryers is usually between 60 and 80%. The power to operate these dryers can be estimated to a good approximation based only on the power to operate the vacuum system, which is 0.06 to 0.12 kW/m^2 tray surface area for vacuums of 680 to 735 mm Hg [1].

11.4.2 Batch Vacuum Rotary Dryers

Upon scaling up a batch vacuum rotary dryer, we find that the heated surface area per internal volume does not remain constant. For example, if we assume that the dryer is a perfect double cone, the heated area increases by a factor of 4.6 when the volume increases by a factor of 10 for geometrical similarity (angles constant) upon scaleup. This means that the ratio of area to volume at the large scale is 46% of the area-to-volume ratio of the small-scale unit with one-tenth the volume. By making the assumption that the time for drying is inversely proportional to the area-to-volume ratio of the dryer, the time for drying in the large-scale dryer can be estimated from the time in the small-scale one [17]:

$$\frac{t_l}{t_s} = \frac{(A/V)_s}{(A/V)_l} \tag{11.4.2}$$

where A is the heated area, V is the internal volume, and the subscripts s and l refer to the small- and large-scale dryers, respectively. Batch vacuum rotary dryers are usually filled to 50 to 65% of their internal volume [1].

11.4.3 Freeze Dryers

The design of a freeze-drying process usually requires a significant amount of development effort. For this work, it is essential to have available a pilot plant scale freeze dryer with a product shelf area of between 0.4 and 2.0 m^2 and layout and characteristics (shelf and ice condenser areas, temperatures, and pressures) similar to those of the expected large-scale production equipment [12]. The two main activities during this development work are the determination of the final product formulation and the determination of the conditions for the freeze-drying cycle.

To formulate the final product, excipients are added to the active component of the product for use as fillers or bulking agents, buffers to control pH, tonicity modifiers for osmotic pressure adjustment, structure modifiers, stabilizers to protect the active molecule, and collapse inhibitors. Commonly used excipients are mannitol, glycine, lactose, sucrose, glucose, and dextran [12].

As is indicated in Figure 11.9, the three major cycles of the freeze-drying process are freezing, primary drying, and secondary drying. The following sequence of testing is typical for determining the design conditions for freeze drying:

1. The maximum allowable product temperature during primary drying is determined, typically by differential scanning calorimetry (DSC). Transition temperatures such as the eutectic temperature and the glass transition temperature can be found by means of DSC. During primary drying, the process should be designed to maintain the product temperature 3 to 4°C below the eutectic and glass transition temperatures, so that no liquid is present and drying is by sublimation only [13].
2. Chamber pressure, shelf temperature, and time for primary drying are determined. In general, the product temperature should not exceed −15°C, or the

heat and mass transfer capacities of the freeze dryer could be overloaded [18]. To allow a high sublimation rate, the chamber pressure should be significantly less than the vapor pressure of ice at the target product temperature; a good rule of thumb is to select a chamber pressure of about 20% of the vapor pressure of ice at the target product temperature [12]. The optimal chamber pressure at a known product temperature can be estimated by the following equation [18]:

$$P_c = 0.29 \times 10^{0.019 T_p} \quad (11.4.3)$$

where P_c is the chamber pressure (torr) and T_p is the product temperature (°C). For most applications of practical interest, the chamber pressure ranges from 50 to 200 mtorr.

The shelf temperature is determined by trial and error in pilot tests, with the objective being to maintain the product temperature constant. A rough rule of thumb is to use an initial temperature difference between the shelf and the vials containing the product corresponding to 100 times the vapor pressure of ice in millibars at the target temperature (1 mm Hg = 1.33 mbar) [12]. A method for estimating the shelf temperature that takes different solute concentrations into account utilizes Figure 11.11, which was derived using Equation (11.4.3) and heat and mass transfer resistances in tubing vials at three different solute concentrations [18]. The time for primary drying can be estimated from the mean value of the difference between the shelf temperature and product temperature at different solid concentration levels using Figure 11.12, which was

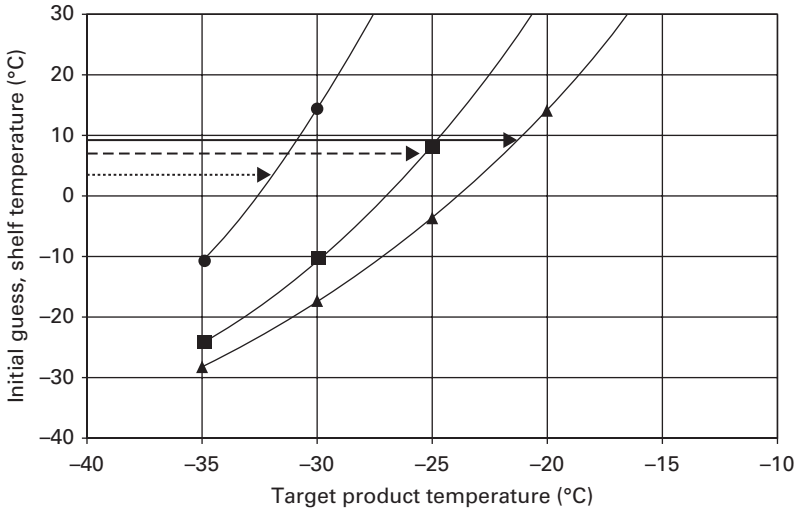

FIGURE 11.11 Freeze dryer initial shelf temperature estimation for given target product temperatures at different solute concentrations (i.e., different dry layer resistance) during primary drying in tubing vials: ●, low dry layer resistance (solids ≤ 1%); ■, medium dry layer resistance (10% > solids > 1%); ▲, high dry layer resistance (solids ≥ 10%). The arrows specify the maximum shelf temperatures above which mass and heat transfer overload of a "typical" manufacturing dryer is likely. *(Calculated data from X. C. Tang and M. J.Pikal, "Design of freeze-drying processes for pharmaceuticals: practical advice,"* Pharm. Res.*, vol. 21, p. 191, 2004.)*

determined by the calculation of heat and mass transfer flows assuming a 1 cm thick frozen cake and heat transfer coefficients and geometry typical for tubing vials [18]. The time for primary drying varies approximately with the initial depth of the frozen solid according to the relationship [12]

$$t = Kd^{1.5} \quad (11.4.4)$$

where K is a constant. Note that the exponent of d is similar, but not identical, to the exponent found in the theoretical equation for vacuum-shelf dryers [Equation (11.4.1)].

3. Chamber pressure and shelf temperature to use for secondary drying are determined. The start of secondary drying is indicated by a sharp increase in product temperature (see Figure 11.9). Since the water desorption rate does not depend on chamber pressure below about 200 mtorr, the chamber pressure in primary drying can also usually be used in secondary drying. The water desorption rate, however, is very sensitive to the product temperature. For amorphous products, the shelf temperature should be increased slowly during secondary drying to avoid collapse; a ramp rate of 0.1 to 0.15°C/min until ambient temperature is reached is generally safe for amorphous products. Since crystalline products do not have any potential for collapse, the ramp rate can be higher (0.3 or 0.4°C/min). Regarding the actual temperature to use, it is advantageous to maintain the shelf temperature at a higher level for a short time rather than at a lower level for a long time. Secondary drying times at the terminal temperature

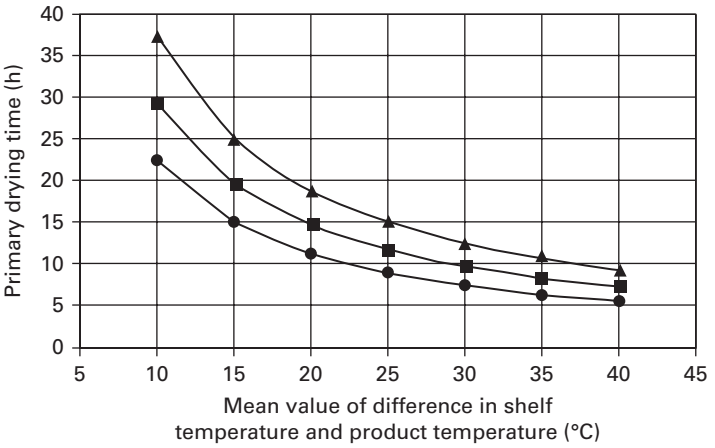

FIGURE 11.12 Primary drying time estimation for a freeze dryer as a function of temperature driving force for different solute concentrations in tubing vials: ●, low dry layer resistance (solids ≤ 1%); ■, medium dry layer resistance (10% > solids > 1%); ▲, high dry layer resistance (solids ≥ 10%). A 1 cm thick frozen cake and heat transfer coefficients and geometry typical for tubing vials are assumed. *(Calculated data from X. C. Tang and M. J. Pikal, "Design of freeze-drying processes for pharmaceuticals: practical advice,"* Pharm. Res.*, vol. 21, p. 191, 2004.)*

of 3-6 hours are generally optimal. The terminal temperature is generally in the range of 40 to 50°C, depending on the formulation, even for proteins [18].

The primary and secondary freeze-drying steps have been mathematically modeled [19, 20]. The modeling is complex, however, and numerical methods generally are required for solutions. Simplified models that allow for analytical solutions have been developed for the primary drying step [21].

11.4.4 Spray Dryers

For the scale-up and design of a large-scale spray dryer, tests in small-sized equipment need to be performed to determine dryer conditions that will cause the largest particles produced to be nonsticky and at the desired moisture level. For biological materials, it is necessary to determine the degree of dryness and operating conditions that will give an active and stable product.

In the sizing of spray dryers, a key variable is the *residence time* of the air in the drying chamber. Residence time is calculated by dividing the chamber volume by the total air flow rate. The minimum residence time of the product can be assumed to be the residence time of the air. However, most of the product passing through the dryer has a residence time much higher than the air residence time. For heat-sensitive products such as biological materials, average air residence times are 35 s or more for drying coarse sprays (mean size 200–275 μm) and are in the range of 20–35 s for drying fine to semicoarse sprays (mean size < 180 μm) [15].

Once the volume of the drying chamber has been determined based on the air residence time, the dimensions of the chamber can be calculated. For spray dryers with cocurrent flow of feed and air, *H:D*, the ratio of cylindrical height to chamber diameter, falls into the following ranges: 0.6:1 to 1:1 for units with rotary wheel atomizers, and 3:1 to 4:1 for units with pressure nozzle atomizers. Because the trajectory of drops from rotary wheel atomizers is horizontal, spray dryers with these atomizers must be large enough in diameter to prevent wall encrustations caused by large drops hitting the chamber wall. The minimum chamber diameter for spray dryers with rotary atomizers should be as follows depending on the mean droplet size [15]:

2 m for 40–80 μm drops
4 m for 80–100 μm drops
5 m for 100–120 μm drops

An alternative way to scale up is to use theoretical correlations, a good example of which was provided by Gluckert [22]. The correlations developed by Gluckert rely on several key assumptions:

1. Because of the large recirculation currents in the dryer, drying conditions are uniform throughout the chamber. The entire chamber is at the gas exit temperature. This assumption has been established except near the atomizer.

2. Drying occurs from the drop surface, which consists of a liquid saturated with the solutes; experimental studies with drops have shown this to be the case. Thus in view of the prior assumption, the temperature-driving force for drying is the difference between the drying gas outlet temperature and the adiabatic saturation temperature of a saturated solution of the material being dried.
3. The convective heat transfer coefficient h can be determined by assuming that a representative drop is in a motionless fluid, with the drop moving at the same speed as the air. For this situation the Nusselt number for heat transfer (hD/k_f, where D is the drop diameter and the subscript f refers to the film around the drop) is 2. This assumption has been substantiated by considerable experimental work.

All these assumptions are helpful in understanding how spray dryers operate. For a spray dryer with pressure nozzle atomizers, for example, the chamber volume V of the large-scale unit can be calculated from the following theoretical correlation:

$$Q = \frac{10.98 k_f V^{2/3} (T - T_s)_{out}}{D_m^2} D_s \sqrt{\frac{\rho_t}{\rho_m}} \tag{11.4.5}$$

where Q = rate of heat transfer to spray (Btu/h)
k_f = thermal conductivity of gas film surrounding drop (Btu/h $k$ft °F)
V = volume of drying chamber (ft^3)
T = gas phase bulk temperature (°F)
T_s = temperature at drop surface (°F)
D_m = maximum drop diameter, assumed to be three times the surface per unit volume average size (ft)
D_s = diameter of pressure nozzle discharge orifice (ft)
ρ_t = density of gas at exit conditions (lb/ft^3)
ρ_m = density of spray jet at the atomizer (lb/ft^3)

This heat transfer rate is the maximum rate that can be achieved if the largest particles from the atomizer are dried as they reach the dryer wall or bottom.

EXAMPLE 11.5

Sizing of a Spray Dryer Estimate the dimensions of a drying chamber for a spray dryer that has an output of 1000 kg/h of a heat-sensitive biological material at 60°C containing 5% moisture and having a mean particle size of 100 μm. The feed contains 40% solids by weight in an aqueous solution at 4°C. The inlet air has a humidity of 0.01 kg/kg dry air and is at 150°C, while the outlet air is at 80°C. Assume the specific heat of the dry solids is 0.3 kcal kg^{-1} K^{-1}and the datum temperature is 0°C.

Solution

We first do material balances on the overall process:

$$\text{Product rate} = 1000\ \frac{\text{kg}}{\text{h}}\ (5\%\text{water})$$

$$\text{Solution feed rate} = \frac{1000(0.95)}{0.4} = 2375\ \frac{\text{kg}}{\text{h}}\ (40\%\text{solids})$$

$$\text{Water evaporation rate} = 2375 - 1000 = 1375\ \frac{\text{kg}}{\text{h}}$$

To size the dryer, we need to find the flow rate of wet gas out. Since we know the humidity of the inlet air on a dry air basis, we use the flow rate G of dry air to write a mass balance for the water:

$$G(\mathscr{H}_2 - 0.01) = 1375$$

or

$$G = \frac{1375}{\mathscr{H}_2 - 0.01}\ \frac{\text{kg dry air}}{\text{h}}$$

where G is the flow rate of dry air and $\mathscr{H}_2$ is the humidity of the outlet air. Using Equations (11.2.3), (11.2.4), and (11.2.5) and a datum temperature $T_0 = 0°\text{C}$ enables us to write

$$\text{Enthalpy of inlet air} = [0.24 + 0.46(0.01)]150 + 597(0.01) = 42.66\ \frac{\text{kcal}}{\text{kg dry air}}$$

$$\text{Enthalpy of outlet air} = (0.24 + 0.46\mathscr{H}_2)80 + 597\mathscr{H}_2 = 19.2 + 633.8\mathscr{H}_2\ \frac{\text{kcal}}{\text{kg dry air}}$$

Since we know the specific heat of the dry solids, we write the enthalpy of the solids and liquids based on the weight of dry solids:

$$\text{Enthalpy of entering feed} = 0.3(4) + 1.0(4)\left(\frac{60}{40}\right) = 7.2\ \frac{\text{kcal}}{\text{kg dry solids}}$$

$$\text{Enthalpy of product leaving dryer} = 0.3(60) + 1.0(60)\left(\frac{5}{95}\right) = 21.2\ \frac{\text{kcal}}{\text{kg dry solids}}$$

Equating the rate of enthalpy in and the enthalpy out gives the equation

$$42.66G + 7.2(950) = (19.2 + 633.8\mathscr{H}_2)G + 21.2(950)$$

Substituting into the foregoing equation for G in terms of $\mathscr{H}_2$ and solving gives

$$\mathscr{Y}_2 = 0.0366 \frac{\text{kg water}}{\text{kg dry air}}$$

$$G = \frac{1375}{0.0366 - 0.01} = 51{,}960 \frac{\text{kg dry air}}{\text{h}}$$

$$\text{Rate of water vapor out} = 0.0366\left(51{,}690\right) = 1892 \frac{\text{kg water}}{\text{h}}$$

To calculate the flow rate of the wet air out, we need to know its density. We do this by first calculating the molar average molecular weight M of the wet air out to obtain

$$\langle M \rangle = 28.3$$

which assumes the molecular weight of dry air to be 28.9. From the ideal gas law at 1 atm and 80°C, the density of the wet air can be calculated, which can then be used to obtain the volumetric flow rate of wet air:

$$\rho_{\text{out}} = \frac{P\langle M \rangle}{RT} = \frac{1\,\text{atm} \times 28.3 \frac{\text{g}}{\text{mol}}}{82.06 \frac{\text{cm}^3\text{atm}}{\text{mol K}} * 353\text{K}} = 0.000977 \frac{\text{g}}{\text{cm}^3} = 0.977 \frac{\text{kg}}{\text{m}^3}$$

$$\text{Total wet air flow rate} = \frac{\left(51{,}960 + 1892\right)\frac{\text{kg}}{\text{h}}}{0.977 \frac{\text{kg}}{\text{m}^3}} = 54{,}840 \frac{\text{m}^3}{\text{h}}$$

For the size of particles produced (mean size of 100 μm), the average air residence time should be in the range of 20 to 35 s. For a conservative design, we select a residence time of 35 s. This gives a spray drying chamber volume V of

$$v = 54{,}840 \frac{\text{m}^3}{\text{h}} \times 35\,\text{s} \times \frac{1\,\text{h}}{3600\,\text{s}} = 533\,\text{m}^3$$

A rotary wheel atomizer is appropriate for a mean particle size of 100 μm. We select a chamber cylindrical height (H) to diameter (D) ratio of 0.8:1, which falls in the 0.6:1 to 1:1 range appropriate for rotary wheel atomizers:

$$\frac{H}{D} = 0.8$$

Height and diameter are related to chamber volume by the equation

$$\frac{\pi D^2}{4} H = 533$$

Solving the two preceding equations for H and D, we obtain

$$H = 7.58 \text{ m}$$
$$D = 9.47 \text{ m}$$

This diameter is larger than the minimum diameter of 5 m recommended for particles with a mean size of 100 to 120 μm.

11.5 SUMMARY

Drying is the process of thermally removing volatile substances (often water) to yield a solid. The drying of biological solids depends on the removal of free water and bound water and must account for the lability of biological activity as a function of temperature.

- The moisture content of a solid in equilibrium with air at a specified relative humidity is given in an equilibrium diagram for some biological solids.
- The psychrometric moisture chart relates moisture content, temperature, and relative humidity of air.
- The time to dry wet solids that are granular, such as crystalline material, by conductive drying on a heated surface is directly proportional to the square of the depth of the solids and inversely proportional to the difference between the heated surface temperature and the boiling point of the evaporating liquid.
- Drying rate curves are divided into initial, changing drying rate (warming up), constant drying rate (surface of solids is saturated), and falling drying rate periods (nonsaturated solids due to moisture content below critical value X_c).
- Drying rate curves have different shapes depending on the type of material being dried (hygroscopic, nonhygroscopic) and on the control of mass transfer (boundary layer, internal diffusion).
- The drying time for the falling rate period for a nonporous solid (continuous and homogeneous) depends on the square of the half-thickness and on the log of the ratio $(X_c - X_e)/(X_m - X_e)$, where X_m is the average moisture content at any time and X_c and X_e are the critical and equilibrium moisture contents, respectively. Moisture content data as a function of time can be used to estimate the moisture liquid diffusion coefficient and the convective heat transfer coefficient.
- *Vacuum-shelf dryers* are commonly used for trays or vials of pharmaceutical products, such as antibiotics; heat is conducted from the shelves, and water is removed by the vacuum system. *Vacuum rotary dryers* tumble the solids,

which are heated by conduction of heat from the walls of the jacket of the dryer; solids aggregation sometimes occurs. In *freeze dryers* both temperature and pressure are controlled so that the sample freezes, and water sublimes into the vapor phase for removal by vacuum while avoiding eutectic and glass transition temperatures of the sample. Freeze drying is popular for proteins, which are heat sensitive. *Spray dryers* disperse liquid solution in fine droplets (atomization) into a large volume of hot air, which drives evaporation from droplets leaving solids; spray drying has successfully dried many heat-sensitive products.

- Theory, empirical correlations, and experimental testing are used to scale up drying operations. Theory and empirical correlations are helpful in estimating dryer size and drying time and are also helpful in analyzing dryer performance and in predicting the effect of changes in operating conditions. Small-scale drying tests in the pilot plant and/or laboratory are an essential element of dryer scale-up and design.

NOMENCLATURE

a	heat transfer area per unit dryer volume (m^{-1})
A	cross-sectional area (m^2)
c_w	concentration of water vapor (mol $liter^{-1}$)
C_{pg}	specific heat of gas (kcal kg^{-1} K^{-1})
C_{pw}	specific heat of water vapor (kcal kg^{-1} K^{-1})
C_s	specific heat of gas and water vapor mixture (kcal kg^{-1} K^{-1})
d	one-half slab thickness for drying from both sides, or total thickness for drying from one side (m)
D	diameter of spray dryer chamber (m)
D_m	maximum drop diameter [Equation (11.4.5)] (ft)
D_s	diameter of pressure nozzle discharge orifice [Equation (11.4.5)] (ft)
$\mathscr{D}$	diffusion coefficient (cm^2 s^{-1})
h	convective heat transfer coefficient (kcal m^{-2} h^{-1} K^{-1})
H	height of spray drying chamber (m)
$\mathscr{H}$	humidity, mass of water per mass of dry air (dimensionless)
H_y	total enthalpy (kcal kg^{-1})
k	thermal conductivity (kcal m^{-1} h^{-1} K^{-1})
M	molecular weight (Daltons)
n	0, 1, 2, . . ., ∞ [Equation (11.2.17)]
N_w	molar flux of water (mol m^{-2} h^{-1})
p	total pressure (atm)
p_w	partial pressure of water (atm)
p_{ws}	partial pressure of water at saturation (atm)
q	heat flux (kcal m^{-2} h^{-1})

Q rate of heat flow (kcal h^{-1})
R gas law constant (0.082058 liter atm mol^{-1} K^{-1})
R_m relative humidity (dimensionless)
t time (s)
T temperature (K)
U overall heat transfer coefficient (kcal m^{-2} h^{-1} K^{-1})
V dryer volume (m^3)
X moisture content, mass of water per mass of dry solids (dimensionless)
X_c critical moisture content, when the drying rate starts to fall (dimensionless)
X_e equilibrium moisture content (dimensionless)
X_m average moisture content (dimensionless)

Greek Letters

λ_0 latent heat, or heat of vaporization, of liquid (kcal kg^{-1}, or kcal mol^{-1})
ρ_m density of spray jet at atomizer [Equation (11.4.5)] (lb ft^{-3})
ρ_s mass of dry solids per volume of wet solids (g cm^{-3})
ρ_t density of gas at spray dryer exit [Equation (11.4.5)] (lb ft^{-3})
ρ_0 mass of water per volume of wet solids (g cm^{-3})

PROBLEMS

11.1 Drying of Insulin Wet insulin crystals containing 32 g water per 100 g of dry insulin need to be dried in air to a moisture level of 5 g water per 100 g of dry insulin. Determine the percentage of bound and unbound water in the wet crystals before drying and the humidity of the air to accomplish the drying. For drying with air at 20°C, what should be the moisture content of the air (g moisture/g dry air)?

11.2 Drying of Wet Antibiotic Crystals in a Vacuum-Shelf Dryer Small-scale drying tests were performed in a vacuum-shelf dryer with wet antibiotic crystals contained in a tray at a solids depth of 2 cm. Water at 70°C was circulating through the shelves, and the absolute pressure was maintained at 100 mm Hg. The wet crystals initially had a water content of 70%. The solids reached dryness after 10 h of drying. It is proposed to dry these crystals in a large-scale dryer at a bed depth of 2.5 cm and using water circulating through the shelves at 70°C. The plant dryer can be operated at an absolute pressure no lower than 150 mm Hg. Estimate how long it will take to reach dryness in the large dryer. For changes in what variable is the estimated drying time the most sensitive?

11.3 Classification of Drying of Biological Materials Drying rate data have been obtained for three biological solids (see Table P11.3). Based on these data, classify the drying for each solid according to whether the following apply: boundary layer control, internal diffusion control, and nonhygroscopic, partially hygroscopic, or hygroscopic solid.

TABLE P11.3

Material 1		Material 2		Material 3	
Moisture content (kg/kg)	Drying rate × 10^4 (kg m^{-2} s^{-1})	Moisture content (kg/kg)	Drying rate × 10^4 (kg m^{-2} s^{-1})	Moisture content (kg/kg)	Drying rate × 10^4 (kg m^{-2} s^{-1})
0.06	0.3	0.03	0.5	0.02	3.0
0.13	0.9	0.07	1.6	0.06	5.5
0.21	1.5	0.12	2.7	0.11	6.7
0.26	2.4	0.18	3.8	0.16	7.7
0.31	3.3	0.22	4.8	0.20	8.3
0.35	4.4	0.26	5.7	0.23	8.6
0.38	5.5	0.29	6.4	0.27	8.6
0.40	6.8	0.32	7.0	0.34	8.6
				0.38	8.6

11.4 Estimation of Drying Time from Drying Rate Data Drying rate data for a biological material are known (see Table P11.4). Determine the drying time for drying the material from 25 to 4 wt% moisture content. The initial material weighs 150 kg, and the material has a surface area of $1 m^2$ per 40 kg of dry material.

TABLE P11.4

Moisture content (kg/kg dry weight)	Drying rate × 10^4 (kg m^{-2} s^{-1})
0.020	0.26
0.060	0.75
0.122	1.49
0.173	2.17
0.222	2.75
0.255	3.16
0.295	3.50
0.345	3.51
0.391	3.49
0.450	3.51

11.5 Convective Drying of Nonporous Biological Solids A 3 mm bed of wet nonporous biological solids was dried in a tray by blowing air with 20% relative humidity across the top of the bed at 70°C and atmospheric pressure. The data in Table P11.5 were obtained for the drying of these solids:

TABLE P11.5

t (min)	X_m, mass water/mass dry solids
0	0.190
10	0.176
20	0.153

TABLE P11.5 **(Continued)**

t (min)	X_m, mass water/mass dry solids
30	0.130
40	0.107
50	0.084
60	0.064
70	0.050
80	0.039
90	0.031
100	0.026
120	0.018
140	0.014
160	0.012

From the drying data, estimate the diffusion coefficient of water in the biological material and the heat transfer coefficient for the convective heat transfer. The wet material has a bulk density of 1.1 g/cm^3.

11.6 Scale-up of a Batch Rotary Vacuum Dryer Drying tests of a biological material were carried out in a pilot scale double-cone rotary vacuum dryer having a volume of 25 liters. The drying time was 8 h. Estimate the drying time and dryer dimensions using a production scale double-cone rotary vacuum dryer with a volume of 500 liters. Assume for both the small and large dryers that each cone has the shape of an equilateral triangle.

11.7 Freeze Drying of a Pharmaceutical Product The data in Table P11.7 were taken in a pilot plant freeze dryer for the primary drying time as a function of cake depth:

TABLE P11.7

Depth (cm)	Time (h)
0.30	1.1
0.50	3.0
0.75	5.8
1.00	10.8

For operation at the same conditions (temperature and chamber pressure), it is desired to use a cake depth of 1.5 cm. Estimate the drying time that would be expected.

11.8 Spray Drying of Yeast Cells A spray dryer with pressure nozzle atomizers has a diameter of 5 m and a height of 15 m. It is desired to spray dry a feed containing yeast cells at a concentration of 30% by weight and 15°C to dry solids at 60°C with 5% moisture and average particle size of yeast cell agglomerates of 150 μm. Tests in a laboratory scale spray dryer have indicated that the air inlet and outlet temperatures should be 160 and 75°C, respectively. The inlet air has a humidity of 0.02 kg per kg of dry air. Estimate the maximum feed rate of yeast cells and the inlet flow rate of air (dry basis). Assume the specific heat of the dry solids is 0.3 kcal kg^{-1} K^{-1} and the datum temperature is 0°C..

REFERENCES

1. Moyers, C. G., and Baldwin, G. W. (1997). Psychrometry, evaporative cooling, and solids drying. In *Perry's Chemical Engineers' Handbook*, 7th ed., R. H. Perry, D. W. Green, and J. O. Maloney, eds., McGraw-Hill, New York, p. 12-1.
2. McCabe, W. L., Smith, J. C., and Harriott, P. (1993). *Unit Operations of Chemical Engineering*, 5th ed., McGraw-Hill, New York.
3. Stephenson, G. A., and Diseroad, B. A. (2000). Structural relationship and desolvation behavior of cromolyn, cefazolin, and fenoprofen sodium hydrates. *Int. J. Pharm*., vol. 198, p. 167.
4. Hsu, C. C., Ward, C. A., Pearlman, R., Nguyen, H. M., Yeung, D. A., and Curley, J. G. (1991). Determining the optimum residual moisture in lyophilized protein pharmaceuticals. *Dev. Biol. Standard*., vol. 74, p. 255.
5. Pikal, M. J., and Rigsbee, D. R. (1997). The stability of insulin in crystalline and amorphous solids: Observation of greater stability for the amorphous form. *Pharm. Res*., vol. 14, p. 1379.
6. McCormick, P. Y. (1993). Drying. In *Kirk-Othmer Encyclopedia of Chemical Technology*, vol. 8, 4th ed., M. Howe-Grant, ed., Wiley-Interscience, New York, p. 475.
7. Bird, R. B., Stewart, W. E., and Lightfoot, E. N. (2002). *Transport Phenomena*, 2nd ed., Wiley, New York.
8. Belter, P. A., Cussler, E. L., and Hu, W.-S. (1988). *Bioseparations*, Wiley, New York.
9. Pakowski, Z., and Mujumdar, A. S. (1995). Basic process calculations in drying. In *Handbook of Industrial Drying*, vol. 1, A. S. Mujumdar, ed., Dekker, New York, p. 71.
10. Marinos-Kouris, D., and Maroulis, Z. B. (1995). Transport properties in the drying of solids. In *Handbook of Industrial Drying*, vol. 1, A. S. Mujumdar, ed., Dekker, New York, p. 113.
11. Van't Land, C. M. (1991). *Industrial Drying Equipment*, Dekker, New York.
12. Snowman, J. W. (1996). Lyophilization. In *Downstream Processing of Natural Products*, M. S. Verrall, ed., Wiley, New York, p. 275.
13. Gatlin, L. A., and Nail, S. L. (1994). Freeze drying: A practical overview. In *Protein Purification Process Engineering*, R. G. Harrison, ed., Dekker, New York, p. 317.
14. Franks, F. (1998). Freeze-drying of bioproducts: Putting principles into practice. *Eur. J. Pharmaceut. Biopharmaceut*., vol. 45, p. 221.
15. Masters, K. (1991). *Spray Drying Handbook*, 5th ed., Wiley, New York.
16. Filkova, I., and Mujumdar, A. S. (1995). Industrial spray drying systems. In *Handbook of Industrial Drying*, vol. 1, A. S. Mujumdar, ed., Dekker, New York, p. 263.
17. Fischer, J. J. (1963). Drying in vacuum tumblers. *Ind. Eng. Chem*., vol. 55, p. 18.
18. Tang, X. C., and Pikal, M. J. (2004). Design of freeze-drying for pharmaceuticals: practical advice. *Pharm. Res*., vol. 21, p. 191.
19. Liapis, A. I., and Bruttini, R. (1995). Freeze drying. In *Handbook of Industrial Drying*, vol. 1, A. S. Mujumdar, ed., Dekker, New York, p. 309.
20. Pikal, M. J., Cardon, S., Bhugra, C., Jameel, F., Rambhatla, S., Mascarenhas, W. J., and Akay, H. U. (2005). The nonsteady state modeling of freeze drying: in-process product temperature and moisture content mapping and pharmaceutical product quality applications. *Pharm. Dev. Technol*., vol. 1, p. 17
21. Velardi, S. A., and Barresi, A. A. (2008). Development of simplified models for the freeze- drying process and investigation of the optimal operating conditions. *Chem. Eng. Res. Design*, vol. 86, p. 9.
22. Gluckert, F. A. (1962). A theoretical correlation of spray-dryer performance. *AIChE. J*., vol. 8, p. 460

/// 12 /// BIOPROCESS DESIGN AND ECONOMICS

This chapter teaches students and practicing engineers the fundamentals of bioprocess design with an emphasis on bioseparation processes. It combines the information presented in earlier chapters for use in the context of integrated processes. The ultimate objective is to enable the reader to efficiently synthesize and evaluate integrated bioseparation processes.

Given a product and a desired annual production rate (process throughput), bioprocess design endeavors to answer the following and other related questions: What are the required amounts of raw materials and utilities needed for a single batch? What is the total amount of resources consumed per year? What is the required size of process equipment and supporting utilities? Can the product be produced in an existing facility or is a new plant required? What is the total capital investment? What is the manufacturing cost? What is the optimum batch size? How long does a single batch take? How much product can be generated per year? Which process steps or resources constitute scheduling and throughput bottlenecks? What changes can increase throughput? What is the environmental impact of the process (i.e., amount and type of waste materials)? Which design is the "best" among several plausible alternatives?

12.1 INSTRUCTIONAL OBJECTIVES

After completing this chapter, the reader should be able to do the following:

- Initiate a process design and choose the appropriate sequencing of processing steps.
- Set up a process flowsheet using the unit procedure concept.
- Become familiar with batch process simulators.
- Schedule batch processes.
- Estimate capital and operating costs.
- Perform profitability analysis.

- Assess the environmental impact of a process.
- Perform process sensitivity analyses.

12.2 DEFINITIONS AND BACKGROUND

Process design is the conceptual work done prior to building, expanding, or retrofitting a process plant. It consists of two main activities, *process synthesis* and *process analysis.* Process synthesis is the selection and arrangement of a set of unit operations (process steps) capable of producing the desired product at an acceptable cost and quality. Process analysis is the evaluation and comparison of different process synthesis solutions. In general, a synthesis step is usually followed by an analysis step, and the results of analysis determine the subsequent synthesis step.

Process design and project economic evaluation require integration of knowledge from many different scientific and engineering disciplines and are carried out at various levels of detail. Table 12.1 presents a common classification of design and cost estimates and typical engineering costs for a $50 million capital investment for a new plant.

Figure 12.1 presents the need for design estimates of various types during the life cycle of product development and commercialization. The trapezoidal shape of the diagram represents the drastic reduction in product candidates as we move from feasibility studies to commercialization. In fact, the chances of commercialization at the research stage for a new product are only about 1 to 3%, at the development stage they are about 10 to 25%, and at the pilot plant stage they are about 40 to 60% [1].

Order-of-magnitude estimates are usually practiced by experienced engineers who have worked on similar projects in the past. They take minutes or hours to complete, but the error in the estimate can be as high as 50%. Table 12.2 presents

TABLE 12.1 Types of Design Estimates, their Cost and Accuracy for a $50 Million Project [1]

Level	Type of estimate	Error (%)	Cost ($1000)
1	Order-of-magnitude estimate (ratio estimate) based on similar previous projects	≤50	
2	Project planning estimate (budget estimation) based on knowledge of major equipment items	≤30	30–100
3	Preliminary engineering (scope estimate) based on sufficient data to permit the estimate to be budgeted	≤25	250–750
4	Detailed engineering (capital approval stage) based on almost complete process data	≤15	1250–2000
5	Procurement and construction (contractor's estimate) based on complete engineering drawings, specifications and site surveys	≤10	3500–7000

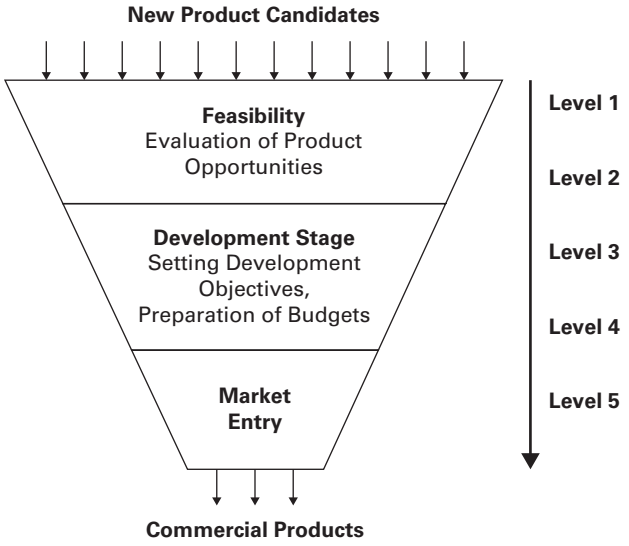

FIGURE 12.1 Types of design estimates during the life cycle of a product [2].

TABLE 12.2 Capital Investments for Cell Culture Facilities

Company	Bioreactor capacity (m^3)	Completion year	Investment ($ millions)	$ million per m^3
Boehringer Ingelheim (Germany)	6 x 15 = 90	2003	296	3.3
Lonza Biologics (Portsmouth, NH)	3 x 20 = 60	2004	207	3.4
Genentech (Oceanside, CA)	6 x 15 = 90	2005	450	5.0
Bristol Myers Squibb (Devens, MA)	6 x 20 = 120	2009	750	6.2
Roche Pharmaceuticals (Switzerland)	6 x 12.5 = 75	2009	375	5.0

a sample of data typically used by experienced engineers for order-of-magnitude estimates. The table lists the capital investment for five large-scale facilities built to manufacture therapeutic monoclonal antibodies using cell culture (by growing mammalian cells in stirred-tank bioreactors). Column #2 displays the number of the production bioreactors, the working volume of each, and the total working volume. For instance, the Genentech facility in Oceanside (former Biogen Idec site) includes six production bioreactors each having a working volume of 15 m^3. Column #4 displays the total capital investment, and column #5 displays the ratio of the total capital investment divided by the total production bioreactor volume. The ratio ranges from 3.3 to 6.2 with an average value of $4.6 million per m^3 of

bioreactor volume. Based on the data of Table 12.2, an engineer may conclude with some confidence that the capital investment for a new 100 m^3 (total production bioreactor volume) cell culture facility would be in the range of $330 million to $620 million and most likely around $460 million. Please note, however, that advances in technology (e.g., cell lines that generate higher product titers and the use of single-use systems) and other factors may render such data obsolete and reduce the accuracy of order-of-magnitude estimates. As a result, cost estimates are progressively refined as new product candidates move through the development lifecycle shown in Figure 12.1.

Most engineers employed by operating companies usually perform level 2 and 3 studies. Such studies take weeks or months to complete using appropriate computer aids. The main objective of such studies is to evaluate alternatives and pinpoint the most cost-sensitive areas—the economic "hot spots"—of a complex process. The results of such analyses are used to plan future research and development and to generate project budgets.

Level 4 and 5 studies are usually performed by the engineering and construction companies hired to build new plants for promising new products that are at an advanced stage of development. Such estimates are beyond the scope of this chapter. Instead, the focus of the material in the rest of this chapter will be on level 1, 2, and 3 studies. It should also be noted that opportunities for creative process design work are usually limited to preliminary studies. By the time detailed engineering work has been initiated, a process is more than 80% fixed. Furthermore, the vast majority of important decisions for capital expenditures and product commercialization are based on results of preliminary process design and cost analysis. This explains why it is so important for a new engineer to master the skills of preliminary process design and cost estimation.

Environmental impact assessment is an activity closely related to process design and cost estimation. Biochemical plants generate a wide range of liquid, solid, and gaseous waste streams that require treatment prior to discharge. The cost associated with waste treatment and disposal has skyrocketed in recent years due to increasingly strict environmental regulations. This cost can be reduced through minimization of waste generation at the source. However, generation of waste from a chemical or biochemical process is dependent on the process design and the manner in which the process is operated. Thus, reducing waste in an industrial process requires intimate knowledge of the process technology. In contrast, waste treatment is essentially an add-on at the end of the process. In addition, minimization of waste generation must be considered by process engineers at the early stages of process development. Once a process has undergone significant development, it is difficult and costly to make major changes. Furthermore, regulatory constraints that are unique to the pharmaceutical industry restrict process modifications after clinical efficacy of the drug has been established. These are only some of the reasons that process synthesis and analysis must be initiated at the early stages of product development.

12.3 SYNTHESIS OF BIOSEPARATION PROCESSES

The development of a flowsheet for the recovery and purification of a biological product is a creative process that draws on the experience and imagination of the engineer. Attempts have been made to capture that experience on the computer in the form of expert systems [3–6] and automate to some extent the process synthesis tasks. Experienced engineers heavily rely on certain *rules of thumb,* also known as *heuristics,* for putting together the skeleton of a recovery and purification process [7]. A few such heuristics follow:

1. Remove the most plentiful impurities first.
2. Remove the easiest-to-remove impurities first.
3. Make the most difficult and expensive separations last.
4. Select processes that make use of the greatest differences in the properties of the product and its impurities.
5. Select and sequence processes that exploit different separation driving forces.

Figure 12.2 provides a generalized structure for creating an initial block diagram representation of a product recovery process. For each product category (intracellular or extracellular) several branches exist in the main pathway. Selection among the branches and alternative unit operations is based on the properties of the product, the properties of the impurities, and the properties of the producing microorganisms, cells, or tissues. Bioprocess synthesis thus consists of sequencing steps according to the five heuristics above and the structure of Figure 12.2. The majority of bioprocesses, especially those employed in the production of high-value and low-volume products, operate in batch mode. Conversely, continuous bioseparation processes are utilized in the production of commodity biochemicals, such as organic acids and biofuels.

12.3.1 Primary Recovery Stages

Primary recovery encompasses the first steps of downstream processing where some purification and broth volume reduction occurs. Primary recovery includes both the solids separation stage and parts of the product isolation stages discussed in Chapter 1 (Table 1.10). According to Figure 12.2, the selection of the first step depends on whether the product is intracellular (remains inside the microorganism after its expression) or extracellular (secreted into the solution). Almost all low molecular weight bioproducts are extracellular, as are many that have a high molecular weight. Recovery and purification is easier for these bioproducts than for intracellular products because of the lower amount of impurities present. Most recombinant eukaryotic proteins produced by prokaryotic microorganisms are intracellular products (see Chapter 3 for definitions of prokaryotic and eukaryotic cells). These proteins accumulate inside the host cell

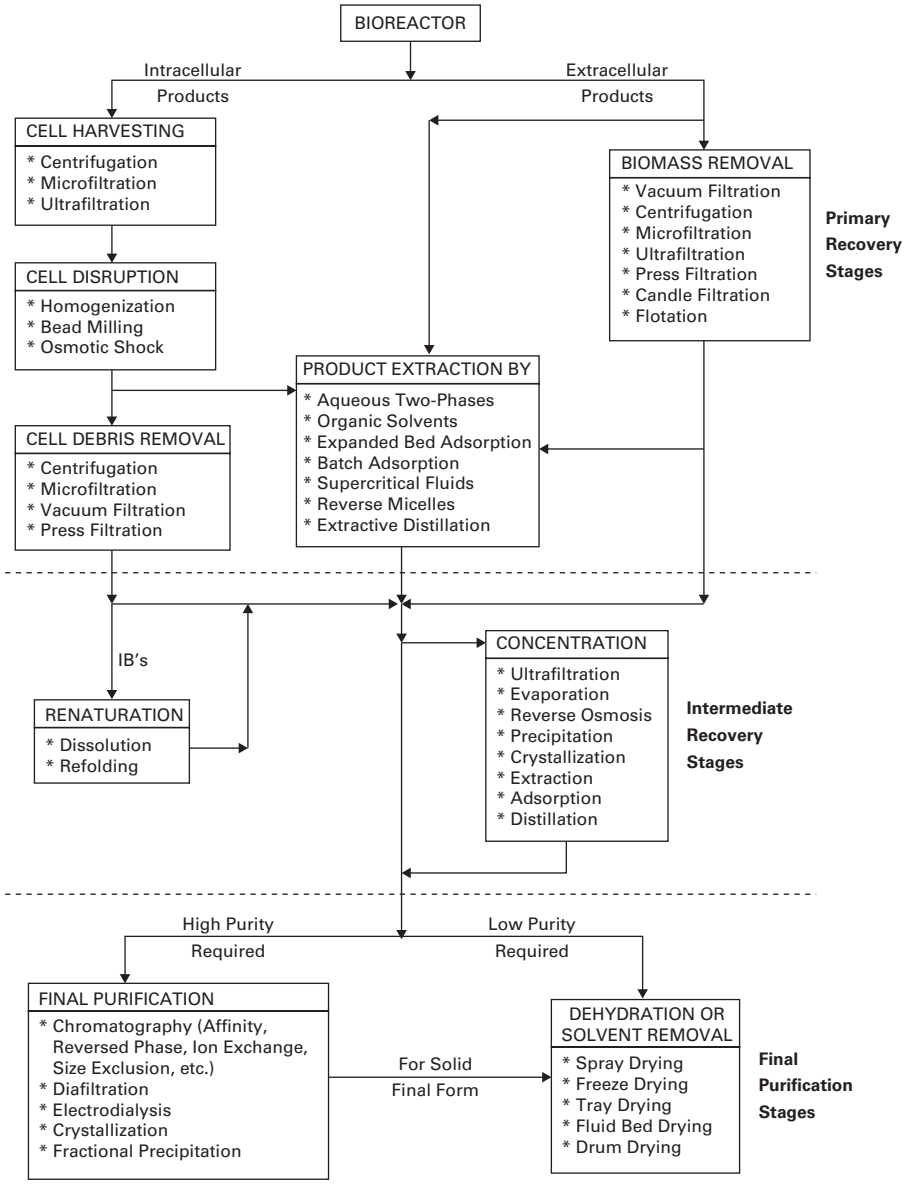

FIGURE 12.2 Generalized block diagram of downstream processing [5].

in either native or denatured form; the denatured intracellular products often form insoluble inclusion bodies (IBs). A brief review of the most common primary recovery steps (described in Chapters 3, 4, 5, and 6) follows, and various rationales for unit operation selection are included. The human insulin process analyzed in this chapter provides additional information on the recovery and purification of intracellular products.

Recovery of Intracellular Products

Cell Harvesting

The first purification step for intracellular products is cell harvesting. Removal of the extracellular liquid is in agreement with the first general heuristic: *Remove the most plentiful impurities first.*

As seen in Figure 12.2, centrifugation and membrane filtration (either microfiltration or ultrafiltration) are the only techniques used for large-scale cell harvesting. As explained in Chapter 5, centrifugation has advantages for large and dense microorganisms (diameter >2 μm and density >1.03 g/cm^3). For instance, centrifugation is very efficient for harvesting yeast. For smaller microorganisms, various coagulation techniques can be used to increase the size of the settling particles (see Chapter 3). Membrane filtration has advantages for harvesting small and light cells. Another advantage of membrane filtration is its superior product recovery. Cell loss during centrifugation is typically 1 to 5%. However, with membrane filtration, essentially all cells are recovered unless there is cell disruption (lysis) or unless the membranes rip.

Cell Disruption

The second step for intracellular products is usually cell disruption, which serves to break open the host cells and release the intracellular product. The various options for cell disruption are presented in Chapter 3. Disruption of bacteria and yeast is carried out either by high-pressure homogenizers or bead mills [8]. For large capacities (several cubic meters per hour) only high-pressure homogenizers are practical. Osmotic shock is often used for release of periplasmic products that accumulate between the cell membrane and the cell wall.

Prior to disruption, the concentrate is often diluted (by 5 to 10%) with a "lysis buffer" to create conditions that minimize product denaturation upon release from the cell. For hard-to-disrupt microorganisms, multiple homogenization passes at 500 to 1000 bar are required. Multiple passes are also required if the product forms inclusion bodies. This allows the IBs to be released and breaks the cell debris into very small particles, facilitating the separation of IBs from cell debris further downstream. Some product degradation also occurs during cell disruption as a result of high shear at interfaces and oxidation.

Removal of Cell Debris

The cell debris generated by cell disruption is usually removed by centrifugation or microfiltration. Other options include rotary vacuum filtration, press filtration, depth filtration, extraction, and expanded-bed adsorption (EBA) chromatography.

Soluble Product. When the product is soluble, it is recovered during cell debris removal either in the light phase of a centrifuge or in the permeate stream of a filter. Centrifuges are only able to efficiently separate fairly large particles of cell debris (>0.5 μm Stokes diameter). Therefore, when a centrifuge is used for cell debris removal, a polishing filtration step must follow the centrifugation in order to remove

small debris particles that might otherwise cause severe problems in processes downstream such as chromatography. Filters of various types (e.g., depth, press, candle, rotary vacuum, membrane microfilters) can be used for polishing. Alternatively, these filters can be used for cell debris removal with no preceding centrifugation step. It is very difficult to predict a priori which filter will perform best for a specific product, so lab and pilot scale testing are typically used to make this decision. In addition, when microfilters are used for cell debris removal, some degree of diafiltration is required to achieve an acceptable product recovery yield.

Insoluble Product. When the product is insoluble and forms inclusion bodies, it must first be separated from the cell debris particles, then dissolved and refolded (see insulin example later in this chapter for additional information on the subject). Fortunately, inclusion bodies usually have a large diameter (0.3–1.0 μm) and high density (1.3–1.5 g/cm^3) [9] and can be separated from cell debris with a disk-stack centrifuge (Chapter 5). The inclusion bodies are recovered in the heavy phase of the centrifuge, while most cell debris particles remain in the light phase. The heavy phase is usually resuspended and recentrifuged two or three times to reach a high degree of inclusion body purity. Resuspension in a solution of a low concentration of a chaotropic agent such as a detergent is often practiced to facilitate the removal of other contaminants. The pH and the ionic strength of the solution are adjusted to reduce the hydrophobicity of the cell debris particles and to enhance their removal in the light phase. Final product purity exceeding 70% is quite common.

Product Extraction/Adsorption

Separation of soluble product from cell debris can be carried out by extraction and/or adsorption. Organic solvents are commonly used as extractants for low molecular weight products, such as various antibiotics. Aqueous two-phase systems have found applications for recovery of proteins. The criteria for extractant selection are as follows: (a) the partition coefficient of the product should be higher than the partition coefficient of the contaminants, (b) the extractant should not degrade the product, (c) the extractant should not be expensive and should be easy to recover or dispose of (see Chapter 6 for more detailed information on extraction).

Alternatively, product separation from debris and simultaneous concentration can be achieved by adsorptive techniques [10]. Adsorbents of various types (e.g., ion exchange, reversed phase, affinity) can be used. This type of purification requires the disrupted cells and product to be mixed in a stirred tank with an adsorbent. A washing step, where most of the cell debris particles and contaminants are washed out, follows product adsorption. Expanded bed adsorption (EBA) chromatography is an alternative technology for separating proteins from cell debris particles [11]. The feed is pumped upward through an expanded bed. Target proteins are bound to the adsorbent while cell debris and other contaminants pass through. A washing step removes all weakly retained material. An elution step follows that releases and further purifies the product (see Chapter 7 for more detailed information on adsorption).

Recovery of Extracellular Products

Biomass Removal

In agreement with the second generic heuristic (*Remove the easiest-to-remove impurities first*), biomass removal is usually the first step of downstream processing of extracellular products. This step can be accomplished by using one (or more) of the following unit operations: rotary vacuum filtration, disk-stack or decanter centrifugation, press filtration, microfiltration, ultrafiltration, and flotation. Since each unit operation has advantages and disadvantages for different products and microorganisms, the selection of the best unit operation(s) for a given system can be difficult.

Rotary Vacuum Filtration. Rotary vacuum filtration, especially with precoat, is the classical method for removal of mycelial organisms [12]. Rotary vacuum filters can operate continuously for long periods of time (see Chapter 4). In addition, the filtrate flux in these units is usually higher than 200 liters m^{-2} h^{-1} and may reach 1000 liters m^{-2} h^{-1}. The most important disadvantage of this type of unit is the problem with disposal of the mixture of filter aid and biomass. Filter aid is added in equal or higher amounts than biomass. Stringent environmental laws have made it costly to dispose of such solid materials. Therefore, if the disposal cost of filter aid is relatively high where a new plant is going to be built, alternative unit operations should be considered for biomass separation. However, if the disposal cost of filter aid is relatively low, a rotary vacuum filter is a good choice. The citric acid process, which is described later in this chapter, offers an example where rotary vacuum filtration is used for biomass removal.

Centrifugation. Disk-stack and decanter centrifuges are frequently used at large scale [13, 14]. Disk-stack centrifuges operate at higher rotational speeds and remove smaller and lighter microorganisms. However, with the use of flocculating agents, the decanter centrifuge performance improves, and choosing between the two types becomes more difficult. It appears that the only criterion being applied when disk-stack is chosen instead of decanter is the ability to remove small, light microorganisms. Centrifugation does not require filter aid, which is a significant advantage over rotary vacuum filtration. In general, the centrifuge paste contains 40 to 60% v/v extracellular liquid. To recover the product dissolved in that liquid, the paste is usually washed and recentrifuged.

Membrane Filtration. With membrane filters (micro- and ultrafilters), the extracellular product passes through the membrane while biomass and other particulate components remain in the concentrate. Concentration is usually followed by diafiltration to prevent product degradation and/or to improve the performance of the subsequent step. (see Chapter 4 for more information on the mode of operation of membrane filters). Membrane filters are used for biomass removal mainly in recovery of low molecular weight products, such as antibiotics from mycelia. For high molecular weight products, gel layer formation often limits application to cases in which the amount of solids is rather small (e.g., cell culture).

12.3.2 Intermediate Recovery Stages

The primary recovery stages just described are followed by the intermediate stages, where the product is concentrated and further purified. Intermediate recovery has similarities to the product isolation stages discussed in Chapter 1 (Table 1.10). If the product is soluble, product concentration is usually the first step. If the product is denatured and insoluble, it is first dissolved and refolded and then concentrated and purified.

Product Concentration

After primary separation, the product is usually in a dilute solution. Volume reduction by concentration is in agreement with heuristics 1 and 2. Common concentration options include ultrafiltration, reverse osmosis, evaporation, adsorption, precipitation, extraction, and distillation.

Ultrafiltration

Ultrafiltration is used extensively for protein solution concentration. The molecular weight cutoff of the membrane is selected to retain the product while allowing undesirable impurities (mainly low molecular weight solutes) to pass through the membrane. The low operating temperature and the purification achieved along with concentration are some of the advantages of ultrafiltration over evaporation. The typical operating transmembrane pressure is 2 to 5 bar and the average flux is 20 to 50 liters m^{-2} h^{-1}.

Reverse Osmosis

Membranes with smaller pore sizes are used for reverse osmosis filters. The process of reverse osmosis may be used when concentrating medium to low molecular weight products (e.g., antibiotics, certain amino acids).

Evaporation

Agitated film evaporators can operate at relatively low temperatures (40 to 50°C) under vacuum. These units compete in the market with ultrafiltration and reverse osmosis for concentrating both low and high molecular weight compounds. Unlike ultrafiltration, however, evaporation lacks the capability to provide purification during concentration. Advantages include the ability to concentrate to a higher final solids concentration and the ability to handle large throughputs [15]. See Chapter 10 for more information about the different types of evaporators.

Precipitation

Precipitation is often used for concentration and purification. Blood protein fractionation (see Chapter 8) and citric acid production (see later: Section 12.6.1) constitute typical applications. Addition of salts, solvents, and polymers and changes in pH, ionic strength, and temperature are commonly used to selectively precipitate

compounds of interest [16]. Precipitation often follows an extraction carried out in a polymer/salt (e.g., PEG and potassium phosphate) aqueous two-phase system. When the product is recovered in the polymer-rich phase, precipitation is accomplished by addition of more polymer. It is important for economic reasons to recover and recycle the precipitating materials. Precipitation is also used to remove contaminants (i.e., nucleic acids) by adding manganese sulfate ($MnSO_4$) and streptomycin sulfate.

Distillation

The process of distillation is used for concentrating and purifying low molecular weight and volatile compounds, such as acetone, ethanol, butanol, acetic acid, etc.

Pervaporation

This membrane-based process has found applications in biofuels for the dehydration of ethanol and other alcohols. One component from a liquid mixture selectively permeates through a membrane, driven by a gradient in partial vapor pressure and leaving the membrane as a vapor [17]. Dehydration of ethanol-water azeotropic solutions (around 90% ethanol) is facilitated by the use of hydrophilic membranes. Hydrophobic membranes are used for removal/recovery of small amounts of organics from aqueous solutions.

Product Renaturation

Eukaryotic proteins produced by prokaryotic microorganisms often form insoluble inclusion bodies in the host cell. Inclusion bodies (IBs) can be dissolved rapidly by using solutions of strong chaotropes, such as 6 M guanidine hydrochloride or urea, in the presence of a reducing agent, such as 0.5 M 2-mercaptoethanol or 50 mM dithiothrietol [18]. The dissolved protein is then allowed to refold to its native conformation by removing the chaotropic agents through diafiltration, dilution, or chromatography, with final protein concentrations in the range of 10 to 100 mg/liter. Dilution is necessary for minimizing intermolecular interactions, which occur during product refolding and can lead to product inactivation. Addition of small amounts of thiols such as reduced glutathione (1–5 mM) and oxidized glutathione (0.01–0.5 mM) and incubation at 35 to 40°C for 5 to 10 h completes the refolding process. Thus, choosing an upstream process that forms IBs entails consideration of the large volumes, hence large waste streams, that are produced. More information on IB solubilization and protein refolding can be found in the insulin example (see later: Section 12.6.2) and also in "Solubilization and Refolding of Proteins in Inclusion Bodies" (in Section 1.4.8).

12.3.3 Final Purification Stages

The final purification steps are dependent on the required final product purity. Final purification includes both the purification and polishing stages discussed in Chapter 1 (Table 1.10). Pharmaceutical products require high purity, while industrial

products require lower purity. For products of relatively low purity, such as industrial enzymes, the final purification step is dehydration or more generally a solvent removal step. For high-purity products, the final purification stages usually involve a combination of chromatographic and filtration steps [19]. If the final product is required in solid form, a dehydration or solvent removal step follows.

Chromatography

Chromatography is typically done later in a process in agreement with the third generic heuristic (*Make the most difficult and expensive separations last*). With the preceding separation steps, a large fraction of contaminants is removed, thereby reducing the volume of material that needs to be treated further. A sequence of chromatographic steps is usually required to achieve the desired final product purity, and the fourth and fifth generic heuristics are good guides for selecting and sequencing such steps [20]. For instance, according to the fifth heuristic, an ion exchange step should not be followed by another step of the same type. Instead, it should be followed by a reversed phase, affinity, or any other chromatography type that takes advantage of a different separation driving force.

Membrane adsorption units combine the high flux of membrane filters with the selective binding of chromatographic resins [21, 22]. As a result, they have advantages compared to traditional column chromatography when operated in flow-through mode for removing small amounts of specific contaminants. The membrane retains certain impurities (e.g., DNA molecule fragments) while the product molecules pass through the membrane. Such membrane systems are typically used as the last step of biopharmaceutical protein purification processes.

Simulated moving bed (SMB) chromatography is the method of choice for handling large volumes of material [23, 24]. It has found applications in the purification of amino acids, high-fructose corn syrup, cheese whey proteins, lactic acid, succinic acid, etc. In SMB systems, multiple columns operate out of phase using a complex system of valves. The feed stream usually passes through two columns, resulting in increased yield and resolution. One column is always out of use for cleaning. SMB systems can handle feed streams of continuous flow, which is the preferred method of operation for the production of high-volume biochemicals.

Membrane filtration steps are commonly employed between chromatographic steps to exchange buffers and concentrate the dilute product solutions. See Chapter 7 for detailed information on chromatographic separation methods and Chapter 4 for the intervening membrane filtration steps. The insulin and monoclonal antibody examples presented later in this chapter provide additional information on selection and operation of chromatographic separation units.

Crystallization and Fractional Precipitation

Crystallization and fractional precipitation can sometimes result in significant purification. Because these processes are cheaper to operate than chromatography, they should always be considered. The crystalline form of a bioproduct is especially

advantageous, since the purity can be quite high and crystals can usually be stored for long periods of time. See Chapters 8 and 9 for a detailed discussion and analysis of precipitation and crystallization. The citric acid process which is analyzed later in this chapter is a good example of a product that is recovered and purified using precipitation and crystallization.

Dehydration or Solvent Removal

Dehydration or solvent removal is achieved with dryers. Spray, fluidized-bed, and tray dryers are used when products can withstand temperatures of 50 to 100°C. Freeze dryers are used for products that degrade at high temperatures. Freeze dryers require high capital expenditures and should be avoided if possible. See Chapter 11 for detailed information on product drying.

12.3.4 Pairing of Unit Operations in Process Synthesis

Besides using rules of thumb, or heuristics, for synthesizing bioseparation processes, it is often advantageous to consider how two unit operations can be paired to improve process efficiency. The following section lists some examples of operations that are logical to pair.

Extraction and Precipitation

The bioproduct is extracted with a solvent and then precipitated. To increase the yield, it is often desirable to concentrate the extract before the precipitation. The major hurdle to overcome for this pairing is to find a solvent that will work with both extraction and precipitation.

Precipitation and Hydrophobic Interaction Chromatography

The pairing of precipitation and hydrophobic interaction chromatography is usually accomplished for protein purification by using ammonium sulfate to precipitate impurities, leaving the desired bioproduct in the mother liquor. The ammonium sulfate is added to a concentration just below that needed to precipitate the bioproduct. After removal of precipitated impurities, the mother liquor can be applied directly to a hydrophobic interaction chromatography column, which was equilibrated to the concentration of ammonium sulfate in the mother liquor prior to the loading. The bioproduct adsorbs to the column under these conditions. The column is eluted with a reverse gradient of ammonium sulfate, and the desired bioproduct is recovered in a fraction from the elution.

Filtration and Extraction

When the bioproduct is contained in the filtrate after filtration, it can often be extracted with an immiscible solvent. For the extraction of small molecules such as antibiotics with organic solvents, the pH must usually be adjusted to obtain the bioproduct in either its free base or free acid form so it will partition into the

organic phase. For the aqueous two-phase extraction of proteins, two polymers or a salt and a polymer must be added. If the additions to the filtrate can be made in-line, the filtration and extraction steps can be carried out simultaneously, reducing the processing time.

12.4 PROCESS ANALYSIS

The flowsheets created during process synthesis must be analyzed and compared on the basis of capital investment, manufacturing cost, environmental impact, and other criteria to decide which ideas to consider further. Methodologies for estimating capital investment and manufacturing cost are presented in the next section of this chapter. In both cases, estimation is based on the results of material and energy balances and equipment sizing. These calculations are typically done using spreadsheets or process simulators. These tools allow the process design team to characterize a processing scenario, and then quickly and accurately redo the entire series of calculations for a different set of assumptions and other input data.

12.4.1 Spreadsheets

Spreadsheet applications, such as Microsoft Excel, have become as easy to use as word processors and graphics packages. In its simplest form, a spreadsheet is an electronic piece of paper with empty boxes, known as cells. The user can enter data in those cells, perform calculations, and generate results. Results from spreadsheets can be easily plotted in a variety of graphs.

12.4.2 Process Simulators and Their Benefits

Process simulators are software applications that enable the user to readily represent and analyze integrated processes. They have been in use in the petrochemical industries since the early 1960's. Established simulators for those industries include Aspen Plus and HYSYS from Aspen Technology, Inc. (Burlington, MA), ChemCAD from Chemstations, Inc. (Houston, TX), and PRO/II from SimSci-Esscor, Inc. (Lake Forest, CA).

The simulators mentioned above have been designed to model primarily continuous processes and their transient behavior. Most biological products, however, are produced in batch and semicontinuous mode [25, 26]. Such processes are best modeled with batch process simulators that account for time-dependency and sequencing of events. The first simulator designed specifically for batch processes was called Batches (from Batch Process Technologies in West Lafayette, IN). It was commercialized in the mid 1980's. All of its operation models are dynamic, and simulation always involves integration of differential equations over a period of time. In the mid 1990's, Aspen Technology (Burlington,

MA) introduced Batch Plus (now called Aspen Batch Process Developer), a recipe-driven simulator that targeted batch pharmaceutical processes. Around the same time, Intelligen, Inc. (Scotch Plains, NJ) introduced SuperPro Designer [27, 28]. SuperPro Designer is a flowsheet-driven simulator which handles material and energy balances, equipment sizing and costing, economic evaluation, environmental impact assessment, process scheduling, and debottlenecking of batch and continuous processes.

Discrete-event simulators have also found applications in the bioprocessing industries. Established tools of this type include ProModel from ProModel Corporation (Orem, UT), Arena and Witness from Rockwell Automation, Inc. (Milwaukee, WI), Extend from Imagine That, Inc. (San Jose, CA), and FlexSim from FlexSim Software Products, Inc. (Orem, UT). The focus of models developed with such tools is usually on the minute-by-minute time-dependency of events and the animation of the process. Material balances, equipment sizing, and cost analysis tasks are usually out of the scope of such models.

The benefits from the use of process simulators depend on the type of product, the stage of development, and the size of the investment. For commodity biological products, such as biofuels, minimization of capital and operating costs are the primary benefits. For high-value biopharmaceuticals, systematic process development that shortens the time to commercialization is the primary motivation. Figure 12.3 shows a pictorial representation of the benefits from the use of such tools at the various stages of the commercialization process.

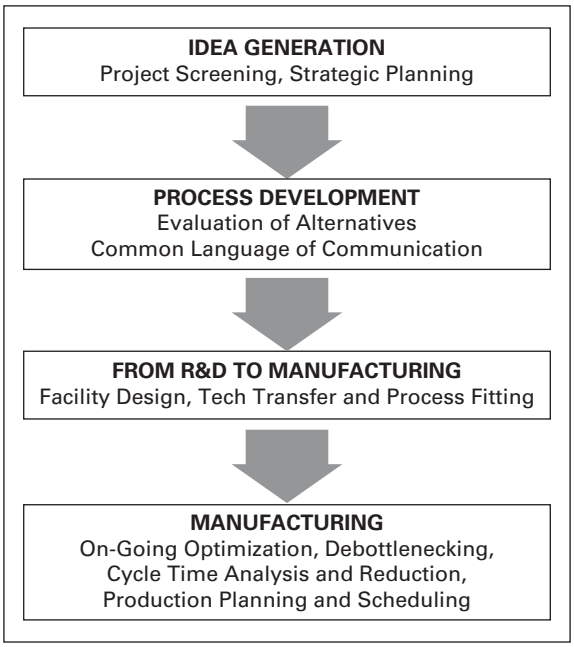

FIGURE 12.3 Benefits of using process simulators.

Idea Generation

When product and process ideas are first conceived, process modeling tools are used for project screening, selection, and strategic planning based on preliminary economic analyses.

Process Development

During this phase, the company's process development groups are looking into the various options available for synthesizing, purifying, characterizing, and formulating the final product. The process undergoes constant changes during development. Typically, a large number of scientists and engineers are involved in the improvement and optimization of individual processing steps. The use of process simulators at this stage can introduce a common language of communication and facilitate team interaction. A computer model of the entire process can provide a common reference and evaluation framework to facilitate process development. The impact of process changes can be readily evaluated and documented in a systematic way. Once a reliable model is available, it can be used to pinpoint the cost-sensitive areas of a complex process. These are usually steps of high capital and operating cost or low yield and production throughput. The findings from such analyses can focus further lab and pilot plant studies in order to optimize those portions of the process. The ability to experiment on the computer with alternative process setups and operating conditions reduces the costly and time-consuming laboratory and pilot plant effort. A simulator can also evaluate the environmental impact of a process. For instance, material balances calculated for the projected large-scale manufacturing reveal environmental hot-spots. These are usually process steps that utilize organic solvents and other regulated materials with high disposal costs. Environmental issues which are not addressed during process development may lead to serious drawbacks during manufacturing.

Facility Design and/or Selection

With process development near completion at the pilot plant level, simulation tools are used to systematically design and optimize the process for commercial production. Availability of a good computer model can greatly facilitate the transfer of a new process from the pilot plant to the large-scale facility. If a new facility needs to be built, process simulators can size process equipment and supporting utilities, and estimate the required capital investment. In transferring production to existing manufacturing sites (technology transfer), process simulators can be used to evaluate the various sites from a capacity and cost point of view and select the most appropriate one.

Manufacturing

In large-scale manufacturing, simulation tools are mainly used for on-going process optimization and debottlenecking studies. Furthermore, tools that are equipped with batch process scheduling capabilities can be used to generate production schedules

on an on-going basis in a way that does not violate constraints related to the limited availability of equipment, labor resources, utilities, inventories of materials, etc.

12.4.3 Using a Biochemical Process Simulator

The minimum requirements for a biochemical process simulator are the ability to handle batch as well as continuous processes and the ability to model the unit operations that are specific to bioprocessing. Because SuperPro Designer (from Intelligen, Inc.) has the ability to satisfy these requirements, we will use it to illustrate the role of such tools in bioprocess design. A functional evaluation version of SuperPro Designer and additional information on bioprocess simulation can be obtained at the website www.intelligen.com. Tutorial videos on the use of SuperPro Designer can be viewed at www.intelligen.com/videos.

To model an integrated process using a simulator, the user starts by developing a flowsheet that represents the overall process. For instance, Figure 12.4 displays the flowsheet of a hypothetical process on the main window of SuperPro Designer. The flowsheet is developed by putting together the required unit operations (sometimes referred to as "unit procedures," as explained later in this section) and joining

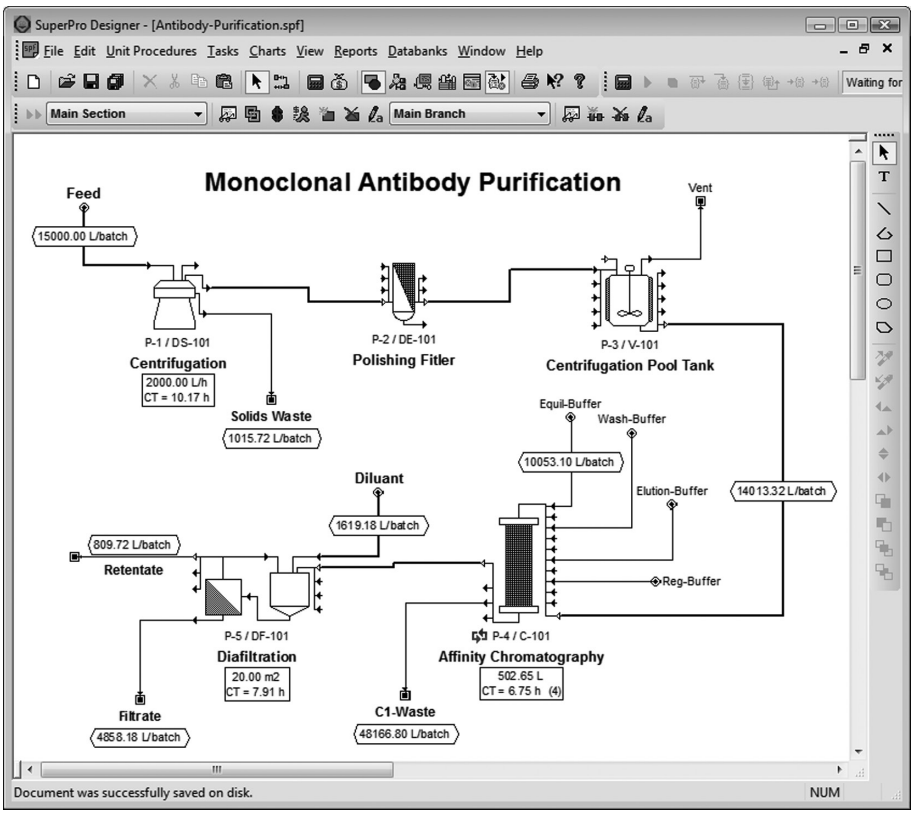

FIGURE 12.4 A flowsheet on the main window of SuperPro Designer (L = liters).

them with material flow streams. Next, the user initializes the flowsheet by registering (selecting from the component database) the various materials that are used in the process and specifying operating conditions and performance parameters for the various operations.

Most biochemical processes operate in batch or semicontinuous mode. This is in contrast to continuous operation, which is typical in the petrochemical and other industries that handle large throughputs. In continuous operations, a piece of equipment performs the same action all the time, which is consistent with the notion of unit operations. In batch processing, on the other hand, a piece of equipment goes through a cycle of operations. For instance, a typical chromatography cycle includes *equilibration, loading, washing, elution,* and *regeneration* (Chapter 7). In SuperPro Designer, the set of operations that comprise a processing step is called a "unit procedure" (as opposed to a "unit operation"). Each unit procedure contains individual tasks (e.g., equilibration, loading) called operations. A unit procedure is represented on the screen with a single equipment icon (e.g., P-4/C-101 in Figure 12.4 represents the affinity chromatography procedure). In essence, a unit procedure is the recipe of a processing step that describes the sequence of actions required to complete that step. Figure 12.5 displays the dialog through which the recipe of a chromatography unit procedure is specified. On the left-hand side of that dialog, the program displays

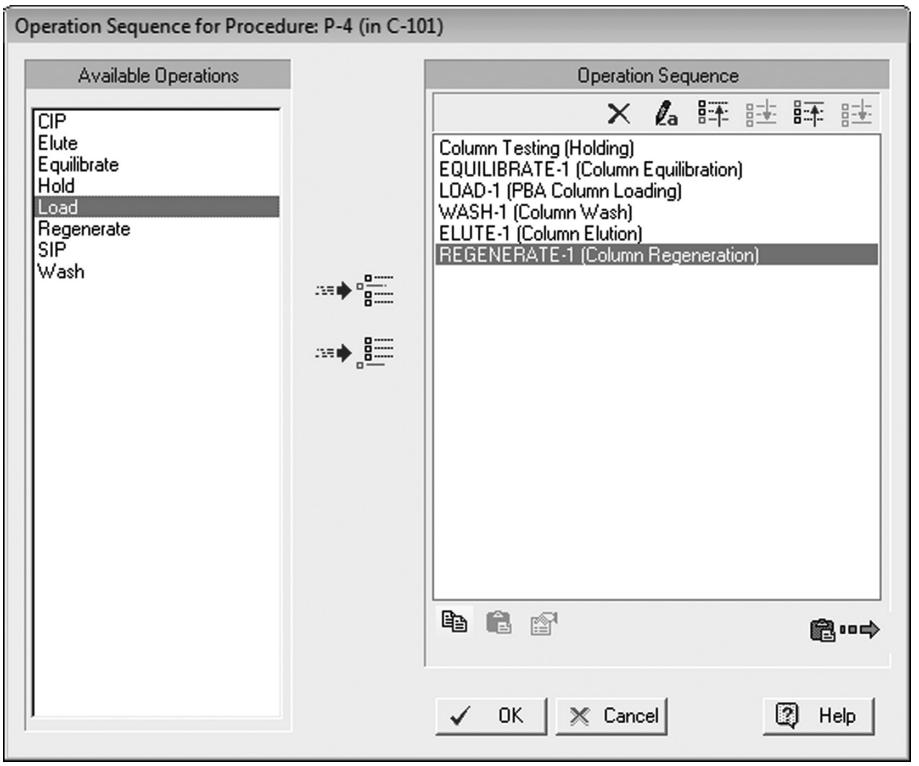

FIGURE 12.5 Window for adding operations to a unit procedure using SuperPro Designer.

the operations that are available in a chromatography procedure; on the right-hand side, it displays the registered operations (i.e. the operations that have been selected for this particular procedure). The significance of the unit procedure is that it enables the user to describe and model the various activities of batch processing steps in detail. Later in this chapter (in the examples, Section 12.6), we will see how the execution of these activities can be visualized as a function of time.

For every operation within a unit procedure, SuperPro includes a mathematical model that performs material and energy balance calculations. Based on the material balances, SuperPro performs equipment-sizing calculations similar to some of the homework problems in this book. If multiple operations within a unit procedure dictate different sizes for a certain piece of equipment, the software reconciles the different demands and selects an equipment size that is appropriate for all operations. In other words, the equipment is sized to ensure that it will not be overfilled during any operation but is no larger than necessary (in order to minimize capital costs). In addition, the software checks to ensure that the vessel contents will not fall below a user-specified minimum volume (e.g., a minimum impeller volume) for applicable operations.

Before any simulation calculations can be done, the user must initialize the various operations by specifying operating conditions and performance parameters through appropriate dialog windows. For instance, Figure 12.6 displays the initialization dialog of a chromatography elution operation. Through this dialog, the user specifies the elution strategy (isocratic or gradient), selects the input and output streams, specifies the eluant volume on a relative (e.g., in terms of bed volumes) or an absolute basis, specifies the fraction of buffer in which the product is recovered, specifies the linear velocity during elution, etc. Through the Labor tab of the same dialog window, the user provides information about labor requirements during this operation. Through the Scheduling tab, the user specifies the sequencing of this operation relative to another operation (either in the same procedure or in a different procedure) or relative to the beginning of the batch. After initialization of the operations, the simulator performs material and energy balances for the entire process and estimates the required sizes of equipment. Optionally, the simulator may be used to carry out cost analysis and economic evaluation calculations. The fundamentals of process economics are described in the next section, and pertinent examples are provided later in this chapter.

Other tasks that can be handled by process simulators include process scheduling, environmental impact assessment, debottlenecking, and throughput analysis. Issues of process scheduling and environmental impact assessment are addressed in Section 12.6. Throughput analysis and debottlenecking is the analysis of the capacity and time utilization of equipment and resources (e.g., utilities, labor, raw materials). The objective is to identify opportunities for increasing throughput with the minimum possible capital investment (see Section 12.6 for additional information on the subject).

Having developed a good model using a process simulator or a spreadsheet, the user may conduct virtual experiments with alternative process setups and operating conditions. This may potentially reduce costly and time-consuming laboratory and

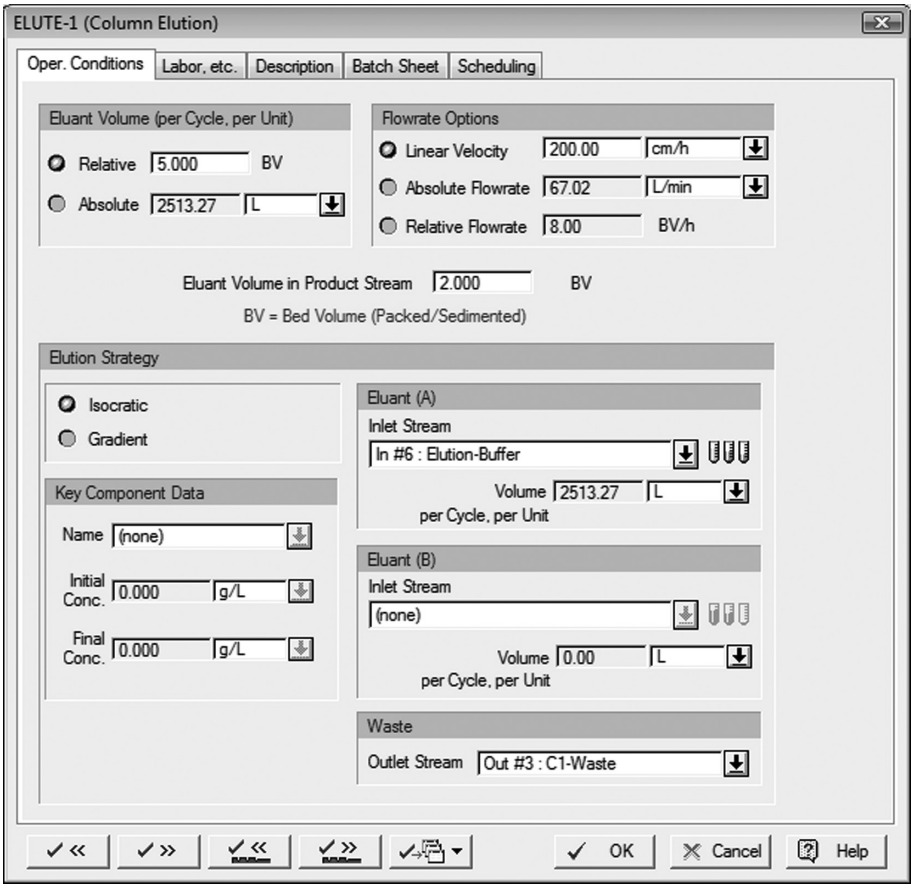

FIGURE 12.6 Dialog window of the elution operation.

pilot plant effort. One must be aware, however, that the GIGO (garbage in, garbage out) principle applies to all computer models. More specifically, if some assumptions and input data are incorrect, the outcome of the simulation will not be reliable. Consequently, validation of the model is necessary. In its simplest form, a review of the results by an experienced engineer can play the role of validation.

12.5 PROCESS ECONOMICS

The preliminary economic evaluation of a project for manufacturing a biological product usually involves the estimation of capital investment, estimation of operating costs, and an analysis of profitability. For biopharmaceuticals, another figure worth considering is the average cost of new drug development, which is in the range of $500 to $1 billion [29, 30]. Much of this figure represents research and development (R&D) spending for all unsuccessful products. In other words, the actual average development cost per successful drug may be $50 to $100 million, but because more than 90% of new projects never reach commercialization, the average overall

R&D cost skyrockets. This order-of-magnitude cost increase reinforces the need for effective process design tools and methodologies that assist engineers and scientists in efficiently evaluating and eliminating nonpromising project ideas at the very early stages of product and process development.

12.5.1 Capital Cost Estimation

The capital investment for a new plant includes three main items: direct fixed capital (DFC), working capital, and start-up and validation cost.

Direct Fixed Capital

The DFC for small- to medium-size biotechnology facilities is usually in the range of $50 to $200 million, whereas for large facilities it is in the range of $250 to $750 million. For preliminary design purposes, the various items of DFC are estimated based on the total equipment purchase cost (PC) using several multipliers sometimes called "Lang Factors." Table 12.3 provides ranges and average values for the multipliers and a skeleton for the calculations. Detailed definitions of the various cost items and additional information can be found in traditional process design textbooks and the technical literature [1, 31–36].

TABLE 12.3 Fixed Capital Cost Estimation

Cost item	Average multiplier	Range of multiplier values
Total plant direct cost (TPDC)		
Equipment purchase cost (PC)		
Installation	0.50 × PC	0.2–1.5
Process piping	0.40 × PC	0.3–0.6
Instrumentation	0.35 × PC	0.2–0.6
Insulation	0.03 × PC	0.01–0.05
Electrical	0.15 × PC	0.1–0.2
Buildings	0.45 × PC	0.1–3.0
Yard improvement	0.15 × PC	0.05–0.2
Auxiliary facilities	0.50 × PC	0.2–1.0
Total plant indirect cost (TPIC)		
Engineering	0.25 × TPDC	0.2–0.3
Construction	0.35 × TPDC	0.3–0.4
Total plant cost (TPC)	TPDC + TPIC	
Contractor's fee	0.05 × TPC	0.03–0.08
Contingency	0.10 × TPC	0.07–0.15
Direct fixed capital (DFC)	TPC + Contractor's fee and contingency	

Notice the wide range of multiplier values for estimating the cost of buildings. Plants for commodity biochemicals, such as ethanol and citric acid, fall on the low end of the range. Conversely, biopharmaceutical facilities with their expensive heating, ventilation, and air conditioning (HVAC) requirements fall on the high end. The average value of 0.45 corresponds to relatively large plants that produce medium to high-value products (e.g., industrial enzymes).

For more accurate estimation of building costs, it is necessary to estimate the process area required based on the footprint of the equipment and the space required around the equipment for safe and efficient operation and maintenance. Then the building cost is estimated by multiplying the area of the various sections (e.g., process, laboratory, office) of a plant by an appropriate unit cost provided in Table 12.4. This table, which was developed by DPS Biometics (Framingham, MA), also provides information on air circulation rates for the various process areas, which determine the sizing and power requirements of HVAC systems.

Table 12.3 indicates a wide range in the equipment installation cost multipliers. Using multipliers that are specific to individual equipment items leads to the most accurate estimates. In general, equipment delivered mounted on skids has a lower installation cost.

For preliminary cost estimates, Table 12.3 clearly shows that the fixed capital investment of a plant is a multiple (usually three to ten times) of its equipment purchase cost. The low end of the range applies to large-scale facilities that produce biofuels and commodity biochemicals. The high end applies to biopharmaceutical facilities.

The equipment purchase cost can be estimated from vendor quotations, published data, company data compiled from earlier projects, and by using process simulators that are equipped with appropriate costing capabilities. Vendor quotations are time-consuming to obtain and are, therefore, usually avoided for preliminary cost estimates. Instead, engineers tend to rely on the other three sources. Figures 12.7 to 12.10

TABLE 12.4 Building Cost Estimation (Year 2012 Prices) [2]

Space function	Unit cost ($/m^2)	Air circulation rates (volume changes/h)
Process areas[a]		
Class 100,000	3000–3750	20
Class 10,000	3750–5200	35–50
Class 1,000	6700–9000	100
Class 100	9000–12000	200–600
Mechanical room (utilities)	450–900	
Laboratory	1500–3000	
Office	750–900	

[a]The class number refers to the maximum number of particles 0.5 μm or larger per cubic foot.

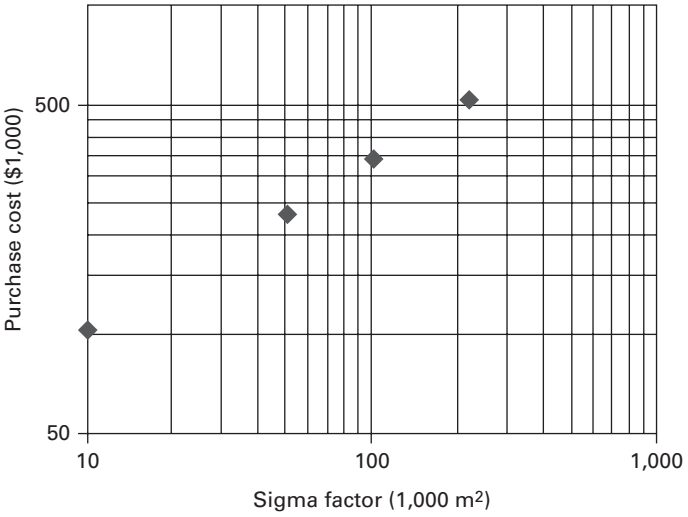

FIGURE 12.7 Purchase cost of disk-stack centrifuges versus Σ factor (2012 prices).

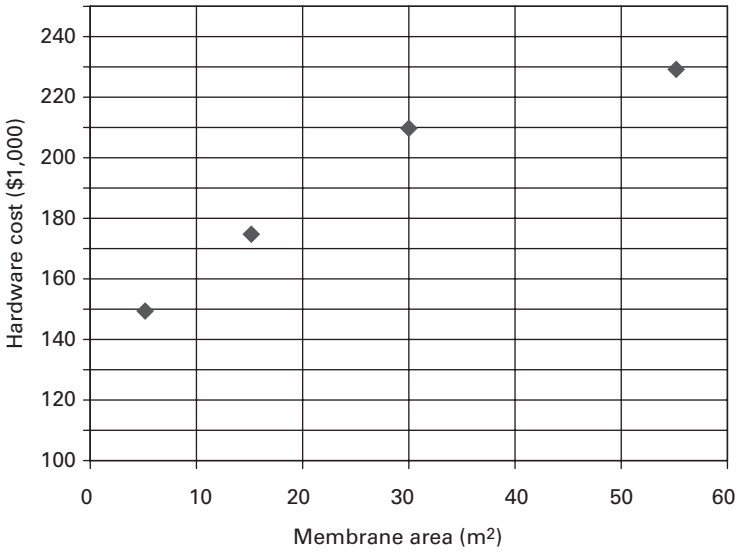

FIGURE 12.8 Purchase cost of membrane filtration systems (2012 prices).

provide equipment cost data for disk-stack centrifuges, membrane filtration systems, chromatography columns, and vertical agitated tanks that meet the specifications of the biopharmaceutical industry. The cost of the membrane filtration systems includes the cost of the skid, tank, pumps and automation hardware and software. The tanks are appropriate for buffer preparation. They include a low-power agitator, but no heating/cooling jacket. The data represent average values from several vendors.

It should be noted that equipment purchase cost is a strong function of industrial application and plant location. The data of Figures 12.7 to 12.10 are applicable to biopharmaceutical facilities in developed countries. The cost of membrane filtration

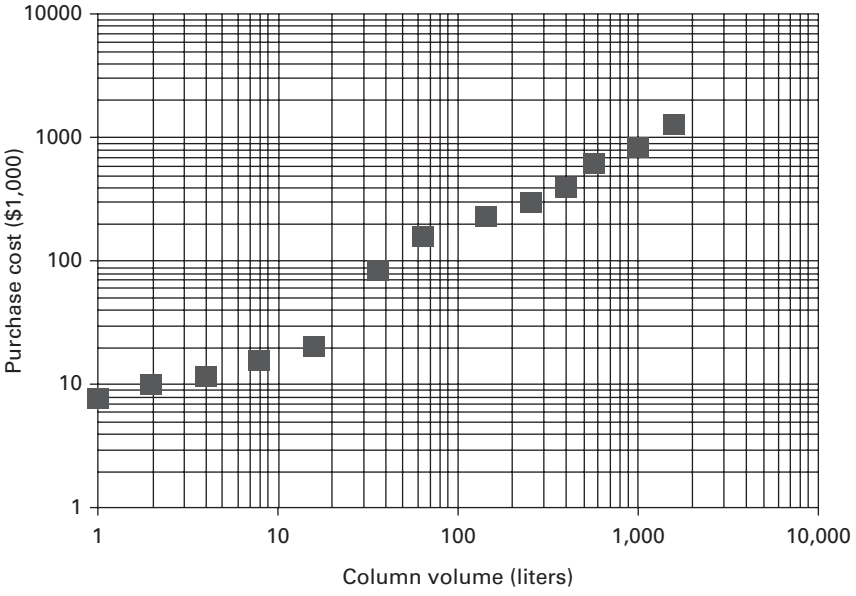

FIGURE 12.9 Purchase costs of chromatography columns made of acrylic-tube and stainless-steel bed supports (2012 prices).

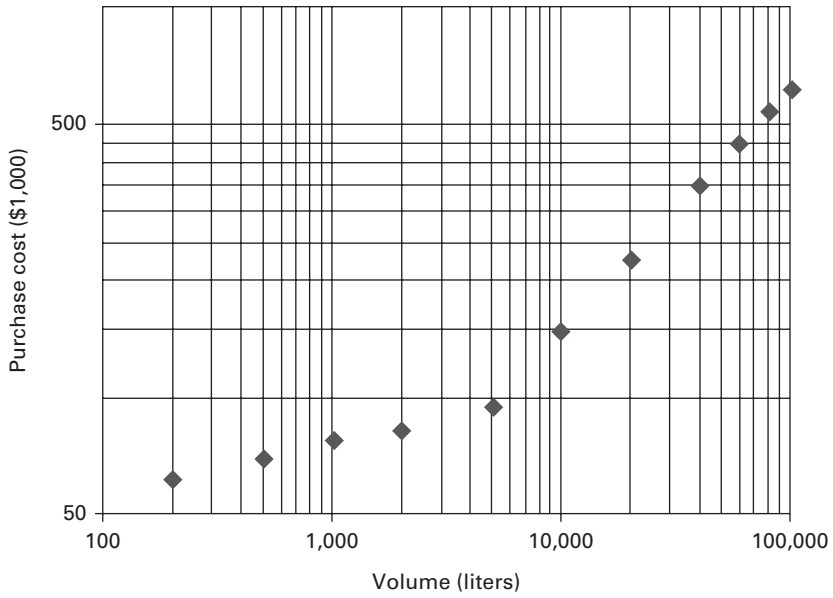

FIGURE 12.10 Purchase cost of agitated tanks made of stainless steel (2012 prices).

systems used in the food, biofuel and water purification industries is more than an order of magnitude lower compared to the biopharmaceutical industry. The much larger equipment scale and the less stringent equipment specifications relative to biopharmaceuticals are responsible for the large difference in cost. The same trend applies to the cost of chromatography columns, storage tanks, reactor vessels, and

most other equipment items. A good source of cost data for equipment used in the biofuel and biomaterial industries is available from the U.S. Department of Energy [37]. Additional sources for bioprocessing equipment cost data are available in the literature [38, 39].

Often, cost data for one or two discrete equipment sizes are available, but the cost for a different size piece of equipment must be estimated. In such cases, the *scaling law* (expressed by the following equation) can be used:

$$\text{Cost}_2 = \text{Cost}_1 \left(\frac{\text{Size}_2}{\text{Size}_1} \right)^a \quad (12.5.1)$$

The mathematical form of the scaling law explains why cost-versus-size data graphed on logarithmic coordinates tend to fall on a straight line. The value of the exponent *a* in Equation (12.5.1) ranges between 0.5 and 1.0, with an average value for vessels of around 0.6 (this explains why the scaling law is also known as the "0.6 rule"). According to this rule, when the size of a vessel doubles, its cost will increase by a factor of $(2/1)^{0.6}$, or approximately 52%. This result is often referred to as the *economy of scale*. In using the scaling law, it is important to make sure that the piece of equipment whose cost is being estimated has a size that does not exceed the maximum available size for that type of equipment.

The price of equipment changes with time owing to inflation and other market conditions. That change in price is captured by the Chemical Engineering Plant Cost Index (CE Index) that is published monthly by *Chemical Engineering* magazine. The index *I* is used to update equipment cost data according to the following equation:

$$\text{Cost}_2 = \text{Cost}_1 \left(\frac{I_2}{I_1} \right) \quad (12.5.2)$$

Another factor that affects equipment purchase cost is the material of construction. For instance, a tank made of stainless steel costs approximately two and one-half to three times as much as a carbon steel tank of the same size. A tank made of titanium costs around 15 times the cost of a carbon steel tank of the same size. Other factors that affect equipment cost include the finishing of the metal surface and the instrumentation that is provided with the equipment.

Working Capital

Working capital accounts for cash that must be available for investments in on-going expenses and consumable materials. These expenses may include raw materials for 1 to 2 months, labor for 2 to 3 months, utilities for a month, waste treatment/disposal for a month, and other miscellaneous expenses. The required amount of working capital for a process is usually 10 to 20% of the DFC.

Start-up and Validation

Start-up and validation costs can also represent a significant capital investment for a biopharmaceutical plant. A value of 20 to 30% of DFC is quite common.

12.5.2 Operating Cost Estimation

The operating cost to run a biochemical plant is the sum of all on-going expenses including raw materials, labor, consumables, utilities, waste disposal and facility overhead. Dividing the annual operating cost by the annual production rate yields the unit production cost (e.g., in dollars per kilogram). The unit cost and selling prices of bioproducts are inversely proportional to market size (see Figure 1.1). Low molecular weight commodity biochemicals and biofuels that are produced in large quantities cost around $1 to $5/kg to make. Citric acid, whose production is analyzed later in this chapter, is a product of this type. Specialty biochemicals that are used as food supplements (e.g., vitamins) and flavoring agents have a manufacturing cost of $5 to $100/kg. The manufacturing cost of therapeutic proteins produced in large quantities is in the range of $1/g to $1000/g. Human serum albumin (HSA) which is extracted from blood plasma and has an annual production volume of more than 500 metric tons lies close to the low end. The manufacturing cost of therapeutic proteins with annual production volume ranging from a few hundreds of kilograms to a few metric tons is in the range of $50 to $1000/g. The insulin and monoclonal antibody processes analyzed later in this chapter represent products of this type. The manufacturing cost of interferons, erythropoietin (EPO), and other therapeutic proteins with very low annual production volume (from hundreds of grams to a few kilograms) is more than $10,000/g [40].

Table 12.5 displays the various types of operating cost, their direct or indirect nature, and ranges for their values relative to the total operating cost. Sometimes cost items are categorized as either fixed or variable. Fixed costs are those that are incurred regardless of the volume of product output. The clearest case of a fixed cost is depreciation, which is part of the equipment-dependent cost. The clearest case

TABLE 12.5 Operating Cost Items and Ranges

Cost item	Type of cost	Range of values (% of total)
Raw materials	Direct	10–80
Labor	Direct	10–50
Consumables	Direct	1–50
Lab/QC/QA	Direct	1–50
Waste disposal	Direct	1–20
Utilities	Direct	1–30
Facility overhead	Indirect	10–70
Miscellaneous	Indirect	0–20

of a variable cost would be the cost of raw materials. Most other costs have a fixed component and a variable component.

It is obvious from the wide range of values in Table 12.5 that industry averages cannot predict the operating cost of a process; a certain level of detailed calculations is required.

Raw Materials

The raw materials cost includes the cost of all fermentation media, recovery chemicals, and cleaning materials. For commodity biochemicals, such as ethanol, the cost of fermentation media is the main component. For high-value products, the solutions used for product recovery and equipment cleaning can be a major part of the raw materials cost. Table 12.6 provides a list of commonly used raw materials in the biochemical industries. Note that the price of a raw material can vary widely depending on its required purity. This can be clearly seen in the case of water. Water for injection (WFI), for instance, costs 100 to 500 times as much as city water. Prices for a wide range of chemicals are available online at www.icis.com.

Labor

Labor is estimated based on the total number of operators, which in turn is calculated by summing up the operator requirements of the various operations as a function of time. As will become clear in the examples in Section 12.6, the labor requirement in a batch manufacturing facility varies with time. In a single-product facility, the number of operators in each shift must be based on maximum demand during that shift. In multiproduct facilities, each product line can employ a certain number of dedicated operators and rely on floating operators during periods of peak demand. In general, smaller facilities tend to utilize a larger number of operators per processing step because these plants are less automated. For instance, a small biotech company may utilize two or three operators to set up a fermentor, whereas in a large, highly automated fermentation facility a single operator may handle the setup of six different fermentors remotely from the control room. In general, a typical biotech company that deals with high-value products will allocate at least one operator to each processing step (centrifugation, membrane filtration, chromatography, etc.) during its operation. The setup of a step may require multiple operators for a short period. The annual cost of an operator (including salary and benefits) varies widely around the globe. It is in the range of $4,000 to $10,000 in developing nations and can exceed $50,000 in developed countries [41].

Consumables

Consumables are items that may be used up, fouled, or otherwise damaged during processing, such as membranes, chromatography resins, activated carbon, etc. These items must be periodically replaced. As the examples later in this chapter will illustrate, the high unit cost of chromatography resins and their frequent replacement can make them a major component of the manufacturing cost. The unit cost of typical ion exchange and hydrophobic interaction chromatography resins used for

TABLE 12.6 Common Bioprocessing Raw Materials (Year 2012 Prices)

Raw material	Comments	Price ($/kg)
C Source		
Glucose	Solution 70% w/v	0.30–0.40
Corn syrup	95% Dextrose equivalent	0.40–0.50
Molasses	50% Fermentable sugars	0.12–0.20
Soybean oil	Refined	1.10–1.30
Corn oil	Refined	1.30–1.40
Ethanol	USP tax free	0.80–0.90
Methanol	Gulf Coast	0.40–0.45
n-Alkanes		0.75–0.90
N Source		
Ammonia	Anhydrous, fertilizer grade	0.30–0.60
Soybean flour	44% protein	0.45–0.50
Cottonseed flour	62% protein	0.50–0.60
Casein	13.5% w/w total N	10.00–12.00
Ammonium sulfate	Technical	0.17–0.25
Ammonium nitrate	Fertilizer grade 33.5% N, bulk	0.20–0.30
Urea	46% N, agricultural grade	0.55–0.65
Yeast	Brewers, debittered	1.25–1.40
Whey	Dried, 4.5% w/w N	1.25–1.40
Salts		
KH_2PO_4	USP, granular	1.65–1.85
K_2SO_4	Granular, purified	2.80–3.00
Na_2HPO_4		1.40–1.80
$MgSO_4 \cdot 7H_2O$		0.45–0.55
$ZnSO_4 \cdot 7H_2O$	Agricultural grade, powder	0.65–0.75
Other		
Process water		0.0001–0.001
RO water		0.005–0.01
Water for injection		0.02–0.5
H_3PO_4 (85% w/w)	Food grade	3.5–4.5
NaOH		0.2–0.5
HCl (37% w/w)		0.7–0.8
H_2SO_4 (98% w/w)		0.15–0.25

the purification of proteins is in the range of $500 to $2,000 per liter of resin. The unit cost of protein-A affinity resins that are commonly used for the purification of monoclonal antibodies is in the range of $5,000 to $15,000 per liter of resin. The replacement frequency of such resins is in the range of 50 to 200 cycles of usage (the high-end resins have a longer useful life). In contrast, the unit cost of polymeric chromatography resins used for the purification of small biomolecules (e.g., amino acids)

is substantially lower (under $100 per liter of resin), and their life is longer (1000 to 2000 h of operation). Likewise, the unit cost of silica-based resins used for water demineralization is around $0.5/liter, and their life is in the range of 2000 to 6000 h of operation (the life strongly depends on the composition of the treated materials).

Regarding membrane filtration operations, the unit cost of MF/UF membranes used in the biopharmaceutical industry (in the form of hollow-fiber cartridges or cassettes) is in the range of $300 to $800/$m^2$. Such membranes typically handle 10 to 50 filtration cycles before disposal. The unit cost of related membranes used in industrial biotechnology (e.g., for production of industrial enzymes) is considerably lower (under $200/$m^2$), and the expected life is more than 2000 h of operation. The cost of membranes used for large-scale water purification is under $50/$m^2$ and their useful life is at least 6000 h of operation. In general, ceramic membranes cost more than polymeric ones, but they last longer.

The cost of disposable bags or containers, also known as single-use systems, is part of the consumables cost as well. Disposable bags have become popular in biopharmaceutical manufacturing because they eliminate the need for cleaning and sterilization in place [42]. Other advantages of single-use systems include increased processing flexibility and shorter validation, start-up and commercialization times. Table 12.7 provides information on disposable bags used for the preparation and storage of buffer solutions and fermentation media. Bags with mixing capability are required for solution preparation. Similar bags are used for inoculum preparation in rocking and stirred tank bioreactors. Bags for stirred tank bioreactors are available with working volumes of up to 2000 liters. A number of biopharmaceuticals are produced exclusively in single-use systems. It should be noted that large disposables bags (larger than 50 liters) utilize appropriate supporting skids. The SuperPro Designer databases provide cost information for such skids as well as for rocking and stirred tank bioreactor bags.

Laboratory/QC/QA

Laboratory, QC, and QA activities include off-line analysis, quality control (QC), and quality assurance (QA) costs. Chemical and biochemical analysis and physical property characterization, from raw materials to final product, are a vital part of biochemical operations. The laboratory/QC/QA cost is usually 10 to 20% of the operating labor cost. However, for certain biopharmaceuticals that require a large number

TABLE 12.7 Disposable Bags for Preparation and Storage of Solutions (Year 2012 prices)

Volume (liters)	Bags for storage ($)	Bags for mixing ($)
50	310	600
100	340	690
200	360	820
500	460	930
1000	650	1180

of very expensive assays, this cost can be as high as the operating labor. For such cases, it is important to account for the number and frequency of the various assays in detail, since changes in lot size that can reduce the frequency of analysis can have a major impact on profit margins.

Waste Treatment and Disposal

The treatment of wastewater and the disposal of solid and hazardous materials is another important operating cost. The amount and composition of the various waste streams is derived from the material balances. Multiplying the amount of each waste stream by the appropriate unit cost yields the cost of treatment and disposal. Treatment of low biological oxygen demand (BOD) wastewater (<1000 mg/liter) by a municipal wastewater treatment facility usually costs \$0.2 to \$0.5/m^3. This is not a major expense for most biotech facilities that deal with high-value products. However, disposal of contaminated solvents (typically generated by chromatography steps) and other regulated compounds can become a major expense because the unit disposal cost can be more than \$1/kg. Waste disposal may also become a problem if an unwanted by-product is generated as part of the recovery chemistry of a process (see the citric acid example, Section 12.6.1). Disposal of single-use systems via incineration costs \$100 to \$200 per metric ton of material.

Utilities

Utilities costs include the cost of heating and cooling agents as well as electricity. The amounts are calculated as part of the material and energy balances. Aerobic fermentors are major consumers of electricity, but downstream processing equipment generally does not consume much electricity. In terms of unit cost, electricity costs \$0.05 to \$0.15/kWh. The cost of heat removal using cooling water is in the range of \$0.002 to \$0.01 per 1000 kcal of heat removed. The cost of cooling using chilled water and refrigerants is in the range of \$0.05 to \$0.1 per 1000 kcal of heat removed. The cost of producing steam for use as a heating medium is around \$5 to \$15/1000 kg depending on pressure (low, medium, high), type of fuel used for its generation, and scale of production. The cost of clean steam (generated utilizing highly purified water) is around \$50 to \$100/1000 kg (depending on the scale of production and level of water purity). Clean steam is used in biopharmaceutical facilities for sterilizing equipment as part of equipment cleaning (e.g., "steam in place" or SIP operations). Note that manufacturers often classify purified water used for buffer preparation and equipment cleaning as a utility and not as a raw material, thus increasing the cost contribution of utilities. The insulin example, presented later in this chapter, describes a methodology for the systematic sizing of systems that supply purified water.

Facility Overhead

Facility overhead costs account for the depreciation of the fixed capital investment, maintenance costs for equipment, insurance, local (property) taxes, and possibly other overhead-type expenses. For preliminary cost estimates, the entire fixed capital

investment is usually depreciated linearly over a 10-year period. In the real world, the U.S. government allows corporations to depreciate equipment in 5 to 7 years and buildings in 25 to 30 years. The value of land cannot be depreciated. The annual maintenance cost can be estimated as a percentage of the equipment's purchase cost (usually 10%) or as a percentage of the overall fixed capital investment (usually 3-5%). Insurance rates depend to a considerable extent upon the maintenance of a safe plant in good repair condition. A value for insurance in the range of 0.5 to 1% of DFC is appropriate for most bioprocessing facilities. The processing of flammable, explosive, or highly toxic materials usually results in higher insurance rates. The local (property) tax is usually 2 to 5% of DFC. The factory expense represents overhead cost incurred by the operation of non-process-oriented facilities and organizations, such as accounting, payroll, fire protection, security, and cafeteria. A value of 5 to 10% of DFC is appropriate for these costs.

Miscellaneous

Included in miscellaneous costs are ongoing R&D, process validation, and other overhead-type expenses that can be ignored in preliminary cost estimates. Other general expenses of a corporation include royalties, advertising, and selling. If any part of the process or any equipment used in the process is covered by a patent not assigned to the corporation undertaking the new project, permission to use the technology covered by the patent must be negotiated, and some form of royalty or license fee is usually required. Advertising and selling covers expenses associated with the activities of the marketing and sales departments.

12.5.3 Profitability Analysis

Estimates of capital investment, operating cost, and revenues of a project provide the information needed to assess its profitability and attractiveness from an investment point of view. There are various measures for assessing profitability. The simplest ones include gross margin, return on investment (ROI), and payback time, and they are calculated by using the following equations:

$$\text{Gross Margin} = \frac{\text{Gross Profit}}{\text{Revenues}} \tag{12.5.3}$$

$$\text{Return on Investment (ROI)} = \frac{\text{Net Profit Per Year}}{\text{Total Investment}} \times 100\ \% \tag{12.5.4}$$

$$\text{Payback Time (years)} = \frac{\text{Total Investment}}{\text{Net Profit Per year}} \tag{12.5.5}$$

where gross profit is equal to annual revenues minus the annual operating cost, and net profit is equal to gross profit minus income taxes plus depreciation. All variables are averaged over the lifetime of a project.

Other measures that are more involved, such as the net present value (NPV) and internal rate of return (IRR), consider the cash flows of a project over its evaluation life and the time value of money. Detailed definitions for NPV and IRR can be found in the literature [31, 36]. The examples presented next demonstrate how these measures facilitate the decision-making process.

12.6 ILLUSTRATIVE EXAMPLES

In this section, SuperPro Designer is used to illustrate the analysis and evaluation of the production of three biological products. The first example analyzes the production of citric acid, a commodity organic acid heavily used in the beverage industry. The second deals with the bacterial production of recombinant human insulin, the first commercial product of modern biotechnology. The third example focuses on the production of monoclonal antibodies (MAbs) from mammalian cells cultured in stirred tank bioreactors. The generation of the flowsheets for the production of all three products was based on information available in the patent and technical literature combined with our engineering judgment and experience with other biological products. We use these examples to draw general conclusions on the manufacturing cost of biological products. The computer files for these examples are available as part of the evaluation version of SuperPro Designer at the website www.intelligen.com. The flowsheets and charts of the examples are available in color format in the readme files of the corresponding SuperPro Designer examples. Additional examples and pertinent publications are available at www.intelligen.com/literature.

12.6.1 Citric Acid Production

A number of organic acids are produced via fermentation. Of these, citric acid is produced in the largest amount (>1,800,000 metric tons per year). Citric acid is marketed as citric acid monohydrate or as anhydrous citric acid. The majority of citric acid (>60%) is used in the food and beverage industries to preserve and enhance flavor. In the chemical industries (which represent 25 to 30% of total utilization), the uses of citric acid include the treatment of textiles, softening of water, and manufacturing of paper. In the pharmaceutical industry (10% of total utilization), iron citrate is used as a source of iron, and citric acid is used as a preservative for stored blood, tablets, and ointments, and in cosmetic preparations [43]. Citric acid is increasingly being used in the detergent industry as a replacement for polyphosphates.

Citric acid was first recovered in 1869 in England from calcium citrate, which was obtained from lemon juice. Its production by filamentous fungi has been known since 1893. The first production via surface culture fermentation was initiated in 1923. Production using stirred tank fermentors began in the 1930's, and presently

this is the preferred method for large-scale manufacturing. The plant considered in this example produces around 18,000 metric tons of crystal citric acid per year, which represents approximately 1% of the current world demand.

Process Description

Upstream Section The entire flowsheet is shown in Figure 12.11. Molasses, the carbon source of fermentation, is diluted with water from about 50% fermentable sugars content to 20% in a blending tank (V-101). Suspended particulate material is then removed by filtration (PFF-101). Metal ions, particularly iron, are subsequently removed by an ion exchange chromatography column (C-101), and the purified raw material solution is then heat-sterilized (ST-101). Nutrients (i.e., sources of ammonium, potassium, phosphorus, magnesium, copper, and zinc) are dissolved in water (V-104) and heat-sterilized (ST-101). The fermentation cycle is 7 days, and the production is handled by seven fermentors that operate in staggered mode. Since the plant operates around the clock, one fermentation batch is initiated daily and another one is completed daily. Each fermentor has a vessel volume of 350 m^3 and generates broth of around 315 m^3. A three-step seed fermentor train (not shown in the flowsheet) supplies inoculum to each production fermentor (FR-101). A pure culture of the mold *Aspergillus niger* is used to inoculate the smallest seed fermentor. When optimum growth of mycelium is reached, the contents of the seed fermentor are transferred to the next stage fermentor, which is approximately ten times larger. Similarly, this larger seed fermentor inoculates the production fermentor with about 10% volume of actively growing mycelium broth. Air is supplied by a compressor (G-101) at a rate that gradually increases from 0.15 VVM (volume of air per volume of liquid per minute) to 1.0 VVM. Cooling water removes the heat produced by the exothermic process (2990 kcal per kg of citric acid formed) and maintains the temperature at 28°C. The fermented broth is discharged into the holding tank (V-105), which acts as a buffer tank between the batch upstream section and the continuous downstream section.

Downstream Section Purification starts with the removal of biomass by a rotary vacuum filter (RVF-101). The clarified fermentation liquor flows to an agitated reactor vessel (V-106) where approximately 1 part of hydrated lime, $Ca(OH)_2$, for every 2 parts of liquor is slowly added in order to precipitate calcium citrate. The lime solution must be very low in magnesium content in order to minimize losses due to generation of relatively soluble magnesium citrate. Calcium citrate is separated by a second rotary vacuum filter (RVF-102), and the citrate-free filtrate (Aq-Waste-1) is sent to a wastewater collection tank. The calcium citrate cake is sent to another agitated reactor vessel (V-107), where it is acidified with dilute sulfuric acid to form a precipitate of calcium sulfate (gypsum). A third filter (RVF-103) removes the precipitated gypsum and yields an impure citric acid solution in the filtrate. Careful control of the pH and temperature of each precipitation step is important for maximizing the yield of citric acid. The resulting solution is concentrated and crystallized using a continuous evaporator/crystallizer (CR-101). The crystals formed are separated

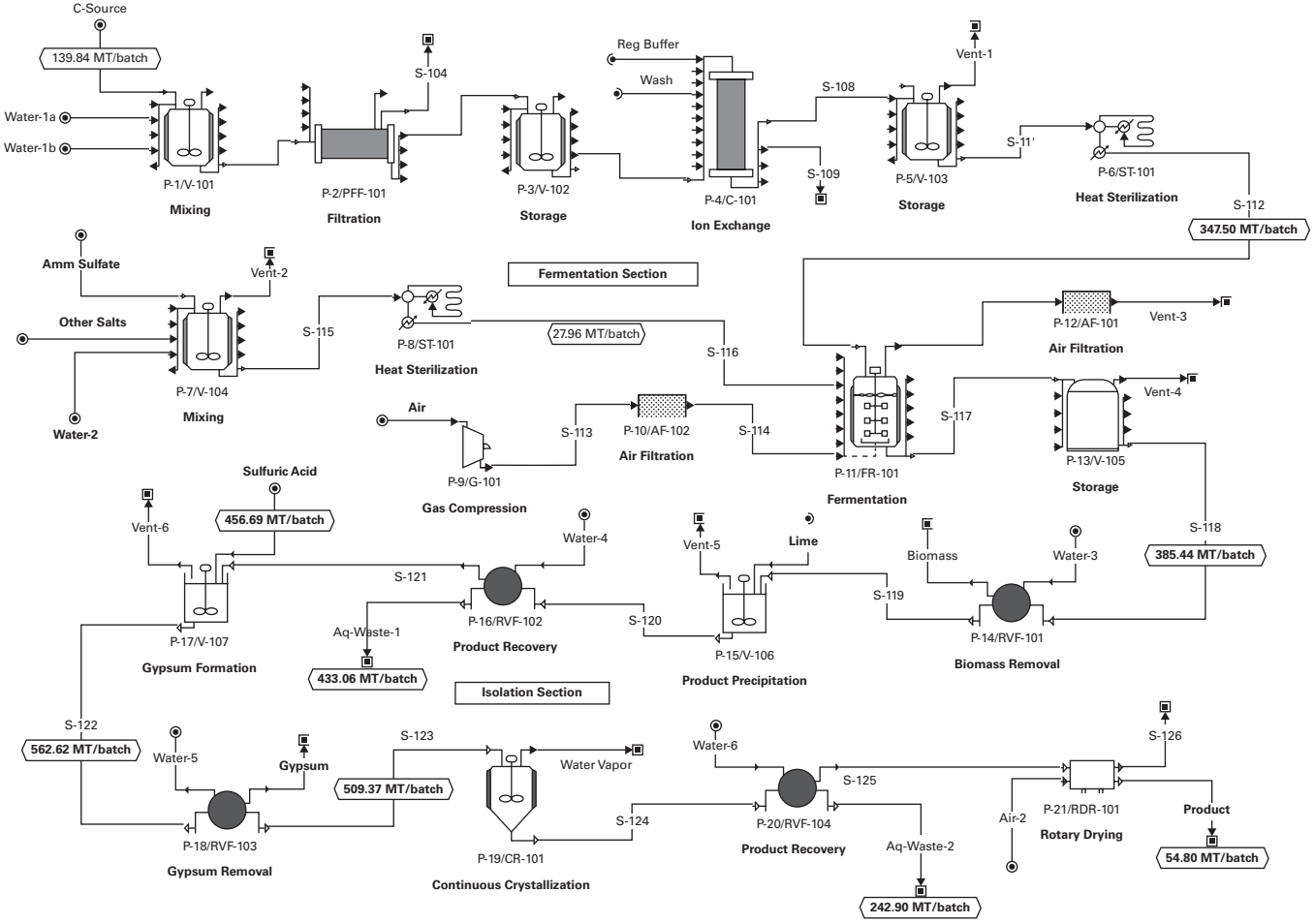

FIGURE 12.11 Citric acid production flowsheet (MT = metric ton).

by rotary vacuum filtration (RVF-104) and dried in a rotary dryer (RDR-101). If the final product is required in high purity, treatment with activated carbon may precede crystallization to remove colorants. In addition, ion exchange is sometimes used to remove metal ions and other ionic species.

Process Scheduling

Figure 12.12 displays the equipment occupancy chart for 14 consecutive batches. The process batch time is approximately 200 h (or 8.3 days). This is the time elapsed from the preparation of raw materials to the final product of a single batch (excluding the time required for inoculum preparation). The duration of each fermentation batch is 160 h (6.7 days). The availability of seven production fermentors operating in staggered mode (out of phase) enable the plant to initiate a new batch every 24 h. The upstream portion of the process (i.e., raw material preparation and fermentation) operates in batch mode. The downstream section (product recovery and purification) operates continuously. The continuous units of the purification train are displayed in Figure 12.12 with aligned blocks that operate back-to-back (lower portion of the chart).

Material Balances

Table 12.8 provides a summary of the overall material balances (expressed as input-output component balance). "CA crystal" stands for crystalline citric acid and represents the final product. Glucose represents the fermentable carbohydrates in

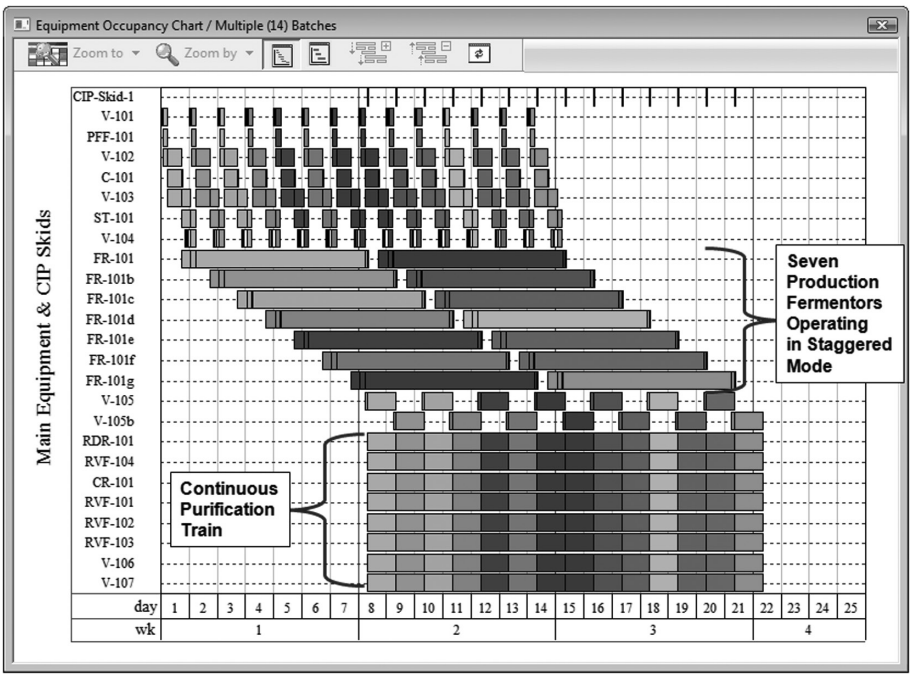

FIGURE 12.12 Equipment occupancy chart for 14 consecutive batches of the citric acid process.

TABLE 12.8 Overall Material Balances for Citric Acid (CA) Production (kg/year)

Component	In	Out	(Out – in)
Ammonium sulfate	278,000	26,000	–252,000
Biomass	0	2,014,000	2,014,000
CA crystal	0	18,250,000	18,250,000
$Ca(OH)_2$	11,717,000	558,000	–11,159,000
Calcium citrate	0	623,000	623,000
CO_2	0	3,861,000	3,861,000
Citric acid	0	657,000	657,000
Glucose	22,934,000	275,000	–22,659,000
Gypsum	0	19,972,000	19,972,000
Impurities	459,000	459,000	0
Nutrients	1,894,000	383,000	–1,511,000
Oxygen	65,171,000	57,994,000	–7,177,000
NaOH	185,000	185,000	0
Sulfuric acid	14,979,000	576,000	–14,403,000
Water	308,879,000	320,663,000	11,784,000
Total	426,496,000	426,496,000	0

molasses (50% w/w). Note the large amounts of $Ca(OH)_2$ and sulfuric acid consumed, and gypsum (calcium sulfate) generated. The quantities of these compounds depend on the chemistry of the purification process and cannot be reduced without changing the recovery technology. Since this gypsum is contaminated with biomass, it has little or no commercial value. A disposal cost of $50/MT (metric ton) was assumed in this example. The large amount of wastewater is also worth noting.

Economic Evaluation

Table 12.9 provides a list of major equipment items along with their purchase costs (generated by SuperPro Designer). The total equipment cost for a plant of this capacity is around $10.4 million. Note that approximately 30% of the equipment cost is associated with the seven production fermentors. The fermentors are made of stainless steel to minimize leaching of heavy metals that affect product formation. The final item, "unlisted equipment," accounts for the cost of the seed fermentors, pumps and other secondary equipment that is not considered explicitly. Table 12.10 displays the various items of the direct fixed capital (DFC) investment. The total DFC for a plant of this capacity is around $43.6 million or approximately 4.2 times the total equipment cost.

Table 12.11 provides a summary of the operating costs. The raw materials cost is the most important, accounting for 40.9% of the overall operating cost. This is quite common for commodity biochemicals. Molasses is the most expensive raw material, accounting for 67% of the raw materials cost. The purification chemicals,

TABLE 12.9 Equipment Specification and Purchase Costs for Citric Acid Production (Year 2012 Prices)

Quantity	Name	Description	Unit cost ($)	Cost ($)
1	AF-101	Air Filter	100,000	100,000
		Rated Throughput = 7.7 m^3/s		
1	AF-102	Air Filter	37,000	37,000
		Rated Throughput = 3.0 m^3/s		
1	C-101	Chromatography Column	150,000	150,000
		Column Volume = 4.66 m^3		
1	CR-101	Crystallizer	542,000	542,000
		Vessel Volume = 130 m^3		
7	FR-101	Fermentor	436,000	3,052,000
		Vessel Volume = 350 m^3		
1	G-101	Centrifugal Compressor	1,560,000	1,560,000
		Compressor Power = 1430 kW		
1	PFF-101	Plate & Frame Filter	145,000	145,000
		Filter Area = 335 m^2		
1	RDR-101	Rotary Dryer	475,000	475,000
		Drying Area = 85 m^2		
1	RVF-101	Rotary Vacuum Filter	154,000	154,000
		Filter Area = 46 m^2		
1	RVF-102	Rotary Vacuum Filter	214,000	214,000
		Filter Area = 83 m^2		
1	RVF-103	Rotary Vacuum Filter	195,000	195,000
		Filter Area = 71 m^2		
1	RVF-104	Rotary Vacuum Filter	137,000	137,000
		Filter Area = 35 m^2		
1	ST-101	Sterilizer	308,000	308,000
		Rated Throughput = 34 m^3/h		
1	V-101	Blending Tank	503,000	503,000
		Vessel Volume = 300 m^3		
1	V-102	Blending Tank	503,000	503,000
		Vessel Volume = 300 m^3		
1	V-103	Blending Tank	503,000	503,000
		Vessel Volume = 300 m^3		
1	V-104	Blending Tank	139,000	139,000
		Vessel Volume = 35 m^3		
2	V-105	Flat Bottom Tank	198,000	396,000
		Vessel Volume = 350 m^3		
1	V-106	Neutralizer	126,000	126,000
		Vessel Volume = 42 m^3		
1	V-107	Neutralizer	94,000	94,000
		Vessel Volume = 15 m^3		
		Unlisted Equipment		1,037,000
		Total		**10,370,000**

TABLE 12.10 Fixed Capital Estimate Summary for Citric Acid Production (Year 2012 Prices in $)

Total plant direct cost (TPDC)		
Equipment purchase cost	10,370,000	
Installation	3,726,000	
Process piping	3,111,000	
Instrumentation	2,074,000	
Insulation	311,000	
Electricals	1,037,000	
Buildings	2,074,000	
Yard improvement	1,556,000	
Auxiliary facilities	1,037,000	
TPDC		25,295,000
Total plant indirect cost (TPIC)		
Engineering	5,059,000	
Construction	7,589,000	
TPIC		12,648,000
Total plant cost (TPC = TPDC + TPIC)		37,943,000
Contractor's fee	1,897,000	
Contingency	3,794,000	
Direct fixed capital (DFC)		43,634,000
TPC + contractor's fee and contingency		

TABLE 12.11 Operating Cost Summary for Citric Acid Production (Year 2012 Prices)

Cost item	**($/kg citric acid crystals)**	**Annual cost ($/year)**	**Proportion of total (%)**
Raw materials	0.57	10,310,000	40.92
Facility-Dependent	0.40	7,223,000	28.67
Labor	0.12	2,102,000	8.34
Consumables	0.00	15,000	0.06
Lab/QC/QA	0.01	210,000	0.83
Waste treatment and disposal	0.09	1,611,000	6.39
Utilities	0.21	3,724,000	14.78
Total	1.40	22,195,000	100.00

sulfuric acid and calcium hydroxide, account for 18.7% and 9.3% of the overall raw materials cost, respectively. The following prices were assumed: \$0.15/kg of molasses, \$0.013/kg of 10% w/w H_2SO_4 solution, \$0.08/kg of $Ca(OH)_2$, and \$0.1/m^3 of process water. The facility-dependent cost is the second most important, accounting for 28.7% of the overall cost. Depreciation of the fixed capital investment and maintenance of the facility are the main contributors to this cost. Utilities are the third largest expense, accounting for 14.8% of the overall cost. Electricity and cooling water utilized by the fermentors are the main contributors to this cost. Labor lies in the fourth position, and the environmental cost (waste treatment/disposal) is fifth. Disposal unit costs of \$1/m^3 and \$50/MT (metric ton) were assumed for liquid and solid (gypsum) waste streams, respectively. The disposal of gypsum accounts for 85% of the overall environmental cost. The overall unit production cost is approximately \$1.4/kg, which is roughly equal to the current (early 2012) selling price of citric acid [44]. This can be explained by noting the excess citric acid production capacity around the world (which keeps profit margins low), and the fact that most operating citric acid plants are rather old and partially depreciated. If depreciation is ignored, the facility-dependent cost is reduced by more than 80%, and the overall unit cost drops to around \$1/kg.

Based on the preliminary evaluation of this project idea, one should not recommend investing in new citric acid production capacity unless there is a combination of favorable conditions. Obviously, availability of inexpensive equipment (e.g., by acquiring an existing facility) and raw materials (e.g., by locating the plant near a source of low-cost molasses) are the most important factors. Development or adoption of a superior technology may also change the attractiveness of citric acid production. Such a technology is actually available; it utilizes extraction for citric acid recovery [45]. Recovery by extraction eliminates the consumption of $Ca(OH)_2$ and H_2SO_4 and the generation of the unwanted $CaSO_4$. Butanol has been used as an extractant, as has tributyl phosphate. Ion pair extraction by means of secondary or tertiary amines dissolved in a water-immiscible solvent (e.g., octyl alcohol) provides an alternative route. Developments in electrodialysis membranes could lead to recovering citric acid directly from the fermentation broth by this technique [46].

12.6.2 Human Insulin Production

Introduction

Insulin facilitates the metabolism of carbohydrates and is essential for the supply of energy to the cells of the body. Impaired insulin production leads to the disease diabetes mellitus, which is a significant cause of death and health problems in industrialized and developing countries [47, 48].

Human insulin is a polypeptide consisting of 51 amino acids arranged in two chains: chain A with 21 amino acids, and chain B consisting of 30 amino acids. The A and B chains are connected by two disulfide bonds. Human insulin has a

molecular weight of 5808 and an isoelectric point of 5.4. Human insulin can be produced by four different methods:

- Extraction from human pancreas
- Chemical synthesis via individual amino acids
- Conversion of pork insulin, or "semisynthesis"
- Fermentation of genetically engineered microorganisms

Extraction from the human pancreas cannot be practiced because the availability of raw material is so limited. Total synthesis, while technically feasible, is not economically viable because the yield is very low. Production based on pork insulin, also known as "semisynthesis," transforms the porcine insulin molecule into an exact replica of the human insulin molecule by substituting a single amino acid, threonine, for alanine in the G-30 position. This technology has been developed and implemented by Novo Nordisk A/S (Denmark). However, this option is also quite expensive because it requires the collection and processing of large amounts of porcine pancreases. In addition, the supply is limited by the availability of porcine pancreas.

At least three alternative technologies have been developed for producing human insulin based on fermentation and utilizing recombinant DNA technology [49].

Two-Chain Method

The first successful technique of biosynthetic human insulin (BHI) production based on recombinant DNA technology was the two-chain method. This technique was developed by Genentech, Inc. (South San Francisco) and scaled up by Eli Lilly and Company (Indianapolis). Each insulin chain is produced as a β-galactosidase fusion protein in *Escherichia coli,* forming inclusion bodies. The two peptide chains are recovered from the inclusion bodies (IBs), purified, and combined to yield human insulin. Later, the β-galactosidase operon was replaced with the tryptophan (Trp) operon, resulting in a substantial yield increase.

Proinsulin Method

The so-called intracellular method of making proinsulin eliminates the need for the separate fermentation and purification trains required by the two-chain method. Intact proinsulin is produced instead. The proinsulin route has been commercialized by Eli Lilly [50]. Figure 12.13 shows the key transformation steps. The *E. coli* cells overproduce Trp-LE′-Met-proinsulin (Trp-LE′-Met is a 121 amino acid peptide signal sequence; proinsulin, with 82 amino acids, is a precursor to insulin) in the form of inclusion bodies, which are recovered and solubilized. Proinsulin is released by cleaving the methionine linker using cyanogen bromide (CNBr). The proinsulin chain is subjected to a folding process to allow intermolecular disulfide bonds to form; and the C peptide, which connects the A and B chains in proinsulin, is then cleaved with enzymes to yield human

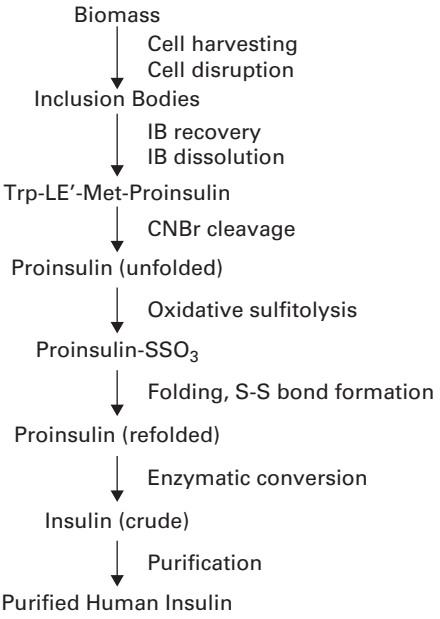

FIGURE 12.13 Human insulin from proinsulin fusion protein.

insulin. A number of chromatography and membrane filtration steps are required to purify the product.

A second (extracellular) method of producing proinsulin was developed by Novo Nordisk A/S. It is based on yeast cells that secrete insulin as a single-chain insulin precursor [47]. Secretion simplifies product isolation and purification. The precursor contains the correct disulfide bridges and is therefore identical to those of insulin. It is converted to human insulin by transpeptidation in organic solvent in the presence of a threonine ester and trypsin followed by de-esterification. Another advantage of the secreted proinsulin technology is that by employing a continuous bioreactor–cell separator loop, it is possible to reuse the cells.

In this example, we analyze a process based on the intracellular proinsulin method. The economics of this process were studied previously by Datar and Rosen [51] and by Petrides et al. [52].

Market Analysis and Design Basis

The annual world demand for insulin and insulin analogs was over 50,000 kg in 2010 and was growing at an annual rate of around 20% [53]. The plant analyzed in this example has a capacity of around 1800 kg of purified biosynthetic human insulin (BHI) per year. This is a relatively large plant for producing polypeptide-based biopharmaceuticals. The plant operates around the clock, 330 days a year. A new batch is initiated every 48 h, resulting in 160 batches per year. The fermentation broth volume per batch is approximately 37.5 m^3.

Process Description

The entire flowsheet for the production of BHI is shown in Figure 12.14. It is divided into four sections: Fermentation, Primary Recovery, Reactions, and Final Purification. *Note:* A "section" in SuperPro is simply a set of unit procedures (processing steps). If you open the file "insulin.spf" in SuperPro, you will see that all of the unit procedures within a given section have their own distinctive color (blue, green, purple, and black for Fermentation, Primary Recovery, Reactions, and Final Purification, respectively).

Fermentation Section

Fermentation media is prepared in a stainless steel tank (BT-101) and sterilized in a continuous heat sterilizer (ST-101). The axial compressor (G-101) and the absolute filter (AF-101) provide sterile air and ammonia to the fermentor at an average rate of 0.5 VVM. A two-step seed fermentor train (not shown in the flowsheet) is used to inoculate the 50 m^3 production fermentor (FR-101) with transformed *E. coli* cells. These cells are used to produce the Trp-LE′-Met-proinsulin precursor of insulin, which is retained in the cellular biomass. The fermentation time in the production fermentor is about 18 h, and the fermentation temperature is 37°C. The final concentration of *E. coli* in the production fermentor is about 30 g/liter (dry cell weight). The Trp operon is turned on when the *E. coli* fermentation runs out of tryptophan. The chimeric protein Trp-LE′-Met-proinsulin accumulates intracellularly as insoluble aggregates (inclusion bodies), and this decreases the rate at which the protein is degraded by proteolytic enzymes. In the base case, it was assumed that the inclusion bodies (IBs) constitute 20% of total dry cell mass. At the end of fermentation, the broth is cooled down to 10°C to minimize cell lysis. After completing each processing step in the fermentation section (and subsequent sections), the equipment is washed to prepare for the next batch of product.

Primary Recovery Section

After the end of fermentation, the broth is transferred into a surge tank (VT-101), which isolates the upstream section from the downstream section of the plant. Three disk-stack centrifuges (DS-101) operating in parallel are used for cell harvesting. Note that a single unit procedure icon in the SuperPro model may represent multiple equipment items operating in parallel (to see the number of equipment items a particular icon represents, right-click on the icon, go to Equipment Data, and look at the "Number of Units" field on the Equipment tab). During centrifugation, the broth is concentrated from 37,000 liters to 9,157 liters, and most of the extracellular impurities are removed. The cell recovery yield is 98%. The cell sludge is diluted with an equal volume of buffer solution (buffer composition: 96.4% w/w water for injection (WFI), 0.7% EDTA, and 2.9% Tris-base) in a blending tank (BT-102). The buffer facilitates the separation of the cell debris particles from inclusion bodies. Next, a high-pressure homogenizer (HG-101) is used to break the cells and release the inclusion bodies. The exit temperature is maintained at around 10°C. The same

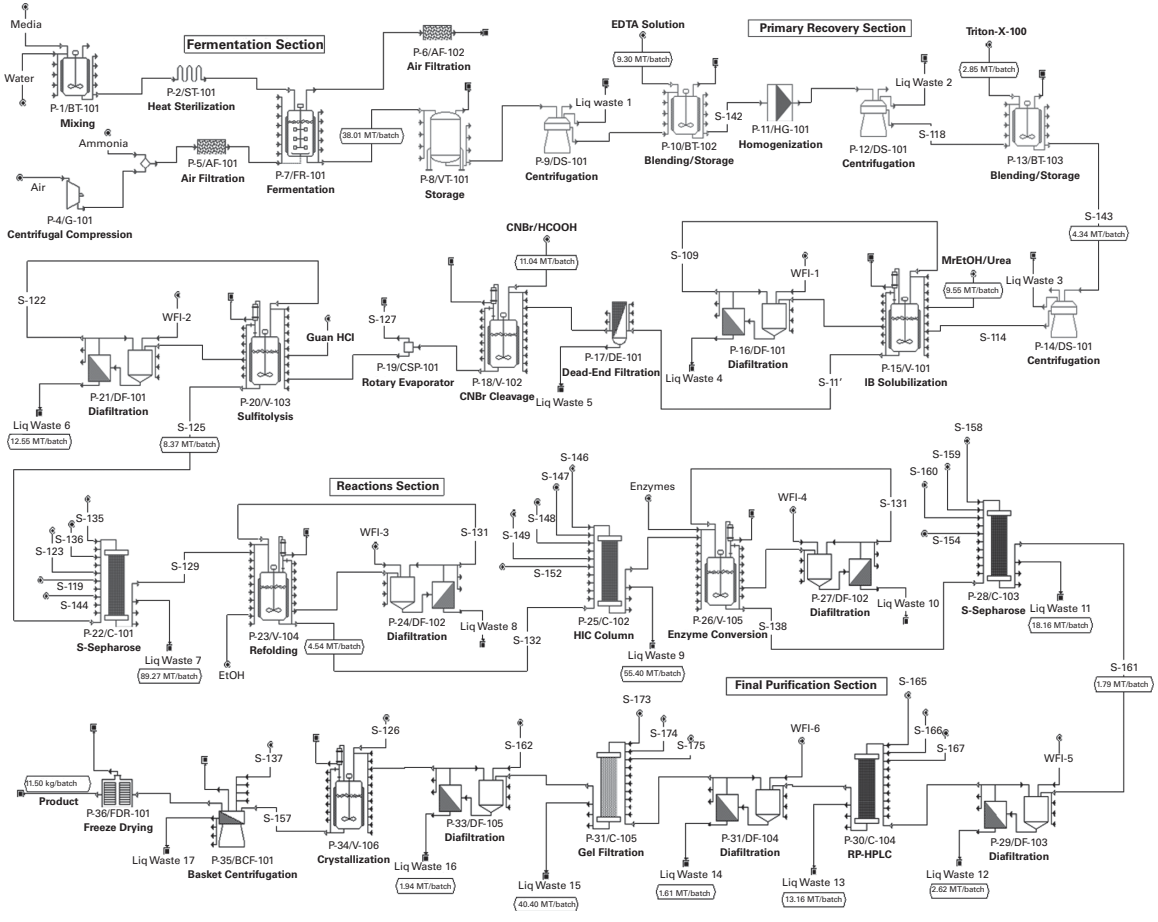

FIGURE 12.14 Insulin production flowsheet (MT = metric ton).

centrifuges as before (DS-101) are then used for inclusion body recovery (P-12). The reuse of these centrifuges can be seen by noting that procedures P-9 and P-12 have the same equipment name, DS-101. The IBs are recovered in the heavy phase (with a yield of 98%) while most of the cell debris particles remain in the light phase. This is possible because the density (1.3 g/cm^3) and size (diameter about 1 μm) of the IBs are significantly greater than that of the cell debris particles. The IB sludge, which contains approximately 20% solids w/w, is washed with WFI containing 0.66% w/w Triton-X100 detergent (the volume of solution is twice the volume of inclusion body sludge) and re-centrifuged (P-14) using the same centrifuges as before (DS-101). The detergent solution facilitates purification (dissociation of debris and soluble proteins from inclusion bodies). The exit temperature is maintained at 10°C. The slurry volume at the end of the primary recovery section is around 1440 liters.

Reactions Section

Inclusion Body Solubilization. The inclusion body suspension is transferred to a glass-lined reaction tank (V-101) and is mixed with urea and 2-mercaptoethanol to final concentrations of 300 g/liter (5 M) and 40 g/liter, respectively. Urea is a chaotropic agent that dissolves the denatured protein in the inclusion bodies, and 2-mercaptoethanol is a reductant that reduces disulfide bonds. A reaction time of 8 h is required to reach a solubilization yield of 95%. The inclusion bodies are composed of 80% w/w Trp-LE′-Met-proinsulin, with the remainder being other (contaminant) proteins. At the end of the solubilization reaction, a diafiltration unit (DF-101) is used to replace urea and 2-mercaptoethanol with WFI and to concentrate the solution. This operation is performed in 6 h with a recovery yield of 98%. All remaining fine particles (biomass, debris, and inclusion bodies) are removed by means of a polishing dead-end filter (DE-101). This polishing filter protects the chromatographic units that are used further downstream. The solution volume at this point is around 2200 liters.

CNBr Cleavage. The chimeric protein is cleaved with CNBr (cyanogen bromide) into the signal sequence Trp-LE′-Met, which contains 121 amino acids, and the denatured proinsulin (82 amino acids) in a glass-lined reactor (V-102). The reaction is carried out in a 70% formic acid solution containing 30-fold molar excess CNBr (stoichiometrically, one mole of CNBr is required per mole of Trp-LE′-Met-proinsulin). The reaction takes 12 h at 20°C and reaches a yield of 95%. The mass of the released proinsulin is approximately 30% of the mass of Trp-LE′-Met-proinsulin. A small amount of cyanide gas is formed as a by-product of the cleavage reaction. Detailed information on CNBr cleavage is available in the patent literature [54]. The formic acid, unreacted CNBr, and generated cyanide gas are removed by applying vacuum and raising the temperature to around 35°C (the boiling point of CNBr). This operation is carried out in a rotary vacuum evaporator (CSP-101) and takes 1 h. Since cyanide gas is toxic, all air exhausted from the vessels is scrubbed with a solution of hypochlorite, which is prepared and maintained in situ [55].

Sulfitolysis. Sulfitolysis of the denatured proinsulin takes place in a glass-lined reactor (V-103) under alkaline conditions (pH 9–11). This operation is designed to unfold proinsulin, break any disulfide bonds, and add SO_3 moieties to all sulfur residues on the cysteines. The product of interest is human proinsulin$(S—SO_3—)_6$ (protein–S–sulfonate). The sulfitolysis step is necessary for two reasons: (1) the proinsulin probably is not folded in the correct configuration when expressed in *E. coli* as part of a fusion protein, and (2) the cyanogen bromide treatment tends to break existing disulfide bonds. The final sulfitolysis mixture contains 50% w/w guanidine HCl (6 M), 0.35% ammonium bicarbonate (NH_4HCO_3), 3% Na_2SO_3, and 1.5% $Na_2S_4O_6$. A reaction time of 12 h is required to reach a yield of 95%. The presence of the denaturing reagent (guanidine HCl) prevents refolding and cross-folding of the same protein molecule onto itself or two separate protein molecules onto each other. Urea may also be used as a denaturing reagent. Upon completion of the sulfitolysis reaction, the sulfitolysis solution is exchanged with WFI to a final guanidine HCl concentration of 20% w/w. This procedure, P-21, utilizes the DF-101 diafilter that also handles buffer exchange after IB solubilization. The human proinsulin$(S—SO_3—)_6$ is then chromatographically purified by means of three ion exchange columns (C-101) operating in parallel and each running four cycles per batch. Each column has a diameter of 140 cm and a bed height of 25 cm. A cation exchange resin is used (SP Sepharose Fast Flow from GE Healthcare Biosciences) operating at pH 4.0. The eluant solution contains: 69.5% w/w WFI, 29% urea, and 1.5% NaCl. Urea, a denaturing agent, is used to prevent incorrect refolding and cross-folding of proinsulin$(S—SO_3—)_6$. The following operating assumptions were made: (1) the column is equilibrated for 30 min prior to loading, (2) the total resin binding capacity is 20 mg/ml, (3) the eluant volume is equal to 5 column volumes (CVs), (4) the total volume of the solutions for column wash, regeneration, and storage is 15 CVs, and (5) the protein of interest is recovered in 1.5 CVs of eluant buffer with a recovery yield of 90%.

Refolding. This operation catalyzes the removal of the SO_3 moiety and then allows disulfide bond formation and correct refolding of the proinsulin to its native form [55]. It takes place in a reaction tank (V-104). This process step involves treatment with mercaptoethanol (MrEtOH), a reductant that facilitates the disulfide interchange reaction. It is added at a ratio of 1.5 mol of mercaptoethanol to 1 mol of SO_3. Dilution to a proinsulin$(S\text{-}SO_3\text{-})_6$ concentration of less than 1 g/liter is required to prevent cross-folding of proinsulin molecules. The reaction is carried out at 8°C for 12 h and reaches a yield of 85%. After completion of the refolding step, the refolding reagents are replaced with WFI, and the protein solution is concentrated using a diafiltration unit (DF-102), which has a product recovery yield of 95% (5% of the protein denatures). The volume of the solution at this point is around 4500 liters. Next, the human proinsulin is chromatographically purified in a hydrophobic interaction chromatography (HIC) column (C-102). The following operating assumptions were made: (1) the column is equilibrated for 30 min prior to loading, (2) the total resin binding capacity is 20 mg/ml, (3) the eluant volume is equal to 6 CVs,

(4) the total volume of the solutions for column wash, regeneration, and storage is 15 CVs, (5) the protein of interest is recovered in 1 CV of eluant buffer with a recovery yield of 90%, and (6) the material of a batch is handled in three cycles.

Enzymatic Conversion. The removal of the C-peptide from human proinsulin is carried out enzymatically (using trypsin and carboxypeptidase B) in a reaction vessel (V-105). Trypsin cleaves at the carboxy-terminus of internal lysine and arginine residues, and carboxypeptidase B removes terminal amino acids. The amount of trypsin used is rate limiting and allows intact human insulin to be formed. Carboxypeptidase is added to a final concentration of 4 mg/liter, while trypsin is added to a final concentration of 1 mg/liter. The reaction takes place at 30°C for 4 h and reaches a conversion yield of 95%. The volume of the solution at this point is around 4300 liters.

Final Purification Section

A purification sequence based on multimodal chromatography, which exploits differences in molecular charge, size, and hydrophobicity, is used to isolate biosynthetic human insulin. A description of all the purification steps follows.

The enzymatic conversion solution is exchanged with WFI and concentrated by a factor of four in a diafilter (DF-102). An ion exchange column (C-103) is used to purify the insulin solution. The following operating assumptions were made: (1) the column is equilibrated for 30 min prior to loading, (2) the total resin binding capacity is 20 mg/mL, (3) the eluant volume is equal to 8 CVs and the eluant is an 11.5% w/w solution of NaCl in WFI, (4) the total volume of the solutions for column wash, regeneration, and storage is 14 CVs, (5) the protein of interest is recovered in 1.5 CV of eluant buffer with a recovery yield of 95%, and (6) the material from each batch is handled in four cycles. The solution volume at this point is around 1780 liters.

Next, the ion exchange eluant solution is exchanged with WFI in a diafilter (DF-103) and is concentrated by a factor of 2.0. A recovery yield of 98% was assumed for this step (2% denatures).

The purification of the insulin solution proceeds with a reversed-phase high-performance liquid chromatography (RP-HPLC) step (C-104). Detailed information on the use of RP-HPLC for insulin purification is available in the literature. Analytical studies with a variety of reversed-phase systems have shown that an acidic mobile phase can provide excellent resolution of insulin from structurally similar insulin-like components. Minor modifications in the insulin molecule, resulting in monodesamido formation at the 21st amino acid of the A chain, or derivatization of amines via carbamoylation or formylation, result in insulin derivatives having significantly increased retention. Derivatives of this nature are typical of the kind of insulin-like components that are found in the charge stream going into the reversed-phase purification. The use of an acidic mobile phase results in the elution of all the derivatives after the insulin peak, while the use of mildly alkaline pH results in derivatives eluted on either side of the parent insulin peak. An ideal pH for insulin purification is in the region of 3.0 to 4.0, since this pH range is far enough below the isoelectric pH of 5.4 to provide for good insulin solubility. An eluant buffer with

an acetic acid concentration of 0.25 M meets these operational criteria because it is compatible with the chromatography and provides good insulin solubility. A 90% insulin yield was assumed in the RP-HPLC step with the following operating conditions: (1) the column is equilibrated for 30 min prior to loading, (2) the total resin binding capacity is 15 mg/ml, (3) the column height is 25 cm, (4) the eluant volume is 6 CVs and its composition is 25% w/w acetonitrile, 1.5% w/w acetic acid, and 73.5% w/w WFI, (5) the total volume of the solutions for column wash, equilibration, regeneration, and storage is 6 CVs, and (5) the protein of interest is recovered in 1 CV of eluant buffer with a recovery yield of 90%.

The RP-HPLC buffer is exchanged with WFI and concentrated by a factor of 2.0 in a diafilter (DF-104) that has a product recovery yield of 98% (2% denatures). Purification is completed by a gel filtration chromatography column (C-105). The following operating assumptions were made: (1) the column is equilibrated for 30 min prior to loading, (2) the sample volume is equal to 5% of the column volume, (3) the eluant volume is equal to 4 CVs, (4) the total volume of the solutions for column wash, depyrogenation, stripping, and storage is 6 CVs, and (5) the protein of interest is recovered in 0.5 CV of eluant buffer with a recovery yield of 90%. The mobile phase is a solution of acetic acid.

Next, a diafilter (DF-105) is used to concentrate the purified insulin solution by a factor of 10. The solution volume at this point is around 180 liters, which contains approximately 12.8 kg of insulin. This material is pumped into a jacketed and agitated tank (V-106). Ammonium acetate and zinc chloride are added to the protein solution until each reaches a final concentration of 0.02 M [51]. The pH is then adjusted to between 5.4 and 6.2. The crystallization is carried out at 5°C for 12 h. Insulin crystallizes with zinc with the following stoichiometry: $insulin_6$-Zn_2. Step recovery on insulin is around 90%.

The crystals are recovered with a basket centrifuge (BCF-101) with a yield of 95%. Finally, the crystals are freeze-dried (FDR-101). The purity of the crystallized end product is between 99.5 and 99.9% as measured by analytical high-performance liquid chromatography (HPLC). Approximately 11.5 kg of product is recovered per batch. The overall recovery yield is around 32%.

Material Balances and Environmental Impact Assessment

Table 12.12 displays the material requirements in kilograms per year, per batch, and per kilogram of main product (MP = purified insulin crystals). The solutions of H_3PO_4 (5% w/w) and NaOH (0.5 M) are used for equipment cleaning. WFI is used for preparing all the buffers utilized in product purification as well as all the cleaning solutions. Note the large amounts of formic acid, urea, guanidine hydrochloride, acetic acid, and acetonitrile required per kilogram of final product. All these materials end up in waste streams.

In the base case, this waste is treated and disposed. However, opportunities may exist for recycling some chemicals for in-process use and recovering others for off-site use. For instance, formic acid (HCOOH), acetonitrile, and urea are good

TABLE 12.12 Raw Material Requirements for Human Insulin Production: 1 Batch = 11.5 kg Main Product (MP = Purified Insulin Crystals)

	Requirement		
Raw material	**kg/year**	**kg/batch**	**kg/kg MP**
Glucose	782,200	4,889	425.1
Salts	71,400	446	38.8
Water	9,715,000	60,719	5,279.9
H_3PO_4 (5% w/w)	3,979,000	24,869	2,162.5
NaOH (0.5 M)	3,842,000	24,013	2,088.0
WFI	51,890,000	324,313	28,201.1
Ammonia	81,600	510	44.3
EDTA	10,420	65	5.7
TRIS base	43,160	270	23.5
Triton-X-100	3,035	19	1.6
MrEtOH	98,660	617	53.6
Urea	3,054,000	19,088	1,659.8
CNBr	15,270	95	8.3
Formic acid	1,752,000	10,950	952.2
Guanidine-HCl	805,600	5,035	437.8
$Na_2O_6S_4$	24,160	151	13.1
NH_4HCO_3	5,551	35	3.0
Sodium sulfite	48,320	302	26.3
Sodium chloride	775,500	4,847	421.5
Acetic acid	975,700	6,098	530.3
Sodium hydroxide	137,200	858	74.6
Enzymes	3	0	0.0
Acetonitrile	764,700	4,779	415.6
Ammonium acetate	181	1	0.1
Zinc chloride	320	2	0.2
TOTAL	78,874,980	492,943	42,866.8

candidates for recycling and recovery. Formic acid is used in large quantities (11 tons/batch) in the CNBr cleavage step (V-102), and it is removed by means of a rotary vacuum evaporator (CSP-101), along with small quantities of CNBr, H_2O, and urea. The recovered formic acid can be readily purified by distillation and recycled in the process. Around 2.2 metric tons per batch of urea is used for the dissolution of inclusion bodies (V-101), and 17 metric tons per batch is used in the first chromatography step (C-101) to purify proinsulin$(S—SO3)_6$ before its refolding. Approximately 90% of the urea appears in just two waste streams (Liq Waste 4 and 8). It is unlikely that these urea-containing streams can be purified economically for

in-process recycling. However, these solutions can be concentrated, neutralized, and shipped off site for further processing and utilization as a nitrogen fertilizer.

Approximately 4.8 metric tons (MT) per batch of acetonitrile is used in the reversed-phase HPLC column (C-104), and most of it ends up in the waste stream of the column (Liq Waste 13) along with 6.8 MT of water, 1.85 MT of acetic acid, and small amounts of NaCl and other impurities. It is unlikely that acetonitrile can be recovered economically to meet the high purity specifications for a step so close to the end of the purification train. However, there may be a market for off-site use.

Process Scheduling

Figure 12.15 displays the scheduling and equipment utilization for six consecutive batches. The batch time is approximately 11 days. This is the time required to go from the preparation of raw materials to final product for a single batch (excluding inoculum preparation). However, since most of the equipment items are utilized for much shorter periods within a batch, a new batch is initiated every 48 h. Multiple bars of the same shade on the same line (e.g., for DS-101, DF-101, and DF-102)

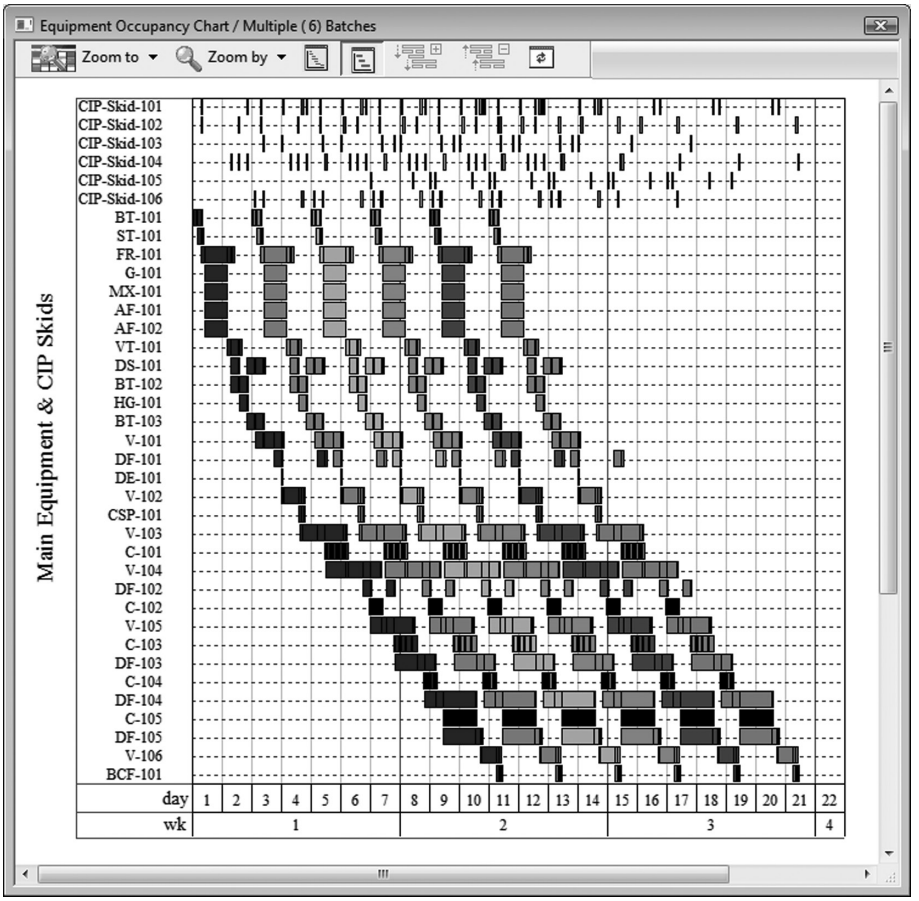

FIGURE 12.15 Equipment occupancy as a function of time for six consecutive batches.

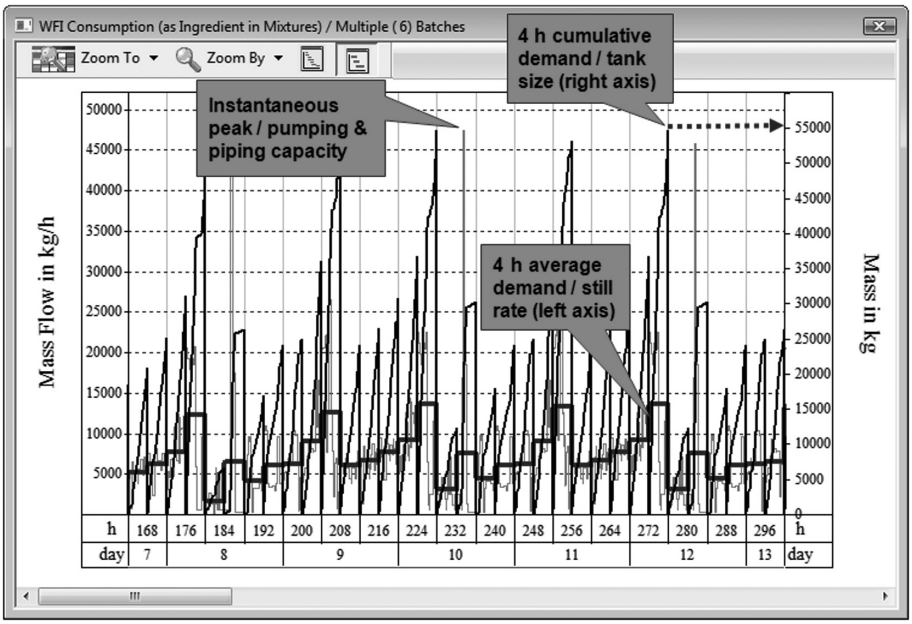

FIGURE 12.16 WFI demand as a function of time.

represent reuse (sharing) of equipment by multiple procedures. White space represents idle time. The equipment with the least idle time between consecutive batches is the *time* (*or scheduling*) *bottleneck* (V-104 in this case) that determines the maximum number of batches per year. Its occupancy time (approximately 45 h) is the minimum possible time between consecutive batches. The production line operates around the clock and processes 160 batches per year.

Process scheduling is closely related to the determination of the annual capacity of a batch process. The last part of this example discusses how changes in scheduling and installation of additional equipment can be used to increase process throughput and reduce manufacturing cost.

Resource Tracking and Utility Sizing

Another characteristic of batch processing is the variable demand for resources (e.g., labor, utilities and raw materials) as a function of time. For instance, Figure 12.16 displays the demand for WFI for six consecutive batches, showing the instantaneous demand, the averaged demand for 4-h intervals, and the cumulative demand for the same 4-h intervals (y-axis on the right hand side of the chart). These charts are useful for sizing utility systems during the design of new facilities. For instance, a WFI system consists of a still that generates distilled water, a surge tank, and a circulation loop for delivering the material around the plant. The chart of Figure 12.16 provides reasonable estimates for the size of the still, the surge tank, and the pumping capacity of the circulation loop. More specifically, the instantaneous demand peak indicates the minimum pumping capacity for the system since this capacity needs to meet the

peak demand (47,500 kg/h). The cumulative demand peak can be used to size the surge tank, which must be large enough to maintain capacity during peak cumulative demand (in this case, the highest demand during any 4-hour interval is 55,000 kg). Finally, the highest averaged demand (step-function line) indicates the size of the still (production capacity of 14,000 kg/h). The trade-off between still rate and surge capacity can be examined by changing the averaging time interval. For example, selecting an interval greater than 4 hours results in a larger surge tank and a lower still rate (e.g., a smaller still) compared to the base case. Figure 12.17 displays the inventory profile of WFI in the surge tank (dark lines) for a tank size of 55,000 kg and a still rate of 14,000 kg/h (as indicated by the findings of Figure 12.16). The still is turned on when the WFI level falls below 35% of the tank's capacity. The still remains on until the tank is full. The operation rate and frequency of the still is depicted by the light step-function lines. Tutorial videos with additional information on WFI system sizing are available at www.intelligen.com/videos.

Sizing of biowaste treatment systems can be handled in a similar manner. Such systems typically involve two tanks that alternate in operation periodically (while one is receiving, the other is treating a batch of waste material). The peak cumulative amount for the alternating period indicates the minimum capacity of each tank.

Economic Evaluation

Table 12.13 shows the results of the economic evaluation. The detailed tables for these calculations are available as part of the evaluation version of SuperPro Designer. For a plant of this capacity, the total capital investment is $178 million. The unit production cost is $61 per gram of purified insulin crystals. Assuming a selling price of $100/g, the project yields an after-tax internal rate of return (IRR) of 35% and a

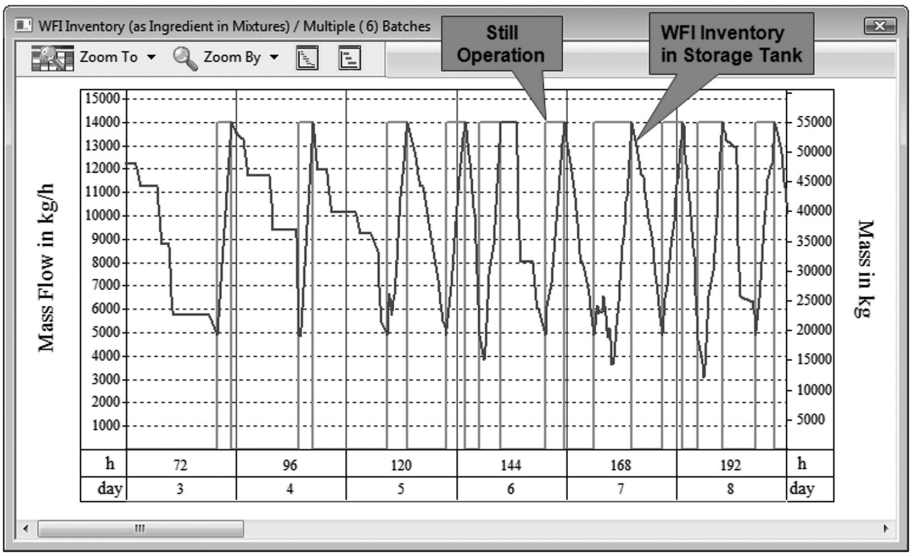

FIGURE 12.17 WFI inventory (dark lines) and operating frequency of still (light blue lines).

TABLE 12.13 Key Economic Evaluation Results for Human Insulin Production

Direct fixed capital	$145 million
Total capital investment	$178 million
Plant throughput	1,803 kg/year
Manufacturing cost	$110 million/year
Unit production cost	$61/g
Selling price	$100/g
Revenues	$180 million/year
Gross profit	$70 million/year
Taxes (40%)	$28 million/year
IRR (after taxes)	35%
NPV (for 7% discount interest rate)	$250 million

net present value (NPV) of $250 million (assuming a discount interest rate of 7%). Based on these results, this project represents a very attractive investment. However, if amortization of up-front R&D costs is considered in the economic evaluation, the numbers change drastically. For instance, a modest amount of $100 million for up-front R&D cost amortized over a period of 10 years reduces the IRR to 16.8% and the NPV to $153 million.

Figure 12.18 breaks down the operating cost. The cost of consumables is the most important, accounting for 31.9% of the overall manufacturing cost. Consumables represent the expense of periodically replacing the resins of the chromatography columns and the membranes of the membrane filters. The cost of raw materials is the second most important, accounting for 27.3% of the overall cost. The facility-dependent cost is third, accounting for 24.1% of the overall cost. This cost item accounts for the depreciation and maintenance of the facility and other overhead expenses. Labor and Lab/QC/QA account for 9.1%. The treatment and disposal of waste materials accounts for 7.3% of the total cost. As mentioned in the material balance section, recycling and reuse of some of the waste materials may reduce this cost.

Figure 12.19 displays the percentage of the operating cost associated with each flowsheet section. Only 7.3% of the overall cost is associated with fermentation. The other 92.7% is associated with the recovery and purification sections. This is common for high-value biopharmaceuticals that are produced from recombinant *E. coli*. Most of the cost is associated with the reactions section because of the large amounts of expensive chemicals and consumables required for purification.

Finally, for each raw material used in the process, Table 12.14 displays the price, annual cost, and contribution to the overall raw materials cost. WFI, urea, and H_3PO_4 (5% w/w) are the top three contributors to the raw materials cost. The H_3PO_4 and NaOH solutions are used for equipment cleaning.

Other assumptions for the economic evaluation include the following: (1) a new manufacturing facility will be built and dedicated to production of 1800 kg/year of purified insulin; (2) the entire direct fixed capital is depreciated linearly over a period of 10 years; (3) the project life-time is 15 years; (4) the unit cost of membranes is $\$800/m^2$ and they are replaced every 50 cycles; (5) the average unit cost of chromatography resins is \$1500/liter; (6) the waste disposal cost is $\$5/m^3$ for low-BOD streams and $\$150/m^3$ for streams containing significant amounts of solvents and other regulated chemicals.

Throughput Increase Options

In the base case, a new batch is initiated every 48 h. Most of the equipment items, however, are utilized for less than 24 h per batch (see Figure 12.15). If the market conditions are favorable, this provides the opportunity for increasing plant throughput without major capital expenditures. A realistic improvement is to initiate a batch every 24 h. This will require a new fermentor of the same size as the original fermentor, whose operation will be staggered relative to the existing unit so that one

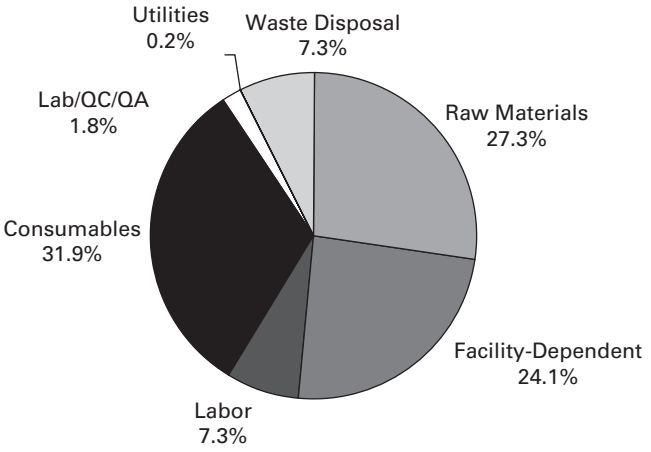

FIGURE 12.18 Breakdown of manufacturing cost for human insulin production.

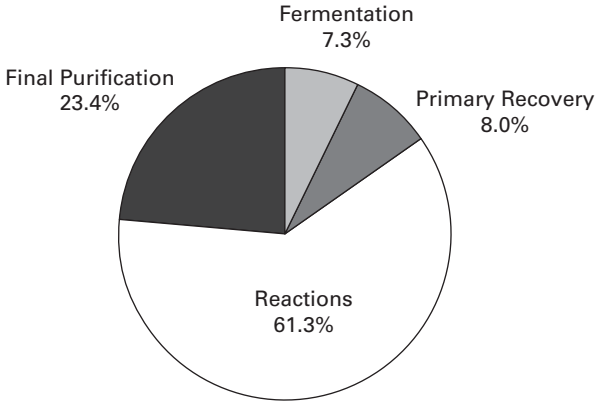

FIGURE 12.19 Cost distribution per flowsheet section for human insulin production.

TABLE 12.14 Cost of Raw Materials for Human Insulin Production (Year 2012 Prices)

Bulk material	Unit cost ($/kg)	Annual cost ($)	%
Glucose	0.60	469,300	1.56
Salts	1.00	71,400	0.24
Water	0.05	485,800	1.61
H_3PO_4 (5% w/w)	1.00	3,979,000	13.19
NaOH (0.5 M)	0.50	1,921,200	6.37
WFI	0.10	5,188,500	17.20
Ammonia	0.70	57,100	0.19
EDTA	18.50	192,700	0.64
TRIS base	6.00	259,000	0.86
Triton-X-100	1.50	4,600	0.02
MrEtOH	3.00	296,000	0.98
Urea	1.52	4,642,200	15.38
CNBr	11.00	168,000	0.56
Formic acid	1.60	2,802,400	9.29
Guanidine-HCl	2.15	1,732,000	5.74
$Na_2O_6S_4$	0.60	14,500	0.05
NH_4HCO_3	1.00	5,600	0.02
Sodium sulfite	0.40	19,300	0.06
Sodium chloride	1.23	954,000	3.16
Acetic acid	2.50	2,439,400	8.08
Sodium hydroxide	3.50	480,300	1.59
Enzymes	500,000	1,691,100	5.60
Acetonitrile	3.00	2,294,200	7.60
Ammonium acetate	15.00	2,700	0.01
Zinc chloride	12.00	3,800	0.01
TOTAL		30,174,100	100.00

fermentor is ready for harvesting every day. Such a production change will also require additional equipment of the following types: (1) disk-stack centrifuges to reduce the occupancy of DS-101 to less than 24 h, (2) two reaction vessels to reduce the occupancy of V-103 and V-104, and (3) membrane filters to reduce the occupancy of DF-104 and DF-105.

The additional capital investment for such a change is around $55 million. This additional investment will allow the plant's capacity to be doubled, and the new unit production cost will be around $55/g. The reduction in the unit production cost is rather small because the majority of the manufacturing cost is associated with consumables and raw materials that scale approximately linearly with production.

12.6.3 Therapeutic Monoclonal Antibody Production

Monoclonal antibodies are large protein molecules that consist of two main regions, the fragment, antigen binding (Fab) region and the fragment, crystallizable (Fc) region. Monoclonal antibodies (MAbs) are the fastest growing segment in the biopharmaceutical industry. MAbs are currently used to treat various types of cancer, rheumatoid arthritis, psoriasis, severe asthma, macular degeneration, multiple sclerosis, and other diseases. More than 20 MAbs and Fc fusion proteins are approved for sale in the United States and Europe and approximately 200 MAbs are in clinical trials for a wide variety of indications [56, 57]. The market size for MAbs in 2010 was in excess of $35 billion [58].

The high-dose demand for several MAbs translates into annual production requirements for purified product in the metric ton range. This example illustrates the analysis of a large-scale MAb process. Again, the modeling and calculations are performed with SuperPro Designer.

Figure 12.20 displays the flowsheet of the overall process. The generation of the flowsheet was based on information available in the patent and technical literature combined with the authors' engineering judgment and experience with such processes [59]. The process in this example produces 1544 kg of purified MAb per year. The flow diagram of Figure 12.20 is a simplified representation of the actual process because it lacks all the buffer preparation and holding activities. Such processes require 20 to 30 buffer solutions for product purification. These solutions are prepared in mixing tanks and then stored in holding tanks located close to the purification train. The tanks required for buffer preparation and holding add to the capital investment of the facility, while the required labor adds to the manufacturing cost. The model files for this example that are part of the evaluation version of SuperPro Designer (available at www.intelligen.com) include the tanks for buffer preparation and holding. In addition, the capital and operating costs associated with buffer preparation activities were considered in the cost analysis results presented in this example. Additional information on this example in the form of two tutorial videos is available at www.intelligen.com/videos.

Process Description

Upstream Section The upstream part is split into two sections: the inoculum preparation section and the bioreaction section. The inoculum is initially prepared in 225 ml T-flasks (TFR-101). Next, the material from the T-flasks is moved to 2.2 liter roller bottles (RBR-101), then to 100 liters, and subsequently to 200 liters rocking bioreactors that utilize disposable bags (BBS-101 and BBS-102). Sterilized media is fed at the appropriate amount in all of these four initial steps (3.6, 11.4, 43.6, 175.4 kg/batch respectively). The broth is then moved to the first stirred seed bioreactor (DSBR-101), which utilizes 1000 liter disposable bags. The second seed bioreactor (SBR-102) is a 5000 liter stainless steel vessel. For the two seed bioreactors, the media powder is dissolved in water-for-injection (WFI) in two prep tanks

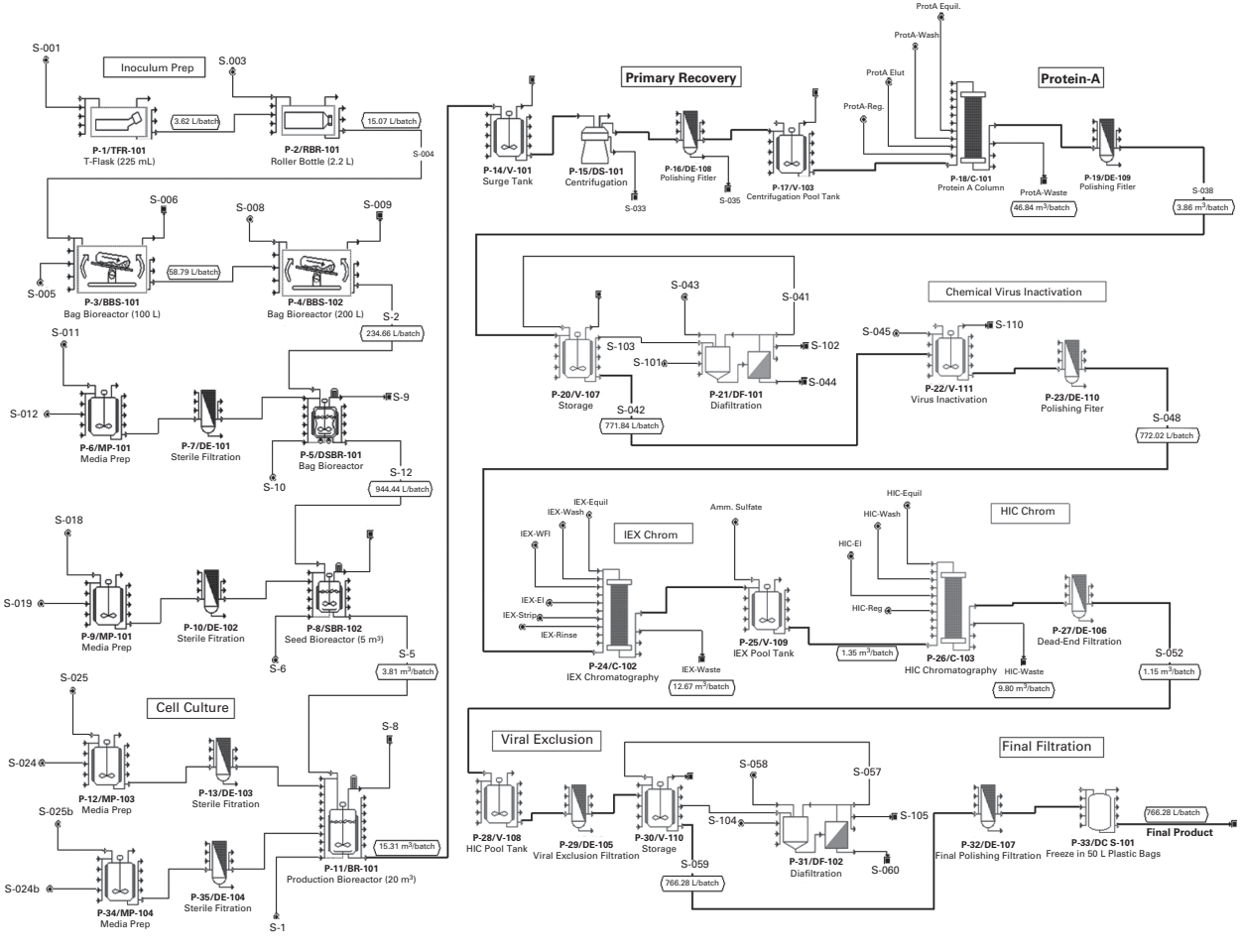

FIGURE 12.20 Monoclonal antibody production flowsheet (L = liters).

(MP-101 & MP-102) and then sterilized/fed to the reactors through 0.2 μm dead-end filters (DE-101 & DE-102). In the cell culture section, serum-free low-protein media powder is dissolved in WFI in a stainless steel tank (MP-103). The solution is sterilized using a 0.2 μm dead-end polishing filter (DE-103). A 20,000 liter stainless stirred-tank bioreactor (BR-101) is used to grow the cells, which produce the therapeutic monoclonal antibody (MAb). The production bioreactor operates in fed batch mode. High media concentrations are inhibitory to the cells, so half of the media is added at the start of the process and the rest is fed at a variable rate during fermentation. The concentration of dry media powder in the initial feed solution is 17 g/liter. The cell culture time is 12 days. The volume of broth generated per bioreactor batch is approximately 15,000 liters, which contains roughly 30.5 kg of product (the product titer is approximately 2 g/liter).

Downstream Section Between the downstream unit procedures there are 0.2 μm dead-end filters to ensure sterility. The generated biomass and other suspended compounds are removed using a disk-stack centrifuge (DS-101). During this step, roughly 5% of MAb is lost in the solids waste stream. The bulk of the contaminant proteins are removed using a Protein A affinity chromatography column (C-101) which processes a batch of material in four cycles. The following operating assumptions were made for each chromatography cycle: (1) resin binding capacity is 15 g of product per liter of resin, (2) the eluant or elution buffer is a 0.6% w/w solution of acetic acid and its volume is equal to 5 column volumes (CVs), (3) the product is recovered in 2 CVs of eluant with a recovery yield of 90%, and (4) the total volume of the solution required for column equilibration, wash and regeneration is 14 CVs. The entire procedure takes approximately 27 h and requires a resin volume of 502 liters. The protein solution is then concentrated five-fold and diafiltered with 2 volumes of buffer (in P-21/DF-101). This step takes approximately 8.4 h and requires a membrane of 21 m^2. The product yield is 97%. The concentrated protein solution is then chemically treated for 1.5 h with Polysorbate 80 to inactivate viruses (in P-22/V-111). The ion exchange (IEX) chromatography step (P-24/C-102) that follows processes one batch of material in three cycles. The following operating assumptions were made for each cycle: (1) the resin's binding capacity is 40 g of product per liter of resin, (2) a gradient elution step is used with a sodium chloride concentration ranging from 0.0 to 0.1 M and a volume of 5 CVs, (3) the product is recovered in 2 CVs of eluant buffer with a MAb yield of 90% and (4) the total volume of the solutions required for column equilibration, wash, regeneration and rinse is 16 CVs. The step takes approximately 22.3 h and requires a resin volume of 210 liters. Ammonium sulfate is then added to the IEX eluate (in P-25/V-109) to a concentration of 0.75 M. This increases the ionic strength of the eluate in preparation for the hydrophobic interaction chromatography (HIC, P-26/C-103) step that follows. Like the IEX step which preceded it, the HIC step processes one batch of material in three cycles. The following operating assumptions were made for each cycle of the HIC step: (1) the resin binding capacity is 40 g of product per liter of resin, (2) the eluant is a sodium chloride (4% w/w) sodium dihydrogen phosphate

(0.3% w/w) solution and its volume is equal to 5 CVs, (3) the product is recovered in 2 CVs of eluant buffer with a recovery yield of 90% and (4) the total volume of the solutions required for column equilibration, wash and regeneration is 12 CVs. The step takes approximately 22 h and requires a resin volume of 190 liters. A viral exclusion step (DE-105) follows. It is a dead-end type of filter with a pore size of 0.02 μm. Finally the HIC elution buffer is exchanged for the product bulk storage (PBS) buffer and concentrated 1.5-fold (in DF-102). This step takes approximately 20 h and requires a membrane area of 10 m^2. The approximately 800 liters of final protein solution is stored in twenty 50 liter disposable storage bags (DCS-101). The overall yield of the downstream operations is 63.2%, and 19.3 kg of MAb are produced per batch.

Process Scheduling and Cycle Time Reduction

Figure 12.21 displays the equipment occupancy chart of the process for four consecutive batches. The schedule represents a plant that has a single production train. The clean in place (CIP) skids, polishing filters and media preparation tanks are not displayed on the chart for the sake of simplicity. The batch time is approximately 50 days. This is the time required from the start of inoculum preparation to the final product purification of a single batch. A new batch is initiated every 2 weeks (14 days). The production bioreactor (BR-101) is the time (scheduling) bottleneck. On an annual basis, the plant processes 20 batches and produces approximately 386 kg of purified MAb. It is clear from the chart that under these conditions the downstream train is underutilized and the cycle time of the process—the time between consecutive batches—is relatively long. The cycle time of the process can

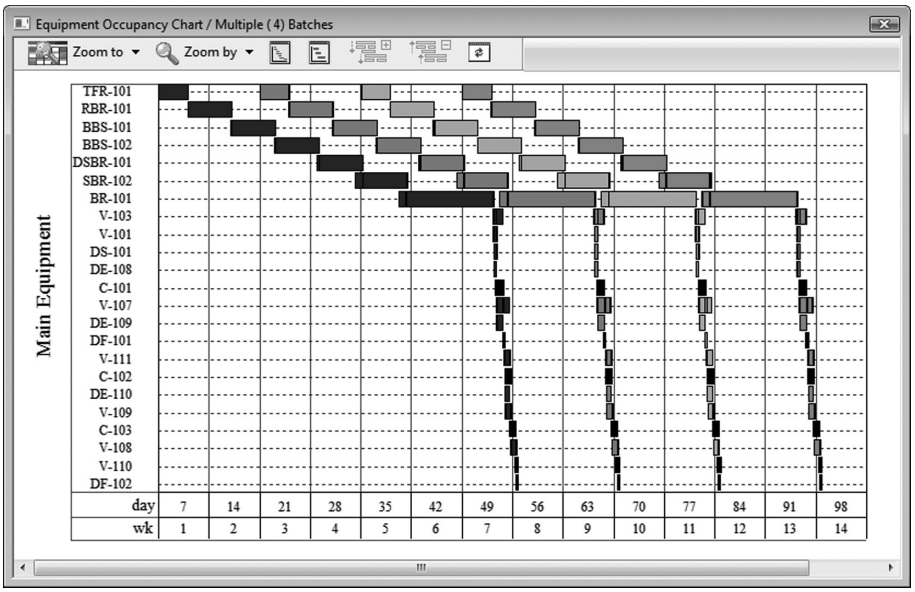

FIGURE 12.21 One bioreactor train feeding one MAb purification train.

be reduced and the plant throughput increased by installing multiple bioreactor trains that operate in staggered mode (out of phase) and feed the same purification train. Figure 12.22 represents a case where four bioreactor trains feed the same purification train. The new cycle time is 3.5 days, which is one fourth of the original. Under these conditions, the plant processes 80 batches per year and produces 1,544 kg of MAb per year. Some biopharmaceutical companies have installed more than four bioreactor trains per purification train in order to achieve cycle times as low as 2 days.

Material Requirements

Table 12.15 provides a summary of the material requirements of the process. Note the large amount of WFI utilized per batch. The majority of WFI is consumed for cleaning and buffer preparation.

Economic Evaluation

Table 12.16 displays the key economic evaluation results generated using the built-in cost functions of SuperPro Designer. The total capital investment (for the case with the four bioreactor trains) is around $477 million. The total annual operating cost is $130 million, resulting in a unit production cost of around $84/g (1,544 kg of purified MAb are produced annually). Assuming a selling price of $200/g, the project yields an after-tax internal rate of return (IRR) of 24.3% and a net present value (NPV) of $560 million (assuming a discount interest rate of 7%).

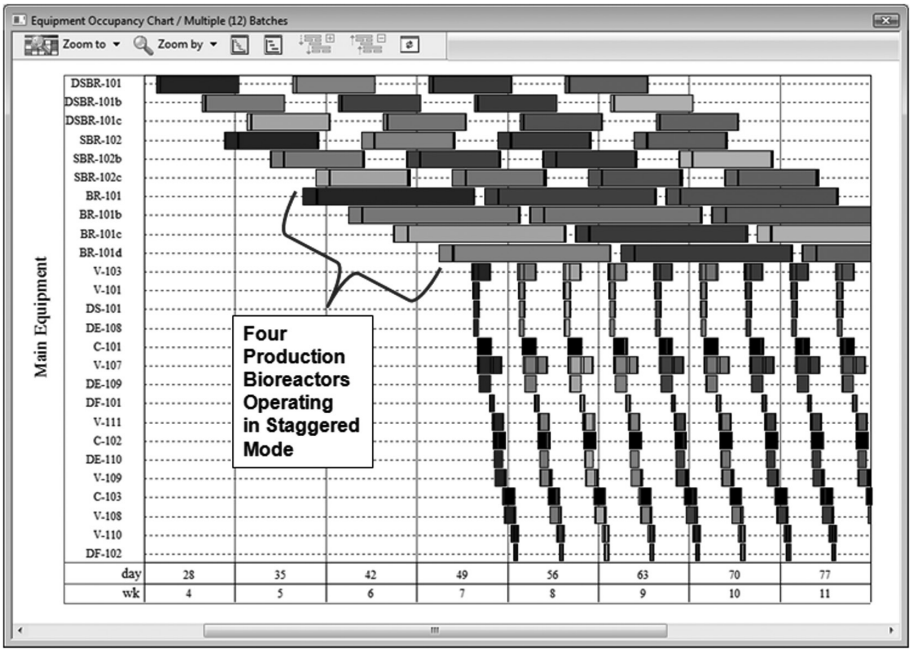

FIGURE 12.22 Four bioreactor trains feeding one MAb purification train.

TABLE 12.15 Raw Material Requirements: 1 Batch = 19.3 kg Main Product (MP = Purified MAb)

Material	kg/yr	kg/batch	kg/kg MP
Inoc. media solution	18,630	232.88	12.066
WFI	8,430,000	105,375.00	5,459.845
Serum free media	37,340	466.75	24.184
H_3PO_4 (5% w/w)	2,277,000	28,462.50	1,474.741
NaOH (0.5 M)	2,054,000	25,675.00	1,330.311
NaOH (0.1 M)	7,815,000	97,687.50	5,061.528
Amm. sulfate	12,160	152.00	7.876
Polysorbate 80	6	0.08	0.004
Protein A equil. buffer	1,967,000	24,587.50	1,273.964
Protein A elution buffer	800,200	10,002.50	518.264
Protein A reg. buffer	480,400	6,005.00	311.140
NaCl (1 M)	184,200	2,302.50	119.301
IEX elution buffer	16,130	201.63	10.447
IEX equil. buffer	664,900	8,311.25	430.635
HIC elution buffer	239,200	2,990.00	154.922
HIC equil. buffer	449,600	5,620.00	291.192
Concentrated PBS	14,370	179.63	9.307
EtOH (10% w/w)	363,000	4,537.50	235.104
TOTAL	25,823,136	322,789.20	16,724.83

TABLE 12.16 Key Economic Evaluation Results for MAb Production

Direct fixed capital	$365 million
Total capital investment	$477 million
Plant throughput	1,544 kg of MAb/year
Manufacturing cost	$130 million/year
Unit production cost	$84/g of MAb
Selling price	$200/g of MAb
Revenues	$309 million/year
Gross profit	$179 million/year
IRR (after taxes)	24.3%
NPV (for 7% discount interest rate)	$560 million

Table 12.17 presents a breakdown of the operating cost contributors. The facility-dependent cost is the most important item, accounting for 46.7% of the manufacturing cost or $39.2/g of final product. This is common for high-value products that are produced in small quantities in expensive facilities. Depreciation of the fixed capital investment and maintenance of the facility are the main contributors to this cost. Consumables are the second most important operating cost, accounting for 18.2% of the total or $15.3/g of final product. Consumables include chromatography resins, membrane filters and disposable bags that need to be replaced on a regular basis. Labor and raw materials costs come third and fourth, accounting for 14.6% and 12.9% of the total cost, respectively. The miscellaneous cost item (4.2% of total) accounts for heating/cooling utilities, electricity, and environmental costs. The cost of WFI, commonly classified as a utility cost in industry, is accounted for in the cost of raw materials in this example. In terms of cost distribution per section, 62% of the cost is associated with the upstream section and 38% with the downstream.

The economic evaluation relies on the following key assumptions: (1) a new manufacturing facility will be built and dedicated to production of 1,544 kg/year of MAb; (2) the entire direct fixed capital is depreciated linearly over a period of 12 years; (3) the project lifetime is 16 years; (4) the unit cost of WFI is $0.15/liter; (5) the cost of the serum free media (in powder form) is $300/kg; (6) all the chemicals used are high purity grade; (7) the unit cost of membranes is $400/m^2; (8) the unit cost of chromatography resins is $6000/liter, $1200/liter, and $2050/liter for columns C-101, C-102, and C-103, respectively; (9) the chromatography resins are replaced every 60, 50, and 50 cycles for columns C-101, C-102, and C-103, respectively.

Sensitivity Analysis

After a model of the entire process has been developed on the computer, tools like SuperPro Designer can be used to ask and readily answer "what if" questions and to carry out sensitivity analysis with respect to key design variables.

TABLE 12.17 Breakdown of the manufacturing cost for MAb production

Cost Item	$million/yr	$/g	%
Raw Materials	16.67	10.8	12.86
Facility-Dependent	60.54	39.2	46.71
Labor	18.89	12.2	14.58
Consumables	23.58	15.3	18.19
Lab/QC/QA	4.45	2.9	3.43
Miscellaneous	5.47	3.5	4.23
TOTAL	129.60	83.9	100.00

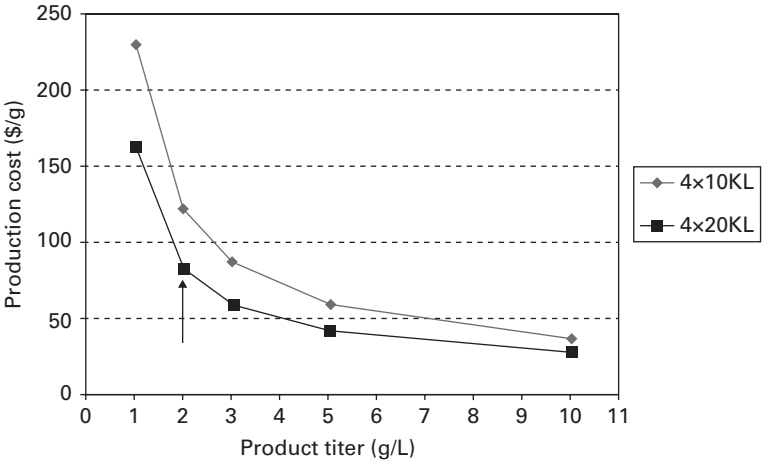

FIGURE 12.23 MAb production cost as a function of product titer and production bioreactor volume (L = liters).

In this example, we looked at the impact of product titer (varied from 1 to 10 g/liter) and bioreactor size (10,000 and 20,000 liters) on unit production cost. Figure 12.23 displays the results of the analysis. All points correspond to four production bioreactors feeding a single purification train. For low product titers, the bioreactor volume has a considerable effect on the unit production cost. For instance, for a product titer of 1 g/liter, going from 10,000 liters to 20,000 liters of production bioreactor volume reduces the unit cost from $230/g to $162/g. On the other hand, for high product titers (e.g., around 5 g/liter), the impact of bioreactor scale is not as important. This can be explained by the fact that at high product titers, the majority of the manufacturing cost is associated with the purification train. It is therefore wise to shift R&D efforts from cell culture to product purification as the product titer in the bioreactor increases. A key assumption underlying the sensitivity analysis is that the composition and cost of the cell culture media is independent of product titer.

12.7 SUMMARY

Process design consists of two main activities, process synthesis and process analysis. Process synthesis is the selection and arrangement of a set of unit operations (process steps) capable of producing the desired product at an acceptable cost and quality. Process analysis is the evaluation and comparison of different process synthesis solutions. In general, a synthesis step is usually followed by an analysis step, and the results of the analysis determine the subsequent synthesis step. Process synthesis and analysis require integration of knowledge from many different scientific and engineering disciplines, and they are carried out at various levels of detail. Some important points to remember when performing process synthesis and analysis are:

- Sequencing of product purification steps is based on experience and rules of thumb (heuristics), in which biomass separation (harvesting or removal) is followed by extraction (isolation) of product and then purification and polishing.
- Process simulators facilitate the analysis of integrated processes by performing material and energy balances, equipment sizing, economic evaluation, cycle time analysis, environmental impact assessment and other tasks.
- Capital costs are estimated based on direct fixed capital, working capital, and start-up and validation costs.
- The cost of a processing step is the sum of the costs of raw materials, labor, consumables, quality control, waste treatment/disposal, utilities, equipment depreciation, equipment maintenance, and overhead. The cost of the entire process is the sum of the costs for all the steps.
- Profitability analysis consists of the calculation of gross margin, return on investment, payback time, net present value, internal rate of return, and other measures.
- Sensitivity analysis uses a process simulator to investigate the impact of changing a specific process variable, such as product titer or scale of production. This activity can help to focus process design or development resources on areas of the process that are likely to have the greatest economic impact.

PROBLEMS

12.1 Tissue Plasminogen Activator Tissue plasminogen activator (tPA) was among the first products of biotechnology to be based on recombinant DNA technology. A medium molecular weight enzymatic protein, tPA is primarily used in the treatment of myocardial infarction (heart attack) patients. First characterized in 1979, the protein was commercially developed by Genentech (now part of Roche Pharmaceuticals), with clinical trial quantities and purities being achieved in late 1984. The current market demand is around 25 kg/year of purified tPA, which generates annual revenues of around $500 million for Roche Pharmaceuticals. The typical dose of tPA is around 100 mg, and this corresponds to a price per dose of around $2000.

The management of your company believes that the annual world demand can increase to more than 200 kg if the price per dose is reduced to around $300. Before committing to the venture, your president would like you, as director of corporate planning, to evaluate a technology for using transgenic goats to produce 50 kg of tPA per year. Based on data from GTC Biotherapeutics, you know that you can buy milk containing tPA at a concentration of 20 g/liter for around $200/g of tPA.

Based on information from the technical and patent literature, develop and evaluate a process that can recover and purify 50 kg of tPA per year from goat milk. More specifically, estimate the capital investment required and the profitability of the project idea.

12.2 Indigo Indigo is a dye that is used by denim manufacturers (to make blue jeans). It has traditionally been produced through chemical synthesis. The chemical route, however, generates large amounts of regulated waste materials that make the process environmentally unattractive. In the late 1990s, Genencor International (a biotechnology

company which is now part of DuPont) commercialized a technology for producing indigo via fermentation.

Based on information from the technical and patent literature, develop and evaluate a process for producing 5,000,000 kg of indigo per year via fermentation. The product must meet the quality specifications of the denim industry. More specifically, estimate the capital investment required and the unit production cost.

12.3 L-Lysine L-Lysine is an amino acid that is produced in large quantities (>100,000 metric tons/year) via fermentation. It is used as an animal feed supplement mainly for poultry and pigs.

Based on information from the technical and patent literature, develop and evaluate a process for producing 15,000,000 kg of L-lysine per year via fermentation. Your analysis should include estimation of capital and operating costs.

12.4 Xanthan Gum Xanthan gum is a water-soluble polysaccharide produced via fermentation. It is used in food products as a thickener, stabilizer, and emulsifier. Xanthan gum is also used for enhanced oil recovery.

Based on information from the technical and patent literature, develop and evaluate a process for producing 10,000,000 kg of xanthan gum per year. The product should meet the specifications of the petroleum industry for enhanced oil recovery. Your analysis should include estimation of capital and operating costs. Also, perform a sensitivity analysis and estimate the unit production cost for plant capacities ranging from 10 to 50 million kg of xanthan gum per year.

12.5 Biodegradable Polymers Because of the capacity limitations of urban landfills, biodegradable plastic packaging materials are of interest as a means to reduce the load on solid waste disposal systems.

Poly-2-hydroxybutyrate (PHB) is a promising biodegradable polyester that can be produced via fermentation. Microorganisms that synthesize PHB include Gram-positive and Gram-negative species and cyanobacteria. Some members of the *Alcaligenes* and *Azotobacter* genera are the most promising because they store high levels of PHB. PHB is synthesized and stored intracellularly as a possible future carbon and energy source. High levels of polymer are obtained under nitrogen and phosphorus limitation. At optimum conditions, PHB can reach 70 to 80% by weight of the cell mass of the organism.

Based on information from the technical and patent literature, design and evaluate a plant that produces 30,000,000 kg of PHB per year. Your analysis should include estimation of capital and operating costs.

12.6 Laundry Enzymes Proteolytic enzymes are used in laundering to hydrolyze and remove proteinaceous stains. The commercially important proteolytic enzymes that are used in detergents are mainly produced by *Bacillus subtilis* and *Bacillus licheniformis*. These enzymes are endo-cleaving, have broad specificity, and are active over a wide pH range; calcium improves their stability at high temperature or extremes of pH. Their molecular weight is around 30,000 and their isoelectric point is in the range of 8.5 to 9.5.

The current world demand for laundry enzymes is around 10,000 metric tons (of pure enzyme) per year, corresponding to a world market of around $300 million.

The marketing department of your company believes that the annual world demand can increase to more than 20,000 metric tons if the selling price is reduced to around \$15/kg of pure enzyme. Before committing to the venture, your company would like you to evaluate the cost structure of the current producers and find out whether it is possible (through the use of genetic engineering and modern separation technologies) to produce such enzymes for less than \$10/kg.

12.7 Therapeutic Proteins from Transgenic Tobacco Transgenic plants (e.g., corn, tobacco, etc.) have the potential to produce complex bioactive proteins at significantly lower cost than production via transgenic animals or mammalian cell cultures. The advantages of transgenic plant production are the following: easy and efficient introduction of stable foreign genes, cost-effective biomass production (\$0.04–\$0.1/kg), no possible contamination with human disease agents, and the ability to perform the complex protein processing needed for many bioactive human therapeutics. Cost-effective biomass production makes this mode of production suitable for high-volume recombinant proteins. The ability to perform complex protein processing is advantageous for production of therapeutic glycoproteins and bioactive peptides. Downstream processing costs are a major portion of the total unit production cost associated with transgenic plant production of high-volume therapeutic proteins. Therefore, primary recovery requires significant volume reduction. Once volume reduction and biomass removal have been achieved, chromatographic purification is required to remove plant protein impurities.

Design a purification process for use in a facility manufacturing 100 metric tons per year of recombinant human serum albumin protein from transgenic tobacco. Assume that the expression level is 0.5 g of product protein per kilogram of tobacco. Assume that biomass production and primary recovery are performed at a separate site. The feed to the purification section is 4000 liters/day (containing 200 g/liter of product protein), and this material is purchased for \$0.7/g of product protein. The process should include the appropriate filtration and chromatographic steps. Assume that a combination of affinity and ion exchange chromatography will provide a product that is more than 90% pure.

12.8 Succinic Acid In a report published by the U.S. Department of Energy [60], succinic acid was identified as one of the top building-block chemicals that could be produced from renewable biomass. Currently, succinic acid uses a petroleum-derived maleic anhydride route for its production, which is costly and environmentally unfriendly. As a result, there is growing interest in new production technologies that are based on fermentation. There are several strains of bacteria which can efficiently transform glucose and other sugars into succinic acid, but separation of the product from the fermentation broth is difficult. Various methods of succinic acid recovery have been proposed, including ion exchange chromatography, precipitation with calcium hydroxide, liquid-liquid extraction with tri-*n*-octylamine, electrodialysis, etc.

Based on information from the technical and patent literature, design and evaluate a process for producing 30,000,000 kg of succinic acid per year via fermentation. Your analysis should include overall material and energy balances, equipment sizing, and estimation of capital and operating costs.

12.9 Riboflavin (Vitamin B_2) Riboflavin is used for human nutrition and therapy, and as an animal feed additive. Its use in animal nutrition helps to keep the animals healthy and fit. Chemical synthesis of riboflavin was replaced by fermentation processes in the 1990s. The annual world demand for riboflavin was around 5,000,000 kg in 2010. Approximately 75% is consumed as an animal feed additive, and the remainder is used for human food and pharmaceutical applications.

Based on information from the technical and patent literature, design and evaluate a fermentation process for producing 1,000,000 kg of riboflavin per year for food and pharmaceutical applications. Your analysis should include overall material and energy balances, equipment sizing, and estimation of capital and operating costs.

12.10 Cheese Whey In whey production, proteins are isolated from the liquid part of the milk that is separated from the curd when making cheese. Whey protein is often sold as a nutritional supplement for protein drinks, energy bars, etc. Such supplements are especially popular in the sport of bodybuilding. Whey proteins also play a vital role in the formulation of amino acid and protein profile of infant formulas, making them nutritionally similar to mother's milk and enhancing their nutritional value to infants. Whey protein is a mixture of the following individual protein components: beta lactoglobulin, alpha-lactalbumin, immunoglobulins, glycomacropeptide, lactoferrin, lactoperoxidase, lysozyme, and bovine serum albumin. The U.S. market for whey proteins is expected to exceed 200,000,000 kg by 2015.

Fresh whey from conventional cheese production is approximately 94% water, less than 1% protein, 4.5% lactose, less than 1% ash and less than 1% fat. The separation of proteins from lactose and other low molecular weight components is accomplished using ultrafiltration systems. Isolation of individual protein components is accomplished with a combination of chromatography and membrane filtration units. Concentration of the lactose solution is done with reverse osmosis units.

Design a plant that processes 200,000 L/day of cheese whey and produces whey protein and purified lactose for infant formula.

12.11 Stevia Sweetener Stevia is a leafy green plant native to subtropical and tropical regions (http://en.wikipedia.org/wiki/Stevia). It is grown around the world for its sweet leaves, which are used in a variety of forms as a high-intensity sweetener. Stevia extracts have 200-300 times the sweetness of sucrose and do not raise blood glucose. Stevia-based sweeteners are used today in dairy products, health drinks and carbonated beverages. Both Coca Cola and PepsiCo have introduced drinks containing stevia-based sweeteners under the commercial names of Truvia and PureVia, respectively. Stevia sweeteners are presently extracted from the leaves of stevia plants. However, recent advances in synthetic biology have enabled the production of stevia sweeteners via fermentation.

Based on information from the technical and patent literature, design and evaluate a fermentation process for producing 5,000,000 kg of stevia sweeteners per year for applications in the beverage industries. Assume that production is accomplished via fermentation in yeast that secretes stevia molecules, reaching a product titer in the fermentation broth of 75 g/liter. The purification train includes a disk-stack centrifuge

for biomass removal and a sequence of chromatography, membrane filtration, crystallization, and drying units for the isolation and purification of the product. Your analysis should include overall material and energy balances, equipment sizing, and estimation of capital and operating cost. Furthermore, estimate the profitability of the investment assuming a selling price for the final product equal to 200 times the current price of sucrose.

12.12 MAb Production in Stirred Tank Bioreactors with Disposable Bags The MAb example in section 12.6.3 analyzes a process for producing 1,544 kg of purified MAb per year using four 20,000 liter stainless steel production bioreactors operating in staggered mode (out of phase) and feeding a single purification train. The product titer is 2 g/liter and the cycle time of each bioreactor is 2 weeks. In the last few years, new cell lines have become available (e.g., PER.C6 from Percivia) that can reach significantly higher product titers (> 20 g/liter). Deployment of such cell lines greatly reduces the volume of the upstream equipment and enables single-use systems to produce metric ton quantities of MAbs. Rocking and stirred tank bioreactors that utilize single-use (disposable) liners (bags) have become popular in the biopharmaceutical industry because they eliminate the need for cleaning and sterilization-in-place. Other advantages of such systems include increased processing flexibility and shorter validation, start-up, and commercialization times. Single-use bioreactors are available with working volume of up to 2,000 liters.

Design a process using the new technologies described above which can produce 1,200 kg of a therapeutic monoclonal antibody per year. Assume you make use of the PER.C6 cell line that can consistently reach 10 g/liter of product titer. For product purification, assume that you need two adsorptive chromatography steps (e.g., affinity and hydrophobic interaction) followed by a polishing ion exchange membrane adsorber that operates in flow-through mode (the product flows through the unit but certain DNA and other charged impurity molecules are retained by the membrane). Your analysis should include overall material and energy balances, equipment sizing, and estimation of capital and operating costs.

REFERENCES

1. Douglas, J. M. (1988). *Conceptual Design of Chemical Processes*, McGraw-Hill, New York.
2. Frohlich, B. T. (1999). Considerations for developing in-house capabilities for cost of goods estimation. In *Biopharmaceutical Process Economics and Optimization* (conference proceedings), September 30–October 1, 1999, International Business Communications, Westborough, MA.
3. Leser, E. W., and Asenjo, J. A. (1992). Rational design of purification processes for recombinant proteins. *J. Chromatog.*, vol. 584, p. 43.
4. Asenjo, J. A., and Andrews, B.A. (2004). Is there a rational method to purify proteins? From expert systems to proteomics. *J. Mol. Recognit.*, vol. 17, p. 236.
5. Petrides, D. P., Cooney, C. L., and Evans, L. B. (1989). An introduction to biochemical process design. In *Chemical Engineering Problems in Biotechnology*, vol. 1, M. L. Shuler, ed., American Institute of Chemical Engineers, New York, p. 351.
6. Petrides, D. P. (1994). BioPro Designer—An advanced computing environment for modeling and design of integrated biochemical processes. *Comput. Chem. Eng.*, vol. 18, p. S621.

7. Nfor, B.K., Ahamed, T., van Dedem, G., van der Wielen, L., van de Sandt, E., Eppink, M., and Ottens, M. (2008). Design strategies for integrated protein purification processes: challenges, progress, and outlook. *J. Chem. Technol. Biotechnol.*, vol. 83, p. 124.
8. Kula, M.-R., and Horst, S. (1987). Purification of proteins and the disruption of microbial cells. *Biotechnol. Prog.*, vol. 3, p. 31.
9. Taylor, G., Hoare, M., Gray, D. R., and Marston, F. A. O. (1986). Size and density of protein inclusion bodies. *Bio/Technology*, vol. 4, p. 553.
10. Palmer, D. E. (1977). High purity protein recovery. *Process Biochem.*, vol. 12, p. 24.
11. Chang, Y.-K., and Chase, H. A. (1996). Development of operating conditions for protein purification using expanded bed techniques: The effect of the degree of bed expansion on adsorption performance. *Biotechnol. Bioeng.*, vol. 49, p. 512.
12. Dlouhy, P. E., and Dahlstrom, D. A. (1968). Continuous filtration in pharmaceutical processing. *Chem. Eng. Prog.*, vol. 64, p. 116.
13. Brunner, K. H., and Hemfort, H. (1988). Centrifugal separation in biotechnological processes. In *Advances in Biotechnological Processes*, vol. 8, A. Mizrahi, ed., Liss, New York, p. 1.
14. Axelsson, H. A. C. (1985). Centrifugation. In *Comprehensive Biotechnology*, vol. 2, M. Moo-Young, ed., Pergamon Press, Oxford, p. 325.
15. Freese H. L. (1993). Evaporation. In *Fermentation and Biochemical Engineering Handbook*, H. C. Vogel, ed., Noyes, Park Ridge, NJ, p. 227.
16. Chan. M. Y. Y., Hoare, M., and Dunnill, P. (1986). The kinetics of protein precipitation by different reagents. *Biotechnol. Bioeng.*, vol. 28, p. 387.
17. Nunes, S.P., and Peinemann, K.-V. (2006). *Membrane Technology in the Chemical Industry*, Wiley-VCH, Weinheim, Germany.
18. Fish, W. W., Danielson, A., Nordling, K., Miller, S. H., Lam, C. F., and Bjork, I. (1985). Denaturation behavior of antithrombin in guanidinium chloride. *Biochemistry*, vol. 24, p. 1510.
19. Bjurstrom, E. (1985). Biotechnology. *Chem. Eng.*, vol. 92, p. 126.
20. Wheelwright, S. M. (1987). Designing downstream processes for large-scale protein purification. *Bio/Technology*, vol. 5, p. 789.
21. Ghosh, R. (2002). Protein separation using membrane chromatography: opportunities and challenges, *J. of Chromatography* A, vol. 952, p. 13.
22. Zhou, J.X., and Tressel, T. (2005). Q membrane chromatography as a robust purification system for large-scale antibody production. *BioProcess Int.*, vol. 3, p. 32.
23. Antia, F.D. (2003). A simple approach to design and control of simulated moving bed chromatographs. In *Scale-Up and Optimization in Preparative Chromatography*, A. S. Rathore and A. Velayudhan, A. eds., Marcel Dekker, New York, p. 184.
24. Holzer, M., Osuna-Sanchez, H. and David, L. (2008). Multicolumn chromatography—a new approach to relieving capacity bottlenecks for downstream processing efficiency, *BioProcess Int.*, vol. 6, p. 74.
25. Korovessi, E., and Linningerr, A.A. (2006). *Batch Processes*, Taylor and Francis, Boca Raton, FL.
26. Heinzle, E., Biwer, A., and Cooney, C. (2006). *Development of Sustainable Bioprocesses*, Wiley, West Sussex, England.
27. Petrides, D.P., Koulouris, A., and Lagonikos, P.T. (2002). The role of process simulation in pharmaceutical process development and product commercialization. *Pharm. Eng.*, vol. 22, p. 56.
28. Toumi, A., Jurgens, C., Junco, C., Maier, B., Papavasileiou, V., and Petrides, D.P (2010). Design and optimization of a large scale biopharmaceutical facility using process simulation and scheduling yools. *Pharm. Eng.*, vol. 20, March/April.
29. DiMasi, J.A., Hansen, R.W., and Grabowski, H.G. (2003). The price of innovation: new estimates of drug development costs. *J. Health Econ.*, vol. 22, p. 151.

30. Gilbert, J., Hensek, P., and Singh, A. (2003). Rebuilding big pharma's business model. *In Vivo: The Business and Medicine Report*, vol. 21, Nov.
31. Peters, M. S., and Timmerhaus, K. D. (1991). *Plant Design and Economics for Chemical Engineers*, 4th ed., McGraw-Hill, New York.
32. Ulrich, G. D. (1984). *A Guide to Chemical Process Design and Economics*, Wiley, New York.
33. Valle-Riestra, J. F. (1983). *Project Evaluation in the Chemical Process Industries*, McGraw-Hill, New York.
34. Garrett, D. E. (1989). *Chemical Engineering Economics*, Van Nostrand Reinhold, New York.
35. Seider, W. D., Seader, J. D., and Lewin, D. R. (1999). *Process Design Principles—Synthesis, Analysis, and Evaluation*, Wiley, New York.
36. Towler, G. and Sinnott, R. (2008). *Chemical Engineering Design; Principles, Practice and Economics of Plant and Process Design*, Butterworth-Heinemann (Elsevier), London.
37. DOE/NETL-2002/1169 (2002). Process Equipment Cost Estimation. Available at http://www.osti.gov/bridge/purl.cover.jsp?purl=/797810-Hmz80B/native/
38. Kalk, J. P., and Langlykke, A. F. (1986). Cost estimation for biotechnology projects. In *Manual of Industrial Microbiology and Biotechnology*, A. L. Demain and N. A. Solomon, eds., American Society for Microbiology, Washington, DC, p. 363.
39. Reisman, H. B. (1988). *Economic Analysis of Fermentation Processes*, CRC Press, Boca Raton, FL.
40. Jagschies, G. (2008). Where is biopharmaceutical manufacturing heading? *BioPharm Int.*, vol. 21, p. 72.
41. Pollak, P., Badrot, A., and Dach, R. (2012). API manufacturing: facts and fiction. *Contract Pharma*, Jan./Feb.
42. Papavasileiou V., Siletti, C., and Petrides, D. (2008). Systematic evaluation of single-use systems using process simulation tools. *BioPharm Int. Suppl.*, Nov., p. 16.
43. Crueger, W., and Crueger, A. (1989). *Biotechnology—A Textbook of Industrial Micro-biology*, 2nd ed., Sinauer, Sunderland, MA.
44. Saleem, H. (2011). China Citric Acid Price Trend Outlook for 2011. Available at http://www.prlog.org/11293569-china-citric-acid-price-trend-outlook-2011.html
45. Roberts L. R. (1979). Citric acid. In *Encyclopedia of Chemical Processing and Design*, vol. 8, J. J. McKetta and W. A. Cunningham, eds., Dekker, New York, p. 324.
46. Blanch, H. W., and Clark, D. S. (1997). *Biochemical Engineering*, Dekker, New York.
47. Barfoed, H. C. (1987). Insulin production technology. *Chem. Eng. Prog.*, vol. 83, p. 49.
48. World Health Organization (2011). The top 10 causes of death by broad income group, 2008, fact sheet no. 310.
49. Ladisch, M. R., and Kohlmann, K. L. (1992). Recombinant human insulin. *Biotechnol. Prog.*, vol. 8, p. 469.
50. Kehoe, J. A. (1989). The story of biosynthetic human insulin. In *Frontiers in Bioprocessing*, S. K. Sikdar, M. Bier, and P. Todd, eds., CRC Press, Boca Raton, FL, p. 45.
51. Datar, R., and Rosen, C.-G. (1990). Downstream process economics. In *Separation Processes in Biotechnology,* J. A. Asenjo, ed., Dekker, New York, p. 741.
52. Petrides, D. P., Sapidou, E., and Calandranis, J. (1995). Computer-aided process analysis and economic evaluation for biosynthetic human insulin production—A case study. *Biotechnol. Bioeng.*, vol. 5, p. 529.
53. Nair, A. (2011). Report from India; Indian firms eager to partner with global manufacturers for biosimilars. *BioPharm Int.*, vol. 24, p. 11.
54. Di Marchi, R. D. (1984). Process for inhibiting undesired thiol reactions during cyanogen bromide cleavage of peptides, U.S. Patent 4,451,396.
55. Bobbitt, J. L., and Manetta, J. (1990). Purification and refolding of recombinant proteins, U.S. Patent 4,923,967.

56. Walsh, G. (2005). Biopharmaceuticals: recent approvals and likely directions. *Trends Biotechnol.*, vol. 23, p. 553.
57. Pavlou, A.K. and Belsey, M.J. (2005). The therapeutic antibodies market to 2008, *Eur. J. Pharm. Biopharm*., vol. 59, p. 389.
58. Rader, R.A. (2012). Top 50 biopharma products, *Contract Pharma*, July/Aug.
59. Kelley, B. (2007). Very large scale monoclonal antibody purification: The case for conventional unit operations. *Biotechnol. Prog*., vol. 23, p. 995.
60. PNNL-14808 (2004). Top Value Added Chemicals From Biomass, Vol. 1. Available at https://www1.eere.energy.gov/bioenergy/pdfs/35523.pdf

/// 13 /// LABORATORY EXERCISES IN BIOSEPARATIONS

Chapters 3 to 11 of this text are organized around the study of various unit operations in the approximate order of their customary application to bioseparations. In this chapter, five of these operations are singled out for further exploration in the laboratory. These are flocculant screening (Chapter 3), crossflow filtration (Chapter 4), centrifugation of cells and lysate (Chapter 5), aqueous two-phase partitioning of a protein (Chapter 6), and gradient-elution ion exchange chromatography of test proteins (Chapter 7). Each section of this chapter is thus an independent laboratory exercise. The instructions can be applied flexibly to the materials and equipment available at a particular laboratory or department. The calculations, reporting, and scale-up applications are applicable to any experiment that follows the generic paradigm of each of the sets of lab instructions. The pattern to be followed consists of becoming acquainted with the equipment and describing it as a unit operation in a report, execution of a predesigned experiment, recording of appropriate data, analysis of the data in the context of this textbook, presenting reduced data in a report, critically analyzing the quality of the results, and, finally applying the actual numerical results to a scale-up to production scale. Process economics may be applied where appropriate.

13.1 FLOCCULANT SCREENING

In this laboratory exercise, a flocculant will be evaluated for its ability to flocculate cells or lysate particles. Lysate particles are smaller and require, typically, higher concentration of flocculant than that required to flocculate whole cells. The flocculant concentration required will be determined by observing the persistence of flocculation and clarity of supernatant, measured as a function of flocculant concentration.

13.1.1 Background

Flocculants are usually polymers with properties, such as charge, that cause them to interact with cells or lysate particles and bind them together. Their effectiveness depends on molecular weight, charge, solubility, and other properties, and their interactions with cells and particles depend, therefore, on pH, ionic strength, temperature, and dry solids concentration.

Unless a great deal is known about the suspended material of interest, or extensive experience has been published, the choice of flocculating conditions usually depends on educated trial and error. Typically, the engineer or scientist chooses a series of flocculants and tests them at different concentrations and ionic strengths, noting the time to observed flocculation, the clarity of the supernatant after centrifugation, and the quality of the flocculated precipitate. An example would be the Cysep series of cationic flocculants 4215, 4218, 4224, and 4225 (Cytec Industries, Inc.), which are listed in order of increasing positive charge; the flocculants in this series do not contain oil or surfactants, thus increasing the compatibility with downstream processing involving membranes and chromatography media.

13.1.2 Objectives

The objectives of this laboratory exercise are to understand flocculation as a unit operation, monitor flocculation through visual observation, and use postcentrifugation data to evaluate the quality of flocculation used to scale a test process to an industrial process.

13.1.3 Procedure

1. From the instructor, obtain samples of cells or cell lysate suspended in broth or buffer and stock solutions of flocculants.
2. Divide each group (three to six persons) according to tasks, such as pH and other preliminary measurements, addition and mixing of flocculants, benchtop centrifugation of flocs, postcentrifuge evaluations (as described later), and using Table 13.1 to keep records.
3. Record sample pH, conductivity, dry weight of solids, source, and type of cells or lysate, as recommended by the instructor.
4. Make (or obtain) a polymer flocculant solution, 0.5% (w/v) if for cells, 3% (w/v) if for lysate.
5. Place 5 ml of cell suspension or lysate into each of six 15 ml centrifuge tubes.
6. Add 0, 1, 2, 3, 4, or 5 ml of polymer solution to each tube. Be sure to label tubes. Do not shake.

TABLE 13.1 Tabulation of Results of Flocculation Experiments

Sample description: _____

Name and concentration of flocculant: _____

	0	1	2	3	4	5
Flocculant solution (ml)						
Flocculation at inversion number						
Still flocculated after 20 inversions?						
Clarity order postcentrifugation						
Pellet volume (ml)						
Optical density of top 2 ml of supernatant						

7. Add water to give a total liquid volume of 10 ml in each tube. Do not shake.
8. Invert tubes 20 times. Record on which inversion each flocculation is first seen and whether breakup of the flocs occurs.
9. Centrifuge the zero-flocculant control at 1000 rpm for 1 min. If it clarifies, resuspend the solids and repeat the centrifugation at lower speed. Using the highest speed at which the zero-flocculant control does not clarify, centrifuge the samples with flocculant for 1 min.
10. Qualitatively judge which supernatant is least cloudy. Score 1 for clearest and 6 for least affected. Record pellet volume and type, using the scale on the centrifuge tube. If time permits, record the optical density at 600 nm for the top 2 ml of the supernatant, including the control.
11. If no flocculation is seen, examine using higher doses of polymer: 3 to 40 g/liter; if "overkill" is seen, examine lower polymer doses, especially below 10 g/liter dry weight of solids in the cell or lysate sample.
12. Record results for the group in Table 13.1.

13.1.4 Report

Write a short report using the following outline.

1. Description of the experiment.
2. Record of all measurements made on sample prior to flocculation test.
3. Complete information about the flocculant solution.
4. Tabular results—use Table 13.1.
5. Identification of optimum conditions for flocculation from the results in the table.
6. A brief design of a unit operation in which you optimally flocculate 100 liters of the product used in the experiment.

13.1.5 Some Notes and Precautions

1. The procedure described here is a laboratory exercise and results in varying the ionic strength to keep the volume constant for centrifugation. Real-world tests with undiluted broth must be performed to find both the optimum polymer dose and ionic strength. The optimum final dose will probably be close to that found in this procedure.
2. No pH adjustment should be required. Flocculation should be found for all biological suspensions at pH 7 (pH is recorded as a standard laboratory practice).
3. Always dilute the as-supplied polymers to 5% or below. Store in the cool and dark for a maximum of 3 days. The Cytec cationic flocculants are stable from pH 3 to 11.
4. The flocculant dose for a given dry weight of whole cells (in any volume) should be approximately constant and less than that for a given dry weight suspension of lysate, which may vary according to the degree and mode of lysis.

13.2 CROSSFLOW FILTRATION

In this laboratory exercise, permeate flux will be measured as a function of solids concentration in a crossflow filtration apparatus operated in batch concentration mode (see Chapter 4). The decline of flux as solids or solutes are concentrated is an important measurement in the monitoring of the progress of a filtration step and in the evaluation of a filtration process for scale-up. These principles apply to both microfiltration and ultrafiltration operations.

13.2.1 Background

Common configurations ("modes") of crossflow filtration unit operations are shown in Figure 4.18. In the *total recycle mode,* there is no net concentration of solids or retained solutes because both the permeate and the retentate are returned to and remixed with the feed. In the *batch concentration mode,* only the retentate is returned to and remixed with the feed. Since permeate is continuously removed from the system, there is an unsteady increase in retained solids or macromolecules in the feed. Again, however, the compositions of the recirculation loop and the material in the feed tank are identical. The batch concentration configuration will be used in this laboratory exercise. *Continuous, or feed-and-bleed, configurations* (Figure 4.20) are designed for steady state operation. Permeate flows are adjusted so that the concentration in the recirculation loop is constant and generally equal to the final desired concentration. Neither the permeate nor the retentate are returned to the feed tank, although the result would be unchanged if the retentate recirculation loop returned directly to the tank.

13.2.2 Objectives

The objectives of this laboratory exercise are to understand crossflow filtration as a unit operation, monitor permeate flux through a batch concentration operation and determine its dependence on the concentration of solids, and use crossflow filtration data to scale a pilot process to an industrial process.

13.2.3 Procedure

1. Test the crossflow filtration unit to ascertain that there are no pressure leaks in the filter cartridge. Be sure to understand the meaning of each pressure (inlet, back pressure, and permeate outlet pressure) and to adhere to the limits specified by the instructor. Be careful not to exceed the back pressure specified by the instructor.
2. Determine the volume of the feed suspension, which consists of a fermentation broth containing *E. coli* cells. The cells are to be concentrated by operating the filter unit in the batch concentration mode.
3. Assign a member of the research team to each task recommended by the instructor, such as flux measurement, pressure and temperature recording, and determining the residual volume in the feed tank and the concentration of solids.
4. Set pressures and temperatures to desired values while operating the unit in total recycle mode (return permeate line to the feed tank).
5. Begin filtration in the batch concentration mode, noting time, feed volume, pressures, and temperatures. At specified intervals, determine the permeate flux by collecting a known volume of permeate in a graduated cylinder while timing with a stopwatch.
6. Determine the concentration of solids in the feed tank, using the same time intervals. Note that this can be calculated by knowing the initial solids content of the whole broth and the volumetric concentration factor derived from the new volume of feed in the tank at each time point. Try to determine the feed volume and permeate flux simultaneously. The solids concentration can be confirmed by a calibrated concentration measurement, such as turbidity, if such a method is specified by the instructor. Record the area of the membrane used.

13.2.4 Report

Prepare an *individual* written report using the following outline.

1. One-paragraph summary.
2. Experimental procedure, including equipment sketch.
3. Graphical summary (with accompanying narrative) of experimental results, plotting permeate flux versus time, feed volume and/or solids concentration

versus time, and permeate flux versus solids concentration. A log scale on the abscissa is useful.

4. Process flow diagram showing membrane filter, proper configuration, and computed feed and permeate rates.
5. Concise written discussion of results, errors, and engineering inaccuracies.
6. A scaling calculation, performed by using the experimental membrane filter area to calculate the membrane area required to achieve a five times concentration of the whole broth from a production scale fermentor. The volume of the production scale fermentor is 180,000 liters, and the fermentation time including turnaround is 4 days. The whole broth contains 2% solids by weight. Assume a *feed-and-bleed* configuration around the filtration unit. Estimate the capital investment required to do the job, using the information in Chapter 12 for the cost of crossflow filters. Discuss the errors and engineering inaccuracies that affect your design.

13.3 CENTRIFUGATION OF FLOCCULATED AND UNFLOCCULATED PARTICULATES

In this laboratory exercise, the concentration of effluent particles will be measured as a function of the flow rate in a continuous centrifugation apparatus. The escape of particles is an important measurement in the monitoring of the success of a centrifugation step and in the evaluation of a centrifugation process for scale-up. These principles apply equally to cell and lysate separations, both of which can be enhanced by flocculation prior to centrifugation. Therefore, the effects of flocculation on particle retention will be evaluated on the basis of "breakthrough curves," which establish allowable flow rates for a given combination of centrifuge and product mixture.

13.3.1 Background

A disk-stack centrifuge (Figure 5.5) can be operated in flowing batch or continuous mode. In the latter case, solids are ejected continuously through a nozzle. In this experiment, the flowing batch mode will be used. The rate at which feed can be pumped into the centrifuge (Q) is determined by the geometry and speed of the centrifuge (Σ factor; see Sections 5.4.1 and 5.4.2) and the sedimentation properties of the particles in the feed (v_g; see Section 5.3.4). It is possible to control v_g by flocculation, the conversion of individual particles to larger hydrodynamic units.

If a disk-stack centrifuge is unavailable, this experiment can also be performed using a bowl centrifuge, such as the Beckman JCF-Z continuous-flow rotor [1], the inner workings of which are shown in Figure 13.1. In this case, the measurements required for determining Σ can be found in Section 5.4.1. If it is not possible to

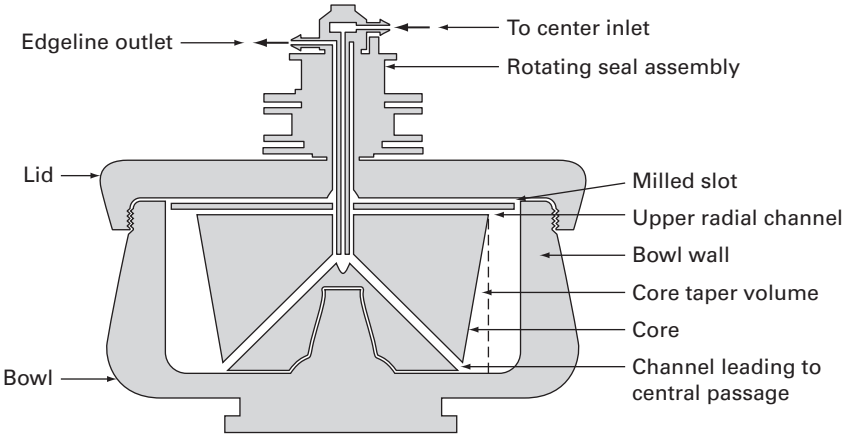

FIGURE 13.1 Cross section of a commercial bowl centrifuge rotor. Feed enters from the right, above the rotary seals, and passes down the central tube to a branched channel that carries the pumped feed to the bottom of the bowl. Feed flows upward in the space between the core and the bowl wall, and the supernatant passes up the flow annulus to the outlet. *(Based on a design by Beckman Coulter, Inc., Spinco Division, 1995.)*

make direct measurements on the centrifuge rotor, whether disk-stack or bowl, these dimensions will be provided by the instructor.

13.3.2 Objectives

The objectives of this laboratory exercise are to understand centrifugation as a unit operation; monitor particle escape through a flowing batch operation; determine its dependence on the properties of solids, with and without flocculation; and use breakthrough centrifugation data to scale a pilot process to an industrial process.

13.3.3 Procedure

1. Obtain from the instructor one of four possible samples in a feed container to be connected to the feed pump for pumping into the centrifuge:
   (a) Unflocculated whole cells (bacteria or yeast) in broth
   (b) Flocculated whole cells in broth
   (c) Unflocculated lysate of cells in broth
   (d) Flocculated lysate of cells in broth
2. Assign a member of the experiment team to each task recommended by the instructor, such as measuring and/or recording the flow rate, collecting samples, diluting samples (if dilution is necessary), reading the spectrophotometer, recording spectrophotometer readings, assisting with cleanup, obtaining the correct measurements and speed of the centrifuge required for determining Σ, collecting the data, and sharing the data with other groups. The bowl and core

combination shown in Figure 13.1 for the Beckman JCF-Z continuous-flow rotor is termed a "large-pellet" rotor, since the filled bowl can accommodate up to 800 ml of solids. This bowl has a top acceleration of 39,900 × *g,* the inner radius of the capture zone is 5.6 cm, and the outer radius is 8.9 cm. The rotor has a volume capacity of 1250 ml, and its internal height is 8.2 cm.

You should determine the ∑ value for the centrifuge from the dimensions and speed. Using the breakthrough Q's, get values for v_g. Use these results to scale up the disk-stack centrifuges (but not the bowl centrifuges).

3. Connect the feed container, via tubing, to the feed pump and the pump to the centrifuge. Pump the suspension through the centrifuge at a controlled flow rate from 500 to 2200 ml/min.
4. Collect the clear liquid coming out of the upper chute of the centrifuge.
5. Measure the optical density (OD) at 600 nm of the clear broth collected at this flow rate.
6. Change the flow rate to another value, and repeat steps 3 to 5. When changing the flow rate, it is advisable to randomly increase or decrease the pump speed rather than simply changing the speed linearly. The pump rate should be allowed to reach a steady state before the feed is switched into the centrifuge inlet. The pump rate can be measured by using a graduated cylinder and a stopwatch.
7. Record and plot the OD versus flow rate for the given feed material using the data table provided (Table 13.2); include the data from other groups. The plot should look like the example breakthrough curve in Figure 13.2.
8. Collect data from the other groups for the other feed materials.

TABLE 13.2 Form for Tabulating Effluent Concentration versus Flow Rate for Plotting in a Graph such as Figure 13.2

Unflocculated whole cells

Flow rate					
Supernatant OD					

Flocculated whole cells

Flow rate					
Supernatant OD					

Unflocculated lysate

Flow rate					
Supernatant OD					

Flocculated lysate

Flow rate					
Supernatant OD					

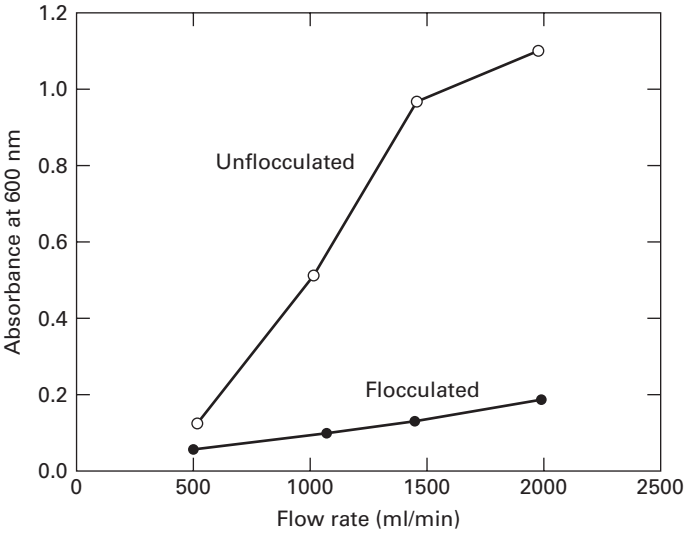

FIGURE 13.2 Breakthrough curves (effluent concentration versus feed flow rate) for flocculated and unflocculated cells in broth in a typical experiment. Note that the flow rate can be more than four times greater for flocculated cells as that for unflocculated cells. This set of breakthrough curves is for *E. coli* treated with Cytec E-2706 cationic flocculant at pH 5 compared with unflocculated suspension. Centrifuge: Alfa Laval at 14,000 rpm.

13.3.4 Report

Each person will prepare an *individual* written report using the following outline:

1. One-paragraph summary.
2. The experimental procedure, including a sketch of the equipment.
3. A table of the data and a graphical summary (with accompanying narrative) of the experimental results (use the format of Table 13.2), plotting the breakthrough OD versus the flow rate for the four different suspensions. Indicate which suspension was used by your group.
4. A process flow diagram showing the rotor components (symbolically), feed (and pumping) configuration, and the given feed and supernatant flow rates and concentrations.
5. A concise written discussion of the results, errors, and engineering inaccuracies.
6. A scaling calculation performed by using the experimental centrifuge to calculate the number of centrifuges required to achieve a 0.07 OD suspension from whole broth from a production-scale fermentor. The production scale fermentor is 180,000 liters, and the fermentation time is 4 days, including the turnaround time. The whole broth contains 1.58 OD units of unflocculated whole cells. Using appropriate relationships, indicate the possible changes that could be made to the centrifuge design to reduce the number of

centrifuges required. State the centrifuge specifications required to perform this job with six mechanically feasible centrifuges. Discuss the errors and engineering inaccuracies that affect your design.

13.4 AQUEOUS TWO-PHASE EXTRACTION

Aqueous two-phase extraction is a technique used in the biochemistry profession and, to a lesser extent, in the biotechnology industry, to isolate and purify a variety of proteins and biological materials, including subcellular particles and whole cells. This technique was developed to its present form by Albertsson [2].

Two-phase aqueous systems are made by combining two incompatible water-soluble polymers (e.g., PEG and dextran) or a polymer and a salt in water, above a "critical" concentration. These systems separate into two immiscible liquid phases, one enriched in one polymer and the other enriched in the other polymer or in salt. Soluble materials added to the system, such as proteins or particulate separands (including living cells), partition themselves between the two phases [3]. This is the basis for extraction. For this experiment, PEG/dextran is the phase system of choice because its physical properties make it suitable for protein extraction without any harmful effects on the protein. The partition coefficients of different separands can be manipulated in this two-polymer system by the addition of acid, base, partitioning ions, nonpartitioning ions, and surfactants.

13.4.1 Physical Measurements

In a single-stage extraction, a dextran solution (heavy phase) along with a certain amount of protein is thoroughly mixed with a solution of PEG (light phase). The protein partitions between the two phases until equilibrium is reached. The equilibrium partition coefficient K is defined as

$$K = y / x \tag{13.4.1}$$

where y = concentration of protein in the extract phase
x = concentration of protein in the raffinate phase.

The objectives of this experiment are as follows:

1. Show that the PEG/dextran mixture forms two phases above certain concentrations.
2. Estimate the phase volume ratios.
3. Determine the equilibrium partition coefficient for a protein.
4. Determine the product yield.

13.4.2 Procedure

1. Use the following aqueous stock solutions:
   (a) 50% (w/w) PEG, MW 8000
   (b) 10 mg/ml hemoglobin, MW 64,500, in 0.1 M Na phosphate buffer, pH 7.8
   (c) 0.1 M Na phosphate buffer, pH 7.8
   (d) 25% (w/w) dextran, MW 480,000
2. Determine the mass of each solution and of dry NaCl needed to combine to form each of the four phase systems for the initial compositions specified in the phase diagram given in Figure 13.3. You will make a total of six phase systems, one each for systems 1, 2, and 4, and three for system 3.
   (a) Plan to add 0.1, 0.2, and 0.5 ml of the hemoglobin solution to phase system 3 and 0.2 ml to each of the other three systems.
   (b) Record all weights.
3. Formulation of the phase systems:
   (a) Place a 15 ml graduated conical tube in a beaker on the balance, and tare it.
   (b) Carefully add the appropriate amounts of PEG, dextran, and buffer stock solutions to the tube. The dextran solution is very viscous, so be sure to wait for the pipette to fill with the appropriate amount.
   (c) Add 0.5 g of NaCl.
   (d) Add the chosen amount of hemoglobin plus 1 ml of buffer (0.1 M Na phosphate, pH 7.8) and enough water for a total final mass of 10 g.

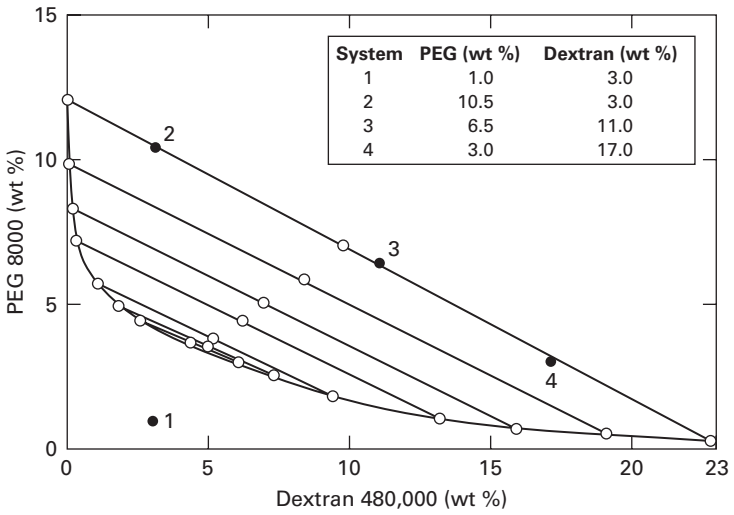

FIGURE 13.3 Phase diagram of the PEG 8000/dextran 480,000 system, indicating the total compositions of systems 1, 2, 3, and 4 by the positions of the corresponding numbered closed circles. Indicated on the tie lines are the experimental data used to construct the phase diagram (open circles), the composition of the two phases (points on the binodal curve), and the composition of the total system (points between the points on the binodal curve). *(Data from P.-Å. Albertsson,* Partition of Cell Particles and Macromolecules, *3rd ed., Wiley, New York, 1986.)*

TABLE 13.3 Compositions of the Six PEG/Dextran Two-Phase Systems

	System					
	1	**2**	**3a**	**3b**	**3c**	**4**
PEG stock, g	0.2	2.1	1.3	1.3	1.3	
Dextran stock, g	1.2	1.2	4.4	4.4	4.4	
Hemoglobin solution, ml	0.2	0.2	0.1	0.2	0.5	0.2
NaCl, g	0.5	0.5	0.5	0.5	0.5	0.5
Buffer, ml	1.0	1.0	1.0	1.0	1.0	1.0

Table 13.3 summarizes the compositions of the six systems. The masses of the PEG and dextran stock solutions required for system 4 should be determined from the table in Figure 13.3.

4. Vortex each phase system. Make sure the NaCl is fully dissolved. If necessary, invert the tube several times to help the salt dissolve.
5. Centrifuge each system at 1500 rpm for 10 min to separate the two phases. Make sure the centrifuge is balanced by checking the volumes of diametrically opposite samples.
6. Use the calibrated markings on the tube to estimate and record the volume of each phase.
7. Remove samples from both the top and bottom phases. Carefully draw up 0.6 to 0.7 ml of the top phase with a pipette, taking care not to disturb the interface. Gently perforate the tube to allow the bottom phase to drain into a tube for diluting and measuring the optical absorbance in the spectrophotometer.
8. Determine the concentration of protein in each phase using a spectrophotometer and the calibration curve (Figure 13.4).
   (a) Set the wavelength (λ) to 405 nm.
   (b) Use pure water to set the blank.
   (c) Make a 1:6 dilution of each sample with pure water.
   (d) Record the absorbance of each phase sample.

13.4.3 Calculations and Report

Each report should be no more than ten pages long and should be written in the format of a scientific paper, which should include the following:

1. *Title page* with your name, date, title of report, and a 100- to 150-word abstract that summarizes the purpose, methods, and results of the experiments.
2. *Introduction,* which gives the background on biphasic aqueous extraction and describes the objectives of the experiments.
3. *Materials and methods*, which describes the materials, equipment, and procedures you used. Provide sketches of the equipment, as appropriate. Cite

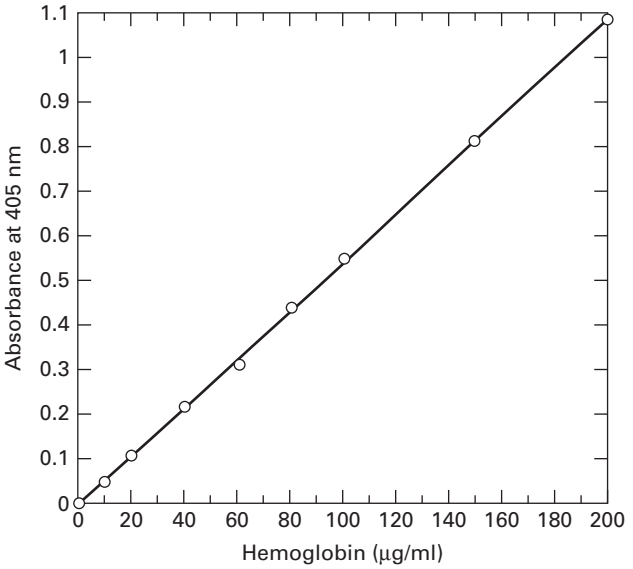

FIGURE 13.4 Hemoglobin calibration curve, absorbance at 405 nm versus the protein concentration.

volumes, concentrations, and other measurements. This section should be written in such a way that the reader could use it as a recipe for repeating your experiments.

4. *Results and discussion,* including the raw data that you measured, together with the calculated results and equations that you used. Present calculated results in tables or figures, as appropriate. Define all symbols used, and number the equations, tables, and figures; refer to these display items by number in your text. Include an error analysis (means, standard errors, confidence limits) and a discussion of the problems or difficulties you encountered, especially those leading to systematic errors. In particular, the following must be included:
   (a) Statement of which of the four systems formed two phases.
   (b) Report of the phase volume ratios for each system and, from the binodal curve on the phase diagram (Figure 13.3), a determination of the equilibrium composition of the upper and lower phases. Calculate the mass ratio of each phase from the phase diagram using the lever rule (see instructions in Section 13.4.4 and Figure 13.5). Explain the trends observed in the phase volume ratios and compare those with the calculated mass ratios.
   (c) Report of the concentration of hemoglobin in both phases. For each phase system, calculate the percentage recovery and the equilibrium partition coefficient K of hemoglobin. Answer the following questions:
      (1) Did K vary as a function of volume ratio?
      (2) Did K vary as a function of protein concentration (explain)?

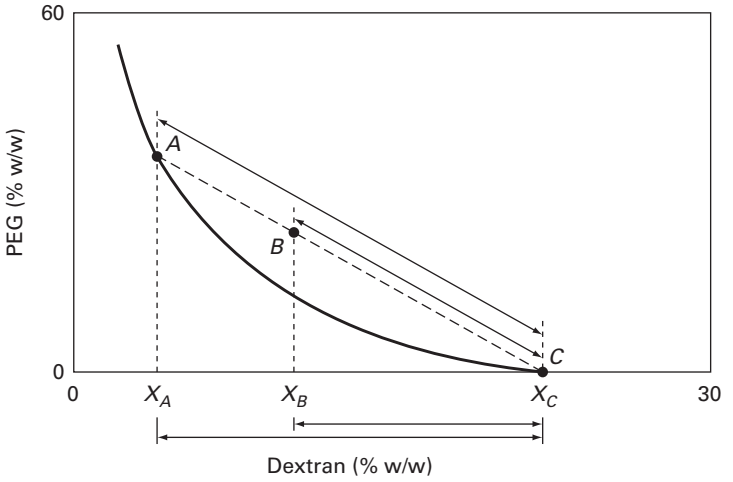

FIGURE 13.5 Phase separation lever rule diagram showing variables used in the inverse lever rule calculations for the purpose of determining phase volume ratios.

(3) What is the significance of the ratio of the mass of hemoglobin in the top phase to that in the bottom phase? What is the extraction factor, and what is the extracted fraction in each case? If these factors varied, why did they vary?
(4) Why was NaCl added to the phase system?

5. *Concluding remarks,* in which your findings are summarized. In particular, explain how the data you obtained would be used in an extraction procedure, and discuss why the PEG/dextran phase system is suitable for protein extraction.
6. *Notation* page with a table of definitions of the dimensions or units for each of the symbols you used.
7. *References* used or relevant to this exercise, including authors, year, article title, journal or book title, volume number, and page numbers.

13.4.4 Inverse Lever Rule

The line connecting points *A* and *C* on the binodal curve in the phase diagram shown in Figure 13.5 is known as a *tie line*. The tie line connects the compositions at which the top and bottom phases are in equilibrium. Since the top and bottom phases are always of some uniform composition, the relative amount of each phase can be calculated using a material balance. If the system consists of a total of *N* moles (or grams), then at any point:

$$N = N_T + N_B \tag{13.4.2}$$

where N_T and N_B are the number of grams in the top and bottom phases, respectively.

Thus for a system of overall composition X_B, referring to Figure 13.5,

$$NX_B = N_T X_A + N_B X_C \tag{13.4.3}$$

Substituting Equation (13.4.2) into Equation (13.4.3), we get

$$\left(N_T + N_B\right) X_B = N_T X_A + N_B X_C \tag{13.4.4}$$

Rearranging leads to

$$\frac{N_T}{N_B} = \frac{X_C - X_B}{X_B - X_A} = \frac{\text{Length of line } BC}{\text{length of line } AB} \tag{13.4.5}$$

This equation is known as the *inverse lever rule.* Thus, the ratio of the masses of the top and bottom phases can be calculated simply as the ratio of the length of two segments of the tie line.

13.5 CHROMATOGRAPHY SCALE-UP

In this laboratory exercise, the elution volume, peak width, resolution, height equivalent of a theoretical plate, and number of theoretical plates will be determined for a small-scale column and a large-scale column, and these will be compared to determine the success of scale-up without significantly changing resolution.

13.5.1 Background

Column chromatography is a common procedure for purifying biological compounds such as proteins, nucleic acids, and antibiotics (see Chapter 7). The basis for separating one dissolved species from another in a mixture depends on the interaction of the solute molecules with the solid support (packing) and the liquid mobile phase. The ionic charge, molecular weight, or relative hydrophobicity may be used as the basis for separation. An ion exchange column is used for separating solutes based on their ionic charge.

13.5.2 Objectives

The goal of this experiment is to obtain hands-on experience in running an ion exchange chromatography column and to learn how to operate the column to separate two different proteins. Equipment used in this experiment will be chromatography columns and other instruments commonly found in purification laboratories. A scale-up calculation will be performed using the Yamamoto (constant resolution) approach.

13.5.3 Procedure

This exercise will require some prelaboratory preparation before the laboratory procedures can be implemented. The prelaboratory preparation will aid in being prepared to make all the appropriate measurements.

Prelaboratory Preparation

Review the small-scale column chromatogram (Figure 13.6) and calculate the resolution (R_s), the gradient slope (G), and the Yamamoto number (Y_m) for the separation of ribonuclease A from cytochrome c. Use the relevant equations, which are given

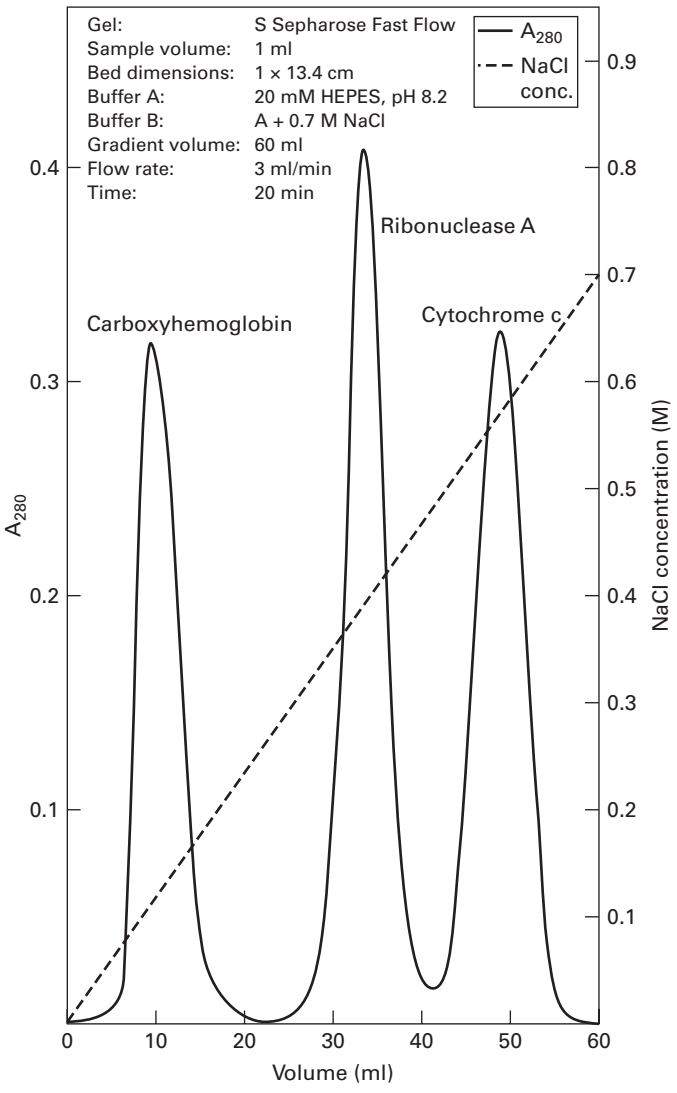

FIGURE 13.6 Small-scale column chromatogram for feed containing carboxyhemoglobin (2.0 mg), ribonuclease A (2.0 mg), and cytochrome C (1.8 mg). *(Courtesy of GE Healthcare Biosciences)*

below. Assume for S Sepharose Fast Flow (the packing that will be used) that $\varepsilon = 0.3$ and d_p = 100 μm. Bring these calculations to the laboratory, and be prepared to review them at the time of the experiment.

Constant Resolution Relationships

The scale-up principle described in Chapter 7 (Section 7.10.2) is based on the principle of having the same resolution at all levels of scale-up. From Equation (7.4.3) for resolution, using average elution volumes instead of average retention times, we write

$$R_s = \frac{V_2 - V_1}{\frac{1}{2}(w_2 + w_1)} \tag{13.5.1}$$

where V_2 and V_1 are the average elution volumes at which components 2 and 1 emerge from the column, respectively, and w_2 and w_1 are the widths of the respective elution peaks. The peak width w is defined in Figure 7.7, and it is calculated as

$$w = 4\sigma \tag{13.5.2}$$

where σ is the standard deviation of the peak.

From the theory for constant resolution, we next define a number, Y_m, which, when held constant, can be used to calculate the scaled operating values. For the purpose of this exercise, the following form is used [see Equation (7.10.11)]:

$$Y_m = \left(\frac{L}{G(1-\varepsilon)ud_p^2} \right)^{1/2} \tag{13.5.3}$$

where L is the bed height, u is the interstitial flow velocity, d_p is the diameter of a resin particle, ε is the void fraction, and G is the normalized gradient slope, which is given by Equation (7.10.18). If we assume that the void fraction and size of the resin particle are not changed with scaleup, then the relationship of interest is simply

$$\left(\frac{Y_{m1}}{Y_{m2}} \right)^2 = 1 = \frac{L_1 G_2 u_2}{L_2 G_1 u_1} \tag{13.5.4}$$

Finally, for constant resolution, the volume of the gradient components to be used in the laboratory column can be determined by writing Equation (7.10.18) as

$$V_g = \frac{V(C_{hi} - C_{low})}{G} \tag{13.5.5}$$

where V is the column volume and V_g is the total gradient volume.

Laboratory Procedure

1. With the help of the instructor, determine the proper operating parameters for the particular column with which you will work. Each group may work with a different set of column parameters. Errors can result from improper chart connections, pumping speed, or calibrations. Assignment of tasks is important.
2. Equilibrate the column with the buffer provided for this purpose, and set up the UV detector and recorder to be sure it is functioning properly.
3. Load the protein mixture onto the column.
4. Separate the proteins from one another by eluting the column with the salt gradient. During this time, record the optical absorbance and conductivity at the outlet, and monitor the elution volume by collecting the eluant in a graduated cylinder.
5. Obtain a copy of the chromatogram (recording of optical density versus time), and record the volumetric data, column parameters, equipment sketch, and any other relevant information needed for completing the report.
6. Reequilibrate the column(s).

13.5.4 Report

Each person will prepare an *individual* written report using the following outline:

1. One-paragraph summary.
2. Experimental procedure, including sketch of equipment.
3. Calculation of R_s, G, and Y_m for the small-scale column using Equations (13.5.1), (13.5.2), (13.5.3), and (7.10.18).
4. Graphical summary, including a copy of the chromatogram you obtained during the experiment with the salt gradient superimposed.
5. Calculation of the values of V_e and w in milliliters, the height equivalent of a theoretical plate (HETP), number of theoretical plates (N), and R_s for the experiment column. Discuss whether the scale-up was or was not successful. N is determined from the following form of Equation (7.4.2):

$$N = \frac{V_e^2}{(w/4)^2} \tag{13.5.6}$$

where w is the peak width and V_e is the volume required to elute a particular separand out of the column. The corresponding plate height is

$$\text{HETP} = \frac{L}{N} \tag{13.5.7}$$

Each of these values should be calculated for each separand.

6. Concise written discussion of results, errors, and measurement inaccuracies.
7. Scaling calculation performed by describing how you would operate a 10 liter column to give the same resolution as the small-scale column or the large-scale column. Include column diameter, bed height, linear and volumetric flow rates, and total gradient volume calculations for the 10 liter column. The column you choose should be available from Millipore (see Table 13.4), and the flow properties of S Sepharose Fast Flow packing should be considered (Figure 13.7). Discuss why you selected your particular design, and list your assumptions and considerations.

   Limit reports to seven pages, including graphs and sketches.

TABLE 13.4 Characteristics of Moduline® Acrylic Biochromatography Columns: Sizes and Pressure Ratings

Diameter × length (mm)	Adjustable length (mm)	Cross-sectional area (cm^2)	Adjustable capacity (liters)	Gage pressure rating (bar)
70 × 500	0–500	38	0–1.9	4
70 × 1000	500–1000	38	1.9–3.8	4
90 × 500	0–500	64	0–3.2	4
90 × 1000	500–1000	64	3.2–6.4	4
140 × 500	0–500	154	0–7.7	4
140 × 1000	500–1000	154	7.7–15.4	4
180 × 500	0–500	254	0–12.6	4
180 × 1000	500–1000	254	12.6–25.4	4
250 × 500	0–500	500	0–25	2
250 × 1000	500–1000	500	25–50	2
350 × 500	0–500	962	0–48	2
350 × 500	0–500	962	0–48	3
350 × 1000	500–1000	962	48–96	2
350 × 1000	500–1000	962	48–96	3
440 × 500	0–500	1520	0–76	1
440 × 500	0–500	1520	0–76	3
440 × 1000	500–1000	1520	76–152	1
440 × 1000	500–1000	1520	76–152	3
630 × 500	0–500	3119	0–156	3
630 × 1000	500–1000	3119	156–312	3

Source: Millipore, Inc., 2002

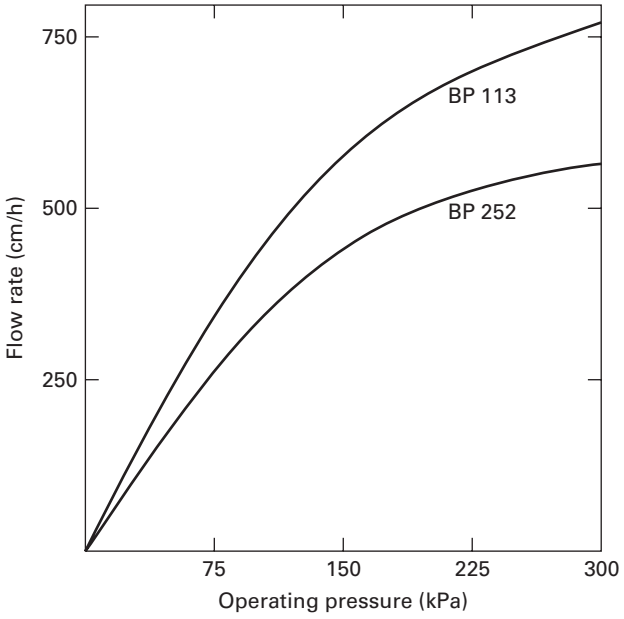

FIGURE 13.7 Pressure–flow characteristics for S Sepharose Fast Flow resin columns. BP 113 column: 15 cm bed height and 100 cm^2 cross-sectional area. BP 252 column: 15 cm bed height and 500 cm^2 cross-sectional area. *(Courtesy of GE Healthcare Biosciences)*

REFERENCES

1. Spinco Division of Beckman Coulter, Inc. (1995). *Beckman Coulter JCF-Z Instruction Manual*, Beckman Coulter, Palo Alto, CA.
2. Albertsson, P.-Å. (1986). *Partition of Cell Particles and Macromolecules*, Wiley, New York.
3. Walter, H., Brooks, D. E., and Fisher, D. (1985). *Partitioning in Aqueous Two-Phase Systems*, Academic Press, Orlando, FL.

APPENDIX

TABLE OF UNITS AND CONSTANTS

UNITS, MECHANICAL

Mass:	1 kg
	2.2046 lb_m
Length:	1 m
	3.2808 ft
	39.370 in.
Volume:	1 m^3
	1000 liters
	35.314 ft^3
	264.17 U.S. gal
Force:	1 newton (N) (kg m s^{-2})
	10^5 dynes (g cm s^{-2})
	0.22488 lb_f
Pressure:	1 atm
	101.33 kPa (kN m^{-2})
	1.0133 bars
	1.0133×10^6 g cm^{-1} s^{-2} (dyne cm^{-2})
	760 mm Hg (torr) at 0°C
	14.696 psia (lb_f $in.^{-2}$)
	29.921 in. Hg at 0°C
Energy:	1 joule (J) (N m)
	10^7 g cm^2 s^{-2} (erg) (dyne cm)
	0.23901 cal
	3.7251×10^{-7} hp h
	2.7778×10^{-7} kW h
	0.73756 ft lb_f
	9.4783×10^{-4} Btu

Power: 1 W ($J\ s^{-1}$)
10^7 g $cm^2\ s^{-3}$ (erg s^{-1})
0.73756 ft $lb_f\ s^{-1}$
1.3410×10^{-3} hp
9.4782×10^{-4} Btu s^{-1}

Viscosity: 1 centipoise (cp) (commonly used unit)
0.01 poise (g $cm^{-1}\ s^{-1}$) (dyne s cm^{-2})
10^{-3} Pa s (N s m^{-2}) (kg $m^{-1}\ s^{-1}$)
6.7197×10^{-4} $lb_m\ ft^{-1}\ s^{-1}$
2.0886×10^{-5} lb_f s ft^{-2}

UNITS, ELECTRICAL

Potential: 1 volt (V)
1 J C^{-1} (C = coulomb)

Charge: 1 electron charge
1.6022×10^{-19}C

UNITS, MAGNETIC

Field strength: 1 A m^{-1}

Flux density: 1 Tesla (T) (N $A^{-1}\ m^{-1}$)

Magnetization: 1 A m^{-1}

Constants

The Gas Constant, R

The gas constant *R* occurs in many forms, depending on the applications. The first two values apply to thermal energy in an ideal gas (often applied to solutions). The remaining values apply to conversions involving pressure explicitly and are useful in osmotic pressure applications (van't Hoff approximation).

8.3145 J g-$mol^{-1}\ K^{-1}$
1.9872 cal g-$mol^{-1}\ K^{-1}$
8.3145×10^3 Pa m^3 g-$mol^{-1}\ K^{-1}$
0.082058 liter atm g-$mol^{-1}\ K^{-1}$
0.73020 ft^3 atm lb-$mol^{-1}\ R^{-1}$

Other Constants

Acceleration of free fall on earth	$g = 9.8066 \text{ m s}^{-2} = 980.66 \text{ cm s}^{-2}$ $= 32.173 \text{ ft s}^{-2}$
Avogadro's number	$N = 6.0221 \times 10^{23}$ molecules g-mol^{-1}
Boltzmann's constant	$k = 1.3807 \times 10^{-23} \text{ J K}^{-1}$
Dielectric constant (relative) for water at 25°C	$\varepsilon_r = 78.3$
Electron charge	$e = 1.6022 \times 10^{-19} \text{ C}$
Faraday's constant	$F = 9.6485 \times 10^{4} \text{ C g-mol}^{-1}$
Hamaker constant (approximate)	$A = 10^{-19} \text{ J}$
Magnetic permeability	$\mu_o = B/H = 4\pi \text{ x } 10^{-7} \text{ T m A}^{-1}$
Permittivity of free space (vacuum)	$\varepsilon_0 = 8.8542 \times 10^{-12} \text{ C}^2 \text{ J}^{-1} \text{ m}^{-1}$ (farads m^{-1})

BIBLIOGRAPHY

Bird, R. B., Stewart, W. E., and Lightfoot, E. N. (2002). *Transport Phenomena,* 2nd ed., Wiley, New York.

Dean, J. A., ed. (1992). *Lange's Handbook of Chemistry,* 14th ed., McGraw-Hill, New York.

Weast, R. C., ed. (1985). *CRC Handbook of Chemistry and Physics,* 66th ed., CRC Press, Boca Raton, FL.

INDEX

acetic acid bacteria, 5–6
adsorption, 245–326
  adsorbent types, 288–293, 314
  affinity, 282–283, 314
  agitated-bed adsorption, 258–259, 305–306, 314
  of antibiotics, 250, 258–259, 290, 305–306
  breakpoint time in fixed beds, 300–304
  breakthrough in fixed beds, 255–257, 300–304, 313
  column dynamics, 251–259, 312–313
  columns, 295
  computer simulation method for scale-up of fixed beds, 304–305
  constant pattern behavior in fixed beds, 257–258, 301
  detectors, 297–298
  effective velocity in fixed beds, 253, 264–268, 313
  equilibrium, 248–250, 312
  Freundlich equilibrium isotherm, 250, 254, 259, 304–305, 312
  of hormones, 250
  ideal adsorption time in fixed beds, 300–304
  mass balance for fixed beds, 251–257, 313–314
  mass transfer coefficient, 252–257, 272–274, 304–305, 312
  Langmuir equilibrium isotherm, 249–250, 253–254, 257, 265–269, 312
  length of unused bed (LUB) method for scale-up of fixed beds, 258, 299–304, 314
  linear equilibrium isotherm, 248–250, 254–257, 264–265, 270–272, 304–305, 312
  linear equilibrium isotherm and negligible dispersion in fixed beds, 254–257, 313
  local equilibrium and negligible dispersion in fixed beds, 253–254, 313
  mixing model for agitated beds, 229–230
  nonlinear equilibrium isotherm, 249–250, 257–258, 265–269, 304–305, 312–313
  periodic countercurrent operation of agitated beds, 258–259, 305–306
  of proteins, 249, 257, 277–279
  Runge-Kutta method to model agitated-bed adsorption, 259
  scale-up, 299–306, 314
  shock wave velocity in fixed beds, 253–254, 266–268, 313
  of steroids, 250
  void fraction in fixed beds, 252
affinity
  chromatography, 292–293, 446, 452, 496–497
  extraction, 225–226
agitated beds, adsorption in. *See* adsorption
alcohols
  denaturation of proteins, 331, 349
  precipitation of proteins, 348–351
  production, 5–6
amino acids
  α-amino acid abbreviations, 8
  α-amino acid structure, 7–8
  analysis, 82–83
  biosynthesis, 5
  p*K* of R group, 8
  reverse osmosis, 450
  size, 4
analytical methods, 48–110
  accuracy, 52, 102
  agarose gel electrophoresis, 72
  amino acid analysis, 79–80, 82
  amino acid sequencing, 79–82
  ampholytes, 69–70
  animal model assays, 55–56, 102
  bioburden, 88–89

analytical methods (*cont.*)
biological activity, 49, 55–59, 102
capillary electrophoresis, 68–69, 72, 102
cell-line-derived bioassays, 56–57, 102
CHNO analysis, 82–83
continuous method of biochemical assay, 57–59, 102
Coomassie blue staining, 73
dilution test for assay of antibiotics, 57
DNA analysis, 66, 72–74, 76
DNA hybridization, 86–87
dry weight, 87
electrolysis reactions in electrophoresis, 65–66
electroosmosis, 61
electrophoresis principles, 60–61
electrophoretic analysis, 60–76, 102
electrospray ionization (ESI) mass spectrometry, 77, 79, 102
endotoxin, 89
enzyme activity, 57–59, 102
enzyme-linkedimmunosorbent assay (ELISA), 84–86
fluorescence detection in electrophoresis, 73–74
gas chromatography, 86
heat generation in electrophoresis, 61–65, 68, 70
HPLC, 52–53, 76–80, 102, 296, 298–299
HPLC and mass spectrometry, coupling of, 80
identity determination, 49–50, 53
in vitro biochemical assays, 57–59, 102
inductively coupled plasma (ICP) coupled with mass spectrometry (MS) or atomic emission spectroscopy (AES), 87
isoelectric focusing, 69–70, 75, 102–103
limit of detection (LOD), 54, 102
limit of quantitation (LOQ), 54
linearity, 53–54, 102
mass spectrometry, 79–80, 102
matrix-assisted laser desorption/ionization (MALDI) mass spectrometry, 79
microbiology assays, 88–90
native gel electrophoresis, 67–68, 102
Northern blot, 77
paper electrophoresis, 70–71
physical/appearance qualities, 49–50
polyacrylamide gel electrophoresis, 66–67, 71–72
precision, 51–52, 102
protein analysis, 66–86, 102
pulsed field electrophoresis, 76
purity, 49–50, 53, 59–87, 102
radioactivity detection in electrophoresis, 74
range, 54–55, 102
RNA analysis, 77
robustness, 55, 102
SDS-PAGE, 66–67, 75, 102
Southern blot, 77
specifications, 49–50, 101
specificity, 52–53, 102
staining in electrophoresis, 72–73
sterility, 88, 102
stopped method of biochemical assay, 57, 102
two-dimensional electrophoresis, 75–76
units of enzyme activity, 57–59
UV absorbance, 80–82
virus and phage, 89–90
Western blot, 66–67, 76–77
animal cells, 4, 114, 131
antibiotics
adsorption, 250, 259, 290, 305–306
analysis of biological activity of, 56–57
biosynthesis routes, 12
in cell lysis, 116
crystallization, 362, 368, 378
drying, 409, 411–412, 417, 426
partition coefficient in solvent extraction, 220–221, 223–226, 228–231, 235, 239
recovery by filtration, 166–167, 450
reverse osmosis, 450
solvent extraction, 220–222, 230–232, 235–236, 448
structure of three well-known antibiotics, 11
antibodies
in affinity chromatography, 292–293
in affinity precipitation, 329
monoclonal, 19, 85, 495–502
production of therapeutic monoclonal antibodies, 495–502
structure, 19
use in ELISA assay, 84–86
use in Western blots, 66–67, 76–77
amylose, 33
aqueous two-phase extraction. *See* extraction

batch operations
in bioprocess design, 445, 454–455
crystallization, 368–373

Beer-Lambert law, 80–81
bench scale preparative separations, 90–101, 103
  density gradient electrophoresis, 91, 93–94
  electrophoresis, 90–96, 103
  free-flow electrophoresis, 91–93
  magneticbioseparations, 96–101, 103
  magnetic separators, 100–101
  recycling isoelectric focusing, 91, 95
  rotating isoelectric focusing, 91, 96
biological activity. *See* analytical methods
bioprocess design and economics, 441–510
  Aspen Batch Process Developer, 455
  batch versus continuous mode, 445
  Batches process simulator, 454
  citric acid production, 472–479
  discrete event simulators, 455
  environmental impact assessment, 444, 487–489
  generalized block diagram of downstream processing, 445–446
  GIGO principle, 460
  heuristics, 445, 447, 449–450, 452, 503
  human insulin production, 479–494
  minimum requirements for a biochemical process simulator, 457
  monoclonal antibody production, 495–502
  pairing of unit operations in process synthesis, 453–454
  process analysis, 442, 454–460, 502
  process economics, 460–472
  process simulators, 457–460, 472–503
  process synthesis, 442, 445–454, 502
  rules of thumb, 445, 447, 449–450, 452, 503
  sensitivity analysis, 501–502
  spreadsheets, 454
  SuperPro Designer biochemical process simulator, 455, 472–502
  throughput analysis and debottlenecking, 459, 493–494
  unit procedure, 457–459
bioproducts, 1–35, 40–42
  categories, 2–4
  documentation, 41–42
  formulation, 42
  GLP and cGMP, 42
  prices, 2
  productions levels, 2
  range of applications, 40–41
  route to market, 40–42
  sales forecasts, 2
Blake-Kozeny equation, 294, 311
blood cells, field-flow fractionation of, 209–210
blood plasma, fractional precipitation of, 349–351
Boltzmann distribution rule, 207
bound water, 408, 411–412, 424
boundary layer in crossflow filtration. *See* filtration
Brønsted model of partitioning in extraction, 221–222

cake filtration, 137–143, 163–168, 176–177, 473
Camp number, 344
Camp and Stein equation for estimation of average shear rate, 341–342
capillary electrophoresis. *See* analytical methods
Carman-Kozeny equation, 206
cefazolin sodium, drying of. *See* drying
cell disruption. *See* cell lysis
cell flocculation, 120–131
  charge of bioparticles, 121–124
  critical flocculation concentration, 126–128, 131
  Debye radius or length, 123–125, 129, 131
  Debye-Hückel constant, 121–123
  DLVO theory, 126–128, 131
  electric double layer, 121–125, 131
  electrolytes, effect of indifferent, 126–128
  electrostatic potential, 122–124
  Gouy-Chapman theory, 122–123
  London forces, 121–122
  polymeric flocculants, 129–131, 511–514
  rate, 129
  Shulze-Hardy rule, 128–129, 131
  temperature, effect of, 126–128
  van der Waals forces, 121–122, 125–126
  zeta potential, 123
cell lysis, 114–120
  alkali treatment, 115
  of animal cells, 115–117, 131
  by antibiotics, 116
  of bacteria, 115–119, 482
  bead or ball mill, 115, 119–120, 131, 446–447
  cell wall digestion, 115–116, 131
  chemical lysis, 114–117
  by detergents, 116–117
  of *E. coli*, 115, 119, 482

cell lysis (*cont.*)
enzyme digestion, 116–117
of eukaryotes, 114–117
high-pressure homogenizer, 117–119, 131, 447, 482–483
in human insulin purification, 482–483
lipid dissolution, 115, 117
mechanical methods, 115, 117–120, 131, 446–447, 482–483
osmotic lysis, 113–116, 131, 446–447
of plant cells, 115, 131
plasma membrane breakage, 116–117
of prokaryotes, 112–113, 114–119, 131
protein release during high-pressure homogenization, 117–119
of red blood cells, 115
by solvents, 115,117
of yeast, 115, 117–119
cells
animal, 114–117
centrifugation, 187–188, 199–200, 482
density, 189
eukaryotic, 113–114, 131
field-flow fractionation, 209–210
flocculation, 111, 120–131, 449, 511–514
inclined settling, 207–209
lysis, 111–112, 114–120, 131, 446–447, 482–483
plant, 114–115
prokaryotic, 112–113, 131
sedimentation radius, 188
settling velocity, 188
centrifugation. *See* sedimentation
chitin, 33
chromatography, gas. *See* analytical methods
chromatography, liquid, 245–326
adsorbent types, 288–293, 314
affinity chromatography, 292–293, 314
column dynamics, 259–279, 312–313
column packing procedures, 296–297
columns, 295–296
computer simulation of, 275–277, 313
detectors, 297–298
dispersion coefficient, 270
dispersion effects, 269–277, 312–313
displacement mode, 246, 279
effectivedispersivity, 252, 270–271, 275–276
efficient separation, maximization, 273–274
elution chromatography, 245–246, 277–279, 306–307, 310, 486–487, 497–498, 526–527
equipment, 295–299, 529
expanded bed, 246, 446–448
frontal mode, 246
Gaussian peak properties, 260–261
gradient elution, 277–279, 306–307, 310, 314, 497, 526–527
height of equivalent theoretical plate (HETP), 261–264, 272–274, 528
HPLC, 49–50, 52–53, 76–80, 296, 298–299, 486–487
in human insulin purification, 483, 485–487
hydrophobic interaction chromatography, 292, 314, 453, 483, 485–486, 496–498
immobilized metal affinity chromatography (IMAC), 293, 314
ion exchange resins, 290–291, 314, 483, 485–486
isocratic elution, 479
mass balance, 251–253, 264, 312
membrane, 279–284, 313
models that consider intraparticle diffusion and fluid phase mass transfer, 271–272
molecular or binary diffusivity in mobile phase, 270, 272–274
moment analysis of, 262–264, 313
in monoclonal antibody purification, 496–498
with negligible dispersion, 264–269
of nucleic acids, 290
on-off chromatography, 245–246, 279
optimum particle size, 274, 294–295
of peptides, 289–290
plate models, 260–261, 313
polymer-based resins, 289–290
pressure drop in fixed beds, 294–295, 311, 314, 530
of proteins, 289–290, 292–293, 306–310, 483, 485–487, 496–498, 525–530
resolution, 261, 306–307, 314, 527
reversed-phase chromatography, 291–292, 483, 486–487
scale-up, 306–311, 314, 535–530
silica-based resins, 288–289
simulated moving bed, 284–288, 313–314
size exclusion (or gel filtration) chromatography, 293, 314, 483, 487
system fluidics, 298–299
vanDeemter equation, 272–274, 313
Yamamoto scale-up equation, 306–308, 527
circular dichroism (CD), 14

citric acid
  bioprocess design of purification process, 473–479
  uses, 472
coagulation. *See* flocculation
coefficient of determination (r^2) for linear least squares fitting, 53–54
concentration polarization in crossflow filtration. *See* filtration
constant rate drying. *See* drying
conventional or dead-end filtration. *See* filtration
cost, 460–472
  air filters, 477
  buildings, 462, 478
  capital cost estimation, 460–465, 476–478, 491–492, 494, 499–501, 503
  chromatography columns, 464, 477
  chromatography resins, 493, 501
  consumables, 466–469, 478, 493, 501, 503
  design estimates, types and cost of, 442–444
  disk centrifuges, 463
  drug development, 460–461
  facility overhead, 470–471, 479, 492–493, 501
  labor, 466–467, 478–479, 492–493, 501, 503
  laboratory/QC/QA, 469–470, 478, 492–493, 503
  maintenance of equipment, 470, 503
  membrane filtration systems, 463
  membranes, 493, 501
  operating cost estimation, 466–471
  raw materials, 467, 476, 478–479, 492–494, 501, 503
  rotary vacuum filters, 477
  scaling law for equipment cost estimation, 465
  six-tenths rule for equipment cost estimation, 465
  start-up and validation, 466, 503
  utilities, 470, 478–479, 493, 501, 503
  vessels, 477
  waste treatment and disposal, 470, 478–479, 492–493, 503
  water for injection (WFI), 501
  working capital, 465, 503
countercurrent stage calculations. *See* extraction
crossflow filtration. *See* filtration
crystallization, 362–383
  advantages of, 362
  of alcohol oxidase, 374
  of antibiotics, 362, 368, 378
  average crystal size, 367
  average linear growth rate for batch experiments, 367
  average mass of crystals, 368
  average nucleation rate from batch experiments, 367
  average surface area of crystals, 368
  batch crystallizers, 368–373, 379
  of citric acid, 473–475
  comparison to precipitation, 362–363
  constant impeller tip speed for scale-up, 377, 379
  constant power per volume for scale-up, 377–379
  contact nucleation, 365
  crystal forms, 363–364
  crystal growth, 366–367, 369–373, 379
  crystal habit, 364
  crystallography, 362
  growth by diffusion, 366
  growth by surface integration, 366
  heterogeneous primary nucleation, 364, 379
  homogeneous primary nucleation, 364, 379
  of human insulin, 375, 487
  kinetics from batch experiments, 367–368
  labile region of crystal nucleation and growth, 365
  linear growth rate, 366, 369
  of lipase, 374–375
  mass transfer coefficient, 366
  metastable region of crystal growth, 365, 375
  minimum speed required for particle suspension, 377, 379
  mixing scale-up, 377–379
  moments analysis of batch experiments, 367–368, 379
  nucleation, 364–365, 367, 370–371, 379
  of ovalbumin, 374
  phase diagram, 365
  primary nucleation, 364, 375, 379
  principles, 363–368
  problems with crystals not meeting specifications, 376
  of proteins, 373–375, 483, 487
  purity of crystals, 362, 376
  rate of mass deposition during growth, 366
  recrystallization, 376
  scale-up and design, 375–379
  scale-up ratios, 376
  secondary nucleation, 364–365, 379

crystallization (*cont.*)
shear nucleation, 364–365
strategy to crystallize proteins, 373–374
supersaturation, 364–366, 371–372, 379

Damköhler number, 274
Darcy equation (or law), 38, 137, 148, 176, 294, 314
Debye radius (or length). *See* cell flocculation
Debye-Hückel constant. *See* cell flocculation
depreciation, 470–471, 503
diafiltration. *See* filtration
diatomite, 153
diffusion
in chromatography and adsorption, 270–276, 282–284, 306–307
in crossflow filtration, 144–148, 177
in crystallization, 366
in drying, 417–418
in eddies, 335
in precipitation, 336–341
in sedimentation, 206
distillation, 446, 450–451
DLVO theory. *See* cell flocculation
DNA
analysis of, 60, 66, 73–74, 76–77
chromatography of, 380–282
purification of plasmids, 33
structure, 31–32
vectors, 32
dryers, 422–436
batch rotary dryers, 407, 423–424, 428, 435–436, 474–475, 477
description and operation, 422–427
fluidized-bed dryers, 446, 453
freeze dryers, 407, 424–426, 428–431, 436, 446, 453, 487
pilot scale, 427, 436
scale-up and design, 427–436
small scale, 427–428, 431, 436
spray dryers, 407, 426–427, 431–436, 446, 453
vacuum-shelf dryers, 407, 422–423, 427, 435
drying, 407–440
adiabatic cooling, 409–411
advantages of freeze drying, 425–426, 453
analytical solution for drying by moisture diffusion, 418–419
of antibiotics, 409, 411–412, 417–418, 426
atomization during spray drying, 426–427, 431, 434, 436
batch rotary drying, 407, 423–424, 428, 435–436, 474–475, 477
bound water, 408, 411–412, 424
boundary layer control of drying rate, 417
capillary flow, 417, 420
of cefazolin sodium, 409, 411–412
in citric acid production, 474–475
collapse of product during freeze drying, 425
by conduction, 413–415, 422, 435
constant rate, 415–417, 419–421, 435
by convection, 413–417, 419–422, 432
critical moisture content, 415–416, 418–420, 435
dielectric or microwave heating, 413
drying periods, 415–417, 435
drying rate curve, 415–417, 435
equilibrium moisture content, 408–412, 415–416, 418–420, 435
excipients in freeze drying, 428
falling rate, 415–418, 435
freeze drying, 407, 424–426, 428–431, 436, 446, 453, 483, 487
freeze-drying cycle, 424–425
gravity flow, 417
heat transfer principles, 412–415
heat transfer coefficient, 413–414, 416–417, 419–421, 432, 435
heat transfer mechanisms, 413
of human insulin, 409, 483, 487
hygroscopic solids, 408, 416–417, 435
liquid diffusion, 417–419, 435
mass transfer coefficient, 416
mass transfer mechanisms, 417–422
mass transfer principles, 415–422
of microorganisms, 426
moisture diffusion coefficient, 418–419, 435
nonhygroscopic solids, 416–417, 435
pilot scale, 427–429, 436
principles, 408–422
of proteins, 409, 418, 425, 431, 483, 487
radiation, 413
reasons for drying, 407
receding front model of drying, 414–415, 424
residence time in spray drying, 431
scale-up and design, 427–436
shrinkage in, 417–418, 420
shrinking core model of drying, 414–415
sizing of a spray dryer, 431–435
small scale, 427–428, 431, 436
of spores, 426

spray drying, 407, 426–427, 431–436, 446, 453
by sublimation, 424, 429, 436
theoretical correlation for spray dryer scale-up, 432
of tissue type plasminogen activator (tPA), 409
unbound or free water, 408, 411–412, 424
vacuum-shelf drying, 407, 422–423, 427–428, 435
vapor diffusion in, 417
wet-bulb temperature, 409, 411, 417, 426

Einstein diffusion equation, 206, 283, 335, 338
electric double layer. *See* cell flocculation
electroosmosis, 61, 92–93
electrophoresis. *See* analytical methods
electrophoretic analysis. *See* analytical methods
electrophoretic mobility, 61, 93–94, 102
electrostatic potential. *See* cell flocculation
elution. *See* chromatography, liquid
endotoxin. *See* analytical methods
engineering analysis, basic principles of
material balance, 37
equilibria, 37–38
flux relationships, 38
enthalpy, 411, 433
environmental impact assessment. *See* bioprocess design and economics
enzyme-linked immunosorbent assay (ELISA). *See* analytical methods
enzymes
active site, 20
analysis of activity, 57–59, 102
aqueous two-phase extraction of, 222–224
lactate dehydrogenase refolding, 29
in proinsulin conversion, 481, 486
error function, 270
erythromycin, 11, 36–37
eukaryotic cells, 113–114, 117, 131
eutectic temperature, 425, 428
evaporation, 384–406
agitated-film evaporator, 399, 403
in bioseparation processes, 446, 450
boiling point elevation in, 386, 402
climbing-film evaporator, 397–398, 402
equipment, 396–403
falling-film evaporator, 398, 402
foaming in, 395, 397, 399
forced-circulation evaporator, 399, 403
fouling in, 385, 397, 399, 396–397, 399, 400
heat transfer, 385–394
heat transfer coefficient, 385–386, 391–393
in insulin purification, 483–484
multi-effect, 400–401
principles, 385–396
scale-up and design, 399–402
vapor-liquid separation, 394–395
excipients, 42, 428
extraction, 219–244
affinity partitioning, 225–226
antibiotic partition in solvent extraction, 221, 230–232, 235–236
aqueous two-phase extraction, 222–226, 239, 446, 454, 520–525
biospecific ligands in aqueous two-phase systems, 225–226, 240
centrifugal extractors, 232, 237–239
column volumetric efficiency of reciprocating-plate extractor, 235
countercurrent stage calculations, 226–232, 240
equilibrium, 220–232
equipment, 232–239
equivalent time in scale-up, 237–239
extraction factor, 228–230, 239
by extractive distillation, 446
height equivalent to a theoretical stage (HETS), 232–236
McCabe-Thiele-type diagram for countercurrent stage calculations, 228, 240
models of partitioning, 221–224
with organic solvents, 219, 221–222, 230–232, 235–237, 446, 448, 453–454
partition coefficient, 220–226, 228–231, 520
partitioning equilibria, 220–232
penicillin partitioning in solvent extraction, 221
phase diagram for aqueous two-phase systems, 222, 239, 521–525
Podbielniak centrifugal extractors, 237–240
principles, 220–232
protein partitioning in aqueous two-phase systems, 223–226, 520–525
with reverse micelles, 446
reciprocating-plate extraction columns, 232–236, 240
scale-up and design of extractors, 232–240
stage efficiency, 232
with supercritical fluids, 446
extractors, 232–240

fatty acids, 9–10
Fick's first law of diffusion, 38
Fick's second law of diffusion, 418
filters
  bomb, 167–168
  conventional or dead-end, 152–156, 447–449, 473–475, 477, 483–484
  crossflow, 156–160, 447–450, 463, 485–487, 496–498
  depth, 169, 171, 447
  flat plate, crossflow, 158–159
  hollow fiber, 158–159
  leaf, 154–155
  Nutsche, 154
  plate-and-frame press, 153–154, 446–449, 473–474, 477
  rotary vacuum filter, 154–156, 164–167, 447–449, 473–474, 477
  rotating cylinder crossflow filters, 158–160
  spiral-woundcrossflow filters, 158–159
  tubularcrossflow filters, 158–159
filtration, 135–184
  air sterile filtration, 170–171
  antibiotic recovery by, 166–167, 449
  batch operation of crossflow filters, 172, 175–177
  boundary layer in crossflow filtration, 143–145, 177
  cake compressibility factor, 141
  in citric acid production, 473–475, 477
  complete recycle in crossflow filtration, 172–173, 177
  concentration polarization in crossflow filtration, 143–149
  configuration of crossflow filters, 157–160
  continuous operation of crossflow filters, 175–177
  conventional or dead-end filtration, 135–143, 152–156, 163–171, 446–449, 473–475, 477, 483–484
  crossflow filtration, 135–136, 143–152, 156–160, 171–177, 446–450, 452, 463, 483–487, 496–498, 514–518
  crossflow filtration modes of operation, 172–177
  diafiltration mode in crossflow filtration, 172–174, 446, 448–449, 451, 483–487, 496–497
  dissolved species in crossflow filtration, 143–149, 177
  feed-and-bleed mode in crossflow filtration, 175
  filter aids, 153
  filter leaf, 154–155, 163–165
  fouling of membranes, 160–162, 172, 177
  in human insulin purification, 483–487
  inertial-lift theory of crossflow filtration, 150, 177
  laminar flow in crossflow filtration, 145–146, 150–152
  liquid sterile filtration, 168–170
  mass transfer coefficient in crossflow filtration, 145–148, 150–152, 177
  media for conventional filtration, 152–153
  membranes, 156–160, 169–171, 493, 501
  microfiltration, 156, 160, 446–449
  in monoclonal antibody purification, 496–498
  by pervaporation, 451
  principles of conventional filtration, 137–143
  principles of crossflow filtration, 143–152
  of proteins, 145–149, 160–162, 173–174, 450–451, 483–487, 496–498
  proteins in membrane fouling, 160–162
  reverse osmosis, 446, 450
  scale-up and design of conventional filters, 163–171, 177
  scale-up and design of crossflow filters, 171–177
  shear-induced diffusion theory of crossflow filtration, 149–152, 177
  specific cake resistance, 137–141
  sterile filtration, 168–171
  suspended particles in crossflow filtration, 149–152, 177
  turbulent flow in crossflow filtration, 146–148
  ultrafiltration, 156, 160–162, 175–176, 446–447, 449–450
  washing of filter cakes, 141–143, 164, 166–168, 176
fixed beds, adsorption in. *See* adsorption
flocculation of cells and bioparticles. *See* cell flocculation
flotation, 446, 449
fouling of membranes. *See* filtration
Fourier's law of heat conduction, 64, 413–415
Freundlich equilibrium isotherm. *See* adsorption
fructose, 5

Gaussian distribution, 260, 262–264
glass transition temperature, 425, 428
GLP and cGMP. *See* bioproducts
glucose, 5
Gouy-Chapman theory. *See* cell flocculation
Graetz solution for mass transfer coefficient, 145–146
Gram-negative bacteria, 112–113
Gram-positive bacteria, 112–113
graphical methods, for multistage extraction, 227–230
growth hormone, human, 21, 56

Hamaker constant, 126–127
heat transfer coefficient. *See* drying; evaporation
heat of vaporization. *See* latent heat
height of the equivalent theoretical plate (HETP). *See* chromatography, liquid
height equivalent to a theoretical stage (HETS). *See* extraction
heterotrophs, 4–5
hormones
  adsorption isotherm for, 250
  human growth hormone, 21, 56
humidity, 408–412
humidity (or psychrometric) chart, 409–410
hybridoma cells
  development of, 19
  recovery by inclined settling, 208

inclusion bodies, 16, 26–28, 35, 43, 446–448, 451, 480, 482–484
insulin (bovine) structure, 14
insulin, human
  alternative production technologies, 480–481
  bioprocess design of purification process, 479–494
  drying of, 409, 493, 487
  properties, 479–480
inverse lever rule, 524–525
ion exchange, 290–291, 314, 483, 485–486
isoelectric focusing. *See* analytical methods
isoelectric point, 69, 330
isotherms, adsorption
  Freundlich, 250, 254, 259, 304, 312
  Langmuir, 249–250, 254, 257, 265–269, 312
  linear, 249–250, 254–257, 264–265, 270–272, 304, 312

ketones, 5–6
Kolmogoroff
  length, 335, 355
  model of mixing, 335, 355

laboratory exercises in bioseparations, 511–530
  aqueous two-phase extraction, 520–525
  centrifugation of flocculated and unflocculated particulates, 516–520
  chromatography scale-up, 525–530
  crossflow filtration of *E. coli* cells, 514–516
  flocculant screening, 511–514
  flocculation of cells and cell lysates, 511–514
Langmuir equilibrium isotherm. *See* adsorption
latent heat, 411, 416
Leveque solution for mass transfer coefficient, 145
linear gradient mixer, 190–191
linear least-squares fitting of data, 53–54
lipids, 5, 9, 113
London forces. *See* cell flocculation
lyophilization. *See* drying, freeze drying
lysis of cells. *See* cell lysis

magnetic bioseparations, 96–101, 103
magnetic permeability, 97–98
magnetic separators, 100–101
mass balance. *See* material balance
mass spectrometry. *See* analytical methods
mass transfer coefficient
  for convection of water evaporated at a solid surface, 416
  in crossflow filtration, 145–148, 150–152, 177
  in crystallization, 366
material balance
  in adsorption, 251–252, 258–259
  in chromatography, 251–252, 271–272, 275–276
  in crossflow filtration, 144
  in crystallization, 367, 369
  in extraction, 227
  in inclined settler, 207–208
  in precipitation for a CSTR, 345–346
  in process synthesis, 475–476, 487–489, 499–400
McCabe-Thiele graphical method for extraction countercurrent stage calculations, 227–229

membrane(s). *See* chromatography, liquid; filtration
microbiology assays. *See* analytical methods
microfiltration. *See* filtration
mixing, 258–259, 305–306, 335, 337–340, 352–354, 377–379
moment(s) analysis. *See* chromatography; crystallization
monoclonal antibodies. *See* antibodies
mother liquor, 334, 376

nucleation
  in precipitation, 335–340, 355
  in crystallization, 364–365, 367, 370–371, 374–376
nucleic acids
  biosynthesis, 5
  chromatography, 290–291
  size, 4
  structure, 31–33
nucleotides, 31
Nusselt number
  for heat transfer, 386–388, 391–393, 432
  for mass transfer, 274

Ohm's law, 38
oligonucleotides, 31–33
operating line for countercurrent extraction, 228
optical rotary dispersion (ORD), 7
organic acids, 4, 5–6, 472–479
osmotic pressure
  in cell disruption, 113–117, 131
  in filtration, 148

paramagnetism, 97–98
particulate products, 34–35
partition coefficient. *See* extraction
payback time, 471–472, 503
Péclet number, 207, 212, 274, 276
penicillin, 2, 116, 221
peptide
  bond, 7–8
  chromatography, 289–290
periplasm, 112–113
perlite, 153
pH, effect of on protein stability, 22–25
phospholipids, 9–10, 112–113
plant cells, 114, 131
plasma membrane of cell, 112–114, 116
Podbielniak centrifugal extractor. *See* extraction
polyacrylamide gel electrophoresis. *See* analytical methods
polypeptide hormones, 21
polysaccharides, 4–5, 33–34
population balances, 345–346, 348, 367, 369–370
precipitation, 327–361
  advantages, 327
  affinity precipitation, 329–330
  aging of precipitates, 335, 343–344
  of albumin, 349–350
  by ammonium sulfate, 333–334, 349
  average particle size, 348
  batch reactor, 352–354
  breakage of precipitate particles, 335, 343, 346–347, 355
  bulk volume of precipitate, 334
  Camp number as indication of particle strength, 344–345
  of α-casein, 337–338
  characteristics of protein precipitates, 334
  in citric acid purification, 473–474
  continuous flow stirred tank reactor (CSTR), 344–348, 352–353, 356
  denaturation of proteins by alcohols, 331, 349–351
  design of precipitation systems, 352–354
  effect of shear rate, 341–347, 352–353, 356
  effect of supersaturation on nucleation rate, 335–336
  flocculation enhancement, 341
  fractional precipitation, 327, 446, 452–453
  of gelatin, 349
  of γ-globulin, 349, 351
  goals, 327, 354
  growth governed by diffusion, 334, 336–341, 355
  growth governed by fluid motion, 334, 341–343, 356
  initial mixing, 335, 355
  of isoagglutinins, 349, 351
  isoelectric precipitation, 348–349, 356
  linear growth rate, 345–346
  mechanical strength of precipitates, 334, 343–344, 352
  methods, 348–352, 356
  model of breakage of protein precipitates, 343, 347
  molecular weight of particles, 337, 340–341, 355–356
  by nonionic polymers, 328–329, 351

nucleation, 335–340, 355
by organic solvents, 331–333, 348–351, 356
particle size distribution in a CSTR, 344–348, 356
of plasma proteins, 349–351
of plasminogen, 349, 351
population density distribution function, 345–348
precipitate formation phenomena, 334–344, 355–356
of proteins, 333–334, 337–341, 343–356
of prothrombin, 349, 351
rate of precipitant addition, 352–353
by salt addition, 331–334, 349–351, 356
salting-in effect, 331–333, 349–351, 355
salting-out, 331–334, 348–349
scale-up, 352–354, 356
of soy protein, 343–345
supersaturation in, 335–336, 353
tubular reactor, 352–353
preparative electrophoresis. *See* bench scale preparative separations
preparative separations. *See* bench scale preparative separations
primary metabolites, 4–9
process economics. *See* bioprocess design and economics
process synthesis. *See* bioprocess design and economics
profit margin (or gross margin), 471–472, 503
profitability analysis, 471–472, 476–479, 491–493, 499–501, 503
prokaryotic cells, 112–113, 131
protein analysis. *See* analytical methods
proteins, 13–31
adsorption, 249, 257, 277–278
analysis of, 58–59, 66–86, 102
antibody structure, 19
aqueous two-phase extraction, 222–226, 448, 520–525
biosynthesis of, 5, 16–18
chromatography, 289–290, 292–293, 306–311, 483, 485–487, 496–498, 525–530
circular dichroism (CD), 14
commercial uses, 19–21
crystallization, 373–375, 483, 487
denaturation, 16, 21–27, 331, 349
density, 189
diafiltration of, 173–174, 483–487, 496–497
disulfide bridges, 16–17, 43
drying, 409, 418, 425, 431, 483, 487
effect of pH on stability of, 22–25
effect of shear on stability of, 25
effect of temperature on stability of, 22–23
folding, 15–16, 28–30, 451, 480–481, 483, 485–486
folding modulators, 30–31
in fouling of membranes, 160–162
functions, 19–21
fusion partners, 26–27
genetic engineering to improve purification, 26, 42–43
α-helix structure, 14–15
inclusion bodies, 16, 26–28, 43, 446–448, 451, 480–484
microfiltration of, 160
molecular weight determination by ultracentrifugation, 204
optical rotary dispersion (ORD), 7
partition coefficient in aqueous two-phase extraction, 223–226
peptide bond, 7–8
posttranslational modifications, 17–18
precipitation, 333–334, 337–344, 348–356
primary structure, 13–14, 43
prosthetic groups, 18–19
quaternary structure, 17, 43
recombinant expression, 25–31, 42–43
refolding, 28–31, 43, 451, 480–481, 483, 485–486
release in high-pressure homogenization, 117–119, 482–483
secondary structure, 14–15, 43
sedimentation radius, 188
sequencing, 79–80
settling velocity, 188
β-sheet structure, 14–15
size, 4
solubility, 328–334
solubilization of inclusion bodies, 26–28, 43, 451, 483–484
stability, 21–25
tertiary structure, 14–17, 43
β-turn structure, 14
ultrafiltration of, 145, 160–162
protoplasts, 118
psychrometric (humidity) chart, 409–410, 435
purification of specific bioproducts. *See* under individual bioproduct (such as insulin, citric acid)
purine bases, 31

purity
  analysis of, 59–87
  definition, 39–40, 43
  of human insulin, 487
pyrimidine bases, 31

relative humidity, 408–409, 411–412, 435
return on investment, 471–472, 491–492, 499–500, 503
Reynolds number, 146–147, 150–151, 187–188, 276, 283, 377–378, 387–388, 390–393
ribonuclease
  chromatography, 526
  thermal denaturation, 22–23
  tertiary structure, 14–17
ribosomes
  density, 189
  sedimentation coefficient, 191–192
  size, 4, 35
RNA
  analysis of, 77
  structure, 31

SDS-PAGE. *See* analytical methods
secondary metabolites
  antibiotics, 9–11
  biosynthesis, 12
sedimentation (includes centrifugation), 185–218
  angle of disks in disk centrifuge, 203
  basket centrifuge, 195–196, 483, 487
  blood cells, 185, 210
  bowl centrifuge with a continuous flow rotor, 516–517
  breakthrough curves, 516
  centrifugal elutriation, 210, 212
  centrifuge equation, 187
  chamber bowl centrifuge, 196
  comparison of production centrifuges, 194–196, 449
  CsCl gradient, 190
  density of cells, DNA, organelles, proteins, and RNA, 169
  diffusion velocity versus sedimentation velocity, 206–207
  disk centrifuge, 194–195, 200–203, 449, 463, 482–484, 516
  engineering analysis of production centrifuges, 194–203, 211–212
  equation of motion, 186–187
  equilibrium sedimentation, 188, 190–191
  equivalent time 192–193, 211
  field-flow fractionation, 209–210, 212
  and flocculation of cells, 205–206, 212, 449
  hindered settling, 188–189, 211
  in human insulin purification, 482–484, 487
  hybridoma cells, 208
  inclined sedimentation, 207–209, 212
  isopycnic sedimentation, 188, 190
  isothermal settling, 207
  low accelerations, 206–210
  molecular weight determination by, 204, 212
  Péclet analysis, 207, 212
  principles, 186–189
  production centrifuges, 194–203, 449, 482–484, 487
  Reynolds number for example bioproducts, 188
  scroll (or decanter) centrifuge, 195–196, 449
  sedimentation coefficient, 191–192, 211
  settling velocity of example bioproducts, 188
  sigma analysis, 193–203, 211–212
  Stokes drag force, 187
  svedberg units, 191
  tubular bowl centrifuge, 195–200
  ultracentrifugation, 203–204, 212
  velocity, 186–189, 191, 194, 199–202, 204, 207–212
shear
  effect on protein stability, 25
  estimation of shear rate, 341–342
Shulze-Hardy rule. *See* cell flocculation
sigma factor, 193–194, 198–199, 202–203, 211–212
single cell proteins, 34–35
small biomolecules, 4–13
Smoluchowski second order precipitation or flocculation equations, 336, 341, 355–356
solubility of proteins, 328–334, 355
  bound water molecules and, 328–329
  Cohn equation, 332–333, 355
  effect of solvents, 331–334
  as function of charge, 329–331
  as function of ionic strength, 332–333
  as function of pH, 330–331
  hemoglobin, 333
  insulin, 330
  Kirkwood model, 331–332
  model for addition of nonionic polymers, 328–329
  molecular size and, 328–329

molecular structure and, 328
specific activity, 39, 43
specific heat, 411, 432
spores, drying of, 426
spray drying, 407, 426–427, 431–436, 446, 453
staged extraction, 226–232, 240
stages of downstream processing, 35–36, 43, 445–454
standard deviation, 51–52
standard error, 52
sterile filtration. *See* filtration
steroids
adsorption, 250
structure, 9–10
Stokes drag force, 187
Stokes-Einstein equation, 38, 204, 337, 339
streptomycin, 11
sucrose, 4–5
sugars, 4, 5, 33–34
sulfitolysis of proinsulin, 483, 485
SuperPro Designer biochemical process simulator. *See* bioprocess design and economics

taxol, 2, 12–13
temperature, effect on protein stability, 22–23
tissue plasminogen activator (tPA)
biochemical assay for, 57–58
equilibrium moisture curve, 409
triple point of water, 424

ultracentrifugation. *See* sedimentation
ultrafiltration. *See* filtration
unit operations
objectives, 36
sequencing of, 445–454
typical, 35–36, 445–454

vaccine, 32, 34
van Deemter equation. *See* chromatography, liquid
van der Waals forces. *See* cell flocculation
Van't Hoff law for osmotic pressure, 116
vinegar, 6
virus, 4, 89–90
vitamins, 3–7

washing of filter cakes. *See* filtration
water in biological solids and in gases, 408–412
bound, 408, 411–412, 424
unbound or free, 408, 411–412, 424
Western blot. *See* analytical methods
wet-bulb (or saturation) temperature, 409–411, 426

yield, 39, 43, 482, 484–487, 497–498

zeta potential. *See* cell flocculation